2023 Experimental Condensed Matter Physics Principal Investigators' Meeting

September 19-21, 2023

Program and Abstracts

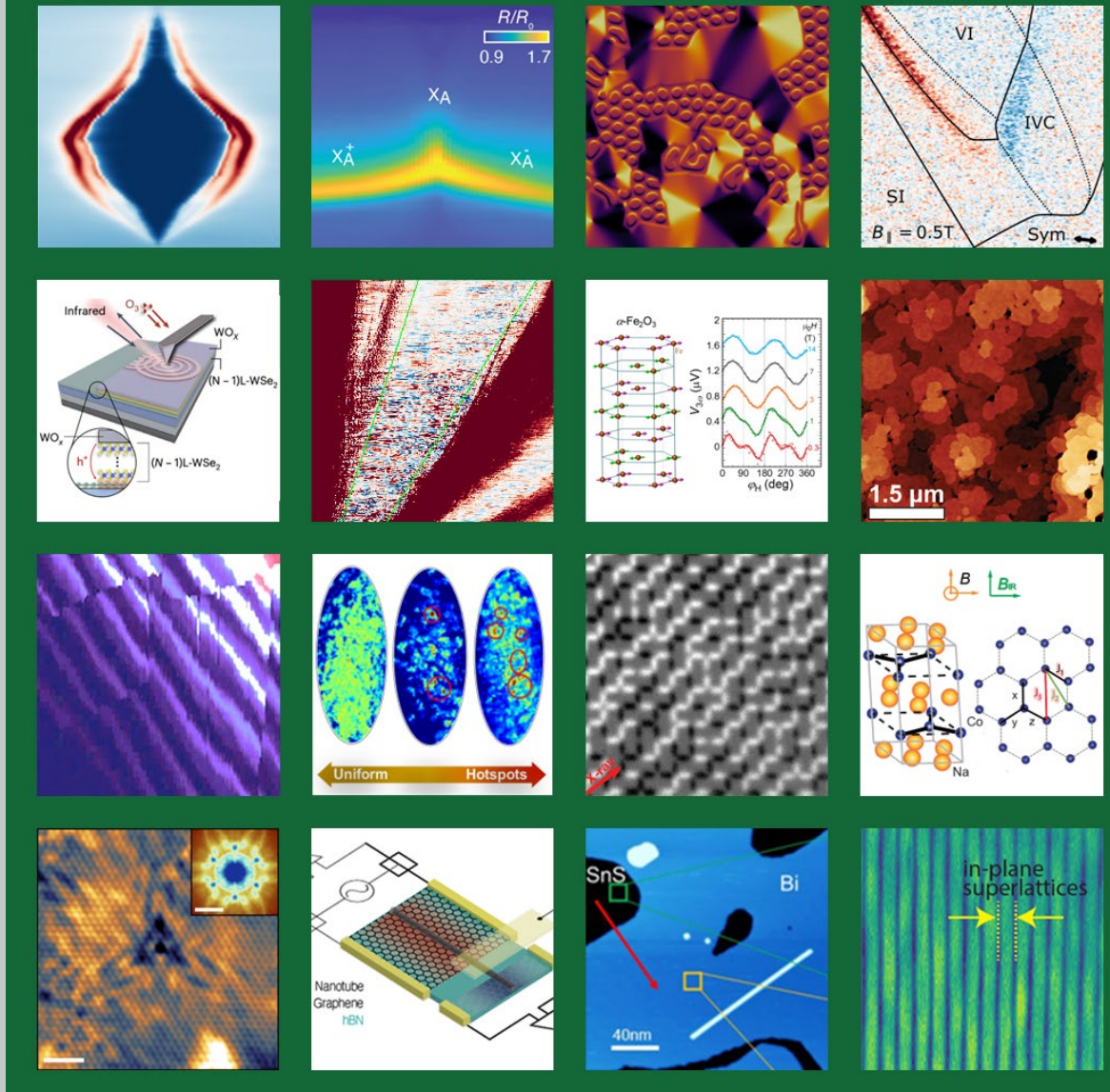

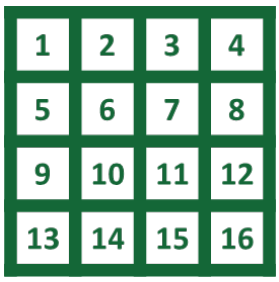

1. Eva Andrei: *Discovery of Field Induced Superconductor to Bose Insulator Transition in Twisted Trilayer Graphene*, phase diagram showing the superconducting dome (dark blue) as a function of moiré band filling.
2. You Zhou: *Giant Optical Nonlinearity in Atomically Thin Semiconductors*, shown is the reflectance spectra of a trilayer WSe_2 as a function of electrostatic doping.
3. Luis Balicas, *Thickness-Driven Giant Anomalous and Topological Hall Effects in* $Fe_{5-x}GeTe_2$, shown is a micromagnetic simulation of the domain structure.
4. Andrea Young: *Intervalley Coherence and Spin Orbit Coupling in Rhombohedral Trilayer Graphene*, shown is the magnetic phase diagram of rhombohedral trilayer graphene measured locally by nanoSQUID on tip microscopy.
5. Dmitri Basov: *Ambipolar Charge-Transfer at van der Waals Interfaces*, shown are the schematics of oxidation-activated charge transfer (OCT) processes.
6. Gleb Finkelstein: *Chiral Andreev Edge States*, shown is a map of nonlocal resistance downstream of a super-conducting contact to graphene in the QH regime.
7. Fengyuan Yang: *Third Harmonic Characterization of Antiferromagnets*, shown is the AFM spin structure of α-Fe_2O_3 in a hexagonal lattice and the in-plane angular dependence of third harmonic Hall voltage.
8. Danna Freedman*: Optically Addressable Molecular Color Center Thin Films on Monolayer Graphene*, shown is an atomic force microscopy image of self-assembled optically addressable molecular qubits and host-matrix molecules on graphene.
9. Sergey Frolov: *"Smoking Gun" Signatures of Topological Milestones through Fine-Tuning in Trivial Materials*, shown are "1/3 charge jumps".
10. Frances Hellman, *Tuning Order-Disorder Transitions in Chiral Phases*, shown is the temporal heterogeneity of fluctuations.
11. Peter Schiffer: *Topological Dynamics in Strings of Magnetic Excitations*, shown is an XMCD-PEEM image of thermally dynamic Santa Fe Ice moments.
12. Dmitry Smirnov: *Disorder-Enriched Magnetic Excitations in a Heisenberg-Kitaev Quantum Magnet* $Na_2Co_2TeO_6$, shown is the average crystal structure of $Na_2Co_2TeO_6$ with each Na site 2/3 occupied.
13. Xavier Roy: 2D Heavy Fermions in a van der Waals Metal, STM topographic image showing standing wave oscillations around a lattice defect.
14. Philip Kim: *Electronic Thermal Conductance in Low-Dimensional Materials with Graphene Nonlocal Noise Thermometry*, show is the schematic of the device in which two graphene thermometers are bridged by a carbon nanotube.
15. Guang Bian: *Synthesis and Characterization of 2D Weyl Semimetals in Epitaxial Bismuthene*, shown is an STM image of epitaxial monolayer bismuthine.
16. Matthew Brahlek: *Epitaxially-Imposed Control of Chiral Transport Phenomena*, shown is spatially resolved x-ray diffraction revealing in-plane superlattices composed of highly-order 1D dislocation arrays in topological insulator (TI) Bi

FOREWORD

This book contains abstracts for presentations made at the 2023 Experimental Condensed Matter Physics (ECMP) Principal Investigators' Meeting sponsored by the Materials Sciences and Engineering Division of the US Department of Energy, Office of Basic Energy Sciences (DOE-BES). The meeting convenes scientists supported within ECMP by the DOE-BES to present the most exciting, new research accomplishments and proposed future research directions in their BES supported projects. The meeting also affords PIs in the program an opportunity to see the full range of research currently being supported. We hope the meeting fosters a collegial environment to 1) stimulate the discussion of new ideas and 2) provide unique opportunities to develop or strengthen collaborations among PIs. In addition, the meeting provides valuable feedback to DOE-BES in its assessment of the state of the program and in identifying future programmatic directions. The meeting was attended by approximately 100 ECMP supported scientists.

The Experimental Condensed Matter Physics program supports research that will advance our fundamental understanding of the relationships between intrinsic electronic structure and properties of complex materials. Research supported by the program focuses on systems whose behavior derives from strong electron correlation, competing or coherent quantum interactions, topology, and effects of interfaces, defects, spin-orbit coupling, and reduced dimensionality. Scientific themes include the interplay of charge, spin, and orbit degrees of freedom resulting in phenomena such as superconductivity, magnetism, and topological protection, and the interactions of these in bulk and reduced-dimensional systems. The program supports synthesis and characterization of new material systems required to explore the central scientific themes. This includes the development of experimental techniques that enable such research. Growth areas include emergent quantum phenomena in topological materials, low-dimensional materials, van der Waals materials, and materials whose functionalities can enable next-generation microelectronics, new clean energy technologies, and quantum technologies.

The meeting was held in a hybrid format and organized into five oral sessions and two poster sessions covering the range of activities supported by the program. Most of the presentations were held by in person participants with the exception of two remote PI talks and a hybrid panel, which featured speakers outside of the ECMP program. Co-chairs for the meeting were Ming Yi (Rice University) and Anand Bhattacharya (ANL). To these two we express our sincere appreciation for their invaluable help in organizing the meeting. We also want to gratefully acknowledge the excellent support provided by Ms. Tia Moua and April Ward of the Oak Ridge Institute for Science and Education and by Ms. Teresa Crockett of BES, for their efforts in organizing the meeting.

Drs. Claudia Cantoni and Tim Mewes
Program Managers, Condensed Matter and Materials Physics
Division of Materials Sciences and Engineering
Basic Energy Sciences

Table of Contents

Foreword iv

Agenda 1

Oral Session 1

Discovery of an unconventional charge density wave intertwined with superconductivity in UTe_2 10

Vidya Madhavan

Complex States, Emergent Phenomena, and Superconductivity in Intermetallic and Metal-Like Compounds 13

Paul Canfield, Sergey Bud'ko, Yuji Furukawa, Adam Kaminski, Makariy Tanatar, Ruslan, Prozorov, Aashish Sapkota, Tyler Slade, and Linlin Wang

Probing the Interplay of Topology, Magnetism and Superconductivity in Intrinsic Magnetic and Superconducting Topologic Materials 17

Ni Ni

Topological Superconductivity in Strong Spin-Orbit Materials 21

Johnpierre Paglione

Superconductivity and magnetism in *d*- and *f*-electron quantum materials 25

M. Brian Maple

Quantum Fluctuations in Narrow Band Systems – Strongly Spin Orbit Coupled Superconductors 31

Filip Ronning, Eric Bauer, Michihiro Hirata, Priscila Rosa, Allen Scheie, and Sean Thomas

Normal State and Superconducting Properties of the Infinite-Layer Nickelates 34

Harold Y. Hwang, Jennifer Fowlie, and Srinivas Raghu

Superconducting nickelate thin films using in-situ synthesis 38

Charles H. Ahn

Study of topological and unconventional superconductivity in low dimensional systems 43

Qi Li

Development of Group-V Network-Based Layered Materials 48

Jin Hu

Science of 100 tesla: Hole pockets, magic gap ratios and nodal quasiparticle states in the cuprates..... 53

Neil Harrison, Mun Chan, Arkady Shekhter, John Singleton, Johanna Palmstrom, Priscila Rosa, Scott Crooker, and Marcelo Jaime

Definitive Majorana Zero Modes in Optimized Hybrid Nanowires 58

Sergey Frolov

Oral Session 2

Symmetry Breaking in Two Dimensional Flat-band Systems for Spin, Charge and Cooper Pair Transport..... 61

Chun Ning (Jeanie) Lau and Marc Bockrath

Synthesis of Electronic-Grade Quantum Heterostructures by Hybrid PLD 66

Chang-Beom Eom

Symmetries, Interactions and Correlation Effects in Carbon Nanostructures..... 72

Gleb Finkelstein

Correlated Topological Quantum Heterostructures 77

Ho Nyung Lee, Matt Brahlek, Gyula Eres, Hu Miao, and T. Zac Ward

Anomalous ac Response Function of Novel Josephson Junctions..... 83

Enrico Rossi, Wei Pan, Javad Shabani

Incompatibility between topological superconductivity and supercurrent injected from Nb. 88

Stephan Kim, Shiming Lei, Leslie Schoop, Robert Cava and N. Phuan Ong

Interface-Induced Superconductivity in Magnetic Topological Insulator-Iron Chalcogenide Heterostructures 91

Cui-Zu Chang

Oral Session 3

Charge-transfer across van der Waals interfaces..... 96

D.N Basov

Indirect excitons in heterostructures 100

Leonid Butov

Van der Waals Heterostructures: Novel Materials and Emerging Phenomena..... 104

Feng Wang, Michael Crommie, Alessandra Lanzara, Steven Louie, Zi Q. Qiu, Mike Zaletel, and Alex Zettl

Quantum Materials **109**

James Analytis, Robert Birgeneau, Alessandra Lanzara, Dunghai Lee, Joel Moore, Joseph Orenstein, and R. Ramesh

Giant optical nonlinearity of Fermi polarons in atomically thin semiconductors **115**

You Zhou

Design, discovery and chemical synthesis of earth abundant magnetic nitrides **120**

Bauers,Sage

Direct Observation of Fractional Quantum Hall Quasiparticle Braiding Statistics via Interferometry **125**

Michael J. Manfra

Topology and molecular arrangement in low-dimensional magnetic materials **129**

Claudia Ojeda-Aristizabal

Large Magneto-Electric Resistance in the Topological Dirac Semimetal α-Sn **134**

Mingzhong Wu

Novel Mechanism for Heat Conduction by Spin-Phonon Hybridized Excitations in a Rare-Earth Magnet **136**

Minhyea Lee

Designing strong stability in non-critical and rare-earth-lean magnetic materials **139**

Laura H. Lewis, Gregory Fiete, George Hadjipanayis, Chaoying Ni, and Julie B. Staunton

Magneto-optical Study of Correlated Electron Materials in High Magnetic Fields **144**

Dmitry Smirnov and Zhigang Jiang

Oral Session 4

Geometry and frustration-induced phenomena in nanomagnet arrays **150**

Peter Schiffer

Broken Symmetries for Control of Electrically-Generated Spin Currents and Torques **154**

Dan Ralph

Hybrid-Magnon Quantum Devices **159**

Axel Hoffmann, Yi Li, Valentine Novosad, Wolfgang Pfaff, André Schliefe, and Jian-Min Zuo

Selective growth of *a*-plane and *c*-plane oriented Kagome antiferromagnet Mn_3Sn thin films on *c*-plane sapphire **164**

Arthur R. Smith

Thickness-driven giant anomalous and topological Hall effects in $Fe_{5-x}GeTe_2$ 169

Luis Balicas

Hanle Hall effect in Pt/insulator boundaries 175

Xiaoshan Xu

Sub-Nanosecond Switching of Antiferromagnets Driven by Interfacial Spin-Orbit Torque 180

Fengyuan Yang

Current Driven Switching of the Neel Vector 185

Fernando Ajejas, Felipe Torres, Ali C. Basaran, Pavel Salev, and Ivan K. Schuller

Oral Session 5

Correlated States of Two-dimensional Electron Systems in AlAs Quantum Wells 188

M. Shayegan

Quantum Fluctuations in Narrow Band Systems – Thrust 1 193

Filip Ronning, Eric Bauer, Michihiro Hirata, Priscila Rosa, Allen Scheie, and Sean Thomas

Synthesis and Studies of Emergent Quantum Properties of Solids 197

I.R. Fisher, A. Kapitulnik, and S.A. Kivelson

The Ground State of Geometrically Frustrated Magnets 202

Arthur P. Ramirez

Unusual ring-like magnons in novel class of Weyl magnets discovered. 205

Jak Chakhalian

Probing electronic and topological properties in 2D atomic crystals and their heterostuctures 206

Eva Y. Andrei

Nanostructure Studies of Correlated Quantum Materials - Shot noise in a strange metal 211

Douglas Natelson

Emergent Quasiparticles in Graphene Heterostructure 216

Philip Kim

Emergent Topological Properties of Landau Flatbands 221

Gabor Csathy

Time, Momentum, and Energy Resolved Pump-Probe Tunneling Spectroscopy 226

H. M. Yoo, M. Korkusinski, D. Miravet, K. W. Baldwin, K. West, L. Pfeiffer , P. Hawrylak , and R. C. Ashoori

Poster Session 1

Optically Addressable Molecular Color Center Thin Films on Monolayer Graphene..... 230

James Rondinelli, David Awschalom, Danna Freedman, Mark Hersam, Jeffrey Long

Search for 3D Topological Superconductors using Laser-Based Spectroscopy..... 234

David Hsieh

Magnetometry Studies of Quantum Correlated Topological Materials in Intense Magnetic Fields 238

Lu Li

Chiral Materials and Unconventional Superconductivity 243

Qiang Li, Mengkun Liu, Weiguo Yin, and Genda Gu

Perfect Coulomb drag in a dipolar excitonic insulator 249

Kin Fai Mak

Correlated Quantum Materials..... 250

Michael A. McGuire, David Mandrus, Andrew F. May, Brenden Ortiz, and Jiaqiang Yan

Tuning magnetic topological insulators using defects..... 255

D. C. Johnston, L. Ke, R. J. McQueeney, P. P. Orth, B. G. Ueland, and D. Vaknin

Dynamics and Driven States in Quantum Magnets..... 260

Thomas F. Rosenbaum

Berry curvature engineering in superconductors..... 265

Badih Antoine Assaf, Yi-Ting Hsu, Xiaolong Liu, and Xinyu Liu

Synthesis and Characterization of 2D Weyl Semimetals in Epitaxial Bismuthene 268

Guang Bian

In-Situ Cryo 4D STEM of Layered Correlated Materials..... 270

Judy J. Cha and Eun-Ah Kim

Epitaxially-Imposed Control of Chiral Transport Phenomena..... 274

Matthew Brahlek

Macroscopic quantum states in antiferromagnets: Bose-Einstein condensation of anti-ferro-magnons 276

Dmytro Bozhko, Zbigniew Celinski, and Valentine Novosad

MXetronics: MXenes as Multifunctional Materials..... 279

Bhoj Raj Gautam, Daniel Autrey, Chandra Mani Adhikari, Shubo Han, Bishnu Prasad Bastakoti, and Binod Kumar Rai

APS CUWiP+: Supporting the Success of All Undergraduate Women+ in Physics 283

Crystal Bailey and Farah Dawood

Update on the activities of the National Academy of Sciences Condensed Matter and Materials Research Committee 287

Colleen N. Hartman

Planar Systems for Quantum..... 289

Jie Shan, Cory R. Dean, James Hone, Allan H. MacDonald, Kin Fai Mak, and Tony F. Heinz

Dynamics of Electron Interactions in Superconductors and Other Novel Materials..... 293

Dan Dessau

Poster Session 2

Digital Synthesis: A pathway to novel states of condensed matter 299

Anand Bhattacharya, Dillon Fong, and Samuel Jiang

Emerging Materials 304

John F. Mitchell, Daniel Phelan, and Nirmal Ghimire

Magnetism and Topology in Kagome and van der Waals Systems..... 309

Ming Yi

Anomalous Proximatized Transport in Metal/Quantum Magnet Heterostructure 314

Haidong Zhou, and Jian Liu

2D magnetic spin LED..... 319

Xiao-Xiao Zhang

High temperature quantum valley Hall effect..... 322

Jun Zhu

Topological Engineering in Carbon-Based Nanostructures 324

Felix R. Fischer

Two Dimensional Heavy Fermions in the van der Waals Metal CeSiI..... 328

Xavier Roy and Abhay Pasupathy

First Observation of Coupled Ferroelectricity and Superconductivity in Few-layer Superconductors 332

Daniel Rhodes and Xiaofeng Qian

Moiré Magnetism in Twisted 2D Magnets 337

Liuyan Zhao

Ultrafast Control of Topological Transport in Quantum Materials..... 341

James McIver

Heterogeneous Integration of 2D-3D Materials for Energy Efficient Electronics..... 345

Nihar R. Pradhan, Anirudha V. Sumant, Jerzy Leszczynski, Dinesh Kumar Sengottuvelu, Mohammed Majdoub, Sasan Nouranian, and Ahmed Al-Ostaz

Exciton Dynamics in 2D WSe_2 Samples..... 348

Birol Ozturk

Incommensurate Interfaces in Intercalated Quantum Materials 350

Joe Checkelsky

Criteria and impact of electronic growth modes of metals on MoS_2 354

Timothy E. Kidd, Pavel V. Lukashev, Paul M. Shand, Andrew J. Stollenwerk

Exploring Chirality-Spin Interplay Enabled by the Inorganic Chiral Nanostructures..... 358

Min Ouyang

Probing the origins of Chirality Induced Spin Selectivity via transport measurements..... 362

Meenakshi Singh

Intervalley coherence and spin orbit coupling in rhombohedral trilayer graphene 364

Andrea Young

Ultrafast and high-endurance switching of sliding ferroelectrics 367

Kenji Yasuda, Evan Zalys-Geller, Xirui Wang, Kenji Watanabe, Takashi Taniguchi, Raymond Ashoori, and Pablo Jarillo-Herrero

Author Index 371

Participant List.....375

Agenda

2023 DOE-BES Experimental Condensed Matter Physics

Principal Investigators' Meeting

Meeting Chairs: Claudia Cantoni and Tim Mewes (DOE-BES)
Meeting Co-Chairs: Ming Yi (Rice University) and Anand Bhattacharya (Argonne National Laboratory)

Tuesday, September 19, 2023	
7:30-8:15 AM	**Breakfast**
8:15-8:30 AM	**Claudia Cantoni and Tim Mewes**, ECMP Program Managers, DOE-BES *Welcome and Introductory Remarks*
Oral Session 1	Session Chair: **Cui-Zu Chang**, Penn State University
8:30-9:00 AM	**Vidya Madhavan**, University of Illinois Urbana-Champaign *Extended Talk: Discovery of an Unconventional Charge Density Wave Intertwined with Superconductivity in UTe_2*
9:00-9:15 AM	**Adam Kaminski**, AMES National Laboratory *A New Fermionic State Revealed*
9:15-9:30 AM	**Ni Ni**, University of California – Los Angeles *Unconventional Pressure-Driven Metamagnetic Transitions in Topological Van der Waals Magnets*
9:30-9:45 AM	**Johnpierre Paglione,** University of Maryland *Tuning Critical Fluctuations and Superconductivity in UTe_2*
9:45-10:00 AM	**Brian Maple**, University of California – San Diego *Suppression of the Conducting Surface State in FeSi*
10:00-10:15 AM	**Sean Thomas,** Los Alamos National Laboratory *UTe_2 Under Stress*
10:15-10:45 AM	**Break**
10:45-11:15 AM	**Harold Hwang**, SLAC National Accelerator Laboratory *Extended Talk: 'Strange Metal' Behavior in $Nd_{1-x}Sr_xNiO_2$*
11:15-11:30 AM	**Charles Ahn**, Yale University *Superconducting NENO Thin Films Using In-Situ Synthesis*
Canceled	**Qi Li**, Penn State University *High T_c and Large Anisotropic H_{c2} in Ultrathin MgB_2 Films*
11:30-11:45 PM	**Jin Hu**, University of Arkansas *Insulator-to-Metal Transition in a P-based Layered Material*

11:45-12:00 PM	**Neil Harrison**, Los Alamos National laboratory *Science of 100 Tesla: Magic Gap Ratio for High-T_c*
12:00-1:15 PM 12:35-1:15 PM	Lunch and Concurrent Keynote Presentation **Sergey Frolov,** University of Pittsburgh *"Smoking Gun" Signatures of Topological Milestones*
Oral Session 2	Session Chair: **Anand Bhattacharya**, Argonne National Laboratory
1:15-1:45 PM	**Marc Bockrath,** Ohio State University *Extended Talk: Quantum Geometry Enabling Superconductivity*
1:45-2:00 PM	**Chang-Beom Eom**, UW–Madison *Electronic-Grade Quantum Epitaxial Heterostructures*
2:00-2:15 PM	**Gleb Finkelstein**, Duke University *Chiral Andreev Edge States*
2:15-2:30 PM	**Ho Nyung Lee**, Oak Ridge National Laboratory *Correlated Electrons Enter the Extreme Quantum Limit*
2:30-3:00 PM	**Break**
3:00-3:15 PM	**Enrico Rossi**, William & Mary *Anomalous ac Response of Novel Josephson Junctions*
3:15-3:30 PM	**Phuan Ong**, Princeton University *Oscillations of Topological Edge Supercurrent in $MoTe_2$*
3:30-3:45 PM	**Cui-Zu Chang**, Penn State University *Interface-Induced Superconductivity in Magnetic Topological Insulator-Iron Chalcogenide Heterostructures*
3:45-5:45 PM	*Poster Session 1*
5:45-6:55 PM 6:15-6:55 PM	**Dinner and Concurrent Keynote Presentation** **Frances Hellman**, Lawrence Berkeley National Laboratory *Hidden Order in Amorphous Materials: Tuning order-disorder transitions in chiral phases*

Wednesday, September 20, 2023	
7:30–8:15am	**Breakfast**
Oral Session 3	Session Chair: **Jun Zhu**, Penn State University
8:15-8:45 AM	**Dimitri Basov**, Columbia University *Extended Talk: Ambipolar Charge-Transfer at van der Waals Interfaces*
8:45-9:00 AM	**Leonid Butov**, University of California San Diego Indirect excitons (IXs) in heterostructures (HS)
9:00-9:15 AM	**Feng Wang**, Lawrence Berkeley National Laboratory *Observation of "Cosmic Sound" in Graphene*
9:15-9:30 AM	**Joe Orenstein**, Lawrence Berkeley National Laboratory *Universal Spin Wavepacket Propagation in 2D Magnets*
9:30-9:45 AM	**You Zhou**, University of Maryland *Giant Optical Nonlinearity in Atomically Thin Semiconductors*
9:45-10:00 AM	**Sage Bauers**, National Renewable Energy Laboratory *A New Cation-Disordered Magnetic Nitride*
10:00-10:30 AM	**Break**
10:30-11:00 AM	**Mike Manfra**, Purdue University *Extended Talk: Direct Observation of Anyonic Braiding Statistics*
11:00-11:15 AM	**Claudia Ojeda-Aristizabal**, California State University Long Beach *Accessing Ground States in Insulating Kitaev Materials*
11:15-11:30 AM	**Mingzhong Wu**, Colorado State University *Large Bilinear Magneto-Electric Resistance in α-Sn*
11:30-11:45 AM	**Minhyea Lee**, University of Colorado Boulder *Novel Mechanism for Heat Conduction by Spin-Phonon Hybridized Excitations in a Rare-Earth Magnet*
11:45-12:00 PM	**Laura Lewis**, Northeastern University *Rare-Earth-Free Permanent Magnets: Prediction, Creation, Validation*
12:00-12:15 PM	**Dmitry Smirnov**, National High Magnetic Field Laboratory *Disorder-Enriched Magnetic Excitations in a Heisenberg-Kitaev Quantum Magnet $Na_2Co_2TeO_6$*
12:15-1:15 PM	Lunch Andrew Schwartz, MSE Division Director, DOE/BES Materials Science and Engineering Division Update Brief ECMP Program Manager Remarks Regarding Acknowledgements
Oral Session 4	Session Chair: **Andrea Young**, University of California Santa Barbara
1:15-1:45 PM	**Peter Schiffer**, Yale University *Extended Talk: Topological Dynamics in Strings of Magnetic Excitations*
1:45-2:00 PM	**Dan Ralph**, Cornell University *New Mechanisms for Electrical Control of Spin Currents*

2:00-2:15 PM	**Axel Hoffmann**, University of Illinois Urbana-Champaign *Unidirectional Microwave Transduction with Short-Wavelength Magnons*
2:15-2:30 PM	**Art Smith**, Ohio University *Selective Growth of a-Plane and c-Plane Oriented Kagome Antiferromagnet Mn_3Sn Thin Films on c-Plane Sapphire*
2:30-3:00 PM	**Break**
3:00-3:15 PM	**Luis Balicas**, National High Magnetic Field Laboratory *Thickness-Driven Giant Anomalous and Topological Hall Effects in $Fe_{5-X}GeTe_2$*
3:15-3:30 PM	**Xiaoshan Xu**, University of Nebraska-Lincoln *Hanle Hall Effect in Pt/Insulator Structures*
3:30-3:45 PM	**Fengyuan Yang**, Ohio State University *Third Harmonic Characterization of Antiferromagnets*
Canceled	**Ivan Schuller**, University of California San Diego *Current Driven Switching of the Neel Vector*
3:45-5:45 PM	**Poster Session 2**
5:45-7:15 PM **6:15-7:15 PM** **Hybrid**	**Dinner and Concurrent Panel Discussion** **The Future of Microelectronics** **Panelists:** • **Debdeep Jena**, David E. Burr Professor of Engineering, Cornell University • **Tina Kaarsberg**, Technology Manager, Advanced Materials and Manufacturing Technologies Office (AMMTO), DOE-EERE • **Vijay Narayanan**, IBM Fellow & Strategist, Senior Manager, PCM and AI Materials, IBM • **Mark Stiles**, Project Leader and NIST Fellow, Alternative Computing Group, Nanoscale Device Characterization Division of the Physical Measurement Laboratory, NIST • **Susan Trolier-McKinstry**, Evan Pugh University Professor and Steward S. Flaschen Professor of Ceramic Science and Engineering, and Professor of Electrical Engineering, Penn State University • **Ian Young**, Senior Fellow and Director, Exploratory Integrated Circuits, Components Research, Intel **Moderator:** • **Axel Hoffmann,** Founder Professor, University of Illinois at Urbana-Champaign

Thursday, September 21, 2023	
7:30–8:15am	**Breakfast**
Oral Session 5	Session Chair: **Ming Yi**, Rice University
8:15-8:30 AM	**Mansour Shayegan**, Princeton University *Many-Body States of 2D Electrons with Anisotropic Valleys*
8:30-8:45 AM	**Filip Ronning**, Los Alamos National Lab *Kondo Quasiparticle Dynamics Observed by Resonant Inelastic X-Ray Scattering*
8:45-9:00 AM	**Ian Fisher**, Stanford University *Emergent Tetragonality in a Fundamentally Orthorhombic Material*
9:00-9:15 AM	**Art Ramirez**, University of California Santa Cruz *The Ground State of Geometrically Frustrated Magnets*
9:15-9:30 AM	**Jak Chakhalian**, Rutgers University *Unusual Ring-Like Magnons in Novel Class of Weyl Magnets Discovered*
9:30-10:00 AM	**Break**
10:00-10:15 AM **Virtual**	**Eva Andrei**, Rutgers University *Discovery of Field Induced Superconductor to Bose Insulator Transition in Twisted Trilayer Graphene*
10:15-10:30 AM **Virtual**	**Doug Natelson**, Rice University *Shot Noise in a Strange Metal: No Quasiparticles?*
10:30-10:45 AM	**Philip Kim**, Harvard University *Electronic Thermal Conductance in Low-Dimensional Materials with Graphene Nonlocal Noise Thermometry*
10:45-11:00 AM	**Gabor Csathy**, Purdue University *The Transition from an Anderson-Type Insulator to Collective Localization in Topological Phases*
11:00-11:15 AM	**Ray Ashoori**, Massachusetts Institute of Technology *Time, Momentum, Energy Resolved Pump-Probe Pulsed Tunneling Spectroscopy*
11:15-11:25 AM	**Concluding Remarks**

Tuesday, September 19, 2023
4:15-6:15 PM

Poster Session 1

Presenter	Institution	Title
Danna Freedman	MIT	*Optically Addressable Molecular Color Center Thin Films on Monolayer Graphene*
Dave Hsieh	Caltech	*A Light-Induced Topological Transition in Tellurium*
Lu Li	Michigan	*Thermodynamic Evidence of Quantum Oscillations in Kondo Insulators*
Qiang Li	BNL	*Ultrafast Melting of Superconductivity*
Kin Fai Mak	Cornell	*Dipolar Excitonic Insulator in a Moiré Lattice*
Michael McGuire	ORNL	*Understanding Distortions in a Kagome Metal*
Rob McQueeney	Ames	*Tuning Magnetic Topological Insulators Using Defects*
Tom Rosenbaum	Caltech	*Domain Wall Tunneling In Driven Quantum Magnets*
Badih Assaf	Notre Dame	*Berry Curvature Engineering in Superconductors*
Guang Bian	Missouri	*Synthesis and Characterization of 2D Weyl Semimetals in Epitaxial Bismuthene*
Judy Cha	Cornell	*In Situ Cryo 4D Stem of Charge Density Waves (CDWs) in TaS_2*
Matthew Brahlek	ORNL	*Epitaxially-Imposed Control of Chiral Transport Phenomena*
Dmytro Bozhko	UCCS	*Macroscopic Quantum States in Antiferromagnets: Bose-Einstein Condensation of Anti-Ferro-Magnons*
Bhoj Gautam	Fayetteville	*Mxetronics: Mxenes as Multifunctional Materials*
Crystal Bailey	APS	*APS CUWiP+: Supporting the Success of All Undergraduate Women+ in Physics*
Colleen Hartman	NAS	*Partial Support of the Condensed Matter and Materials Research Committee*
Jie Shan	Cornell	*Fractional Chern Insulator in Moiré $MoTe_2$*
Dan Dessau	Colorado	*A 'Strange Metal' Nickelate*

Wednesday, September 20, 2023
4:00-6:00 PM

Poster Session 2

Presenter	Institution	Title
Anand Bhattacharya	ANL	*Tunable Superconductivity and its Origin at $KtaO_3$ Interfaces*
John Mitchell	ANL	*Stripes and Metals Meet in the Middle*
Ming Yi	Rice-University	*Emergent Phases in Magnetic Kagome Lattices*
Haidong Zhou	University-of-Tennessee	*Anomalous Proximitized Transport in Metal/Quantum Magnet Heterostructure $Bi_2Ir_2O_7/Yb_2Ti_2O_7$*
Xiao-Xiao Zhang	University of Florida	*Spin Led Realized with 2D Magnetic Heterostructures*
Jun Zhu	Penn-State	*High Temperature Quantum Valley Hall Effect*
Felix Fischer	UC Berkeley	*Robust Metallicity in Bottom-Up Synthesized GNR*
Xavier Roy	Columbia	*2D Heavy Fermions in a van der Waals Metal*
Daniel Rhodes	UW–Madison	*First Observation of Coupled Ferroelectricity and Superconductivity in Few-layer Superconductors*
Liuyan Zhao	University-of-Michigan	*Moiré Magnetism in Twisted 2D Magnets*
James McIver	Columbia	*Ultrafast Control of Topological Transport*
Nihar Pradhan	Jackson State	*Heterogeneous Integration of 2D-3D Materials for Energy Efficient Electronics*
Birol Ozturk	Morgan-State-University	*Quantum Properties of Defects in 2D Semiconductors*
Joe Checkelsky	MIT	*Structurally Modulated vdW Superlattice*
Tim Kidd	University-of-Northern-Iowa	*Surface Criteria for Quantized Growth Modes*
Min Ouyang	University of Maryland	*Interfacial Chirality Induced Spin Polarization in Semiconductors*
Meenakshi Singh	Co-School-of-Mines	*Characterizing CISS Materials with Magneto-Transport Measurements*
Andrea Young	UCSB	*Intervalley Coherence and Spin Orbit Coupling in Rhombohedral Trilayer Graphene*
Ray Ashoori	MIT	*Ultrafast High Endurance Ferroelectric Memory*

Oral Session 1

Discovery of an unconventional charge density wave intertwined with superconductivity in UTe_2

Vidya Madhavan, University of Illinois, Urbana-Champaign

Keywords: Superconductors, scanning tunneling microscopy, topology, single crystals,

Research Scope

Over the past few decades there is has been an intense search for topological superconductors (TSs). Some of the interest in realizing and exploring these materials stems from the possibility of realizing exotic particles such as Majorana fermions. But even beyond this, there are many experimental and theoretical unknowns about these new phases. Our goal is to investigate TSs with low temperature scanning tunneling microscopy (STM) and spectroscopy (STS). We are deploying a variety of tuning knobs such magnetic fields and temperature to obtain answers to fundamental questions on the nature of superconductivity and the low energy excitations of these systems.

Recent Progress

A pair density wave (PDW) phase is an exotic state of matter where the cooper pair density and the superconducting gap oscillate as a function of position. PDWs can occur as a daughter phase of an existing charge density wave (CDW) state and superconductivity or as the parent phase with the CDW being the daughter order. In the former case, even if superconductivity is destroyed with field, the CDW continues to survive, as is seen in almost all known superconducting materials with a high temperature CDW phase (for example, transition metal dichalcogenides, Kagome superconductors etc.). In the latter case, the CDW would disappear if either the PDW or superconductivity is destroyed. We have carried out STM studies of the charge density wave phase in the triplet superconductor UTe_2. We show that UTe_2 hosts an unusual CDW which gets suppressed with magnetic fields and disappears close to the superconducting H_{c2} (Fig.1)[1]. One possible hypothesis that explains the magnetic field sensitivity, and the concomitant disappearance of the CDW and superconductivity is that the CDW arises from and is intertwined with a pair density wave (PDW) and uniform superconductivity in this system. To test this hypothesis, we generate real space maps of the amplitude and phase as a function of field[2]. The maps reveal that the melting of the CDW occurs by the generation of topological defects or dislocations in the CDW with an increasing magnetic field. Moreover, there is a direct correspondence between the regions of suppressed CDW order parameter and the location of the topological defects. Our theory shows that this behavior is consistent with the presence of a parent PDW phase on the surface UTe_2.

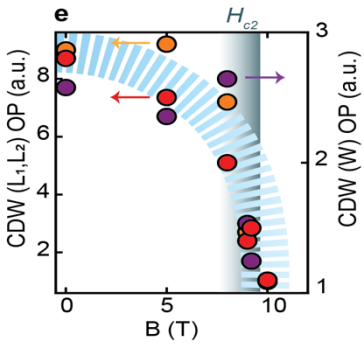

Fig. 1 Magnetic field dependence of the CDW order parameter.

Future Plans

1) We have ordered a vector magnet for our system. It will be installed in January 2024 and will allow us to make STM measurement in a parallel field that will provide further data to determine the order parameter of UTe_2.

2) We have set up a new molecular beam epitaxy system to grow UTe_2 films. The system has been designed and built. We are currently testing the system.

References

1. Aishwarya, A., May-Mann, J., Raghavan, A. et al. Magnetic-field-sensitive charge density waves in the superconductor UTe_2, Nature 618, 928–933 (2023). https://doi.org/10.1038/s41586-023-06005-8
2. Anuva Aishwarya, Julian May-Mann, Sheng Ran, Shanta R. Saha, Johnpierre Paglione, Nicholas P. Butch, Eduardo Fradkin, Vidya Madhavan, Visualizing the Melting of the Charge Density Wave in UTe2 by Generation of Pairs of Topological Defects with Opposite Winding, arXiv:2306.09423

Publications

1. Yulia Maximenko, Yueqing Chang, Guannan Chen, Mark R. Hirsbrunner, Waclaw Sweich, Taylor L. Hughes, Lucas K. Wagner, Vidya Madhavan, *Nanoscale Studies of Electric Field Effects on Monolayer 1T'-WTe_2*, *npj Quantum Mater*., **7**, 29, (2022), DOI: https://doi.org/10.1038/s41535-022-00433-x.
2. Z. Wang, Cheng-Yi Huang, Chia-Hsiu Hsu (+), Hiromasa Namiki, Tay-Rong Chang, Feng-Chuan Chuang, H. Lin, Takao Sasagawa, Vidya Madhavan, Yoshinori Okada, *Observation of a van Hove Singularity of a Surface Fermi Arc with Prominent Coupling to Phonons in a Weyl Semimetal*, Phys. Rev. B, **105**, 075100, (2022), DOI: https://doi.org/10.1103/PhysRevB.105.075110.
3. Zhenyu Wang, Jorge Olivares Rodriguez, Hiromasa Namiki, Vivek Pareek, Keshav Dani, Takao Sasagawa, Vidya Madhavan, Yoshinori Okada, *Visualizing Superconductivity in a Doped Weyl Semimetal with Broken Inversion Symmetry*, Phys. Rev. B, **104**, 115102, (2021), DOI: https://doi.org/10.1103/PhysRevB.104.115102.
4. Guannan Chen (+), Anuva Aishwarya (+), Mark R. Hirsbrunner, Jorge Olivares Rodriguez, Lin Jiao, Lianyang Dong, Nadya Mason, Dale Van Harlingen, John Harter, Stephen D. Wilson, Taylor L. Hughes, Vidya Madhavan, *Evidence for a Robust Sign-Changing S-Wave Order Parameter in Monolayer Films of Superconducting Fe(Se,Te)/Bi_2Te_3*, npj Quantum Materials, **7,** 110, (2022) DOI: https://doi.org/10.1038/s41535-022-00513-y
5. Yue Yu, Vidya Madhavan, S. Raghu, *Majorana Fermion Arcs and the Local Density of States in UTe_2*, Physical Review B, Volume 105, 174520, (2022) DOI: https://doi.org/10.1103/PhysRevB.105.174520
6. Anuva Aishwarya, Julian May-Mann, Arjun Raghavan, Liamei Nie, Marisa Romanelli, Sheng Ran, Shanta R. Saha, Johnpierre Paglione, Nicholas P. Butch, Eduardo Fradkin, Vidya Madhavan, *Magnetic-Field Sensitive Charge Density Wave Orders in the Superconducting Phase of UTe_2*, Nature **618**, 928–933 (2023). https://doi.org/10.1038/s41586-023-06005-8
7. Anuva Aishwarya, Julian May-Mann, Sheng Ran, Shanta R. Saha, Johnpierre Paglione, Nicholas P. Butch, Eduardo Fradkin, Vidya Madhavan, *Visualizing the Melting of the Charge Density Wave in UTe2 by Generation of Pairs of Topological Defects with Opposite Winding,* arXiv:2306.09423

Program Title: Complex States, Emergent Phenomena, and Superconductivity in Intermetallic and Metal-Like Compounds

Principle Investigators: Paul Canfield (FWP leader), Sergey Bud'ko, Yuji Furukawa, Adam Kaminski, Makariy Tanatar, Ruslan Prozorov, Aashish Sapkota, Tyler Slade, Linlin Wang, Division of Materials Science and Engineering, Ames Laboratory, Iowa State University, Ames, IA 50011

Keywords

Magnetism, Superconductivity, Topology, non-Fermi liquid behavior, Emergent quantum phases.

Research Scope

Our FWP focuses on discovering, understanding and ultimately controlling new and extreme examples of complex states, emergent phenomena, and superconductivity. Materials manifesting specifically clear or compelling examples (or combinations) of superconductivity, strongly correlated electrons, novel electronic topologies, quantum criticality, and exotic, bulk magnetism are of particular interest given their potential to lead to revolutionary steps forward in our understanding of their complex, and potentially energy relevant, properties. The experimental work consists of new materials development and crystal growth, combined with detailed and advanced measurements of microscopic/spectroscopic, thermodynamic, transport and electronic properties, at extremes of pressure, temperature, magnetic field, and resolution. The theoretical work focuses on understanding and modeling transport, thermodynamic and spectroscopic properties using world-leading and advanced phenomenological approaches to superconductors and electronic band structures.

The priority of this FWP is the development and understanding of model systems combined with agile and flexible response to, and leadership in, a rapidly-changing new-materials landscape. To accomplish this goal, our combined synthetic, characterization and theory efforts operate both in series and in parallel. This work supports the DOE mission by directly addressing the Grand Challenge of understanding the Emergence of Collective Phenomena: Strongly Correlated Multiparticle Systems and is a key contributor to fulfilling the Ames Laboratory Scientific Strategic Plan for preeminence in solid-state materials discovery, synthesis, and design; this FWP designs, discovers, characterizes and understands systems that shed light on how remarkable properties of matter emerge from complex correlations of the atomic or electronic constituents and, as a result, provides better control of these properties. These efforts directly address research priorities identified in the Basic Research Needs Workshops on *Quantum Materials for Energy Relevant Technology* and *Synthesis Science for Energy Relevant Technology*.

Recent Progress

For this contractors meeting, we will primarily present our discovery and progress in studying the spin textured Fermi arcs that emerge upon transition to AFM state in some of the cubic rare-earth mono-pnictides [1]. This work is the culmination of over a decade of effort, and building, to create a laser ARPES system that can reach temperatures below 3 K with high momentum and energy resolution that could then study the effect of local moment ordering on model, intermetallic compounds. NdBi undergoes AFM transition at T_N=24.5 K. We found that upon establishing long range magnetic order in this material, in addition to other changes in the band structure, pairs of very sharp surface states appear, first as a single band, but upon further cooling this band splits into two, one electron-like and one hole-like. At E_F, the hole-like band forms an arc, rather than a closed contour in momentum space. Both the energy separation and curvature of these bands display strong temperature dependences. Furthermore, circular dichroism data revealed that the two bands in a pair have opposite spin polarization and spin textures. The observed magnetic splitting is highly unusual, as it creates bands of opposing curvature, that change with temperature and follow the antiferromagnetic order parameter. This is completely different from previously reported cases of magnetic splitting such as traditional Zeeman or Rashba, where the curvature of the bands is temperature independent. This is likely a new Fermionic state created by new type of magnetic band splitting in the presence of a long-range AFM order that is not readily explained by existing theoretical ideas. Because the surface states are spin/momentum locked and intimately linked to the AFM order, they can be controlled by the application of magnetic fields such as those present in ultrafast laser pulses, thereby this class of materials potentially opens new avenues for terahertz spintronics.

We extended these studies to other compounds within the monopnictide family and found similar effects also in NdSb, CeBi, whereas we did not detect these states in SmBi down to lowest temperatures. It appears that the strength of the effect (intensity of the surface states and their energy separation) depends on the magnetic moment of the rare-earth element. [2] We further found that these states form domains in real space, due to three possible orientations of the AFM ordering vector at the sample surface. [3]

Future Plans

The RSb and RBi APRES studies have clearly illustrated that we can detect and quantify complex and novel changes in band structure and topology associated with local moment ordering. We have ongoing collaborations with STM groups (Madrid and Geneva) to study the QPI and spin textures we have discovered in our ARPES data. We are continuing to expand our studies to heavier rare earth members of the RBi and RSb families and also embarking on dilution studies such as $(Nd_{1-x}La_x)Sb$ and $(Nd_{1-x}La_x)Bi$. More broadly, we plan to search for other cleavable, model systems that will let us examine the interaction between local and itinerant moment ordering or hybridization with the conduction band.

More widely, we will use NMR, ARPES, London penetration depth, as well as ambient and high-pressure measurements of resistivity and magnetization to study, and even create, new superconductors. In many of these cases we can gain insight into the nature, and symmetry, of the superconducting gap by studying the effects of chemical substitution as well as electron irradiation on these properties. We are studying novel superconductors ranging from FeAs materials like $CaKFe_4As_4$, to U-based heavy Fermion systems like UTe_2, to potentially unconventional gapped materials like $Rh_{17}S_{15}$, to pressure induced superconductivity in Re_3Ge_7 and even superhydride systems.

We continue to develop pressure and strain dependent measurements. We will apply pressure to tune itinerant magnetic systems to and through quantum phase transitions often with the goal of identifying quantum critical points that may have emergent states associated with them. We currently can perform temperature and field dependent NMR, electrical transport, a.c. specific heat and magnetization for pressures under 2.5 GPa; we can measure temperature and field dependent electrical transport and magnetization in anvil cell configurations up to 50 GPa. The FWP is currently installing a single crystal x-ray diffraction unit that can perform diffraction studies on samples in diamond anvil cells (DACs) so that we can add in-house, pressure dependent, structural data to our capabilities, thus allowing for direct structure-property correlation.

Beyond superconductivity, we will continue to develop new, fragile magnetic systems with the intent of discovering new quantum critical systems and mastering new emergent phases that may be in proximity to their quantum critical points. The discovery and development of these new systems will be accomplished by implementation of new algorithms for the discovery of low dimensional crystal structures as well as on the use of band structure theory to identify antiferromagnetic systems that respond strongly to pressure, stress, and/or substitution. (A detailed discussion of some of these algorithms can be found in "New Materials Physics" [4])

References

[1] B. Schrunk, Y. Kushnirenko, B. Kuthanazhi, J. Ahn, L.-L. Wang, E. O'Leary, K. Lee, A. Eaton, A. Fedorov, R. Lou, V. Voroshnin, O. J. Clark, J. Sánchez-Barriga, S. L. Bud'ko, R. Slager, P. C. Canfield and A. Kaminski, "*Emergence of Fermi arcs due to magnetic splitting in an antiferromagnet*", Nature **603**, 610–615 (2022).

[2] Y. Kushnirenko, B. Schrunk, B. Kuthanazhi, L.-L. Wang, J. Ahn, E. O'Leary, A. Eaton, S. L. Bud'ko, R.-J. Slager, P. C. Canfield, and A. Kaminski, "*Rare-earth monopnictides: Family of antiferromagnets hosting magnetic Fermi arcs*," *Phys. Rev. B* **106**, 115111 (2022).

[3] Y. Kushnirenko, B. Kuthanazhi, L.-L. Wang, B. Schrunk, E. O'Leary, A. Eaton, P. C. Canfield, A. Kaminski "*Directional effects of antiferromagnetic ordering on the electronic structure in NdSb*", arXiv:2305.17085 (2023), PRB - under consideration.

[4] P. C. Canfield, "New Materials Physics", *Rep. Prog. Phys.* 83 016501 (2020).

Publications

The FWP published roughly 50 papers per year on a wide range of materials, states and phase transitions. We publish in Physical Review Letters, Physical Review B, and Nature and Science families of journals. Above, in References, list the recent RBi and RSb APRES papers; below is a selection of other recent publications.

[1] R.A. Ribeiro, S.L. Bud'ko, L. Xiang, D.H. Ryan, P.C. Canfield, "Small-moment antiferromagnetic ordering in single-crystalline La_2Ni_7," *Physical Review B,* 105, 014412 *(*2022). https://link.aps.org/doi/10.1103/PhysRevB.105.014412

[2] E.H. Krenkel, M.A. Tanatar, M. Loncykowski, R. Gasset, E.I. Timmons, S. Ghimire, K.R. Joshi, Y. Lee, L. Ke, S. Chen, C. Petrovic, P. P. Orth, M.S. Scheurer, R. Prozorov, "Possible unconventional pairing in $(Ca,Sr)_3(Ir,Rh)_4Sn_{13}$ superconductors revealed by controlling disorder," *Physical Review B,* 105, 094521 *(*2022). https://doi.org/10.1103/PhysRevB.105.094521

[3] L.-L. Wang, "Highly Tunable Band Inversion in AB_2X_4 (A=Ge, Sn, Pb; B=As, Sb, Bi; X=Se, Te) Compounds," *Physical Review Materials,* 6, 094201 *(*2022). https://doi.org/10.1103/PhysRevMaterials.6.094201

[4] M. Xu, J. Schmidt, E. Gati, L. Xiang, W.R. Meier, V.G. Kogan, S.L. Bud'ko, P.C. Canfield, "Superconductivity and phase diagrams of $CaK(Fe_{1-x}Mn_x)_4As_4$ single crystals," *Physical Review B,* 105, 214526 *(*2022). https://doi.org/10.1103/PhysRevB.105.214526

[5] D.V. Ambika, Q.-P. Ding, K. Rana, C.E. Frank, E.L. Green, S. Ran, N.P. Butch, Y. Furukawa, "Possible coexistence of antiferromagnetic and ferromagnetic spin fluctuations in the spin-triplet superconductor UTe_2 revealed by ^{125}Te NMR under pressure," *Physical Review B,* 105, L220403 *(*2022). https://doi.org/10.1103/PhysRevB.105.L220403

[6] K. Rana, D.V. Ambika, S.L. Bud'ko, A.E. Bohmer, P.C. Canfield, Y. Furukawa, "Interrelationships between nematicity, antiferromagnetic spin fluctuations and superconductivity: Role of hotspots in $FeSe_{1-x}S_x$ revealed by high pressure ^{77}Se NMR study," *Physical Review B,* 107, 134507 *(*2023). https://doi.org/10.1103/PhysRevB.107.134507

[7] T.J. Slade, R.S. Dissanayaka Mudiyanselage, N. Furukawa, T.R. Smith, J. Schmidt, L.-L. Wang, C.-J. Kang, K. Wei, Z. Shu, T. Kong, R. Baumbach, G. Kotliar, S.L. Bud'ko, W. Xie, P.C. Canfield, "$Mn(Pt_{1-x}Pd_x)_5P$: Isovalent Tuning of Mn Sublattice Magnetic Order," *Physical Review B,* 107, 134429 *(*2023). https://doi.org/10.1103/PhysRevB.107.134429

[8] M. Xu, S.L. Bud'ko, R. Prozorov, P.C. Canfield, "Unusual coercivity and zero field stabilization of fully saturated magnetization in single crystals of $LaCrGe_3$," *Physical Review B,* 107, 134437 *(*2023). https://doi.org/10.1103/PhysRevB.107.134437

[9] V.S. Minkov, V. Ksenofontov, S.L. Bud'ko, E.F. Talantsev, M.I. Eremets, "Magnetic flux trapping in hydrogen-rich high-temperature superconductors," *Nature Physics, (*2023). https://doi.org/10.1038/s41567-023-02089-1

[10] V.G. Kogan, R. Prozorov, "Effects of scattering on the field-induced Tc enhancement in thin superconducting films in a parallel magnetic field," *Physical Review B,* 107, L020501 *(*2023). https://doi.org/10.1103/PhysRevB.107.L02050

Probing the Interplay of Topology, Magnetism and Superconductivity in Intrinsic Magnetic and Superconducting Topologic Materials

Ni Ni

Department of Physics and Astronomy, University of California, Los Angeles

Keywords: Magnetism, topological materials, 2D and layered materials, single crystal

Program Scope

The overarching goal of this proposal is to addressing the grand challenge of basic energy science by discovering new intrinsic magnetic topological materials, and characterizing them through thermodynamic, transport, X-ray, and neutron measurements. Of particular interest in this research is to probe the interplay of band topology, structure, electronic and spin degrees of freedom in these materials through chemical doping, external pressure and uniaxial strains. The proposed research will accelerate the discovery of these materials and advance our understanding of the interplay of the topology and magnetism, potentially enabling us to manipulate the emergent phenomena arising from the interlay.

Recent Progress

During the funding period from 09/01/2021 to 08/20/2023, we have 14 papers published or under review. In this session, I will report some selected works.

I) Unconventional pressure-driven metamagnetic transitions in topological van der Waals magnets [1]: Activating metamagnetic transitions between ordered states in van der Waals magnets and devices bring great opportunities in spintronics. We show that external pressure, which enhances the interlayer hopping without introducing chemical disorders, triggers multiple metamagnetic transitions upon cooling in the topological van der Waals magnets $Mn(Bi_{1-x}Sb_x)_4Te_7$, where the antiferromagnetic interlayer superexchange coupling competes with the ferromagnetic interlayer coupling mediated by the antisite Mn spins (Fig. 1). The temperature-pressure phase diagrams reveal that while the ordering temperature from the paramagnetic to ordered states is almost pressure-independent, the metamagnetic transitions show non-trivial pressure and temperature dependence, even re-entrance. For these highly anisotropic magnets, we attribute the former to the ordering temperature being only weakly dependent on the intralayer parameters, the latter to the parametrically different pressure and temperature

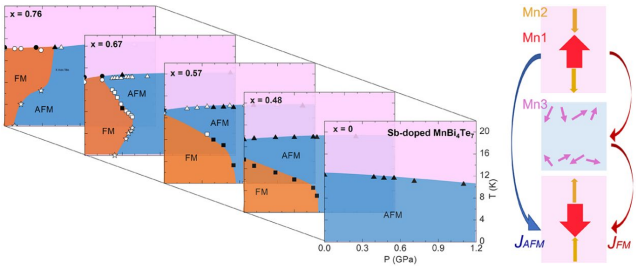

Fig. 1 $Mn(Bi_{1-x}Sb_x)_4Te_7$: Left: the temperature-pressure phase diagrams of. Right: the competing interactions.

dependence of the two interlayer couplings. Our independent probing of these disparate magnetic interactions paves an avenue for efficient magnetic manipulations in van der Waals magnets. This work has just been accepted by Nano Letter.

II) Magnetic dilution effect and topological phase transitions in $(Mn_{1-x}Pb_x)Bi_2Te_4$ [2]:As the first intrinsic antiferromagnetic (AFM) topological insulator (TI), MnBi2Te4 has provided a material platform to realize various emergent phenomena arising from the interplay of magnetism and band topology. Here by investigating $(Mn_{1-x}Pb_x)Bi_2Te_4$ ($0 \le x \le 0.82$) single crystals via the x-ray, electrical transport, magnetometry and neutron measurements, chemical analysis, external pressure, and first-principles calculations, we reveal the magnetic dilution effect on the magnetism and band topology in $MnBi_2Te_4$ (Fig. 2). With increasing x, both lattice parameters a and c expand linearly by around 2%. All samples undergo the paramagnetic to A-type antiferromagnetic transition with the Neel temperature decreasing lineally from 24 K at x=0 to 2 K at x=0.82. Our neutron data refinement of the x=0.37 sample indicates that the ordered moment is 4.3(1)μ_B/Mn at 4.85 K and the amount of the MnBi antisites is negligible within the error bars. Isothermal magnetization data reveal a slight decrease of the interlayer plane-plane antiferromagnetic exchange interaction and a monotonic decrease of the magnetic anisotropy, due to diluting magnetic ions and enlarging the unit cell. For x=0.37, the application of external pressures enhances the interlayer antiferromagnetic coupling, boosting the Neel temperature at a rate of 1.4 K/GPa and the saturation field at a rate of 1.8 T/GPa. Furthermore, our first-principles calculations reveal that the band inversion in the two end materials, $MnBi_2Te_4$ and $PbBi_2Te_4$, occurs at the Γ and Z point, respectively, while two gapless points appear at x= 0.44 and x= 0.66, suggesting possible topological phase transitions with doping.

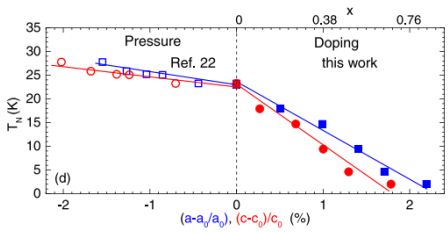

Fig. 2 Neel temperature vs. the change of lattice parameters for the pressure work and strain.

III) Growth, characterization and Chern insulator state in $MnBi_2Te_4$ via the chemical vapor transport method [3]: As the first intrinsic antiferromagnetic topological insulator, $MnBi_2Te_4$ has provided a platform to investigate the interplay of band topology and magnetism as well as the emergent phenomena arising from such an interplay. Here we report the chemical-vapor-transport (CVT) growth and characterization of $MnBi_2Te_4$, as well as the observation of the field-induced quantized Hall conductance in 6-layer devices (Fig. 3). Through comparative studies between our CVT-grown and flux-grown $MnBi_2Te_4$ via magnetic, transport, scanning tunneling microscopy, and angle-resolved photoemission

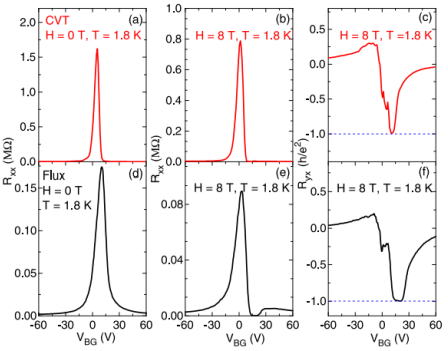

Fig. 3 Observation of Chern insulator state in CVT and flux grown $MnBi_2Te_4$.

spectroscopy measurements, we find that CVT-grown $MnBi_2Te_4$ is marked with higher Mn occupancy on the Mn site, slightly higher Mn_{Bi} antisites, smaller carrier concentration, and a Fermi level closer to the Dirac point. Furthermore, a 6-layer device made from the CVT-grown sample shows by far the highest mobility of 2500 cm2Vs in $MnBi_2Te_4$ devices with the quantized Hall conductance appearing at 1.8 K and 8 T. Our study provides a route to obtain high-quality single crystals of $MnBi_2Te_4$ that are promising to make superior devices and realize emergent phenomena, such as the layer Hall effect and quantized anomalous Hall effect, etc.

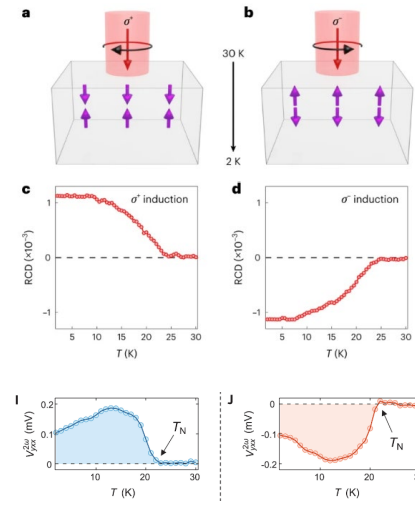

Fig. 4 Top: The prepared two AFM states of 6-layer $MnBi_2Te_4$. Middle: The RCD in the two AFM states. Bottom: The nonlinear Hall voltage as a function of temperature for these two AFM states.

IV) Our collaborations with other groups have been fruitful. Here I will discuss a couple of them on $MnBi_2Te_4$. In collaboration with Suyang Xu's group at Harvard, **A)** We have discovered helicity-dependent optical control of fully compensated antiferromagnetic order in two-dimensional even-layered $MnBi_2Te_4$ (Fig. 4), a topological axion insulator with neither chirality nor magnetization. To understand this control, we study an antiferromagnetic circular dichroism, which appears only in reflection but is absent in transmission. We show that the optical control and circular dichroism both arise from the optical axion electrodynamics, providing the possibility to optically control a family of PT-symmetric antiferromagnets [4]. **B)** Quantum geometry has two parts, the real part quantum metric and the imaginary part Berry curvature. We have discovered a new nonlinear Hall effect induced by quantum metric by interfacing even-layered $MnBi_2Te_4$ (a PT-symmetric antiferromagnet (AFM)) with black phosphorus. This novel nonlinear Hall effect switches direction upon reversing the AFM spins and exhibits distinct scaling that suggests a non-dissipative nature (Fig. 4). Like the AHE brought Berry curvature under the spotlight, our results open the door to discovering quantum metric responses [5].

Future Plans

Discovering new intrinsic MBT topological insulators in the 2-2-5 or 3-2-6 ratios. Investigating the pressure effect in $MnBi_6Te_{10}$ and $MnBi_8Te_{13}$. Investigating the origin of the large anomalous hall effect in $EuAg_4Sb_2$ and related materials. Investigating the effect of band structure, potential non-coplanar magnetic structures on the anomalous Hall effect in $EuAg_4Sb_2$ and related materials. Exploring and charactering new proposed magnetic topological materials. Close collaborations with other groups to investigate the magnetic and topological properties as well as emergent phenomena in devices for materials made in our group.

References

1. Tiema Qian, Eve Emmanouilidou, Chaowei Hu, Jazmine C. Green, Igor I. Mazin, Ni Ni, Unconventional pressure-driven metamagnetic transitions in topological van der Waals magnets, Nano Lett., **22,** 5523 (2022)
2.Tiema Qian, Yueh-Ting Yao, Chaowei Hu, Erxi Feng, Huibo Cao, Igor I. Mazin, Tay-Rong Chang, Ni Ni, Magnetic dilution effect and topological phase transitions in (Mn1−xPbx)Bi2Te4, Phys. Rev. B **106,** 045121 (2022)
3. Chaowei Hu, Anyuan Gao, Bryan Stephen Berggren, Hong Li, Rafal Kurleto, Dushyant Narayan, Ilija Zeljkovic, Dan Dessau, Suyang Xu, and Ni Ni, Growth, characterization and Chern insulator state in MnBi2Te4 via the chemical vapor transport method, Phys. Rev. Mater, **5**, 124206 (2021)
4. Jian-Xiang Qiu, Christian Tzschaschel, Junyeong Ahn, Anyuan Gao, Houchen Li, Xin-Yue Zhang, Barun Ghosh, Chaowei Hu, Yu-Xuan Wang, Yu-Fei Liu, Damien Bérubé, Thao Dinh, Zhenhao Gong, Shang-Wei Lien, Sheng-Chin Ho, Bahadur Singh, Kenji Watanabe, Takashi Taniguchi, David C. Bell, Hai-Zhou Lu, Arun Bansil, Hsin Lin, Tay-Rong Chang, Brian B. Zhou, Qiong Ma, Ashvin Vishwanath, Ni Ni & Su-Yang Xu, Axion optical induction of antiferromagnetic order, Nature Materials, **22**, 583 (2023)
5. Anyuan Gao, Yu-Fei Liu, Jian-Xiang Qiu, Barun Ghosh, Thaís V. Trevisan, Yugo Onishi, Chaowei Hu, Tiema Qian, Hung-Ju Tien, Shao-Wen Chen, Mengqi Huang, Damien Bérubé, Houchen Li, Christian Tzschaschel, Thao Dinh, Zhe Sun, Sheng-Chin Ho, Shang-Wei Lien, Bahadur Singh, Kenji Watanabe, Takashi Taniguchi, David C. Bell, Hsin Lin, Tay-Rong Chang, Chunhui Rita Du, Arun Bansil, Liang Fu, Ni Ni, Peter P. Orth, Suyang Xu, Quantum metric nonlinear Hall effect in a topological antiferromagnet, Science, **381**, 181 (2023)

Publications

1. Chaowei Hu, Anyuan Gao, Bryan Stephen Berggren, Hong Li, Rafal Kurleto, Dushyant Narayan, Ilija Zeljkovic, Dan Dessau, Suyang Xu, and Ni Ni, Growth, characterization and Chern insulator state in MnBi2Te4 via the chemical vapor transport method, Phys. Rev. Mater, **5**, 124206 (2021)
2.Tiema Qian, Morten H. Christensen, Chaowei Hu, Amartyajyoti Saha, Brian M. Andersen, Rafael M. Fernandes, Turan Birol, Ni Ni, Revealing the competition between charge-density-wave and superconductivity in CsV3Sb5 through uniaxial strain, Phys. Rev. B, **104**, 144506 (2021) (Editors' suggestion)
3.Chaowei Hu, Makariy A. Tanatar, Ruslan Prozorov, Ni Ni, Unusual dynamic susceptibility arising from soft ferromagnetic domains in MnBi8Te13 and Sb-doped MnBi2nTe3n+1 (n=2, 3), J. Phys. D:Appl Phys, **55**, 054003 (2021)
4. Tiema Qian, Eve Emmanouilidou, Chaowei Hu, Jazmine C. Green, Igor I. Mazin, Ni Ni, Unconventional pressure-driven metamagnetic transitions in topological van der Waals magnets, Nano Lett., **22,** 5523 (2022)
5.Tiema Qian, Yueh-Ting Yao, Chaowei Hu, Erxi Feng, Huibo Cao, Igor I. Mazin, Tay-Rong Chang, Ni Ni, Magnetic dilution effect and topological phase transitions in (Mn1−xPbx)Bi2Te4, Phys. Rev. B **106,** 045121 (2022)
6. Jian-Xiang Qiu, Christian Tzschaschel, Junyeong Ahn, Anyuan Gao, Houchen Li, Xin-Yue Zhang, Barun Ghosh, Chaowei Hu, Yu-Xuan Wang, Yu-Fei Liu, Damien Bérubé, Thao Dinh, Zhenhao Gong, Shang-Wei Lien, Sheng-Chin Ho, Bahadur Singh, Kenji Watanabe, Takashi Taniguchi, David C. Bell, Hai-Zhou Lu, Arun Bansil, Hsin Lin, Tay-Rong Chang, Brian B. Zhou, Qiong Ma, Ashvin Vishwanath, Ni Ni & Su-Yang Xu, Axion optical induction of antiferromagnetic order, Nature Materials, **22**, 583 (2023)
7. Anyuan Gao, Yu-Fei Liu, Jian-Xiang Qiu, Barun Ghosh, Thaís V. Trevisan, Yugo Onishi, Chaowei Hu, Tiema Qian, Hung-Ju Tien, Shao-Wen Chen, Mengqi Huang, Damien Bérubé, Houchen Li, Christian Tzschaschel, Thao Dinh, Zhe Sun, Sheng-Chin Ho, Shang-Wei Lien, Bahadur Singh, Kenji Watanabe, Takashi Taniguchi, David C. Bell, Hsin Lin, Tay-Rong Chang, Chunhui Rita Du, Arun Bansil, Liang Fu, Ni Ni, Peter P. Orth, Suyang Xu, Quantum metric nonlinear Hall effect in a topological antiferromagnet, Science, **381**, 181 (2023)
8. Yujin Cho, Jin Ho Kang, Liangbo Liang, Madeline Taylor, Xiangru Kong, Subhajit Ghosh, Fariborz Kargar, Chaowei Hu, Alexander A. Balandin, Alexander A. Puretzky, Ni Ni, and Chee Wei Wong, Phonon modes and Raman signatures of MnBi2nTe3n+1(n = 1, 2, 3, 4) magnetic topological heterostructures, Phys. Rev. Res. **4**, 013108 (2022)
9. Nathan J. McLaughlin, Chaowei Hu, Mengqi Huang, Shu Zhang, Hanyi Lu, Hailong Wang, Yaroslav Tserkovnyak, Ni Ni, and Chunhui Rita Du, Quantum Imaging of Magnetic Phase Transitions and Spin Fluctuations in Intrinsic Magnetic Topological Nanoflakes, Nano Lett., **22**, 5810 (2022)
10. N Sirica, P. P. Orth, M. S. Scheurer, Y. M. Dai, M. -C. Lee, P. Padmanabhan, L. T. Mix, L. X. Zhao, G. F. Chen, B. Xu, R. Yang, B. Shen, C. -C. Lee, H. Lin, T. A. Cochran, S. A. Trugman, J. -X. Zhu, M. Z. Hasan, N. Ni, X. G. Qiu, A. J. Taylor, D. A. Yarotski, R. P. Prasankumar, Photocurrent-driven transient symmetry breaking in the Weyl semimetal TaAs, Nature Materials, **21**, 62 (2022)

Project Title: Topological Superconductivity in Strong Spin-Orbit Materials

Principal Investigator: Johnpierre Paglione, University of Maryland

Keywords: topological superconductivity, topological materials

Research Scope

The search for an efficient material platform for topological quantum computation has recently focused on superconductors that exhibit unconventional properties that exhibit chiral or non-trivial topological aspects with promise of hosting novel phenomena, including emergent Majorana quasiparticles. This program continues to explore the nature of superconductivity in topological materials lacking inversion symmetry using a joint experimental and theoretical effort to focus on understanding the topological superconducting state of the non-centrosymmetric material YPtBi. Our previous work has led to a new understanding of "high-spin" superconductivity arising from a spin-3/2 band structure [1,2], which is the first time such physics has been considered theoretically for a superconductor, and has sparked a flurry of activity understanding j=3/2 physics. More recently, our discovery of spin-triplet pairing in UTe_2 has sparked an intense race to identify its multi-component order parameter and topological properties. Following these advances, our program is focused on further exploring these materials using an established in-house synthesis and characterization program and an extensive collaboration network in order to elucidate the potential of these materials to form the next generation platform for quantum technologies. The main focus of the program investigates the interplay of topological superconductivity with magnetic and other ground states in the XYZ family [3], and extends previous studies of the UTe_2 system [4,5] to further explore the topological nature of superconductivity and its ramifications. In this abstract, we focus on our progress in understanding the topological superconductor UTe_2.

Recent Progress

Our discovery of superconductivity in nearly–ferromagnetic UTe_2 in 2018 is one of our surprising but grand accomplishments in the last few years. This superconductor is a strong candidate for spin-triplet pairing, based on an extremely large, anisotropic upper critical field H_{c2}; temperature-independent nuclear magnetic resonance (NMR) Knight shift; and power law behavior of electronic specific heat and nuclear spin-lattice relaxation rate in the superconducting state. In addition, UTe_2 closely resembles ferromagnetic superconductors, but in this case having a paramagnetic normal state that harbors spin fluctuations that drive the superconductivity. Our discovery launched an intense race with several groups worldwide now investigating various aspects of this material, producing upwards of ~80 papers to date. Our work in the last reporting period has focused on elucidating both the superconducting state, and the normal state from which this exotic superconductivity arises:

a) We studied the temperature dependence of electrical resistivity for currents directed along all crystallographic axes, focusing particularly on an accurate determination of the resistivity along the c-axis by using transport geometries that allow extraction of two resistivities along with the primary axes directions. Measurement of the absolute values of resistivities in all current directions reveals a surprisingly (given the anticipated highly anisotropic band structure) nearly isotropic transport behavior at temperatures above Kondo coherence, but with

a qualitatively distinct behavior at lower temperatures, as shown in **Figure. 1**. This work has been published in Phys. Rev. B (Eo, 2022).

b) We have worked with collaborator Andrew Wray to study the nature of the uranium f-electron state, providing crystals and sample characterization in support of resonant inelastic x-ray scattering, x-ray absorption spectroscopy, and atomic-multiplet-based modeling to shed light on the orbital states. The first two data sets are found to agree strongly with predictions for a $5f^2 6d^1$-like valence electron configuration with weak intra-dimer magnetic correlations. This work is now published in Phys. Rev. B (Liu, 2022).

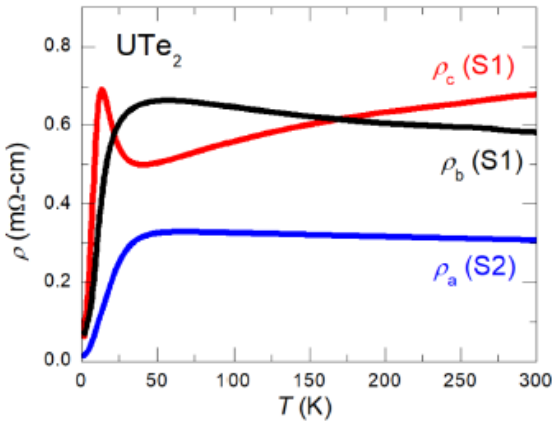

Figure 1: Electrical resistivity anisotropy of UTe2 extracted using a generalized Montgomery measurement technique. [Eo, PRB (2022)].

c) Our experiments using muon spectroscopy in collaboration with Jeff Sonier (SFU) have shed light on the anomalous low-temperature magnetic state of UTe_2 by probing the internal magnetism, showing the existence of magnetic clusters that gradually freeze into a disordered spin frozen state at low temperatures. These findings suggest that inhomogeneous freezing of magnetic clusters is linked to the ubiquitous low-temperature behavior of the specific heat and shed light on the intrinsic low-temperature properties of UTe2. This work is published in Nature Comm. (Sundar, 2023).

d) We are continuing close collaborations with B. Ramshaw (Cornell) to perform ultrasound experiments probing the superconducting state. The first phase of this is complete, which established a method of doing resonant ultrasound on irregular shaped crystals, and is being followed by measurements to probe the symmetry of the order parameter, one of the key questions about this system. This work is submitted for publication (Theuss, 2023).

e) We have been collaborating with two STM groups – V. Madhavan (UIUC) and J.C.S. Davis (Oxford/Cornell) – to study a new found charge ordered phase in UTe2. In particular, the UIUC group discovered a charge density wave (CDW) phase that lives above the superconducting state, and the Oxford group has found a pair-density wave (PDW) state that onsets in the superconducting state. Both works are published in Nature (2023).

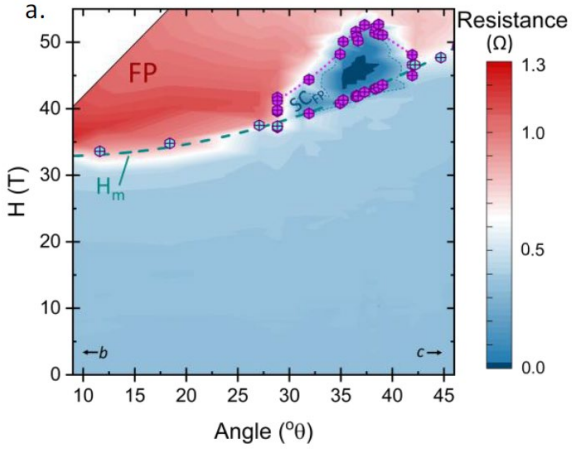

Figure 2: Extremely large magnetic fields give rise to an unprecedented high field superconductor in UTe2 samples that lack a zero-field parent phase. This orphan superconductivity exists at fields between 37 T and 52 T, and presents is a challenge to existing theoretical explanations [Frank, Nature Phys. under review (2023)].

f) Our most recent work with the group of N. Butch (NIST) on the high-field superconducting "Lazarus" phase has produced an astonishing find – that non-superconducting samples (produced by tuning the growth method) still robustly possess high field-induced superconductivity. Shown in Figure 2, the angle dependence of the magnetoresistance (b to c, degrees) of "entrant" magnetic field-induced superconductivity in

non-superconducting UTe_2 at 0.5 K reproduces the famous Lazarus phase, suggesting this phase is succinctly different than the ambient zero-field phase that is fully suppressed by disorder. This work is under review (Frank, 2023).

g) Finally, we recently reported the observation of applied pressure tuning of a magnetic energy scale in UTe2, previously identified as a peak in the c-axis electrical transport. Upon increasing pressure, the characteristic c-axis peak moves to a lower temperature before vanishing near the critical pressure of about 15 kbar, and follows previous magnetic markers indicating the tuning of a magnetic energy scale. The observed Fermi-liquid behavior at ambient pressure is violated near the critical pressure, exhibiting nearly linear resistivity in temperature and an enhanced pre-factor. Our results provide an important window into the evolution of magnetic quantum criticality in this system. This work is submitted (Kim, 2023).

Future Plans

The main effort is focused on elucidating the superconductivity of UTe_2, including continued work on thermodynamic and spectroscopic measurements aimed at identifying the exact pairing symmetry of this superconductor as well as the opportunities to observe, isolate and manipulate Majorana fermions to establish a platform for future quantum technologies. We are also working very closely with the groups of V. Madhavan (UIUC) and J.C.S. Davis (Oxford/Cornell) on STM studies of a newly discovered charge ordered phase in UTe_2 that may have implications for both normal and superconducting states of this material. Ongoing experiments are probing the sample dependence and correlation with other experiments on the normal state properties. Continued work on the RPtBi series is aimed in the same direction, with projects focused on further elucidating this exotic superconducting phase and its implications. In particular, we are probing further substitution series including both magnetic ion and heavy fermion mixing of the j=3/2 superconducting state.

References

[1] H. Kim, K. Wang, Y. Nakajima, R. Hu, S. Ziemak, P. Syers, L. Wang, H. Hodovanets, J. D. Denlinger, P. M. R. Brydon, D. F. Agterberg, M. A. Tanatar, R. Prozorov, and J. Paglione, "Beyond triplet: Unconventional superconductivity in a spin-3/2 topological semimetal," *Sci. Adv.* **4**, eaao4513 (2018). [http://dx.doi.org/10.1126/sciadv.aao4513].

[2] H. Kim, J. Lee, H. Hodovanets, K. Wang, J. D. Sau, and J. Paglione, "Quantum oscillations of the j=3/2 Fermi surface in the topological semimetal YPtBi," *Phys. Rev. Res.* **4**, 033169 (2022). [http://dx.doi.org/10.1103/PhysRevResearch.4.033169].

[3] Y. Nakajima, R. Hu, K. Kirshenbaum, A. Hughes, P. Syers, X. Wang, K. Wang, R. Wang, S. R. R. Saha, D. Pratt, J. W. W. Lynn, and J. Paglione, "Topological RPdBi half-Heusler semimetals: A new family of noncentrosymmetric magnetic superconductors," *Sci. Adv.* **1**, e1500242–e1500242 (2015). [http://dx.doi.org/10.1126/sciadv.1500242].

[4] S. Ran, C. Eckberg, Q.-P. Ding, Y. Furukawa, T. Metz, S. R. Saha, I.-L. Liu, M. Zic, H. Kim, J. Paglione, and N. P. Butch, "Nearly ferromagnetic spin-triplet superconductivity," *Science* **365**, 684–687 (2019). [http://dx.doi.org/10.1126/science.aav8645].

[5] S. Ran, I.-L. Liu, Y. S. Eo, D. J. Campbell, P. M. Neves, W. T. Fuhrman, S. R. Saha, C. Eckberg, H. Kim, D. Graf, F. Balakirev, J. Singleton, J. Paglione, and N. P. Butch, "Extreme magnetic field-boosted superconductivity," *Nat. Phys.* **15**, 1250–1254 (2019). [http://dx.doi.org/10.1038/s41567-019-0670-x].

Publications

1. Florian Theuss, Gregorio de la Fuente Simarro, Avi Shragai, Gael Grissonnanche, Ian M. Hayes, Shanta Saha, Tatsuya Shishidou, Taishi Chen, Satoru Nakatsuji, Sheng Ran, Michael Weinert, Nicholas P. Butch, Johnpierre Paglione, B. J. Ramshaw., "*Resonant Ultrasound Spectroscopy for Irregularly-Shaped Samples and its Application to Uranium Ditelluride*", arXiv:2303.03473.
2. Corey E. Frank, Sylvia K. Lewin, Gicela Saucedo Salas, Peter Czajka, Ian Hayes, Hyeok Yoon, Tristin Metz, Johnpierre Paglione, John Singleton, Nicholas P. Butch, "*Orphan High Field Superconductivity in Non-Superconducting Uranium Ditelluride* " arXiv:2304.12392.
3. Anuva Aishwarya, Julian May-Mann, Arjun Raghavan, Laimei Nie, Marisa Romanelli, Sheng Ran, Shanta R. Saha, Johnpierre Paglione, Nicholas P. Butch, Eduardo Fradkin, Vidya Madhavan, "*Magnetic-field sensitive charge density wave orders in the superconducting phase of UTe_2*", Nature 618, 928–933 (2023).
4. Qiangqiang Gu, Joseph P. Carroll, Shuqiu Wang, Sheng Ran, Christopher Broyles, Hasan Siddiquee, Nicholas P. Butch, Shanta R. Saha, Johnpierre Paglione, J. C. Séamus Davis, Xiaolong Liu, "*Detection of a Pair Density Wave State in UTe_2*", Nature 618, 921–927 (2023).
5. S. Sundar, N. Azari, M. Goeks, S. Gheidi, M. Abedi, M. Yakovlev, S.R. Dunsiger, J.M. Wilkinson, S.J. Blundell, T.E. Metz, I.M. Hayes, S.R. Saha, S. Lee, A.J. Woods, R. Movshovich, S.M. Thomas, P.F.S. Rosa, N.P. Butch, J. Paglione, J.E. Sonier, "*Ubiquitous Spin Freezing in the Superconducting State of UTe_2*", Nature Comm. Phys. 6, 24 (2023).
6. S. Liu, Y. Xu, E. C. Kotta, L. Miao, S. Ran, J. Paglione, N. P. Butch, J. D. Denlinger, Y.-D. Chuang, L. A. Wray "*Identifying f-electron symmetries of UTe_2 with O-edge resonant inelastic X-ray scattering*" Phys. Rev. B 106, L241111 (2022).
7. C. W. Chuang, S. Souma, A. Moriya, K. Nakayama, A. Ikeda, M. Kawaguchi, K. Obata, S. R. Saha, H. Takahashi, S. Kitagawa, K. Ishida, K. Tanaka, M. Kitamura, K. Horiba, H. Kumigashira, T. Takahashi, S. Yonezawa, J. Paglione, Y. Maeno, T. Sato, "*Fermiology of a topological line-nodal compound $CaSb_2$ and its implication to superconductivity*", Phys. Rev. Materials 6, 104203 (2022).
8. H. Kim, J. Lee, H. Hodovanets, K. Wang, J.D. Sau, J. Paglione, "*Quantum Oscillations of the j=3/2 Fermi Surface in Topological Semimetal YPtBi"*, Phys. Rev. Research 4, 033169 (2022).
9. A. Ikeda, S.R. Saha, D. Graf, P. Saraf, D.S. Sokratov, Y. Hu, H. Takahashi, S. Yamane, A. Jayaraj, J. Slawinska, M. Buongiorno Nardelli, S. Yonezawa, Y. Maeno, J. Paglione, "Quasi-two-dimensional Fermi surface of superconducting line-nodal metal CaSb2", Phys. Rev. B 106, 075151 (2022).
10. Y.S. Eo, S. R. Saha, H. Kim, S. Ran, J. A. Horn, H. Hodovanets, J. Collini, W. T. Fuhrman, A. H Nevidomskyy, N. P. Butch, M. S. Fuhrer, J. Paglione, *"c-axis transport in UTe2: evidence of three-dimensional conductivity component",* Phys. Rev. B 106, L060505 (2022).

Project Title: Superconductivity and magnetism in *d*- and *f*-electron quantum materials

Principal Investigator: M. Brian Maple
Mailing address: Department of Physics, University of California, San Diego, La Jolla, California 92093
Email: mbmaple@ucsd.edu

Keywords: magnetism, superconductivity, single crystals, semiconductors, magnetotransport

Research Scope

The general theme of this research program is the investigation of emergent phases and phenomena in correlated electron and topological quantum materials. Although our objective is to develop an understanding of the physics of quantum materials on a fundamental level, these materials also have potential applications in technology; e.g., energy sector (superconductivity (SC), thermoelectric cooling and electric power generation, magnetic refrigeration), sensors, spintronics, quantum computing. A major goal of our research involves finding and investigating new examples of emergent phenomena and phases in the vicinity of a quantum critical point (QCP), a value of a nonthermal control parameter $\boldsymbol{\delta}$ such as chemical composition, pressure and magnetic field, where a second order phase transition, often magnetic, is suppressed to 0 K. Emergent phenomena of interest in our research include unconventional spin-singlet *d*-wave and spin-triplet *p*-wave SC, high temperature SC, charge and spin ordered phases, "hidden order", topological insulator behavior, topological Kondo insulator (TKI) behavior, heavy fermion behavior, non-Fermi liquid behavior. A combination of materials synthesis and physical properties measurements are employed to characterize these phenomena, map out complex phase diagrams in which they reside, determine how different phases are related to one another, probe the underlying physics, and, when possible, test relevant theoretical models. We are also interested in studying quantum matter under extreme conditions of pressure, P (megabar range), magnetic field, B (45 T – static, 65 T – pulsed), and temperature, T (mK region). The emphasis of our current research is on two extraordinary quantum materials: the correlated *d*-electron small gap semiconductor FeSi which has a conducting surface state (CSS) and is a candidate for a *d*-electron topological Kondo insulator [1] and the correlated *f*-electron compound UTe_2 which exhibits unconventional SC and is a candidate for a spin triplet chiral topological SCor [2]. Recent research on FeSi and UTe_2 and progress in developing a nitrogen vacancy center microscope for imaging the magnetization of materials in diamond anvils cells (DACs) at high pressures are briefly described below.

Recent Progress

Possible 2-dimensional magnetism in the conducting surface state of FeSi

The correlated *d*-electron small gap semiconductor FeSi has been studied for decades. Its unusual T-dependent electronic and magnetic properties are reminiscent of those of *f*-electron Kondo insulators such as SmB_6. This led to the proposal that FeSi may be a *d*-electron counterpart of an *f*-electron Kondo insulator. Our group reported the existence of a conducting surface state (CSS)

in FeSi below ~19 K, suggesting the possibility that FeSi could be a topological insulator. Given the evidence that SmB_6 is a TKI, it seems possible that FeSi could be a TKI, as well.

Several years ago, hysteresis in the magnetoresistance *MR* and an anomalous Hall effect were found in SmB_6 below the onset temperature of its low-temperature resistivity plateau, leading the authors to propose the existence of a ferromagnetic (FM), topologically non-trivial surface state with a quantized conductance value of e^2/h stemming from the chiral edge channels of FM domain walls [3]. Considering the resemblances between FeSi and SmB_6 in behavior of the resistivity in magnetic fields and a report of a spin-orbit coupled FM surface state originating from the Zak phase in FeSi nanofilms, we embarked on a search for evidence of magnetic ordering in the CSS of FeSi single crystals. To affect this search, we carried out electrical resistance $R(T)$ measurements on rod-shaped FeSi single crystals previously studied in our lab [1, publication 9] as a function of T, B, and angle (θ) between the electrical current and B.

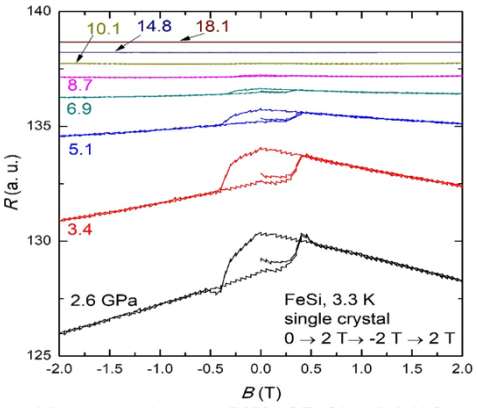

Magnetoresistance $R(B)$ of FeSi at 3.3 K for several pressures between 2.6 and 18.1 GPa

In the temperature range where the CSS exists, the *MR* exhibits a hysteresis loop bounded within ± 0.5 T, suggesting two-dimensional magnetic ordering. The hysteretic *MR* is asymmetric in B and anisotropic with respect to θ. Further exploration of $R(\theta)$ at a fixed field of 9 T reveals an initial progressive rotation of the axis for two-fold rotational symmetry from 2 K to 10 K, then a stabilized axis for two-fold symmetry until at $T > 40$ K, the anisotropy vanishes, coincident with the disappearance of the CSS. These observations point to a possible magnetically ordered surface state that has been reported in similar systems such as FeSi nanofilms and bulk SmB_6.

In a set of experiments on FeSi under pressure in a DAC, R vs B measurements were performed at 3.3 K as a function of P. The area of the hysteresis loop in $R(B)$ was found to decrease with P and vanish near the critical pressure P_{cr} where the CSS collapses and the energy gap of the semiconducting phase of FeSi closes. For pressures above P_{cr}, FeSi exhibits metallic behavior. The sign of $R(B)$ changes from negative in the semiconducting region for $P < P_{cr}$ to small and positive in the metallic region $P > P_{cr}$.

Experiments on the unconventional superconductivity of UTe_2

Experiments on UTe_2 have yielded evidence for unconventional SC characterized by spin-triplet pairing of electrons, multiple SCing order parameters, time-reversal symmetry breaking, and in-gap chiral surface states. UTe_2 has an enormous reentrant upper critical field $H_{c2}(T)$ of the order of 40 T, considering its low SCing critical temperature T_c of only 2 K. In addition, there is a pocket of SC, the so-called 'Lazurus' phase, between 40 T and 60 T for magnetic fields oriented at angles between 23º and 45º between the b and c crystalline axes [4]. The compound UTe_2 has attracted a great deal of attention, driven by an interest in developing a fundamental understanding of its

unconventional SC and because it is regarded as a candidate for topological SC with potential for robust quantum computing. We have been preparing single crystals of UTe_2 for several research projects with collaborators, in addition to our own experiments, described below, that address the nature and origin of the SC of UTe_2.

Neutron scattering experiments on UTe_2 and it alloys

One of the projects involves a series of neutron scattering experiments on single crystals of pure and chemically substituted UTe_2 compounds prepared in our lab in collaboration with Professor Pengcheng Dai and his group at Rice University. Two neutron scattering experiments have been carried out that have yielded surprising results that were reported in two papers, one in *Physical Review Lett*ers which identified the AFM nature of the spin fluctuations and another in *Nature* that revealed coupling of the AFM spin fluctuations and the SC [5]. Similar work has been reported by several other neutron scattering groups. Further neutron scattering experiments in collaboration with Professor Dai on UTe_2 and its alloys are planned for the future.

Symmetry of the superconducting order parameter of UTe_2

Experiments to study the symmetry of the superconducting order parameter of UTe_2 using Josephson junctions are currently underway at Pennsylvania State University in collaboration with Professor Ying Liu and his group. Although it is widely believed that the SC of UTe2 is characterized by odd-parity, spin-triplet pairing symmetry, direct evidence for it is still lacking, especially in low magnetic fields. These experiments probe the symmetry of the OP in UTe2 through Josephson coupling between In, an s-wave superconductor, and UTe2. The orientation dependence of the Josephson coupling has revealed that the pairing state in UTe2 must be that of odd-parity B1u in zero magnetic fields. Features were also observed in the single-particle tunneling spectra that were attributed to the formation of Andreev surface bound states on the (1-10) surface of UTe2. These results are relevant to developing a fundamental understanding of other SCing properties of UTe2 and the SCing mechanism. A paper reporting the initial results of this investigation has recently been submitted for publication.

Upper critical magnetic field measurements on $U_{1-x}Th_xTe_2$ alloys

Initial experiments to investigate the SCing phases in high magnetic fields of the $U_{1-x}Th_xTe_2$ system have been carried out at the Pulsed Field Facility of the NHMFL at LANL. It will be interesting to see if Th substitution reduces the $H_{c2}(T)$ of UTe_2 and how it affects the reentrant SC and the field induced phase that forms at high fields when the field is oriented at angles between 23º and 45º with respect to the *b* and *c* axes. This experiment will provide information that may yield insight into the mechanism responsible for reentrant SC in high fields and the origin of the high field SCing phase as well as the relationship between the high and low field SCing phases.

XRD and RIXS measurements on UTe_2 under high pressure

Our group recently performed XRD and Resonant Inelastic X-ray Diffraction (RIXS) measurements on UTe_2 under high pressure to 30 GPa at HPCAT at ANL in collaboration with Professor Russell Hemley and his group. These measurements were undertaken to explore the *T* vs *P* phase space to higher *P* to determine the *P*-dependence of the lattice parameters *a*, *b*, and *c*, and volume of the body-centered orthorhombic unit cell of UTe_2, search for possible crystallographic phase transitions, and obtain information about changes in the U valence. We observed a transition from the body-centered orthorhombic structure (space group Immm) to a body-centered tetragonal structure (space group I4/mmm) at ~5-7 GPa and evidence for an initial change in U valence toward 4+, and then back toward 3+ with increasing pressure. In the meantime, XRD measurements on UTe_2 under pressure which also reveal a structural phase transition from the body-centered orthorhombic to a body-centered tetragonal structure at high pressure were reported at pressures between ~4 GPa and ~5 GPa, independently, by two other groups. One of these groups also reported a new superconducting phase above ~6 GPa in the tetragonal phase with a $T_c \approx 2$ K that appears to be associated with conventional SC in a weakly correlated electron metal. The XRD and RIXS data are currently being analyzed.

Development of a nitrogen vacancy microscope for magnetization measurements at ambient and high pressures

Nitrogen vacancy (NV) center magnetometry is an optical measurement technique that is highly sensitive to weak magnetic fields. As such, NV microscopes can be powerful instruments for studying magnetic properties under high pressure, as it is notoriously difficult to adapt standard magnetometry methods for high pressure studies with DACs. This motivated us to build a prototype custom NV widefield microscope that will be integrated with our DACs to allow magnetic imaging in addition to electrical transport measurements that will be performed at high pressure. This microscope probe will be incorporated in our DynaCool PPMS which is capable of achieving magnetic fields up to 9 T and cooling to a temperature of 2 K. Our work has progressed in the following manner:

1. Our room temperature prototype widefield NV magnetometry microscope has been completed.
2. Work on developing the open-source QUDI software for NV widefield imaging data analysis and hardware integration has been completed.
3. Our prototype NV magnetometer probe incorporating a DAC is currently being assembled/tested using 3D printed parts and carbon fiber rods.
4. Our next step is to integrate our Almax easyLab DAC into our DynaCool PPMS for measurements down to 2 K and magnetic fields up to 9T using NV widefield imaging.

Future Plans

Examples of future research include the following:

- Synthesis of single crystals of various materials for ongoing and new research conducted in our lab and labs of collaborators; e.g., FeSi, MnSi, $FeSb_2$, $URu_{2-x}M_xSi_2$ (M = Fe, Co), UTe_2, $U_{1-x}Th_xTe_2$, $Y_{1-x}Pr_xBa_2Cu_3O_7$.
- Hall effect and thermal conductivity measurements on FeSi single crystals.
- Search for quantum oscillations (SdH and dHvA) in FeSi single crystals.
- Electrical transport measurements on FeSi single crystals at high pressure to determine how the gaps close and the CSS collapses and search for new emergent phases such as SC and exotic types of magnetic order.
- Extend XRD and RIXS measurements at high pressures to other correlated *f*-electron materials; e.g., $U_{1-x}Th_xTe_2$, UFe_4P_{12}, $CeFe_4P_{12}$, $PrRu_4P_{12}$, $CeOs_4Sb_{12}$, etc.
- Electrical resistivity measurements at high pressure on UTe_2 and $U_{1-x}Th_xTe_2$ single crystals to determine the T vs P phase diagrams and search for other emergent phases.
- Continuation of investigations of studies that have been initiated on UTe_2 and $U_{1-x}Th_xTe_2$; e.g., neutron scattering experiments with Prof. Dai's group, superconducting order parameter studies with Prof. Liu's group, measurements at high fields and high pressures at the NHMFL in LANL.
- Search for new correlated 5*f* electron U-based compounds that exhibit emergent phenomena and unconventional superconductivity.
- Measurements of the electrical resistivity of correlated electron materials into the megabar region to search for emergent phenomena and unconventional forms of superconductivity.
- Continue development and testing of NV microscope for magnetization measurements.

References

1. Yuankan Fang, Sheng Ran, Weiwei Xie, Shen Wang, Ying Shirley Meng, and M. Brian Maple, "Evidence for a conducting surface ground state in high-quality single crystalline FeSi," *Proceedings of the National Academy of Sciences* **115**, 8558 (2018).

2. Sheng Ran, Chris Eckberg, Qing-Ping Ding, Yuji Furukawa, Tristin Metz, Shanta R. Saha, I-Lin Liu, Mark Zic, Hyunsoo Kim, Johnpierre Paglione, and Nicholas P. Butch, "Nearly ferromagnetic spin-triplet superconductivity," *Science* **365**, 684 (2019).

3. Yasuyuki Nakajima, Paul Syers, Xiangfeng Wang, Renxiong Wang and Johnpierre Paglione, "One-dimensional edge state transport in a topological Kondo insulator," *Nature Physics* **12**, 213 (2016).

4. Sheng Ran, I-Lin Liu, Yun Suk Eo, Daniel J. Campbell, Paul M. Neves, Wesley T. Fuhrman, Shanta R. Saha, Christopher Eckberg, Hyunsoo Kim, David Graf, Fedor Balakirev, John Singleton, Johnpierre Paglione and Nicholas P. Butch, "Extreme magnetic field-boosted superconductivity," *Nat. Phys.* **15**, 1250 (2019).

5. Chunruo Duan, R. E. Baumbach, Andrey Podlesnyak, Yuhang Deng, Camilla Moir, Alexander J. Breindel, M. Brian Maple, E. M. Nica, Qimiao Si, and Pengcheng Dai, "Resonance from antiferromagnetic spin fluctuations for superconductivity in UTe_2," *Nature* **600**, 636 (2021).

Publications

1. A. M. Konic, R. B. Adhikari, D. L. Kunwar, A. A. Kirmani, A. Breindel, R. Sheng, M. B. Maple, M. Dzero, and C. C. Almasan, "Evolution of non-Kramers doublets in magnetic field in $PrNi_2Cd_{20}$ and $PrPd_2Cd_{20}$," *Physical Review B* **104**, 205139 (2021)

2. Chunruo Duan, R. E. Baumbach, Andrey Podlesnyak, Yuhang Deng, Camilla Moir, Alexander J. Breindel, M. Brian Maple, E. M. Nica, Qimiao Si, and Pengcheng Dai, "Resonance from antiferromagnetic spin fluctuations for superconductivity in UTe_2," *Nature* **600**, 636 (2021).

3. J. D. Denlinger, J.-S. Kang, L. Dudy, J. W. Allen, Kyoo Kim, J.-H. Shim, K. Haule, J. L. Sarrao, N. P. Butch and M. B. Maple, "Global perspectives of the bulk electronic structure of URu_2Si_2 from angle-resolved photoemission," *Electronic Structure* **4**, 013001 (2022).

4. D. L. Kunwar, S. R. Panday, Y. Deng, S. Ran, R. E. Baumbach, M. B. Maple, Carmen C. Almasan, and M. Dzero, "Heat capacity of $URu_{2-x}Os_xSi_2$ at low temperatures," *Physical Review B* **105**, L041106 (2022).

5. K. Götze, M. J. Pearce, M. J. Coak, P. A. Goddard, A. D. Grockowiak, W. A. Coniglio, S. W. Tozer, D. E. Graf, M. B. Maple, P.-C. Ho, M. C. Brown, and J. Singleton, "Pressure-induced shift of effective Ce valence, Fermi energy and phase boundaries in $CeOs_4Sb_{12}$," *New Journal of Physics* **24**, 043044 (2022).

6. Alejandro Ruiz, Brandon Gunn, Yi Lu, Kalyan Sasmal, Camilla M. Moir, Rourav Basak, Hai Huang, Jun-Sik Lee, Fanny Rodolakis, Timothy J. Boyle, Morgan Walker, Yu He, Santiago Blanco-Canosa, Eduardo H. da Silva Neto, M. Brian Maple, and Alex Frano, "Stabilization of three-dimensional charge order through interplanar orbital hybridization in $Pr_xY_{1-x}Ba_2Cu_3O_{6+\delta}$," *Nature Communications* **13**, 6197 (2022).

7. N. Pouse, Y. Deng, S. Ran, D. Graf, Y. Lai, J. Singleton, F. F. Balakirev, R. E. Baumbach, and M. B. Maple, "Anisotropy of the *T* vs. *H* phase diagram and the HO/LMAFM phase boundary in $URu_{2-x}Fe_xSi_2$," *Frontiers in Electronic Materials* **2**, 991754 (2022).

8. P.-C. Ho, D. E. MacLaughlin, M. B. Maple, Lei Shu, A. D. Hillier, O. O. Bernal, T. Yanagisawa, P. K. Biswas, Jian Zhang, Cheng Tan, S. D. Hishida, and T. McCullough-Hunter, "Muon spin rotation and relaxation in $Pr_{1-x}Nd_xOs_4Sb_{12}$: Superconductivity and magnetism in Pr-rich alloys," *Physical Review B* **106**, 144508 (2022).

9. Alexander Breindel, Yuhang Deng, Camilla M. Moir, Yuankan Fang, Sheng Ran, Hongbo Lou, Shubin Li, Qiaoshi Zeng, Lei Shu, Christian T. Wolowiec, Ivan K. Schuller, Priscila F. S. Rosa, Zachary Fisk, John Singleton, and M. Brian Maple, "Probing FeSi, a *d*-electron topological Kondo insulator candidate with magnetic field, pressure, and microwaves," *Proceedings of the National Academy of Sciences* **120**, e2216367120 (2023).

10. Andrea Marino, Denise S. Christovam, Chun-Fu Chang, Johannes Falke, Chang-Yang Kuo, Chi-Nan Wu, Martin Sundermann, Andrea Amorese, Hlynur Gretarsson, Eric Lee-Wong, Camilla M. Moir, Yuhang Deng, M. Brian Maple, Peter Thalmeier, Liu Hao Tjeng, and Andrea Severing, "Fe substitution in URu_2Si_2: Singlet magnetism in an extended Doniach phase diagram," *Physical Review B* **108**, 085128 (2023).

Quantum Fluctuations in Narrow Band Systems – Strongly Spin Orbit Coupled Superconductors

Filip Ronning, Eric Bauer, Roman Movshovich, Priscila Rosa, Sean Thomas (Los Alamos National Lab), and Philip Moll (Max Planck Institute for the Structure and Dynamics of Matter)

Keywords: Superconductivity, Magnetism, Topological superconductivity, Single crystals, and Nanofabrication

Research Scope

Narrow band systems, whose renormalized electronic bandwidth is comparable to other relevant energy scales in the material, inherently have strong interactions and a proliferation of quantum fluctuations. 4*f*- and especially 5*f*-materials possess strong Coulomb repulsion, large spin-orbit coupling, and multiple competing energy scales, which generate coherent narrow bands and topologically non-trivial states of matter. This complexity provides a rich environment for discovering new states of matter, as well as providing ideal representatives that enable the understanding of quantum matter that arises across the periodic table more generally.

Superconductivity is one such state of matter that emerges in narrow band systems. In this second thrust we aim to exploit the small energy scales and complex order parameters in materials with strong spin-orbit coupling to create novel quantum-coherent devices from this technologically underexplored class of superconductors for both fundamental and applied interests. In the next three years we will emphasize phase sensitive probes of the order parameter and demonstrate the effects of the increased kinetic inductance in devices made from strongly spin-orbit coupled superconductors.

Recent Progress

Strongly spin-orbit coupled superconductors based on uranium are excellent candidates to host topological superconducting phases and have small energy scales that make them amenable to tuning with applied pressure and stress. We measured resistivity and heat capacity while applying uniaxial stress σ to three crystallographic directions of superconducting UTe_2 [1]. We find that the critical temperature T_c of the single observed bulk superconducting transition decreases with stress along [100] and [110] but increases with stress along [001]. Aside from its effect on T_c, we notice that *c*-axis stress leads to a significant piezoresistivity, which we associate with a changing electronic structure which shifts the zero-pressure resistivity peak at $T^* \approx 15$K to lower temperatures under stress. Finally, we show that an in-plane shear stress σ_{xy} does not induce any observable splitting of the superconducting

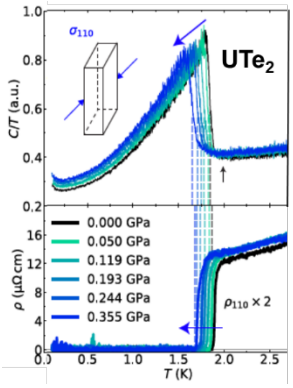

Heat capacity (top) and resistivity (bottom) of UTe_2 for stress applied along [110].

transition over a stress range of $\sigma_{xy} \approx 0.17$GPa. The lack of splitting of the single transition temperature of our high-quality crystals, particularly for stress applied along the [110] direction implies a single component order parameter whose behavior under uniaxial strain mirrors that found under hydrostatic pressure. In addition, our Kerr effect measurements failed to find evidence for broken time reversal symmetry at the superconducting transition in samples grown from either salt flux or by chemical vapor transport [2]. Instead, we observe a field-trainable signal that varies in magnitude between samples and between different locations on a single sample, which is a sign of inhomogeneous magnetic regions. These results are consistent with penetration depth measurements done in collaboration with Kam Moler's group that suggests a B_{3u} superconducting order parameter [3], and from muSR measurements done in collaboration with Jeff Sonier's group which shows that the low energy spin fluctuations vanish in cleaner crystals, and no evidence of broken time reversal symmetry was found [4]. Finally, our high pressure measurements using a diamond anvil cell showed that the crystal structure of UTe_2 transforms from the orthorhombic structure (*Immm*) at ambient pressure to a body-centered tetragonal (*I4/mmm*) structure above 5 GPa, with possibly an increased localization of the 5*f*-electrons [5].

Future Plans

We aim to make novel superconducting devices from strongly spin-orbit coupled materials that take advantage of the changing phase of the order parameter as well as its sensitivity to strain. Following up on our recent work that showed T_c of $CeIrIn_5$ could be controlled in microstructured devices using substrate defined strain variations, we will exploit our microstructuring capability and the large effective masses in *f*-electron based superconductors to demonstrate large kinetic inductances of such devices. We will also study the critical currents across interfaces made from strongly spin-orbit coupled superconductors to create novel π junctions.

References

1. C. Girod, C.R. Stevens, A. Huxley, E.D. Bauer, F.B. Santos, J.D. Thompson, R.M. Fernandes, F. Ronning, P.F.S. Rosa, and S.M. Thomas, *Thermodynamic and electrical transport properties of UTe_2 under uniaxial stress*, Physical Review B **106**, L121101 (2022).

2. M.O. Ajeesh, M. Bordelon, C. Girod, S. Mishra, F. Ronning, E.D. Bauer, B. Maiorov, J.D. Thompson, P.F.S. Rosa, and S.M. Thomas, *The fate of time-reversal symmetry breaking in UTe_2*, ArXiv:2305.00589 (2023).

3. Y. Iguchi, H. Man, S.M. Thomas, F. Ronning, P.F.S. Rosa, and K.A. Moler, *Microscopic imaging homogeneous and single phase superfluid density in UTe_2*, Physical Review Letters **130**, 196003 (2023).

4. N. Azari, M. Yakovlev, N. Rye, S.R. Dunsiger, S. Sundar, M.M. Bordelon, S.M. Thomas, J.D. Thompson, P.F.S. Rosa, J.E. Sonier, *Absence of Spontaneous Magnetic Fields Due to Time-Reversal Symmetry Breaking in Bulk Superconducting UTe_2*, ArXiv:2308.09773 (2023).

5. L.Q. Huston, D.Y. Popov, A. Weiland, M.M. Bordelon, P.F.S. Rosa, R.L. Rowland, II, B.L. Scott, G. Shen, C. Park, E.K. Moss, S.M. Thomas, J.D. Thompson, B.T. Sturtevant, and E.D. Bauer, *Metastable phase of UTe_2 formed under high pressure above 5 GPa,* Physical Review Materials **6**, 114801 (2022).

Publications (Supported by this thrust over the past 2 years)

1. M.R. van Delft, M.D. Bachmann, C. Putzke, C. Guo, J.A.W. Straquadine, E.D. Bauer, F. Ronning, and P.J.W. Moll, *Controlling superconductivity of $CeIrIn_5$ microstructures by substrate selection*, Appl. Phys. Lett. **120**, 092601 (2022).

2. C. Girod, C.R. Stevens, A. Huxley, E.D. Bauer, F.B. Santos, J.D. Thompson, R.M. Fernandes, F. Ronning, P.F.S. Rosa, and S.M. Thomas, *Thermodynamic and electrical transport properties of UTe_2 under uniaxial stress*, Physical Review B **106**, L121101 (2022).

3. L.Q. Huston, D.Y. Popov, A. Weiland, M.M. Bordelon, P.F.S. Rosa, R.L. Rowland, II, B.L. Scott, G. Shen, C. Park, E.K. Moss, S.M. Thomas, J.D. Thompson, B.T. Sturtevant, and E.D. Bauer, *Metastable phase of UTe_2 formed under high pressure above 5 GPa,* Physical Review Materials **6**, 114801 (2022).

4. S.M. Thomas, C. Stevens, F.B. Santos, S.S. Fender, E.D. Bauer, F. Ronning, J.D. Thompson, A. Huxley, P.F.S. Rosa, *Spatially inhomogeneous superconductivity in UTe_2*, Physical Review B **104**, 224501 (2021).

5. Y. Iguchi, H. Man, S.M. Thomas, F. Ronning, P.F.S. Rosa, and K.A. Moler, *Microscopic imaging homogeneous and single phase superfluid density in UTe_2*, Physical Review Letters **130**, 196003 (2023).

6. A. Weiland, F. B. Santos, J.D. Thompson, E.D. Bauer, S. M. Thomas, and P.F.S. Rosa, *Differences in the resistive and thermodynamic properties of the single crystalline chiral superconductor candidate SrPtAs,* Physical Review Materials **7**, 054802 (2023).

7. S. Sundar, N. Azari, M. R. Goeks, S. Gheidi, M. Abedi, M. Yakovlev, S. R. Dunsinger, J. M. Wilkinson, S. J. Blundell, T. E. Metz, I. M. Hayes, S. R. Saha, S. Lee, A. J. Wooks, R. Movschovich, S. M. Thomas, N. P. Butch, P.F.S. Rosa, J. Paglione, and J. E. Sonier, *Ubiquitous spin freezing in the superconducting state of UTe_2,* Communication Physics **6**, 24 (2023).

8. N. Azari, M. R. Goeks, M. Yakovlev, M. Abedi, S. R. Dunsiger, S. M. Thomas, J. D. Thompson, P. F. S. Rosa, and J. E. Sonier, *μ^+ Knight shift in UTe_2: Evidence for relocalization in a Kondo lattice,* Physical Review B **108**, L081103 (2023).

9. S. Mishra, Y. Liu, E.D. Bauer, F. Ronning, and S.M. Thomas, *Anisotropic magnetotransport properties of the heavy-fermion superconductor $CeRh_2As_2$,* Physical Review B **106**, L140502 (2022).

10. S.S. Philip, J. Yang, D. Louca, P.F.S. Rosa, J.D. Thompson, K.L. Page, *Bismuth kagome sublattice distortions by quenching and flux pinning in superconducting $RbBi_2$*, Physical Review B **104**, 104503 (2021).

Normal State and Superconducting Properties of the Infinite-Layer Nickelates

Harold Y. Hwang[1,2], Jennifer Fowlie[1,2], and Srinivas Raghu[1,3]

[1]Stanford Institute for Materials & Energy Sciences, SLAC National Accelerator Laboratory, Menlo Park, CA 94025

[2]Department of Applied Physics, Stanford University, Stanford, CA 94305

*[3]Department of Physics, Stanford University, Stanford, CA 94305 *hyhwang@slac.stanford.edu*

Keywords:

Superconductivity, thin film heterostructures, transition metal compounds, magnetotransport, pulsed-laser deposition

Research Scope

A central aim of modern materials research is the control of materials and their interfaces to atomic dimensions. In the search for emergent phenomena and ever-greater functionality in devices, transition metal oxides have enormous potential. They host a vast array of properties, such as orbital-ordering, unconventional superconductivity, magnetism, and ferroelectricity, as well as quantum phase transitions and couplings between these states. This research effort is pursued via the SLAC FWP#10069 "Atomic Engineering Oxide Heterostructures: Materials by Design." Our broad objective is to develop the science and technology arising in heterostructures of these novel materials. Using atomic-scale growth techniques we explore the properties of novel interface phases, metastable films, and freestanding crystalline membranes. Magnetotransport, magnetic, x-ray, and optical probes are used to determine the static and dynamic electronic and magnetic structure. The experimental efforts are guided and analyzed theoretically, particularly with respect to superconductivity and new states of emergent order. A wide set of tools, ranging from analytic field theory methods to exact computational treatments, are applied towards the understanding and design of quantum materials more broadly. Our specific current research topics are the investigation of unconventional superconductivity in the infinite-layer nickelates, dynamic strain control of states in oxide membranes, dilute/low-dimensional superconductivity and high-mobility transport in $SrTiO_3$ heterostructures, and the fate of 2D electrons with interactions and disorder.

Recent Progress

Finding unconventional superconductors in proximity to various strongly correlated electronic phases has been a recurring theme in materials as diverse as heavy fermion compounds, cuprates, pnictides, and twisted bilayer graphene. The discovery of superconductivity in the infinite-layer nickelates[1] was motivated by looking for an analog of the cuprates. The synthesis of the nickelates is in and of itself interesting – it involves the removal of planes of oxygen from a 3D nickel oxide using soft chemistry techniques. An initial picture of the phenomenology,

electronic properties, and magnetic structure is emerging. Notable aspects are a doping-dependent superconducting dome[2], strong magnetic fluctuations[3], and charge stripe instabilities[4]. These features are strongly reminiscent of other unconventional superconductors, despite key differences in the electronic structure and the absence of a proximate correlated insulator. Here we highlight our current research on two aspects of these materials.

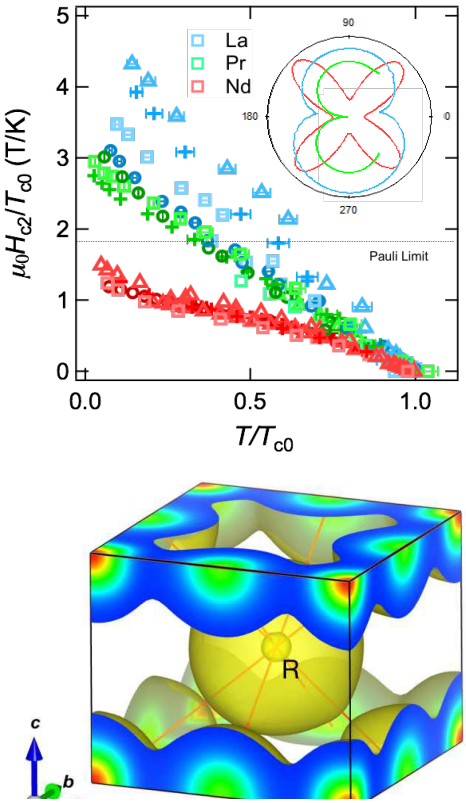

Fig. 1: (top) Rare-earth dependence of the perpendicular H_{c2}, with the in-plane angular magnetoresistance shown in the inset. (bottom) DFT electron density distribution of $NdNiO_2$, from which the crystal field structure is calculated.

Following the initial studies of Nd-based nickelates, the subsequent development of rare-earth variants with Pr (Ref. 5) and La (Publication #6) in place of Nd has created an emerging family of superconducting infinite-layer nickelates. There is increasing attention to the fact that the nickelates have the additional feature of electron-like bands arising from hybridization between the rare-earth 5*d* and Ni 3*d* orbitals. In this context, physical effects of the rare-earth site and its variation are of considerable interest. We find that there are significant differences in the magnitude and anisotropy of the superconducting upper critical field (H_{c2}) across the La-, Pr-, and Nd-nickelates (Fig. 1a). These distinctions originate from the 4*f* electron characteristics of the rare-earth ions in the crystal field of the lattice (Fig. 1b): they are absent for La^{3+}, nonmagnetic for the Pr^{3+} singlet ground state, and magnetic for the Nd^{3+} Kramer's doublet. The unique polar and azimuthal angle-dependent magnetoresistance found in the Nd-nickelates can be understood to arise from the magnetic contribution of the Nd^{3+} 4*f* moments. This leads to surprisingly tunable H_{c2} via rare-earth composition.

An ongoing challenge in studies of the nickelates has been their propensity to form a high density of extended defects, arising from lattice mismatch with the substrate. This has particularly impacted transport studies, for which these defects often dominate scattering. We have made a significant breakthrough in the materials control of the infinite-layer nickelates, by using substrates that balance the strain imposed on the precursor perovskite with that of the infinite-layer phase (Publication #1). This enables the reproducible stabilization of high-quality $Nd_{1-x}Sr_xNiO_2$ thin films essentially free from extended defects, with markedly enhanced superconductivity. Measurements of these samples reveals a normal state phase diagram exhibiting a logarithmic upturn of resistivity in the underdoped region driven by electron-electron correlations, a fan of *T*-linear normal-state resistivity near optimal doping, and a Fermi-liquid ground state in the

overdoped region (Fig. 2). This is quite different from initial measurements of the nickelates, and surprisingly similar to the "strange metal" phenomenology of other correlated systems, including the cuprates. The latter is striking when considering the marked distinctions between the two materials in terms of fermiology, band alignment, and the ground state of the parent compound. This might argue for an underlying connection in the superconducting mechanism between the two systems that is robust to these notable differences, opening doors to further resolve critical features underlying unconventional superconductivity.

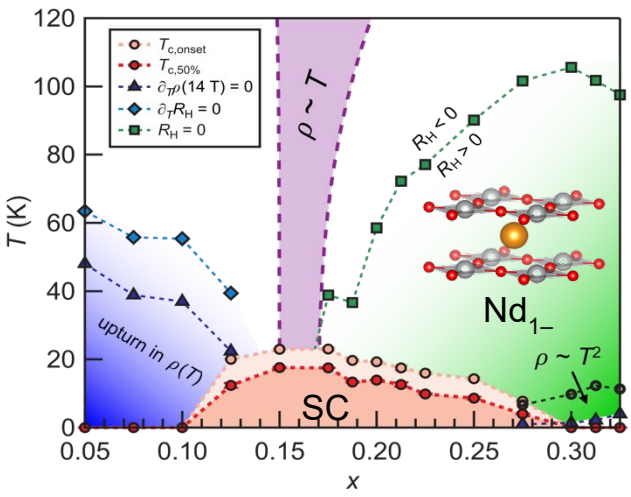

Fig. 2: Phase diagram of $Nd_{1-x}Sr_xNiO_2$ free of extended defects, emphasizing features in the resistivity and Hall effect.

Future Plans

A number of collaborative efforts are underway of the improved $Nd_{1-x}Sr_xNiO_2$ thin films, including high-field transport and time-resolved optical spectroscopy. Furthermore, we are embarking on a careful study of the superfluid density using mutual inductance measurements, both in terms of doping- and temperature- dependence. Finally, efforts are ongoing to allow for the operando resistivity measurements during topotactic reduction, to better understand the structural transition and refine its optimization.

References

1. D. F. Li, K. Lee, B. Y. Wang, M. Osada, S. Crossley, H. R. Lee, Y. Cui, Y. Hikita, and H. Y. Hwang, "Superconductivity in an Infinite-Layer Nickelate," *Nature* **572**, 624 (2019).

2. D. F. Li, B. Y. Wang, K. Lee, S. P. Harvey, M. Osada, B. H. Goodge, L. F. Kourkoutis, and H. Y. Hwang, "Superconducting Dome in $Nd_{1-x}Sr_xNiO_2$ Infinite Layer Films," *Physical Review Letters* **125**, 027001 (2020).

3. H. Lu, M. Rossi, A. Nag, M. Osada, D. F. Li, K. Lee, B. Y. Wang, M. Garcia-Fernandez, S. Agrestini, Z. X. Shen, E. M. Been, B. Moritz, T. P. Devereaux, J. Zaanen, H. Y. Hwang, K. J. Zhou, and W. S. Lee, "Magnetic Excitations in Infinite-Layer Nickelates," *Science* **373**, 213 (2021).

4. M. Rossi, M. Osada, J. Choi, S. Agrestini, D. Jost, Y. Lee, H. Lu, B. Y. Wang, K. Lee, A. Nag, Y.-D. Chuang, C.-T. Kuo, S.-J. Lee, B. Moritz, T. P. Devereaux, Z.-X. Shen, J.-S. Lee, K.-J. Zhou, H. Y. Hwang, and W.-S. Lee, "A Broken Translational Symmetry State in an Infinite-Layer Nickelate," *Nature Physics* **18**, 869 (2022).

5. M. Osada, B. Y. Wang, B. H. Goodge, K. Lee, H. Yoon, K. Sakuma, D. F. Li, M. Miura, L. F. Kourkoutis, and H. Y. Hwang, "A Superconducting Praseodymium Nickelate with Infinite-Layer Structure," *Nano Letters* **20**, 5735 (2020).

Publications

1. K. Lee, B. Y. Wang, M. Osada, B. H. Goodge, T. C. Wang, Y. Lee, S. P. Harvey, W. J. Kim, Y. Yu, C. Murthy, S. Raghu, L. F. Kourkoutis, and H. Y. Hwang, "Linear-in-Temperature Resistivity for Optimally Superconducting (Nd,Sr)NiO_2," *Nature* **619**, 288 (2023).

2. B. Y. Wang, T. C. Wang, Y.-T. Hsu, M. Osada, K. Lee, C. Jia, C. Duffy, D. F. Li, J. Fowlie, M. R. Beasley, T. P. Devereaux, I. R. Fisher, N. E. Hussey, and H. Y. Hwang, "Effects of Rare-Earth Magnetism on the Superconducting Upper Critical Field in Infinite-Layer Nickelates," *Science Advances* **9**, eadf6655 (2023).

3. R. Xu, K. J. Crust, V. Harbola, R. Arras, K. Y. Patel, S. Prosandeev, H. Cao, Y.-T. Shao, P. Behera, L. Caretta, W. J. Kim, A. Khandelwal, M. Acharya, M. M. Wang, Y. Liu, E. S. Barnard, A. Raja, L. W. Martin, X. W. Gu, H. Zhou, R. Ramesh, D. A. Muller, L. Bellaiche, and H. Y. Hwang, "Size-Induced Ferroelectricity in Antiferroelectric Oxide Membranes," *Advanced Materials* **35**, 2210562 (2023).

4. J. Fowlie, M. Hadjimichael, M. M. Martins, D. F. Li, M. Osada, B. Y. Wang, K. Lee, Y. H. Lee, Z. Salman, T. Prokscha, J.-M. Triscone, H. Y. Hwang, and Andreas Suter, "Intrinsic Magnetism in Superconducting Infinite-Layer Nickelates," *Nature Physics* **18**, 1043 (2022).

5. Y. Yu, H. Y. Hwang, S. Raghu, and S. B. Chung, "Theory of Superconductivity in Doped Quantum Paraelectrics," *npj Quantum Materials* **7**, 63 (2022).

6. M. Osada, B. Y. Wang, B. H. Goodge, S. P. Harvey, K. Lee, D. F. Li, L. F. Kourkoutis, and H. Y. Hwang, "Nickelate Superconductivity without Rare-Earth Magnetism: (La,Sr)NiO_2," *Advanced Materials* **33**, 2104083 (2021).

7. V. Harbola, R. J. Xu, S. Crossley, P. Singh, and H. Y. Hwang, "Fracture and Fatigue of Thin Crystalline $SrTiO_3$ Membranes," *Applied Physics Letters* **119**, 053102 (2021).

8. V. Harbola, S. Crossley, S. S. Hong, D. Lu, Y. Birkhölzer, Y. Hikita and H. Y. Hwang, "Giant Strain Gradient Elasticity in $SrTiO_3$ Membranes: Bending versus Stretching," *Nano Letters* **21**, 2470 (2021).

9. Z. Y. Chen, B. Y. Wang, A. G. Swartz, H. Yoon, Y. Hikita, S. Raghu, and H. Y. Hwang, "Universal Behavior of the Bosonic Metallic Ground State in a Two-Dimensional Superconductor," *npj Quantum Materials* **6,** 15 (2021).

10. B. Y. Wang, D. F. Li, B. H. Goodge, K. Lee, M. Osada, S. P. Harvey, L. F. Kourkoutis, M. R. Beasley, and H. Y. Hwang, "Isotropic Pauli-Limited Superconductivity in the Infinite-Layer Nickelate $Nd_{0.775}Sr_{0.225}NiO_2$," *Nature Physics* **17**, 473 (2021).

Superconducting nickelate thin films using in-situ synthesis

Charles H. Ahn, Yale University, New Haven, CT 06511

Department of Applied Physics, Department of Physics, Department of Mechanical Engineering and Materials Science, Yale University

Keywords: superconductivity, thin film heterostructures, Ni-based superconductors, molecular beam epitaxy, x-ray scattering

Research Scope

The goals of the project are to develop new materials systems that exhibit novel electronic and magnetic functionalities and visualize their lattice, electronic, and magnetic structures using advanced synchrotron techniques. Our approach takes advantage of the unique properties of complex oxides, in which the strong coupling between order parameters gives rise to a variety of complex physical phenomena, such as magnetism, metal-insulator transitions, and superconductivity. In this project, we study the physical and electronic structures of complex oxide heterostructures based on the rare-earth nickelates and explore the effects of lattice distortion, dimensional confinement, and chemical composition.

Discovered in 2019, the superconducting infinite-layer nickelates represent a novel class of unconventional superconductors that are spurring intense research interest due to their electronic and structural similarities to cuprate superconductors[1]. Several groups have achieved success in synthesizing superconducting nickelates, and key to this success is addressing the challenges of synthesizing a highly doped nickelate perovskite parent phase, followed by topotactic reduction to the infinite-layer superconducting phase using CaH_2 reduction. In this work we apply an all-in-situ synthesis thin film processing technique to induce superconductivity in a new nickelate composition that results in samples with atomically smooth surfaces and high Tc. This technique relies on two factors: the unique properties of the rare-earth element Eu and its 4f electrons as a dopant, and the use of metallic Al deposited on top to reduce the samples to the infinite-layer superconducting phase. The resulting films of $Nd_{1-x}Eu_xNiO_2$ have an onset superconducting temperature as high as 21K and an unusually large upper critical magnetic field. With its Eu doping, $Nd_{1-x}Eu_xNiO_2$ may have salient differences from the currently studied Sr doped nickelate superconductors. Also, the in-situ reduction technique using Al, instead of CaH_2, addresses an outstanding question of the role of hydrogen in nickelate superconductivity. We note that this *in situ* process is easy to implement and produces films of extremely high quality, which may make this approach broadly amenable to the exploration of new superconducting compositions in this class of materials.

Recent Progress

We develop this new superconductor in two steps. First, we discover an *in-situ* process to synthesize infinite-layer nickelates via the deposition of metallic aluminum in ultra-high vacuum (UHV) (**Fig. 1**) using in-situ synchrotron diffraction to visualize the process. Thin films of $NdNiO_3$, which is the fully oxidized parent of the superconducting phases, are grown to a thickness of 15-unit cells using oxide molecular beam epitaxy (MBE) at Yale. The thin films are then transferred in air to the x-ray scattering chamber 33-ID-E at the Advanced Photon Source. The $NdNiO_3$ thin films are subsequently reduced by depositing Al over a range of deposition temperatures, using either a continuous or stepwise deposition process. The film physical and electronic structure is assessed *in situ* by measuring crystal truncation rod (CTR) diffraction and diffraction-based X-ray absorption near edge structure (dXANES)[2] using tunable synchrotron radiation (**Fig. 2**). As the coverage of Al is systematically increased, CTR measurements are consistent with a phase transition from oxygen-deficient $NdNiO_{3-x}$ to $NdNiO_2$ as indicated by a monotonic change in lattice constant from 3.75Å to 3.30Å. Changes in the electronic structure measured by dXANES at

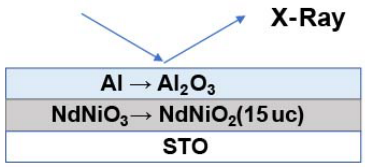

$2Al + 3NdNiO_3 \rightarrow Al_2O_3 + 3NdNiO_2$
$\Delta H = -8.09$ eV

Figure 1. Metallic aluminum as the reducing agent. The first step is to use a systematic route to reduction using Al as the reducing agent. The reduction is driven by a large thermodynamic driving force of -8.09 eV per Al. This large reducing power ensures the removal of 1.5 oxygens from $NdNiO_3$ for each atom of Al deposited. A balance of film thickness and temperature controls

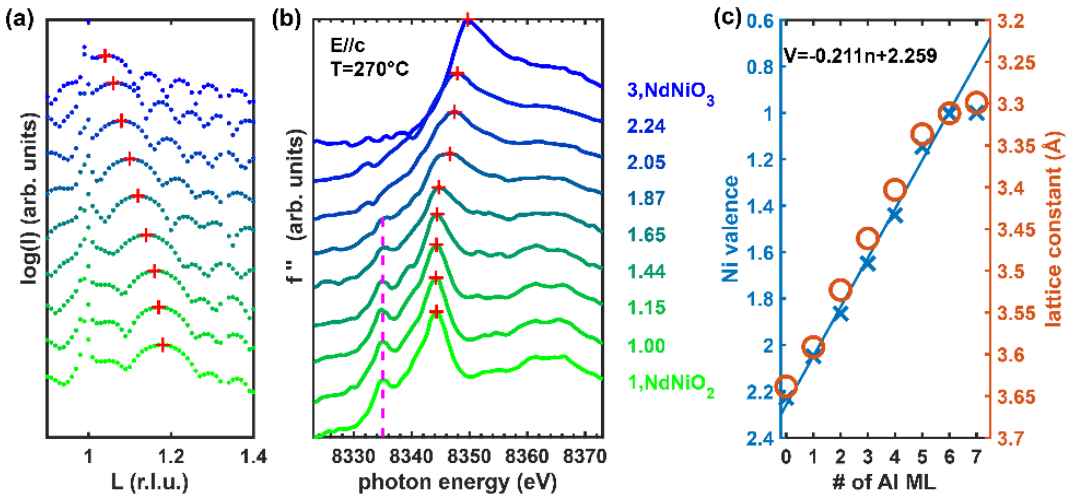

Figure 2. **Physical and electronic structure during reduction. (a)** CTR scans along the (00L) direction show a change of out-of-plane lattice parameter for a 15-unit-cell $NdNiO_{3-x}$ thin film during reduction after Al is sequentially deposited onto the nickelate thin film. **(b)** The imaginary part of the Ni anomalous scattering factor, f''_{Ni}, across the K edge shows a shift of white line energy during reduction. The f''_{Ni} is achieved using the dXANES technique taken at the corresponding diffraction peak marked in (a). The white line energy is marked in each curve, and the dashed lines are guides for the eye marking the energy of a pre-edge feature that grows in intensity during reduction. The numbers in corresponding color are the average Ni valences extracted using the Principal Component Analysis method. **(c)** A fit of Ni valence and out-of-plane lattice constant vs Al coverage

the Ni K edge show a monotonic 5eV shift of the white line energy and characterizes a change of the Ni valence from 3+ for $NdNiO_3$ to 1+ for $NdNiO_2$. We establish a relation between Ni valence and the lattice constant of $NdNiO_{3-x}$ and show that the *in-situ* nickelate reduction process is a straightforward extension of the thin film growth process for the parent perovskite compound and can be directly controlled by the amount of aluminum. An important feature of this reduction process is that it eliminates the role of hydrogen in the reduction process, which has been a question regarding films reduced using CaH_2.

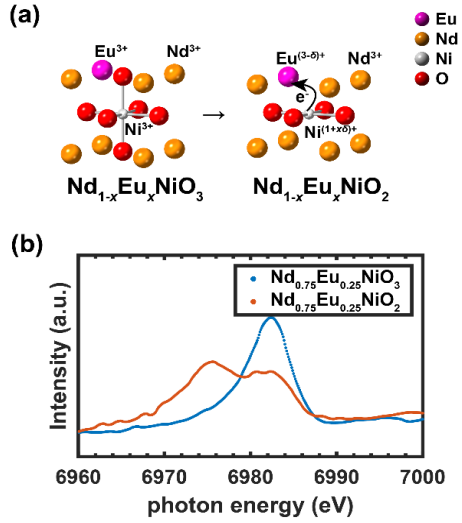

Figure 3. Eu valence changes before and after reduction. (a) The multivalent nature of Eu allows it to dope after reduction. (b) Both Eu^{2+} and $Eu^{3+}$are observed after reduction at the Eu L_3 edge dXANES.

Next, we extend the reduction process to the synthesis of other nickelates and discover a new superconducting nickelate. Rather than dope the square planar nickel layers with strontium, we use the polyvalent property of Eu on the Nd site to dope holes into the nickelate parent compound $NdNiO_3$. As described above, we start with fully oxidized thin films of $Nd_{1-x}Eu_xNiO_3$ and reduce them to $Nd_{1-x}Eu_xNiO_2$ using the *in-situ* aluminum process. In the fully oxidized parent compound, Eu starts out with a valence of 3+ (**Fig. 3**), as expected for a lanthanide on the A-site of the perovskite structure, like Nd. As the perovskite is reduced using metallic Al deposition, the valence of the Eu goes from pure 3+ to a mixture of 3+ and 2+ as measured using dXANES at the Eu L3 edge in Fig. 3. The resulting films of $Nd_{1-x}Eu_xNiO_2$ show superconductivity with an onset temperature as high as 21K. Another interesting property of the Eu based nickelates is that the magnetic field response shows an unusually high upper critical magnetic field, possibly due to Eu as a 4*f* dopant (**Fig. 4**) with a high magnetic moment. The new mixed-rare-earth nickelate superconductor is a potentially new class of superconducting nickelate with possible differences from the strontium doped materials. By expanding the library of dopants for the nickelates, we have introduced additional opportunities for understanding the underlying physics of unconventional superconductivity in this system.

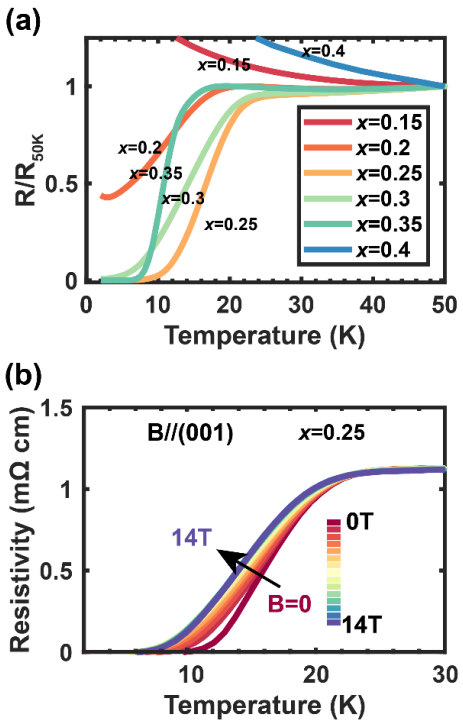

Figure 4. Magneto transport properties of $Nd_{1-x}Eu_xNiO_2$ as a function of temperature. (a) $Nd_{1-x}Eu_xNiO_2$ shows a superconducting transition for $0.2<x<0.35$. (b) For $x = 0.25$ $Nd_{1-x}Eu_xNiO_2$ thin films show a weak field dependence and robust superconductivity in magnetic fields up to 14T.

Our work also contributes to the debate on the role of hydrogen impurities in nickelate superconductivity. A recent *Nature* article[3] asserts the critical role of hydrogen intercalation in nickelate superconductivity. Our work demonstrates superconductivity without hydrogen intercalation in the nickelates, which rules out the necessity of hydrogen to induce superconductivity and realigns the discussion of nickelate superconductivity in relation to the cuprates.

In addition to being supported by the U.S. DOE, Office of Science, Office of Basic Energy Sciences under award no. DE-SC0019211, this research used resources of the Advanced Photon Source, a U.S. Department of Energy (DOE) Office of Science user facility operated for the DOE Office of Science by Argonne National Laboratory under Contract No. DE-AC02-06CH11357.

Future Plans

Our recent result shows the potential of UHV synthesis and surface-sensitive characterization on superconducting nickelates. Despite the advances in UHV synthesis, surface-sensitive characterization (e.g., ARPES) on superconducting nickelates has not yet been fully achieved because thin oxide capping layers are needed after synthesis. In the future, we will explore alternative UHV-compatible methods on the reduction of nickelate thin films. Our experience with synthesizing a new superconducting nickelate compound in UHV may enable breakthroughs on combinatorial in-situ synthesis and ARPES measurements of this system. With this experimental setup, we can unveil the band structure of square-planar nickelates and enable the engineering of other superconducting nickelates.

The new Eu doped nickelate superconductor has novel properties that merit further attention. For example, the superconducting transition is notably robust up to our highest measured field of 14T, and the large superconducting upper critical field may be related to Eu 4f doping. In addition, the strength of the Eu self-doping effect needs more study. We observe multiple valences of Eu for x = 0.25 $Nd_{1-x}Eu_xNiO_2$ and show that on average a Eu ion contributes 0.6 holes, but the self-doping effect may change as a function of Eu substitution level. Therefore, more work is needed to understand the role of Eu in superconducting $Nd_{1-x}Eu_xNiO_2$ thin films and its magnetoresistance behavior as a superconductor.

References

1. Danfeng Li, Kyuho Lee, Bai Yang Wang, Motoki Osada, Samuel Crossley, Hye Ryoung Lee, Yi Cui, Yasuyuki Hikita, and Harold Y. Hwang, *Superconductivity in an infinite-layer nickelate,* Nature, **572**, 624 (2019).

2. E.D. Specht and F.J. Walker, *Oxidation state of a buried interface: Near-edge x-ray fine structure of a crystal truncation rod,* Physical Review B **47**, 13743 (1993).

3. Xiang Ding, Charles C. Tam, Xuelei Sui, Yan Zhao, Minghui Xu, Jaewon Choi, Huaqian Leng, Ji Zhang, Mei Wu, Haiyan Xiao, Xiaotao Zu, Mirian Garcia-Fernandez, Stefano Agrestini, Xiaoqiang Wu, Qingyuan Wang, Peng Gao, Sean Li, Bing Huang, Ke-Jin Zhou and Liang Qiao, *Critical role of hydrogen for superconductivity in nickelates,* Nature **615**, 50 (2023).

Publications

1. Wenzheng Wei, Dung Vu, Zhan Zhang, Frederick J. Walker, and Charles H. Ahn, *Superconducting $Nd_{1-x}Eu_xNiO_2$ thin films using in situ synthesis*, Science Advances **9**, eadh3327 (2023).

2. Wenzheng Wei, Kidae Shin, Hawoong Hong, Yeongjae Shin, Arashdeep Singh Thind, Yingjie Yang, Robert F. Klie, Frederick J. Walker, and Charles H. Ahn, *Solid state reduction of nickelate thin films*, Phys. Rev. Materials **7**, 013802 (2023).

3. Chong Liu, Ryan P. Day, Fengmiao Li, Ryan L. Roemer, Sergey Zhdanovich, Sergey Gorovikov, Tor M. Pedersen, Juan Jiang, Sangjae Lee, Michael Schneider, Doug Wong, Pinder Dosanjh, Frederick J. Walker, Charles H. Ahn, Giorgio Levy, Andrea Damascelli, George A. Sawatzky, Ke Zou, *High-order replica bands in monolayer $FeSe/SrTiO_3$ revealed by polarization-dependent photoemission spectroscopy*, Nature Communications **12**, 4573 (2021).

Study of topological and unconventional superconductivity in low dimensional systems

Qi Li

Department of Physics, Pennsylvania State University, University Park, PA 16802

Keywords: superconductivity, topological superconductivity, 2D and layered crystals, thin film heterostructures, magnetotransport

Research Scope

The goal of the project is to study proximity-induced superconductivity in two-dimensional quantum materials and unconventional superconductivity. The focus of the research is on the interplay between superconductivity, Rashba spin orbit coupling, topological bands, and low filling Landau level states. The systems to be studied include 2D electron systems at transition metal oxides interfaces in (111) orientation with large Rashba spin-orbit coupling (SOC) and 2D materials with Dirac bands. Superconductors to be used include Nb and MgB_2. MgB_2 has the highest T_c for an s-wave superconductor and the goal is to increase the temperature of the topological superconducting states. In addition, Dirac nodal line has been predicted and observed by ARPES on its *M*-plane (10-10), which supports the prospect of an intrinsic topological superconductor. Furthermore, MgB_2 has very large H_{c2} which can reach the states where the 2D system is in low Landau level quantum Hall states while MgB_2 is still superconducting in the required magnetic field. This provides a possibility that superconductivity can be induced in low Landau level states. The overall goal of this project is to explore the superconductivity in topological or quantum limit states in metal oxide 2D electron systems with large Rashba SOC and other 2D materials.

Recent Progress

1. Anisotropic high upper critical field in ultrathin MgB_2 film

Ultrathin superconducting films with high transition temperature and high critical magnetic field are desirable for many potential applications, such as hybrid superconductor-topological material structure for quantum computing, and single photon detectors. MgB_2 is one of the highest T_c *s*-wave superconductors and therefore is very promising for these applications. In this work, we studied the superconducting transition of ultrathin MgB_2 film with film thickness in the nanometer scale. Fig. 1 shows the superconducting transitions of a nominal 3 nm and 6 nm films. The T_c of the nominal 3 nm- thick film is above 30 K. Fig. 2 (a) (b) display the resistance as a function of temperature in high magnetic fields for the perpendicular and parallel field directions. Fig.2 (c) shows the upper critical field as a function of reduced T_c. The upper critical field exhibits a good agreement with the phenomenological Ginzburg-Landau expression for a 2D superconducting

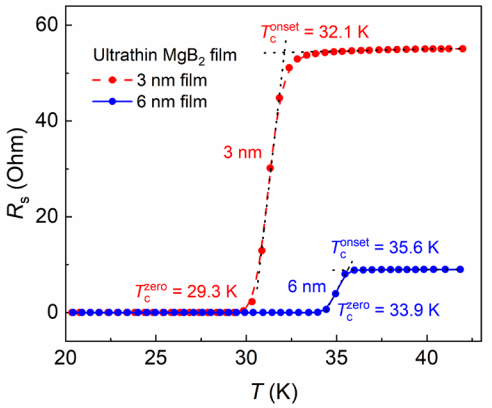

Fig. 1. Superconducting transition curves of two ultrathin MgB_2 films with film thickness of 3 nm and 6 nm. The 3 nm-thick film exhibits an onset T_c of 32.1 K and a zero resistance T_c of 29.3 K. The 6 nm- thick film exhibits an onset T_c of 35.6 K and a zero resistance T_c of 33.9 K.

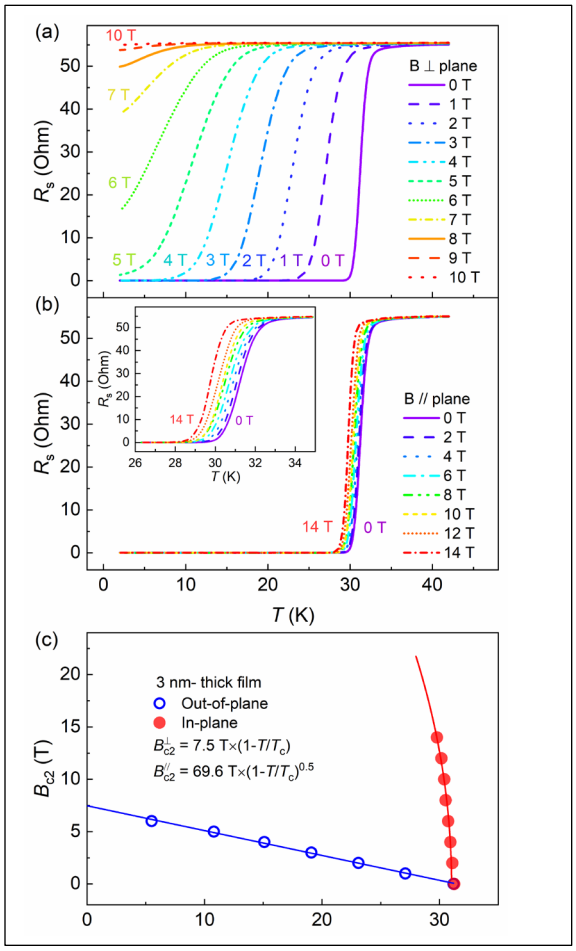

Fig. 2. Anisotropic superconductivity of a 3 nm- thick MgB_2 film. (a) Superconducting transition with magnetic field applied perpendicular to the film plane. (b) Superconducting transition with the magnetic field applied parallel to the film plane. Inset, zoom-in of the superconducting transition region. (c) Out-of-plane and in-plane upper critical fields show pronounced anisotropy and follow the Ginzburg-Landau formula for a 2D film, *i.e.*, $B_{c2}^{\perp} \propto 1 - T/T_c$ for an out-of-plane magnetic field and $B_{c2}^{\parallel} \propto (1 - T/T_c)^{0.5}$ for an in-plane magnetic field. The extrapolation of upper critical field yields $B_{c2}^{\perp}(0\ \mathrm{K}) = 7.5$ T and $B_{c2}^{\parallel}(0\ \mathrm{K}) = 70$ T in the 3 nm- thick film. The large anisotropy indicates that the superconductivity of ultrathin MgB_2 film is strongly 2D in nature. The angular dependence of the upper critical field $B_{c2}(\theta)$ shows a sharp cusp feature when the magnetic field is parallel to the film. The 2D Tinkham model could describe the trend of angular dependent upper critical field, which once again indicates the 2D superconducting nature of the MgB_2 films.

2. Tilted *ab*-axis MgB_2 films with anomalous upper critical field anisotropy

It has been predicted and experimentally shown that Dirac nodal lines exist along the *M*-plane (10-10) in MgB_2. It is further predicted that it would be an intrinsic topological superconductor.[1] Moreover, MgB_2 has well-documented two-energy gaps, with a small gap of ~2.3 meV due to π band contributions and a larger σ band gap ~7.1 meV that is largely accessible only from the *M*-planes. Therefore, *ab*-axis MgB_2 thin films have been very desirable. This direction also has very large H_{c2} due to the intrinsic layered structures which can be used for studying the proximity effect to quantum Hall states. Previously, in collaboration with other groups, we have

achieved tilted ⟨0001⟩ as 19° relative to the normal of the substrate surface when grown on miscut MgO substrate. A greater tilt toward an epitaxial *M*-plane film would be desired for device creation.

Toward this effort, MgB_2 films were grown on *M*-plane sapphire using hybrid physical-chemical vapor deposition (HPCVD). The resulting MgB_2 film produces bi-directional grains that tilt the MgB_2 *C*-plane 37° relative to the substrate surface and significantly exposes the MgB_2 *M*-plane. This is confirmed by x-ray diffraction, cross sectional TEM, and AFM. These twinned tilted grains have a unique influence on the anisotropy of the electrical properties of the film.

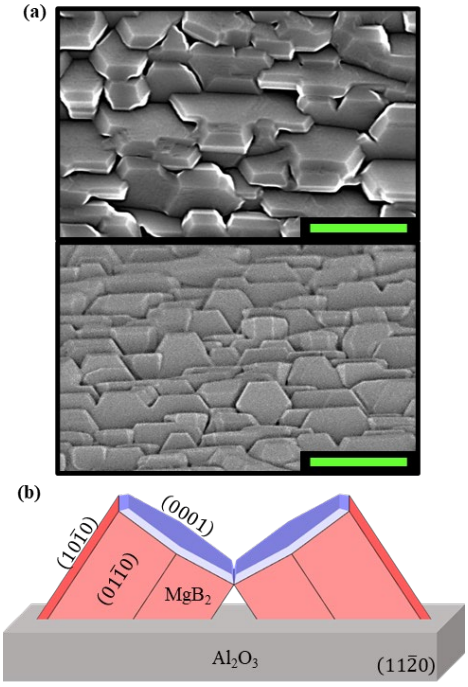

Fig. 3 (a) SEM images viewing the film from the top-down (top) and angled 60° (bottom) indicate two opposing directions to the grains in the film. (b) Individual grain structure schematic.

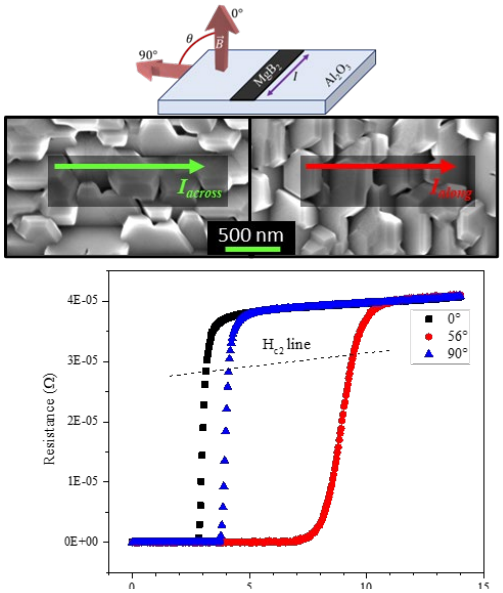

Fig. 4 Experimental setup with film morphology relative to magnetic field $\vec{B}$ angle. Current direction is referenced as across (left SEM image) or along (right SEM image) the grains. Resistance versus field at 20 K illustrates anisotropy of the I_{across} H_{c2}, measured at 80% of the transition, when the field is at perpendicular to the substrate versus aligned to $\langle 0001 \rangle_{MgB2}$.

Most prominent of these effects is shown in the angular dependence of H_{c2}. The H_{c2} maximum is at approximately 56° and a local minimum exists at 90° when current is applied across the grains (I_{across}), shown in Fig. 5. This is contrary to 90° as the maximum H_{c2} for an average film. The result indicates that the crystal anisotropy dominates the H_{c2} maximum, while the thin film shape anisotropy still dominates the H_{c2} minimum. Comparison of the two current directions is shown in Fig. 5. Additionally, we see a second peak present in the I_{across} due to good field alignment with the twinned grain's *C*-plane.

This is best illustrated when comparing the H_{c2} with I_{across} and I_{along}, [Fig. 5], where I_{along} follows traditional anisotropy because of a lack of field alignment with the crystallographic planes

in the grains of the film so anisotropy follows the film's bulk. Additionally, we see a second peak present in the I_{across} due to good field alignment with the twinned grain's *C*-plane. Understanding the morphology of these films provides invaluable insight that may be utilized toward the realization of *M*-plane MgB_2 films and their physical properties for quantum device applications.

3. Shubnikov-de Hass oscillations in 2D electron systems at $KTaO_3$ (001) interface.

$KTaO_3$ is a band insulator with 5d electron band instead of 3d electron band in $SrTiO_3$. It has recently attracted special interests due to its strong spin-orbit coupling. Previously, we have developed a process to create two-dimensional electron system at (001)-oriented $KTaO_3$ interface and studied the magnetoresistance behavior in high pulsed magnetic field up to 60 T at Los Alamos National Lab. Shubnikov-de Hass (*SdH*) oscillation was observed with relatively large amplitude of oscillations. Fast Fourier transformation (FFT) and other analysis related to SdH oscillations have been performed during this period.

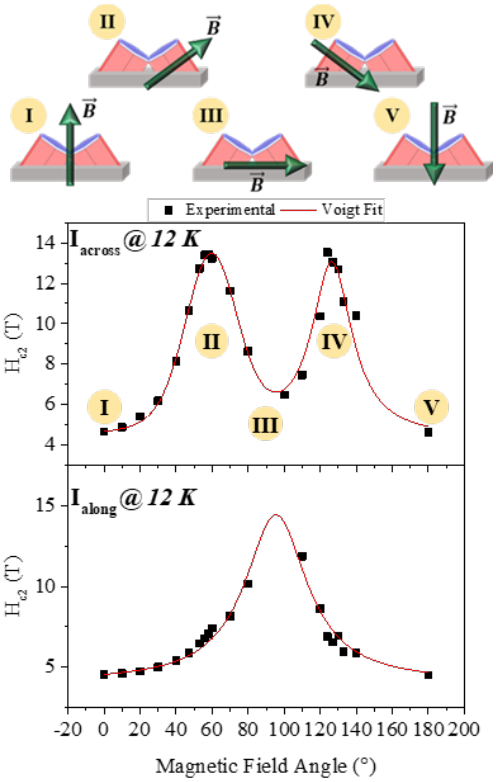

Fig. 5 H_{c2} as a function of the angle of magnetic field for the two current directions. Significant difference in the H_{c2} anisotropy is clearly seen.

4. Hybrid structure of MgB_2 thin films on epitaxial and transferred graphene

We have explored the growth of superconductor MgB_2 thin films on epitaxial buffer layer and monolayer graphene on SiC substrates, as well as on transferred graphene. Varieties of growth modes have been observed on different type of graphene. These will be explored further for both Josephson effect of MgB_2 through graphene as well as using graphene as a protecting layer for other topological materials growth with MgB_2.

Future Plans

Future plan will follow the proposal on (1) Study SdH oscillations on high mobility metal oxide interface electron gases to reveal the band structures, Rashba SOC, and other quantum states after the system reaching the lowest Landau levels. (2) Inducing superconductivity in the above systems. (3) Study possible epitaxial growth of a-axis MgB_2 films. (4) Study possible topological superconducting state in MgB_2. (5) study the growth and magnetotransport properties of hybrid MgB_2/graphene structures.

References

1. Zhou, X. *et al.* Observation of topological surface states in the high-temperature superconductor MgB 2. *Phys. Rev. B* **100**, 184511 (2019).

Publications and submitted manuscripts

1. Jue Jiang, Weiwei Zhao, Fei Wang, Renzhong Du, Ludi Miao, Ke Wang, Qi Li, Cui-Zu Chang, Moses H.W. Chan, "Long-Range Superconducting Proximity Effect in Nickel Nanowires" submitted to Phys. Rev. Research 4, 023133 (2022). https://doi.org/10.1103/PhysRevResearch.4.023133
2. Shalini Kumari, Dhiren K. Pradhan, Shi Liu, M. M. Rahaman, Peng Zhou, Kevin Roccapriore, Dillip K. Pradhan, Gopalan Srinivasan, Qi Li, Ram S. Katiyar, Philip D. Rack, J. F. Scott, and Ashok Kumar "Room-temperature large magnetoelectricity in a transition metal doped ferroelectric perovskite" Phys. Rev. B 104, 174415 (2022) DOI:10.1103/PhysRevB.104.174415
3. Tej B. Limbu, Shalini Kumari, Ziqiao Wang, Chetan Dhital, Qi Li, Yongan Tang, and Fei Yan, "Anomalous Enhancement of Ferromagnetism in Chemically-Reduced 2D $Ti_3C_2T_x$ MXene Nanosheets", Journal of Chemistry and Physics 285, 126155 (2022). https://doi.org/10.1016/j.matchemphys.2022.126155
4. Z. Wang, W. Yang, K. Chen, X.X. Xi, and Qi Li. "Anisotropic high upper critical field in ultrathin MgB2 films". *IEEE Trans. Appl. Supercond.* 33, (2023). DOI: 10.1109/TASC.2023.3264173
5. Ziqiao Wang, Autumn Heltman, Shalini Kumari, Lunhui Hu, Zhu Lin, Rojin Taheri, Nasim Alem, Lin Jiao, Shalinee Chikara, Alexey Suslov, John Singleton, Fedor Balakirev, Chaoxing Liu, and Qi Li "Shubnikov-de Haas Oscillations into the Quantum Limit in Two-Dimensional Electron Systems at $SrTiO_3$ (111) Interfaces" submitted to Science Advance (2023)
6. P. A. Rondomanski, A. Heltman, C. Chen, A. R. Richardella, J. L. Gray, J. M. Redwing, and Q. Li, *Exposure of the MgB2 M-plane via HPCVD Grown Tilted C-plane Films*, Appl.Phys. Lett., to be submitted (2023)
7. P. A. Rondomanski, A. Heltman, J. Glaser, J. M. Redwing, and Q. Li, Tilted ab-axis *MgB2 films and anomalous Upper Critical Field Anisotropy IEEE Trans. Supercond. submitted* (2023)
8. Patrick Rondomanski, Anushka Bansal, Chengye Dong, Ke Wang, Jennifer Gray, Jeffrey Shallenberger, Joshua Robinson, Qi Li, and Joan Redwing, Magnesium Intercalation Underneath Epitaxial Graphene via Physical and Chemical Vapor Deposition, to be submitted (2023).

Development of Group-V Network-Based Layered Materials

Jin Hu, University of Arkansas

Keywords: magnetism, transport, layered crystals, topological materials, group-V

Research Scope

Recent breakthroughs in topological quantum materials have revolutionized our understanding of quantum states of matter. These emergent quantum materials offer enormous potential to identify, engineer, and control a wide range of physical properties for applications in a new generation of technologies. Electronic correlations are known to drive fascinating phenomena such as high temperature superconductivity, heavy fermion, metal-to-insulator transition, etc. Therefore, extending the topological quantum physics to the regime of interacting electronic system is expected to produce new quantum states and exotic phenomena. This project aims for the realization of this vision, by establishing Group-V network-based layered material platforms with interacting topological electronic states, and based on which to explore novel electronic states and properties. Two types of material platform are investigated: the Sb-layer based *Ln*SbTe (*Ln* = lanthanides) compounds, and the P-layer based *Ln*PS compounds.

Recent Progress

We recently made progress on the development of *Ln*SbTe and *Ln*PS compounds. Three important achievements are: (1) For *Ln*SbTe materials, we established the evolution of the structural, magnetic and electronic properties for $SmSb_xTe_{2-x}$ with various Sb contents [1]; (2) We further extended the study to the Se-based compounds and developed the new non-magnetic LaSbSe material as the baseline for future studies on magnetic *Ln*SbSe materials [2]; (3) For *Ln*PS materials, we discovered exotic giant negative magnetoresistance and the corresponding field-driven insulator-to-metal transition in GdPS [3].

(i) Evolution of the structural, magnetic and electronic properties in $SmSb_xTe_{2-x}$

The ZrSiS-family compounds belong to topological nodal-line semimetal and show rich phenomena due to the presence of two types of Dirac states. In addition to those non-magnetic compounds, the magnetic version *Ln*SbTe exhibits long-range magnetic order brought in by magnetic lanthanide element *Ln*, and thus provides a platform to study the interplay between magnetism and topological states. Our earlier work [4] has demonstrated that SmSbTe is a magnetic topological semimetal with possible enhanced electronic correlations. Here we extended the study to the composition dependence, particularly the effects of Sb/Te stoichiometry on the properties of $SmSb_xTe_{2-x}$. We have successfully grown single crystals for $SmSb_xTe_{2-x}$ with various Sb content x (from ~0.2 to ~1) using a chemical vapor transport technique, and characterized their structural, magnetic and electronic properties. As shown in Figs. 1a and 1b, we found that, with gradual replacing the Sb atom by Te, the tetragonal SmSbTe, which is characterized by the Sb square net, undergoes a structure distortion around $x = 0.8$. Such structure

evolution by reducing Sb content is accompanied by changes in magnetic and electronic properties. As shown in Fig. 2c, our magnetization and specific heat measurements have established multiple antiferromagnetic transitions that vary with Sb content. Furthermore, $SmSb_xTe_{2-x}$ becomes more insulating-like when Sb content is reduced (Fig. 2d). With such tunable properties, $SmSb_xTe_{2-x}$ materials provide a good platform to study and design various quantum states that arising from the interplay between lattice, spin, and topology.

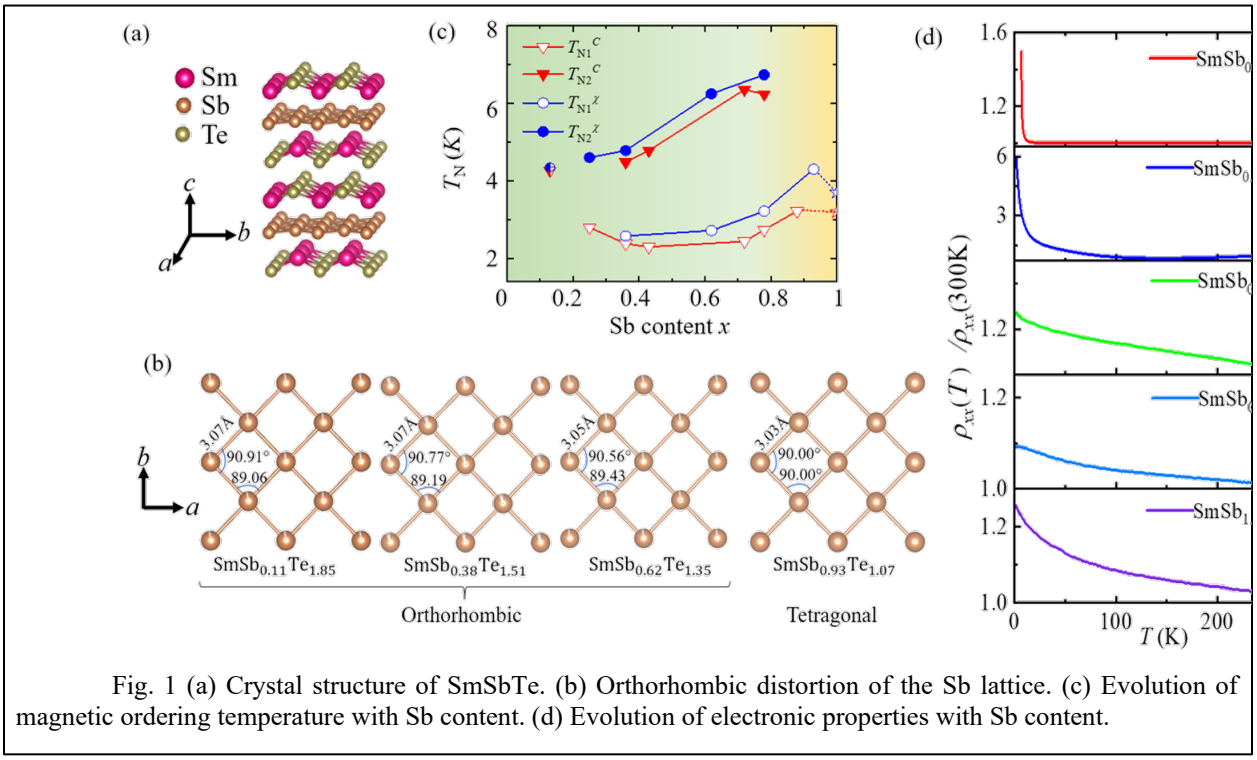

Fig. 1 (a) Crystal structure of SmSbTe. (b) Orthorhombic distortion of the Sb lattice. (c) Evolution of magnetic ordering temperature with Sb content. (d) Evolution of electronic properties with Sb content.

(ii) Crystal Growth and Electronic Properties of LaSbSe

In topological materials, spin-orbit coupling (SOC) is an important parameter that efficiently tunes electronic band structures and consequently topology. Also SOC is relatively easily tunable by elementary substitutions. In *Ln*SbTe, replacing Te with other chalcogen elements is one simple route to modify SOC. Extending from tellurides to selenides, those *Ln*SbSe compounds provide additional opportunities to investigate the topological materials and topological physics. Under this motivation we have investigated the previously unexplored non-magnetic LaSbSe [2]. We have successfully grown single crystals for LaSbSe using a chemical vapor transport technique (Fig. 2b, inset). We found that this material exhibits metallic transport behavior with small positive magnetoresistance, non-compensated charge carriers (10^{19} - 10^{20} cm^{-3}), and relatively low carrier mobilities (~10^2 cm^2/Vs) for electrons and holes (Figs. 2b-2e). Those transport characteristics are distinct from that of many other topological quantum materials. Our heat capacity measurements also revealed a small Sommerfeld coefficient (~2 mJ mol/K^2) for LaSbSe, which is comparable with LaSbTe (Fig. 2f) but is distinct from its magnetic telluride

sibling compounds *Ln*SbTe. Those results establish the non-magnetic LaSbSe as baseline for the future studies on *Ln*SbTe magnetic *Ln*SbSe compounds.

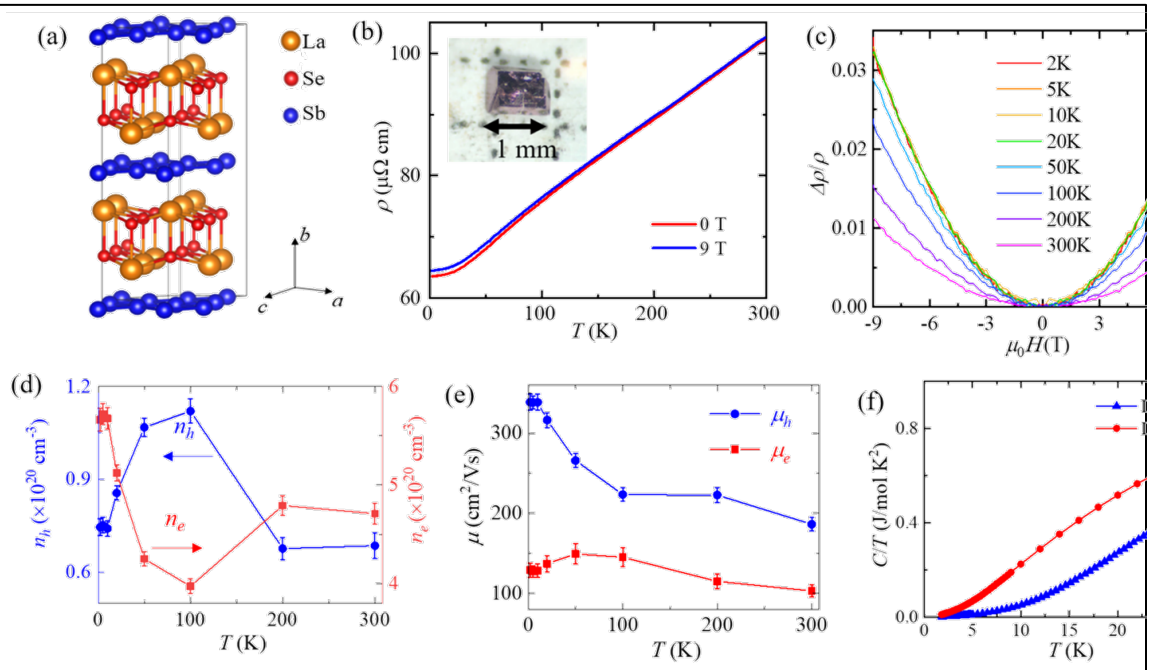

Fig. 2 (a) Crystal structure of LaSbSe. (b) Temperature dependent resistivity measured under 0 and 9 T magnetic fields. Inset: image of a LaSbSe single crystal. (c) Magnetoresistance at various temperatures. (d) Temperature dependent carrier concentrations. (e) Temperature dependent carrier mobilities. (f) Comparison of heat capacity.

(iii) Insulator to metal transition in GdPS

Compared to the layered *Ln*SbTe that is based on Sb network, *Ln*PS represents another related layered material family based on P network (Figs. 3a). We have successfully grown single crystals for GdPS (Figs. 3b, inset) and discovered exotic magnetotransport phenomena. As shown in Figs. 3b-3d, GdPS displays semiconductor-like temperature dependent transport behavior under zero magnetic field (Fig. 3b). However, with the applications of magnetic field, the resistivity for GdPS is strongly suppressed, which eventually leads to metallic transport above 5 T. Correspondingly, GdPS shows giant negative magnetoresistance (MR) reaching > 95% (Fig. 3c). Importantly, such negative MR is isotropic, and essentially does not vary with magnetic field orientations. The giant negative, isotropic MR is not seen in other materials. To understand the nature of such exotic transport phenomenon, we have performed collaborative investigations on electronic band structure and high field transport/magnetization. We found that GdPS reaches a real metallic state with a well-defined Fermi surface under magnetic field, which indicates a true insulator-to-metal transition driven by magnetic field. This transition can be attributed to the strong splitting of the bands when the Gd spins gradually rotate toward the orientation of the external magnetic field. Although GdPS in the antiferromagnetic ground is a band insulator/semiconductor with a band gap ~0.3 eV (Fig. 3e), under magnetic field, the splitting of the band causes some

bands to approach and eventually cross the Fermi energy (Fig. 3f), leading to a metallic state. Interestingly, such spin polarization is nearly isotropic to the orientation of the magnetic field. Therefore, the response to magnetic field is also isotropic, which leads to the giant negative, isotropic MR in GdPS.

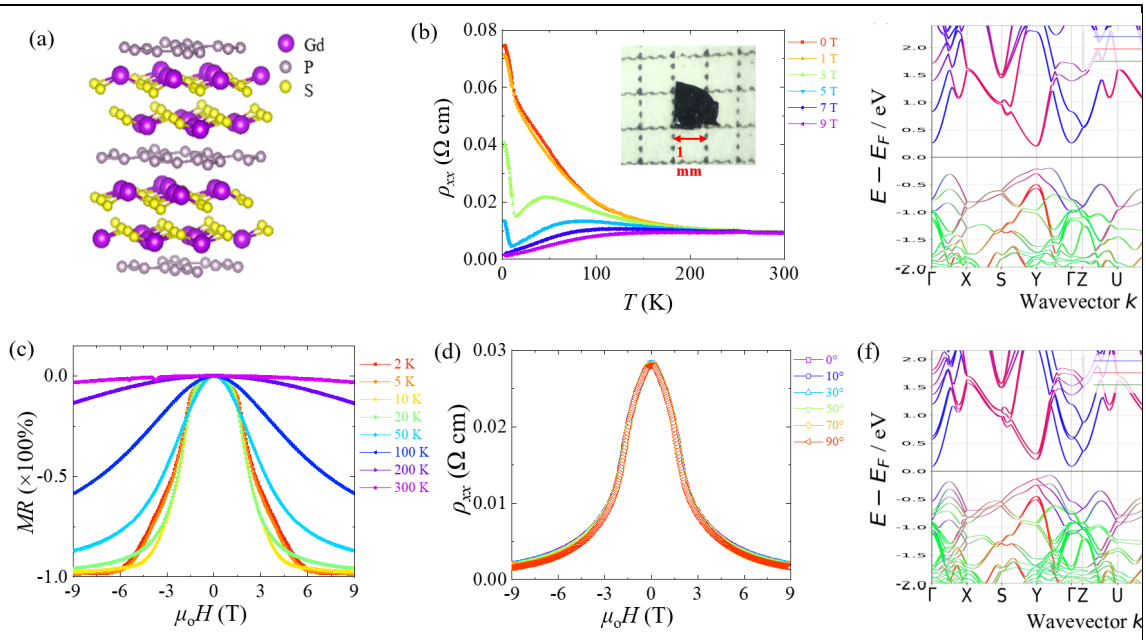

Fig. 3 (a) Crystal structure of GdPS. (b) Temperature dependent resistivity measured under various magnetic fields. Inset: image of a GdPS single crystal. (c) Magnetoresistance at various temperatures. (d) Magnetoresistance at various magnetic field orientations. (e) Band structure of antiferromagnetic ground state. (f) Band structure of the polarized ferromagnetic state.

Future Plans

For both *Ln*SbTe and *Ln*PS materials, we will extend the study to other rare earth-based compounds as well as Se- and S- substitution. For *Ln*SbTe, we will continue to focus on the impact of stoichiometry on transport and magnetism, to find out and understand the phenomena resulting from the interplay between charge, spin, electron interaction, and topology. For *Ln*PS, we will focus on tuning of the magnetotransport by other parameters, such as composition and pressure.

References

[1] K. Pandey, R. Basnet, J. Wang, B. Da, and J. Hu, *Evolution of electronic and magnetic properties in the topological semimetal $SmSb_xTe_{2-x}$*, Phys. Rev. B **105**, 155139 (2022).

[2] K. Pandey, L. Sayler, R. Basnet, J. Sakon, F. Wang, and J. Hu, *Crystal Growth and Electronic Properties of LaSbSe*, Crystals **12**, 1663 (2022).

[3] G. Acharya, In preparation.

[4] K. Pandey *et al.*, *Magnetic Topological Semimetal Phase with Electronic Correlation Enhancement in SmSbTe*, Adv. Quantum Technol. **4**, 2100063 (2021).

Publications

1. Y. Li, X. Hu, A. Fereidouni, R. Basnet, K. Pandey, J. Wen, Y. Liu, H. Zheng, H. O. H. Churchill, J. Hu, A. K. Petford‐Long and C. Phatak, *Visualizing the Effect of Oxidation on Magnetic Domain Behavior of Nanoscale Fe_3GeTe_2 for Applications in Spintronics*, ACS Applied Nano Material, **6**, 4390 (2023)

2. Arthur R. C. McCray, Yue Li, Rabindra Basnet, Krishna Pandey, Jin Hu, Daniel Phelan, Xuedan Ma, Amanda K. Petford‐Long, Charudatta Phatak, *Thermal Hysteresis and Ordering Behavior of Magnetic Skyrmion Lattices*, Nano Letters, **22**, 7804 (2022)

3. Yue Li, Rabindra Basnet, Krishna Pandey, Jin Hu, Wei Wang, Xuedan Ma, Arthur R. C. McCray, Amanda K. Petford‐Long, Charudatta Phatak, *Field‐Dependent Magnetic Domain Behavior in van der Waals Fe3GeTe2*, JOM, **74**, 2310 (2022)

4. Krishna Pandey, Rabindra Basnet, Jian Wang, Bo Da, Jin Hu, *Evolution of electronic and magnetic properties in the topological semimetal $SmSb_xTe_{2-x}$*, Physical Review B, **105**, 155139 (2022)

5. K. Pandey, L. Sayler, R. Basnet, J. Sakon, S. Guo, F. Wang, J. Hu, *Crystal Growth and Electronic Properties of LaSbSe*, Crystals, **2**, 1663 (2022)

6. R. Basnet, D. Ford, K. TenBarge, J. Lochala and J. Hu, *Emergence of Ferrimagnetism in Li‐intercalated $NiPS_3$*, Journal of Physics: Condensed Matter, **34**, 434002 (2022)

7. R. Basnet, K. Kotur, M. Rybak, C. Stephenson, S. Bishop, C. Autieri, M. Birowska, J. Hu, *Controlling magnetic exchange and anisotropy by non‐magnetic ligand substitution in layered MPX_3 (M = Ni, Mn; X = S, Se),* Physical Review Research, **4**, 023256, (2022)

8. F. Mazzola, B. Ghosh, J. Fujii, G. Acharya, D. Mondal, G. Rossi, A. Bansil, D. Farias, J. Hu, A. Agarwal, A. Politano and I. Vobornik, *Discovery of a Magnetic Dirac System with a Large Intrinsic Nonlinear Hall Effect*, Nano Letters, **23**, 902 (2022)

9. C. Cropek, V. Nguyen, S. Karki Chhetri, J. Hu, S. Guo, J. Wang, Synthesis, *Crystal and Electronic Structures, Nonlinear Optical Properties, and Magnetic Properties of Two Thiophosphates: $KInP_2S_7$ and $KCrP_2S_7$*, Crystals, 12, 1505 (2022)

10. Zhengyang Ye, Wanyue Peng, Fei Wang, Ashiwini Balodhi, Rabindra Basnet, Jin Hu, Alexandra Zevalkink, Jian Wang, *Quasilayered Crystal Structure Coupled with Point Defects Leading to Ultralow Lattice Thermal Conductivity in n‐Type $Cu_{2.83}Bi_{10}Se_{16}$*, ACS Applied Energy Materials, **4**, 11325 (2022)

Science of 100 tesla: Hole pockets, magic gap ratios and nodal quasiparticle states in the cuprates

PIs: Neil Harrison, Mun Chan, Arkady Shekhter, John Singleton, Johanna Palmstrom, Priscila Rosa, Scott Crooker, Marcelo Jaime

Keywords: Cu-based superconductors, magnetotransport, strong magnetic fields, thermodynamics

Research Scope

Our FWP involves a coordinated research effort in which we tackle pressing questions in condensed matter physics that can only be answered by use of the strongest available non-destructive pulsed magnetic fields of order 100 T. Our specific Thrusts focus on (1) the *control of orbital degrees of freedom in two dimensions*, (2) the *overcoming of intrinsic energy scales in correlated quantum matter*, and (3) "*strange metal" and pseudogap states of matter*. In Thrust 1 we are concerned primarily with fundamental changes in properties in interacting systems of electrons in strong magnetic fields brought on by orbital quantization, with prominent examples of this today being monolayer materials such as the transition metal dichalcogenides, or in noncentrosymmetric semimetals. In both of these examples, spin-orbit interaction effects are expected to be significant. In Thrust 2 we are concerned primarily with the role of strong magnetic fields coupling to spin degrees of freedom, leading to the destruction of phases or the creation of novel emergent phases in a magnetic field. Examples of such behavior are found in Kondo insulators, in the magnetic field-induced superconducting states of unconventional spin-triplet candidate uranium-based superconductors, or in candidate Kitaev spin liquid systems. Of interest in all three of these examples also is the possible realization of Majorana fermion states. Finally, Thrust 3 concerns identifying the fundamental origin of the Planckian resistivity (where the resistivity scattering rate scales with temperature divided by Planck's constant) and pseudogap states. The most robust examples of these are found in unconventional superconductors such as the cuprates, thereby requiring very strong magnetic fields.

In the present extended abstract, we focus Thrusts 1 and 2 with regards to recent research on the Cu-based high temperature superconductors. Specifically, the dichotomy that arises from studies of angle-dependent magnetoresistance oscillations in the pseudogap regime in very strong magnetic fields, and what one learns on considering the thermodynamics and strange metal behavior.

Recent Progress

We first discuss the result of recent angle-dependent magnetoresistance measurements. Superconductivity is conventionally understood as resulting from pair condensation of coherent electronic quasiparticles on a Fermi-surface. The cuprates, regarded as antiferromagnetically ordered Mott insulators when undoped, become high-temperature superconductors with small amounts of hole-doping. Many aspects of this evolution, not only the origins of the high-temperature superconductivity, but also the nature or even the very existence of a Fermi surface from which the pairing should derive, remain unresolved. We have made a significant milestone

by detecting angle-dependent magnetoresistance oscillations in the pseudogap region of the phase diagram above the superconducting temperature T_c of an underdoped cuprate, $HgBa_2CuO_{4+\delta}$ (Hg1201)[1] (see Fig. 1). The angle-dependent magnetoresistance oscillations (AMROs) provide direct evidence of a coherent close-contoured Fermi-surface in advance of the superconducting transition. The Fermi-surface is small, enclosing only a fraction of the expected free carrier density.

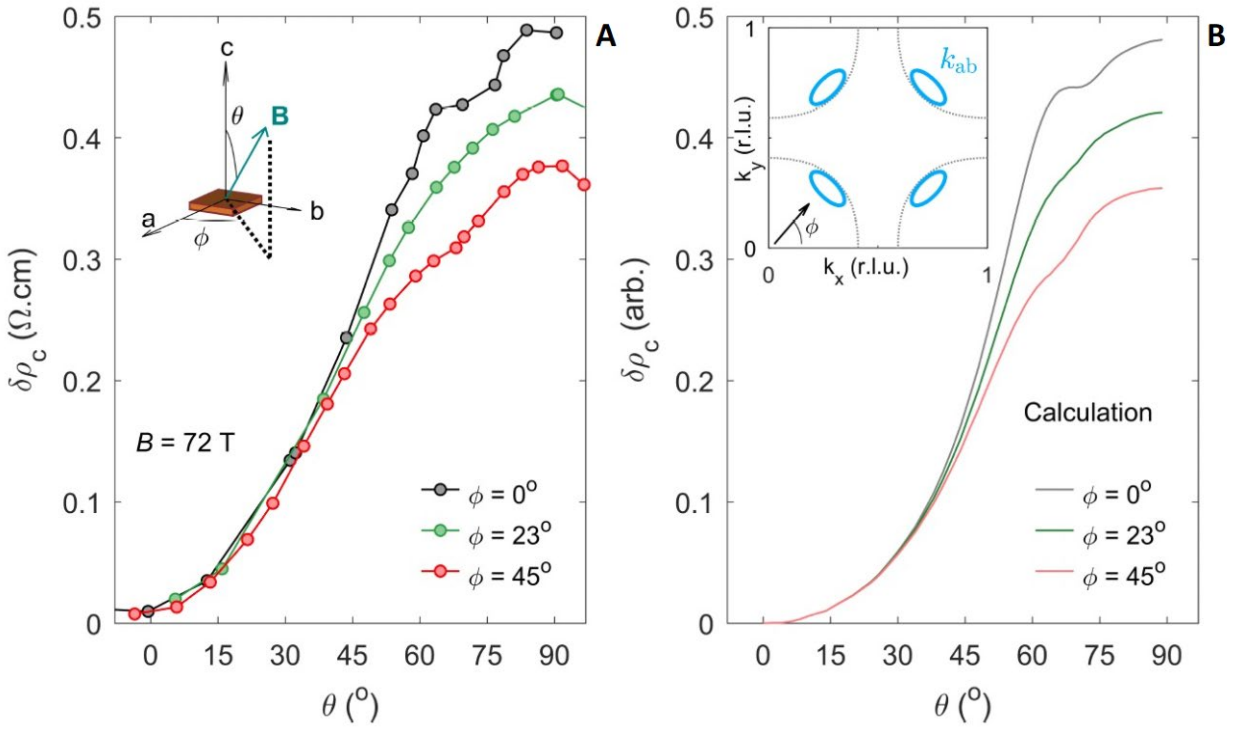

Fig. 1. (A) In interlayer resistivity, $\delta\rho_c$, at B = 72 T and T = 85 K as a function of the polar angle θ for three different azimuthal angles φ = 0°, 23° and 45° (see inset, which is a schematic defining the tilt and azimuthal angles of the applied magnetic field), for 10% hole doping. Each point is taken from measurements during a separate 72.5 T pulsed magnetic field shot. (B) Calculated $\delta\rho_c(\theta)$ for a Fermi-surface comprising elliptical pockets located at the nodal regions shown in the inset. The calculations were made assuming the Boltzmann transport equation.

The absence of long-range broken translational symmetry that would naturally produce small pockets, suggests an unconventional Fermi-surface, perhaps featuring fractionalized quasiparticles. We anticipate that these surprising results will help illuminate the physics of doped-Mott insulators[2], and its relation to unconventional superconductivity and the longstanding debate over the nature of the cuprate pseudgap phase.

In a separate effort that stemmed from data analysis that was initiated during the covid lockdown, we performed a thermodynamic analysis which shows that certain thermodynamics aspects of the phase diagram show a strong similarity to what happens in a cold atomic Fermi gas on crossing over from the Bardeen-Schrieffer-Cooper (BCS) to the Bose-Einstein condensation (BEC) regime by tuning the interactions[3]. BCS and BEC occur at opposite limits of a continuum of pairing interaction strength between fermions. Whether the crossover occurs in other systems such as the high temperature superconducting cuprates has remained an open question. We uncover here experimental evidence for a physical situation strongly resembling a BCS-BEC

crossover in the cuprates by identifying a universal magic gap ratio $2\Delta/k_BT_c \approx 6.5$ (where Δ is the pairing gap) at which paired fermion condensates become optimally robust. At this gap ratio, corresponding to the unitary point in a cold atomic Fermi gas, the measured condensate fraction N_0 and the height of the jump $\delta\gamma(T_c)$ in the coefficient γ of the fermionic specific heat at T_c are strongly peaked. In the cuprates, $\delta\gamma$(Tc) is peaked at this gap ratio when Δ corresponds to the antinodal spectroscopic gap, thus reinforcing its interpretation as the pairing gap. We find the peak in $\delta\gamma(T_c)$ also to coincide with a normal state maximum in γ, which is consistent with a pairing fluctuation pseudogap above T_c.

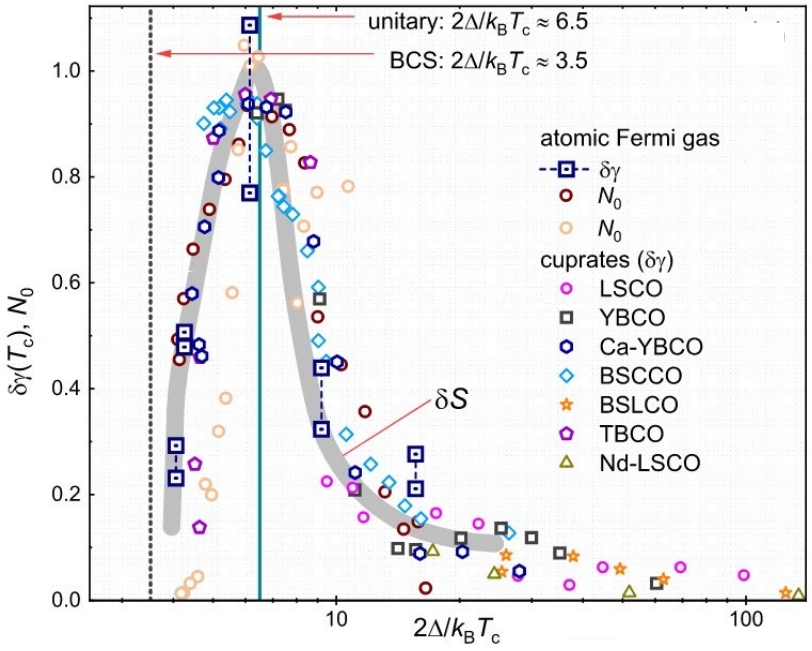

Fig. 2. $\delta\gamma(T_c)$, condensation fraction, N_0, and difference in entropy across Tc, δS, [rescaled to unity] plotted versus $2\Delta/k_BT_c$. Data shown are for a cold atomic Fermi gas, and for cuprates in which $\delta\gamma(T_c)$ measurements exist as a function of doping.

The latter results are not without their controversy. For example, angle-resolved photoemission measurements, which are performed at a similar temperature to our AMRO measurements but at zero magnetic field, find no evidence for small hole pockets. Instead, they find extended gapless regions which are commonly referred to as Fermi arcs[4]. Meanwhile, despite the similarity in the behavior of $\delta\gamma(T_c)$ to that in a cold atomic Fermi gas, suggesting a crossover into a BEC regime at low hole dopings, angle-resolved photoemission measurements find no evidence for a significant shift in the chemical potential[5].

Future Plans

Ultimately, a complete understanding of the high-T_c cuprates must reconcile both of the above observe phenomena. A presently on-going study of our is finding that the thermodynamic properties, including the normal state specific heat, magnetic susceptibility and nuclear magnetic resonance Knight shift, must at zero magnetic field be described as a nodal metal. The origin of this nodal metal still remains a mystery, and it is as yet unclear how precisely this relates to the observation of small hole pockets in strong magnetic fields. There is clearly a need to measure the hole pockets over an extended range in temperature and over a range in hole doping. This is another direction in which some of the future high magnetic field experiments are going.

Another effort is the direct study of quantum criticality in the cuprates that is responsible for the anomalous relaxation dynamics as manifest in the transport behavior in the strange metal state. Our recent efforts focus on the Hall transport in the strange metal state near quantum critical point in the LSCO cuprates. The *T*-linear resistivity and the *T*-inverse Hall resistivity at low magnetic fields are the hallmark of the strange metal behavior. The question that motivates this line of research is: how does quantum criticality in the cuprates manifest itself in the Hall resistivity at very high magnetic fields?

Another effort is the development of the resonant probes of thermodynamic properties of ultra-small size samples that are specifically designed for pulsed magnet systems. The resonant measurements magnetotropic susceptibility has been established as a viable magnetic anisotropy probe in pulsed magnetic fields. The thermal impedance spectroscopy will, for the first time, allow reliable measurements of the specific heat in 100 T fields and is at this time under active development and testing.

References

1. M. K. Chan, R. D. McDonald, B. J. Ramshaw, J. B. Betts, A. Shekhter, E. D. Bauer, and N. Harrison. Extent of Fermi-surface reconstruction in the high-temperature superconductor $HgBa_2CuO_{4+\delta}$. Proc. Natl. Acad. Sci. **117**, 9782–9786 (2020).

2. P. A. Lee, N. Nagaosa, and X.-G. Wen, Doping a mott insulator: *Physics of high-temperature superconductivity*. Rev. Mod. Phys. **78**, 17–85 (2006).

3. N. Harrison, and M. K. Chan. Magic gap ratio for optimally robust Fermionic condensation and its implications for High-T_c superconductivity. Phys. Rev. Lett. **129**, 017001 (2022).

4. B. Keimer, S. A. Kivelson, M. R. Norman, S. Uchida, J. Zaanen, *From quantum matter to high-temperature superconductivity in copper oxides*. Nature **518**, 179 (2015).

5. J. Sous, Y. He, and S. A. Kivelson *Absence of a BCS-BEC crossover in the cuprate superconductors*. npj Quantum Materials volume **8**, 25 (2023).

Publications

L. Ding, X. Xu, H. O. Jeschke, X. Bai, E. Feng, A. S. Alemayehu, J. Kim, F.-T. Huang, Q. Zhang, X. Ding, N. Harrison, V. Zapf, D. Khomskii, I. I. Mazin, S.-W. Cheong, and H. Cao, Field-tunable toroidal moment in a chiral-lattice magnet, Nature Communications **12**, 5339 (SEP 2021).

R. Schonemann, G. Rodriguez, M. Jaime, R. Schönemann, G. Rodriguez, D. Rickel, F. Balakirev, R. D. McDonald, J. A. Evans, B. Maiorov, C. Paillard, L. Bellaiche, A. V. Stier, M. B. Salamon, K. Gofryk & M. Jaime, *Magnetoelastic standing waves induced in UO_2 by microsecond magnetic field pulses*, Proceedings of the National Academy of Sciences of the United States of America **118**, 1091 (DEC 2021).

J. Li, M. Goryca, J. Choi, X. Xu & S. A. Crooker, Many-body exciton and intervalley correlations in heavily electron-doped WSe_2 monolayers, Nano Letters **22**, 426 (JAN 2022).

M. Wartenbe, P. H. Tobash, J. Singleton, L. E. Winter, S. Richmond & N. Harrison, Pseudogap in elemental plutonium, Physical Review B **105**, L041107 (JAN 2022).

S. Regmi, G. Dhakal, F. C. Kabeer, N. Harrison, F. Kabir, A. P. Sakhya, K. Gofryk, D. Kaczorowski, P. M. Oppeneer, and M. Neupane, Observation of multiple nodal lines in SmSbTe, Physical Review Materials **6**, L031201 (MAR 2022).

N. Harrison & M. K. Chan, Magic gap ratio for optimally robust fermionic condensation and its implications for high-T_c superconductivity, Physical Review Letters **129**, 017001 (JUN 2022).

D. V. Tuan , S.-F. Shi, X. Xu, S. A. Crooker, and H. Dery, *Six-body and eight-body exciton states in monolayer WSe_2*, Physical Review Letters **129**, 076801 (AUG 2022).

M. O. Ajeesh , S. M. Thomas , S. K. Kushwaha, E. D. Bauer, F. Ronning, J. D. Thompson, N. Harrison, and P. F. S. Rosa, *Ground state of $Ce_3Bi_4Pd_3$ unraveled by hydrostatic pressure*, Phys. Rev. B **106**, L161105 (OCT 2022).

A. Legros, K. W. Post, Prashant Chauhan, D. G. Rickel, Xi He, Xiaotao Xu, Xiaoyan Shi, Ivan Božović, S. A. Crooker, and N. P. Armitage, *Evolution of the cyclotron mass with doping in $La_{2-x}Sr_xCuO_4$*, Phys. Rev. B **106**, 195110 (NOV 2022).

M. M. Bordelon, C. Girod, F. Ronning, K. Rubi, N. Harrison, J. D. Thompson, C. dela Cruz, S. M. Thomas, E. D. Bauer, and P. F. S. Rosa, *Interwoven atypical quantum states in $CeLiBi_2$*, Phys. Rev. B **106**, 214433 (DEC 2022).

Definitive Majorana Zero Modes in Optimized Hybrid Nanowires

Sergey Frolov, University of Pittsburgh

Keywords: topological superconductivity, transport, nanostructures, quantum wells

Research Scope

Researchers around the world have been excited about Majorana Zero Modes (MZM). While encouraging experiments are abundant, and a 'mission accomplished' has been issued on several occasions, there has not been a definitive demonstration of MZM in any platform. The reasons for that largely fall under two categories. First, MZM and topological superconductivity put rather stringent requirements on materials in terms of crystalline defects, mean free path, and various interactions such as spin-orbit, superconductivity and magnetism – which need to coexist in just the right proportion. This in practice eliminates many approaches even if they nominally appear promising. The second reason why MZM have not been firmly established is that we have found other excitations that look so much like MZM, but are not of a topological origin. These alternative non-Majorana phenomena are all related to trivial Andreev bound states.

The goal of this project is to firmly establish Majorana Zero Modes in superconductor-semiconductor hybrid devices. We are developing optimized two-shell hybrid superconductor-semiconductor nanowires, with a tunnel barrier shell added in between the semiconductor core and the superconductor outer shell. And we are using the powerful three-terminal experimental measurement technique that allows to distinguish Majorana and Andreev states. Once Majorana modes are established, this opens doors to a large number of exciting and long-awaited experiments that explore and leverage all of the predicted Majorana properties, from teleportation to fractional Josephson effect and braiding.

Recent Progress

At the start we were planning to use InSb nanowires with CdTe shells for this project. However, the grower in Eindhoven no longer provides us with these materials. We are transitioning to analogous InAs nanowires with ZnTe barriers grown in Grenoble, France. Preliminary DFT calculations on trilayers confirm that ZnTe can serve as an effective tunnel barrier based on the favorable band alignment between InAs, ZnTe and Al superconductor metal. The new nanowires show great promise, their crystalline quality is on par with InSb nanowires, the ZnTe shells are lattice matched and can be grown in a wide range of thicknesses. Basic transport properties of InAs nanowires reveal high electron mobility and relatively straightforward superconductor contacts. We have tested shadow-defined InAs/Sn Josephson junctions which yield high critical currents. So far it appears that InAs nanowires should satisfy the basic requirements for Majorana devices and enable us to carry on to the main objectives of the program, including three-terminal device measurements of subgap spectra in hybrid devices.

In various nanoscale devices based on nanowires and quantum wells, we studied the emergence of dramatic signatures of topological superconductivity, Majorana modes and related effects such as the fractional Josephson effects and braiding. We used literature as our guide of what patterns in transport measurements are reported as smoking gun evidence of these phenomena. We found multiple examples of patterns compatible with exotic topological effects, but in samples explicitly not under topological conditions. These results serve as a critical exploration of the experimental method widely used in the community and they help establish the adequate criteria for making a claim of a major discovery in our field.

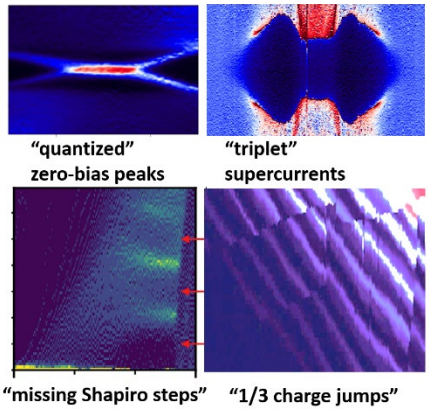

Future Plans

We plan to elaborate devices for transport measurements based on the optimized InAs nanowires with ZnTe shells. After identifying the effect of shells grown under different conditions on transport in nanowire core, we shall proceed to adding a layer of superconductor such as Al or Sn on the exterior of the shell. In these devices, we shall perform studies of induced superconductivity and how it depends on the shell thickness. Once a range of shell thicknesses suitable for tuning induced superconductivity is identified, we shall proceed to tunneling spectroscopy measurements, and identifying correlations between nanowire ends.

Oral Session 2

Symmetry Breaking in Two Dimensional Flat-band Systems for Spin, Charge and Cooper Pair Transport

PI: Chun Ning (Jeanie) Lau
co-PI: Marc Bockrath
Department of Physics, The Ohio State University, Columbus, OH 43210

Keywords: 2D and layered crystals, superconductivity, quantum Hall, moiré physics, transport

Research Scope

Electronic bands with very low or vanishing energy dispersion, known as flat bands, have strongly reduced electronic kinetic energy relative to the energy scale of interactions. This favors the emergence of correlated ground states, including correlated insulators, Chern insulators, superconductors, and ferromagnetism. Such flat band systems had been realized in a number of ways, including two-dimensional materials in quantizing magnetic fields, few-layer rhombohedral-stacked graphene, and more recently in two-dimensional material bilayers in which a moiré lattice is achieved by a small twist angle, or intrinsic lattice mismatch between the two layers. Building on past accomplishments, this program aims at the investigation of graphene-based flat band systems, including magic angle twisted bilayer graphene (tBLG), twisted, Bernal-stacked and rhombohedral-stacked few-layer graphene (FLG) heterostructures.

Our efforts consist of three thrusts, focusing on three distinct phases of correlated electronic phenomena. The first thrust focuses on flat-band superconductivity in twisted bilayer and twisted multilayer graphene, focusing on understanding the unconventional (non-kinetic energy origin) contribution to the superfluid stiffness and BEC-BCS crossover in these new classes of superconductors. The second thrust focuses on flat-band magnetism, focusing on emergent magnetism, and spin transport and dynamics in antiferromagnetic and ferromagnetic insulator in few-layer graphene and twisted graphene. The third thrust focuses on novel correlated insulating and metallic states, including those at fractional filling factors $N \pm 1/3$ in twisted bilayer graphene (where N is an integer), and fractional quantum Hall states in few-layer graphene.

We plan to perform low temperature transport measurements on ultra-clean devices that are either suspended or encapsulated by hexagonal BN. The aforementioned phenomena and processes will be investigated by tuning a large number of experimental "knobs", including twist angle, charge density, perpendicular displacement field, bias, temperature, and in-plane and perpendicular magnetic fields. This program aims to reveal further insight into the properties flat band systems and their varied and tunable correlated electron phases, and is expected lead to advances in the fundamental knowledge of correlated and/or topological states in flat band systems, with relevance for quantum information sciences and novel nanodevices.

Recent Progress

1. Evidence for Dirac Flat Band Superconductivity Enabled By Quantum Geometry

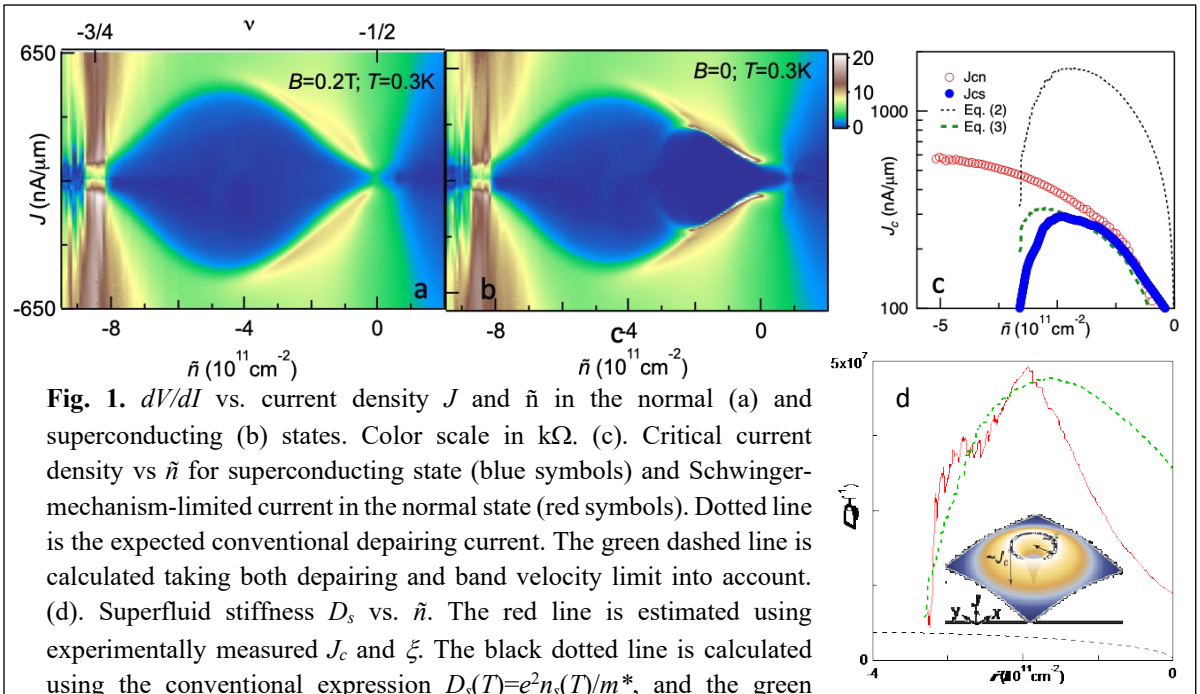

Fig. 1. *dV/dI* vs. current density J and ñ in the normal (a) and superconducting (b) states. Color scale in kΩ. (c). Critical current density vs $\tilde{n}$ for superconducting state (blue symbols) and Schwinger-mechanism-limited current in the normal state (red symbols). Dotted line is the expected conventional depairing current. The green dashed line is calculated taking both depairing and band velocity limit into account. (d). Superfluid stiffness D_s vs. $\tilde{n}$. The red line is estimated using experimentally measured J_c and ξ. The black dotted line is calculated using the conventional expression $D_s(T)=e^2n_s(T)/m^*$, and the green dotted line using $D_s(0,\tilde{n}) \approx b\frac{e^2}{\hbar^2}\Delta(0,\tilde{n})$ with b=0.33. Inset: Supercurrent density circulating around a vortex core with radius ξ.

In a flat band superconductor, the charge carriers' group velocity v_F is extremely slow. Superconductivity therein is particularly intriguing, being related to the long-standing mysteries of high temperature superconductors and heavy fermion systems. Yet the emergence of superconductivity in flat bands would appear paradoxical, as a small v_F in the conventional BCS theory implies a vanishing coherence length, superfluid stiffness, and critical current. Here, using twisted bilayer graphene (tBLG), we explore the profound effect of vanishingly small velocity in a superconducting Dirac flat band system. Using Schwinger-limited non-linear transport studies, we demonstrate an extremely slow normal state drift velocity $v_n \sim 1000$ m/s for filling fraction ν between -1/2 and -3/4 of the moiré superlattice. In the superconducting state, the same velocity limit constitutes a new limiting mechanism for the critical current, analogous to a relativistic superfluid. Importantly, our measurement of superfluid stiffness, which controls the superconductor's electrodynamic response, shows that it is not dominated by the kinetic energy, but instead by the interaction-driven superconducting gap, consistent with recent theories on a quantum geometric contribution. We find evidence for small pairs, characteristic of the BCS to Bose-Einstein condensation (BEC) crossover, with an unprecedented ratio of the superconducting transition temperature to the Fermi temperature exceeding unity.

This work provides experimental evidence that the superfluid stiffness in ultra-flat band tBLG is dominated by quantum geometric contributions, calls for a deeper understanding of how superconductivity arises in flat bands with nontrivial topology and how well-known BCS relations are modified when quantum geometric effects dominate, and points to a possible new guiding principle for the search of high-T_c superconductors. This work was published by *Nature*[1], and was reported by several news media.

2. Gate Tunable Magnetism and Giant Magnetoresistance in Suspended Rhombohedral-stacked Few-Layer Graphene

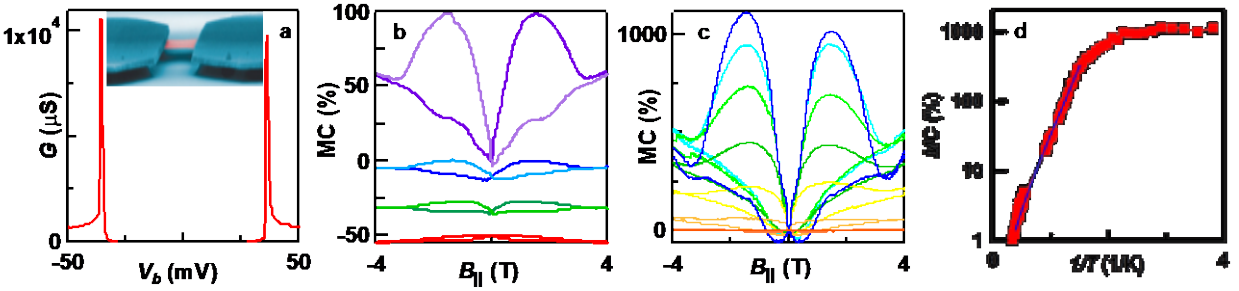

Fig. 15. (a). Two-terminal G vs bias voltage at the CNP, showing a~40 meV gap. Inset: False-color SEM image of a suspended graphene device. (b). Magnetoconductance (MC) vs. $B_{||}$ at T=0.26K and V_g=-4.8, 12.2 and -11.3V, respectively. The curves are offset for clarity. (c). MC($B_{||}$) at V_g=-3.8V and temperatures ranging from 0.28 (blue) to 4.2K (red). (d). MC at V_g=-3.8V vs T in Arrhenius scale. The blue line is an Arrhenius fit with characteristic T~ 4.5K.

Conventionally, magnetism arises from the strong exchange interaction among the magnetic moments of *d*- or *f*-shell electrons. It can also emerge in perfect lattices from non-magnetic elements, such as that exemplified by the Stoner criterion. Here we report tunable magnetism in suspended rhombohedral-stacked few-layer graphene (r-FLG) devices with flat bands. At small doping (n~10^{11} cm^{-2}), we observe prominent conductance hysteresis and giant magnetoconductance that exceeds 1000% as a function of magnetic fields. Both phenomena are tunable by density and temperature, and disappear at n>10^{12} cm^{-2} or T>5K. These results are confirmed by first principles calculations, which indicate the formation of a half-metallic state in doped r-FLG, in which the magnetization is tunable by electric field. Our combined experimental and theoretical work demonstrate that magnetism and spin polarization, arising from the strong electronic interactions in flat bands, emerge in a system composed entirely of carbon atoms. This work is published by *Nano Letters*[2].

3. Tuning Spin Transport in a Graphene Antiferromagnetic Insulator.

Long-distance spin transport through anti-ferromagnetic insulators (AFMIs) is a long-standing goal of spintronics research. Unlike conventional spintronics systems, monolayer graphene in quantum Hall regime (QH) offers an unprecedented tunability of spin-polarization and charge carrier density in QH edge states. Here, using gate-controlled QH edges as spin-dependent injectors and detectors in an all-graphene electrical circuit, for the first time we demonstrate a selective tuning of ambipolar spin transport through graphene ν=0 AFMIs. By modulating polarities of the excitation bias, magnetic fields, and charge carriers that host opposite chiralities,

we show that the difference between spin chemical potentials of adjacent edge channels in the spin-injector region is crucial in tuning spin-transport observed across graphene AFMI. We demonstrate that non-local response vanishes upon reversing directions of the co-propagating edge channels when the spin-filters in our devices are no longer selective for a particular spin-

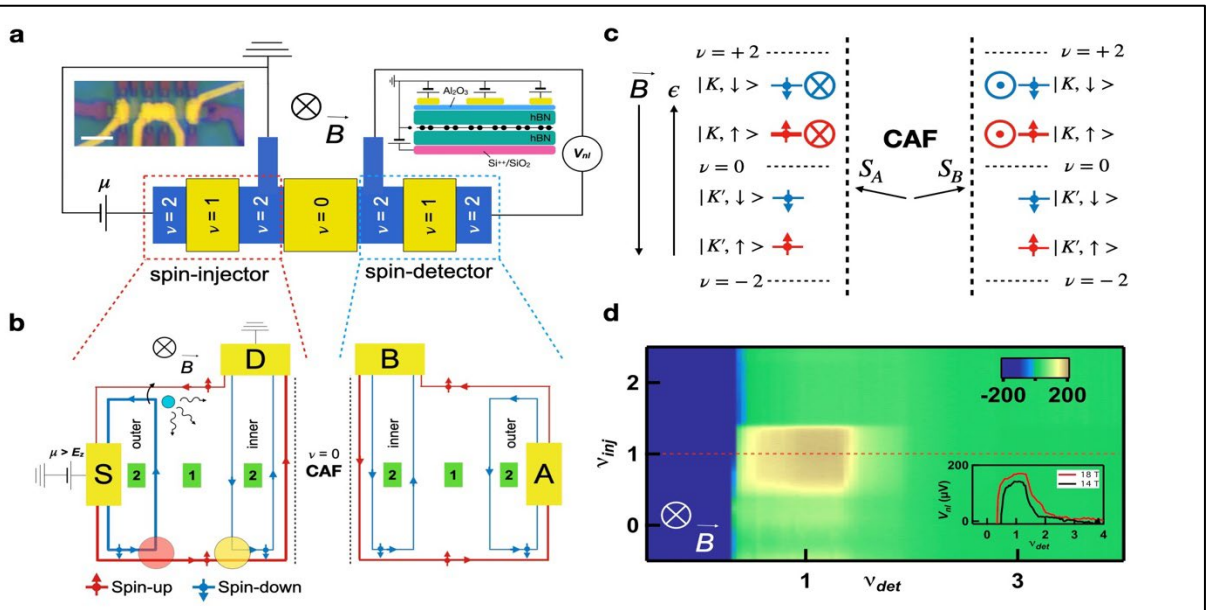

Figure 3. | **Theoretical and experimental setup for spin transport detection. a)** All-graphene electric circuit proposed to perform spin-transport measurements. Blue regions are "bare" back-gated. Yellow regions are gated independently with both bottom and top gates. Dashed red- (blue-) line boxes show injection (detection) region, respectively. **b)** Schematics illustrating QH edge states inside the spin-injection and spin-detection regions. Solid red (blue) lines demonstrate QH edge channels with ↑(↓)-spin polarization. Thicker (thinner) lines refer to the "hot" ("cold") edges, that carry high (low) chemical potential, respectively. **c)** Configuration of 0th LL states near graphene easy-plane CAF ν=0 region. CAF state is sandwiched between the two inner QH states at fillings ν=+2 that host two co-propagating edge channels (marked by circles) with spin angular momentum imbalance indicated by a thicker ↑-polarized red line. **d)** Experimental measurements of the non-local signal (in μV) at B=18 T and T=1.8 K. The inset in the right lower corner shows line traces at B=18 T (red) and B=14 T (black) taken along the red dashed line.

polarization. Our results establish a versatile set of methods to tune pure spin transport via an anti-ferromagnetic media and open a pathway to explore their applications for a broad field of antiferromagnetic spintronics research. This work is published by *Physical Review Applied*[3].

Future Plans

Apart from the general direction outlined in the first section, our immediate plans for the next year include investigation of

- superfluidity and superconductivity in twisted bilayer and trilayer graphene
- correlated insulating states in graphene-based moiré systems
- magnetism in graphene-based moiré systems

References

[1] H. Tian, X. Gao, Y. Zhang, S. Che, T. Xu, P. Cheung, K. Watanabe, T. Taniguchi, M. Randeria, F. Zhang, C. N. Lau, and M. W. Bockrath, *Evidence for Dirac flat band superconductivity enabled by quantum geometry*, Nature **614,** 440 (2023).

[2] Y. Lee, S. Che, J. Velasco, Jr., X. Gao, Y. Shi, D. Tran, J. Baima, F. Mauri, M. Calandra, M. Bockrath, and C. N. Lau, *Gate-Tunable Magnetism and Giant Magnetoresistance in Suspended Rhombohedral-Stacked Few-Layer Graphene*, Nano Lett. **22,** 5094 (2022).
[3] P. Stepanov, D. L. Shcherbakov, S. Che, M. W. Bockrath, Y. Barlas, D. Smirnov, K. Watanabe, T. Taniguchi, R. K. Lake, and C. N. Lau, *Tuning Spin Transport in a Graphene Antiferromagnetic Insulator,* Physical Review Applied **18,** 014031 (2022).

List of 2-year Publications

1. H. Tian, X. Gao, Y. Zhang, S. Che, T. Xu, P. Cheung, K. Watanabe, T. Taniguchi, M. Randeria, F. Zhang, C. N. Lau, and M. W. Bockrath, *Evidence for Dirac flat band superconductivity enabled by quantum geometry*, Nature **614,** 440 (2023).

2. Y. Lee, S. Che, J. Velasco, Jr., X. Gao, Y. Shi, D. Tran, J. Baima, F. Mauri, M. Calandra, M. Bockrath, and C. N. Lau, *Gate-Tunable Magnetism and Giant Magnetoresistance in Suspended Rhombohedral-Stacked Few-Layer Graphene*, Nano Lett. **22,** 5094 (2022).

3. P. Stepanov, D. L. Shcherbakov, S. Che, M. W. Bockrath, Y. Barlas, D. Smirnov, K. Watanabe, T. Taniguchi, R. K. Lake, and C. N. Lau, *Tuning Spin Transport in a Graphene Antiferromagnetic Insulator,* Physical Review Applied **18,** 014031 (2022).

4. C. N. Lau, M. W. Bockrath, K. F. Mak, and F. Zhang, Reproducibility in the fabrication and physics of moiré materials, Nature 602, 41 (2022).

5. D. Y. Wang, M. Karaki, N. Mazzucca, H. D. Tian, G. X. Cao, C. N. Lau, Y. M. Lu, M. Bockrath, K. Watanabe, and T. Taniguchi, Spin-orbit coupling and interactions in quantum Hall states of graphene/WSe2 heterobilayers, Phys. Rev. B 104, L201301 (2021).

Synthesis of Electronic-Grade Quantum Heterostructures by Hybrid PLD

Chang-Beom Eom
University of Wisconsin-Madison

Keywords: Thin Film Synthesis, Quantum Heterostructures, Electronic-Grade, Heterointerfaces, Superconductivity

Program Scope

Quantum materials such as unconventional superconductors, interfacial 2D electron gases (2DEGs), and multiferroics have been fertile ground for new discoveries. Our overarching theme is developing novel synthesis routes to create a new generation of epitaxial quantum thin film heterostructures for studies of fundamental science and development of new applications. These heterostructures can be of comparable or higher quality than available bulk single crystals, but these novel systems are usually sensitive to constraints of thin film heterostructures, including interaction with the substrate, the difficulty in controlling stoichiometry and point defects, and the challenge of forming atomically perfect interfaces.

Our hypothesis is that designing substrate interactions, controlling and identifying point defects, the creation of atomically perfect interfaces and fabricating and stacking of free-standing single crystal membranes will reveal new phenomena in complex oxides and unconventional superconductors, and will discover fundamental intrinsic properties of quantum materials arising from dimensionality, anisotropy, and electronic correlations. We have already demonstrated static strain engineering of the Fe-based superconductor $BaFe_2As_2$, made the first direct observation of the two-dimensional hole gas (2DHG) at an oxide interface, are developing a hybrid pulsed laser deposition, and have begun to understand a route to new discoveries through control of highly perfect and defect free films and heterostructures and free-standing membranes. This approach overcomes conventional thin film growth limitations of epitaxial and orientational lattice match, and the clears the way for nearly limitless possibilities in materials design. The **thrusts** of our proposed work expand into new materials systems with synthesis and experimental measurements:

Fabrication of Novel Quantum Material Platforms

Novel Hybrid PLD Synthesis Route - builds on our chemical PLD process but with expanded capabilities for stoichiometry and point defect control in electronic grade quantum heterostructures involving elements with a very large vapor pressure mismatch

Complex oxide membranes **-** free-standing membranes of complex oxides films and heterostructures for assembling stacked and twisted heterostructures that expand quantum heteromaterials, allowing for dynamic strain control

Fundamental Science of Novel Quantum Materials Platform

$LaAlO_3$ / $KTaO_3$ interface superconductivity – a strong spin-orbit superconducting system with not yet understood orientation dependence, studied with hybrid PLD heterostructures.

$Ba(Pb_xBi_{1-x})O_3$ superconducting films and membranes with strong spin-orbit coupling – our recently discovered spin hall effect in this unusual superconducting system has implications for the microscopic mechanism, and offers opportunities for superconducting spintronics.

Strain-controlled pnictide superconducting free-standing membranes – investigation of fundamental magnetic, nematic, structural, and superconducting properties by dynamic strain manipulation, building on our epitaxial strain results.

Recent Progress

The discovery of interfacial superconductivity at $KTaO_3$ (111) heterointerfaces offers fresh insights into the interplay of quantum paraelectricity, strong spin-orbit coupling, and superconductivity. Future progress relies on innovations in the synthesis of ever-cleaner samples to investigate the intrinsic quantum phenomena free of extrinsic effects due to crystalline imperfections. Recently, we reported superconducting heterostructures based on electronic-grade epitaxial (111) $KTaO_3$ thin films grown by a novel hybrid synthesis route that synergistically combines thermal evaporation of K_2O suboxide and pulsed laser deposition of Ta_2O_5 facilitated by an ultrathin $SmScO_3$ template. The two-dimensional electron gas at the heterointerface between $LaAlO_3$ and the $KTaO_3$ thin film exhibits significantly higher electron mobility, superconducting transition temperature and critical current density than those in bulk single crystal $KTaO_3$-based heterostructures. Cross-sectional STEM shows a lower density of point defects and cleaner interface in heteroepitaxial $KTaO_3$ thin films in contrast to bulk single crystal $KTaO_3$ substrates. Our hybrid approach opens new synthesis routes to epitaxial growth of other alkali metal-based oxides that lie beyond the capabilities of conventional approaches.

Fig. 1a shows the calculated stability phase diagram of K-Ta-O near the stoichiometric $KTaO_3$ as a function of K partial pressure and temperature; here, the oxygen (O_2) partial pressure is fixed at 10^{-6} Torr based on the potential phase diagram as a function of K and O_2 partial pressures. We used commercially available potassium oxide (K_2O) as K source due to the unstability of elemental K. We estimate the source temperatures for achieving stoichiometric $KTaO_3$ synthesis by calculating partial pressures of all gas species (Fig. 1b) at source temperatures from 500-1000 K. We identify three

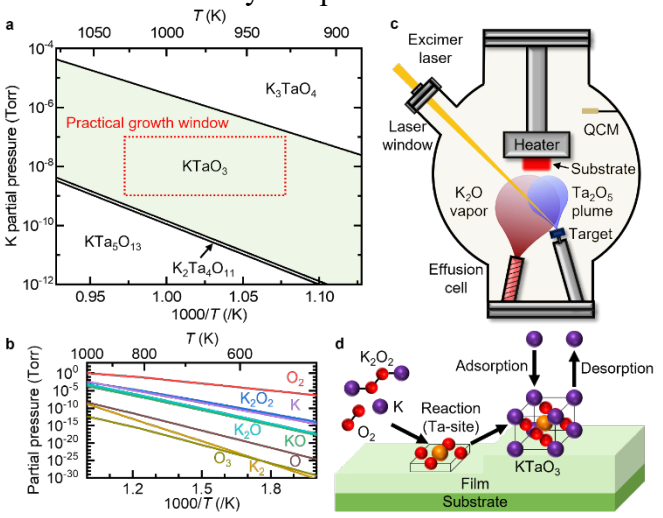

Fig. 1 | Thermodynamics-guided epitaxial growth of $KTaO_3$ thin films by hybrid PLD. a, Phase region of $KTaO_3$ as a function of K partial pressure and temperature at fixed O_2 partial pressure of 10^{-6} Torr. Practical experimental parameters within the $KTaO_3$ growth window are marked by a red box. **b**, Vapor pressure of gas species in the K-O system. **c**, Schematic illustrating the hybrid PLD method for $KTaO_3$ thin film growth. QCM: quartz crystal microbalance. **d**, Schematic illustrating the adsorption-controlled growth of $KTaO_3$ thin films.

major gas species as O_2, K_2O_2, and K with the calculated equilibrium partial pressures ≈$1.7x10^{-3}$, $9.2x10^{-7}$, and $3.9x10^{-7}$ Torr, respectively, at a source temperature of 750 K. These values set the upper limits for the partial pressures of gas species.

These analyses indicated that the practical growth window of $KTaO_3$ should be in the range of 10^{-7}-10^{-9} Torr K partial pressure and 950-1000 K substrate temperatures (red box, Fig. 1a). Fig. 1c schematically depicts the hybrid PLD experimental setup. As with MBE, K is supplied by thermal evaporation of a K_2O effusion cell directed at the substrate. In contrast, Ta is supplied by ablating a ceramic target of tantalum pentoxide (Ta_2O_5) with a pulsed excimer laser as in PLD. Fig. 1d schematically illustrates the adsorption-controlled growth of $KTaO_3$. In adsorption-controlled growth, the volatile species (K in this case) is provided with sufficiently large overpressure to avoid for K deficiency while excess K readily evaporates from the K-terminated surface.

We grew ≈8-10 nm thick epitaxial $KTaO_3$ thin films on single crystal substrates of $SrTiO_3$ (001), $SrTiO_3$ (111), $KTaO_3$ (111), and on $KTaO_3$ (111) with an ≈1 nm-thick $SmScO_3$ template layer. An increased substrate temperature of 1023 K enhances stoichiometry, but results in surface roughening. To address these issues, we grew a thin $SmScO_3$ template on $KTaO_3$ (111) substrates, and grew stoichiometric and smooth $KTaO_3$ thin films at low substrate temperature. The $SmScO_3$ template serves three purposes (i) stabilizing the $KTaO_3$ surface by suppressing K evaporation from the $KTaO_3$ substrate surface at high temperature and high vacuum, (ii) inhibiting the migration of native defects from the $KTaO_3$ substrate to the filmClick or tap here to enter text. that may deteriorate the superconductivity and (iii) suppressing the leakage of charge carriers from the film to the substrate area where more disorder is expected.

We characterized the interfacial structure with scanning transmission electron microscopy High-angle annular dark field (HAADF) cross-sectional images of the heterostructures confirm atomically-sharp interfaces of $SmScO_3/KTaO_3$ (111) substrate and $LaAlO_3/KTaO_3$ (111) thin film, which means that thin $SmScO_3$ template could protect the unstable (111) surface of the KTO substrate under the highly reducing atmosphere of ≈10^{-6} Torr at 973 K. The $KTaO_3$ thin film is fully epitaxial to the $KTaO_3$ substrate through the underlying $SmScO_3$ template without any misfit dislocations, facilitated by a small 2.6% lattice mismatch between $SmScO_3$ and $KTaO_3$ (111). The crystal structure of ≈1 nm-thick $SmScO_3$ film appears to adopt a (psuedo-)cubic structure. This allows the $KTaO_3$ (111) thin film to be coherently grown with the desired cubic structure due to the (pseudo-)cubic $SmScO_3$ template.

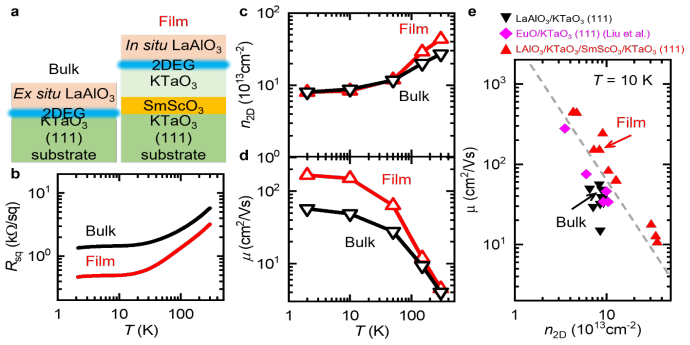

Fig. 2 | Electrical transport measurements of $KTaO_3$ (111). a, Schematic illustrating the structures of the measured samples. In the bulk case, the $LaAlO_3$ overlayer is always grown *ex situ*, which inevitably creates the 2DEG in the first few nm of $KTaO_3$ with high defect density. In the case of $KTaO_3$ thin film, the $LaAlO_3$ layer is grown *in situ* and the surface of $KTaO_3$ has low defect density, which results in enhanced μ. **b-d**, Temperature dependence (2-300 K) of **b**, R_{sq}, **c**, n_{2D}, **d**, μ of $LaAlO_3/KTaO_3$ (111) (Bulk) and $LaAlO_3/KTaO_3/SmScO_3/KTaO_3$ (111) (Film) heterostructures. The measurements in **b-d** are performed in a Van der Pauw geometry. **e**, Distribution of μ and n_{2D} estimated from Hall measurements at T = 10 K. The samples shown in **b-d** marked with arrows. Purple diamonds are data at T = 10 K from different growth conditions of EuO

These lower defect concentrations improve the normal state and superconducting state properties of the 2DEG at the $LAlO_3/KTaO_3$ interface. We compared two different heterostructures: $LaAlO_3/KTaO_3$ (111) substrate (denoted as "Bulk") and $LaAlO_3/KTaO_3/SmScO_3/KTaO_3$ (111) substrate (denoted as "Film") (Fig. 2). As shown in Fig. 2a, 2DEGs are created at the $LaAlO_3/KTaO_3$ interface. The amorphous $LaAlO_3$ layer is grown *in situ* in the case of $LaAlO_3/KTaO_3/SmScO_3/KTaO_3$ (111) heterostructures to produce clean $LaAlO_3/KTaO_3$ interfaceClick or tap here to enter text.. Fig. 2b shows the R_{sq}-T data of the "Bulk" and "Film" samples. The Film sample shows much lower R_{sq} in the normal state (Fig. 2b) despite having nearly the same n_{2D} as the Bulk sample at 10 K (Fig. 3c). We attribute the lower R_{sq} to the high carrier mobility (μ) of the Film sample (≈150 cm^2/Vs at 10 K) compared to the Bulk sample (≈48 cm^2/Vs at 10 K). We tested multiple samples with the similar structures and summarize their properties at 10 K in a μ-n_{2D} diagram (Fig. 2e). This clearly demonstrates that the $LaAlO_3/KTaO_3/SmScO_3/KTaO_3$ (111) (red up-triangles, Fig. 2e) samples generally possess higher μ within the same n_{2D} range compared to the $LaAlO_3/KTaO_3$ (111) samples (black down-triangles, Fig. 2e). We attribute the differences in μ to the lower point defect concentrations, which control the low temperature mobility.

We patterned Hall bars along the [11-2] and [1-10] on the Bulk and Film samples to investigate the superconductivity in $KTaO_3$. Fig. 3a shows the R_{sq} vs. T data at $T < 2$ K along the [11-2]. The Film sample shows a T_c ≈1.5 K, which is 25% higher than the T_c ≈1.2 K exhibited by the Bulk sample. The V-I curves at T = 0.5 K (Fig. 3b) confirm the enhanced superconductivity in the Film sample with a critical current I_c (≈12.3 μA), substantially larger than I_c of the Bulk sample (≈3.9 μA) possessing the same n_{2D}. The R_{sq}-T, V-I data suggests that reduced disorder (*i.e.*, higher μ) eliminates signatures of disorder-induced inhomogeneities[41] observed in the superconductivity of $KTaO_3$ (111) such as anisotropic transport, residual resistance, and step-like V-I curves which appear to be highly sensitive to μ.

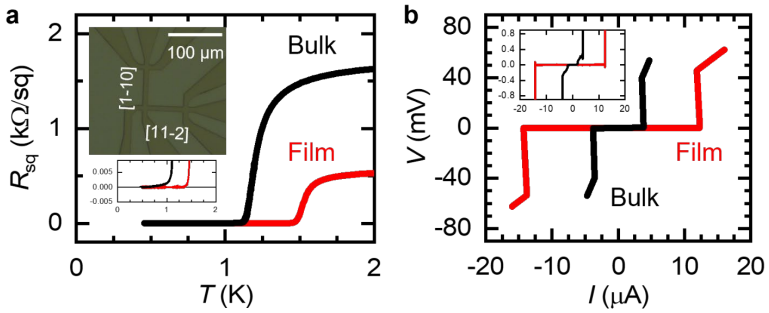

Fig. 3 | Superconductivity of $KTaO_3$ (111). a, Temperature dependence of R_{sq} along the [11-2] on Hall bars. The insets show an optical micrograph of Hall bars (top) and a magnified view near the transition (bottom). **b**, V-I curves along the [11-2] measured at T = 0.5 K on Hall bars. The inset shows a magnified view near the transition.

Future Plans

(1) Fabrication of freestanding membranes made of electronic-grade $KTaO_3$

We plan to fabricate freestanding membranes made of electronic-grade $KTaO_3$ (KTO) grown by hybrid PLD. We choose 001- and 111-orientations as the model systems to examine the complex interplay of dynamic (or static) strain, dimensionality, and doping. Our findings will have implications on the understanding of i) the detailed processes through which superconductivity emerges in the KTO system, ii) the interplay of ferroelectricity, spin-orbit coupling, and superconductivity and the resulting phase diagrams, and iii) novel applications derived from therein. This task will be achieved by employing a judiciously chosen composition of sacrificial

and reaction barrier layers, namely $0.15Ba_3Al_2O_6$-$0.85Sr_3Al_2O_6$ (BSAO) (BSAO) and $0.3BaZrO_3$-$0.7SrTiO_3$ (BSZT), during the growth of $KTaO_3$ (001) and (111) heterostructures.

(2) Nonreciprocal transport in BPBO (Diode effects and Spin Orbit Torque),
Our observation of giant spin-orbit torque (SOT) in the normal state of $BaPb_{1-x}Bi_xO_3$ (BPBO), a known superconductor, demonstrated its potential for spintronics and hinted at a hidden spin-orbit coupling (SOC). But a triplet superconducting state must be induced for superconducting BPBO to produce a net torque which could be accomplished with a ferromagnetic interface. Such interfaces, as well as unit cell-level distortions can lead to nonreciprocal responses, which we will investigate through spin orbit torque and superconducting diode effects in which current in one direction shows no voltage drop, while current in the opposite direction (opposite polarity) shows a finite, non-zero voltage[2]. We intend to extract the nonlinearities from sensitive IV curves, as we did in our previous work. Our plan for next year is to isolate the detailed nonreciprocal transport dependencies on BPBO. The current results are a convolution of superconducting diode effects in the longitudinal resistance and torque driven dependence on the anomalous Hall effect. We first intend to evaluate any superconducting diode effects in isolated BPBO thin films.

Publications (which acknowledge DOE support)

1. Kitae Eom, Muqing Yu, Jinsol Seo, Dengyu Yang, Hyungwoo Lee, Jung-Woo Lee, Patric Irvin, Sang Ho Oh, Jeremy Levy, Chang-Beom Eom, "Electronically reconfigurable complex-oxide heterostructure free-standing membranes" *Science Advances*, **7**, eabh1284 (2021) https://doi.org/10.1126/sciadv.abh1284
2. S. Ryu, H. Zhou, T. R. Paudel, N. Campbell, J. Podkaminer, C. W. Bark, T. Hernandez, D. D. Fong, Y. Zhang, L. Xie, X. Q. Pan, E. Y. Tsymbal, M. S. Rzchowski, and C. B. Eom "Electronic reconstruction at the polar (111)-oriented oxide interface", accepted for publication in *APL Materials* (2022) https://arxiv.org/abs/2110.02305
3. Kitae Eom, Hanjong Paik, Jinsol Seo, Neil Campbell, Evgeny Y. Tsymbal, Sang Ho Oh, Mark Rzchowski, Darrell G. Schlom, and Chang-Beom Eom, "Oxide two-dimensional electron gas with high mobility at room-temperature" *Advanced Science,* 2105652 (2022). https://doi.org/10.1002/advs.202105652
4. Megan Briggeman, Hyungwoo Lee, Jung-Woo Lee, Kitae Eom, François Damanet, Elliott Mansfield, Jianan Li, Mengchen Huang, Andrew J. Daley, Chang-Beom Eom, Patrick Irvin and Jeremy Levy, "One-dimensional Kronig–Penney superlattices at the $LaAlO_3/SrTiO_3$ interface" *Nature Physics*, **17**, 782 (2021). https://doi.org/10.1038/s41567-021-01217-z
5. Lu Guo, Shun-Li Shang, Neil Campbell, Mark Rzchowski, Zi-Kui Liu, and Chang-Beom Eom, "Searching for a route to *in situ* synthesis of epitaxial $Pr_2Ir_2O_7$ thin films guided by thermodynamic calculations" *npj Computational Materials*, **7**, 144 (2021) https://doi.org/10.1038/s41524-021-00610-9
6. J.H. Kang, Philip J. Ryan, Jong-Woo Kim, Jonathon Schad, Jacob P. Podkaminer, Neil Campbell, Joseph Suttle, Tae Heon Kim, Liang Luo, Di Cheng, Yesusa G. Collantes, Eric E. Hellstrom, Jigang Wang, Robert McDermott, Mark S. Rzchowski, and Chang-Beom Eom, "Local Atomic Configuration Control of Superconductivity in the Undoped Pnictide

Parent Compound $BaFe_2As_2$" *ACS Appl. Electron. Mater.* **4**, 1511 (2022) https://doi.org/10.1021/acsaelm.2c00291

7. S. Lindemann, J. Irwin, G.-Y. Kim, B. Wang, K. Eom, J. J. Wang, J. M. Hu, L. Q. Chen, S. Y. Choi, C. B. Eom, M. S. Rzchowski, "Low-Voltage Magnetoelectric Coupling in Membrane Heterostructures" *Science Advances* **7,** eabh2294 (2021) https://doi.org/10.1126/sciadv.abh2294
8. "Quantum Coherence Tomography of Lightwave–Controlled Superconductivity" L. Luo, M. Mootz1, J. H. Kang, C. Huang, K. Eom, J. W. Lee, C. Vaswani, Y. G. Collantes, E. E. Hellstrom, I. E. Perakis, C. B. Eom and J. Wang, *Nature Physics*, (2022) https://doi.org/10.1038/s41567-022-01827-1
9. C. Vaswani, J. H. Kang, M. Mootz, L. Luo, X. Yang, C. Sundahl, D. Cheng, C. Huang, R. H. J. Kim, Z. Liu, Y. G. Collantes, E. E. Hellstrom, I. E. Perakis, C. B. Eom & J. Wang, "Light quantum control of persisting Higgs modes in iron-based superconductors" *Nat. Commun.* **12**, 258 (2021). https://doi.org/10.1038/s41467-020-20350-6
10. Michael Patton, Gautam Gurun, Ding-Fu Shao, Gahee Noh, Joseph A. Mittelstaedt, Marcel Mazur, Jong-Woo Kim, Philip J. Ryan, Evgeny Y. Tsymbal, Si-Young Choi, Daniel C. Ralph, Mark S. Rzchowski, Tianxiang Nan, Chang-Beom Eom, "Symmetry Control of Unconventional Spin-Orbit Torques in IrO_2", *Advanced Materials*, 2301608 (2023) https://doi.org/10.1002/adma.202301608

Symmetries, Interactions and Correlation Effects in Carbon Nanostructures

Gleb Finkelstein, Physics Department, Duke University, Durham, NC 27708

Keywords: topology-quantum Hall, superconductivity, 2D and layered crystals, magnetotransport, Josephson junctions

Research Scope

1) The PI's group had performed some of the early studies of the superconducting proximity in the quantum Hall regime. The highlights included: the first detection of the supercurrent in a Josephson junction made from a quantum Hall (QH) region [Science 2016]; creating a QH-based SQUID [Science Advances 2019]; and most recently, the first detection of the chiral Andreev edge states and their interference [Nature Physics 2020]. Our efforts in the current funding cycle continued to focus on the superconductor- quantum Hall hybrid structures.

2) The PI's group was the first to realize ballistic mutlti-terminal graphene-based Josephson junctions, which we studied in a series of papers [Nano Letters 2019, 2021, 2022]. It had been predicted that the Andreev bound states in such structures could emulate energy band structures of topological materials. We are working to realize these predictions.

3) We have started a new collaborative effort on studying the anisotropic superconductivity of the $KTaO_3$ (111) interface [Science Advances, 2023].

Recent Progress

1. Multiterminal Josephson Junctions and the Superconducting Triode

Multiterminal Josephson junctions (MTJJ) with a normal region connected to several (>2) superconducting leads have received renewed attention in the past few years. This interest is driven in part by predictions that Andreev bound states in such structures could emulate energy band structures of topological materials. We have recently reported on the three and four-terminal graphene Josephson junctions, in which *ballistic* coupling between the terminals was achieved [Nano Letters, 2019]. We have further reported on the synchronized dynamics in these structures [Nano Letters, 2020, 2021]. Most recently, we used the MTJJ to realize a nearly ideal *superconducting diode*, described below [Nano Letters, 2023].

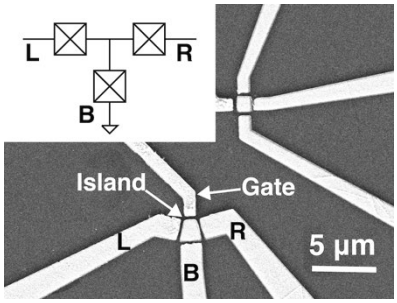

Figure 1. SEM image of two triodes. We measure the I-V curves of the Left-Bottom junction of the lower device, while applying the control bias to the Right junction.

While traditional diodes exploit P-N interfaces in semiconducting materials, a flurry of theoretical interest has focused on developing their superconducting analogues. This interest is

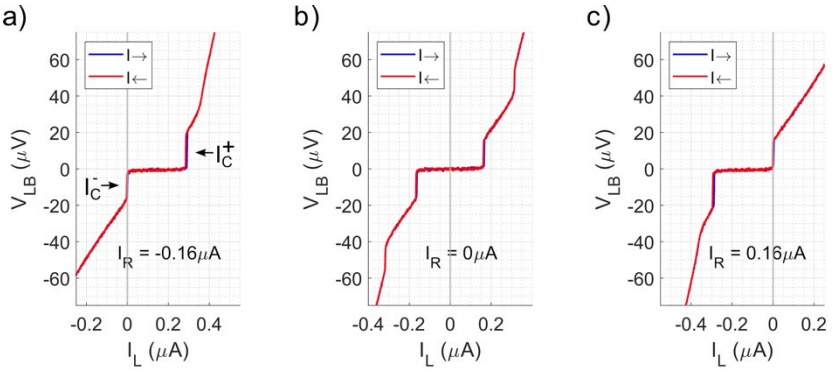

Figure 2. I-V curves of the left-bottom (LB) junction at three values of the control bias applied to the right (R) junction. The curves are completely symmetric at zero control bias (b) and reach a nearly perfect asymmetry for both negative (a) and positive (c) control currents. Importantly, no hysteresis is observed between the two current sweep directions.

driven by the search of novel materials which break both the inversion and time-reversal symmetry, thereby intrinsically enabling the superconducting diode effect (SDE). Unfortunately, the intrinsic SDE is typically small. Somewhat higher SDE can be achieved in properly designed nanostructures, in which an external magnetic field is applied to break the time-reversal symmetry. However, magnetic field is often undesired for integrating the diodes in superconducting circuits. We have succeeded in creating superconducting diodes which can operate at zero magnetic field and achieve efficiency approaching 100%. Our devices are based on multiterminal Josephson junctions made in graphene, which we first reported a few years ago.

We utilize the developments in the multi-terminal Josephson junctions to achieve the SDE at zero external magnetic field. The structure is based on three graphene Josephson junctions tied at the central superconducting island (Fig. 1). Initally, the I-V curves are symmetric (Fig. 2, center). By applying a dissipationless control current in one of the junctions, we break the time-reversal symmetry and tune the I-V curves of the other two junctions, achieving the SDE efficiencies approaching 100% (left and right panels of Fig. 2). Our devices are further tunable by electrostatic gating, which allows us to adjust the scale of the rectified supercurrent from tens of nA to a μA.

2. Chiral Andreev Edge States

At the interface between a superconductor and a quantum Hall (QH) system, the QH edge states are expected to be proximitized, turning into chiral Andreev edge states (**CAES**). These are dispersive states composed of both the electron and the hole components, which are the eigenstates of the system. An electron approaching the superconducting region must be converted to a linear combination of CAES, interfering while propagating along the interface (Figure 3a). Semi-classically, one can think of an electron propagating along the interface with the superconductor, which could be Andreev-reflected as a hole flowing in the same chiral direction. The hole could then be Andreev-reflected as an electron, etc. We have reported the first measurement that directly detected the CAES [Nature Physics, 2020] and actively continued this line of research in this funding cycle [Preprint, under review in PRL].

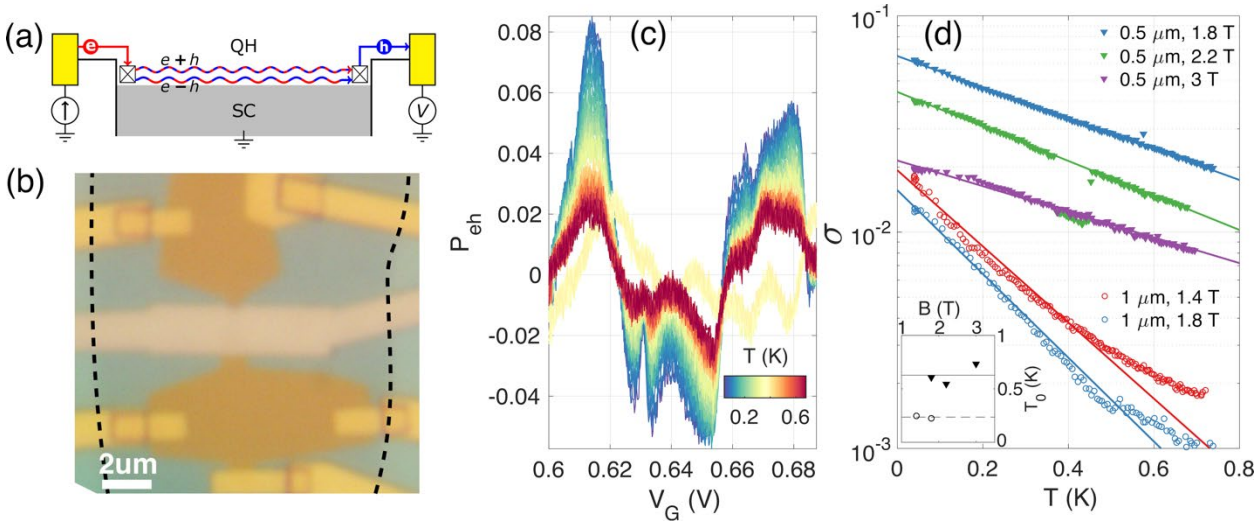

Figure 3. a) Schematic of the measurement schematics and the chiral Andreev edge states, which are shown as skipping trajectories along the QH-SC interface. b) Image of the sample with graphene regions (brown), a superconducting contact (gray, in the center), and normal contacts (gold). The superconductor forms two interfaces with graphene, 0.5 and 1 micron long. c) Typical trace of resistance measured downstream of the superconducting contact and translated to the electron-hole conversion efficiency, P_{eh}. The negative signal corresponds to Andreev reflections, while the positive signal corresponds to normal reflections. d) The dependence of the standard deviation $\sigma(P_{eh})$ on temperature shows a clear exponential trend.

Following our experiment observing the chiral Andreev edge states, several theoretical papers explored their properties. However, the exact mechanism of the Andreev e-h conversion remains open: the role of the disorder, superconducting vortices, and graphene have been discussed. To address these questions, we performed a systematic study of the conversion probability vs temperature, T, magnetic field, B, and interfacial length, L (Figure 3). We found that the dependences of the electron-hole conversion probability on magnetic field and temperature nearly factorize. We suggested a simple phenomenological expression involving exponential decays as a function of B, T and L, and a prefactor determined by the configuration of superconducting vortices. The expression captured the observed dependencies very well and can be interpreted in terms of the CAES losses, which are determined by the magnetic field, and decoherence, which is controlled by the temperature.

3. Quantum Hall based interferometer

In the past few years, there had been a renewed interest to the quantum Hall interferometers, driven primarily by the properties of the quasiparticles in the fractional QH effect. In order to the explore the coherence properties of the CAES, we intend to incorporate them into one or both arms of the QH interferometer. To this end, we have developed a simple method to make QH interferometers in graphene with etched quantum point contacts and self-aligned side gates (Figure 4) [Nano Letters, 2022]. Our interferometers demonstrate very high visibility of interference patterns and are compatible with the superconducting contact technology.

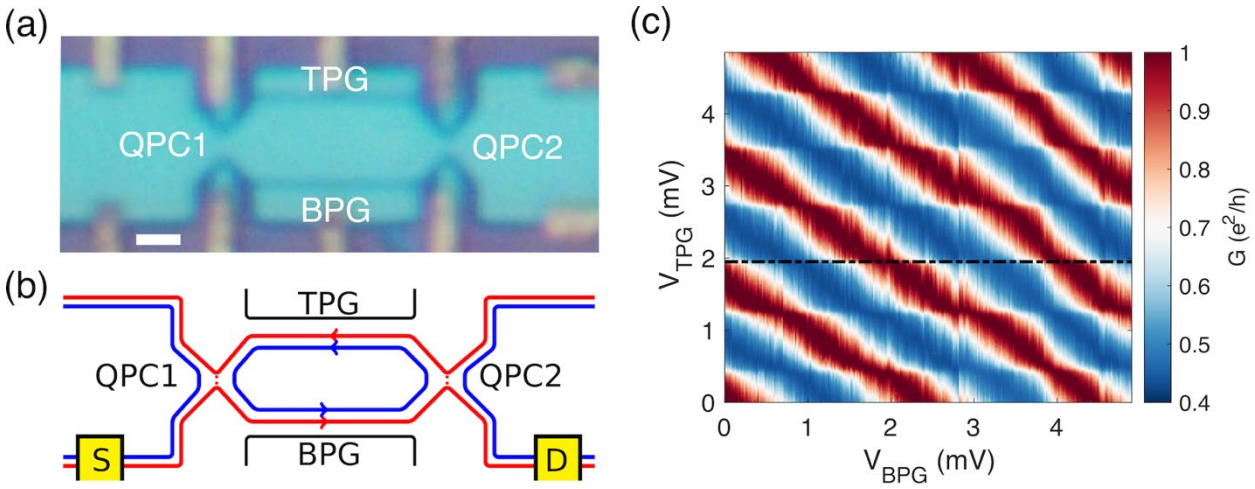

Figure 4. a) Image of the QH interferometer, defined by two quantum point contacts (QPC 1 and 2), and the top and bottom plunger gates (TPG and BPG). The outline is etched in graphene and the self-alighned side gates are formed by graphene regions detached from the main device. b) Schematics of the edge states configuration: bulk filling factor ν=2, QPC pass one spin channel. c) Conductance map measured vs plunger gate voltages, showing a high-contrast interference pattern.

4. 2D superconductivity in $KTaO_3$

In this extension of the core research projects, the PI's group collaborated with the group of Kaveh Ahadi (NCSU) to study the recently discovered anisotropic superconductivity in $KTaO_3$ (111) interfaces. Our paper on this topic has just been published [Science Advances, 2023].

Future Plans

1) Our recent studies of the CAES highlight the need to develop a realistic understanding of the QH-superconductor interfaces. First, the vortices in the type II superconductor result in losses by absorbing the single particle edge states. Second, the electron and hole amplitudes of the CAES acquire opposite phases due to local fluctuations of electric field, resulting in efficient dephasing. We intend to further study the loss and decoherence processes by incorporating superconducting contacts inside QH interferometers of Figure 4. These studies will have implications for the future development of the more complex devices, which will further explore the physics of superconducting correlations in the chiral states.

2) We plan to continue our search for the predicted topological effects in the multiterminal Josephson junctions. We have observed intriguing new synchronization effects in the Josephson triode samples of Figure 1. Beyond the basic physics, the Josephson triodes may show promise as small signal rectifiers and mixers in quantum circuits. For these applications, it is extremely important that our triodes operate at zero magnetic field, so they should not be disruptive to the qubit operation. While the near perfect diode efficiency of our devices is compelling, integration into realistic quantum circuits will require reaching GHz frequencies. Ballistic graphene devices

may likely be suitable for the purpose, and I plan to further explore the properties of our triodes in the microwave regime.

Publications

1. Lingfei Zhao, Zubair Iftikhar, Trevyn F.Q. Larson, Ethan G. Arnault, Kenji Watanabe, Takashi Taniguchi, Francois Amet and Gleb Finkelstein, *Loss and decoherence at the quantum Hall superconductor interface*, under review in PRL. Preprint https://arxiv.org/abs/2210.04842

2. Ethan G. Arnault, Athby H. Al-Tawhid, Salva Salmani-Rezaie, David A. Muller, Divine P. Kumah, Mohammad S. Bahramy, Gleb Finklestein, and Kaveh Ahadi, *Anisotropic Superconductivity at KTaO3(111) interfaces*, Science Advances 9, eadf1414 (2023). https://doi.org/10.1126/sciadv.adf1414

3. J. Chiles, E.G. Arnault, C.-C. Chen, T.F.Q. Larson, L. Zhao, K. Watanabe, T. Taniguchi, F. Amet, G. Finkelstein, *Nonreciprocal Supercurrents in a Field-Free Graphene Josephson Triode*, Nano Lett. 23, 5257–5263 (2023). https://doi.org/10.1021/acs.nanolett.3c01276.

4. Lingfei Zhao, Ethan G. Arnault, Trevyn F. Q. Larson, Zubair Iftikhar, Andrew Seredinski, Tate Fleming, Kenji Watanabe, Takashi Taniguchi, Francois Amet, and Gleb Finkelstein, *Graphene-based quantum Hall interferometer with self-aligned side gates*, Nano Letters 22, 9645–9651 (2022). https://doi.org/10.1021/acs.nanolett.2c03805

5. E. G. Arnault, S. Idris, A. McConnell, L. Zhao, T. Larson, K. Watanabe, T. Taniguchi, G. Finkelstein, and F. Amet, *Dynamical Stabilization of Multiplet Supercurrents in Multi-terminal Josephson Junctions*, Nano Letters 22, 7073 (2022). https://doi.org/10.1021/acs.nanolett.2c01999

6. E.G. Arnault, T.F.Q. Larson, A. Seredinski, L. Zhao, S. Idris, A. McConnell, K. Watanabe, T. Taniguchi, I. Borzenets, F. Amet, G. Finkelstein, *Multiterminal Inverse AC Josephson Effect*, Nano Lett. 21 (2021) 9668–9674. https://doi.org/10.1021/acs.nanolett.1c03474

7. A. Seredinski, E.G. Arnault, V.Z. Costa, L. Zhao, T.F.Q. Larson, K. Watanabe, T. Taniguchi, F. Amet, A.K.M. Newaz, G. Finkelstein, *One-dimensional edge contact to encapsulated MoS2 with a superconductor*, AIP Advances. 11, 045312 (2021). https://doi.org/10.1063/5.0045009

8. G. Zhang, C.-H. Chung, C.-T. Ke, C.-Y. Lin, H. Mebrahtu, A.I. Smirnov, G. Finkelstein, H.U. Baranger, Nonequilibrium quantum critical steady state: Transport through a dissipative resonant level, Phys. Rev. Research. 3, 013136 (2021). https://doi.org/10.1103/PhysRevResearch.3.013136

Correlated Topological Quantum Heterostructures

Ho Nyung Lee (PI), Matt Brahlek, Gyula Eres, Hu Miao, and T. Zac Ward; Oak Ridge National Laboratory, Oak Ridge, TN 37831

Keywords: Thin film heterostructure, transition metal compounds, ARPES, pulsed laser deposition, molecular beam epitaxy

Research Scope

The combination of symmetry, correlation and topology is predicted to realize novel quantum states of matter. Despite a variety of experimental attempts to reshape the wave function topology and to induce entangled quantum states that intertwine charge, spin and orbital degrees of freedom, only a handful of materials have been identified and continue to be debated and explored as candidate correlated topological materials. The overarching goal of this project is to understand how to combine correlated and topological states of matter by exploiting the interplay between symmetry, correlation, and topology in oxide- and chalcogenide-based quantum heterostructures. To address this goal, we focus on three specific aims: (1) Design topological phases in correlated oxides by interrogating the role of lattice geometry and symmetry, (2) Understand how to control topological wavefunctions by manipulating magnetic orders and heterogeneities. (3) Reveal the role of polyhedral lattice symmetry and sublattice disorder in governing the behavior of symmetry-driven correlated states. Underpinning this work is a unique combination of expertise and experimental capabilities based on integrating precision synthesis by pulsed-laser deposition (PLD) and molecular-beam epitaxy (MBE) with advanced characterizations tools, including 3D spin- and angle-resolved photoemission spectroscopy (ARPES). Interfacial magnetism and electronic structure is investigated by neutron scattering and x-ray and optical spectroscopy. The objective of this work is to advance the understanding of the interplay between symmetry, correlation, and topology, generating fundamental knowledge for the development of novel correlated topological quantum materials for next-generation information and energy technologies.

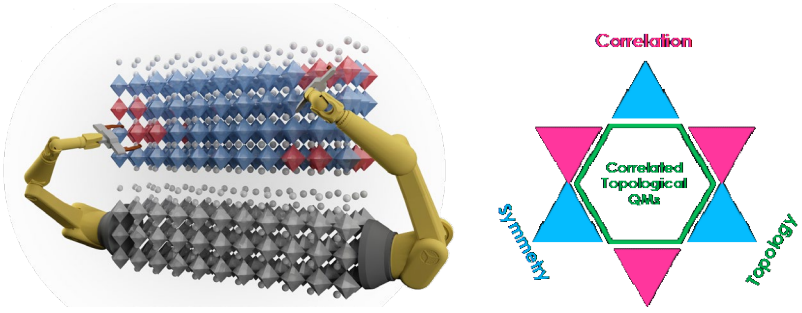

Fig.1. Precision synthesis of quantum heterostructures. The goal of the project is to discover emergent quantum phenomena by exploiting the interplay between symmetry, correlation, and topology in oxide- and chalcogenide-based quantum heterostructures.

Recent Progress

The research in this project is focused on the discovery of new correlated and topological materials and their emergent phenomena arising from well-controlled, functionally cross-coupled interfaces. Special emphasis was on understanding and controlling the interplay between correlation and spin-orbit coupling in 4*d* correlated oxide heterostructures grown by pulsed laser deposition (PLD) by deliberately controlling the degree of epitaxial strain. This project has also developed a novel synthesis route for growing high-quality delafossite thin films on triangular substrates. This rational design of interfacial layer allowed tailoring of magnetism and transport properties. The interface between magnetic materials and topological insulators in thin films grown by molecular-beam epitaxy (MBE) was also studied to understand the formation of exotic phases of matter that enable functionality through manipulation of strong spin polarized transport. This project also emphasizes the use and advancement of ARPES to understand topological materials. The use of wide range of characterization methods, including microstructural imaging, local spectroscopy, neutron scattering, optical and soft x-ray spectroscopy, in combination with theory plays a key role in performing this research. A few research accomplishments achieved over the last two years are highlighted as follows:

Discovery of correlated oxide Dirac semimetal that enters the extreme quantum limit

Quantum materials (QMs) with strong correlation and nontrivial topology are indispensable to next-generation information and computing technologies. Exploitation of topological band structure is an ideal starting point to realize correlated topological QMs. We discovered for the first time that strain-induced symmetry modification in correlated oxide $SrNbO_3$ thin films creates an emerging topological band structure [1]. Dirac electrons in strained $SrNbO_3$ films revealed ultra-high mobility ($\mu_{max} \approx 100{,}000$ cm^2/Vs), exceptionally small effective mass ($m^* \sim 0.04m_e$), and non-zero Berry phase. Strained $SrNbO_3$ films reach the extreme quantum limit, exhibiting a sign of fractional occupation of Landau levels and giant mass enhancement. Our results suggest that symmetry-modified $SrNbO_3$ is a rare example of correlated oxide Dirac semimetals, in which strong correlation of Dirac electrons leads to the realization of a novel correlated topological QM.

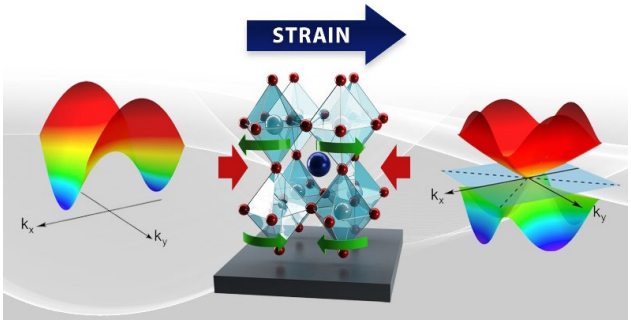

Fig. 2. Bi-axial strain (red arrows) alters crystal symmetry (green arrows) in $SrNbO_3$, which changes band dispersion (left and right), leading to highly mobile electrons.

Emergent Orders in Kagome Superconductors and Magnets

Emergent electronic order in the geometrically frustrated kagome lattice is a new quantum frontier. The characteristic electronic structures of the kagome lattice, including flat-band, Dirac-fermion

and van Hove singularities, are found to be a rich platform to realize correlated and topological quantum states, including unconventional pairing and charge density waves, quantum Hall effects, and chiral Weyl fermions. Using ARPES, we established the quasi-nested Fermi surface and van Hove singularities in AV_3Sb_5 (A=K, Rb, Cs), supporting a Fermi surface driven unconventional charge density wave (CDW) [2–4]. By careful analyze the single-particles spectral function determined by ARPES, we extracted the doping, temperature, and momentum dependent electron-phonon couplings, which is then used to calculate then superconducting transition. A remarkable consistency is observed, supporting a conventional superconductivity in AV_3Sb_5. Furthermore, using resonant and high-pressure x-ray scattering, we established conjoint CDWs in CsV_3Sb_5, which couple with superconductivity at low temperature [3]. We have also combined ARPES, x-ray and theoretical calculations to study of the kagome magnet, where a novel spin-phonon coupling driven CDW is revealed (to appear in *Nature Commun.*). Our studies significantly deepen our understanding of correlated topological quantum states.

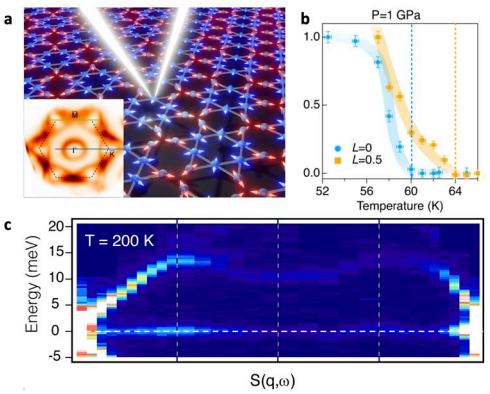

Fig. 2. Nature of emergent orders in kagome materials. (a) Photon-based spectroscopy reveals the nature of kagome superconductor and magnet. Inset shows ARPES data revealing the Fermi surface topology of RbV_3Sb_5. (b) High-pressure x-ray scattering reveals conjoined CDW. (c) Phonon dynamical structure factor uncovers a novel spin-phonon driven CDW in the kagome magnet FeGe.

Kinetic control of surfaces drives bulk magnetic properties

Understanding the effects of the interfacial modification to the functional properties of magnetic topological insulator thin films is crucial for developing novel technological applications from spintronics to quantum computing. Polarized neutron reflectometry revealed that the surface oxidation of the intrinsic magnetic topological insulator $MnBi_2Te_4$ is kinetically limited to the topmost layer, determining the bulk magnetism. In addition, a large electronic and magnetic response is discovered from the intrinsic magnetic topological insulator $MnBi_2Te_4$ by controlling the propagation of surface oxidation [5]. It is shown that the formation of the surface oxide layer is confined to the top 1–2 unit cells but drives large changes in the overall magnetic response. Specifically, a dramatic reversal of the sign of the anomalous Hall effect is observed to be driven by finite thickness magnetism, which indicates that the film splits

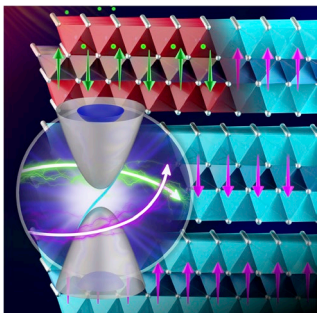

Fig. 3. Schematic showing the oxidation of the $MnBi_2Te_4$ surface which dramatically impacts the bulk-derived magnetic properties. This is represented as the color change across the crystal structure. Inset: changing the magnetic properties affects the band structure and the emergence of the quantized electronic states.

into distinct magnetic layers each with a unique electronic signature. These data reveal a delicate dependence of the overall magnetic and electronic response of $MnBi_2Te_4$ on the stoichiometry of the top layers. This study suggests that perturbations resulting from surface oxidation may play a non-trivial role in the stabilization of the quantum anomalous Hall effect in this system and that understanding targeted modifications to the surface may open new routes for engineering novel topological and magnetic responses in this fascinating material.

Future Plans

This project will focus on understanding how to co-design correlated and topological states of matter by exploiting the interplay between symmetry, correlation, and topology in oxide- and chalcogenide-based quantum heterostructures. Semi-Dirac fermion in transition-metal-oxide heterostructures will be studied using a combined approach with PLD, *in situ* spin- and angle-resolved photoemission spectroscopy, and quantum transport. A particular focus will be on understanding the role of octahedral symmetry in $SrNbO_3$ and $CaNbO_3$ as well as their alloys to understand the nature of band dispersion combined with theoretical predictions. Revealing emergent phenomena that arise from strongly correlated electrons with spin-orbit coupling in correlated delafossites with triangular lattices. The plasmonic excitations in highly conducting delafossite thin films will be also studied by core-loss electron-energy loss spectroscopy uniquely available in ORNL's monochromatically aberration-corrected scanning transmission microscopy. Development of oxide-based membranes via remote epitaxy will be conducted with a particular focus on studying the interfacial phenomena and extreme strain effect as well as creating twisted interfaces to discover exotic electronic and magnetic phenomena. Also, investigation on the interplay between topological surface state and magnetic ordering in magnetic topological insulators will be conducted by combining transport and spectroscopy. Using finite thickness control of $MnBi_2Te_4$ will enable accessing exotic physics, including quantum anomalous Hall where time reversal symmetry is broken and axionic phases when time reversal is preserved. This study will also enable us to understand how magnetic order couples with the topological states to induce macroscopic quantum phenomena. *In situ* spin-ARPES and *ex situ* x-ray and transport studies of correlated and topological states in 2D materials systems, including oxide thin films, chalcogenides thin films, and van der Waals materials, will be continued to understand intertwined orders and emergent topological superconductivity as well as uncovering new mechanisms and materials exhibiting high-temperature superconductivity and quantum anomalous Hall effects.

References

1. J. M. Ok, N. Mohanta, J. Zhang, S. Yoon, S. Okamoto, E. S. Choi, H. Zhou, M. Briggeman, P. Irvin, A. R. Lupini, Y.-Y. Pai, E. Skoropata, C. Sohn, H. Li, H. Miao, B. Lawrie, W. S. Choi, G. Eres, J. Levy, and H. N. Lee, *Correlated oxide Dirac semimetal in the extreme quantum limit*, Sci. Adv. **7**, eabf9631 (2021).
2. H. X. Li *et al*., *Observation of unconventional charge density wave without acoustic phonon anomaly in kagome superconductors AV_3Sb_5 (A= Rb, Cs)*, Phys. Rev. X **11**, 031050 (2021).
3. H. X. Li *et al*., *Discovery of conjoined charge density waves in the Kagome superconductor CsV_3Sb_5*. Nature Commun. **13**, 6348 (2022).

4. C. Mielke III *et al., Time-reversal symmetry-breaking charge order in a correlated kagome superconductor*. Nature **602**, 245 (2022).
5. A. Mazza, J. Lapano, H. Meyer III, C. Nelson, T. Smith, Y.-Y. Pai, K. Noordhoek, B. Lawrie, T. Charlton, R. Moore, T. Ward, M.-H. Du, G. Eres, and M. Brahlek, *Surface-driven evolution of the anomalous Hall effect in magnetic topological insulator $MnBi_2Te_4$ thin films,* Adv. Funct. Mater. **32***,* 2202234 (2022).

Publications

1. J. M. Ok, N. Mohanta, J. Zhang, S. Yoon, S. Okamoto, E. S. Choi, H. Zhou, M. Briggeman, P. Irvin, A. R. Lupini, Y.-Y. Pai, E. Skoropata, C. Sohn, H. Li, H. Miao, R. G. Moore, B. Lawrie, W. S. Choi, G. Eres, J. Levy, and H. N. Lee, *Correlated oxide Dirac semimetal in the extreme quantum limit*, Sci. Adv. **7**, eabf9631 (2021).

2. J. M. Ok, S. Yoon, A. R. Lupini, P. Ganesh, A. Huon, M. F. Chisholm, and H. N. Lee, *Twin-domain formation in epitaxial triangular lattice delafossites*, ACS Appl. Mater. Interfaces, **13**, 22059 (2021).

3. J. Zhang, J. M. Ok, Y.-Y. Pai, J. Lapano, E. Skoropata, A. R. Mazza, H. X. Li, A. Huon, S. Yoon, B. Lawrie, M. Brahlek, T. Z. Ward, G. Eres, H. Miao, and H. N. Lee, *Extremely large magnetoresistance in high-mobility $SrNbO_3/SrTiO_3$ heterostructures*, Phys. Rev. B **104**, L161404 (2021).

4. A.R. Mazza, Q. Lu, G. Hu, H. Li, J. F. Browning, T. R. Charlton, M. Brahlek, T. Z. Ward, H. N. Lee, P. Ganesh, and G. Eres, *Reversible hydrogen-induced phase transformations in $La_{0.7}Sr_{0.3}MnO_3$ thin films characterized by in situ neutron reflectometry*, ACS Appl. Mater. Interfaces **14**, 10898 (2022).

5. A.R. Mazza, J. Lapano, H.M. Meyer, C.T. Nelson, T. Smith, Y.-Y. Pai, K. Noordheok, B.J. Lawrie, T.R. Charlton, R.G. Moore, T.Z. Ward, M.-H. Du, G. Eres, and M. Brahlek, *Surface-driven evolution of the anomalous Hall effect in magnetic topological insulator $MnBi_2Te_4$ thin films*, Adv. Funct. Mater. **33**, 2202234 (2022).

6. A. Huon, J. M. Ok. S. Yoon, A. R. Lupini, and H. N. Lee, *Solid-phase epitaxy of a $CuAlO_2$ template on c-Al_2O_3 for delafossite growth,* APL Mater. **10**, 08111 (2022).

7. H. Li, G. Fabbris, A. H. Said, J. P. Sun, Y.-X. Jiang, J.-X. Yin, Y. Y. Pai, S. Yoon, A. R. Lupini, C. S. Nelson, Q. W. Yin, C. S. Gong, Z. J. Tu, H. C. Lei, J.-G. Cheng, Z. M. Hasan, Z. Wang, B. Yan, R. Thomale, H. N. Lee, and H. Miao, *Discovery of conjoined charge density waves in the kagome superconductor CsV_3Sb_5*, Nature Commun. **13**, 6348 (2022).

8. Q. Zhang, G. Hu, V. Starchenko, G. Wan, E. M. Dufresne, Y. Dong, H. Liu, H. Zhou, H. Jeen, K. Saritas, J. T. Krogel, F. A. Reboredo, H. N. Lee, A. R. Sandy, R. C. Alamazan, P. Ganesh, and D. Fong, *Phase transition dynamics in a complex oxide heterostructure*, Phys. Rev. Lett. **129**, 235701 (2022).

9. Y. Zhong, S. Li, H. Liu, Y. Dong, K. Aido, Y. Arai, H. Li, W. Zhang, Y. Shi, Z. Wang, S. Shin, H. N. Lee, H. Miao, T. Kondo, and K. Okazaki, *Testing electron–phonon coupling for the superconductivity in kagome metal CsV_3Sb_5*, Nature Commun. **14**, 1945 (2023).

10. Q. Zhang, G. Wan, V. Starchenko, G. Hu, E. M. Dufresne, H. Zhou, H. Jeen, I. C. Almazan, Y. Dong, H. Liu, A. R. Sandy, G. E. Sterbinsky, H. N. Lee, P. Ganesh, and D. Fong*, Intermittent defect fluctuations in oxide heterostructures*, Adv. Mater. DOI: 10.1002/adma.202305383 (2023).

Anomalous ac Response Function of Novel Josephson Junctions

Enrico Rossi[1], Wei Pan[2], Javad Shabani[3]
[1]William & Mary, [2]Sandia National Lab, [3]New York University

Keywords: topological superconductivity, quantum wells, thin film heterostructures, semiconductors, molecular beam epitaxy.

Research Scope

Josephson junctions (JJs) are superconducting devices formed by two superconducting leads separated by a non-superconducting material. JJs can be used to create high quality qubits and very sensitive quantum sensors. The discovery of materials with non-trivial topological properties has led to the realization of novel JJs with anomalous, and still not well understood, properties. At the same time, it has been proposed that heterostructures formed by semiconductor quantum wells with strong spin-orbit coupling, and superconductors, can be designed to realize planar JJs that in the presence of an external magnetic field can be driven into a superconducting topological state. JJs in such state are called "topological JJs". Topological JJs support non-Abelian bound states and are therefore a physical realization of topological protected qubits, qubits that are expected to be fault-tolerant due to the topological protection of the quantum states used to encode the information. Two of the main challenges that have emerged in studying novel JJs are: identify reliable experimental signatures to detect unambiguously the topological character of the JJ, and understand how the unusual properties of topological materials affect the JJ's response.

Recent Progress

Under microwave radiation of frequency f the voltage-current (V-I) of a JJ exhibits steps (Shapiro steps) for values of the voltage equal to a multiple of hf/2e, where h is the Planck's constant, and e is the electron's charge. It had been proposed that in a topological JJ the odd Shapiro steps should be absent and therefore that the response of a JJ under ac bias could provide a signature for the topological character of a JJ. However, in 2021 we showed[1] that in high quality planar JJs based on InAs/Al heterostructures, see Fig.1(a), grown via molecular beam epitaxy (MBE), the odd Shapiro steps are missing even when no external magnetic field is present, a situation in which the JJ is unambiguously in a topologically trivial phase. This prompted us to further study how the Shapiro steps of planar JJs based on InAs/Al heterostructures depend on the strength and direction of an in-plane magnetic field.

We find[2] that the evolution of the Shapiro steps with external magnetic field, B, is complex, and strongly dependent on the interplay of the many Andreev Bound states (ABSs) present in a planar junction. Contrary to the naïve expectation, the odd steps are missing for B=0, when the JJ is non topological, and reappear at a crossover value of B that depends on the direction of the field, the frequency of the microwave radiation, and the strength of the spin-orbit coupling in the InAs quantum well, see Fig. 1. We interpret this behavior by theoretically analyzing the Andreev bound

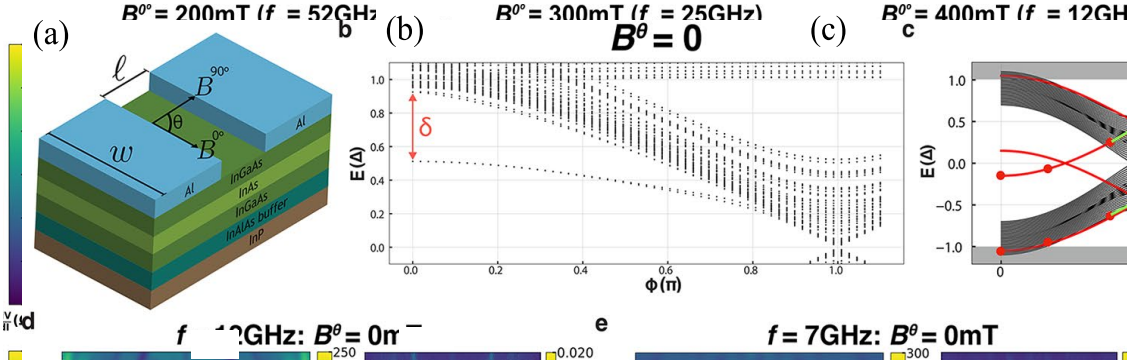

Figure 1. (a) Schematic of a Josephson Junction based on Al/InAs heterostructures grown via MBE. (b) dV/dI as a function of bias dc current and microwave (RF) power in the absence of magnetic field and for RF frequency f=3.5 GHz. The dark blue regions show the Shapiro steps. We see that the first odd step is missing. (c) Same as (b) for the case when an in-plane magnetic field B=400 mT, in the direction perpendicular to the current, is present. We see that the first odd Shapiro step has reappeared.

states spectrum and the transitions, Landau-Zener processes, induced by the nonadiabatic dynamics of the junction. For small B Landau-Zener processes take place only between the highest energy occupied ABSs and the lowest energy un-occupied ABSs that have a very small probability to transition into the continuum of states above the superconducting gap. In this situation the Landau-Zener transitions are responsible for the absence of odd Shapiro steps and the apparent "topological" behavior of the JJ. As B increases the occupied ABSs can transition to many more unoccupied states that in turn can transition into the continuum suppressing the apparent "topological" behavior of the JJ and causing the reappearance of the odd Shapiro steps, Fig.1(c). We also found that the crossover value of B for the reappearance of the odd Shapiro steps strongly depends on the direction of B, as shown in Fig. 2. Our analysis reveals that this is due to several factors: the dependence of the JJ's critical current on the direction of B, the presence of strong spin-orbit coupling in the quantum well, and the dependence on the direction of B of the transition probabilities between different ABSs.

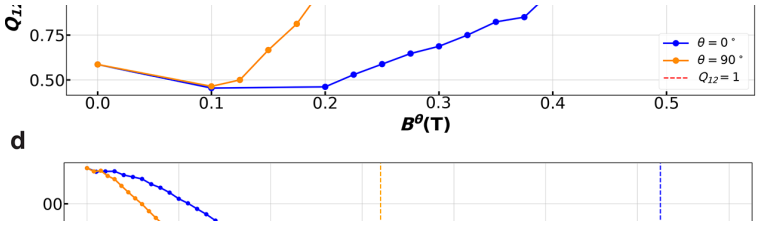

Figure 2. Ratio Q_{12} between the first and second Shapiro step as a function of the strength of the magnetic field for two different directions of B. We identify the value for which Q_{12}=1 as the crossover magnetic field. We see the strong dependence of such value on the direction of B.

Our results highlight the complex phenomenology of missing Shapiro steps in planar JJs and how such phenomenology can be used to infer the structure and properties of the ABSs in such junctions. More in general, they underscore the importance of combining signatures in the microwave response with other additional correlated signatures to make claims about the topological character of a Josephson junction.

In recent years gapless topological materials such as Dirac and Weyl semimetals have attracted a lot of attention due to their unusual electronic band structure and expected electronic properties. In a Dirac semimetal the 3D bulk states' band touch at isolated points (Dirac points), while on the 2D surface topologically protected states are present. By placing a superconductor on the surface of a Dirac semimetal, superconducting correlations can be induced among both the surface and bulk states, resulting in a multiband superconductor.

Superconducting pairing in multiple bands can give rise to novel and interesting phenomena. Leggett modes are exemplary of the unusual effects that can be present in multiband superconductors. A Leggett mode describes the collective periodic oscillation of the relative phase between the phases of the superconducting condensates formed by electrons in different bands. It can be thought of as the mode arising from an inter-band Josephson effect. The experimental observation of Leggett modes is challenging for several reasons: (i) multiband superconductors are rare; (ii) they describe charge fluctuations between bands and therefore are hard to probe directly; (iii) their mass gap is often larger than the superconducting gaps and therefore are strongly overdamped via relaxation processes into the quasiparticle continuum.

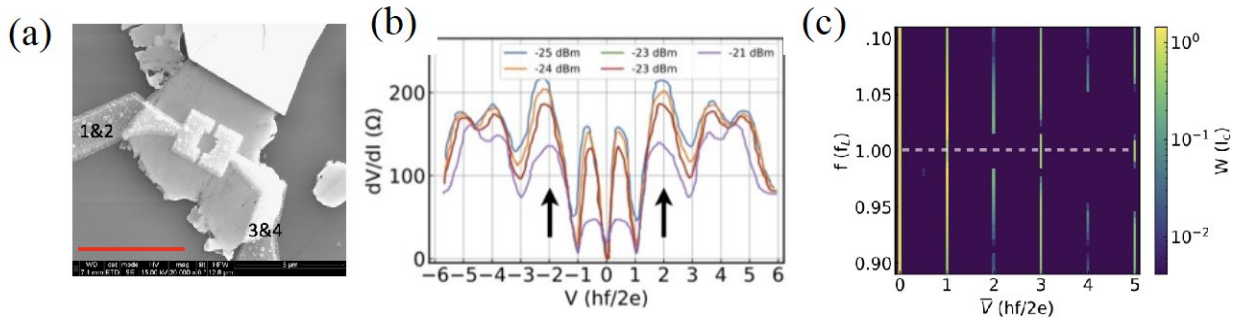

Figure 3. (a) Scanning electron microscope (SEM) image of a SQUID formed by depositing superconducting Al on the Dirac semimetal Cd_3As_2. (b) Measured dV/dI as a function of bias voltage V for a Al/Cd_3As_2 SQUID. The arrows point to the unusual presence of maxima, rather than minima, when V=2(hf/2e), where f is the RF frequency. (d) Theory results for the width, W, of the minima of the dV/dI as function of V and f: W is suppressed for V=2(hf/2e) when f is close to the frequency of the Leggett mode, f_L.

We have shown[3] that the Leggett mode of a two-band superconductor, and its frequency, can be detected unambiguously in ac driven superconducting quantum interference devices (SQUIDs). In particular we find that for JJs and SQUIDs under microwave radiation, when the frequency of the radiation is close to the resonant frequency of the Leggett mode, f_L, the *even* Shapiro steps are strongly suppressed. In addition, we have shown that for f~ f_L the evolution of a SQUID's Shapiro steps structure with the magnetic flux also possesses unique qualitative features. We have then used the results to analyze the measurements of a SQUID formed by two JJs based on heterostructures formed by superconducting Al placed on Cd_3As_2, an exemplar Dirac semimetal. The experimental results show the theoretically predicted unique signatures of Leggett modes and therefore allow us to conclude that a Leggett mode is present in the two-band superconducting state of Dirac semimetal Cd_3As_2.

Future Plans

By patterning the area of the Al layer close to the normal region of an Al/InAs JJ it is in principle possible to increase the region in parameters' space in which planar Al/InAs-based JJs are in a topological state, the robustness of such state, and realize a Josephson diode effect. We plan to study these type of junctions, in particular their response in the dc and ac regime in the presence of an external magnetic field.

Recently we have observed a strong superconducting diode effect in SQUIDs formed by JJs based on Al/Cd_3As_2 heterostructures even in the absence of any external magnetic field. This suggests that in these devices an intrinsic mechanism might be present to break time-reversal symmetry. We will study such effect in these devices with the goal to understand it, and enhance it for possible technological applications, such as the realization of ideal, dissipationless, diodes and isolators. Along the same line of research we plan to finalize and publish our work on the ac Josephson diode effect in asymmetric SQUIDs, including the case in which one of the JJs forming the SQUID is topological.

We will continue refining the MBE growth processes to obtain superconductor-semiconductor heterostructures based on InAs/GaSb double quantum wells (DQWs) designed to realize a quantum spin Hall insulating state. We will characterize via transport measurements, scanning transmission electron microscopy, and atomic force microscopy, structures in which Al is grown epitaxially on InAs/GaSb DQWs. We will develop new growth structures designed to add an etching stop layer of InAs thin quantum well before Al is epi-grown to allow the use of the photoresist developers to etch Al. We also plan to finalize the characterization and theoretical description of JJs formed by superconducting leads attached to InAs/GaSb DQWs.

We will continue the ongoing theory-experiment work to understand the role played by disorder in high quality super-semi heterostructures designed to realize, in the presence of an external magnetic field, topological superconducting states, with a focus to identify critical values of the disorder strength below which such states are robust.

References

1. Matthieu C. Dartiailh, Joseph J. Cuozzo, William Mayer, Joseph Yuan, Kaushini S. Wickramasinghe, Enrico Rossi, Javad Shabani, *Missing Shapiro steps in topologically trivial Josephson Junction on InAs quantum well*, Nature Communications, **12**, 78 (2021).
2. Elfeky, Joseph J. Cuozzo, Neda Lotfizadeh, William F. Schiela, William M. Strickland, Dylan Langone, Enrico Rossi, Javad Shabani, *Reemergence of missing Shapiro steps in the presence of in-plane magnetic field*, ACS Nano, **17**, 4650 (2023).
3. Joseph J. Cuozzo, Wenlong Yu, Paul Davids, Tina M. Nenoff, Daniel B. Soh, Wei Pan, Enrico Rossi, *Leggett Modes in Dirac Semimetals*, arXiv:2205.15995 (2022)

Publications

1. D. P. Cummings, D. L. Perry, L. J. Jauregui, J. Deitz, J. F. Klem, W. Pan, and P. Lu, *Observation of Focused Ion Beam-Induced Artifacts in Transmission Electron Microscopy Samples Leading to the Epitaxial Growth of AlGaSb Quantum Dots on the GaSb Substrate*, Microscopy and Microanalysis, **29**, 138 (2023).

2. B. H. Elfeky, J. J. Cuozzo, N. Lotfizadeh, W. F. Schiela, S. M. Farzaneh, W. M. Strickland, D. Langone, E. Rossi, and J. Shabani, *Evolution of 4π-Periodic Supercurrent in the Presence of an In-Plane Magnetic Field,* ACS Nano, **17**, 4650 (2023).

3. S. M. Farzaneh, M. Hatefipour, W. F. Schiela, N. Lotfizadeh, P. Yu, B. H. Elfeky, W. M. Strickland, A. Matos-Abiague, and J. Shabani, *Magneto-anisotropic weak antilocalization in near-surface quantum wells*, arXiv:2208.06050 (2022).

4. A. Lau, S. Peotta, D. I. Pikulin, E. Rossi, and T. Hyart, *Universal suppression of superfluid weight by disorder independent of quantum geometry and band dispersion*, SciPost Physics, **13,** 086 (2022).

5. D.-X. Qu, J. J. Cuozzo, N. E. Teslich, K. G. Ray, Z. Dai, T. T. Li, G. F. Chapline, J. L. DuBois, and E. Rossi, *Phase-Slip Lines and Anomalous Josephson Effects in a Tungsten Clusters-Topological Insulator Microbridge,* arXiv:2301.00086 (2022).

6. J. J. Cuozzo, W. Pan, J. Shabani, and E. Rossi, *Microwave-Tunable Diode Effect in Asymmetric SQUIDs with Topological Josephson Junctions*, arXiv:2303.16931 (2023).

7. S. A. A. Ghorashi, J. Cano, E. Rossi, and T. L. Hughes, *Higher-Order Nodal Hinge States in Doped Superconducting Topological Insulator,* arXiv:2211.00682, accepted for publication in Physical Review B. (2022).

8. X. Hu, E. Rossi, and Y. Barlas, *Effect of Inversion Asymmetry on Bilayer Graphene's Super- conducting and Exciton Condensates*, arXiv:2304.04825 (2023).

9. E. Chatterjee, W. Pan, and D. Soh, *Ultra-high-precision detection of single microwave photons based on a hybrid system between a Majorana zero mode and a quantum dot*, Physical Review Research, **5**, 013034 (2023).

10. Ke Wang, Han Fu, K. Levin, *Simulating Cosmological Evolution by Quantum Quench of an Atomic BEC,* arXiv:2304.02131 (2023).

Incompatibility between topological superconductivity and supercurrent injected from Nb.

Stephan Kim, Shiming Lei, Leslie Schoop, Robert Cava and N. Phuan Ong, Princeton University

Keywords: Topological superconductivity, transition metal compounds, proximity effect, edge supercurrent

Research Scope: To date, the layered chalcogenide $MoTe_2$ is the only Weyl semimetal that becomes a superconductor (T_c = 0.1 K). In its superconducting state, $MoTe_2$ features an unusual edge supercurrent that was detected [1] by periodic edge oscillations of the critical current I_c as the magnetic field H is varied (this is caused by Little-Parks fluxoid quantization). We describe experiments that utilize this topologically protected edge supercurrent to "eavesdrop" on the supercurrent response in $MoTe_2$ when an *s*-wave supercurrent is injected from Nb contacts. Figure 1 shows the anomalous features observed [2]. First, as $|H|$ approaches zero, the critical current function $I_c(H)$ (boundary of black regions in Fig. 1a) displays a prominent and narrow "central peak" caused by proximitization of the bulk states by the *s*-wave Nb pairing potential. As H is cycled back and forth (green arrows), the central peak position leads the zero-crossing of H (instead of lags). We call this unusual behavior antihysteretic [2]. Concurrently, whenever $|H|$ is reduced towards zero, the oscillations display very large phase noise. However, once H crosses 0, the noise is suppressed (Fig. 1b). These features reflect strong incompatibility between the injected supercurrent and the intrinsic pairing amplitude in the topological superconductor as well as the field-induced switching of the device gap function $\hat{\mathbf{\Psi}}$ between *s*-wave symmetry and the symmetry $\boldsymbol{F_{\alpha\beta}}$ intrinsic to pristine $MoTe_2$.

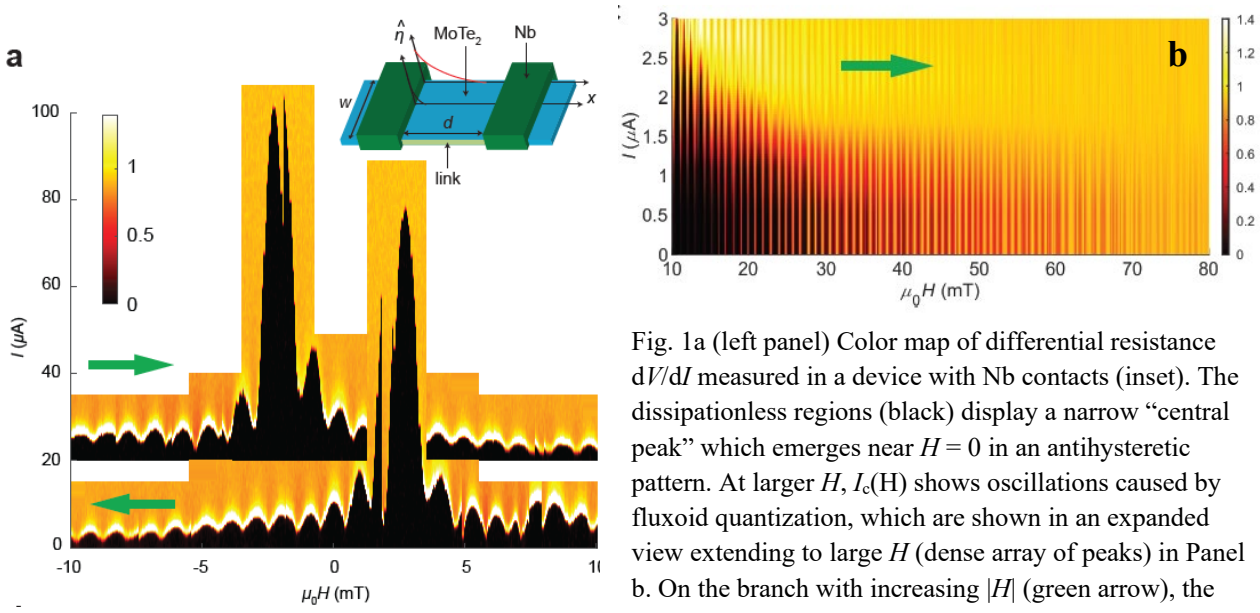

Fig. 1a (left panel) Color map of differential resistance dV/dI measured in a device with Nb contacts (inset). The dissipationless regions (black) display a narrow "central peak" which emerges near H = 0 in an antihysteretic pattern. At larger H, I_c(H) shows oscillations caused by fluxoid quantization, which are shown in an expanded view extending to large H (dense array of peaks) in Panel b. On the branch with increasing $|H|$ (green arrow), the phase noise is suppressed. (Kim *et al*. [2]).

Considerable insight [2] on the incompatibility is provided by correlating the phase-noise asymmetry with the behavior of I_c. Despite long-standing interest in how incompatible pairing potentials co-exist and compete to form Cooper pairs, investigators have lacked a way to probe the competition. Here, the existence of the topological edge supercurrent provides a window that unveils many unsuspected features.

Recent Progress: By exploring these features in 8 devices with layouts designed to systematically test inferences, we succeeded in associating features in the color map with supercurrent flowing either in the bulk (e.g. the central peak) or along the edges (periodic peaks in Fig. 1). Using these bulk- and edge-specific features as guides, we arrive at the following picture. On the inbound branch ($|H|$ decreasing), edge-state pairing is initially incompatible with that in the bulk which leads to large phase noise in the edge oscillations, while the gap function $\hat{\Psi}$ adopts the $\boldsymbol{F_{\alpha\beta}}$ symmetry. The central peak emerges when $|H|$ becomes too weak to suppress *s*-wave pairing in the bulk, causing the gap function $\hat{\Psi}$ to switch to *s*-wave symmetry (Fig. 1a). Close to $H = 0$, $\hat{\Psi}$ switches back to $\boldsymbol{F_{\alpha\beta}}$ symmetry when the vortices transition to a vortex solid. Finally, as H crosses to the positive branch, the vortex solid persists. Now, compatibility between pairing in the bulk and at the edges ensures the absence of phase noise as shown in Fig. 1b.

Future Plans: The features uncovered provide the potential to explore the physics of competing pair condensates in great detail and to understand the relation between paired states in the bulk vs. the edge. We will adopt new device designs to obtain more information from the correlations and to test the inferences derived from them**.**

The research was supported by DOE award DE-SC0017863.

References

1. Wudi Wang, Stephan Kim, Minhao Liu, F. A. Cevallos, R. J. Cava, and N. P. Ong, "Evidence for an edge supercurrent in the Weyl superconductor $MoTe_2$," *Science* **368**, 534-537 (2020).
2. Stephan Kim, Shiming Lei, Leslie M. Schoop, R. J. Cava and N. P. Ong, "Eavesdropping on competing condensates by the edge supercurrent in a Weyl superconductor." *Nature Physics*, *in review*.

Publications supported by DOE award DE-SC0017863

1. Wudi Wang, Stephan Kim, Minhao Liu, F. A. Cevallos, R. J. Cava, and N. P. Ong, "Evidence for an edge supercurrent in the Weyl superconductor $MoTe_2$," *Science* **368**, 534-537 (2020). 10.1126/science.aaw9270
2. Shiming Lei, Jingjing Lin, Yanyu Jia, Mason Gray, Andreas Topp, Gelareh Farahi, Sebastian Klemenz, Tong Gao, Fanny Rodolakis, Jessica L. McChesney, Christian R. Ast, Ali Yazdani, Kenneth S. Burch, Sanfeng Wu, N. Phuan Ong, Leslie M. Schoop, "High mobility in a van der Waals layered antiferromagnetic metal," *Science Advances* **6,** eaay6407 (2020), DOI: 10.1126/sciadv.aay6407.
3. Ruidan Zhong, Tong Gao, N. P. Ong, R. J. Cava, "Weak-field induced nonmagnetic state in a Co-based honeycomb," *Science Advances* **6,** eaay6953 (2020), DOI: 10.1126/sciadv.aay6953
4. Peter Czajka, Tong Gao, Max Hirschberger, Paige Lampen-Kelley, Arnab Banajee, Jiaqiang Yan, David Mandrus, Stephen E. Nagler, N. P. Ong, "Oscillations of the thermal conductivity in the spin liquid state of α-$RuCl_3$," *Nature Physics,* 17(8), 915–919 (2021). doi.org/10.1038/s41567-021-01243-x
5. Zheyi Zhu, Stephan Kim, Shiming Lei, Leslie M. Schoop, R. J. Cava and N. P. Ong, "Phase tuning of multiple Andreev reflections of Dirac fermions and Josephson supercurrent in Al-MoTe2-Al junctions," *Proc. Nat. Acad. Sci.* **119**, e2204468119 (2022). doi.org/10.1073/pnas.2204468119
6. Peter Czajka, Tong Gao, Max Hirschberger, Paula Lampen-Kelley, Arnab Banerjee, Nicholas Quirk, David G. Mandrus, Stephen E. Nagler, and N. P. Ong, The planar thermal Hall conductivity in the Kitaev magnet α-RuCl3, *Nature Materials* **22**, 36-41 (2023), doi.org/10.1038/s41563-022-01397-w
7. Stephan Kim, Shiming Lei, Leslie M. Schoop, R. J. Cava and N. P. Ong, "Eavesdropping on competing condensates by the edge supercurrent in a Weyl superconductor," *in review*.

Interface-Induced Superconductivity in Magnetic Topological Insulator-Iron Chalcogenide Heterostructures

PI: Cui-Zu Chang, Department of Physics, The Pennsylvania State University, University Park, PA 16802

Keywords: Topological insulators, interfacial superconductivity, thin film heterostructures, topological superconductivity, molecular beam epitaxy

Research Scope

The current program is focusing on the molecular beam epitaxy (MBE) growth of $(Bi,Sb)_2Te_3$/FeTe and Cr-doped $(Bi,Sb)_2Te_3$/FeTe (i.e. QAH/FeTe) heterostructures, which we will then use to explore the topological interfacial superconductivity and Majorana physics towards topological quantum computations.

Recent Progress

In the first year of our project (09/01/2022 to 08/30/2023), we have published 3 high-profile papers, including one in *Review of Modern Physics* (#1 in **Publications**), one in *Physical Review Letters*(#2 in **Publications**), and 1 in *Nano Letters* (#3 in **Publications**). Two more papers with *primary* DOE support are currently under review (#4 & #5 in **Publications**). In the following, we will focus on these two papers and discuss our recent research progress:

The search for the chiral topological superconducting (TSC) phase has attracted a great deal of attention in the past decade because of both the elegant physics of the subject and its potential application in topological quantum computation. The chiral TSC phase has been proposed to be present in hybrid structures where a quantum anomalous Hall (QAH) insulator is proximally coupled to a conventional *s*-wave superconductor [1,2]. A primary barrier to the growth of magnetic TI films/heterostructures with the QAH state [3] on *s*-wave superconductors (or vice versa) lies in the difficulty of achieving an atomically sharp interface due to a host of experimental challenges such as chemical reactivity and uncontrolled nucleation. Moreover, the superconductivity is usually suppressed and even disappears once a magnetic TI layer is grown on top, primarily owing to their contrasting spin orders[4].

Over the past year, we used molecular beam epitaxy (MBE) to synthesize $(Bi,Sb)_2Te_3$/FeTe heterostructures with an atomically sharp interface, in which the chemical potential of the ternary TI $(Bi,Sb)_2Te_3$ can be tuned by varying the Bi/Sb ratio. By performing *in-vacuo* angle-resolved photoemission spectroscopy (ARPES) and *ex-situ* electrical transport measurements, we find that the superconducting transition temperature and the upper critical magnetic field are suppressed when the chemical potential approaches the Dirac point. This strongly suggests a direct link between the interfacial superconductivity and the Dirac electrons of the TI layer. We provide a scenario to understand the chemical potential dependence of interfacial superconductivity as the

complex competition between bicollinear antiferromagnetic order in the FeTe layer and the Ruderman-Kittel-Kasuya-Yosida (RKKY) interaction mediated by surface Dirac electrons of the TI layer[5]. This paper is now under review in *Nature Communications*.

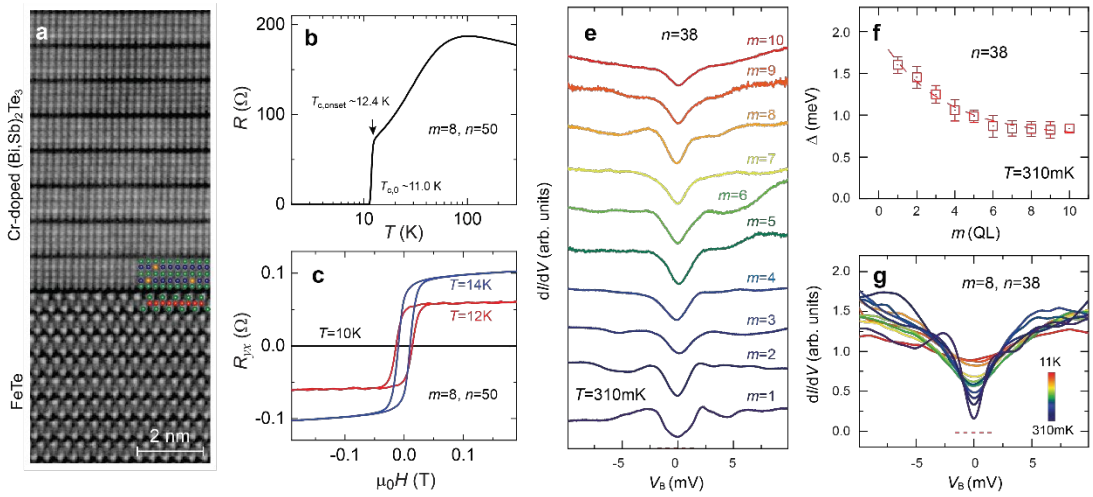

Fig. 1| Coexistence of ferromagnetism and superconductivity in Cr-doped (Bi, Sb)2Te3/FeTe heterostructures**. a**, Cross-sectional STEM image of the (8,50) heterostructures grown on heat-treated $SrTiO_3$ (100) substrate. **b**, Temperature dependence of the sheet longitudinal resistance R of the (8,50) heterostructure. **c**, Magnetic field $\mu_0 H$ dependence of the Hall resistance R_{yx} at T=10K (black), T=12K (red), and T=14K (blue). **d**, m dependence of the dI/dV spectra on the surface of the (m,38) heterostructure (setpoint: V_B=+10mV, I_t=300pA, T =310 mK). **e**, m dependence of the superconducting gap D on the surface of the (m,38) heterostructure. The values of the superconducting gap D are determined by fitting the dI/dV spectra. The error bars are the results of the fitting process and spatial distribution. The dashed line is a guide to the eyes. **f**, Temperature dependence of the dI/dV spectra on the surface of the (8, 38) heterostructure (setpoint: V_B=+10mV, I_t=300pA).

Besides $(Bi,Sb)_2Te_3$/FeTe heterostructures, we also employed MBE to grow a ferromagnetic TI Cr-doped $(Bi, Sb)_2Te_3$ layer with the QAH state on the antiferromagnetic FeTe layer. Our measurements reveal an atomically sharp interface in these Cr-doped $(Bi, Sb)_2Te_3$/FeTe heterostructures (Fig. 1a). By performing electrical transport, reflective magnetic circular dichroism (RMCD), magnetic force microscopy (MFM), scanning tunneling microscopy and spectroscopy (STM/S), and ARPES measurements, we demonstrated the trifecta occurrence of superconductivity, ferromagnetism, and topological band structure(Figs. 1b to 1g). Moreover, we found that the upper critical magnetic field of the interface-induced superconductivity is very high (>40 T) and isotropic at T =1.5 K, which may be responsible for the coexistence of superconductivity and ferromagnetism in these heterostructures. The QAH/FeTe heterostructures with robust interface-induced superconductivity and atomically sharp interfaces provide an ideal platform for the exploration of chiral TSC and Majorana physics and thus constitute an important step toward scalable topological quantum computation. This paper is now under review in *Science*.

Future Plans

We will pursue the following projects:

(1) We will optimize the growth parameters for $(Bi,Sb)_2Te_3$/FeTe and Cr-doped $(Bi,Sb)_2Te_3$/FeTe (i.e. QAH/FeTe) heterostructures and explore the superconducting mechanisms in these two systems.

(2) We will initiate the MBE growth of $MnBi_2Te_4$/FeTe and explore if the interface-induced superconductivity can also emerge in heterostructures formed by two antiferromagnetic materials.

(3) Based on $(Bi,Sb)_2Te_3$/FeTe and Cr-doped $(Bi,Sb)_2Te_3$/FeTe (i.e. QAH/FeTe) heterostructures, we will fabricate the Josephson junction devices and explore the topological interfacial superconductivity and Majorana physics.

References

1. Qi, X. L., Hughes, T. L. & Zhang, S. C. *Chiral Topological Superconductor from the Quantum Hall State*. Phys. Rev. B **82**, 184516 (2010).

2. Wang, J., Lian, B., Qi, X. L. & Zhang, S. C. *Quantized topological magnetoelectric effect of the zero-plateau quantum anomalous Hall state*. Phys. Rev. B **92**, 081107 (2015).

3. Chang, C. Z., Zhang, J. S., Feng, X., Shen, J., Zhang, Z. C., Guo, M. H., Li, K., Ou, Y. B., Wei, P., Wang, L. L., Ji, Z. Q., Feng, Y., Ji, S. H., Chen, X., Jia, J. F., Dai, X., Fang, Z., Zhang, S. C., He, K., Wang, Y. Y., Lu, L., Ma, X. C. & Xue, Q. K. *Experimental Observation of the Quantum Anomalous Hall Effect in a Magnetic Topological Insulator*. Science **340**, 167-170 (2013).

4. Yi, H. M., Hu, L. H., Wang, Y. X., Xiao, R., Cai, J. Q., Hickey, D. R., Dong, C. Y., Zhao, Y. F., Zhou, L. J., Zhang, R. X., Richardella, A. R., Alem, N., Robinson, J. A., Chan, M. H. W., Xu, X. D., Samarth, N., Liu, C. X. & Chang, C. Z. *Crossover from Ising-to Rashba-type superconductivity in epitaxial Bi_2Se_3/monolayer $NbSe_2$ heterostructures*. Nature Mater. **21**, 1366-1372 (2022).

5. Liu, Q., Liu, C. X., Xu, C. K., Qi, X. L. & Zhang, S. C. *Magnetic Impurities on the Surface of a Topological Insulator*. Phys. Rev. Lett. **102**, 156603 (2009).

Publications

1. **Chang, C.-Z**., Liu, C.-X. & MacDonald, A. H. *Colloquium: Quantum anomalous Hall effect*. Rev. Mod. Phys. **95**, 011002 (2023).

2. Zhou, L.-J., Mei, R., Zhao, Y.-F., Zhang, R., Zhuo, D., Yan, Z.-J., Yuan, W., Kayyalha, M., Chan, M. H. W., Liu, C.-X. & **Chang, C.-Z**. *Confinement-Induced Chiral Edge Channel Interaction in Quantum Anomalous Hall Insulators*. Phys. Rev. Lett. **130**, 086201 (2023).

3. Tay, H., Zhao, Y. F., Zhou, L. J., Zhang, R. X., Yan, Z. J., Zhuo, D. Y., Chan, M. H. W. & **Chang, C. Z.** *Environmental Doping-Induced Degradation of the Quantum Anomalous Hall Insulators*. Nano Lett. **23**, 1093-1099 (2023).

4. H. Yi, L.-H. Hu, X. Wu, Y.-F. Zhao, L.-J. Zhou, Z. Yan, R. Zhang, W. Yuan, Z. Wang, D. R. Hickey, A. R. Richardella, J. Singleton, L. E. Winter, M. H. W. Chan, N. Samarth, C.-X. Liu, and **C.-Z. Chang**. *Dirac-Fermion-Assisted Interfacial Superconductivity in Epitaxial Topological Insulator/Iron Chalcogenide Heterostructures*. Nature Commun. (2023, in press)

5. H. Yi, Y.-T. Chan, J. Cai, X. Wu, Z.-J. Yan, Y.-F. Zhao, L.-J. Zhou, R. Zhang, R. Mei, R. Xiao, K. Wang, A. R. Richardella, J. Singleton, L. E. Winter, M. H. W. Chan, N. Samarth, X.Xu, W. Wu, C.-X. Liu, and **C.-Z. Chang**. *Interface-Induced Superconductivity in Magnetic Topological Insulator-Iron Chalcogenide Heterostructures.* Science (2023, under review)

Oral Session 3

Charge-transfer across van der Waals interfaces

D.N Basov (Columbia University)

Keywords: light-matter interfaces, van der Waals materials, graphene, scanning probe microscopy

Research Scope

The ability to control charge carrier density and electrostatic landscapes in 2D materials is a key enabling technology for tailoring material properties and quantum ground states at the nanoscale. For example, the generation of surface plasmon polaritons (SPPs) in graphene hinges on extrinsic sources of free carriers typically achieved by means of electrostatic gating. Alternatively, proximal high work function materials integrated in 2D heterostructures offer a reliable method for injecting free carriers into graphene (and other 2D materials) without external contacts. The PI has systematically investigated charge transfer across a variety of van der Waals interfaces including but not limited to: graphene-$RuCl_3$, graphene-WO_x, graphene-ZrO_x, WSe_2-$RuCl_3$ and several others. The PI utilized multi-messenger optical nano-spectroscopy and nano-imaging to investigate a multitude of effects promoted by charge transfer across vdW interfaces.

Recent Progress

The PI has investigated charge-transfer doping via the work-function mismatch between graphene and proximal transition-metal oxide (TMO) layers. This method has allowed the PI to implement ambipolar charge-transfer in vdW nanostructures. This study was published in *Nature Materials* in 2023 [Publication 1]. Specifically, our team has demonstrated the creation of WO_x/graphene and ZrO_x/graphene interfaces using oxidation-activated charge transfer (OCT). In our approach, charge-neutral graphene is first covered with transition-metal dichalcogenides (TMDs), including WSe_2 and $ZrSe_2$. Subsequent oxidization, using UV-ozone treatment, transforms these TMDs into TMOs: a high-work-function compound WO_x promoting hole doping in a proximal graphene layer, and a low-work-function compound ZrO_x for electron doping to produce p- and n-type charge-transfer plasmons, respectively (Fig. 1). To the best of our knowledge, the n-type charge transfer at the ZrO_x/graphene interface is the first demonstration of electron-doping graphene via a van der Waals (vdW) charge-transfer interface.

Our team has developed an electrostatic model that is suitable to predict and tailor the magnitude of OCT-induced charge transfer at vdW interfaces. This new design principle is broadly applicable to vdW heterostructures. Our detailed analysis of plasmon dispersion using nano-infrared (nano-IR) imaging together with our electrostatic model verified the presence of charge transfer at both WO_x/graphene and ZrO_x/graphene interfaces with opposite signs of charge carriers. Specifically, our team has found that charge-transfer plasmons residing at these interfaces operate at the near-intrinsic limit of graphene and at previously unattainable exceptionally high carrier densities. Notably, these plasmonic devices also operate without the need for gating, allowing for the generation of a high carrier density without the risk of electrical breakdown. Our team has

further demonstrated that the charge transfer process produces laterally abrupt boundaries between electron-doped or hole-doped and charge-neutral regions by circumventing fabrication-related nanoscale disorder or blurred doping profiles due to electric field fringing.

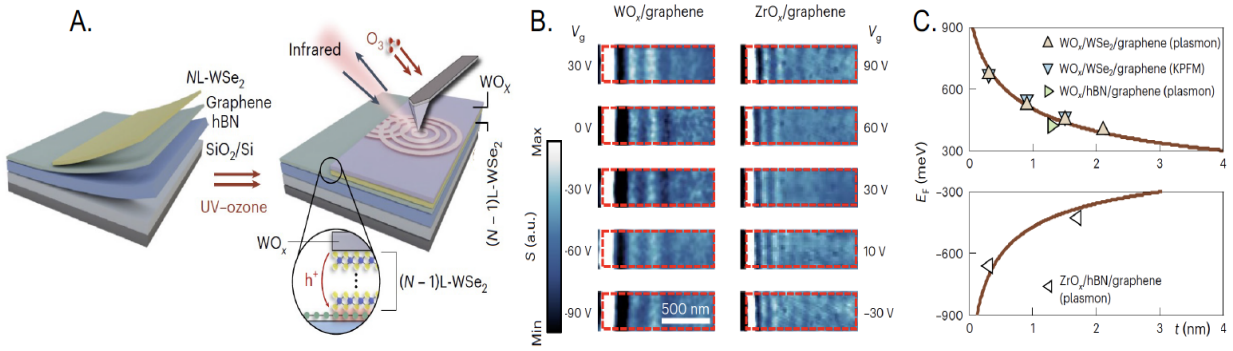

Figure 1. Charge-transfer plasmon polaritons at the graphene/TMO interface. Panel A: Schematic of WO_x/graphene plasmonic devices. A subsequent UV-ozone treatment at room temperature converts the topmost monolayer of WSe_2 into WO_x, resulting in the formation of charge-transfer plasmons at the WO_x/graphene interface. Panel B: Gate-dependent near-field images of graphene plasmons at the WO_x/graphene (left) and ZrO_x/graphene (right) interfaces. The contrasting gate dependence of the two interfaces verifies the ambipolar nature of SPPs. Panel C: Tunable charge transfer at the WO_x/graphene and ZrO_x/graphene interfaces achieved by inserting spacer layers. Adapted from Kim et al. Nature Materials **22**, 838–843 (2023)

WO_x/graphene and ZrO_x/graphene structures allowed us to implement plasmonic cavities with sharp features and designer doping profiles, which are essential for practical nano-scale opto-electronic circuits. For example, our team has demonstrated the elusive plasmonic whispering-gallery modes in suspended graphene/TMO heterostructures. Our team has also developed a comprehensive numerical model that accurately predicts the salient features of the plasmonic whispering-gallery modes observed in nano-IR imaging of our devices. The plasmonic signatures of low-loss whispering-gallery modes open pathways for tailored strong light-matter coupling in vdW materials integrated quantum cavities, plasmonic sensors, and cavity optomechanical systems.

In parallel, the PI has conducted detailed studies of emergent nano-optical and electronic phenomena in graphene/α-$RuCl_3$ heterostructures. Here, heterostructures illuminated with mid-IR light are observed to host three types of charge-transfer plasmon polaritons. The analysis of mid-IR nanoscopy data reveals several remarkable properties of this graphene/α-$RuCl_3$ heterostructure, including charge-transfer-induced carrier density in graphene ($> 4 \times 10^{13}$ cm^{-2}). Finally, the PI observed an acute sensitivity of interfacial charge transfer on interlayer separation, providing another tuning knob for nanoscale electrostatic engineering in 2D. The magnitude and spatial dependence of interfacial charge transfer is solidly supported by DFT calculations. [Publication 6].

Future Plans

Nano-optical experiments carried out by the PI for the first generation of vdW charge transfer structures □-$RuCl_3$/graphene determined that the carrier density at that charge transfer interface can be as high as 4×10^{13} cm^{-2}. The in-depth analysis of the SPPs in □-$RuCl_3$/graphene also suggests the emergence of the weak electronic response attributable to □-$RuCl_3$. Our future plans include the exploration of more complex multi-layer structures with "amplified" charge transfer between monolayer graphene (G), bilayer graphene (BLG) and □-$RuCl_3$ (R) where the electronic response of □-$RuCl_3$ is likely to become enhanced. The PI has already fabricated and performed preliminary characterization for numerous trilayers. The PI will carry out SPP imaging at cryogenic temperature. At low T, the contribution of phonons to SPP losses is suppressed and the number of plasmonic fringes increases. This aspect of cryogenic SPPs enhances the fidelity of findings extracted from plasmonic data. Recent self-consistent Hartree-Fock calculations by Shi and MacDonald revealed the importance of the angular orientation between graphene and □□$RuCl_3$ for the emergent physics at the graphene/□-$RuCl_3$ interface [arXiv:2305.1211]. The PI will systematically investigate this conjecture. Fabricating multiple structures with varied angular alignment of layers is a tedious task. The PI will circumvent this obstacle by employing structures with graphene in the form of an extended beam assembled on the surface of □□$RuCl_3$, developed in the group of C.R. Dean (Columbia) and reported in Ref.[1]. Finally, recent advances in nano-THz spectroscopy and imaging implemented by the PI will allow him to visualize propagating magnon-polariton modes in vdW (anti)ferromagnets integrated in various multi-layer heterostructures.

References

1. Maëlle Kapfer, Bjarke S. Jessen, Megan E. Eisele, Matthew Fu, Dorte R. Danielsen Thomas P. Darlington, Samuel L. Moore, Nathan R. Finney, Ariane Marchese, Valerie Hsieh, Paulina Majchrzak, Zhihao Jiang, Deepnarayan Biswas5, Pavel Dudin, José Avila, Kenji Watanabe, Takashi Taniguchi, Søren Ulstrup, Peter Bøggild, P. J. Schuck, Dmitri N. Basov, James Hone, Cory R. Dean *Programming twist angle and strain profiles in 2D materials* Science 381, 677 (2023)

Publications

1. B. S. Y. Kim, A. J. Sternbach, M. S. Choi, Z. Sun, F. L. Ruta, Y. Shao, A. S. McLeod, L. Xiong, Y. Dong, T. S. Chung, A. Rajendran, S. Liu, A. Nipane, S. H. Chae, A. Zangiabadi, X. Xu, A. J. Millis, P. James Schuck, C. R. Dean, J. C. Hone, and D. N. Basov, *Ambipolar charge-transfer graphene plasmonic cavities*, Nature Materials **22**, 838–843 (2023).

2. D. Halbertal, L. Klebl, V. Hsieh, J. Cook, S. Carr, G. Bian, C. R. Dean, D. M. Kennes, D. N. Basov, *Multilayered Atomic Relaxation in van der Waals Heterostructures.* Phys Rev X. 13, 011026 (2023)

3. A. J. Sternbach, S. L. Moore, A. Rikhter, S. Zhang, R. Jing, Y. Shao, B. S. Y. Kim, S. Xu, S. Liu, J. H. Edgar, A. Rubio, C. Dean, J. Hone, M. M. Fogler, D. N. Basov, *Negative refraction in hyperbolic hetero-bicrystals.* Science 379, 555 (2023).

4. D. Halbertal, S. Turkel, C. J. Ciccarino, J. B. Hauck, N. Finney, V. Hsieh, K. Watanabe, T. Taniguchi, J. Hone, C. Dean, P. Narang, A. N. Pasupathy, D. M. Kennes, D. N. Basov, *Unconventional non-local relaxation dynamics in a twisted trilayer graphene moiré superlattice.* Nat Commun. 13, 7587 (2022), doi:10.1038/s41467-022-35213-5

5. Y. Shao, A. J. Sternbach, B. S. Y. Kim, A. A. Rikhter, X. Xu, U. De Giovannini, R. Jing, S. H. Chae, Z. Sun, S. H. Lee, Y. Zhu, Z. Mao, J. C. Hone, R. Queiroz, A. J. Millis, P. J. Schuck, A. Rubio, M. M. Fogler, D. N. Basov, *Infrared plasmons propagate through a hyperbolic nodal metal*. Sci Adv. 8, eadd6169 (2022).

6. D. J. Rizzo, S. Shabani, B. S. Jessen, J. Zhang, A. S. McLeod, C. Rubio-Verdú, F. L. Ruta, M. Cothrine, J. Yan, D. G. Mandrus, S. E. Nagler, A. Rubio, J. C. Hone, C. R. Dean, A. N. Pasupathy, D. N. Basov, *Nanometer-Scale Lateral p–n Junctions in Graphene/α-RuCl3 Heterostructures.* Nano Lett. 22, 1946–1953 (2022).

7. D. J. Rizzo, S. Shabani, B. S. Jessen, J. Zhang, A. S. McLeod, C. Rubio-Verdú, F. L. Ruta, M. Cothrine, J. Yan, D. G. Mandrus, S. E. Nagler, A. Rubio, J. C. Hone, C. R. Dean, A. N. Pasupathy, D. N. Basov, *Nanometer-Scale Lateral p–n Junctions in Graphene/α-RuCl3 Heterostructures*. Nano Lett. 22, 1946–1953 (2022).

8. X. Yan, J. Li, L. Gu, C. A. Gadre, S. L. Moore, T. Aoki, S. Wang, G. Zhang, Z. Gao, D. N. Basov, R. Wu, X. Pan, *Curvature-Induced One-Dimensional Phonon Polaritons at Edges of Folded Boron Nitride Sheets.* Nano Lett. 22, 9319 (2022)

9. Y. Dong, L. Xiong, I. Y. Phinney, Z. Sun, R. Jing, A. S. McLeod, S. Zhang, S. Liu, F. L. Ruta, H. Gao, Z. Dong, R. Pan, J. H. Edgar, P. Jarillo-Herrero, L. S. Levitov, A. J. Millis, M. M. Fogler, D. A. Bandurin, D. N. Basov, *Fizeau drag in graphene plasmonics.* Nature. 594, 513–516 (2021).

Indirect excitons in heterostructures

Leonid Butov, University of California San Diego

Keywords: 2D exciton and light-matter phenomena, moiré physics, quantum wells, optical spectroscopy, spintronics

Research Scope

A spatially indirect exciton (IX), also known as an interlayer exciton, is a bound pair of an electron and a hole confined in separated layers in a heterostructure.

- Long lifetimes of IXs allow them to cool below the temperature of quantum degeneracy. This gives an opportunity to realize quantum excitonic systems.

- Due to IX built-in dipole moment, IX energy is effectively controlled by voltage. This gives an opportunity to create tailored potential landscapes for IXs by voltage.

- Long IX lifetimes allow them to travel over large distances. This gives an opportunity to study exciton transport by imaging spectroscopy.

Due to these properties, IXs are explored as a platform for basic studies of cold excitons – cold bosons in semiconductor materials. The goal of this project is to explore IXs in GaAs heterostructures, which form the lowest-disorder platform for IXs, and in van der Waals heterostructures composed of atomically thin layers of transition-metal dichalcogenides (TMD), which are characterized by high IX binding energies and can bring the quantum IX phenomena to high temperatures.

In this contribution, we present (1) the realization of ultracold neutral electron-hole plasma and finding of the Fermi edge singularity due to Cooper-pair-like excitons, (2) finding of the long-distance decay-less transport of IXs in TMD heterostructures, and (3) finding of the long-distance decay-less spin transport in TMD heterostructures.

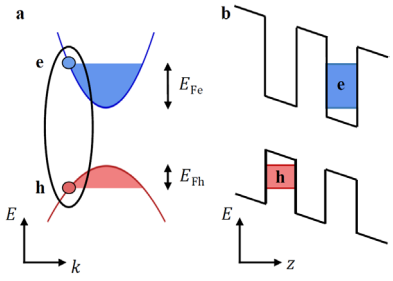

Fig. 1. (a) Diagram showing Cooper-pair-like excitons (oval) with electrons (e) and holes (h) at the Fermi energy in a neutral dense e-h system. (b) Diagram of the coupled quantum well heterostructure. Electrons and holes are confined in separated layers. This allows the realization of cold and dense e-h system. From [1].

Recent Progress

1. Fermi edge singularity in neutral electron-hole system due to Cooper-pair-like excitons [1]. In neutral dense electron-hole (e-h) systems at low temperatures, theory predicted Cooper-pair-like excitons exist at the Fermi energy and form a BCS-like condensate. Optical excitations create e-h systems with the density

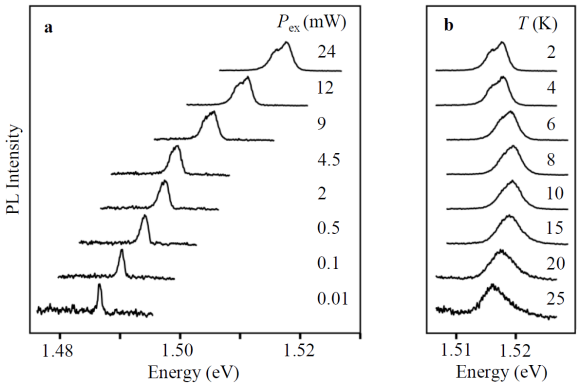

Fig. 2. (a) PL spectra vs the laser excitation power P_{ex} at $T = 2$ K. The e-h densities are $n \approx 11, 9, 7, 5, 4, 3, 1$, and 0.3×10^{10} cm^{-2} (top to bottom). The spectra show the crossover from hydrogen-like IXs at low n to an e-h plasma with the Fermi edge singularity due to Cooper-pair-like IXs at high n. (b) PL spectra vs temperature at $P_{ex} = 24$ mW. The Fermi edge singularity vanishes at high temperatures. From [1].

controlled via the excitation power. However, the intense optical excitations required to achieve high densities cause substantial heating that prevents the realization of simultaneously dense and cold e-h systems in conventional semiconductors. We found that the separation of electron and hole layers in coupled quantum well heterostructure (Fig. 1) enables the realization of a simultaneously dense and cold e-h system. We found a strong enhancement of photoluminescence intensity at the Fermi energy of the neutral dense ultracold e-h system that demonstrates the emergence of an excitonic Fermi edge singularity due to the formation of Cooper-pair-like excitons at the Fermi energy (Fig. 2). We found a crossover from the hydrogen-like excitons to the Cooper-pair-like excitons with increasing density, consistent with the theoretical prediction of a smooth transition (Fig. 2).

2. Long-distance decay-less transport of IXs in a van der Waals heterostructure [2]. Long lifetimes of IXs allow implementing both quantum exciton systems and long-range exciton transport. Van der Waals heterostructures composed of atomically thin layers of TMD offer the opportunity to explore IXs in moiré superlattices. The moiré IXs in TMD heterostructures form the materials platform for exploring the Bose-Hubbard physics and superfluid and insulating phases in periodic potentials. IX transport in TMD heterostructures was intensively studied and diffusive IX transport with $1/e$ decay distances $d_{1/e}$ up to 3 μm was realized in earlier works. We found in a $MoSe_2/WSe_2$ heterostructure the IX long-range transport with $d_{1/e}$ exceeding 100 μm and diverging at the optical excitation resonant to spatially direct excitons (Fig. 3). The IX long-range transport vanishes at high temperatures. With increasing IX density, we found IX localization, then IX long-range transport, and then IX reentrant localization (Fig. 3). The results are in qualitative agreement with the Bose-Hubbard theory of bosons in periodic potentials predicting superfluid and insulating phases.

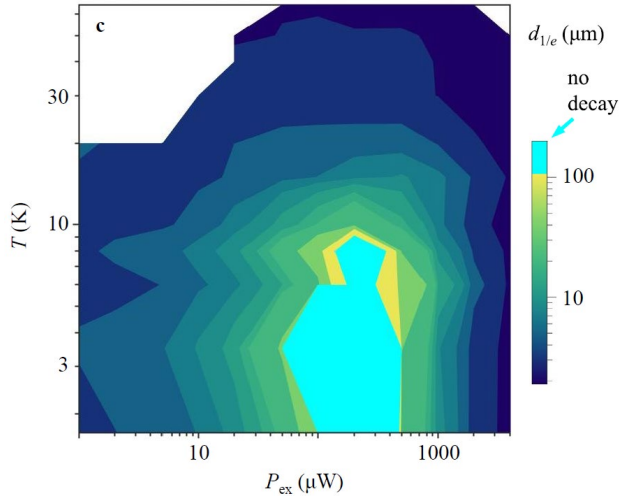

Fig. 3. IX transport decay distance $d_{1/e}$ in $MoSe_2/WSe_2$ heterostructure vs excitation power and temperature. The data with diverging $d_{1/e}$ are presented by cyan color. From [2].

3. Long-distance decay-less spin transport in IXs in a van der Waals heterostructure [3]. We explored IXs in TMD HS as spin transport carries. TMD heterostructures also offer coupling of spin and valley transport. Earlier studies led to the realization of spin transport with 1/*e* decay distances $d^{s}_{1/e}$ up to a few μm in IXs in TMD HS. We found the long-distance spin transport with $d^{s}_{1/e}$ exceeding 100 μm and diverging so spin currents show no decay in the heterostructure (Fig. 4). We found that the suppression of spin relaxation is caused by the suppression of IX scattering. This mechanism enables the long-distance decay-less spin transport. With increasing IX density, we found spin localization, then long-distance spin transport, and then reentrant spin localization. This agrees with the Bose-Hubbard theory.

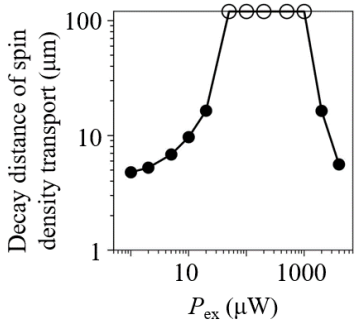

Fig. 4. The 1/*e* decay distance $d^{s}_{1/e}$ of spin density transport in IXs vs. excitation power. The data with diverging $d^{s}_{1/e}$ are presented by circles on the edge. From [3].

Future Plans

GaAs heterostructures form the lowest-disorder platform for studying IXs. We plan to study the ultracold neutral dense e-h system realized in coupled quantum well heterostructures (Fig. 1) and explore the Cooper-pair-like excitons and BCS-like exciton condensation at high densities. In addition to photoluminescence measurements, we also plan to explore this system in absorption measurements, which allow accessing new collective states.

IXs in van der Waals heterostructures based on single-atomic-layers of TMD are characterized by high binding energies, significantly higher than in GaAs heterostructures. Due to this property, theoretical predictions indicate that TMD heterostructures can bring the IX quantum phenomena studied in GaAs heterostructures at low temperatures, such as condensation and superfluidity, to high temperatures. Furthermore, IXs in moiré superlattices provide the experimental realization of the 2D Bose-Hubbard model for bosons with repulsive dipolar interaction. We plan to explore quantum phenomena in cold exciton gases in TMD heterostructures.

References

1. D.J. Choksy, E.A. Szwed, L.V. Butov, K.W. Baldwin, L.N. Pfeiffer, *Fermi edge singularity in neutral electron–hole system*, Nature Physics, DOI: https://doi.org/10.1038/s41567-023-02096-2 (2023).

2. L.H. Fowler-Gerace, Zhiwen Zhou, E.A. Szwed, D.J. Choksy, L.V. Butov, *Transport and localization of indirect excitons in a van der Waals heterostructure*, arXiv:2307.00702 (2023).

3. Zhiwen Zhou, E.A. Szwed, D.J. Choksy, L.H. Fowler-Gerace, L.V. Butov, Long-distance decay-less spin transport in indirect excitons in a van der Waals heterostructure, prepare for publication

Publications

1. D.J. Choksy, E.A. Szwed, L.V. Butov, K.W. Baldwin, L.N. Pfeiffer, *Fermi edge singularity in neutral electron–hole system*, Nature Physics, DOI: https://doi.org/10.1038/s41567-023-02096-2 (2023).

2. L.H. Fowler-Gerace, Zhiwen Zhou, E.A. Szwed, D.J. Choksy, L.V. Butov, *Transport and localization of indirect excitons in a van der Waals heterostructure*, arXiv:2307.00702 (2023).

3. L.H. Fowler-Gerace, D.J. Choksy, L.V. Butov, *Voltage-controlled long-range propagation of indirect excitons in a van der Waals heterostructure*, Phys. Rev. B **104**, 165302 (2021).

4. D.J. Choksy, Chao Xu, M.M. Fogler, L.V. Butov, J. Norman, A.C. Gossard, *Attractive and repulsive dipolar interaction in bilayers of indirect excitons*, Phys. Rev. B **103**, 045126 (2021).

5. J.R. Leonard, Lunhui Hu, A.A. High, A.T. Hammack, Congjun Wu, L.V. Butov, K.L. Campman, A.C. Gossard, *Moiré pattern of interference dislocations in condensate of indirect excitons*, Nat. Commun. **12**, 1175 (2021).

Van der Waals Heterostructures: Novel Materials and Emerging Phenomena

Feng Wang, Michael Crommie, Alessandra Lanzara, Steven Louie, Zi Q. Qiu, Mike Zaletel, Alex Zettl

Materials Science Division, LBNL

Keywords: 2D and layered crystals, moiré physics, 2D exciton and light-matter phenomena, nanofabrication and 2D assembly

Research Scope

This program aims to exploit extraordinary new scientific opportunities enabled by designing van der Waals (vdW) heterostructures that allow creation of novel functional materials with unprecedented flexibility and control. The key innovation here is that van der Waal bonded materials with different dimensionality and wide-ranging properties can be integrated together to form a new class of materials – vdW-bonded heterostructures (vdW heterostructures) - in which each constituent can be engineered separately. In this program, we will design and create novel vdW heterostructures composed of rich 0D, 1D, and 2D vdW units and their 3D assemblies. With such dimensionally diverse vdW heterostructure materials we will elucidate the moire superlattice effects and discover novel quantum phases; we will understand non-equilibrium quantum transport of novel energy, charge, spin, and valley excitations; and we will reveal and control quantum phenomena in heterostructures of different dimensionality.

Recent Progress:

We have made important progress in exploring a variety of novel quantum phenomena that can arise in van der Waals heterostructures. Here we highlight two studies. (1) Observation of energy wave of Dirac fluid in monolayer graphene. (2) Discovery of intralayer charge-transfer moire excitons in transition metal dichalcogenide (TMDC) superlattices.

Observation of energy wave of Dirac fluid in monolayer graphene:

Ultraclean graphene provides an attractive platform to explore Dirac fluid physics, where relativistic electrons and holes form a strongly interacting plasma. The electron-electron scattering can dominate over electron-impurity and electron-phonon scatterings in graphene over a substantial temperature range, and the many-body system can be well described by a relativistic hydrodynamic theory[1]. Such hydrodynamic Dirac fluid is predicted to host intriguing collection excitations that are governed by the strong electron-electron scattering and do not depend on the microscopic details of interactions. The most striking example is the energy wave, where heat propagates ballistic as a wave rather than through diffusion. This energy wave, also known as the electronic second sound, is analogous to the cosmic sound in high energy physics, which gives rise to the large-scale fluctuations observed in the cosmic microwave background radiation, a relic of the "big bang" creating the universe. Such cosmic sound is predicted to propagate at a universal speed of $c/\sqrt{D}$, where D is the dimensionality. For Dirac electrons in graphene, the energy sound speed should have a value of $V_F/\sqrt{2}$.

In a collaborative study between Wang and Zettl, we observed for the first time the energy wave in ultraclean graphene[2]. Building upon the on-chip terahertz spectroscopy developed previously by our program[3], we performed spatial-temporal terahertz imaging to directly probe the propagation of energy wave in graphene. Figure 1a shows a cross-section view of the graphene device. Fig. 1b shows a top view of the whole device and an illustration of spatial-temporal imaging technique. A 532 nm femtosecond laser is focused to a narrow line with lateral width around 1 μm to create an ultrafast local thermal excitation of the electron system in graphene. In the hydrodynamic regime, this transient heat pulse can propagate as energy waves along the graphene channel (white arrow). When the energy wave reaches the waveguide nanogap, it can generate a transient electrical signal (i.e. a THz pulse) in the waveguide. Here the metallic nanogap in the waveguide acts as a THz nanoantenna that converts the local charge oscillation associated with the energy wave in weakly doped graphene to a strong THz electrical signal. This terahertz pulse will propagate along the waveguide and be detected by the GaAs photoconductive detector. By scanning the position of the line excitation and triggering the GaAs detector using a time-delayed pulse, we can measure the THz electrical signal $E(t, x)$ as a function of the pump position (x) and the time delay (t). This spatial-temporal mapping directly probes the propagation behavior of the energy wave.

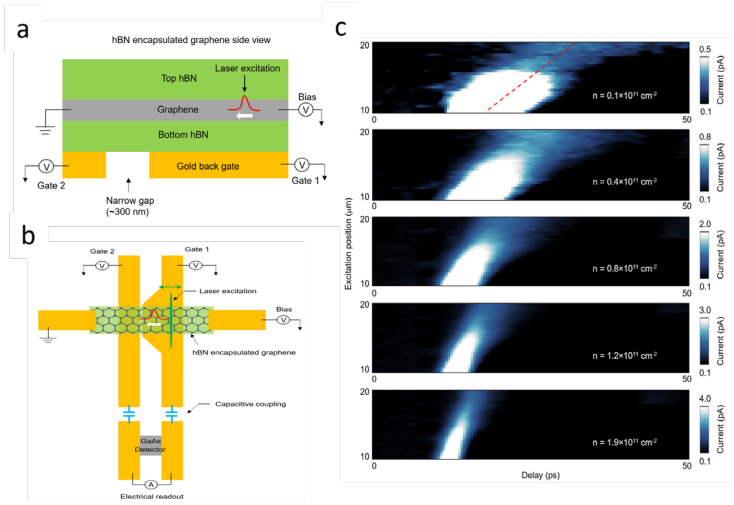

Fig. 1: (a) The side view and (b) top view of an on-chip terahertz spectroscopy device for measuring the hydrodynamic energy wave in graphene. The local pump beam heats the Dirac fluid and launches the energy wave in graphene. The induced electron temperature increase in the graphene below the metal waveguide is probed by terahertz pulses generated by the probe beam. (c) Spatial-temporal imaging data reveal the demon propagation at various carrier densities for (**a**) n = 0.1×10^{11} cm^{-2}. (**b**) n = 0.4×10^{11} cm^{-2}. (**c**) n = 0.8×10^{11} cm^{-2}. (**d**) n = 1.2×10^{11} cm^{-2}. (**e**) n = 1.9×10^{11} cm^{-2}. Red dash line in panel a marks $V_F/\sqrt{2}$ ($V_F = 10^6$ m/s).

Figure 1c shows the spatial-temporal evolution of the measured THz signal at different electron densities. The graphene temperature is at 300 K in these measurements. A propagating energy wave is clearly observed in all carrier densities. At extremely low carrier density (n ~ 0.1×10^{11} cm^{-2}), the energy mode has a velocity close to $V_F/\sqrt{2}$ (red dash line in Figure 6a), where $V_F = 1 \times 10^6\ m/s$[7]. This propagation speed is a defining signature of the energy wave in charge neutral Dirac liquid. Our first observation of energy waves of Dirac fluid opens new opportunities to explore collective hydrodynamic excitations in low dimensional materials.

Elucidating the nature of moire excitons in WS_2/WSe_2 heterostructures:

Excitonic physics in transition metal dichalcogenide (TMD) moiré superlattices have garnered great interest due to recent identification of multiple new resonances in the photoluminescence and absorption spectra. For example, in the WS_2/WSe_2 heterostructure, the WSe_2 A exciton peak splits into multiple emergent peaks when the twist-angle between the layers is reduced to less than ~2° (Fig. 2a).[4] The microscopic nature of the moiré excitons, however, has been a mystery because, so far, optical probes do not have the spatial resolution required to resolve the electron and hole positions of individual excitons states in the superlattice unit cell.

In a collaborative study between Louie and Wang, we elucidate the nature of the moire exciton states of TMDC moire heterostructures[5]. Louie's group developed a novel computational scheme to solve the large-scale Bethe-Salpeter equation of the entire moiré superlattice, which enables us to study for the first time the microscopic electron-hole distributions in different moiré exciton states. Combined with micro-reflection spectroscopy by Wang group, we establish the nature of moiré exciton resonances in rotationally aligned WS_2/WSe_2 heterostructures. Our calculation reveals that different moiré excitons are modulated differently by the moiré superlattice and exhibit distinct characters. Notably, the lowest energy moiré resonance (peak I) is described by a Wannier-type exciton with a tightly bound electron and hole pair (Fig. 2b), while the highest energy moiré resonance (peak III) is characterized by an intralayer charge-transfer exciton with the electron and hole densities spatially separated in the moiré superlattice (Fig. 2c). To our knowledge, this is the first identification of an intralayer charge-transfer exciton in 2D materials. The different characters of the different moiré exciton resonances are confirmed experimentally through their dependences on the carrier doping and magnetic field in the moiré heterostructure.

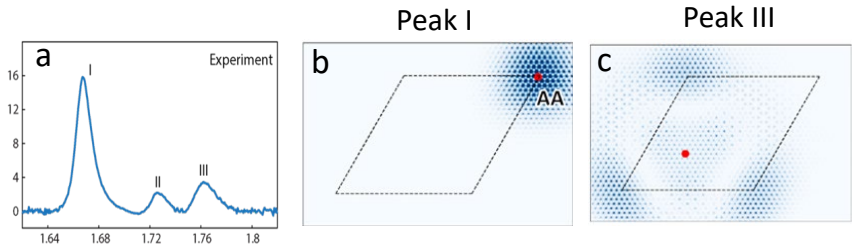

Fig. 2 : (a) Multiple moire exciton peaks have been observed previously in the WS_2/WSe_2 moire heterostructure (ref. 4). We show that the different moire exciton have completely different microscopic structures. (b) Property of moire exciton resonance I. The red dot shows the hole position with the highest probability. The blue shade shows the corresponding electron distribution when the hole is at the red dot position. Peak I shows tightly a bound electron-hole pair, as in typical Wannier excitons. (b) Property of the moire exciton resonance III. The electrons are mostly localized at moire sites away from the hole position, corresponding to a new type in-plane charge transfer exciton unique to the moire heterostructure.

Our study shows that novel exciton states with highly unusual electron-hole correlations, including intralayer charge-transfer excitons, can be present in TMD moiré superlattices. They can give rise to intriguing electron-exciton interactions and can lead to new ways for electrical control of moiré excitons.

Future Plans

We propose to push the frontiers of vdW heterostructure research with unique and collaborative efforts of our team members. Specifically, we will design and create a new class of artificial quantum materials that are enabled by integrating 0D, 1D, and 2D vdW materials with widely varying properties into vdW heterostructures. Using these artificial quantum materials, we will advance vdW heterostructure research in three closely connected directions.

(1) We aim to achieve systematic understanding of the atomic reconstruction, interlayer interaction, and electronic structure of moiré systems at a microscopic level by combining state-of-the-art *ab initio* calculations**,** analytical theory of strong correlation, atomically precise structural characterization**,** and electrical/optical/x-ray spectroscopy characterizations.

(2) Beyond new quantum phases in the ground state, we will characterize and control non-equilibrium quantum transport of novel charge, spin, valley, and energy excitations in 2D vdW heterostructures. For example, we will further explore the propagation as well as focusing of the energy wave of the Dirac liquid and their response to magnetic fields, and we will investigate ultrafast dynamics of the different type of moire exciton states.

(3) 0D, 1D, and hybrid-dimension vdW heterostructures can give rise to completely new quantum phenomena thanks to the quantum confinement and enhanced correlation. We will investigate novel quantum and topological properties of 0D vdW molecules and 1D vdW chains that are stabilized in carbon and boron nitride nanotubes.

References

1. Lucas, A.; Fong, K. C., Hydrodynamics of electrons in graphene. *Journal of Physics: Condensed Matter* **2018,** *30* (5), 053001.

2. Zhao, W. Y.; Wang, S. X.; Chen, S.; Zhang, Z. C.; Watanabe, K.; Taniguchi, T.; Zettl, A.; Wang, F., Observation of hydrodynamic plasmons and energy waves in graphene. *Nature* **2023,** *614* (7949), 688.

3. Gallagher, P.; Yang, C. S.; Lyu, T.; Tian, F.; Kou, R.; Zhang, H.; Watanabe, K.; Taniguchi, T.; Wang, F., Quantum-critical conductivity of the Dirac fluid in graphene. *Science (New York, N.Y.)* **2019,** *364* (6436), 158-162.

4. Jin, C.; Regan, E. C.; Yan, A.; Iqbal Bakti Utama, M.; Wang, D.; Zhao, S.; Qin, Y.; Yang, S.; Zheng, Z.; Shi, S.; Watanabe, K.; Taniguchi, T.; Tongay, S.; Zettl, A.; Wang, F., Observation of moiré excitons in WSe2/WS2 heterostructure superlattices. *Nature* **2019,** *567* (7746), 76-80.

5. Naik, M. H.; Regan, E. C.; Zhang, Z. C.; Chan, Y. H.; Li, Z. L.; Wang, D. Q.; Yoon, Y.; Ong, C. S.; Zhao, W. Y.; Zhao, S. H.; Utama, M. I. B.; Gao, B. N.; Wei, X.; Sayyad, M.; Yumigeta, K.; Watanabe, K.; Taniguchi, T.; Tongay, S.; da Jornada, F. H.; Wang, F.; Louie, S. G., Intralayer charge-transfer moire excitons in van der Waals superlattices. *Nature* **2022,** *609* (7925), 52.

Publications

1. Chatterjee, S.; Wang, T. G.; Berg, E.; Zaletel, M. P., Inter-valley coherent order and isospin fluctuation mediated superconductivity in rhombohedral trilayer graphene. *Nature Communications* **2022,** *13* (1).
2. Hong, J. P.; Soejima, T.; Zaletel, M. P., Detecting Symmetry Breaking in Magic Angle Graphene Using Scanning Tunneling Microscopy. *Physical Review Letters* **2022,** *129* (14).
3. Naik, M. H.; Regan, E. C.; Zhang, Z. C.; Chan, Y. H.; Li, Z. L.; Wang, D. Q.; Yoon, Y.; Ong, C. S.; Zhao, W. Y.; Zhao, S. H.; Utama, M. I. B.; Gao, B. N.; Wei, X.; Sayyad, M.; Yumigeta, K.; Watanabe, K.; Taniguchi, T.; Tongay, S.; da Jornada, F. H.; Wang, F.; Louie, S. G., Intralayer charge-transfer moire excitons in van der Waals superlattices. *Nature* **2022,** *609* (7925), 52-+.
4. Stonemeyer, S.; Dogan, M.; Cain, J. D.; Azizi, A.; Popple, D. C.; Culp, A.; Song, C. Y.; Ercius, P.; Cohen, M. L.; Zettl, A., Targeting One- and Two-Dimensional Ta-Te Structures via Nanotube Encapsulation. *Nano Letters* **2022,** *22* (6), 2285-2292.
5. Su, C.; Zhang, F.; Kahn, S.; Shevitski, B.; Jiang, J. W.; Dai, C. H.; Ungar, A.; Park, J. H.; Watanabe, K.; Taniguchi, T.; Kong, J.; Tang, Z. K.; Zhang, W. Q.; Wang, F.; Crommie, M.; Louie, S. G.; Aloni, S.; Zettl, A., Tuning colour centres at a twisted hexagonal boron nitride interface. *Nature Materials* **2022,** *21* (8), 896-+.
6. Yang, M.; Li, Q.; Wang, T.; Hong, B.; Klewe, C.; Li, Z.; Huang, X.; Shafer, P.; Zhang, F.; Hwang, C.; Yan, W. S.; Ramesh, R.; Zhao, W. S.; Wu, Y. Z.; Zhang, X. X.; Qiu, Z. Q., Current switching of the antiferromagnetic Neel vector in Pd/CoO/MgO(001). *Physical Review B* **2022,** *106* (21).
7. Zhang, Z. C.; Regan, E. C.; Wang, D. Q.; Zhao, W. Y.; Wang, S. X.; Sayyad, M.; Yumigeta, K.; Watanabe, K.; Taniguchi, T.; Tongay, S.; Crommie, M.; Zettl, A.; Zaletel, M. P.; Wang, F., Correlated interlayer exciton insulator in heterostructures of monolayer WSe2 and moire WS2/WSe2. *Nature Physics* **2022,** *18* (10), 1214-+.
8. Zhao, W. Y.; Wang, S. X.; Chen, S.; Zhang, Z. C.; Watanabe, K.; Taniguchi, T.; Zettl, A.; Wang, F., Observation of hydrodynamic plasmons and energy waves in graphene. *Nature* **2023,** *614* (7949), 688-+.
9. Popple, D.; Dogan, M.; Hoang, T. V.; Stonemeyer, S.; Ercius, P.; Bustillo, K. C.; Cohen, M.; Zettl, A., Charge-induced phase transition in encapsulated HfTe2 nanoribbons. *Physical Review Materials* **2023,** *7* (1).
10. Ai, P.; Moreschini, L.; Mori, R.; Latzke, D. W.; Denlinger, J. D.; Zettl, A.; Ojeda-Aristizabal, C.; Lanzara, A., Linearly dispersive bands at the onset of correlations in KxC60 films. *Physical Review Research* **2023,** *5* (2).

Project Title: Quantum Materials

Principal Investigators: James Analytis, Robert Birgeneau, Alessandra Lanzara, Dunghai Lee, Joel Moore, Joseph Orenstein, and R. Ramesh

Affiliations: Lawrence Berkeley National Lab and University of California, Berkeley

Keywords: spintronics/magnonics, 2D exciton and light-matter phenomena, 2D and layered crystals, antiferromagnets, scanning probe microscopy.

Program Scope: Quantum materials are a fertile ground for discovery of new phases and phenomena with potential to advance energy, transportation, medical and information technologies. In these materials, quantum effects are intensified by the combination of frustration, strong interaction and low-dimensionality. Competing spin, orbital, and lattice interactions yield a multiplicity of nearly degenerate ground states and complex phase diagrams that can be challenging to characterize. The challenges and opportunities presented by this class of materials motivates the overarching goal of our Quantum Materials FWP: to understand, manipulate, and control interacting forms of order in condensed matter systems that arise through interactions shaped by quantum physics. The current research Quantum Materials FWP is organized into two themes.

- Theme 1: *Non-locality and coherence in magnetic quantum materials.* The goal of this part of the program is to extend our understanding of spin dynamics in condensed matter to new regimes and classes of materials.
- Theme II: *Superconductivity and intertwined phases in strongly correlated quantum materials*. The goal of this theme is to achieve a deeper understanding how different forms of order, such as nematic, spin and charge density phases, compete, coexist, or collaborate with superconductivity.

Both themes are pursued by combining bulk crystal growth and thin-film heterostructure synthesis with advanced characterization that includes: spin- and time-resolved ARPES; a suite of optical probes spanning terahertz to visible wavelengths; X-ray and neutron scattering; transport, thermodynamic, and scanning microscopy probes; and theoretical modelling.

Recent Progress

In this abstract for our presentation at the ECMP Meeting we feature progress and future plans in Theme I. Harnessing electron spin is one of the central goals of condensed matter physics. A particularly exciting direction is the coupling of spin to charge and lattice degrees of freedom as a route to transduction in quantum systems. To this end, it is essential to understand and control the generation, propagation, and detection of spin information. Recent progress in magnetically ordered systems has shown promise in using propagating spin waves – collective excitations of the electron spins – to transport information over large distances (*1*). Increasingly, attention has focused on quasi-two-dimensional (2D) systems in which planar ferromagnetic order couples either ferro- or anti-ferromagnetically from layer to layer. Of particular interest are systems in

which magnetocrystalline anisotropy favors alignment of spin parallel to the layers (*2*). Compared with easy-axis systems, such easy-plane magnets exhibit highly tunable spin dynamics and potentially a form of dissipationless spin transport known as spin superfluidity (*3*).

We use temporal and spatially resolved optical techniques to probe the spin transport. In our pump/probe measurement scheme, the pump pulse excites a spin wavepacket whose propagation is detected by a time-delayed and spatially-separated probe pulse through the magneto-optic Kerr effect or optical birefringence. The range of wavevectors that comprise the spin wavepacket is determined by the Fourier transform of the real space excitation density, which is typically Gaussian. Since the size of the focused laser spot is diffraction limited, the excited wavevectors are typically within the range of inverse micrometers. In this long wavelength regime, the propagation of spin is dominated by magnetic dipole interactions, drastically altering the properties that arise from short-ranged exchange interactions alone (*4*). Excitations in this regime are referred to as magnetostatic spin waves (MSWs) although they are fully dynamic; the term arises because their dispersion relations can be obtained within the magnetostatic approximation, $\nabla \times H = 0$, which is valid because spin wave velocities are much smaller than the speed of light.

Spin Wavepackets in the Kagome Ferromagnet Fe3Sn2: Propagation and Precursors: We chose the easy-plane kagome ferromagnet Fe_3Sn_2 for our initial study of spin propagation because of its weak magnetocrystalline anisotropy (*5*). Figures 1a and 1b show snapshots of magnetization maps measured at a pump-probe time delay of 220 ps, showing clear evidence of anisotropic propagation. The anisotropic propagation we observe in Fe_3Sn_2 differs qualitatively from the isotropic group velocity predicted by Damon and Eshbach (*4*). In the theoretical component our work, we show that anisotropy emerges when the DE formalism is extended to biaxial XY magnets in which there is a hard axis perpendicular to the plane and an easy axis within the plane. Fig. 1c shows the calculated spin wave frequency in the k_x, k_y plane for fixed $k_z = 1\ \mu^{-1}$. Line cuts through this plane defined by $k_x = 0$ (purple) and $k_y = 0$ (orange) plotted in Fig. 1d show forward propagation along the y direction and backward along x, with a saddle point at $\boldsymbol{q} = 0$. These predictions are unique to biaxial ferromagnets and are distinct from the uniaxial (DE) case, in which there are no forward propagating reciprocal modes.

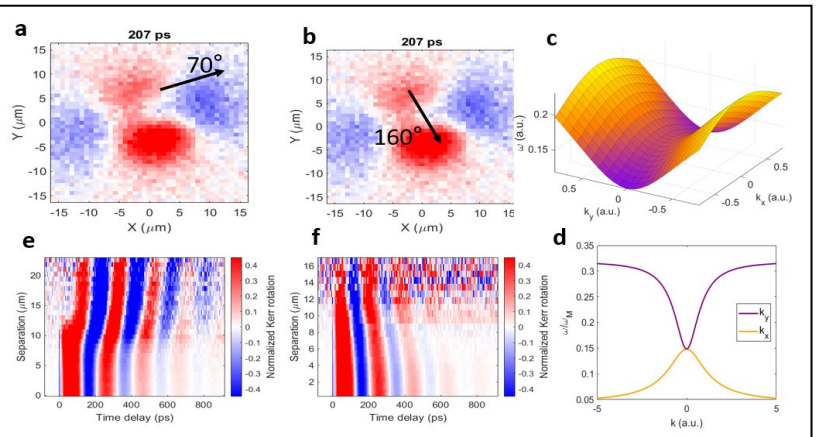

Figure 1: (a,b) Snapshot of spin wavepacket propagation at 207 ps after pump pulse showing two principal axes; (c,d) Theoretically predicted magnon dispersion; (e,f) Phase front trajectories for the two principal axes verifying the prediction of saddle point dispersion.

The prediction of a saddle dispersion relation was tested by measuring the trajectory of the spin wavepacket phase fronts as a function of pump/probe separation along the two principal axes of propagation. The results are presented in Figs. 1e, f as color plots in the time-separation plane. The slope of the lines of constant phase distinguishes forward vs. backward propagating modes. In agreement with our theoretical prediction for the biaxial ferromagnet, modes with wavevector perpendicular to $\boldsymbol{M}$ are forward propagating, and backward propagating for wavevectors parallel to $\boldsymbol{M}$.

Universal spin wavepacket transport in van der Waals antiferromagnets: Two-dimensional van der Waals antiferromagnets are currently under intense investigation as platforms for the generation, propagation, and detection of spin information. Recently, it was shown that in the insulating van der Waals (vdW) semiconductor, CrSBr, strong spin-exciton coupling enables readout of magnon density and propagation using photons of visible light (*6*). This exciting observation came with a puzzle: photogenerated magnons were observed to propagate 10^3 times faster than the velocity inferred from neutron scattering, leading to a conjecture that spin wavepackets are carried along by coupling to much faster elastic modes. In our work, we showed, through a combination of theory and experiment, that the propagation mechanism is, instead, coupling via the long-range dipole-dipole interaction. This mechanism is an inevitable consequence of Maxwell's equations, and as such, will dominate the propagation of spin at long wavelengths in the entire class of vdW magnets currently under intense investigation. Moreover, identifying the mechanism of spin propagation provides a set of optimization rules, as well as caveats, that are essential for any future applications of these promising systems.

The conclusion that dipole-dipole coupling is responsible for spin wave propagation in CrSBr is based on our discovery of salient features of the spin dynamics predicted by our theory of

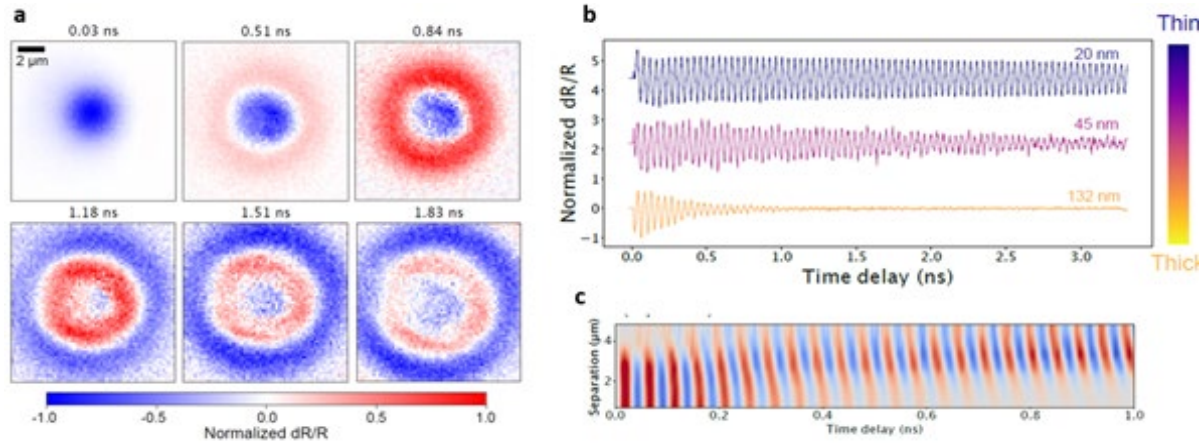

Figure 2: Three key features of magnon propagation in CrSBr that validate the dipole coupling mechanism. (a) Snapshots of spin wavepacket propagation in CrSBr showing isotropic group velocity; (b) Wavepacket amplitude measured with pump/probe overlap. The amplitude decays faster in thicker crystals because the group velocity is proportional to thickness; (c) The slope of the phase front trajectories verifies the prediction of negative group velocity.

magnetostatic modes in biaxial magnets: (1) near isotropy of spin wave propagation in the lower magnon band; (2) dependence of group velocity on sample thickness; (3) and the observation that the group and phase velocity of the spin wavepacket are opposite in sign.

Future directions

- *Magnons is CrSBr as a probe of quantum materials:* The extraordinary features of magnon propagation in CrSBr – large coherence length and sensitive readout via optics – can be used as probe of collective modes in metals, superconductors, and magnets. Fig. 3 shows two approaches in which materials under test are placed in contact with CrSBr: (left side) thin samples in which the group velocity is zero can be used to probe spin transport and damping;(right side) thick samples can be used as a platform to measure transmission of spin information.

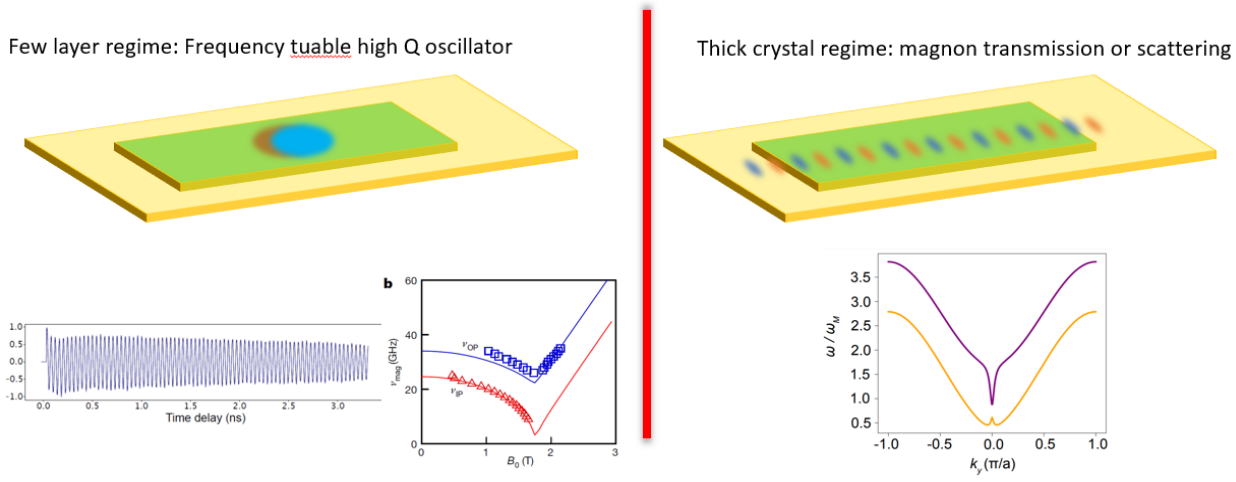

Figure 3: Projected use of magnons in CrSBr as a probe of spin dynamics in correlated metals, superconductors, and magnets.

- *Magnon propagation in noncolinear antiferromagnets:* We have discovered that magnons can be optically generated and detected in $EuIn_2As_2$, a fascinating system in which helical and antiferromagnetic order coexist (*7*). As it appears that magnetocrystalline anisotropy is extremely weak in this system, we will investigate the possibility of propagation via Goldstone modes of the helix.

References

1. P. Pirro, V. I. Vasyuchka, A. A. Serga, B. Hillebrands, Advances in coherent magnonics. *Nature Reviews Materials*. **6**, 1114–1135 (2021).

2. R. Lebrun, A. Ross, S. A. Bender, A. Qaiumzadeh, L. Baldrati, J. Cramer, A. Brataas, R. A. Duine, M. Kläui, Tunable long-distance spin transport in a crystalline antiferromagnetic iron oxide. *Nature*. **561**, 222–225 (2018).
3. E. B. Sonin, Spin currents and spin superfluidity. *Adv. Phys.* **59**, 181–255 (2010).
4. R. W. Damon, J. R. Eshbach, Magnetostatic modes of a ferromagnet slab. *J. Phys. Chem. Solids*. **19**, 308–320 (1961).
5. N. Kumar, Y. Soh, Y. Wang, Y. Xiong, Magnetotransport as a diagnostic of spin reorientation: Kagome ferromagnet as a case study. *Phys. Rev. B Condens. Matter*. **100**, 214420 (2019).
6. Y. J. Bae, J. Wang, A. Scheie, J. Xu, D. G. Chica, G. M. Diederich, J. Cenker, M. E. Ziebel, Y. Bai, H. Ren, C. R. Dean, M. Delor, X. Xu, X. Roy, A. D. Kent, X. Zhu, Exciton-coupled coherent magnons in a 2D semiconductor. *Nature*. **609**, 282–286 (2022).
7. S. X. M. Riberolles, T. V. Trevisan, B. Kuthanazhi, T. W. Heitmann, F. Ye, D. C. Johnston, S. L. Bud'ko, D. H. Ryan, P. C. Canfield, A. Kreyssig, A. Vishwanath, R. J. McQueeney, L.-L. Wang, P. P. Orth, B. G. Ueland, Magnetic crystalline-symmetry-protected axion electrodynamics and field-tunable unpinned Dirac cones in EuIn2As2. *Nat. Commun.* **12**, 999 (2021).

Publications

1. Chen, Su-Di, Makoto Hashimoto, Yu He, Dongjoon Song, Jun-Feng He, Ying-Fei Li, Shigeyuki Ishida, Hiroshi Eisaki, Jan Zaanen, Thomas P. Devereaux, Dung-Hai Lee, Dong-Hui Lu, and Zhi-Xun Shen. 2022. "Unconventional Spectral Signature of Tc in a Pure D-Wave Superconductor." *Nature* 601 (7894): 562–67.

2. Chen, Xiang, Yu-Tsun Shao, Rui Chen, Sandhya Susarla, Tom Hogan, Yu He, Hongrui Zhang, Siqi Wang, Jie Yao, Peter Ercius, David A. Muller, Ramamoorthy Ramesh, and Robert J. Birgeneau. 2022. "Pervasive beyond Room-Temperature Ferromagnetism in a Doped van Der Waals Magnet." *Physical Review Letters* 128 (21): 217203.

3. Junquera, Javier, Yousra Nahas, Sergei Prokhorenko, Laurent Bellaiche, Jorge Íñiguez, Darrell G. Schlom, Long-Qing Chen, Sayeef Salahuddin, David A. Muller, Lane W. Martin, and R. Ramesh. 2023. "Topological Phases in Polar Oxide Nanostructures." *Reviews of Modern Physics* 95 (2). American Physical Society: 025001.

4. Lee, Changmin, Yue Sun, Linda Ye, Sumedh Rathi, Kevin Wang, Yuan-Ming Lu, Joel Moore, Joseph G. Checkelsky, and Joseph Orenstein. 2023. "Spin Wavepackets in the Kagome Ferromagnet Fe3Sn2: Propagation and Precursors." *Proceedings of the National Academy of Sciences of the United States of America* 120 (21). Proceedings of the National Academy of Sciences: e2220589120.

5. Lee, Changmin, Praveen Vir, Kaustuv Manna, Chandra Shekhar, J. E. Moore, M. A. Kastner, Claudia Felser, and Joseph Orenstein. 2022. "Observation of a Phase Transition within the Domain Walls of Ferromagnetic Co3Sn2S2." *Nature Communications* 13 (1): 3000.

6. Rees, Dylan, Baozhu Lu, Yue Sun, Kaustuv Manna, Rüstem Özgür, Sujan Subedi, Horst Borrmann, Claudia Felser, J. Orenstein, and Darius H. Torchinsky. 2021. "Direct Measurement of Helicoid Surface States in RhSi Using Nonlinear Optics." *Physical Review Letters* 127 (15). American Physical Society: 157405.

7. Sun, Yue, Changmin Lee, Hung-Yu Yang, Darius H. Torchinsky, Fazel Tafti, and Joseph Orenstein. 2021. "Mapping Domain-Wall Topology in the Magnetic Weyl Semimetal CeAlSi." *Physical Review. B, Condensed Matter* 104 (23). American Physical Society: 235119.

8. Takasan, Kazuaki, Takahiro Morimoto, Joseph Orenstein, and Joel E. Moore. 2021. "Current-Induced Second Harmonic Generation in Inversion-Symmetric Dirac and Weyl Semimetals." *Physical Review. B, Condensed Matter* 104 (16). American Physical Society: L161202.

9. Wu, S., Z. Xu, S. C. Haley, S. F. Weber, A. Acharya, and E. Maniv. 2022. "Highly Tunable Magnetic Phases in Transition-Metal Dichalcogenide." *Physical Review X*. APS. https://journals.aps.org/prx/abstract/10.1103/PhysRevX.12.021003.

10. Zhang, Hongrui, David Raftrey, Ying-Ting Chan, Yu-Tsun Shao, Rui Chen, Xiang Chen, Xiaoxi Huang, Jonathan T. Reichanadter, Kaichen Dong, Sandhya Susarla, Lucas Caretta, Zhen Chen, Jie Yao, Peter Fischer, Jeffrey B. Neaton, Weida Wu, David A. Muller, Robert J. Birgeneau, and Ramamoorthy Ramesh. 2022. "Room-Temperature Skyrmion Lattice in a Layered Magnet (Fe0.5Co0.5)5GeTe2." *Science Advances* 8 (12): eabm7103.

11. Zhang, Hongrui, Yu-Tsun Shao, Rui Chen, Xiang Chen, Sandhya Susarla, David Raftrey, Jonathan T. Reichanadter, Lucas Caretta, Xiaoxi Huang, Nicholas S. Settineri, Zhen Chen, Jingcheng Zhou, Edith Bourret-Courchesne, Peter Ercius, Jie Yao, Peter Fischer, Jeffrey B. Neaton, David A. Muller, Robert J. Birgeneau, and Ramamoorthy Ramesh. 2022. "A Room Temperature Polar Magnetic Metal." *Physical Review Materials* 6 (4). American Physical Society: 044403.

12. Zou, Changwei, Zhenqi Hao, Xiangyu Luo, Shusen Ye, Qiang Gao, Miao Xu, Xintong Li, Peng Cai, Chengtian Lin, Xingjiang Zhou, Dung-Hai Lee, and Yayu Wang. 2022. "Particle–hole Asymmetric Superconducting Coherence Peaks in Overdoped Cuprates." *Nature Physics* 18 (5). Nature Publishing Group: 551–57.

13. Sunko, V., Sun, Y., Vranas, M., Homes, C. C., Lee, C., Donoway, E., Wang, Z.-C., Balguri, S., Mahendru, M. B., Ruiz, A., Gunn, B., Basak, R., Blanco-Canosa, S., Schierle, E., Weschke, E., Tafti, F., Frano, A., & Orenstein, J. (2023). Spin-carrier coupling induced ferromagnetism and giant resistivity peak in EuCd2P2. *Physical Review. B, Condensed Matter*, *107*(14). https://doi.org/10.1103/physrevb.107.144404

Giant optical nonlinearity of Fermi polarons in atomically thin semiconductors

You Zhou, Department of Materials Science and Engineering

University of Maryland, College Park, MD 20742

Keywords: 2D exciton, and light-matter phenomena, 2D and layered crystals, semiconductors, optical spectroscopy, moiré physics

Research Scope

In this grant period, we explore how the strong interactions between excitons and free carriers in atomically thin semiconductors can lead to giant nonlinear optical effects. Realizing strong nonlinear optical responses is a long-standing goal of both fundamental and technological importance. Recently significant efforts have focused on exploring excitons in solids as a pathway to achieving nonlinearities even down to few-photon levels. However, a crucial tradeoff arises as strong light-matter interactions require large oscillator strength and a short radiative lifetime of the excitons, which limits their interaction strength and nonlinearity. Here we experimentally demonstrate strong nonlinear optical responses by exploiting the coupling between excitons and carriers in an atomically thin semiconductor of trilayer tungsten diselenide.[1] By controlling the electric field and electrostatic doping of the trilayer, we observe the hybridization between intralayer and interlayer excitons along with the formation of Fermi polarons due to the interactions between excitons and free carriers. We find substantial optical nonlinearity can be achieved under both continuous wave and pulsed laser excitation, where the resonance of the hole-doped Fermi polaron blueshifts by as much as ~10 meV. Intriguingly, we observe a remarkable asymmetry in the optical nonlinearity between electron and hole doping, which is tunable by the applied electric field. We attribute these features to the strong interactions between excitons and free charges with optically induced valley polarization. Our results establish that atomically thin heterostructures are a highly versatile platform for engineering nonlinear optical response with applications to classical and quantum optoelectronics and open avenues for exploring many-body physics in hybrid Fermionic-Bosonic systems.

Recent Progress

In our experiments, we fabricated dual-gated homotrilayer WSe_2, first investigating their basic excitonic properties and then exploring their optical nonlinearity (Fig. 1a & b). As we apply electric field, we observe the photoluminescence (PL) of the intralayer momentum direct exciton X_A, corresponding to the K-K transition, and the lower energy X_I with a finite Stark shift, which are the momentum-indirect excitons at the band edge (Fig. 1c). Next, we measure the reflectance of the trilayer under an electric field (Fig. 1d). In addition to the intralayer X_A excitons at 1.71 eV, we observe an additional strong reflectance contrast at 1.78 eV (IX_D), which exhibits a substantial Stark effect of almost 100 meV. The finite reflection contrast and linear Stark effect of IX_I suggest that it corresponds to interlayer exciton at the direct K-K transition with larger

oscillator strength than those momentum-indirect excitons observed in PL. From the slope of the Stark effect, we estimate the electron-hole displacement to be 1.35 nm. Interestingly, as the energy of IX_D approaches that of the intralayer exciton X_A under a higher electric field, we observe an apparent anti-crossing behavior of X_A and IX_D near the electric field of 0.05 V/nm. The observed anti-crossing can be fitted using a simple coupled oscillator model, from which we estimate a coupling strength of $W = 10 \pm 2$ meV between X_A and IX_D. Lastly, we further characterize how electrostatic doping influences the optical response of the excitons while keeping the electric field at zero (Fig. 1e). With doping, the reflectance from neutral interlayer excitons diminishes as they lose their oscillator strength, while the charged intralayer excitons emerge, i.e., trions or Fermi polarons, which redshifts with increasing doping levels.

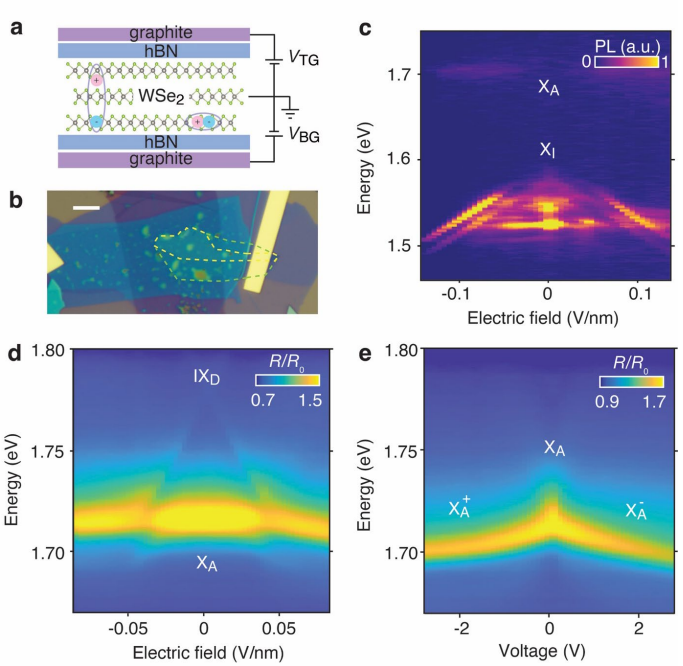

Fig. 1. Dual-gated WSe_2 homotrilayer van der Waals heterostructure and their optical characteristics under gating at T = 4 K. a, a schematic of device where homotrilayer WSe_2 is encapsulated with two hBN of 15~20 nm thick**. b,** an optical image of the homotrilayer WSe_2 device (Scale bar: 5 μm). The trilayer region is indicated by the yellow dashed line. **c,** Photoluminescence map of the WSe_2 trilayer with electric field. The bright emission with a stark shift from 1.5 to 1.58eV with electric field corresponds to the indirect exciton X_I. The upper weaker emission at 1.7eV corresponds to the momentum direct K-K intralayer exciton X_A. **d,** Reflectance spectra with electric field of the WSe_2 trilayer. The high energy momentum direct K-K interlayer exciton shows a Stark shift of ~100 meV and hybridize with X_A when they become energy degenerate around the electric field of 0.05 V/nm. **e,** Doping density dependent reflectance spectra of the WSe_2 trilayer. With increasing doping concentration, the intralayer trion or Fermi polaron (X_A^- /X_A^+) shifts toward lower energy.

Next, we study the system's nonlinear optical response by measuring the trilayer's reflectance spectra under different laser pumping. Figs. 2a-c show the reflectance spectra of the sample, probed with a broadband halogen lamp, while we excite the system with a 635nm continuous wave (CW) laser of different power. When the trilayers are electron-doped or intrinsic, optical pumping does not alter the reflectance spectra significantly. Intriguingly, however, in the hole-doped regime, optical pumping leads to a dramatic blueshift of the exciton energies on the order of a few millielectronvolts under microwatts excitation (Fig. 2b). Fig. 2d shows the reflectance spectra change induced by the optical pumping, relative to the reflectance spectra without pumping, under symmetric gating where we vary the doping concentrations without applying an electric field. We observe a striking asymmetry between the electron and hole sides. Figure 2e shows how the reflectance contrast of the X_A^+ evolves as we increase the average power of the

resonant excitation laser. A blueshift of as much as 10 meV is induced under tens of microwatts of optical pumping.

The observed large Stark effect and anti-crossing can be understood by examining the crystal and band structure of trilayer WSe_2. In trilayers, each monolayer is rotated by 180 degrees with respect to the neighboring layer, resulting in alternating K and K' points between layers (Figs. 3a, b). The sizeable spin-orbit coupling in the valence band dictates that the direct tunneling between the neighboring layers would be much weaker than that between the top and bottom layers across the middle layer. Such tunneling between the top and bottom layer leads to finite oscillator strength of interlayer K-K excitons IX_D and their avoided crossing with intralayer excitons X_A.

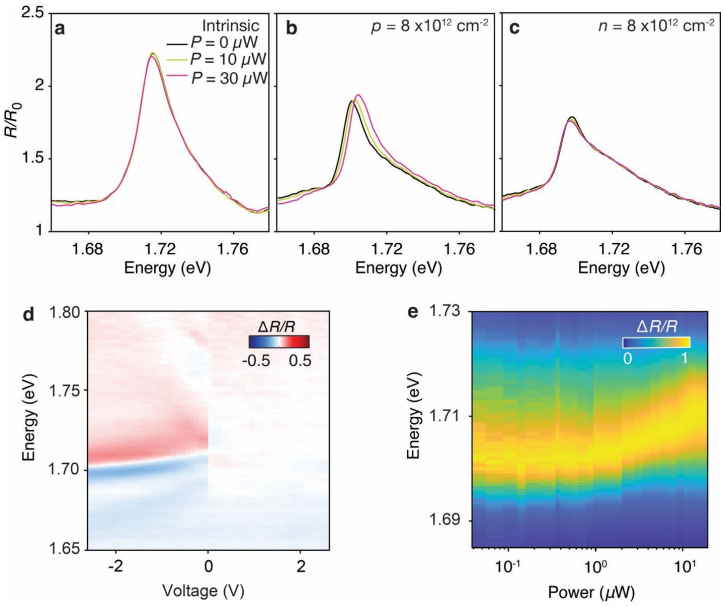

Fig. 2. Nonlinearity in hole doped homotrilayer WSe_2 at $T = 4$ K . a, b, c, Reflectance contrast R/R_0 of the trilayer under 0 μW, 10 μW, 30 μW CW (635nm) laser excitation with different doping levels, where R_0 is the reflectance of a reference region near the trilayer region with bare hBN on SiO_2 on the sample. **d,** Relative change in the sample reflectance induced by 30 μW of CW laser pumping under different doping. The color map is obtained by normalizing the reflectance change induced by the CW excitation with respect to the reflectance without optical pumping, $\Delta R/R = \frac{R_{(30\mu W)}}{R_{(No\ Pump)}} - 1$. The color contrast (red at higher energy, blue at lower energy) refers to the peak blue shift. **e,** Peak shift of the X_A^+ as a function of the pulsed laser excitation power (718-720nm, resonant with X_A^+), at hole doping of $8 \times 10^{12} cm^{-2}$.

We attribute the observed strong optical nonlinearity to the interactions between intralayer excitons and free carriers. In particular, excitons created by optical pumping can induce a valley population imbalance of resident carriers between K and Γ valleys, via mechanisms such as exciton-carriers scattering (Fig. 3c, d). Under zero electric field, the energy difference between K and Γ is rather small in trilayers, and Γ point is spin-degenerate[2]. As a result, holes at the Γ point could be efficiently scattered into the K valley by excitons such as X_A and X_I, via Coulombic and exchange interactions. This creates a net accumulation of valley population at both K and K', which induces phase space filling and, consequently, the observed blueshift. Such a blueshift induced by exciton-charge interactions does not occur in the intrinsic regime because of the lack of free carriers. Meanwhile, free electrons will experience a much higher energetic barrier for population transfer into K valleys due to the much larger energy splitting of Q and K valleys in the conduction band. This explains the observed strong asymmetry of optical nonlinearity on the electron vs. hole side. Another possible mechanism for optically induced valley polarization

could be that the accumulation of X_I excitons with finite dipole moments creates an effective displacement field across the trilayer by introducing a relative energy shift between K and Γ. In both proposed mechanisms, X_I can play an important role in the exciton-carrier interaction, which could underly the dynamics of the nonlinearity (Figs. 2d). Based on the lifetime of X_I^+ and the sample's absorption at the laser excitation, we estimate the density of the X_I^+ to be at least ten times smaller than the resident carriers, but comparable to the required valley polarization to induce the observed blueshift by phase space filling, therefore consistent with our observations.

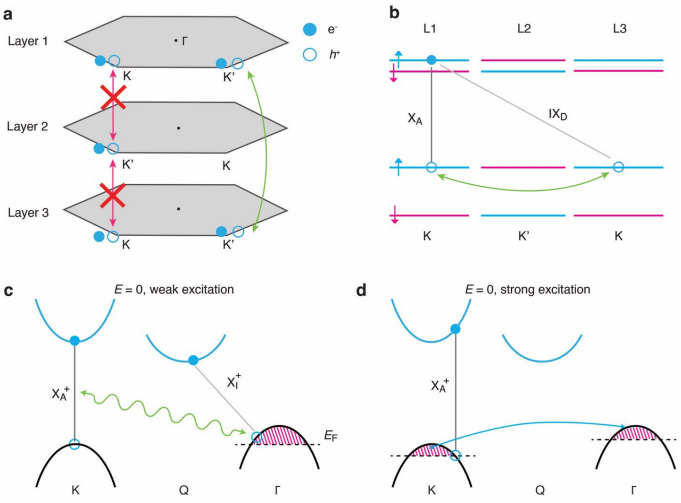

Fig. 3. Electronic band structure of trilayer WSe_2. a, The crystal structures of natural trilayer WSe_2 dictates alternating K and K' valleys among neighboring layers. The strong spin-orbit coupling of holes leads to weak tunneling among neighboring layers but strong tunnelling between the top and bottom layer. **b,** The tunnelling of holes between top and bottom layer results in the hybridization of intralayer K-K excitons X_A and interlayer K-K excitons IX_D. **c, d,** Band structures and carrier populations of hole-doped trilayer WSe_2 in the absence of electric field. **c,** Optical excitation generates both momentum intralayer X_A^+ and momentum indirect X_I of higher population. Intralayer Fermi polaron X_A^+ can interact with X_I and the free holes in the system. **d,** Under strong optical excitation, the interaction between intralayer excitons and free charges can induce a population transfer of carriers from the Γ to the K valley. The energy difference between Γ and K is small. The additional free carriers in K valley leads to phase space filling and optically induced blueshift of X_A^+.

Future Plans

We plan to explore how confining the holes and excitons in a moiré superlattice could further enhance the optical nonlinearity via quantum confinement. We also plan to further investigate the low carrier density regime, where the electron correlation effect becomes important and intricate interplay between optical nonlinearity and Wigner crystals could emerge. We also plan to explore the intriguing possibility of realizing distinct moiré lattice geometries in Γ vs. K valleys, such as Kagome, triangular, and honeycomb[3]. The optical control of the population at the Γ vs. K valleys may open new avenues for realizing dynamically tunable moiré and correlated systems.

References

1. L. Gu, L. Zhang, R. Ni, DS Wild, M. Xie, S. Park, H. Jang, K. Watanabe, T. Taniguchi, M. Hafezi, & Y. Zhou. *Giant optical nonlinearity of Fermi polarons in atomically thin semiconductors*. *arXiv*:2306.11199 (2023)
2. H. C. P. Movva, T. Lovorn, B. Fallahazad, S. Larentis, K. Kim, T. Taniguchi, K. Watanabe, S. K. Banerjee, A. H. MacDonald, & E. Tutuc. *Tunable Γ-K Valley Populations in Hole-Doped Trilayer WSe_2.* Phys. Rev. Lett. **120**, 107703 (2018).
3. A., Mattia, & A. H. MacDonald. *Γ valley transition metal dichalcogenide moiré bands.* Proceedings of the National Academy of Sciences 118, e2021826118 (2021).

Publications

1. D.G. Suarez-Forero, R. Ni, S. Sarkar, M.J. Mehrabad, E. Mechtel, V. Simonyan, A. Grankin, K. Watanabe, T. Taniguchi, H. Jang, S. Park, M. Hafezi & Y. Zhou. *Chiral optical nanocavity with atomically thin mirrors*. arXiv:2308.04574 (2023).

2. L. Gu, L. Zhang, R. Ni, DS Wild, M. Xie, S. Park, H. Jang, K. Watanabe, T. Taniguchi, M. Hafezi, & Y. Zhou. *Giant optical nonlinearity of Fermi polarons in atomically thin semiconductors*. *arXiv*:2306.11199 (2023).

3. B. Gao, D.G. Suarez-Forero, S. Sarkar, T.S. Huang, D. Session, M.J. Mehrabad, R. Ni, M. Xie, J. Vannucci, S. Mittal, K. Watanabe, T. Taniguchi, A. Imamoglu, Y. Zhou & M. Hafezi. *Excitonic Mott insulator in a Bose-Fermi-Hubbard system of moiré WS_2/WSe_2 heterobilayer*. arXiv:2304.09731 (2023).

4. L. Zhang, R. Ni, Y. Zhou. *Controlling quantum phases of electrons and excitons in moiré superlattices*. Journal of Applied Physics **133**, 080901 (2023). [Invited]

Design, discovery and chemical synthesis of earth abundant magnetic nitrides

Project PI: Sage Bauers, National Renewable Energy Laboratory

Keywords: ferromagnets, polycrystalline materials, materials discovery, metastability

Research Scope

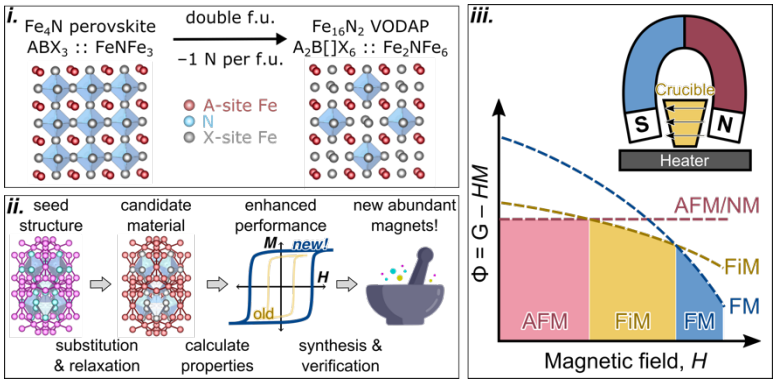

Fig 1: This project pursues three research thrusts enabling designed magnetic materials. (i.) understanding how chemical substitutions in magnetic antiperovskite nitrides leads to different structural distortions and magnetic exchange interactions. (ii.) developing workflows to predict and prepare new families of metal-rich nitrides containing ferrous elements. (iii.) employing unconventional thermodynamic handles and synthetic control to prepare new magnetic materials.

Permanent magnets are required in vast quantities to deploy technologies related to energy conversion and electric mobility. New magnetic materials are required both to strengthen supply chains and to increase performance over current state of the art. Major materials advances in earth abundant materials suitable for permanent magnets have all but stopped in the past few decades.[1] This program is discovering new magnetic nitrides, which we hypothesize hold untapped potential as a chemical family for permanent magnets. Nitrogen's position on the periodic table imparts an intermediate electronegativity. This makes N more electron-withdrawing than the anions conventionally found in permanent magnets (B and C), affording both increased magnetic strength of $>d^5$ ions and stronger structural distortions away from high symmetry structures at dilute concentrations, both necessary ingredients for high performance magnets. Conversely, N is not as anionic as O, so it is less likely to drive transition metals into high oxidation states or form rigid ionic structures favoring antiferromagnetic correlation through super exchange.

We elect to pursue two approaches for discovering new magnetic nitrides. In the first approach, we draw inspiration from the strongest known ferromagnet, $Fe_{16}N_2$.[2] While it is often described as an interstitial nitride based on cubic close packed (ccp) Fe, we instead view $Fe_{16}N_2$ through the lens of a vacancy-ordered double antiperovskite (VODAP). This establishes a slew of chemically intuitive spaces—other antiperovskites (APs)—to begin searching for new high-performance magnetic nitrides. For the second approach, we are employing high-throughput predictive workflows to identify altogether new nitride families that are rich in 3*d* metals. We previously developed similar complementary computational and experimental workflows to predict and synthesize new nitrides,[3] which are being amended for high fidelity in magnetic chemistries.

The primary reason that promising nitrides are underutilized for permanent magnet applications lies in their synthesis. Conventional metallurgical processing based on nucleation, gaseous

diffusion, and high temperature sintering naturally precludes synthesis of materials with low or positive formation enthalpies and even operationally stable materials that cannot survive high-temperature processing because of, for example, volatilized N_2. To this end, we are developing new nitride synthesis approaches, which are in turn guided by high dimensional computational phase diagrams, to prepare new magnetic materials under gentle reaction conditions.

Recent Progress

Thrust 1: Chemical modifications in the AP family

Inspired by reports of myriad magnetic properties in alloyed and off-stoichiometric derivatives of Mn_3GeN, we have elected to first study APs in this system. While there are several reports on Mn_3GeN dating back to the 1970's, incomplete literature data leaves several questions regarding how compositional changes influence its properties. The initial hypothesis guiding this work is that the varying magnetism of nitride APs arises from a competition between local AFM moments in X_6B octahedra and itinerant ferromagnetic (FM) moments from *A* site electrons (*cf.* **Fig 1*i***), providing several avenues to control the net magnetic properties.

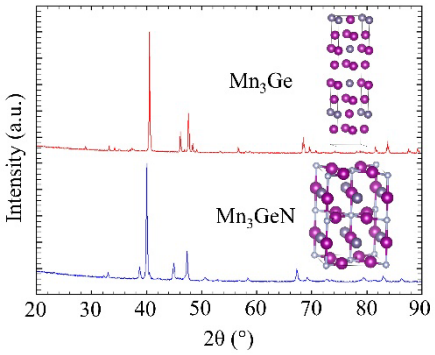

Fig 2: X-ray diffraction of Mn_3GeN AP and Mn_3Ge achieved by topotactic denitridation of the AP phase.

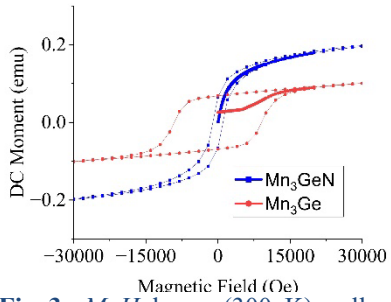

Fig 3: *M–H* loops (300 K) collected from Mn_3GeN AP (blue, canted AFM) and the new Mn_3Ge phase (red, hard FM).

We prepared Mn_3GeN as bulk powders and subsequently studied how denitriding the AP induces change to the magnetic properties (**Fig 2**). We find AP Mn_3GeN is a canted antiferromagnet (AFM) at room temperature with a small hysteresis. Prior reports on Mn_3GeN noted the PM–AFM transition was concomitant with a structural distortion to tetragonal symmetry. Within our model, the tetragonal phase results from Mn_6N octahedral rotations, likely disrupting the inter-octahedral superexchange interaction strength and thus favoring ferrimagnetic order. Similar disruptions might arise from intra-octahedral modifications, for example by denitriding. We note that this is conceptually similar to creating a VODAP from a stoichiometric perovskite (**Fig 1*i***). Surprisingly, when Mn_3GeN is gently denitrided to Mn_3Ge, a new polymorph is formed in which the baseline AP metal lattice is almost entirely "locked" into place. The new phase is a hard FM with an impressive room temperature coercive field, H_C, of 1 T and T_C over 350 K (**Fig 3**).

Thrust 2: Structural design of magnetic nitrides

To expand the number of magnetic nitride candidates requires rational methods to predict stable new chemistries and structures. We've amended our prior nitride search algorithms,[3] based on ionic substitution, to be suitable for magnetic materials with less ionic character, by making

substitutions based on the structural prototypes atoms share. While our original algorithm only predicted 6 new stable ternary nitrides not containing alkaline metals or Zn—elements that are generally undesirable for magnetism because they help drive transition metals into high oxidation states in ternary nitrides—the updated approach yields 49 such candidates. Only 1 of the original 6 compounds contained 2 transition metals: $MnCoN_2$. For this reason, $MnCoN_2$ is explored first.

$MnCoN_2$ was originally predicted in the *R*3*m* structure with Mn and Co tetrahedrally coordinated by nitrogen. However, subsequent calculations found several lower energy polymorphs with a ground state in the rocksalt-derived α-$NaFeO_2$ prototype. We synthesize $MnCoN_2$ using high-throughput thin film approaches. The ternary $MnCoN_2$ material's magnetism is significantly altered from the binaries. While MnN is AFM with T_N = 650 K and CoN is paramagnetic, $MnCoN_2$ displays AFM correlations with $T_N \approx 15$ K (**Fig 4**). $MnCoN_2$ exhibits the face-centered cubic symmetry of a simple rocksalt structure, suggesting a significant degree of cation antisite disorder as is common in ternary nitrides. Both binaries also exhibit face-centered cubic (or nearly) symmetry (MnN is distorted rocksalt and CoN is zincblende), so more work is required to unequivocally determine the structure. Our proposal to answer these questions using X-ray absorption spectroscopy (XAS) at Brookhaven National Laboratory was recently awarded time.

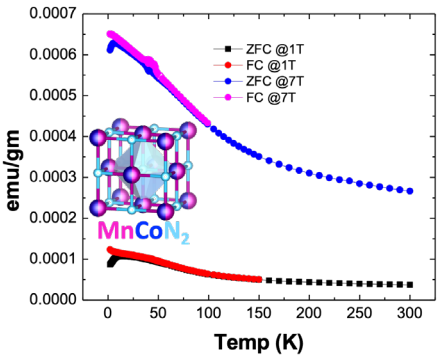

Fig 4: Field-cooled (FC) and zero-field-cooled (ZFC) magnetization of $MnCoN_2$, which has starkly different magnetism than MnN and CoN binary compounds.

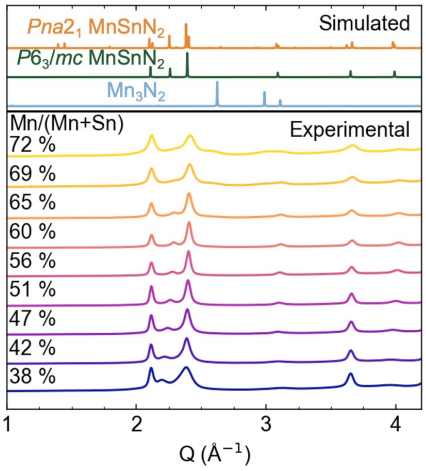

Fig 5: Diffraction of various Mn-Sn-N compositions shows wurtzite is stable over a large phase-width.

Thrust 3: Designing metastable magnetic nitride synthesis by controlling chemical potentials

Because of its chemical and predicted structural similarities to other nitrides our team has discovered, the first metastable magnetic material we studied was $MnSnN_2$. $MnSnN_2$ was predicted to be a magnetic semiconductor with a wurtzite (WZ)-derived crystal structure (*Pna*2$_1$), like chemically analogous AFM semiconductors $MnSiN_2$ and $MnGeN_2$. We used thin film approaches with high μ_N during synthesis to achieve the first experimental realization of metastable $MnSnN_2$. The material exhibited sufficient cation anti-site disorder such that the diffraction signature is of simple WZ (*P*6$_3$/*mc*, Fig 5). Semiconducting properties of WZ-$MnSnN_2$ are comparable to $MnSiN_2$ and $MnGeN_2$, but an AFM ordering transition is surprisingly not observed until ca. 10 K—over 400 K below $MnSiN_2$ and $MnGeN_2$.

To understand the origins of the T_N discrepancy, we compared the *magnetic* ordering energy of *atomically* ordered and disordered $MnSnN_2$ using Monte Carlo + DFT. Fig 6 shows the evolution

of magnetic energy from cation-ordered and -disordered $MnSnN_2$ as spins are computationally quenched. The disordered supercell remains in a paramagnetic state throughout the simulation,

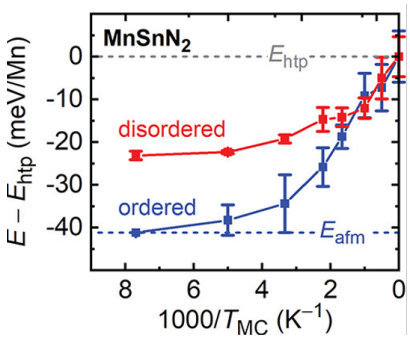

Fig 6: Monte Carlo + DFT comparison of magnetic ordering energy for cation-ordered and -disordered $MnSnN_2$.

whereas the ordered atomic structure adopts magnetic order around 600 K, in relatively good agreement with experiments on ordered MnSiN2 and MnGeN2. Synthesizing MnGeN2 as thin films yields similar results to MnSnN2: cation disordered material and TN ≈ 25 K. Thus, in these wurtzite-based materials anti-site disorder appears to significantly frustrate magnetic order, which we propose can be an important design consideration—and tool—for both promoting and inhibiting magnetism in complex materials.

Future Plans

Thrust 1: we will continue investigating Mn_3AN alloys (*A* = Al, Si, Ga, Ge) and continue denitridation studies to further test our exchange hypothesis against known compounds. We will also explore $(3d)_3PMN$ (*3d* = Fe, Co, Ni and *PM* = precious metal) APs, since their broad predicted stability and ferromagnetism affords low-hanging opportunities to study systematic changes to AP metal sites. We are particularly interested in learning how magnetic anisotropy can be instilled into APs with high magnetization by decorating a predominantly ferrous element matrix with 5*d* elements providing strong orbital momentum, together leading to a high performing material.

Thrust 2: we will synthesize candidate metastable ferromagnetic materials predicted by our expanded substitution algorithms. For example, we predicted a series of $Mn_{12}M_{12}N_4$ (*M* = Hf, Nb, Ta) compounds, which have a compelling structure (shown in Fig 1*ii*) comprising a ferrous matrix punctuated by M_6N octahedra. Denitriding could lead to isolated M_6N polyhedra akin to $Fe_{16}N_2$, but with heavy *M* elements that may help produce high coercivity through spin orbit coupling. Another family of predicted materials are $(3d)_8M_{16}N_4$ (*3d* = Fe, Co, Ni and *M* = Ti, Nb, Hf), which have a similar structure but the 3*d* metals form isolated tetrahedra.

Thrust 3: many predicted magnetic nitrides are barely above the thermodynamic ground state such that perturbation to the Gibbs energy by a field during synthesis could assist with their realization (Fig 1*iii*). Thus, we are building a custom furnace giving the ability to prepare materials in a 14 T field. Heat flow modeling of a manufacturable design is promising up to 1000 K, and manufacturing is imminent. In addition, we are continuing work on soft synthesis approaches, such as topotactic denitridation, to provide routes to phases incompatible with ceramic synthesis.

References

1. R. W. McCallum, L. H. Lewis, R. Skomski, M.J. Kramer, I.E. Anderson, *Practical Aspects of Modern and Future Permanent Magnets*, Annual Reviews of Materials Research **55**, 451 (2014)
2. J. P. Wang, *Environment-friendly bulk $Fe_{16}N_2$ permanent magnet: Review and prospective*, Journal of Magnetism and Magnetic Materials **497**, 165962 (2020).
3. W. Sun, C. J. Bartel, E. Arca, S. R. Bauers, B. Matthews, B. Orvañanos, B. R. Chen, M. F. Toney, L. T. Schelhas, W. Tumas, J. Tate, A. Zakutayev, S. Lany, A. M. Holder, G. Ceder, *A map of the inorganic ternary metal nitrides*, Nature Materials **18**, 732 (2019).

Publications

1. C. L. Rom, et al., *Combinatorial synthesis of cation-disordered manganese tin nitride $MnSnN_2$ thin films with magnetic and semiconducting properties*, Chemistry of Materials **35**, 2936 (2023).

2. S. Dugu, et al., *Circling back on recently predicted metal-metal-nitrides: experimental synthesis, structure, and magnetic properties of thin film $MnCoN_2$*, In Preparation (working title).

3. S. O'Donnell, et al., *Ambient-pressure synthesis of ferromagnetic Mn_3Ge with >1 T coercive field using topotactic chemistry*, In Preparation (working title).

4. S. Bauers, et al., *Earth abundant magnetic materials for electrified mobility*, In Preparation (working title)

Direct Observation of Fractional Quantum Hall Quasiparticle Braiding Statistics via Interferometry

Michael J. Manfra, Purdue University and Microsoft Quantum Lab, West Lafayette

Keywords: anyonic braiding statistics, topology-fractional quantum Hall effect, Fabry-Perot interferometry, molecular beam epitaxy

Research Scope

Interferometric measurements focused on direct observation of anyonic statistics in the fractional quantum Hall regime beyond the primary Laughlin state at ν=1/3. Current work is focused on ν=2/3, the particle-hole symmetric partner to ν=1/3, and ν=2/5, a principal daughter state of ν=1/3 in the Halperin-Haldane hierarchy. Additional work extends our techniques to putative non-Abelian fractional states, e.g., ν=5/2, in the N=1 Landau level.

Recent Progress

We have extended our experimental techniques to investigate edge mode transport and anyonic braiding statistics at the ν=2/3 and ν=2/5 fractional quantum Hall states. At ν=2/3 we first focused on transmission of edge modes through quantum point contacts. Unexpectedly we discovered a half-integer conductance plateau under small but finite source-drain bias. This intermediate plateau with $G=0.5e^2/h$ was found to be consistent with full reflection of a counterpropagating -1/3 edge mode. This novel structure was attributed to the sharp confinement potential in our screening well design. This result was published in *Physical Review Letters* in 2023 as an editor's suggestion.

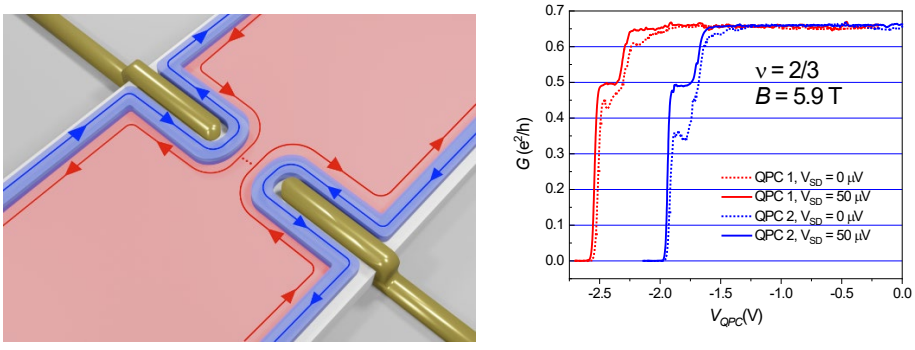

Figure 1: a) schematic diagram of counterpropagating charged edge modes at ν=2/3. b) plot of conductance of individual QPCs at ν=2/3. With 50mV of bias, an intermediate plateau at $G=0.5e^2/h$ is observed, indicating a fully reflected -1/3 charge mode.

At ν=2/5 we were able to demonstrate that Fabry-Perot interferometry may be extended to states with multiple edge modes to *quantitatively* investigate anyon braiding. A key aspect of this work was demonstration of *independent* interference of the inner and outer charge modes. Independent interference of both modes is a necessary requirement for analysis of fractional statistics for states

with complex multimode edge structure. At ν=2/5 we determine the anyon charge to be e*=e/5, where e is the fundamental charge of the electron, and the anyonic statistical phase to be -4π/5, consistent with theoretical expectations. This demonstration paves the way for interferometric measurements at ν=5/2. The work is currently under review at PRX and was the subject of a Journal Club for Condensed Matter Physics in June 2023 [1].

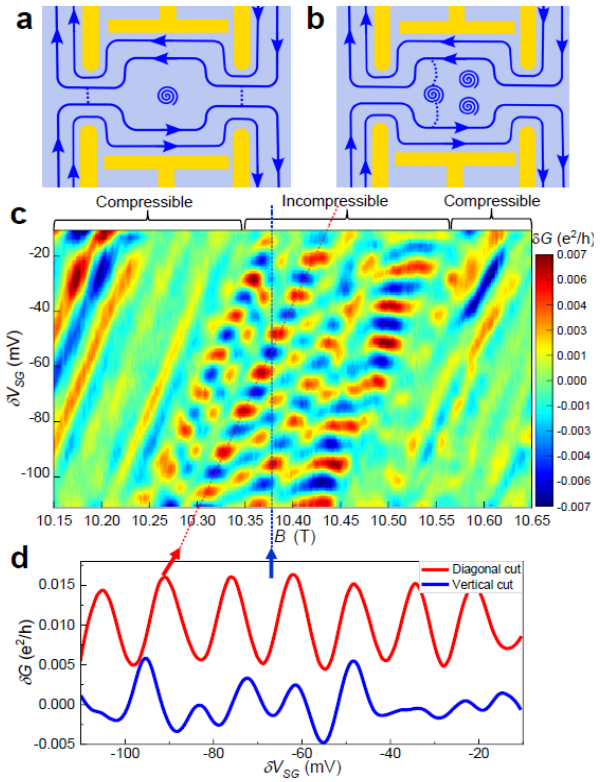

Figure 2: a) Schematic of interference for the inner mode at ν= 2/5. b) Schematic of resonant tunneling when the bulk is compressible, and many quasiparticles are present inside the interferometer. c) Conductance for the inner mode at ν=2/5. There is a central region where a checkerboard-pattern forms with discrete jumps in the oscillation pattern indicative of anyonic statistics. d) Vertical cut of conductance (blue) in the incompressible regime. Since this cut intersects several of the discrete jumps in phase, the behavior is non-sinusoidal. On diagonal cuts parallel to (but in between) the discrete jumps in phase (red), the quasiparticle number is fixed, so the conductance oscillates sinusoidally due to the continuously varying Aharonov-Bohm phase. Red and blue dashed lines in c) in a indicate where each cut is taken.

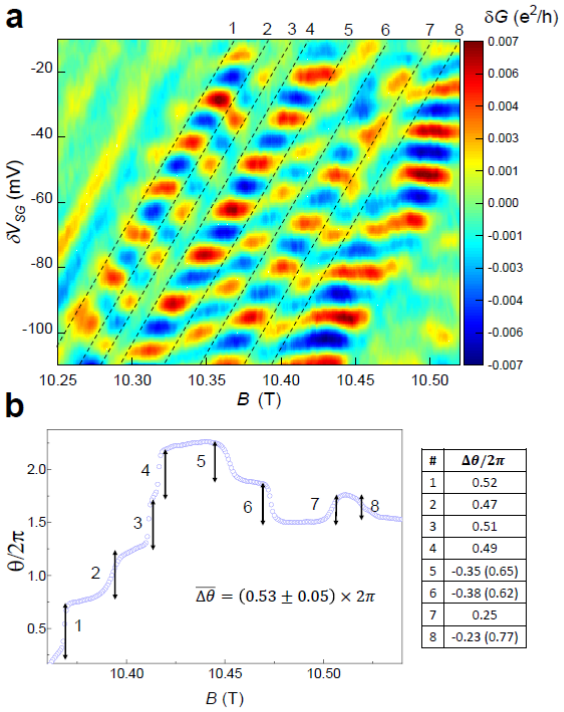

#	Δθ/2π
1	0.52
2	0.47
3	0.51
4	0.49
5	-0.35 (0.65)
6	-0.38 (0.62)
7	0.25
8	-0.23 (0.77)

Figure 3: a) Conductance versus side gate voltage and magnetic field for the inner mode at ν =2/5 (zoomed in view on the incompressible region with dashed lines indicating the positions of discrete jumps in phase. b) Phase extracted via Fourier transform versus magnetic field. Discrete steps in the phase correspond to the discrete jumps visible in a). The values of each phase jump (calculated from the difference of θ on each plateau between the jumps) is indicated in the table to the right of the plot.

Future Plans

Our plans focus on new experiments at ν=5/2 to probe non-Abelian statistics. We are designing new heterostructures that provide sufficient screening to operate as interferometers but are also extremely low disorder, as needed for the fragile states in the N=1 Landau level. Our first generation of etched trench-gate devices are currently under test at low temperatures. We also have begun design of devices that interface different filling factors such as ν=3 and ν=5/2 or ν=2 and ν=5/2. Conductance measurements in this configuration may expose the underlying topological order of the ν=5/2.

Reference

1. Steven A. Kivelson, and Charles M. Marcus, *Progress measuring fractional quantum numbers in quantum Hall interferometers*, DOI:10.36471/JCCM_June_2023_01.

Publications

1. J. Nakamura, S. Liang, G. C. Gardner, and M. J. Manfra, *Fabry-Perot interferometry at the ν=2/5 fractional quantum Hall state*, arXiv: 2304:12415, submitted to *Physical Review X* (2023).

2. J. Nakamura, S. Liang, G. C. Gardner, and M. J. Manfra, *Half-integer conductance plateau at the ν=2/3 fractional quantum Hall state in a quantum point contact,* Phys. Rev. Lett. **130**, 076205 (2023)

3. J. Nakamura, S. Liang, G. C. Gardner, and M. J. Manfra, *Impact of bulk-edge coupling on observation of anyonic braiding statistics in quantum Hall interferometers*, Nature Communications, **13**, 344 (2022)

Topology and molecular arrangement in low-dimensional magnetic materials

Claudia Ojeda-Aristizabal, Department of Physics and Astronomy, California State University Long Beach

Keywords: magnetism, topology, 2D and layered crystals, graphene, transition metal compounds, topological materials, transport, ARPES.

Research Scope

Our current research aims to understand and control properties derived from topologically protected phases, molecular arrangement and Moiré patterns in low dimensional materials that present a long-range magnetic order. Research efforts are organized into two thrusts. The first thrust focuses on layered ferromagnets such as VI_3, but most importantly, on two-dimensional Dirac semimetals such as $PtTe_2$ and $PdTe_2$ that when substituted with a magnetic element like Cr, become high transition temperature ferromagnets (T*c* up to 220 K). These materials have the important property of keeping the air-stability of their transition metal dichalcogenide (and topological) parent crystals. This effort intents to bring light on the intriguing interplay between magnetism and Dirac fermion physics in two dimensional materials but also, should provide details on the electronic structure of exfoliatable, metallic, air-stable ferromagnets. Additionally, this thrust has developed efforts to measure through specialized transport methods, quantum materials that are highly insulating and that present magnetically ordered ground states as well as more thrilling states such as spin liquids, which is the case of α-$RuCl_3$.

A second thrust of our research is centered on molecular solids made of C_{60} or metal-Phthalocyanines (MPc). MPc are versatile planar molecules that can host almost any transition metal from the periodic table, some of which transform these molecules into magnetic building blocks that are fundamentally different from those studied in the first thrust of our research program. C_{60} and MPc can form thin films on two-dimensional materials where molecular arrangements and Moiré patterns may have a profound impact on their electronic structure. Such patterns may result from a periodical variation of the orientation of the molecules on the substrate or simply from the non-commensurability of the molecular thin film unit cell with the one of the substrate. We have performed preliminary studies of the arrangement of Cu-phthalocyanines (CuPc) on graphene finding encouraging results. We have also performed ARPES measurements on a thin film of K_xC_{60} on hexagonal layered Bi_2Se_3, demonstrating the existence of a quantum phase transition induced by intercalation doping.

Recent Progress

Polarization dependent photoemission as a probe of the magnetic ground state in the layered ferromagnet VI3

VI_3 is a van der Waals layered semiconductor that presents ferromagnetism with a magnetic state that is fundamentally different from the one in the first Cr reported layered ferromagnets [1]. There is yet no consensus on the exact mechanism responsible for a band gap in VI_3. In this material,

crystal field effects split the vanadium d-orbitals into a lower t_{2g} triplet and an upper e_g doublet state. Trigonal distorsions cause an additional split of the t_{2g} levels, leading to two possible scenarios for the ground state in VI_3. A first scenario, where V d^2 electrons fully occupy the lower energy level that resulted from the t_{2g} level splitting. The second scenario where one of the Vd^2 electrons partially occupies the higher energy level that resulted from the t_{2g} level splitting. This last one is at first sight a metallic state, however spin-orbit coupling can potentially split further the half-filled orbital that together with electronic correlations, leas to a Mott insulator. In this work, we made use of circularly polarized light to put in evidence through Angle Resolved Photoemission Spectroscopy ARPES, the preferred ground state in VI3, revealed by the circular dichroic signal of the valance band. Our data pointed to orbitals oriented in the out-of-plane direction, consistent with the second scenario. Our measurements put in evidence in an indirect way, the importance of spin – orbit coupling in VI_3, which plays an essential role in the observed perpendicular magnetic anisotropy in this material, crucial for electronic applications.

Electronic transport mechanisms in a thin crystal of the Kitaev candidate α-RuCl3 probed through guarded high impedance measurements

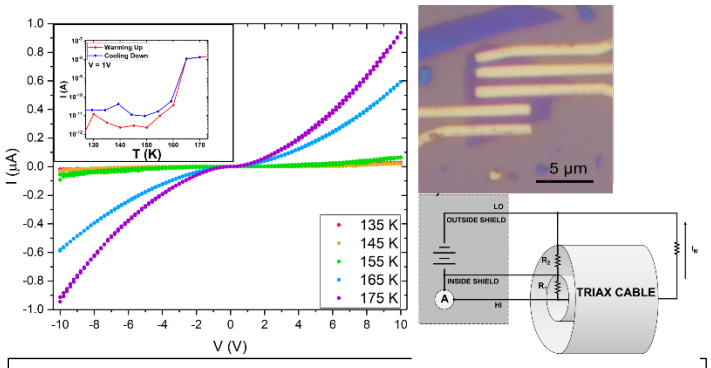

Figure 1: Left: IV characteristics at different temperatures showing a structural phase transition in α-$RuCl_3$ at ~160 K. The inset shows the change of the current across the device. Top Right: 100 x optical image of the measured device. Bottom right: Circuit schematic of the guarded setup with triax lines.

Among the different materials that can host Kitaev physics, α-RuCl3 has played a starring role, bringing scientists a step closer to the thrilling ground states predicted in the frame of the Kitaev model, of interest for fault-tolerant topological quantum computing. α-RuCl3, like other candidates for the experimental realization of the Kitaev model, is highly insulating, reducing the experimental probes available to study the ground states in these materials. In this work, we made use of a specialized technique to reach, through electronic transport measurements, temperatures where α-$RuCl_3$ is highly insulating and becomes a zig-zag antiferromagnet, finding evidence of the transport mechanism ruling our thin crystals. Our experimental setup, equipped with a guard terminal, triaxial lines and a metallic sample shield, allows us to clearly identify different transport regimes in a wide range of temperatures and bias electric fields, as well as the localization length of the impurities in our samples. We found through electronic transport, clear evidence of a structural phase transition. Most importantly, we found that below 7K, the magnetic order temperature for α-$RuCl_3$, the electronic transport mechanism in our device deviates from Efros Shklovskii variable range hopping. Our work demonstrates the possibility of reaching, through specialized high impedance measurements, the thrilling ground states predicted for α-RuCl3 in the frame of the Kitaev-Heisenberg model, at temperatures where

this material is highly insulating, and paves the way for the study of other insulating quantum materials.

Coexistence of bulk type-II and surface Dirac cones in $PtTe_2$ and $PdTe_2$ probed through Angle Resolved Photoemission Spectroscopy (ARPES)

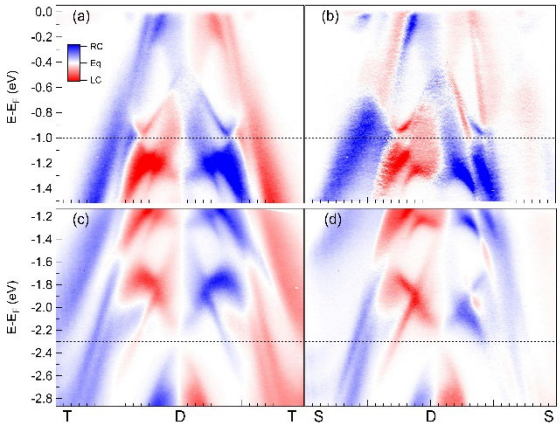

Figure 2: Left: Circular polarization dependent photoemission for PtTe2 (a) and (b) show the dichroic signal for T-D-T and S-D-S respectively (near the type-II Dirac cone). (c) and (d) show the dichroic signal for the Dirac surface state. Dirac points are indicated with pointed lines.

$PtTe_2$ and $PdTe_2$ are among the transition metal dichalcogenides that were first predicted to recreate type-II Dirac fermions, exotic particles prohibited in free space [2]. These materials are layered and air-stable, which makes them suitable for different technological applications. Most importantly, they have the particularity of not only hosting type-II Dirac particles at the bulk but also topologically protected chiral states at the surface. In this work, we provide a careful characterization of the electronic structure of $PtTe_2$ and $PdTe_2$ through Angle Resolved Photoemission Spectroscopy ARPES and Density Functional Theory DFT calculations, stressing the important role played by the different symmetries associated to their crystallographic space group, discernible in our data. Space group $P\bar{3}m1$ has a primitive Bravais lattice with inversion symmetric three-fold rotation and mirror symmetry. This is can be identified in the ARPES measured band structure and DFT data, that fulfills $E_o(k_x, k_y, k_z)=E_o(-k_x, -k_y, -k_z)$. Additionally, by using circularly polarized light, we show the different character of Dirac dispersions that derive from those symmetries. One, a type-II Dirac cone that lives in the bulk, formed by four bands, protected by the symmetries of the crystal and hosting exotic type-II Dirac fermions. The second, a surface state formed at the bandgap between two bands, topologically protected and hosting chiral Dirac fermions. Our work not only provides a useful reference for the characterization of other transition metal dichalcogenides with topological properties, but more generally, it illustrates the use of circular dichroism in ARPES for the distinction of states with dissimilar orbital and topological properties .

Linearly dispersive bands at the onset of correlations in K_xC_{60} films

We have reported in the past the first observation of highly dispersive bands in thin film of fullerenes. Our finding, in collaboration with the Lanzara and Zettl groups at UC Berkeley, revealed that in a thin film of C_{60} molecules the electronic structure is not dominated by the electronic interactions within a single molecule. Instead, long range interactions between the molecules in a thin film have a profound effect shaping the electronic structure of this material [3]. Additionally, light polarization studies of the photoemission provided information on the orbital makeup of the C_{60} band manifolds [4]. In this work, we have analyzed the dependence of the

photoemission of a C_{60} thin film upon doping with potassium, finding that K_xC_{60} is ruled by fundamentally different physics depending on the K doping. Most importantly, we find that upon doping, the C_{60} thin film undergoes a Mott transition from a molecular insulator to a correlated metal, which challenges the commonly accepted band-filling picture as the explanation for K_3C_{60} metallicity, where superconductivity occurs.

Future Plans

Electronic transport in CuPc/graphene/hBN heterostructures: we have performed preliminary characterization of CuPc on graphene through transmission electron microscopy TEM and atomic force microscopy AFM finding an organized arrangement of the molecules on graphene. Our preliminary electronic transport measurements are encouraging, and show the possible effect of CuPc's magnetic moment, leading to an asymmetry in the magnetoresistance of the device. Measurements on additional samples are currently in progress. We plan to use mesoscopic electronic transport techniques to bring light on important properties at the interface between graphene and the metallo-organic molecules, such as macroscopic magnetic moments, electronic correlations or enhanced spin-orbit coupling, a crucial ingredient for the design of quantum materials.

Electronic transport in Cr alloys of PtTe2 and PdTe2: Taking advantage of the air stability and layered character of these materials, we will perform electronic transport experiments to probe the magnetic ordered states in the new families of layered ferromagnets $Cr_xPt_{1-x}Te_2$ and $Cr_xPd_{1-x}Te_2$ through anomalous Hall effect. Nanofabrication techniques will allow us to assess the dependence of the electronic transport on the number of layers of $Cr_xPt_{1-x}Te_2$.

ARPES studies of the air-stable layered ferromagnet $Cr_xPt_{1-x}Te_2$: A question of interest is the evolution of the characteristic topologically protected states for $PtTe_2$ and $PdTe_2$ as Cr is substituted in the Pt and Pd sites. It is well known that in type-II Dirac semimetals, three dimensional Dirac points are protected by time reversal T and inversion P symmetries. These Dirac points, made of energetically degenerate Weyl modes are stabilized at the same crystal momentum by a C_3 rotational symmetry. To a first approximation, one would think that the introduction of a magnetic element such as Cr breaks time reversal symmetry, pulling apart the individual Weyl modes in momentum space [5].Our preliminary ARPES measurements show that instead of an antagonist role, Cr benefits the experimental reach of the type-II Dirac cone characteristic of the parent crystal, by introducing electron doping and bringing the type-II cone closer to the Fermi level. Our DFT calculations show the resilience of the tilted Dirac dispersion in the kz direction, characteristic of type-II excitations. Also, it looks like the topologically protected surface states characteristic of PtTe2, endure the Cr substitution.

References

[1] Tai Kong, Karoline Stolze, Erik I. Timmons, Jing Tao, Danrui Ni, Shu Guo, Zoë Yang, Ruslan Prozorov, and Robert J. Cava, "VI3 a new layered ferromagnetic semiconductor" Adv. Mat. 31, 1808074 (2019)

[2] H. Huang, S. Zhou, and W. Duan, Type-ii dirac fermions in the PtSe2 class of transition metal dichalcogenides, Phys. Rev. B 94, 121117 (2016).
[3] Drew W. Latzke*, C. Ojeda-Aristizabal*, Sinead M. Griffin, Jonathan Denlinger, Jeffrey B. Neaton, Alex Zettl and Alessandra Lanzara "Observation of highly dispersive bands in pure thin film C60" Phys. Rev. B 99, 045425 (2019).
[4] Drew W. Latzke*, C. Ojeda-Aristizabal*, Jonathan Denlinger, Ryan Reno, Alex Zettl and Alessandra Lanzara "Orbital character effects in the photon energy and polarization dependence of pure C60 photoemission" ACS Nano 13 (11), 12710 (2019).
[5] J. Cano, B. Bradlyn, Z. Wang, M. Hirschberger, N. P. Ong, and B. A. Bernevig, Chiral anomaly factory "Creating Weyl fermions with a magnetic field" Phys. Rev. B 95, 161306 (2017).

Publications

1. Derek Bergner, Tai Kong, Ping Ai, Daniel Eilbott, Claudia Fatuzzo, Samuel Ciocys, Nicholas Dale, Conrad Stansbury, Drew W. Latzke, Everardo Molina, Ryan Reno, Robert J. Cava, Alessandra Lanzara and Claudia Ojeda-Aristizabal "Polarization dependent photoemission as a probe of the magnetic ground state in the layered ferromagnet VI3" **Appl. Phys. Lett. 121, 183104 (2022)**
2. Paul Anderson, Yifan Huang, Yuanjun Fan, Sara Qubbaj, Sinisa Coh, Qin Zhou and Claudia Ojeda-Aristizabal "Signature of multilayer graphene strain-controlled domain walls in quantum Hall effect" **Phys. Rev. B 105, L081408 (Letter) (2020)**
3. Patrick Barfield, Vinh Tran, Vikram Nagarajan, Maya Martinez, Amirari Diego, Derek Bergner, Alessandra Lanzara, James G. Analytis and Claudia Ojeda-Aristizabal "Electronic transport mechanisms in a thin crystal of the Kitaev candidate α-RuCl3 probed through guarded high impedance measurements" **Appl. Phys. Lett. 122, 243102 (2023)**
4. Ping Ai, Luca Moreschini, Ryo Mori, Drew W. Latzke, Jonathan D. Denlinger, Alex Zettl, Claudia Ojeda-Aristizabal and Alessandra Lanzara "Linearly dispersive bands at the onset of correlations in KxC60 films" **Phys. Rev. Research 5, L022042 (Letter) (2023)**
5. Ivan Pelayo, Derek Bergner, Archibald J. Williams, Jiayuwen Qi, Mahfuzun Nabi, Warren L. Huey, Ziling Deng, Luca Moreschini, Jonathan Denlinger, Alessandra Lanzara, Wolfgang Windl, Joshua Goldberger and Claudia Ojeda-Aristizabal "Coexistence of bulk type-II and surface Dirac cones in PtTe2 and PdTe2 probed through Angle Resolved Photoemission Spectroscopy (ARPES)" In Preparation
6. Master thesis dissertations by Everardo Molina (2021), Maya Martinez (2022), Derek Bergner (2023) and Patrick Barfield (2023).

Large Magneto-Electric Resistance in the Topological Dirac Semimetal α-Sn

Mingzhong Wu, Department of Physics and Department of Electric and Computer Engineering, Northeastern University, Boston, MA 02115

Keywords: Spintronics, topological materials, topological Dirac semimetals, topological surface states, and magnetoresistance

Research Scope

Explore topological surface and bulk states in topological Dirac semimetal α-Sn thin films grown by sputtering, as well as the potential applications of those topological states in spintronic devices.

Recent Progress

The spin-momentum locking of surface states in topological materials can produce a resistance that scales linearly with magnetic and electric fields. Such a bilinear magneto-electric resistance (BMER) effect offers a new approach for information reading and field sensing applications, but the effects demonstrated so far are too weak or for low temperatures. This presentation reports the first observation of BMER effects in topological Dirac semimetals; the BMER responses were measured at room temperature and were substantially stronger than those reported previously. The experiments used topological Dirac semimetal α-Sn thin films grown on

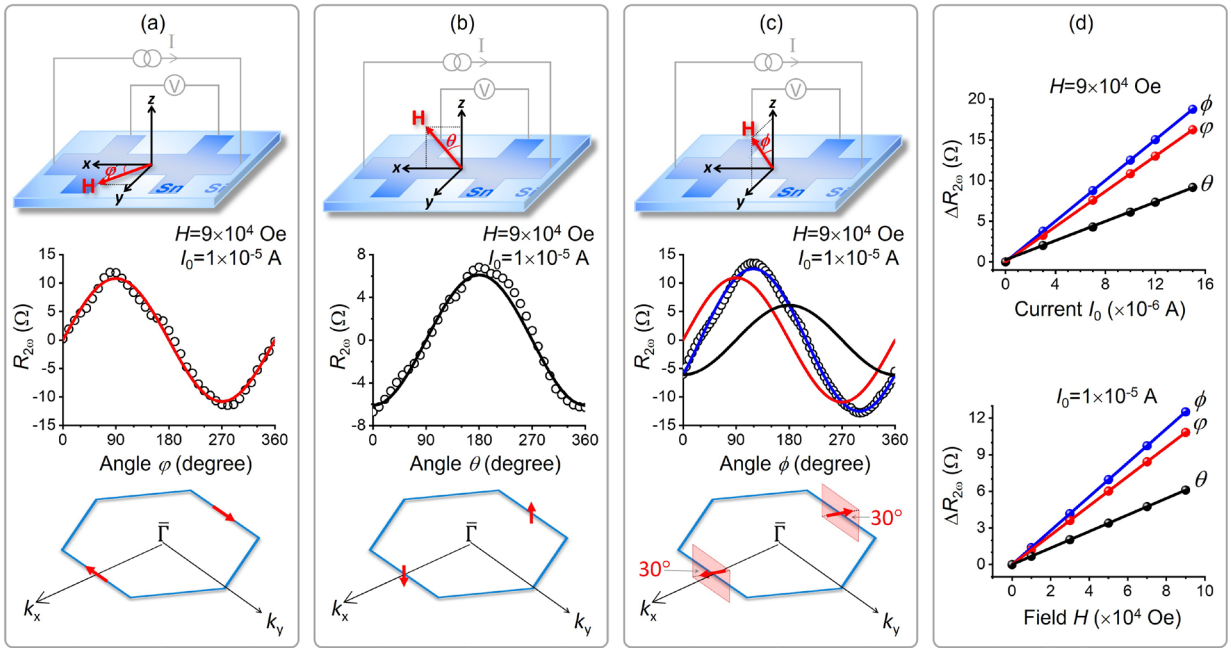

Second-harmonic resistance ($R_{2\omega}$) as a function of the magnetic field angle for a 4-nm-thick α-Sn film. The circles show the data, the curves show sinusoidal fits, and the lines show linear fits. The field strength H and the current amplitude I_0 are indicated. In (c), the red curve shows the fit in (a), and the black curve shows the fit in (b); the blue curve is the sum of the red and black curves. In (d), $\Delta R_{2\omega}$ is the amplitude of the sinusoidal $R_{2\omega}$ vs. angle response.

silicon substrates. The films showed BMER responses that are 10^6 times larger than previously measured at room temperature and are also larger than those previously obtained at low temperatures. These results represent a major advance toward realistic BMER applications. Significantly, the data also yield the first characterization of three-dimensional Fermi-level spin texture of topological surface states in α-Sn.

Future Plans

Study how the BMER varies with the film thickness, the Fermi level, and temperature, aiming at maximizing the BMER effect.

References

1. Yuejie Zhang, Vijaysankar Kalappattil, Chuanpu Liu, M. Mehraeen, Steven S.-L. Zhang, Jinjun Ding, Uppalaiah Erugu, Zhijie Chen, Jifa Tian, Kai Liu, Jinke Tang, and Mingzhong Wu, "Large magneto-electric resistance in the topological Dirac semimetal α-Sn," *Science Advances* **8**, eabo0052 (2022).

Novel Mechanism for Heat Conduction by Spin-Phonon Hybridized Excitations in a Rare-Earth Magnet

Minhyea Lee, University of Colorado Boulder

Keywords: magnetism, single crystals, rare earth compounds, thermal transport

Research Scope

Bridging theoretical spin models for exotic quantum magnetism and real materials is a central objective in modern condensed matter physics. In real materials, the crystalline lattice plays a profound role, although its impact on magnetism is often overlooked. Leveraging intense magnetic fields and inherent magnetic anisotropies, we investigate generic contributions from the underlying lattice (phonons) that are not specific to particular systems in a range of unconventional quantum magnets. This, in turn, offers a suite of experimental probes for pinning down highly sought after entangled and unconventional magnetic states. In recent work, we devised a simple description of heat conduction via hybridized quasiparticles formed by acoustic phonons and Zeeman-split spin-flip excitations. Having established the rare-earth insulating magnets as an excellent model system for investigating phonon-spin coupling, studies of novel physical phenomena involving interactions between crystal electric field splitting and phonons are in progress.

Recent Progress

Quasi 2-dimensional rare-earth (RE) delafossites (AREX_2, where A= alkali metal, RE = rare earth ions X=O, S, Se) have attracted great interest because of quantum spin-liquid-like signatures reported in neutron scattering experiments. Compared to their 3d-electron counterparts, 4f RE magnets exhibit much smaller scales of crystal electric field (CEF) splitting, of which separations are often comparable to the Zeeman splitting under moderately high magnetic field [1], and hence offer an excellent playground to search for field-induced magnetic phase transitions. We investigated thermal conductivity of $CsYbSe_2$ under magnetic field and found highly non-monotonic field dependence [Fig. 1] that can be explained by new hybridized spectra of acoustic phonons and Zeeman-split spin-flip excitations (SFEs). Such hybridization is enabled by the g-factor modulation resulting from distortion of the $YbSe_6$ octahedron [See Fig. 1**a**]. Using the dispersion and group velocity of new excitations [Fig. 1**b**], we calculate thermal conductivity in the framework of the relaxation time approximation with Debye weight [2]. Our minimalistic model captures the key features of the magneto thermal conductivity in

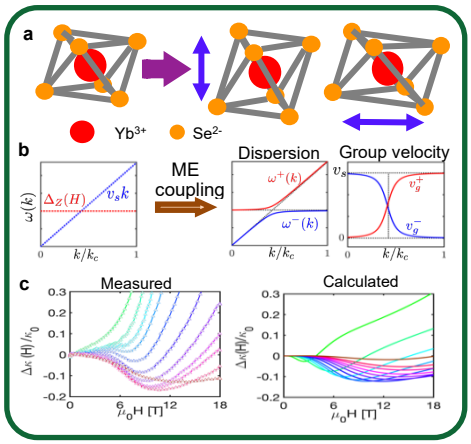

Figure 1 a. Phonon-induced distortion mediate the magnetoelastic coupling via g-factor modulation, which directly modulates Zeeman gap **b.** Acoustic phonon-SFE hybridized spectra and corresponding group velocity. **c.** Field dependence of the measured fractional thermal conductivity and calculated results using dispersion in **b**.

CsYbSe2. Our model can be applied to any system with non-zero magnetoelastic coupling in the presence of Zeeman splitting and does not depend on the details of materials. Hence it can be utilized to understand field dependence of thermal conductivity in a wide range of quantum magnets. This result was submitted and is currently under revision.

Future Plans

Encouraged by experimentally identifying a new type of spin-phonon coupling, our near future plans are to involve searching for the spectroscopic signatures of interactions between CEF spectra and other degrees of freedom, especially for spin exchange and spin-phonon interactions that can be related to thermal transport, magnetic susceptibility and heat capacity. Recently we have performed infrared spectroscopy on $CsErSe_2$ under magnetic field, as shown in Fig. 2. We find that the single-magnetic ion CEF calculation [3] agrees very well with the data, which offers a great insight: we place a particular focus on magnetic properties at the level-repulsion-free ground state energy crossing point in H || c configuration [green circle on Figure 2b]. At this crossing field, the ground state magnetization will change discontinuously (*i.e.* first-order like) and hence diverging magnetic susceptibility as a function of field. Knowing the system's small spin exchange energy sale (J_{ex} ~ 0.5 K), the transition here is likely to be placed near a critical point with enhanced magnetic frustration, potentially leading to a field-induced quantum disordered state. In order to examine this hypothesis, our investigations of the magnetic phase diagram of $CsErSe_2$ with magnetic susceptibility and heat capacity at dilution refrigerator temperature (< 100 m K) are in progress.

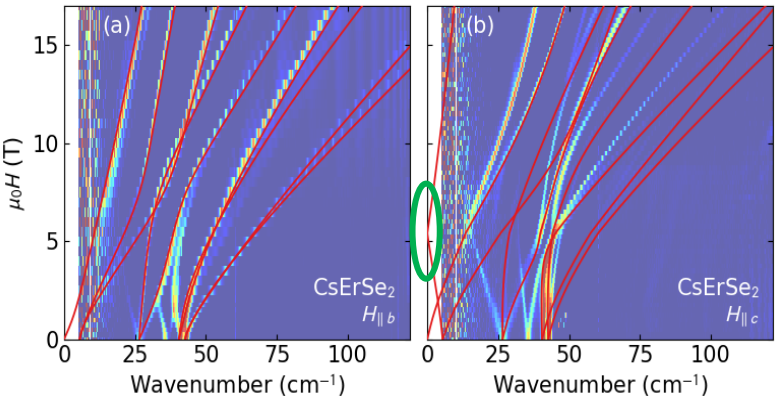

Figure 2 $CsErSe_2$ simulated single-ion CEF spectra as a function of applied field up to 18 T (red lines) overlaid with the Infra-red spectroscopy data for different field directions of H applied to the ab-plane (a) and the c-axis (b) respectively. The ground-state energy level crossing is marked on the right panel with the green ellipsoid at ~ 6.2 T.

References

1. Christopher A. Pocs, Peter E. Siegfried, Jie Xing, Athena S. Sefat, Michael Hermele, B. Nor- mand, and Minhyea Lee. "Systematic extraction of crystal electric-field effects and quantum magnetic model parameters in triangular rare-earth magnets." Phys. Rev. Res. 3, 043202 (2021).

2. R. Berman, Thermal Conduction in Solid, Oxford University Press, 1976, Oxford, UK

3. A. Scheie, V. O. Garlea, L. D. Sanjeewa, J. Xing, and A. S. Sefat. "Crystal-field Hamiltonian and anisotropy in $KErSe_2$ and $CsErSe_2$." Phys. Rev. B 101, 144432 (2020).

Publications

1. C. A. Pocs, P.E. Siegfried, J. Xie, A. S. Sefat, M. Hermele, B. Normand and Minhyea Lee, "Extracting quantum magnetic model parameters in a triangular rare-earth magnet: systematic characterization of crystal electric field effects from magnetic susceptibility and resonant torsion magnetometry", *Phys. Rev. Research* **3**, 043202 (2021)

2. K. Feng, I. A. Leahy, O. Oladehin, K. Wei, Minhyea Lee and R. Baumbach, "Magnetic ordering in $TbAuAl_4Ge_2$ and $GdAuAl_4Ge_2$: Layered compounds with triangular lanthanide nets", *J. Mag. Mag. Mater*. **564**, 170006 (2022).

3. I. A. Leahy, K. Feng, R. Dery, R. Baumbach and Minhyea Lee, "Field-induced magnetic states in the metallic rare-earth layered triangular antiferromagnet $TbAuAl_4Ge_2$", *Phys. Rev. B* **106**, 094426 (2022).

4. K. Feng, C. Bush, O. Oladehin, Minhyea Lee and R. Baumbach, "Complex Antiferromagnetic Order in the Metallic Triangular Lattice Compound $SmAuAl_4Ge_2$", Submitted (2023).

5. C. A. Pocs, I. A. Leahy, J. Xie, A. S. Sefat, M. Hermele, and Minhyea Lee, " Heat Conduction via Hybridized Quasiparticles of Acoustic Phonon and Spin-Flip Excitations in a Rare-Earth Magnet", Under Revision and to be submitted (2023).

Designing strong stability in non-critical and rare-earth-lean magnetic materials

Laura H. Lewis[1], Gregory Fiete[2], [1]College of Engineering, [2]College of Science, Northeastern University, Boston MA

George Hadjipanayis[3], Chaoying Ni[4], [3]Department of Physics and Astronomy, [4]Department of Materials Science and Engineering, University of Delaware, Newark DE

Julie B. Staunton[5], [5]Department of Physics, University of Warwick, Coventry, UK

Keywords: magnetism, polycrystalline materials, ferro/ferrimagnets, transmission electron microscopy, transition metal compounds

Research Scope

In support of a clean energy economy as well as a secure critical mineral and materials supply chain, there is great interest to develop strong rare-earth-free permanent magnets for use in advanced applications. This project seeks to delineate fundamental strategies and design principles, derived from tightly coordinated computational, theoretical, and experimental efforts to stabilize high magnetic anisotropy in non-critical and rare-earth-lean ferromagnetic materials, in bulk form. This goal is approached by examining the nanometer-scale crystal lattice condition as impacted by thermal, chemical, strain, and magnetic field energy contributions during synthesis and processing. Research is focused on two families of ferromagnetic materials that demonstrate particularly promising magnetic performance with reduced critical element content: i) chemically ordered TM-X (TM = Mn, Fe, Ni; X = Al, Pd, Pt) compounds and ii) $Sm(Fe,Co)_{12}$-based materials. This extended abstract will focus in depth on recent scientific advances for activity i) above (TM-X compounds); however, the publication list includes contributions from both activities i) and ii).

Recent Progress

Overview: Experimental progress and computational insight have been achieved towards obtaining ordered FeNi in industrially relevant timeframes and amounts. The chemically ordered form of FeNi, a meteoritic mineral known as tetrataenite, possesses a large magnetocrystalline anisotropy energy (MAE) that is a significant fraction of that of the best NdFeB supermagnets, yet contains no critical elements[1]. However, this compound is extraordinarily challenging to synthesize: extremely slow kinetics and unfavorable thermodynamic driving forces restrict its natural formation to only the most slowly cooled (~0.1 K/Myr) meteorites. Chemical order is achieved in equiatomic FeNi through a first-order nucleation-and-growth process, transforming the parent disordered fcc (A1) FeNi structure to the tetragonal ordered $L1_0$ (prototype AuCu-I)-type superlattice structure, Figure 1. The magnitude of magnetocrystalline anisotropy energy *K* of

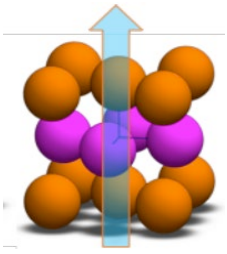

Figure 1. Unit cell of $L1_0$-type FeNi (tetrataenite) with uniaxial magnetocrys-talline anisotropy along the superlattice ordering

$L1_0$ FeNi is determined in large part by the degree of lattice crystallographic order S[2] which can vary from unity (perfect sublattice order) to zero (completely randomly occupied alloy lattice). The goal to accelerate formation of tetrataenite through increasing thermodynamic driving forces and decreasing kinetic barriers is approached by augmenting thermal energy with magnetic and strain energies during processing, using a custom-built apparatus[3]. To this end, FeNi-based samples were annealed at mild temperatures under simultaneous magnetic- and stress-field conditions for a period of 6 weeks.

Results: While detection of Fe-Ni superlattice chemical order is very challenging using standard X-ray and neutron diffraction methods, it can be clearly resolved, albeit with little information on spatial extent or distribution, using Mössbauer spectroscopy. To this end, processed specimens were examined with simultaneous conversion X-ray and backscattered γ-ray ^{57}Fe Mössbauer spectroscopy (CXMS); additionally, meteorite-derived tetrataenite was also studied with CXMS to provide Mössbauer fitting parameters for data analysis. Results provided quantification of up to 22 vol% of the tetragonal tetrataenite phase in the magnetic- and strain-field-processed samples, with the remainder identified as the cubic disordered FeNi alloy[4]. In contrast, all precursor samples consist only of the cubic FeNi alloy; data are summarized in Figure 2. The $L1_0$ phase hyperfine magnetic field distributions obtained from the synthetic tetrataenite spectra are wider than that of the meteorite, indicating that the degree of induced chemical order is low. This conclusion is corroborated by the low measured magnetocrystalline anisotropy energy. Furnishing independent verification of these results, transmission electron microscopy (TEM) and *in-situ* TEM experiments have also identified regions of atomic order in these processed specimens, Figure 3.

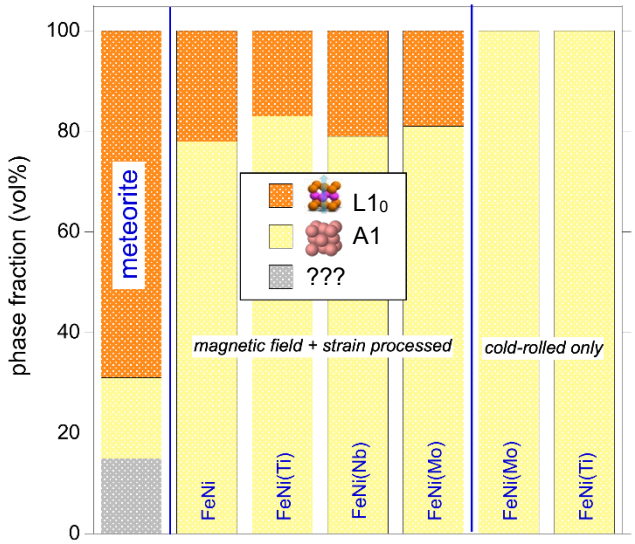

Figure 2. Quantification of phase fractions in FeNi synthetic and natural materials.

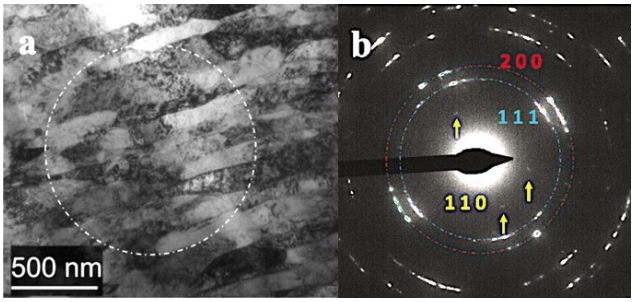

Figure 3. a) TEM image of annealed FeNi sample. b) SAED in the area circled in Fig 3a.

Complementing and informing experimental efforts on magnetism and ordering in TM-X compounds, a first-principles-based holistic approach for modeling atomic ordering in rare-earth-free, multi-component ferromagnetic alloys and associated

magnetocrystalline anisotropy energy was applied to unequivocally confirm that the state of the magnetic order has a profound impact on the nature of predicted chemical order. For example, it is noted that $L1_0$ atomic ordering of Fe and Ni, necessary for high MAE in FeNi and in elementally modified compounds $Fe_{50}Ni_{50-y}X_y$ (X=Pt, Pd, Al, P), is only obtained when the materials are in their ferromagnetic state. These results confirm that annealing FeNi-based samples in an applied magnetic field should promote desired chemical ordering by altering the magnetic state of the material, as was indeed experimentally validated. Most interestingly – and extremely relevant to the objectives of this program – often the addition of light, unconstrained elements (such as Al) provide the greatest MAE enhancement. In parallel, computational methods were applied to investigate intriguing disconnects between reported experimental and computational linkages between FeNi's atomic order parameter S and resultant magnetocrystalline anisotropy energy K. This work confirms that decreasing long-range order consistently decreases the predicted MAE (Figure 4 (left)), a result in agreement with experiment as well as with computational reports from other research groups, providing confidence in our method and approach. The computed uniaxial anisotropy constant K of $L1_0$-type FeNi is found to remain robust to high temperatures. Figure 4 (right) depicts the computed increase in K as a function of order parameter S for two FeNi compositions. Also included in Figure 4 (right) is the reported anisotropy constant for a $L1_0$-type FeNi thin film of $S = 0.60$[5], represented by the green dot. Additionally, for the first time for this system, the dominant MAE coefficients K_1 and K_2 that contribute to the overall anisotropy energy K have been calculated for finite temperatures and imperfect chemical order. Discrepancies between computation and experiment for these investigations confirm the existence of factors contributing to MCA in ordered FeNi that are yet to be discovered.

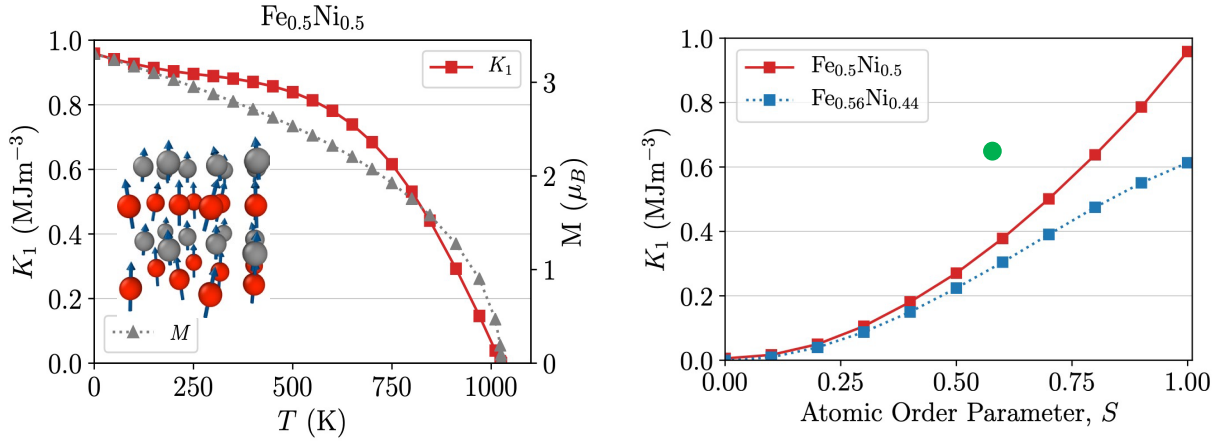

Figure 4. (left) Finite-temperature calculation of the magnetocrystalline anisotropy constant K and the magnetic moment M for equiatomic $L1_0$-type FeNi. (right) Magnetocrystalline anisotropy constant for two different com-positions of $L1_0$-type FeNi as a function of lattice order parameter S. It can be seen that the computed value of K is much smaller than the experimental value reported by Shima *et al.* [5] for a thin film form, represented by the green data marker.

Future Plans

Overall, these results shed light on the subtlety of magnetic anisotropy in this system and suggest routes for improving its hard magnetic properties during synthesis. Future efforts will seek to determine origins of these effects and how combined magnetic and strain energies alter the Fe-Ni thermodynamic landscape. It is recognized that magnitude of the magnetic field applied during the described thermal treatment step is much too small to produce an appreciable Zeeman energy; therefore some other factor(s) must be in play. Preliminarily it is contemplated that these external energies alter the structure and arrangement of the exchange-split 3*d* bands and impact the electronic free energy of the system. Elucidation of the origins of these effects will suggest targeted refinements to the processing conditions of FeNi that will foster greater atomic order and increased magnetocrystalline anisotropy, leading to an enhanced magnetic energy product. Highlighted outcomes include postulated anisotropy contributions attributed to a nanocrystalline microstructure as well as the potential for realization of yet-larger magnetocrystalline anisotropy in well-ordered synthetic samples.

References

1. L. H. Lewis, A. Mubarok, E. Poirier, N. Bordeaux, P. Manchanda, A. Kashyap, R. Skomski., J. Goldstein, F. E. Pinkerton, R. K. Mishra, and R. C. Kubic Jr., *Inspired by Nature: Investigating Tetrataenite for Permanent Magnet Applications*, Journal of Physics: Condensed Matter **26,** 064213 (2014).

2. S. S. A. Razee, J. B. Staunton, B. Ginatempo, F. J. Pinski, and E. Bruno, *Ab Initio Theoretical Description of the Interrelation between Magnetocrystalline Anisotropy and Atomic Sshort-Range Order*, Phys. Rev. Lett. **82**, 5369 (1999).

3. N. Maât, I. McDonald, R. Barua, B. Lejeune, X. Zhang, G. M. Stephen, A. Fisher, D. Heiman, I. V. Soldatov, R. Schäfer, and L. H. Lewis, *Creating, Probing and Confirming Tetragonality in Bulk FeNi Alloys*, Acta Materialia **196** 776 (2020).

4. L. H. Lewis and P. Stamenov, *Accelerating Nature: Induced Atomic Order in Equiatomic FeNi,* Advanced Science, in review.

5. T. Shima, M. Okamura, S. Mitani, and K. Takanashi, *Structure and Magnetic Properties for $L1_0$-ordered FeNi Films Prepared by Alternate Monatomic Layer Deposition,* J. Magn. Magn. Mat. **310**, 22213 (2007).

Publications

1. C. D. Woodgate, D. Hedlund, L. H. Lewis, J. B. Staunton, *Interplay Between Magnetism and Short-Range Order in Ni-Based High-Entropy Alloys: CrCoNi, CrFeCoNi, and CrMnFeCoNi*, Physical Review Materials **7**, 053801 (2023).

2. A. M. Gabay, C.-Y. Han, C.-Y. Ni, G. C. Hadjipanayis, *Re-investigation of High-Temperature Phase Equilibria in Fe-rich Sm–Fe–Ti Alloys*, Journal of Alloys and Compounds **947**, 169520 (2023).

3. A. M. Gabay, C.-Y. Han, C.-Y. Ni, G. C. Hadjipanayis, *Assessment of Directionally Solidified Eutectic Sm–Fe(Co)–Ti Alloys as Permanent Magnet Materials*, IEEE Transactions on Magnetics, accepted.

4. C. Han, B.T. Lejeune, X. Zhang, C. Ni, L.H. Lewis, *$L1_0$ Ordering in MnAl and FeNi Influenced by Magnetic Field and Strain,* Microscopy and Microanalysis **29** (Suppl 1), 1346 (2023).

5. C. Han, A.M. Gabay, C.-Y. Ni, G. C. Hadjipanayis, *Structural Characteristics and Phase Evolution of Calcium-reduced $(Sm,Zr)(Fe,Co,Ti)_{12}$ Particles*, Microscopy and Microanalysis **29** (Suppl 1), 1328 (2023).

6. A.M. Gabay, C. Han, C.-Y. Ni, G. C. Hadjipanayis, *Phase Equilibria in Iron-Rich Sm–Fe–Ti and Sm–(Fe,Co)–Ti Alloys at 1100–1200 °C,* Journal of Alloys and Compounds **965,** 171444 (2023).

Magneto-optical Study of Correlated Electron Materials in High Magnetic Fields

Principal Investigator: Dmitry Smirnov[1]; Co-PI: Zhigang Jiang [2]

[1] National High Magnetic Field Laboratory, Tallahassee, FL 32310

[2] Georgia Institute of Technology, Atlanta, GA 30332

Keywords: General: magnetism, topology, 2D exciton and light-matter phenomena, **Material Forms:** single crystals, 2D and layered crystals, thin film heterostructures, **Material Classes:** topological materials, transition metal compounds, antiferromagnets, semiconductors, **Techniques:** optical spectroscopy, transport

Research Scope

This program is aimed at studying electronic structure, low-energy excitations, and many-body effects in novel quantum materials via high-field magneto-optical spectroscopy. The current research is mostly focused on the spectroscopy of the exotic quantum states and excitations in quantum magnets. We also continue optical spectroscopy studies of Dirac and Weyl fermions in topological materials and excitonic states in atomically-thin van der Waals semiconductors.

Recent Progress

Disorder-Enriched Magnetic Excitations in a Heisenberg-Kitaev Quantum Magnet $Na_2Co_2TeO_6$ (Xiang *et al.* Phys. Rev. Lett. **131**, 076701 (2023))

Kitaev-type quantum spin liquid (QSL) systems have become one of the central themes of today's condensed matter physics as a potential platform for realization of exotic states with fractionalization of quantum spins into Majorana fermions, which is of particular interest to the quantum computing community. Because of the essential role of spin-orbit coupling (SOC), most of research on Kitaev QSL has been focused on candidate systems with heavy 4*d* or 5*d* ions, like the most studied case of α-$RuCl_3$. Recent theoretical studies recognized another promising avenue, 3*d* Co-based honeycomb-structure compounds with effective pseudospin 1/2 [1]. Among them, Co-based honeycomb $Na_2Co_2TeO_6$ with antiferromagnetic (AFM) ordering below T_N = 25 K has been recently proposed to host a magnetic-field induced quantum-spin disordered state within a complex temperature-field (T-B) phase diagram [2].

We have performed a systematic optical magneto-spectroscopy study of single-crystal $Na_2Co_2TeO_6$ to probe the magnetic excitations in a broad magnetic field range at low temperatures. Our far-infrared absorption and electron spin resonance (ESR) experiments reveal a multitude of in-plane excitation modes across the AFM to spin-polarized (SP) magnetic phases (Fig.1). The measurements with polarized light provide strong evidence that the multiple high-field in-plane magnetic excitations are one-magnon in nature. This is in sharp contrast to the expectation for a pristine sample: the four Co atoms in the unit cell support a maximum of four magnon branches in

the SP state and practically only one dominant optically-active mode is expected. These expectations are satisfied for α-$RuCl_3$, but apparently not for $Na_2Co_2TeO_6$.

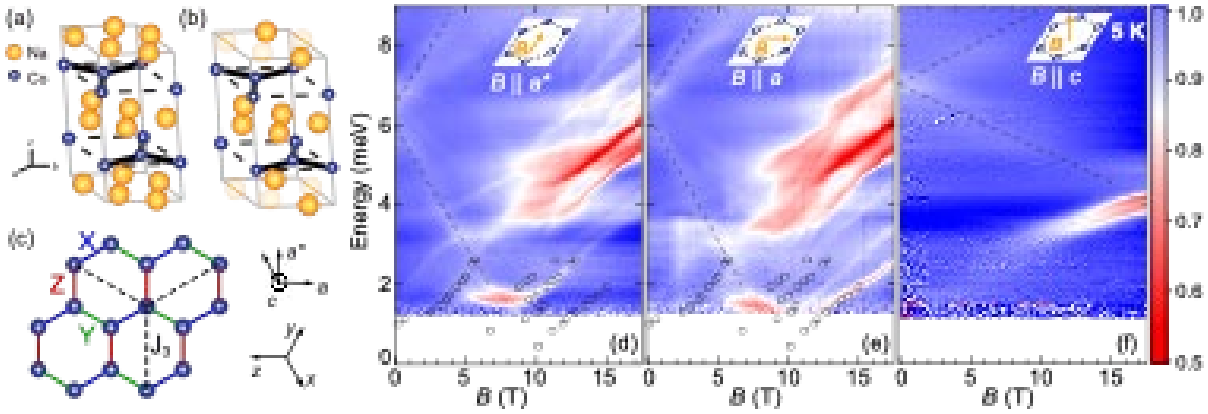

Figure 2: (a) Average crystal structure of $Na_2Co_2TeO_6$ with each Na site 2/3 occupied; Te and O atoms are omitted for clarity. (b) Representative structure showing Na-occupation disorder. (c) Honeycomb lattice of Co^{2+} ions with nearest neighbor *X*, *Y*, *Z* and third neighbor J_3 bonds indicated. Crystallographic (*a,a*,c*) and cubic (*x,y,z*) coordinates are shown. (d)–(f) Normalized magneto-transmission measured on single-crystal $Na_2Co_2TeO_6$ at T=5 K with $B \parallel a$ (d), $B \parallel a^*$ (e), and $B \parallel c$ (f). Black circles are excitation modes extracted from the ESR spectra measured on $Na_2Co_2TeO_6$ powder samples.

These findings are explained within a microscopic theoretical model that takes into account intrinsic Na disorder (i.e. contributions from different possible Na occupancies). The model takes into account different unique possible Na occupancies, one of which is depicted in Fig. 1(b). At first consideration, one might expect disorder in the interlayer Na atoms to have little impact on the Co crystal fields. However, the SOC in *3d* Co is relatively weak, which makes the local magnetic couplings strongly dependent on the relative locations of the Na atoms around each Co. The random couplings lead to a significant distribution of the excitation energies over several meV, which is compatible with the experimental observations. The nearest neighbor interactions are found to be considerably smaller than previous estimates as well as compared to dominant third neighbor interactions, which do not have bond-orientation dependence.

Our results not only provide the new information on exotic magnetic excitations in $Na_2Co_2TeO_6$ and reveals a key role of Na-occupation disorder. In a more general context, our work outlines the fragility of spin-orbit moments in 3*d* Co-based honeycomb-structure materials and further emphasizes the necessity to consider disorder in the spin environment in the search for practicable materials potentially hosting Kitaev QSL states.

Anomalous temperature evolution of the Dirac band in $ZrTe_5$ across topological phase transition (Jiang *et al.* Phys. Rev. B **108**, L041202 (2023) (Editors' Suggestion Letter))

Zirconium pentatelluride ($ZrTe_5$) is a van der Waals material with the layer stacking direction along the *b* axis of the crystal. The recent interest in $ZrTe_5$ originates from the theoretical prediction of a room-temperature quantum spin Hall insulator phase in its monolayer limit and a three-dimensional topological insulator (TI) phase in its bulk form. The prediction has sparked intensive

experimental investigations into both the electronic and topological properties of $ZrTe_5$. However, different topological phases, i.e. weak or strong TIs (WTI or STI) and Dirac or Weyl semimetals, have all been reported in $ZrTe_5$ from different experiments. Such a discrepancy may result from the sensitive dependence of the topological phase on the lattice constants. In addition, many theoretical calculations have predicted that volume expansion can result in a topological phase transition (TPT) in $ZrTe_5$, featuring a band gap closure and then reopening across the TPT. These results invite controllable measurements across the TPT to reconcile the experimental observations.

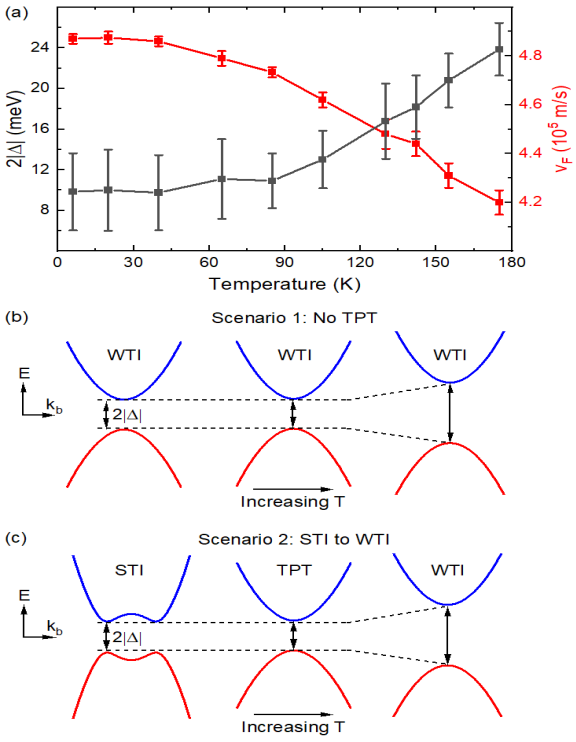

Figure 2: (a) Temperature dependence of the extracted Fermi velocities and band gaps of $ZrTe_5$ from LL spectroscopy measurements. (b,c) Schematic drawings of the band structure evolution as a function of temperature for two possible scenarios that can describe our experimental results.

In our work, we examine the temperature evolution of the Dirac band in semiconducting $ZrTe_5$ using magnetoinfrared spectroscopy, which can directly probe the band structures of different carriers with high accuracy by tracing their Landau level (LL) transitions. Specifically, we find that the band gap of $ZrTe_5$ is temperature independent at low temperatures and increases with temperature at elevated temperatures (Fig. 2(a)). Although such an observation seems to support a WTI phase at all temperatures (Fig. 2(b)) and defy the previously reported TPT at an intermediate temperature in $ZrTe_5$, we show that it is also possible to explain the observation by considering the effect of conduction-valence band mixing and band inversion with a STI phase at low temperatures (Fig. 2(c)). The key to distinguishing these two scenarios is to identify the topological phase of $ZrTe_5$ at the base temperature. Based on our previous works [3,4], where we demonstrate a STI phase in $ZrTe_5$ at low temperatures, we lean to the second scenario (Fig. 2(c)) as the plausible picture.

Future Plans

We will continue to apply high-field optical magneto-spectroscopy to probe and understand electronic states and low-energy excitations in novel quantum materials. One of the near-future goals is to complete the Raman spectroscopy study of Co crystal field excitations in $Na_2Co_2TeO_6$ and related systems. Other directions of ongoing or planned research and the systems of interest include quantum magnets with a honeycomblike spin lattice, for example, $Ba_2Ni(PO_4)_2$ and $Na_3Co_2SbO_6$. We will continue magneto-spectroscopy studies of optically excited states and many-body effects in atomically-thin 2D semiconductors with strong SOC and their parent van der Waals crystals.

References

1. H. Liu and G. Khaliullin, *Pseudospin exchange interactions in d^7 cobalt compounds: Possible realization of the Kitaev model*, Phys. Rev. B **97**, 014407 (2018)
2. G. Lin, J. Jeong, C. Kim, Y.Wang, Q. Huang, T. Masuda, S.Asai, S. Itoh, G. Günther, M. Russina, Z. Lu, J. Sheng, L. Wang, J. Wang, G. Wang, Q. Ren, C. Xi, W. Tong, L. Ling, Z. Liu, L. Wu, J. Mei, Z. Qu, H. Zhou, J.-G. Park, Y. Wan, J. Ma, *Field-induced quantum spin disordered state in spin-1/2 honeycomb magnet $Na_2Co_2TeO_6$* , Nat. Commun. **12**, 5559 (2021)
3. Y. Jiang, J. Wang, T. Zhao, Z. L. Dun, Q. Huang, X.S. Wu, M. Mourigal, H.D. Zhou, W. Pan, M. Ozerov, D. Smirnov, Z. Jiang, *Unraveling the Topological Phase of $ZrTe_5$ via Magnetoinfrared Spectroscopy*. Physical Review Letters. **125**, 046403 (2020).
4. J. Wang, Y. Jiang, T. Zhao, Z. L. Dun, A. L. Miettinen, X.S. Wu, M. Mourigal, H.D. Zhou, W. Pan, D. Smirnov Z. Jiang, *Magneto-transport evidence for strong topological insulator phase in $ZrTe_5$*, Nature Communications **12**, 6758 (2021)

Publications

[1] L. Xiang, R. Dhakal, M. Ozerov, Y. Jiang, B. S. Mou, A. Ozarowski, Q. Huang, H. Zhou, J. Fang, S. M. Winter, Z. Jiang, D. Smirnov, *Disorder-Enriched Magnetic Excitations in a Heisenberg-Kitaev Quantum Magnet $Na_2Co_2TeO_6$*, Phys. Rev. Lett. **131**, 076701 (2023)

[2] Y. Jiang, T. Zhao, L. Zhang, Q. Chen, H. Zhou, M. Ozerov, D. Smirnov, Z. Jiang, *Revealing temperature evolution of the Dirac band in $ZrTe_5$ via magnetoinfrared spectroscopy*, Phys. Rev. B **108**, L041202 (2023) (Editor's Suggestion Letter)

[3] Y. Jiang, M. Ermolaev, G. Kipshidze, S. Moon, M. Ozerov, D. Smirnov, Z. Jiang, S. Suchalkin, *Giant g-factors and fully spin-polarized states in metamorphic short-period InAsSb/InSb superlattices*, Nature Communications **13**, 5960 (2022)

[4] Y. Jiang, M. Ermolaev, S. Moon, G. Kipshidze, G. Belenky, S. Svensson, M. Ozerov, D. Smirnov, Z. Jiang, S. Suchalkin, *g-factor engineering with InAsSb alloys toward zero band gap limit*, Phys. Rev. B, accepted as a Letter

[5] D. Chen, Z. Lian, X. Huang, Y. Su, M. Rashetnia, L. Ma, L. Yang, M. Blei, L. Xiang, T. Taniguchi, K. Watanabe, S. Tongay, D. Smirnov, Z. Wang, C. Zhang, Y. Cui, S. Shi, *Excitonic insulator in a heterojunction moire superlattice,* Nature Physics **18**, 1171 (2022)

[6] W. Zheng, L. Xiang, F.A. de Quesada, Z. Lu, M. Wilson, A. Sood, F. Wu, D. Shcherbakov, S. Memaran, R. Baumbach, G.T. McCanfless, J.Y. Chan, S. Liu, J.H. Edgar, C.H. Lui, E.J.G. Santos, A. Lindenberg, D. Smirnov, L. Balicas, *Thickness- and Twist-Angle-Dependent Interlayer Excitons in Metal Monochalcogenide Heterostructures*, American Chemical Society Nano **16**, 18695 (2022)

[7] X. Wang, J. Cao, H. Liang, Z. Lu, A. Cohen, A. Haldar, H. Kitadai, Q. Tan, K.S. Burch, D. Smirnov, W. Xu, S. Sharifzadeh, L. Liang, X.I. Ling, *Electronic Raman scattering in the 2D antiferromagnet $NiPS_3$*, Science Advances, 8 (2), eabl7707 (2022)

[8] A. Ramanathan, J. Kaplan, D.-C. Sergentu, J.A. Branson, M. Ozerov, A.I. Kolesnikov, S.G. Minasian, J. Autschbach, J.W. Freeland, Z. Jiang, M. Mourigal, H.S. La Pierre, *Chemical design of electronic and magnetic energy scales of tetravalent praseodymium materials*, Nature Communications **14**, 3134 (2023)

[9] H. Zhang, C.K. Xing, K. Noordhoek, Z. Liu, T.H. Zhao, L. Horák, Q. Huang, L. Hao, J. Yang, S. Pandey, E. Dagotto, Z. Jiang, J.-H. Chu, Y. Xin, E.S. Choi, H.D. Zhou, J. Liu, *Anomalous magnetoresistance by breaking ice rule in $Bi_2Ir_2O_7/Dy_2Ti_2O_7$ heterostructure*, Nature Communications **14**, 1404 (2023)

[10] V.S. Prudkovskiy, Y.R. Hu, K. Zhang, Y. Hu, P. Ji, G. Nunn, J. Zhao, C. Shi, A. Tejeda, D. Wander, A. De Cecco, C.B. Winkelmann, Y. Jiang, T. Zhao, Z. Jiang, L. Ma, C. Berger, W.A. de Heer, *An epitaxial graphene platform for zero-energy edge state nanoelectronics,* Nature Communications **13**, 7814 (2022)

Oral Session 4

Geometry and frustration-induced phenomena in nanomagnet arrays

Principal Investigator: Peter Schiffer, Yale University, New Haven, CT 06520

Keywords: Magnetism, Topology, Nanostructures, Ferromagnets, Scanning Probe Microscopy

Research Scope

This program encompasses studies of lithographically fabricated "artificial spin ice" arrays of nanometer-scale single-domain ferromagnetic islands in which the array geometry results in frustration of the interactions between the islands. Artificial spin ice offers a wide range of opportunities for studying the mechanism by which nature accommodates frustration. Since the arrays are created lithographically, we can easily vary the array characteristics, including the geometry of the lattice, the nature of the moments, and the level and type of lattice disorder. We can probe the local properties of the arrays by imaging individual moments, and we can also probe thousands of moments simultaneously, allowing us to gain insight into the collective properties of the system and observe novel phenomena that are not accessible in other systems [1].

This research program focuses on the properties of these systems, probing the collective behavior of different geometries, and exploring arrays of more complex nanomagnet shapes. Specific thrusts include examinations of new lattice geometries, low-frequency dynamics of the moments, finite size effects in smaller arrays, and magnetic moments that are not simple dipoles. The research program uses permalloy as the ferromagnetic material, taking advantage of its well-understood magnetic properties and low magnetocrystalline anisotropy.

Recent Progress

The past two years of this program have included several projects, exploring a wide range of physics within different artificial spin ice systems [2-9]. All work has been done in close collaboration with the groups of Chris Leighton at the University of Minnesota and Cristiano Nisoli at Los Alamos National Laboratory, as well as a collaboration with the group of Scott Crooker at Los Alamos National Laboratory. Much of the work has also involved x-ray magnetic circular dichroism – photoemission electron microscopy (XMCD-PEEM) data-taking at the Advanced Light Source. In this abstract, we describe three of the recent projects: topologically complex thermally excited strings in the Santa Fe ice lattice, collective behavior of a new magnetic object with six possible moment states, and entropy-driven ordering in Tetris ice.

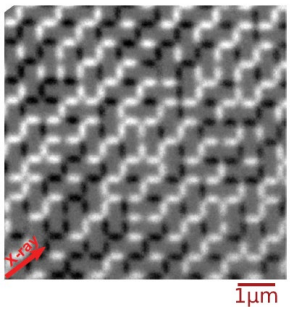

Left: XMCD-PEEM image of Santa Fe Ice moments, where the black and white colors indicate the moment directions. **Below:** Illustration and taxonomy of various string motions, where the strings are formed of local magnetic excitations. Island moments are shown as arrows, and the flipped moments as solid arrows. (Top) Trivial string motions. (Bottom) Nontrivial string motions. The tables list the motions illustrated.

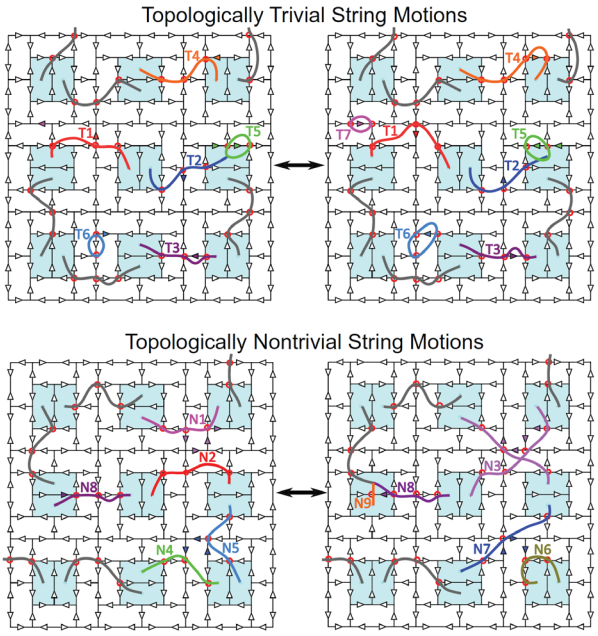

Topologically trivial motions	
Wiggle	Energy increase (T1)
	Energy decrease (T1)
	No energy change (T2,T3)
Grow (T4)	
Shrink (T4)	
Loop	Wiggle (T5)
	Grow (T6)
	Shrink (T6)
	Creation (T7)
	Annihilation (T7)

Topologically nontrivial motions	
Merge (N1,N2→N3)	
Split (N3→N1,N2)	
Reconnection (N4,N5↔N6,N7)	
Adjacent reconnection (N8)	
Strings on adjacent interior plaquette	Creation (N9)
	Annihilation (N9)

Topological Kinetic Crossover in Santa Fe Ice: Artificial spin ice arrays can be designed so that the frustration arises from the location of the excitations among the vertices, leading to a range of exotic behavior. We have studied one such vertex-frustrated lattice, dubbed Santa Fe Ice. Our previous work demonstrated that the disordered magnetic state is naturally described within a framework of thermally activated emergent strings [4]. Our new results demonstrate a crossover temperature between two kinetic regimes, visible from real-space XMCD-PEEM data [8]. At high temperature, all types of string motions are observed. Below the crossover, however, the kinetics is almost entirely limited to topologically trivial moves of the strings, and the system cannot explore the full phase space of magnetic moment configurations. Because of the topological nature of strings, the entirety of the possible configurations of the system can be partitioned into topological sectors, each one pertaining to specific configurations. These sectors are the so-called 'homotopy classes" for the strings, an important mathematical construct in the study of topology. Above our crossover temperature, the system can cut between these homotopy classes. Below the crossover temperature, however, changes to string topology are suppressed. Despite still fluctuating thermally, the system thus tends to stay in a specific sector, or homotopy class. These results explicitly demonstrate how system topology can break ergodicity, an underlying assumption of thermodynamics.

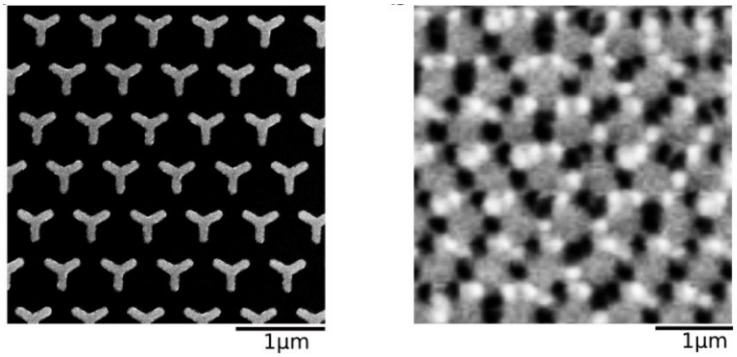

SEM and MFM images of magnetic tripod ice.

Collective behavior of magnetic tripods: Previous studies of artificial spin ice have focused on stadium-shaped islands or nanowires whose magnetization can be described by Ising-like binary moments. A few studies have looked at effective XY and quadrupolar moments by altering the island shape – but always staying within paradigms of types of moments that have been studied in atomic magnetic systems. In our group's recent work, we created a new object, a magnetic tripod, that has three-fold symmetry with six possible magnetic states [9]. We explore its collective behavior by realizing interacting triangular arrays of these objects which individually map well onto theoretical models for Potts or clock states. To our knowledge there has been no prior experimental realization of a 6-state object of this nature, and certainly no realization of interacting arrays of such objects. After thermalizing these arrays, which we have named " magnetic tripod ice", we demonstrate collective ferromagnetic behavior that has qualitative differences with the well-studied kagome ice system of similar geometry. We thus demonstrate the importance of the tripod moment as an emergent variable.

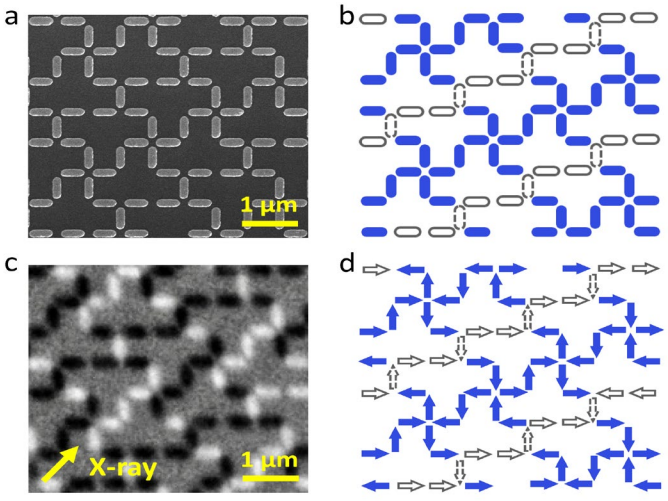

a. Scanning electron microscopy image of nanomagnet array with tetris ice structure. **b.** Schematic showing the two stripes of nanomagnet islands (ordered and disordered in blue and grey, respectively). **c.** XMCD-PEEM image of the nanomagnet array from the Advanced Light Source. The islands that have a magnetization component along (opposite to) the X-ray direction yield black (white) contrast. **d.** Magnetic moment configuration map corresponding to (c).

Entropically-induced ordering in Tetris ice: Long-range ordering is generally understood to occur at low energies to optimize the energetics of interactions among the constituents of a system. As a system lowers its energy, it also lowers its entropy, and ordered systems generally have zero residual entropy. By contrast, "entropy-driven" order can occur under very special circumstances, where increasing entropy in one aspect of a system can lead to ordering in another. We have found such entropy-induced ordering in vertex-frustrated tetris artificial spin

ice [6]. In this system, one subset of magnetic moments orders globally, driven by maximizing entropy in the other subset. We demonstrate these results via synchrotron-based x-ray circular magnetic dichroism photoemission electron microscopy measurements of the moments in a tetris array. Monte Carlo simulations confirm that ordering is driven by entropic effects rather than energetics.

Future Plans

Our immediate future plans are to study the physics of other lattices of magnetic tripods, which should reveal interesting physics associated with the objects' unusual symmetry. We also are looking at the low frequency dynamics of artificial spin ice through various time-dependent measurements. Finally, we are continuing investigations of novel topological effects in these systems.

References and Publications

1. "Artificial spin ice: Paths forward", Peter Schiffer and Cristiano Nisoli, Applied Physics Letters **118**, 110501 – 1-6 (2021).

2. "Field-Induced Magnetic Monopole Plasma in Artificial Spin Ice", M. Goryca, X. Zhang, J. Li, A. L. Balk, J. D. Watts, C. Leighton, C. Nisoli, P. Schiffer, and S. A. Crooker, Physical Review X **11**, 011042 – 1 - 11 (2021).

3. "Experimental Realization of the 1D Random Field Ising Model", N. S. Bingham, S. Rooke, J. Park, A. Simon, W. Zhu, X. Zhang, J. Batley, J. D. Watts, C. Leighton, K. A. Dahmen, and P. Schiffer, Physical Review Letters **127**, 207203 – 1-6 (2021).

4. "String Phase in an Artificial Spin Ice", Xiaoyu Zhang, Ayhan Duzgun, Yuyang Lao, Shayaan Subzwari, Nicholas S. Bingham, Joseph Sklenar, Hilal Saglam, Justin Ramberger, Joseph T. Batley, Justin D. Watts, Daniel Bromley, Rajesh V. Chopdekar, Liam O'Brien, Chris Leighton, Cristiano Nisoli and Peter Schiffer Nature Communications **12**, 6514 – 1-7 (2021).

5. "Magnetic field dependent thermodynamic properties of square and quadrupolar artificial spin ice", M. Goryca, X. Zhang, J. D. Watts, C. Nisoli, C. Leighton, P. Schiffer, and S. A. Crooker, Physical Review B **105**, 094406 – 1-11 (2022).

6. "Entropy-driven order in an array of nanomagnets", Hilal Saglam, Ayhan Duzgun, Aikaterini Kargioti, Nikhil Harle, Xiaoyu Zhang, Nicholas S. Bingham, Yuyang Lao, Ian Gilbert, Joseph Sklenar, Justin D. Watts, Justin Ramberger, Daniel Bromley, Rajesh V. Chopdekar, Liam O'Brien, Chris Leighton, Cristiano Nisoli and Peter Schiffer, Nature Physics **18**, (2022).

7. "Collective Ferromagnetism of Artificial Square Spin Ice", N. S. Bingham, X. Zhang, J. Ramberger, O. Heinonen, C. Leighton, and P. Schiffer, Physical Review Letters **129**, 067201 (2022).

8. "Topological Kinetic Crossover in a Nanomagnet Array", Xiaoyu Zhang, Grant Fitez, Shayaan Subzwari, Nicholas S. Bingham, Ioan-Augustin Chioar, Hilal Saglam, Justin Ramberger, Chris Leighton, Cristiano Nisoli, and Peter Schiffer, Science, **380**, 526-531 (2023).

9. "Artificial Magnetic Tripod Ice", Xiaoyu Zhang, Ioan-Augustin Chioar, Grant Fitez, Anthony Hurben, Michael Saccone, Nicholas S. Bingham, Justin Ramberger, Chris Leighton, Cristiano Nisoli, and Peter Schiffer, Physical Review Letters **in press** (2023).

Broken Symmetries for Control of Electrically-Generated Spin Currents and Torques

Dan Ralph, Cornell University

Keywords: spintronics, thin film heterostructures, ferromagnets, antiferromagnets

Research Scope

The focus of this project is to understand mechanisms for controlling the direction of the spin polarization within electrically-generated spin currents. Strategies for coupling electric fields and spin currents are of both fundamental interest (e.g., they can arise from spin Berry curvature in topological materials) and practical interest because such spin currents can exert spin-transfer torques to drive efficient magnetic switching in magnetic memory technologies. Previous studies of electrically-induced spin currents have focused on samples made from high-symmetry heavy metals or topological insulators, in which the direction of spin polarization is constrained by symmetry to lie strictly in-plane and perpendicular to the applied electric field. This "conventional" orientation can drive efficient magnetic switching for samples with in-plane magnetic anisotropy, but it is inefficient for switching nanoscale samples with perpendicular magnetic anisotropy (PMA) that are required for high-density magnetic memory applications. For switching of nanoscale PMA samples, an important goal of the spintronics field is to generate unconventional spin currents that flow in the out-of-plane direction with a strong component of spin polarization perpendicular to the plane (Fig. 1). This orientation enables such spin currents to apply out-of-plane torques that should be far more efficient for switching PMA samples – by a factor of approximately 100 – compared to in-plane torques. The generation of electrically-induced spin currents with this type of unconventional direction of spin polarization requires spin-source materials with reduced symmetry, which can be achieved in principal by, e.g., using materials with low crystalline symmetry, ferromagnetic order, or antiferromagnetic order.

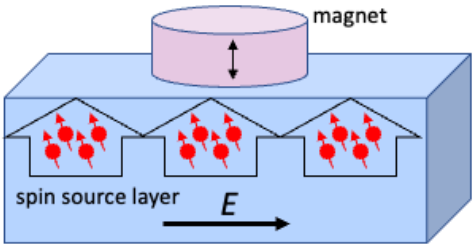

Fig. 1. Goal: Spin-source layers in which an electric field generates an upward-flowing spin current with a strong out-of-plane component of spin polarization.

Recent Progress

I will report measurements of electrically-induced spin currents generated by two rutile materials with tetragonal crystal symmetry, IrO_2 and RuO_2 (references 1, 2). When these materials are grown in thin films for which the growth direction is along one of the crystal axes (e.g., a (001) or (100) orientation), by symmetry the electrically-generated spin polarization is constrained to point in only the conventional direction, in plane and perpendicular to the electric field. However, by implementing a growth direction tilted away from a crystal axis (e.g., a (101) or (111) orientation), this symmetry constraint is relaxed for a tetragonal material, and in theory other

components of spin polarization can be produced in either or both the out-of-plane direction and an unconventional in-plane direction (parallel to the electric field). IrO_2 and RuO_2 have the same crystal structures but IrO_2 is non-magnetic while RuO_2 is a collinear antiferromagnet with a Néel vector along the [001] axis. The comparison between the two materials therefore allows a comparison of the spin currents generated with and without the additional lowering of symmetry provided by antiferromagnetic order. We find that appropriately-tilted IrO_2 films can produce unconventional spin-polarizations in both the in-plane and out-of-plane directions, consistent with the constraints allowed by symmetry, but the out-of-plane spin component is about a factor of 10 weaker than predicted by density functional theory calculations. Appropriately-tilted antiferromagnetic RuO_2 films can produce a considerably stronger component of out-of-plane spins, with a spin-vector orientation closely parallel to the antiferromagnetic Néel vector. This suggests that the mechanism of spin-current generation in RuO_2 is not spin-orbit coupling, but a recently-proposed mechanism related to a spin-split band structure induced by the antiferromagnetic order in RuO_2.[3]

The experiments for both IrO_2 and RuO_2 consist of growing single-crystal films on differently-oriented TiO_2 substrates to control the film growth direction, then capping with a magnetic permalloy layer and fabrication of test samples. Electric fields are applied in the sample plane to induce spin currents, which are measured quantitatively by detecting the magnetic deflection of the permalloy layer when it absorbs the spin current. This magnetic deflection is quantified electrically using two separate methods developed under previous funding, spin-torque ferromagnetic resonance (ST-FMR) and the 2nd-harmonic Hall technique. Measurements as a function of changing the direction of an in-plane magnetic field allow a determination of all vector components of the spin polarization for the spin current that is incident from the spin source layer into the permalloy.

Measurements on IrO_2 were performed in collaboration with the group of Chang-Beom Eom and Mark Rzchowski at the Univ. of Wisconsin, with theory help from the group of Evgeny Tsymbal at the Univ. of Nebraska.[1] We studied three growth orientations of the IrO_2: (001), (110), and (111). As shown in Fig. 2, the symmetry constraints for these orientations are that (001) films should produce a spin polarization pointing only in the conventional (x) direction, (110) films may produce both x and y components, and (111) films

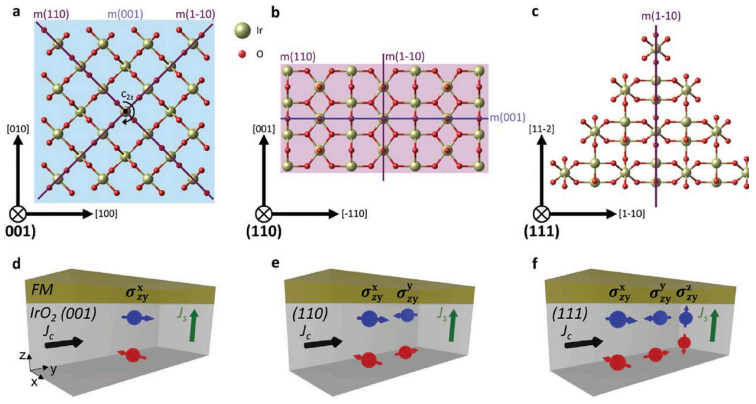

Fig. 2. Depictions of the (001), (110), and (111) surfaces of IrO_2, and the different components of electrically-generated spin currents allowed by symmetry constraints.

should allow x, y, and z components. Theoretical predictions for the magnitudes of the spin currents can be made by calculating the components of the spin Hall conductivity tensor for a single orientation, and then performing a rotation operation appropriate for a film growth direction.

The results of the IrO_2 measurements were qualitatively consistent with the theoretical predictions. All spin components that were forbidden by theory were indeed found to be zero to measurement accuracy, and the components allowed by symmetry were measured to be nonzero. The dependence on the angle of in-plane magnetic field for the signals due to each of the components of spin current was also in agreement with theory. In regard to quantitative comparisons, the conventional (y) spin components for all three crystal orientations were in reasonable agreement with predictions, as were the unconventional in-plane (x) component for the (110) and (111) films. However, the unconventional component of primary interest, the out-of-plane (z) spin polarization was small, corresponding to a spin current density per unit electric field of just 18 $(\hbar/2e)(\Omega\text{cm})^{-1}$ compared to a predicted value of 200 $(\hbar/2e)(\Omega\text{cm})^{-1}$. This experiment therefore confirms the primary hypothesis of the project that the orientation of electrically-induced spin currents can be manipulated simply by controlling the growth direction of a non-cubic crystal, but quantitative agreement with theory is lacking so far.

The experiment on RuO_2 was performed in collaboration with the groups Darrell Schlom and David Muller at Cornell, and once again with the theory group of Evgeny Tsymbal at the Univ. of Nebraska.[2] In this case, we compared (001)-oriented films (for which only spin currents with conventional (x) orientation are allowed) to (101) films. We found that the (101)-oriented films produced out-of-plane spin polarizations as large a 70 $(\hbar/2e)(\Omega\text{cm})^{-1}$, much stronger than for IrO_2. (Ref. 2 also presented data for (101)-oriented IrO_2 with no measurable out-of-plane-oriented spin current.) Furthermore, by comparing the in-plane and out-of-plane spin currents, we found that the angle of the electrically-induced spin polarization was closely aligned to the Néel vector of the RuO_2. This suggests that the antiferromagnetism in RuO_2 is central to this result, and furthermore the result is in agreement with a recently-proposed mechanism for producing electrically-generated spin currents based on momentum-dependent spin-splitting in the band structure of RuO_2, depicted schematically in Fig. 3. Within the rutile structure of RuO_2, the oxygen atoms coordinating the Ru atoms with up spins are rotated by 90 degrees relative to the oxygen atoms coordinating the Ru atoms with down spins. This leads to non-spherical Fermi surfaces in which the states occupied by up

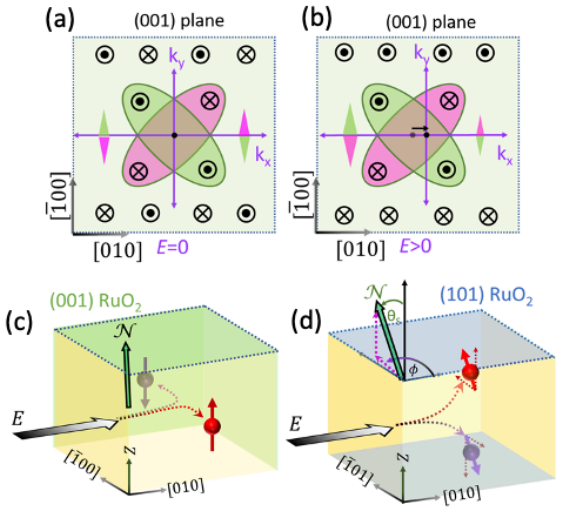

Fig. 3. Illustration of spin-current generation by the spin-splitter mechanism in RuO_2.

electrons are rotated by 90 degrees relative to the states with down electrons (Fig. 3(a)). When an electric field is applied to shift the Fermi surfaces, this naturally leads to strong electrically-induced spin currents. For example, in Fig. 3(b), an electric field along [010] produced more spins pointing out of the page moving upward in the figure (along $[\bar{1}10]$) and more spin pointing into the page moving downward in the figure. The result is a strong spin current flowing transverse to the applied electric field with a spin orientation parallel to the Néel vector. This spin current arises from exchange and inter-atomic coordination interactions rather than spin-orbit interactions. Because exchange and coordination interactions are generally stronger than spin-orbit interactions, this mechanism is exciting as a potential strategy for producing even stronger electric-field induced torques on magnets compared to the spin-orbit torques that have been the focus within the spintronics field for the past decade.

The out-of-plane spin current we measured in RuO_2 was approximately a factor of 50 smaller than the prediction for a sample of RuO_2 with a single antiferromagnetic domain. This is not surprising because the domain formation in our samples is uncontrolled, and a mix of differently-oriented domains can give cancelling contributions to the out-of-plane-oriented spin current. A challenge for the future is to characterize and control the domain configuration to favor one of the two possible domain configurations over the other, and see if this allows a large enhancement of the net electrically-generated spin current.

Future Plans

We are working toward measurements of additional orientations of IrO_2 and RuO_2 to check whether the results for all different orientations are fully consistent with simple matrix rotations of a single spin Hall conductivity tensor. We will also see if we can adjust the balance of oppositely-oriented antiferromagnet domains in RuO_2 by a combination of injecting spin current and annealing. We have new measurements underway of electrically-generated spin-currents produced by other low-symmetry crystals, to establish a basis for a more systematic comparison with theory. These include the delafossites $PdCoO_2$ (nonmagnetic) and $PdCrO_2$ (antiferromagnetic), and the pyrochlore $Bi_2Ir_2O_7$ (nonmagnetic).

References

1. Arnab Bose, Nathaniel J. Schreiber, Rakshit Jain, Ding-Fu Shao, Hari P. Nair, Jiaxin Sun, Xiyue S. Zhang, David A. Muller, Evgeny Y. Tsymbal, Darrell G. Schlom, and Daniel C. Ralph, *Tilted spin current generated by the collinear antiferromagnet ruthenium dioxide*, Nature Electronics **5**, 267–274 (2022).

2. Michael Patton, Gautam Gurung, Ding-Fu Shao, Gahee Noh, Joseph A. Mittelstaedt, Marcel Mazur, Jong-Woo Kim, Philip J. Ryan, Evgeny Y. Tsymbal, Si-Young Choi, Daniel C. Ralph, Mark S. Rzchowski, Tianxiang Nan, and Chang-Beom Eom, *Symmetry Control of Unconventional Spin-Orbit Torques in IrO_2*, Advanced Materials **35**, 2301608 (2023).

3. Rafael González-Hernández, Libor Šmejkal, Karel Výborný, Yuta Yahagi, Jairo Sinova, Tomáš Jungwirth, and Jakub Železný, *Efficient electrical spin splitter based on nonrelativistic collinear antiferromagnetism*, Phys. Rev. Lett. **126**,127701 (2021).

Publications

1. Xiaoxi Huang, Shehrin Sayed, Joseph Mittelstaedt, Sandhya Susarla, Saba Karimeddiny, Lucas Caretta, Hongrui Zhang, Vladimir A. Stoica, Tanay Gosavi, Farzad Mahfouzi, Qilong Sun, Peter Ercius, Nicholas Kioussis, Sayeef Salahuddin, Daniel C. Ralph, and Ramamoorthy Ramesh, *Novel Spin–Orbit Torque Generation at Room Temperature in an All-Oxide Epitaxial $La_{0.7}Sr_{0.3}MnO_3/SrIrO_3$ System*, Adv. Mater. **33**, 2008269 (2021).
(May 7, 2021)

2. S. Karimeddiny and D. C. Ralph, *Resolving Discrepancies in Spin-Torque Ferromagnetic Resonance Measurements: Lineshape vs. Linewidth Analyses*, Phys Rev. Appl. **15**, 064017 (2021).
(June 7, 2021)

3. Thow Min Cham, Saba Karimeddiny, Vishakha Gupta, Joseph A. Mittelstaedt, and Daniel C. Ralph, *Separation of Artifacts from Spin-Torque Ferromagnetic Resonance Measurements of Spin-Orbit Torque for the Low-Symmetry van der Waals Semi-Metal $ZrTe_3$*, Adv. Quantum Technol. **4**, 2100111 (2021).
(Dec. 17, 2021)

4. Arnab Bose, Rakshit Jain, Jackson J. Bauer, Robert A. Buhrman, Caroline A. Ross, and Daniel C. Ralph, *Origin of transverse voltages generated by thermal gradients and electric fields in ferrimagnetic-insulator/heavy-metal bilayers*, Phys. Rev. B **105**, L100408 (2022).
(March 28, 2022)

5. Arnab Bose, Nathaniel J. Schreiber, Rakshit Jain, Ding-Fu Shao, Hari P. Nair, Jiaxin Sun, Xiyue S. Zhang, David A. Muller, Evgeny Y. Tsymbal, Darrell G. Schlom, and Daniel C. Ralph, *Tilted spin current generated by the collinear antiferromagnet ruthenium dioxide*, Nature Electronics **5**, 267–274 (2022).
(May 5, 2022)

6. David Burke, Raghunath Dasari, Vinod Sangwan, Alexander Oanta, Zoheb Hirani, Chloe Pelkowski, Yongjian Tang, Ruofan Li, Daniel Ralph, Mark Hersam, Stephen Barlow, Seth Marder, and William Dichtel, *Synthesis, Hole Doping, and Electrical Properties of a Semiconducting Azatriangulene-Based Covalent Organic Framework*, J. Am. Chem. Soc. **145**, 11969−11977 (2023).
(May 22, 2023)

7. Michael Patton, Gautam Gurung, Ding-Fu Shao, Gahee Noh, Joseph A. Mittelstaedt, Marcel Mazur, Jong-Woo Kim, Philip J. Ryan, Evgeny Y. Tsymbal, Si-Young Choi, Daniel C. Ralph, Mark S. Rzchowski, Tianxiang Nan, and Chang-Beom Eom, *Symmetry Control of Unconventional Spin-Orbit Torques in IrO_2*, Advanced Materials **35**, 2301608 (2023).
(June 5, 2023)

8. Rakshit Jain, Max Stanley, Arnab Bose, Anthony R. Richardella, Xiyue S. Zhang, Timothy Pillsbury, David A. Muller, Nitin Samarth, and Daniel C. Ralph, *Thermally-generated spin current in the topological insulator Bi_2Se_3*, in review at Science Advances. (arXiv:2210.05636)

9. Xiaoxi Huang, Xianzhe Chen, Yuhang Li, John Mangeri, Hongrui Zhang, Maya Ramesh, Hossein Taghinejad, Peter Meisenheimer, Lucas Caretta, Sandhya Susarla, Rakshit Jain, Christoph Klewe, Tianye Wang, Rui Chen, Cheng-Hsiang Hsu, Hao Pan, Jia Yin, Padraic Shafer, Ziqiang Qiu, Davi R. Rodrigues, Olle Heinonen, Dilip Vasudevan, Jorge Iniguez, Darrell G. Schlom, Sayeef Salahuddin, Lane W. Martin, James G. Analytis, Daniel C. Ralph, Ran Cheng, Zhi Yao, and Ramamoorthy Ramesh, *Manipulating chiral-spin transport with ferroelectric polarization*, in review at Nature Materials.

Hybrid-Magnon Quantum Devices

Axel Hoffmann[1,2,3], Yi Li[4], Valentine Novosad[4], Wolfgang Pfaff[2,3], André Schleife[1,3,5], and Jian-Min Zuo[1,3]

1. Materials Science and Engineering, University of Illinois Urbana-Champaign, Urbana, IL 61801
2. Department of Physics, University of Illinois Urbana-Champaign, Urbana, IL 61801
3. Materials Research Laboratory, University of Illinois Urbana-Champaign, Urbana, IL 61801
4. Materials Science Division, Argonne National Laboratory, Lemont, IL 60439
5. National Center for Supercomputing Applications, University of Illinois Urbana-Champaign, Urbana, IL 61801

Keywords: magnetism, spintronics/magnonics, superconductivity, thin film heterostructures, microwave spectroscopy

Research Scope

Magnons, the quanta of collective spin excitations in magnetically ordered media, have emerged as an exciting candidate for quantum information processing and quantum transduction. Magnons exhibit unique features for microwave quantum engineering, *i.e.*, ultra-small wavelength down to the nanometer scale and the potential for non-reciprocity, which are highly desired for nm-sized quantum gates and noise-isolated qubit operations with on-chip integration. Although quantum operations of magnons have been demonstrated in bulk magnets, the quantum property of propagating magnons in magnetic films remains a fundamental challenge in both physics and materials science and is key for building magnon-based quantum information devices.

Our main objective is the development of a materials strategy for realizing hybrid magnonic quantum systems around magnetic materials that can be integrated into on-chip quantum systems. We will optimize magnon-photon coupling and test our main hypothesis that reduced magnetic damping is key, since it directly determines magnon coherence. We will pursue a multipronged approach based on investigating low-damping metallic alloys and developing new synthesis approaches for low-damping magnetic insulators. Furthermore, we aim to utilize a unique advantages of magnetic systems, namely their inherently non-reciprocal dynamics. We will address this objective by proper engineering of hybrid magnon systems through geometric constraints as well as interfacial symmetry breaking, which both can tune chiral interactions. Lastly, we will integrate these new material systems in prototypical quantum information systems with superconducting qubits with the goal to demonstrate new quantum coherent functionality.

The main program scope is nonreciprocal magnon propagation for noise isolation in quantum information systems. This program will overcome three major challenges: 1) low-damping (down to 10^{-4}) magnetic thin film and device platforms to provide efficient coherent magnonic operations, 2) magnon nonreciprocity with sufficient isolation for coherent magnon-qubit transduction at mK

temperatures, and 3) developing quantum modalities that maintain state-of-the-art coherence in the presence of magnetic fields and may be integrated with magnetic devices.

Recent Progress

Towards the objective of optimizing damping, we focus on two material systems; thin films of amorphous transition metal alloys and yttrium iron garnet. The first one has the advantage of large magnetization allowing very strong coupling to microwave photons, while the second system has very low damping, which is hard to maintain for epitaxial thin films at sub-K temperatures. For the amorphous transition metal alloys we focused on whether amorphization of $Co_{25}Fe_{75}$ via doping with boron can result in a reduction of damping. We observed a transition to an amorphous phase at around 6% B concentration, which coincides with a reduction of magnetic damping. We complemented these experimental results with first-principles calculations of amorphous alloys, which suggests a possible increase of the electronic density of states upon doping. Therefore, the experimentally observed reduced damping is most likely due to reduced magnetic anisotropy or decreased electronic scattering times.

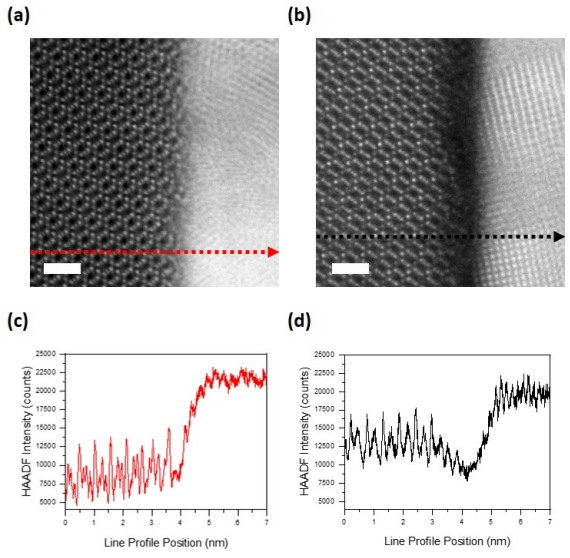

Fig. 1: Atomic-resolution STEM images for YIG/Py (a) with ion-milling and (b) without ion-milling. The corresponding line profile intensity (c) and (d) shows the different interface. The scale bar is 1 nm in (a) and (b).

For the epitaxial $Y_3Fe_5O_{12}$ (YIG) thin films we explored the detailed interfacial structure with permalloy ($Ni_{80}Fe_{20}$, Py) films using aberration-corrected scanning transmission electron microscopy (STEM) (see Fig. 1), in order to understand the experimentally observed antiferromagnetic interfacial exchange coupling. These experimental results were accompanied by first-principles simulations to investigate at the atomic level how Ni interdiffusion at the interface can possibly change electronic and magnetic properties and their influence on magnetic damping. These simulations provide predictions about the energetically favored Ni defect position, which we are currently testing experimentally.

Towards the objective of utilizing non-reciprocal spin-wave transduction we investigated the chiral coupling of a ground-signal-ground microwave antenna to magnons in the underlying ferromagnetic films. Using a simple model we established that the chiral selectivity is optimized, when the wavelengths of the excited spin waves match the thickness of the ferromagnetic layer. Indeed, experimental measurements show pronounced non-reciprocities up to 30 dB with a single transmission band in a broad frequency range, see Fig. 2 [8]. Furthermore, we investigated whether several different non-reciprocal phenomena can interfere constructively. Toward this end

we performed micromagnetic simulations, which indicate that non-reciprocities due to exchange bias as well as dipolar coupling in synthetic antiferromagnets can interfere constructively with dipolar-chiral coupling from suitable microwave antennae.

Lastly, towards new functionality, we successfully demonstrated time-domain manipulation of hybrid magnonic states in a chip-embedded magnon-superconducting-resonator hybrid circuit. We experimentally show the programming and gating of the hybrid states of two remotely coupled YIG spheres on a superconducting circuit with multiple microwave pulses and detecting their states independently using a pair of vertical microwave antennas, see Fig. 3. This is the first demonstration of time-domain control of remotely coupled magnonic resonators and is a significant advance towards magnon-magnon entanglement with coherent magnon interference. Coherent Rabi-like magnon excitation oscillations between the two remote YIG spheres were observed with a 30-MHz magnon-magnon coupling strength and a magnon T_1 of 161.5±3.4 ns and T_2 of 168.9±9.1 ns at an operating frequency of 5 GHz. This is a record magnon coherence and dephasing time in cavity magnonics at cryogenic temperature. With coherent microwave pulses, a complete cancellation of hybrid magnonic excitations with an anti-phase magnon drive was achieved. Additionally, parametric amplification of microwave input > 20 dB was demonstrated, by pumping the hybrid magnon modes into nonlinear states. This demonstrates a realistic hybrid magnonic system for building circuit integrated distributed quantum magnonic modules for quantum magnon operations and remote magnon entanglement.

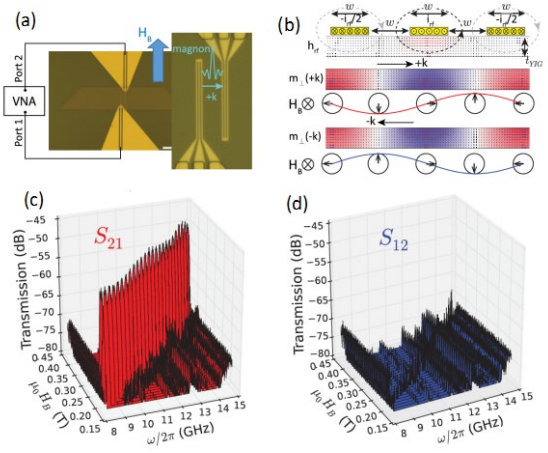

Fig. 2: (a) Optical image of a YIG delay line. (b) micromagnetic simulation of the chiral magnetic field of the antenna and magnon dynamic magnetizations for opposite propagation directions. (c) and (d) Broadband non-reciprocal microwave transmission with constant isolation of at least 30 dB. Adapted from Ref. 8.

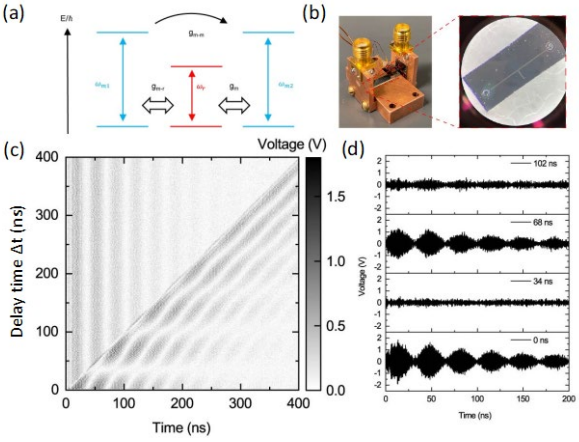

Fig. 3: (a), (b) Coherent coupling of two remote YIG spheres mediated by a superconducting resonator. (c), (d) Full constructive and destructive magnon interference with two microwave pulse excitations.

In addition, we are developing field-compatible Josephson circuits made from thin Al with hybrid magnon devices. We acquired preliminary data from a device that combines a nonlinear Josephson circuit including a SNAIL (Superconducting Nonlinear Asymmetric Inductive eLement)

that is coupled to a cavity-magnon system. We have shown that the Josephson circuit can be operated in an in-plane magnetic field of 300 mT, sufficient to match the Kittel mode of YIG to the few-GHz cavity resonances. This device will demonstrate parametrically time-controlled, quantum-limited magnons and superconducting qubit interactions.

Future Plans

We will characterize the magnetic damping over a wide temperature range down to the mK regime to identify the materials best suited for exploring single magnon physics. In parallel, we have developed designs for field-tolerant superconducting quantum devices, which we plan to validate experimentally. In order to emphasize the non-reciprocity of magnons in quantum information, we will integrate superconducting resonators with magnetic thin films, such as CoFeB and YIG, to achieve coherent excitation of short-wavelength propagating magnons and their strong coupling with microwave photons. We will fabricate superconducting resonators with sub-micron antennas to couple with short-wavelength propagating magnons. Using our previous demonstration of nonreciprocal magnon excitation and transduction, this will allow for unidirectional quantum state transfer mediated by propagating magnons. In addition to this we will use non-linear effects and three-wave mixing for fast dynamic control of the coupling between magnon and superconducting resonator modes. Lastly, to pursue magnon-qubit interactions for real quantum magnonics, we will couple our hybrid magnonic circuits to a superconducting qubit with our set-up dilution fridges for quantum microwave experiments. The qubit will be operated in the continuous-wave (CW) condition with ultralow-power, where the excited number of photon/magnon quanta is suppressed down to the single quantum limit. The resolution of the quantized magnon state will be reflected by the discretized resonance states of the qubits that reflects different excited numbers of magnon/photon quanta. We will explore the field-dependent operation of superconducting qubits.

In addition, we plan to cultivate time-domain coherent magnon operations with our signature remote magnon-magnon coupled superconducting circuit in the following directions: (1) to explore multi-pulse interference control of magnon states, which is inspired by the diffraction of light through a multi-slit grating; (2) to achieve time-domain gating of magnon-magnon interaction in order to achieve dynamic control of magnon states; (3) to further explore the potential of magnon-based parametric amplification of microwaves. Direction (1) is to fully cultivate the limit of coherent magnon interaction by increasing the number of magnon pulses. Direction (2) is the prerequisite for any practical gating application of quantum magnonics in quantum computing. Direction (3) is to cultivate the nonlinearity in superconducting kinetic inductance and magnon-photon interaction for single-magnon or single-photon operations. The goal is to explore new protocols for coherent magnon operations with multiple magnon nodes and create entanglement with the help of magnon interactions and control.

Towards the integration of quantum devices with magnon modes, we will investigate the performance of thin-Al devices coupled to magnons in magnetic field. Of particular interest is the

degree of coherence that can be achieved when operating in parameter regimes that are required for coupling magnon modes to microwave resonators. Because Al devices are hard to operate in magnetic fields, we will additionally pursue the development of quantum devices based on field-compatible superconductors that have intrinsic nonlinearity based on kinetic inductance. We will investigate Al-free devices that can act as sources of quantum states and quantum-limited couplers.

Publications

1. Y. Xiong, J. Inman, Z. Li, K. Xie, R. Bidthanapally, J. Sklenar, P. Li, S. Louis, V. Tyberkevych, H. Qu, Z. Xiao, W. K. Kwok, V. Novosad, Y. Li, F. Ma, and W. Zhang, *Tunable Magnetically Induced Transparency Spectra in Magnon-Magnon Coupled $Y_3Fe_5O_{12}$/Permalloy Bilayers*, Phys. Rev. Appl. **17**, 044010 (2022).

2. J. Inman, Y. Xiong, R. Bidethanapally, S. Louis, V. Tyberkevych, H. Qu, J. Sklenar, Valentine Novosad, Yi Li, X. Zhang, and W. Zhang, *Hybrid Magnonics for Short-Wavelength Spin Waves Facilitated by a Magnetic Heterostructure*, Phys. Rev. Appl. **17**, 044034 (2022).

3. M. Lonsky, M.-W. Yoo, Y.-S. Huang, J. Qian, J.-M. Zuo, and A. Hoffmann, *Structural and magnetic properties of Pt/Co/Mn-based multilayers*, Phys. Rev. Mater. **6**, 054413 (2022).

4. A. Hoffmann, *Spin transport modified by magnetic order*, J. Magn. Magn. Mater. **563**, 169896 (2022).

5. Y. Li, J.-C. Qian, Z.-H. Jiang, T.-H. Lo, D. Ding, T. Draher, T. Polakovic, W. Pfaff, A. Schleife, J.-M. Zuo, W.-K. Kwok, V. Novosad, and A. Hoffmann, *Hybrid-Magnon Quantum Devices: Strategies and Approaches,* 2022 IEEE International Electronic Devices Meeting, 154.6.1 (2022).

6. A. R. C. McCray, Y. Li, E. Qian, Y. Li, W. Wang, Z. Huang, X. Ma, Y. Liu, D. Y. Chung, M. G. Kanatzidis, A. K. Petford-Long, and C. Phatak, *Direct Observation of Magnetic Bubble Lattices and Magnetoelastic Effects in van der Waals $Cr_2Ge_2Te_6$*, Adv. Funct. Mater. **33**, 2214203 (2023).

7. Y. Guan, S. Haas, H. Schlömmer, and Z. Jiang, *Plasmons in Z_2 topological insulators*, Phys. Rev. B **107**, 155414 (2023).

8. Y. Li, T.-H. Lo, J. Lim, J. E. Pearson, R. Divan, W. Zhang, U. Welp, W.-K. Kwok, A. Hoffmann, and V. Novosad, *Unidirectional Microwave Transduction with Chirality Selected Short-Wavelength Magnon Excitations*, Appl. Phys. Lett. **123**, 022406 (2023).

9. Z. Jiang, J. Lim, Y. Li, W. Pfaff, T.-H. Lo, J. Qian, A. Schleife, J.-M. Zuo, V. Novosad, and A. Hoffmann, *Integrating Magnons for Quantum Information*, Appl. Phys. Lett., submitted; srXiv:2305.03164.

10. Y. Li, T. Draher, A. H. Comstock, Y. Xiong, Md. A. Haque, E. Easy, J.-C. Qian, T. Polakovic, J. E. Pearson, R. Divan, J.-M. Zuo, X. Zhang, U. Welp, W.-K. Kwok, A. Hoffmann, M. C. Beard, D. Sun, W. Zhang, and V. Novosad, *Tunable Magnon-Photon Coupling by Magnon Band Gap in a Layered Hybrid Perovskite Antiferromagnet*, Phys. Rev. Res., submitted; arXiv:2307.14447.

Abstract Title: **Selective growth of *a*-plane and *c*-plane oriented Kagome antiferromagnet Mn_3Sn thin films on *c*-plane sapphire**

PI: **Arthur R. Smith**
Address: **Ohio University**
Nanoscale & Quantum Phenomena Institute
Department of Physics & Astronomy
Athens, OH 45701
E-mail: **smitha2@ohio.edu**

Keywords: spintronics/magnonics, topological materials, antiferromagnets, scanning tunneling microscopy, molecular beam epitaxy

1. Research Scope

The overall scope of this research project is to investigate the spin as well as topological properties of a certain class of antiferromagnetic materials referred to as Kagome antiferromagnets. These materials have been found to exhibit fascinating properties in electron transport including the anomalous Hall, topological Hall, and anomalous Nernst effects [1,2,3]. Such materials include manganese-tin (Mn_3Sn), iron-tin (Fe_3Sn_2 and FeSn), and others. Our research approach is to fabricate thin films using molecular beam epitaxy (MBE) and then study the films using scanning tunneling microscopy (STM) and ultimately spin-polarized scanning tunneling microscopy (SP-STM). The instrumentation we employ in this project includes two MBE/STM labs. The goal of each lab is to independently grow by MBE the selected or desired films on suitable substrates and then transfer directly through UHV into adjoining STM analysis chambers. The idea is to avoid inadvertent exposure to ambient atmosphere and thus explore pristine surfaces. The sample grown by MBE must first be explored using an array of additional equipment for the initial characterization, prior to the STM studies. Since we recently began growing these Kagome antiferromagnets, until now the work has not yet included STM measurements, but that is the next step for our project.

2. Recent Progress

Progress on the molecular beam epitaxial growth of Mn_3Sn

Our initial studies of the MBE growth of Mn_3Sn in summer 2020 were aimed at answering the question 'can we achieve a crystalline or semi-crystalline, well-ordered, and epitaxially well-oriented film?' We began simply by co-depositing Mn and Sn onto a *c*-plane sapphire (0001) substrate at a Mn:Sn flux ratio of 3.1:1. We were lucky in that our first set of films showed primarily a *c*-oriented crystalline structure in x-ray diffraction along with some other smaller peaks in the 2θ spectrum. The film was produced at an elevated temperature of 524 +/- 5 °C, and the reflection high energy electron diffraction showed a clear diffraction pattern only after cooling down and waiting for about one day. The Mn_3Sn RHEED streak spacings were contracted compared to sapphire, revealing the larger Mn_3Sn lattice constant to within a small difference from accepted values (see Fig. 1). Rutherford backscattering showed a slight Mn-deficiency (Mn:Sn =

2.47:1) for the measured film, while the transmission electron microscopy revealed a mound-like, discontiguous film with voids down to the substrate [4].

We also investigated MBE growth at different temperatures while increasing the Mn:Sn flux ratio up to 3.3:1. Although this time RBS gave us a ratio of 3.3:1 (matching the flux ratio), depositing at a lower substrate temperature (453 +/- 5 °C) we discovered surprisingly that the film crystal structure changed to [11$\underline{2}$0] (*a*-plane) orientation, *c*-axis *in-plane* (see Fig. 2).

Amazing was that the RHEED streak spacing hardly changed relative to the sapphire (0001) substrate. Calculating the lattice constant from the RHEED streak spacings, we obtained a value along sapphire's *a*-axis close to the expected value for the *b*-value of Mn_3Sn but a value along sapphire's *b*-axis compressed by more than 9% compared to the *c*-value of Mn_3Sn. To understand the unexpected results, we turned to theoretical calculations via our project theory collaborators. First-principles calculations helped us to find models for the possible film structures, and we discovered a model which agrees extremely well with our experimental observations [5].

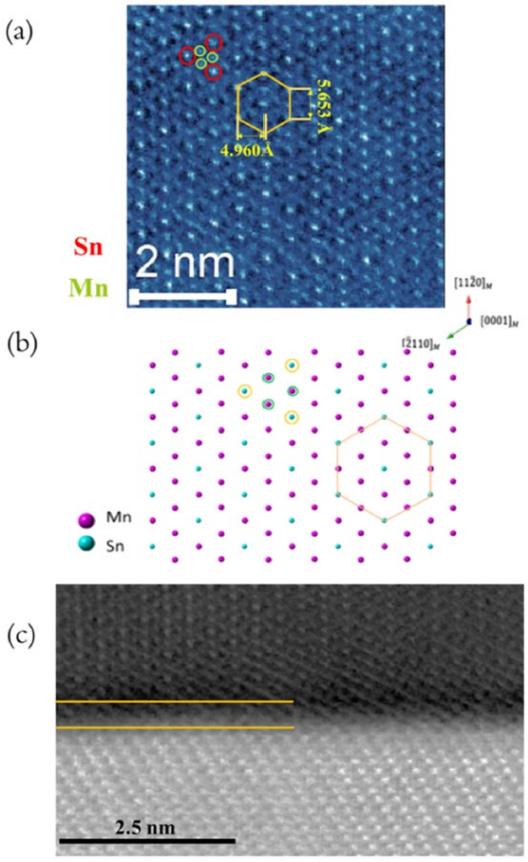

Fig. 2 *a*-plane results: (a) lattice image showing the *c*-plane standing upright. Numbers in the image were calculated after calibration using the sapphire lattice; (b) model corresponding to the lattice image shown in (a); (c) lattice image at the interface between sapphire and Mn_3Sn. [5]

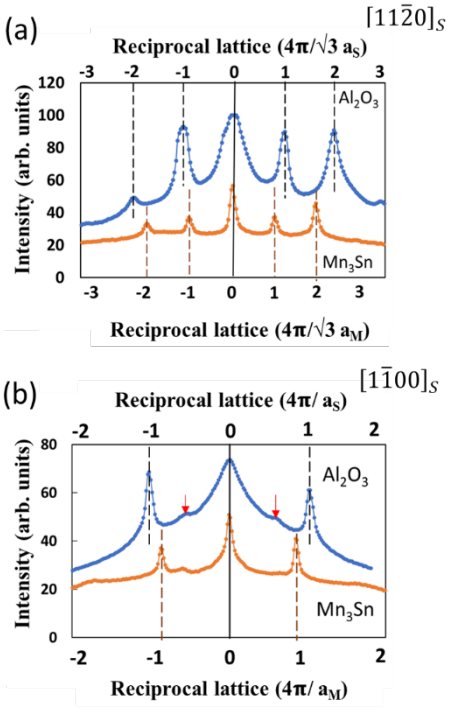

Fig. 1 *c*-plane results: Line profiles of the RHEED patterns for annealed Al_2O_3 and Mn_3Sn in both (a) [11$\underline{2}$0]$_S$ and (b) [1$\underline{1}$00]$_S$ directions. The red arrows indicate Kikuchi lines. [4]

Still, the film that we grew with *a*-plane orientation was found to be discontiguous although considerably smoother compared to the *c*-plane oriented film. To attempt to solve this problem, we tried a new growth trick. The idea was based on work published in 1996 in *Science* where it was reported that atomically smooth and contiguous silver films could be grown on GaAs (110) cleaved

surfaces (overcoming the usual growth kinetics which lead to highly rough Ag films) by employing a 2-step growth procedure: 1. depositing 1.5 nm of Ag at a cryogenic temperature, followed by 2. warming up to room temperature (anneal step) [6]. In our Mn_3Sn case, we deposited a seed layer (about 3 nm) of Mn + Sn at room temperature and waited overnight. The results were stupendous, with a highly crystalline layer emerging the next day. We then deposited a thicker layer on top of this template layer, also at room temperature, and examined the results using RHEED and XRD. The results show greatly improved crystalline orientation for these 2-step films along with atomic force microscopy which shows a smooth contiguous film. We have also explored annealing the film to higher temperatures to gain better crystallinity, and the results for that are encouraging [7].

Progress towards scanning tunneling microscopy of Mn_3Sn

Our most important goal is to explore the surfaces of the Kagome lattices using STM and spin-polarized STM at low temperatures and under applied magnetic fields. We are steadily progressing towards this goal. We have 2 MBE/STM systems where these studies are very soon to be possible (see Fig. 3). Note that all our STM systems include home-built scan heads including all the internal electronic wiring to accommodate the MBE sample holders. An important part of the students' training is in learning STM construction. Both STM systems in the 2 separate labs are currently undergoing developments and modifications. Lab 1 is nearly to the test phase for our variable low-temperature (20-300 K) low-field (0-1T, *in-plane* or *out-of-plane*) STM. Lab 2 is close to testing our variable ultra-low-temperature (1.5-300 K), high-field (0-4.5T) STM.

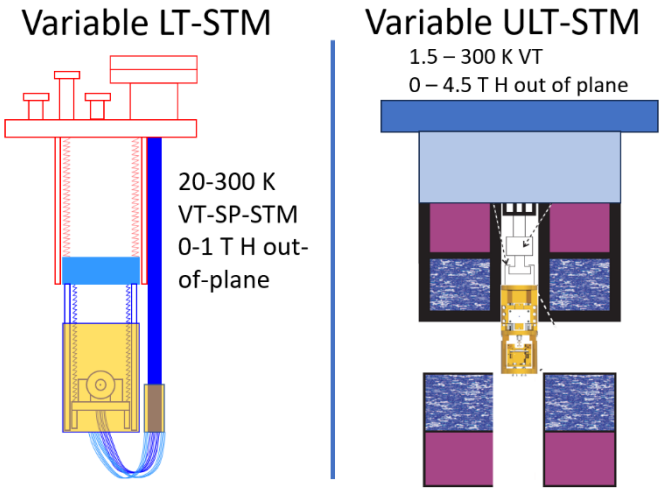

Fig. 3 Schematic design of variable low-temperature STM and variable ultra-low-temperature STM systems for investigations of spin-polarized surfaces under temperature

What has been achieved with both low-temperature STM developments is quite amazing and significant and includes for Lab 1's STM: a) completed construction and receipt of the OFHC gold-coated copper bundles for STM cooling and temperature control; b) design and construction of an OFHC gold-coated heat shield which can be raised and lowered to enable sample transfer and tip-sample approach; c) near completion of all STM electrical wiring; d) final connections to the various vacuum feedthroughs; and e) readying for connection to our new *RHK R10* electronics. And for Lab 2's STM, the progress includes: a) de-coupling the scan head from the 4.2 K magnet cryostat to allow the temperature to be controlled at the tip of an ultra-low-temperature flow cryostat (1.5-300 K); b) re-designing and re-building the STM scanner with better rigidity; c) adding a temperature sensor; and d) connecting the STM to our *RHK R9plus* electronics.

At the same time, in Lab 1 we continue to use our fully operational room-temperature STM. This RT-STM system has steadily worked to give good results for many years.

3. Future Plans

We are now poised for investigation of these Kagome lattice materials using ultra-low variable-temperature and low variable-temperature STM under applied magnetic fields. The MBE growth of the Mn_3Sn material has been achieved already on sapphire substrates, and publication are happening for that already. The progress with custom, home-built STM constructions is extremely good, and in all likelihood, we will be performing low-temperature STM studies by the end of 2023. The goals include to observe the Kagome spin lattice using spin-polarized STM on both the *a*-plane and the *c*-plane surfaces. The unusual non-collinear spin structures will be ideally explored using this method with both spin and spatial resolution at the atomic scale. By utilizing the applied magnetic field, we can manipulate the spin orientation of the tip and thus we can adjust the spin sensitivity to the surface along different directions. Beyond this will be the capacity to vary the temperature from 2 K to 300 K, allowing us to look at phase transitions and temperature-dependent field effects.

4. References

[1] Large anomalous Hall effect in a non-collinear antiferromagnet at room temperature, S. Nakatsuji, N. Kiyohara, and T. Higo, *Nature* **527**, 212 (2015).

[2] Anomalous and topological Hall effects in epitaxial thin films of the noncollinear antiferromagnet Mn_3Sn, J. M. Taylor, A. Markou, E. Lesne, P. K. Sivakumar, C. Luo, F. Radu, P. Werner, C. Felser, and S. S. P. Parkin, *Phys. Rev. B* **101**, 094404 (2020).

[3] Anomalous Nernst and Righi-Leduc Effects in Mn_3Sn: Berry Curvature and Entropy Flow, X. Li, L. Xu, L. Ding, J. Wang, M. Shen, X. Lu, Z. Zhu, and K. Behnia, *Phys. Rev. Lett.* **119**, 056601 (2017).

[4] Exploring the Interfacial Structure and Crystallinity for Direct Growth of Mn_3Sn (0001) on Sapphire (0001) by Molecular Beam Epitaxy, Sneha Upadhyay, Tyler Erickson, Hannah Hall, Ashok Shrestha, David C. Ingram, Kai Sun, Juan Carlos Moreno Hernandez, Gregorio Hernandez Cocoletzi, Noboru Takeuchi, and Arthur R. Smith, *Surfaces & Interfaces***,** under reconsideration after minor revision (2023).

[5] Molecular beam epitaxy and crystal structure of majority *a*-plane-oriented and substrate-strained Mn_3Sn thin films grown directly on sapphire (0001), Sneha Upadhyay, Tyler Erickson, Hannah Hall, Ashok Shrestha, David C. Ingram, Kai Sun, Juan Carlos Moreno Hernandez, Gregorio Hernandez Cocoletzi, Noboru Takeuchi, and Arthur R. Smith, *Journal of Vacuum Science & Technology A* **41**, 042710 (2023).

[6] Formation of Atomically Flat Silver Films on GaAs with a "Silver Mean" Quasi Periodicity, Arthur R. Smith, Kuo-Jen Chao, Qian Niu, and Chih-Kang Shih, *Science* **273**, 226 (1996).

[7] Epitaxial Template growth of *a*-plane Mn_3Sn, Sneha Upadhyay, Tyler Erickson, Hannah Hall, Ashok Shrestha, David C. Ingram, Kai Sun, Juan Carlos Moreno Hernandez, Gregorio Hernandez Cocoletzi, Noboru Takeuchi, and Arthur R. Smith, *Manuscript in preparation* (2023).

5. Publications of DOE sponsored research (2021-2023)

Papers listed below are shown in reverse chronological order, with the numbering defined based on paper #1 = A.R. Smith's first paper. Full publication list can be seen at: http://www.phy.ohiou.edu/~asmith/publist.html.

2023

107. Exploring the Interfacial Structure and Crystallinity for Direct Growth of Mn_3Sn (0001) on Sapphire (0001) by Molecular Beam Epitaxy, Sneha Upadhyay, Tyler Erickson, Hannah Hall, Ashok Shrestha, David C. Ingram, Kai Sun, Juan Carlos Moreno Hernandez, Gregorio Hernandez Cocoletzi, Noboru Takeuchi, and Arthur R. Smith, *Surfaces & Interfaces***,** under reconsideration after minor revision (2023).

106. A Study of the Structure, Structural Transition, Interface Model, and Magnetic Moments of CrN Grown on MgO(001) by Molecular Beam Epitaxy, Khan Alam, Rodrigo Ponce-Pérez, Kai Sun, Andrew Foley, Noboru Takeuchi, and Arthur R. Smith, *Journal of Vacuum Science & Technology A* **41**, 053411 (2023).

105. Molecular beam epitaxy and crystal structure of majority a-plane-oriented and substrate-strained Mn_3Sn thin films grown directly on sapphire (0001), Sneha Upadhyay, Tyler Erickson, Hannah Hall, Ashok Shrestha, David C. Ingram, Kai Sun, Juan Carlos Moreno Hernandez, Gregorio Hernandez Cocoletzi, Noboru Takeuchi, and Arthur R. Smith, *Journal of Vacuum Science & Technology A* **41**, 042710 (2023).

2021

104. Investigating the magnetic and atomic interface configuration for a model Fe/CrN bilayer system, Khan Alam, Rodrigo Ponce-Pérez, Kai Sun, Andrew Foley, Noboru Takeuchi, and Arthur R. Smith, *Journal of Vacuum Science & Technology A* **39**, 063209 (2021).

103. Noncollinear magnetic configurations and substrate-mediated interactions in Mn trimers on the GaN(000-1) surface, Diego Hunt, María Andrea Barral, Arthur R. Smith, and Valeria Ferrari, *Physical Review B* **103**, 094418 (2021).

102. Surface structures of magnetostrictive $D0_3$-Fe_3Ga(001), Ricardo Ruvalcaba, Joseph P. Corbett, Andrada-Oana Mandru, Noboru Takeuchi, Arthur R.Smith, and Jonathan Guerrero-Sanchez, *Applied Surface Science* **553**, 149488 (2021).

Thickness-driven giant anomalous and topological Hall effects in $Fe_{5-x}GeTe_2$

Luis Balicas, National High Magnetic Field Laboratory, and Florida State University

Keywords: magnetism, topology, 2D and layered crystals, nanostructures, ferro/ferrimagnets,

Research Scope

$Fe_{5-x}GeTe_2$ is a promising two-dimensional (2D) van der Waals (vdW) magnet for practical applications, given its remarkable magnetic properties. These include Curie temperatures above room temperature, and topological spin textures – TST (both merons and skyrmions), responsible for a pronounced anomalous Hall effect (AHE) and its topological counterpart (THE), which can be harvested for spintronics. Here, we show that both the AHE and THE can be amplified considerably by just adjusting the thickness of exfoliated $Fe_{5-x}GeTe_2$, with THE becoming observable even in zero magnetic field. Using a complementary suite of techniques, including electronic transport, Lorentz transmission electron microscopy, and micromagnetic simulations, we reveal the emergence of substantial coercive fields upon exfoliation, which are absent in the bulk, implying thickness-dependent magnetic interactions that affect the TST. We detected a 'magic' thickness t ~30 nm where the formation of TST is maximized, inducing large magnitudes for the topological charge density (~6.45 x 10^{20} cm^{-2}), and the concomitant anomalous ($\rho_{xy}^{\mathrm{A,max}} \cong$ 22.6 μΩ cm) and topological ($\rho_{xy}^{\mathrm{u,T}} \cong 15$ μΩ cm) Hall resistivities at $T \sim 120$ K. These values for $\rho_{xy}^{\mathrm{A,max}}$ and $\rho_{xy}^{\mathrm{u,T}}$ are higher than those found in magnetic topological insulators and, so far, the largest reported for 2D magnets. The hitherto unobserved THE under zero magnetic field could provide a platform for the writing and electrical detection of TST aiming at energy-efficient devices based on vdW ferromagnets.

Recent Progress

The study of magnetism in the two-dimensional (2D) limit has been pivotal for the development of critical phenomena and strongly correlated phases in ultrathin compounds[1]. Magnetism in van der Waals (vdW) like compounds has seen a remarkable recent resurgence due to the advent of layered magnetic compounds displaying a magnetic ground state even when exfoliated down to the monolayer limit[2]. Among known vdW layered magnets, the metallic ferromagnets belonging to the $Fe_{n-x}GeTe_2$ family, and its doped variants, display the highest known Curie temperatures (T_c). Despite being centrosymmetric, implying *a priori* the absence of the Dzyaloshinskii–Moriya interaction, these compounds are prone to display topological spin textures, such as skyrmions and

merons[3] and complex domain boundaries between stripe domains. Topological spin textures such as skyrmions, are vortex-like nanometric spin textures that carry an integer topological number, or topological charge, describing how many times the magnetic moments composing it wrap around a sphere. In contrast, merons are characterized by a half integer topological charge. Such textures are characterized by a finite value of the scalar field spin chirality, $\chi_{ijk} = \overrightarrow{S_i} \cdot \left(\overrightarrow{S_j} \times \overrightarrow{S_k}\right)$, which is a fictitious magnetic field that bends the electronic orbits, generating the so-called topological Hall effect (THE)[4]. In fact, we have recently shown that spin chirality also leads to an unconventional (topological) Hall like response even in a configuration that lacks Lorentz force[3,5].

We evaluatee the unconventional THE ($\rho_{xy}^{\mathrm{u,T}}$) and AHE (ρ_{xy}^{A}) responses of $Fe_{5-x}GeTe_2$ as a function of both the crystal thickness t within 12 nm ≤ t ≤ 65 nm and temperature. For fields parallel to electrical currents flowing along a planar direction, we find a coercive field $\mu_0 H_c^{ab} > 10$ $\mu_0 H_c^c$, where $\mu_0 H_c^{ab}$ and $\mu_0 H_c^c$ are the coercive fields seen in the THE and AHE responses for $\mu_0 H$ parallel to the *ab*-plane and the *c*-axis, respectively. This implies a rotation of the magnetic hard axis of $Fe_{5-x}GeTe_2$ upon exfoliation, from the *c*-axis towards the *ab*-plane, in contrast to what is observed for bulk samples. Experimentally, we find that this reorientation leads to a very large enhancement of both ρ_{xy}^{A} and $\rho_{xy}^{\mathrm{u,T}}$, with both quantities peaking at a thickness $t \cong 30$ nm. Our micromagnetic simulations indicate that there is a maximum in the topological charge density around this thickness, located between the complete spin homogeneity of very thin films due to an exchange-dominated regime, and the spin inhomogeneity intrinsic to thick films, dominated by the dipolar interactions. We also observe the emergence of a very pronounced hysteresis in the THE, particularly in a temperature range where hysteresis remains completely absent in the longitudinal magnetoresistivity. This implies that the hysteresis observed at higher temperatures is not dominated by the movement and pinning of ferromagnetic domain walls. Instead, we argued that remnant chiral spin textures provide a Hall-like signal even after the external magnetic field is suppressed. This is supported by both our Lorentz transmission electron microscopy (LTEM) measurements that reveal remnant skyrmions upon magnetic field removal, and our micromagnetic simulations indicating that the maximum meron density, and, hence, topological charge-density, peaks at $\mu_0 H = 0$ T. The ensemble of our observations is consistent with intrinsic anomalous and topological Hall responses modulated by the evolution of the spin textures as a function of thickness, temperature, and magnetic field. They also point to the possibility of writing remnant

topological spin textures with a magnetic field and electrically detecting them via a topological Hall voltage. This exposes the potential of $Fe_{5-x}GeTe_2$ for the development of magnetic memory elements and spintronics in general.

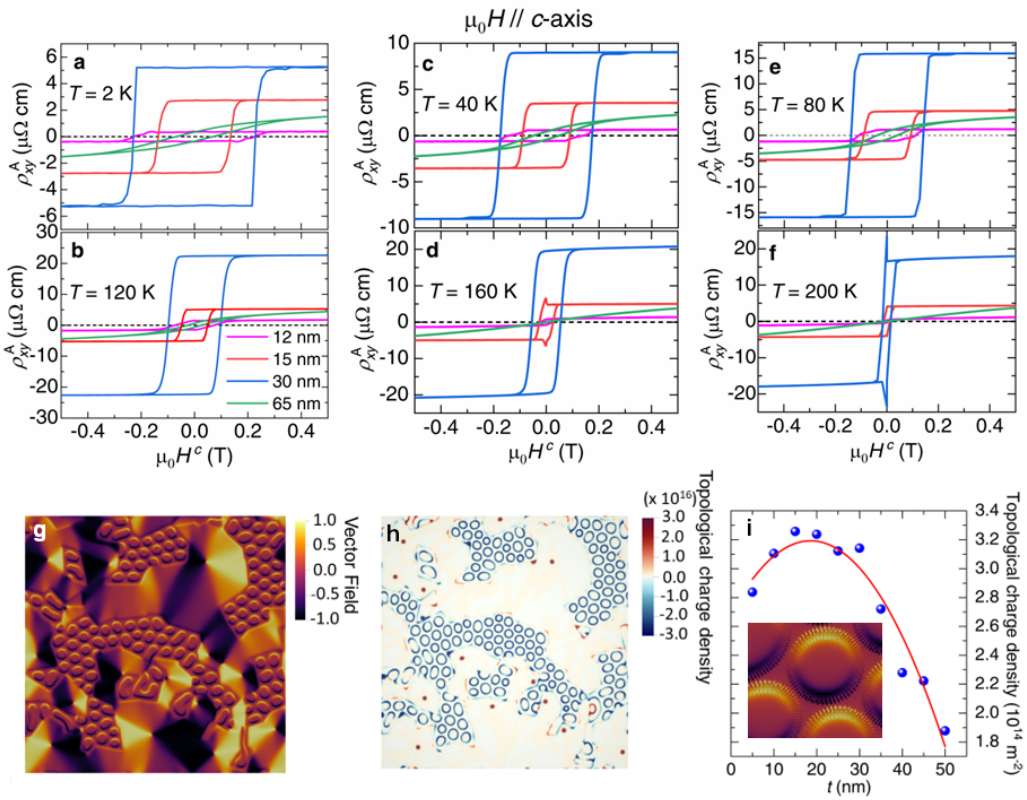

Fig. 1| Anomalous Hall response ρ_{xy}^{A} and micromagnetic simulations. **a-f**, ρ_{xy}^{A} as function of $\mu_0 H$ applied along the *c*-axis for six temperatures, 2, 40, 80, 120, 160 and 200 K, respectively. Magenta, red, blue, and green traces correspond to crystal thicknesses of 12, 15, 30 and 65 nm, respectively. Note the increased loop squareness with the increase of the coercive field $\mu_0 H_c^c$ as T is lowered, and the increase in the AHE response as the number of layers, n, decreases. The maximum values occurred for an $Fe_{5-x}GeTe_2$ crystal of 30 nm thickness. **g**, Snapshot of the magnetization domains obtained via micromagnetic simulations at zero field and 0 K, including domains with their magnetization oriented within the conducting planes and domains with the magnetization oriented perpendicular to the planes. Several domain walls meet at a planar spin vortex that contains a meron at its center. The application of a transverse magnetic field stabilizes skyrmions in domains characterized by an out-of-plane magnetization component[35]. **h**, Calculated topological charge density associated with domain structure shown in **g**. **i**, Topological charge density as a function of sample thickness, showing a maximum for 15 nm ≤ t ≤ 25 nm, nearly in agreement with the t-dependence of $\rho_{xy}^{A}(t)$. The slight fluctuation in the values of the topological charge (blue dots) are due to several realizations (~10 times) of the random spin seeds that were subsequently averaged for each thickness. The red line is a simple fit to an order-3 polynomial. **Inset:** magnified image of a simulated magnetic skyrmion.

Future Plans

Currently, we are finalizing a thorough study on Fe_3GaTe_2 (T_c ~ 380 K) grown by us via chemical vapor transport, indicating enormous anomalous and topological Hall responses. Our goals are to understand the mechanism leading to the "writing" of spin textures and its evolution as a function of temperature, particularly above room T. We will use imaging techniques coupled to transport and transvers electric fields, to explore our ability to manipulate and move this spin textures.

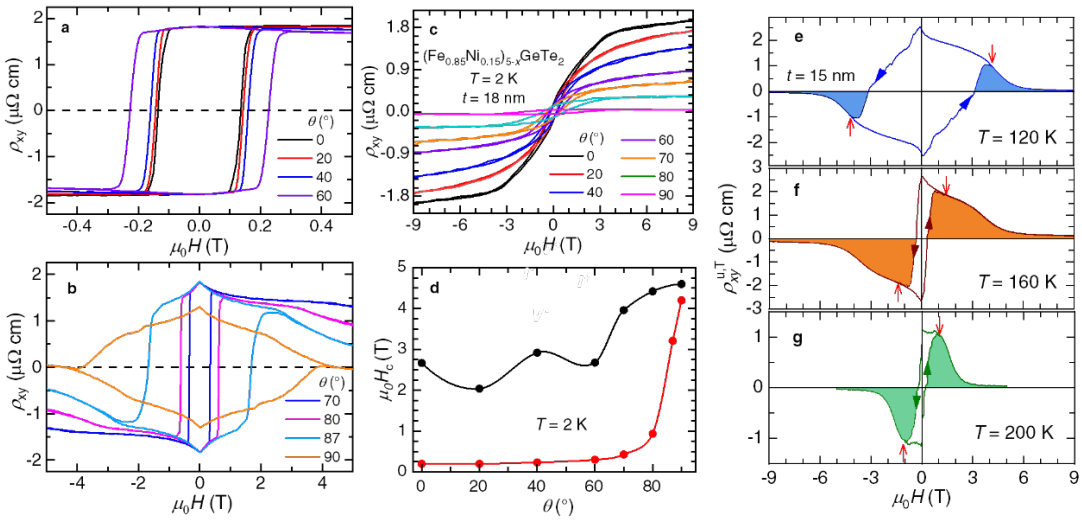

Fig. 2| Coercivity as a function of magnetic field orientation and emergence of the unconventional THE. a-b, Raw Hall resistivity ρ_{xy} as a function of the angle θ between $\mu_0 H$ and the *c*-axis of a t = 15 nm thick $Fe_{5-x}GeTe_2$ crystal. We observed an increase by more than one order of magnitude in the coercive field H_c as $\mu_0 H$ is rotated towards the *ab*-plane. **c**, Raw ρ_{xy} measured from a Ni-doped $Fe_{5-x}GeTe_2$ crystal (composition $(Fe_{0.85}Ni_{0.15})_{5-x}GeTe_2$) of thickness t = 18 nm. Note the similar values of the saturating anomalous Hall response with respect to the value for the t = 15 nm thick $Fe_{5-x}GeTe_2$ crystal. In contrast, $(Fe_{0.85}Ni_{0.15})_{5-x}GeTe_2$ displays one order of magnitude larger values for $\mu_0 H_c^c$, probably due to the disorder inherent to its alloy character. **d**, Coercive fields, $\mu_0 H_c$, as a function of the angle θ between $\mu_0 H$ and the interlayer *c*-axis for both $(Fe_{0.85}Ni_{0.15})_{5-x}GeTe_2$ (t = 18 nm, black markers) and $Fe_{5-x}GeTe_2$ (t = 15 nm, red markers) at T = 2 K. For both compounds, H_c increases rapidly as θ surpasses 70°, but for both samples it displays similar values around θ = 90°. **e**, **f**, and **g**, Unconventional THE response $\rho_{xy}^{u,T}$ resulting from an unconventional measurement geometry, namely magnetic field parallel to the electrical current using a Hall geometry for the voltage leads, and for three temperatures T = 120 K, 160 K, and 200 K, respectively. We note extremely large coercive fields $\mu_0 H_c^{ab}$ (indicated by red arrows) that are over one order of magnitude larger than $\mu_0 H_c^c$ at the same temperatures, and the broad peak in $\rho_{xy}^{u,T}$ for fields beyond $\mu_0 H_c^{ab}$.

References

1. Q. H. Wang *et al*., *The Magnetic Genome of Two-Dimensional van der Waals Materials*, ACS Nano **16**, 6960 (2022).
2. B. Huang *et al*., *Layer-dependent ferromagnetism in a van der Waals crystal down to the monolayer limit*, Nature **546**, 270 (2017)
3. B. W. Casas *et al*., *Coexistence of Merons with Skyrmions in the Centrosymmetric Van Der Waals Ferromagnet* $Fe_{5-x}GeTe_2$. Adv. Mater. **35**, 2212087 (2023).
4. N. Verma, Z. Addison, and M. Randeria, *Unified theory of the anomalous and topological Hall effects with phase-space Berry curvatures*, Sci. Adv. **8**, eabq2765 (2022).
5. J. Macy *et al*., Magnetic field-induced non-trivial electronic topology in $Fe_{3-x}GeTe_2$. Appl. Phys. Rev. **8**, 041401 (2021).

Publications

1. B. W. Casas Y. Li, A. Moon, Y. Xin, C. McKeever, J. Macy, Amanda K. Petford-Long, C. M. Phatak, E. J. G. Santos, E. S. Choi, L. Balicas, *Coexistence of Merons with Skyrmions in the Centrosymmetric Van Der Waals Ferromagnet $Fe_{5-x}GeTe_2$*. Adv. Mater. **35**, 2212087 (2023).

2. Q. Zhang, Md. S. Hossain, B. Casas, W. Zheng, Z.-J. Cheng, Z. Lai, Y.-H. Tu,G. Chang, Y. Yao, S. Li, Y.-X. Jiang, S. Mardanya, T.-R. Chang, J.-Y. You, Y.-P. Feng, G. Cheng, J.-X. Yin, N. Shumiya, T. A. Cochran, X. P. Yang, M. Litskevich, N. Yao, K. Watanabe, T. Taniguchi, H. Zhang, L. Balicas, and M. Z. Hasan, Ultrahigh supercurrent density in a two-dimensional topological material, Phys. Rev. Mater. 7, L071801 (2023)

3. N. Shumiya, Md S. Hossain, J.-X. Yin, Z. Wang, M. Litskevich, C. Yoon, Y. Li, Y. Yang, Y.-X. Jiang, G. Cheng, Y.-C. Lin, Q. Zhang, Z.-J. Cheng, T. A. Cochran, D. Multer, X. P. Yang, B. Casas, T.-R. Chang, T. Neupert, Z. Yuan, S. Jia, H. Lin, N. Yao, L. Balicas, F. Zhang, Y. Yao, and M. Z. Hasan*, Evidence of a room-temperature quantum spin Hall edge state in a higher-order topological insulator,* Nat. Mater. **21**, 1111 (2022).

4. J. Macy, D. Ratkovski, P. P. Balakrishnan, M. Strungaru, Y.-C. Chiu, A. Flessa Savvidou, A. Moon, W. Zheng, A. Weiland, G. T. McCandless; J. Y. Chan, G. S. Kumar; M. Shatruk, A. J. Grutter, J. A. Borchers, W. D. Ratcliff, E. S. Choi, E. J. G. Santos, L. Balicas, *Magnetic field-induced non-trivial electronic topology in $Fe_{3-x}GeTe_2$*, Appl. Phys. Rev. **8**, 041401 (2021).

5. D. Sun, V. S. Minkov, S. Mozaffari, Y. Sun, Y. Ma, S. Chariton, V. B. Prakapenka, M. I. Eremets, L. Balicas, F. F. Balakirev, *High-temperature superconductivity on the verge of a structural instability in lanthanum superhydride*, Nat. Commun. **12**, 6863 (2021).

6. L. Alahmed, B. Nepal, J. Macy, W. Zheng, B. Casas, A. Sapkota, N. Jones, A. R Mazza, M. Brahlek, W. Jin, M. Mahjouri-Samani, S. S.-L. Zhang, C. Mewes, L. Balicas, T. Mewes, and P. Li, *Magnetism and spin dynamics in room-temperature van der Waals magnet Fe_5GeTe_2*, 2D Mater. **8**, 045030 (2021).

7. H.-Y. Yang, X. Yao, V. Plisson, S. Mozaffari, J. P. Scheifers, A. Flessa Savvidou, E. S. Choi, G. T. McCandless, M. F. Padlewski, C. Putzke, P. J. W. Moll, J. Y. Chan, L. Balicas, K. S. Burch, and F. Tafti, *Evidence of a coupled electron-phonon liquid in $NbGe_2$*, Nat. Commun. **12**, 5292 (2021).

8. I. F. Gilmutdinov, R. Schönemann, D. Vignolles, C. Proust, I. R. Mukhamedshin, L. Balicas, and H. Alloul, Interplay between strong correlations and electronic topology in the underlying kagome lattice of $Na_{2/3}CoO_2$, Phys. Rev. B **104**, L201103 (2021).

9. P. Kong, V. S. Minkov, M. A. Kuzovnikov, A. P. Drozdov, S. P. Besedin, S. Mozaffari, L. Balicas, F. F. Balakirev, V. B. Prakapenka, S. Chariton, D. A. Knyazev, E. Greenberg, and M. I. Eremets, *Superconductivity up to 243 K in the yttrium-hydrogen system under high pressure*, Nat. Commun. **12**, 5075 (2021).

Hanle Hall effect in Pt/insulator boundaries

Xiaoshan Xu

Department of Physics and Astronomy, University of Nebraska-Lincoln

Keywords: spintronics, ferroelectrics and multiferroics, magnetotransport

Research Scope

The overarching goal of this project is to realize the non-volatile electric-field control of spin transport across interfaces [1] and in spin-orbit coupled materials, which is crucial for the operations in spin-based circuitry. Particularly, this project exploits non-volatile control using interfaces with ferroelectrics in both spin-polarized charge current and in non-magnetic spin-orbit coupled materials, especially the recently discovered molecular ferroelectrics that have large polarizations and small switching fields. The specific aims are 1: elucidate the effect of polarization on the spin transport through the ferromagnet/molecular ferroelectrics interfaces; 2: gain fundamental understanding on the effect of polarization on the charge/spin conversion in spin-orbit coupled materials at the interfaces with molecular ferroelectrics. 3: characterize spin transport in crystalline molecular ferroelectrics.

Recent Progress

Previously, we have demonstrated the ferroelectric control of spin-polarized charge current in a magnetic tunneling junction, using proton-transfer type molecular ferroelectrics as the tunneling barrier, employing the electrostatic effect (energy landscape change) due to the polarization reversal [2]. To study the effect of polar interface on spin/charge conversion in spin-orbit coupled materials, we investigated the spin transport, including the spin Hall effect (SHE), inverse spin Hall effect (ISHE), and the spin-Hall Hanle effects (SHHEs) of Pt thin films grown on various polar and non-polar insulators. Our results show that SHHEs offer a self-contained way to extract spin-transport properties such as spin Hall angle θ_{SH}, spin diffusion length λ_s, spin

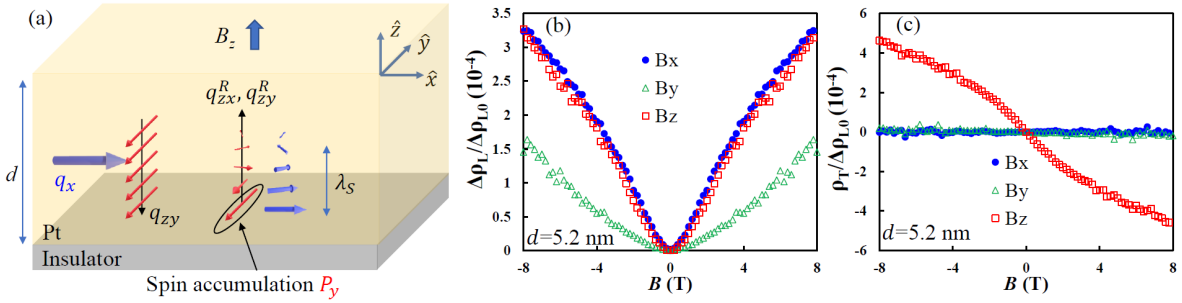

Figure 1. (a) Schematic of the spin Hall Hanle effects (SHHEs) in a Pt/insulator heterostructure. Applied magnetic field causes precession of spin polarization during the diffusion from the interface and manifests in the magnetoresistance and the Hall effect. (b) Measured change of longitudinal resistivity normalized with the zero-field resistivity. B_x, B_y, and B_z are the magnetic field along the x, y, and z directions, respectively. (c) Measured transverse Hall resistivity normalized with the zero-field longitudinal resistivity.

relaxation time τ_s. [3] Comparison between SHHEs at polar and non-polar interfaces suggests great potential of controlling spin/charge conversion using ferroelectric polarization.

SHE and the ISHE have been widely used for both the generation and detection of pure spin current. On the other hand, it is difficult to probe SHE and ISHE as bulk effects in heavy metals using magneto-transport, because the modulation by a magnetic field is limited by the short timescale of momentum relaxation. In contrast, at the boundary of the heavy metals, the spin accumulation and diffusion (spin-current reflection) may be more effectively manipulated by a magnetic field via spin precession according to the Hanle effect [Fig. 1(a)], because it is the spin relaxation that determines the timescale of the process. Dyakonov predicted a longitudinal effect [4], which was later observed in Pt and β-phase Ta thin films and named Hanle magnetoresistance. On the other hand, spin precession is also expected to rotate the spin polarization and generate a transverse charge current corresponding to a Hall effect. However, this Hanle Hall effect has not been experimentally demonstrated and often overlooked.

To resolve the puzzle of missing Hanle Hall effect, we deposit Pt thin films on Al_2O_3 substrates using pulsed laser deposition to enhance τ_s for reaching the strong-precession condition. We observed non-quadratic and non-linear field dependence for the longitudinal (magnetoresistance) and the transverse (Hall) effects respectively, indicating the strong precession condition. The dual effects, which we refer to as the spin-Hall Hanle effects (SHHEs), can be fit using the same set of parameters (θ_{SH}, λ_s, and τ_s), suggesting that SHHE can be reliably employed in extracting the spin transport properties without complications from the magnetic interfaces, such as spin memory loss [5] and proximity-induced magnetism.

Figure 1(b) shows the change of longitudinal resistivity $\Delta\rho_L=\rho_L-\rho_{L0}$ normalized with respect to the zero-field value ρ_{L0} in a 5.2-nm-thick Pt film, where B_x, B_y and B_z represent the magnetic field applied along the x, y, and z direction respectively. Overall, $\Delta\rho_L$ increases with the magnetic field, consistent with the expectation from the SHHE. As illustrated in Fig. 1(a), the longitudinal charge current (q_x) in the Pt film generates a spin current (q_{zy}, polarization along $\hat{y}$, current flow along $\hat{z}$) via SHE toward the Pt/Al_2O_3 interface. The reflected spin current (q_{zy}^R) generates a longitudinal charge current q_x^R via the ISHE before the spin polarization relaxes. The Hanle effect may be observed when an external magnetic field causes the precession of the spin polarization of resulting in q_{zx}^R and transverse charge current q_y^R. In addition, q_x^R will be reduced, which increases the longitudinal resistivity, as observed in Fig. 1(b).

The anisotropy in Fig. 1(b) also agrees with SHHE in that $\Delta\rho_L(B_y)/\rho_{L0}$ is smaller than $\Delta\rho_L(B_x)/\rho_{L0}$ and $\Delta\rho_L(B_z)/\rho_{L0}$ while the latter two are similar. When the magnetic field is parallel to the initial polarization direction ($\hat{y}$) of q_{zy}, no spin precession is caused by the external magnetic field and the SHHE does not contribute to $\Delta\rho_L(B_y)/\rho_{L0}$. Hence the difference $\Delta\rho_L(B_z)$-$\Delta\rho_L(B_y)$ is attributed to the longitudinal SHHE. Figure 1(b) also reveals the strong-precession behavior of the longitudinal SHHE that was not observed before. A numeric simulation shows that, at low field (weak precession), the longitudinal SHHE is quadratic ($\propto B_z^2$); at high field (strong precession),

the effect saturates when the precession angle is so large that q_x^R vanishes, consistent with the reduced slope of $\Delta\rho_L(B_x)/\rho_{L0}$ and $\Delta\rho_L(B_z)/\rho_{L0}$ at high field in Fig. 1(b).

Figure 1(c) shows the normalized transverse resistivity ρ_T/ρ_{L0}, which has non-trivial field dependence only in B_z. In addition, $\rho_T(B_z)/\rho_{L0}$ exhibits a non-linear relation with a large slope at low field and a smaller slope at high field. As illustrated in Fig. 1(a), with B_z, the spin precession leads to non-zero q_{zx}^R, which generates a non-zero q_y^R (Hall signal) via ISHE. At low field (weak precession), the effect is linear ($\propto B_z$). At high field (strong precession), the transverse effect is expected to vanish because the projection of q_y^R cancels due to the large precession angle. This overall nonlinear effect is consistent with the observation in Fig. 1(c).

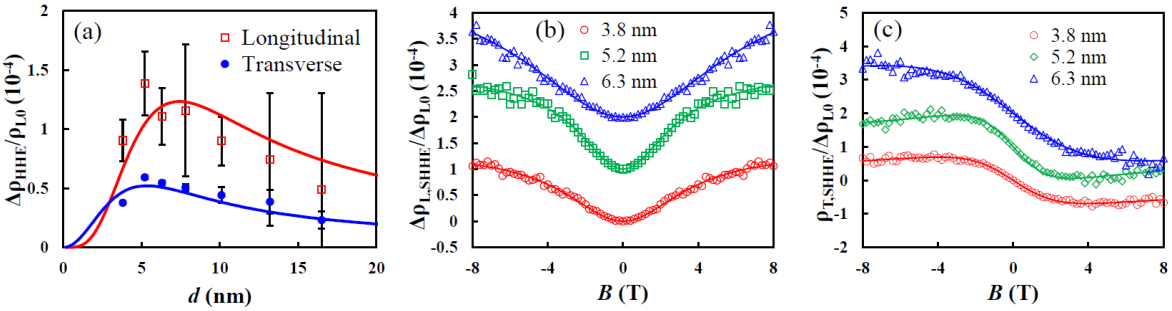

Figure 2. (a) Longitudinal and transverse SHHE measured at 4 T and 1 T respectively, as a function of Pt thickness. (b) Measured longitudinal SHHE (symbols) as the difference between the magnetoresistance in B_z and that in B_y. (c) Measured transverse SHHE (symbols) as the measured Hall effect with the linear background subtracted. The data are shifted vertically in both (b) and (c) for clarity. The lines in (b) and (c) are fit of the data. For each Pt film thickness, the fit uses the same set of parameters.

A scaling rule pointed out by Dyakonov [4] needs to be considered to extract the spin transport parameters. Considering the spin-precession nature, the SHHEs are expected to scale with the spin precession time τ_s^* defined as $\frac{1}{\tau_s^*} = \frac{1}{\tau_s}\left[1 + \left(\frac{2\lambda_s}{d}\right)^2\right]$ [4]. Indeed, numerical simulation shows that the field dependence "scaled" with τ_s^* of SHHE maintains roughly the same curve shape despite that the value of d/λ_s changes over orders of magnitude. Therefore, one needs to estimate λ_s from the thickness dependence of SHHE, which can then be used to extract τ_s (out of τ_s^*) and θ_{SH}. We then measured the thickness dependence of SHHE in the epitaxial Pt films. The experimental $\Delta\rho_{L,SHHE}/\rho_{L0}$ is calculated as $[\Delta\rho_L(B_z) - \Delta\rho_L(B_y)]/\rho_{L0}$. Figure 2(a) shows the thickness dependence of experimental $\Delta\rho_{L,SHHE}/\rho_{L0}$ at 4 T field. Meanwhile, the experimental $\Delta\rho_{T,SHHE}/\rho_{L0}$ is calculated by subtracting the linear contribution from $\rho_T(B_z)/\rho_{L0}$; the result at 1 T field is displayed in Fig. 2(a). Fitting the thickness dependence of both longitudinal and transverse SHHE leads to λ_s=1.63 ± 0.26 nm. The λ_s values are comparable to the value reported in polycrystalline Pt/sapphire at 300 K and single crystalline Pt/Fe/MgO.

With the estimation of λ_s, we fit the field dependence of SHHE and derive the value of θ_{SH}, τ_s. Figure 2(b) and 2(c) shows fittings of both longitudinal and transverse SHHE signals from three different Pt/Al_2O_3 films. For each film, same set of parameters (θ_{SH}, λ_s, τ_s) have been used

to fit both longitudinal and transverse SHHE. We found that θ_{SH} and τ_s are 0.022±0.006 and 1.8±0.9 ps, respectively in our Pt thin films. One salient difference between this work and previous work is that the spin relaxation time τ_s is roughly one order of magnitude longer in the epitaxial Pt films used in this work, which is critical for reaching the strong-precession condition of SHHE.

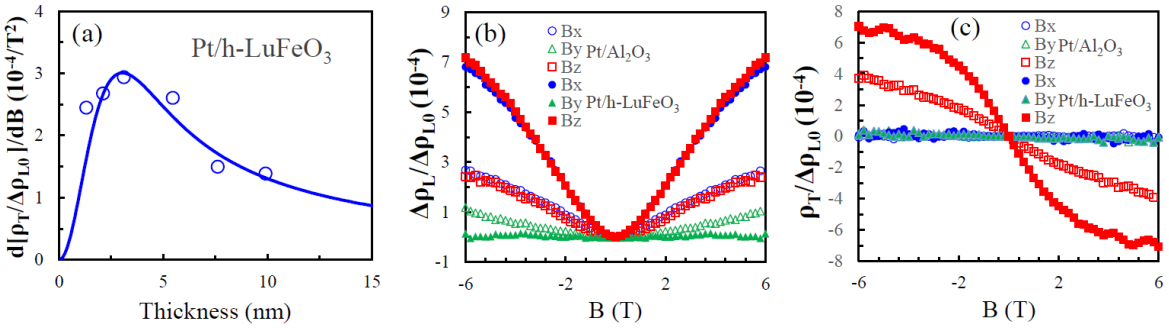

Figure 3. (a) Thickness dependence of the low-field slope of the Hall effect for Pt/h-$LuFeO_3$. The fitting reveals a spin diffusion length λ_s = 0.9 ± 0.2 nm. Measured transverse Hall resistivity normalized with the zero-field longitudinal resistivity. Field dependence of the normalized longitudinal resistivity (magnetoresistance) (b) and transverse resistivity (Hall effect) (c) of a Pt (5.4 nm)/h-$LuFeO_3$ and a Pt (5.2 nm)/Al_2O_3 samples.

Furthermore, we studied SHHEs with a Pt/h-$LuFeO_3$ interface, where h-$LuFeO_3$ is ferroelectric with polarization about 10 $\mu C/cm^2$. Figure 3(a) shows the thickness dependence of the Hanle Hall effect $\rho_T(B_z)$ slope. By fitting the slope, we found the spin diffusion length as λ_s = 0.9 ± 0.2 nm. Figure 3(b) and (c) show the MR (i.e., field dependence of ρ_L) and the Hall effect (i.e., field dependence of ρ_T) in Pt (5.4 nm)/h-$LuFeO_3$ and in Pt (5.2 nm)/Al_2O_3 [3]. Remarkably, we found that the magnitude of both MR and Hall effect are much larger in Pt(5.4 nm)/h-$LuFeO_3$ than that in Pt(5.2 nm)/Al_2O_3, implying that the spin Hall angle θ_{SH} is substantially larger in the Pt/h-$LuFeO_3$.

Future Plans

1. Comprehensive study on the Pt interface with isomorphic ferroelectric materials, i.e., hexagonal ferrites and manganites.
2. Study the effect of polarization switching on the Pt/ferroelectric interface.

References

[1] X. Xu, *A Brief Review of Ferroelectric Control of Magnetoresistance in Organic Spin Valves*, J. Mater. **4**, 1 (2018).

[2] Y. Yin, Y. Yin, X. Jiang, M. A. Koten, J. E. Shield, X. Chen, Y. Yun, A. T. N'Diaye, X. Hong, and X. Xu, *Spin Rectification and Electrically Controlled Spin Transport in Molecular-Ferroelectrics-Based Spin Valves*, Phys. Rev. Appl. **13**, 064011 (2020).

[3] J. Li, A. H. Comstock, D. Sun, and X. Xu, *Comprehensive Demonstration of Spin Hall Hanle Effects in Epitaxial Pt Thin Films*, Phys. Rev. B **106**, 1 (2022).

[4] M. I. Dyakonov, *Magnetoresistance Due to Edge Spin Accumulation*, Phys. Rev. Lett. **99**, 126601 (2007).

[5] J.-C. Rojas-Sánchez, N. Reyren, P. Laczkowski, W. Savero, J.-P. Attané, C. Deranlot, M. Jamet, J.-M. George, L. Vila, and H. Jaffrès, *Spin Pumping and Inverse Spin Hall Effect in Platinum: The Essential Role of Spin-Memory Loss at Metallic Interfaces*, Phys. Rev. Lett. **112**, 106602 (2014).

Publications

[1]Jing Li, Andrew H. Comstock, Dali Sun, and Xiaoshan Xu, *Comprehensive demonstration of spin Hall Hanle effects in epitaxial Pt thin films*, Physical Review B **106**, 184420 (2022).

[2]Xuanyuan Jiang, Xiao Wang, Pratyush Buragohain, Andy T. Clark, Haidong Lu, Shashi Poddar, Le Yu, Anthony D. DiChiara, Alexei Gruverman, Xuemei Cheng, and Xiaoshan Xu, *Persistent opto-ferroelectric responses in molecular ferroelectrics*, Physical Review Materials **6**, 074412 (2022).

[3]Yu Yun, Pratyush Buragohain, Ming Li, Zahra Ahmadi, Yizhi Zhang, Xin Li, Haohan Wang, Jing Li, Ping Lu, Lingling Tao, Haiyan Wang, Jeffrey E. Shield, Evgeny Y. Tsymbal, Alexei Gruverman and Xiaoshan Xu, *Intrinsic ferroelectricity in Y-doped HfO2 thin films*, Nature Materials **21**, 903–909 (2022).

[4]Yifan Yuan, Yuanyuan Ni, Xuanyuan Jiang, Yu Yun, Jing Li, and Xiaoshan Xu, *Highly Oriented Organic Ferroelectric Films with Single-Crystal-Level Properties from Restrained Crystallization*, Crystal Growth Design, **22**, 2124–2131 (2022).

Project Title: Sub-Nanosecond Switching of Antiferromagnets Driven by Interfacial Spin-Orbit Torque

Principle Investigator: **Fengyuan Yang**
Affiliation: Department of Physics, The Ohio State University, Columbus, OH 43210

Keywords: spintronics, thin film heterostructures, antiferromagnets, magnetotransport

Research Scope:

The goal of this DOE research project is to investigate fast spin-orbit torque (SOT) switching of antiferromagnets (AFM) enabled by their interface with heavy metals (HM) or topological insulators (TI) driven by electrical pulses with duration down to 0.3 nanosecond. Compared to ferromagnets (FM), AFMs offer numerous advantages such as low damping loss, robustness against stray magnetic field, ultrafast picosecond speed, terahertz dynamics, and abundancy for spintronics. Recent breakthroughs in electrical switching of AFMs have led to the emergence of antiferromagnetic spintronics as one of the most exciting frontiers in condensed matter physics. SOT has become the preferred choice for controlling both FMs and AFMs with high scalability and novel functionalities. Given the infancy of the new field of antiferromagnetic spintronics, the electrical switching of AFMs at fast time scales (~ns) has been essentially unexplored, which is needed for the understanding of ultrafast AFM spin dynamics and the development of high-speed AFM spintronic devices. This project has the following aims to uncover the fast switching behaviors of AFM spins and the underlying mechanisms: (1) achieve spin-orbit torque switching of AFM insulators (e.g., Fe_2O_3 and NiO) and semiconductor (MnTe) enabled by an adjacent TI layer (e.g., Bi_2Se_3); (2) probe electrical switching in HM/AFM and TI/AFM bilayers using pulses with duration ranging from quasi-DC to 0.3 ns and understand the time-energy scales of fast AFM switching.

This research project focuses on AFM insulators and semiconductor with high Néel temperatures and moderate anisotropies, which ensure AFM stability and allow for electrical switching at room temperature. TIs can provide high charge-to-spin conversion efficiency and giant SOT due to the surface spin-momentum locking. This project will demonstrate electrical switching of AFMs by an adjacent TI with high charge-to-spin conversion efficiency.

Recent Progress

- **Third Harmonic characterization of Spin/Magnetic Interactions in Antiferromagnetic Heterostructures**

Lock-in detection technique has been widely used to investigate current-induced spin torque contributions in HM/FM systems by measuring the first and second harmonic voltages.[1] Supported primarily by this DOE grant, we reported, for the first time, harmonic measurements in HM/AFM bilayer Pt/α-Fe_2O_3.[2] As compared to HM/FM bilayers where spin torques only contribute to the second harmonic signals, our results show that for HM/AFMs, the damping-like SOT, as well as the magnetoelastic effect, appear in the third harmonic response. Our theoretical modeling, together with the temperature-dependent harmonic measurements, indicate that magnetoelastic effect could have an important contribution to current-induced AFM switching.

We used Pt(5 nm)/α-Fe_2O_3(30 nm) bilayers patterned into a 5 μm wide Hall cross (Fig. 1a) for the harmonic measurement with a 4 mA ac current at 17 Hz while the first (1ω), second (2ω), and third (3ω) harmonic voltages are recorded by a lock-in amplifier. Figure 1b schematically illustrates the two spin sublattices $\boldsymbol{m}_{\mathbf{A(B)}}$ of α-Fe_2O_3 with the in-plane magnetic field applied at an angle φ_H relative to the $\boldsymbol{x}$ axis. We define the unit vector of Néel order $\boldsymbol{n} = \frac{\boldsymbol{m_A} - \boldsymbol{m_B}}{|\boldsymbol{m_A} - \boldsymbol{m_B}|}$ and net magnetization $\boldsymbol{m} = \boldsymbol{m_A} + \boldsymbol{m_B}$ (Fig. 1c). Figure 1d shows the φ_H-dependence of first harmonic voltage $V_{1\omega}$. Based on the theory of spin Hall magnetoresistance (SMR), when the current is applied along the $\boldsymbol{x}$ direction, the generated spin current with spin polarization $\boldsymbol{\sigma}$ is along the $\boldsymbol{y}$ direction. Depending on the relative angle between $\boldsymbol{\sigma}$ and $\boldsymbol{n}$, the transverse voltage $V_{1\omega} \propto n_x n_y$. For our α-Fe_2O_3 films, the spin-flop transition occurs at the critical field of <1 T, where the Néel order is perpendicular to the magnetic field. Then,

$$V_{1\omega} = -V_{\mathrm{TSMR}} \sin 2\varphi_H. \qquad (1)$$

Such transvers SMR (TSMR) has been demonstrated in many Pt/AFM bilayer systems. Fitting the angular-dependent $V_{1\omega}$ curves in Fig. 1d with Eq. (1), we extract V_{TSMR} for each value of the magnetic field, as shown in Fig. 1e. V_{TSMR} saturates near $\mu_0 H$ = 1 T, indicating single domain AFM state at $\mu_0 H$ > 1 T.

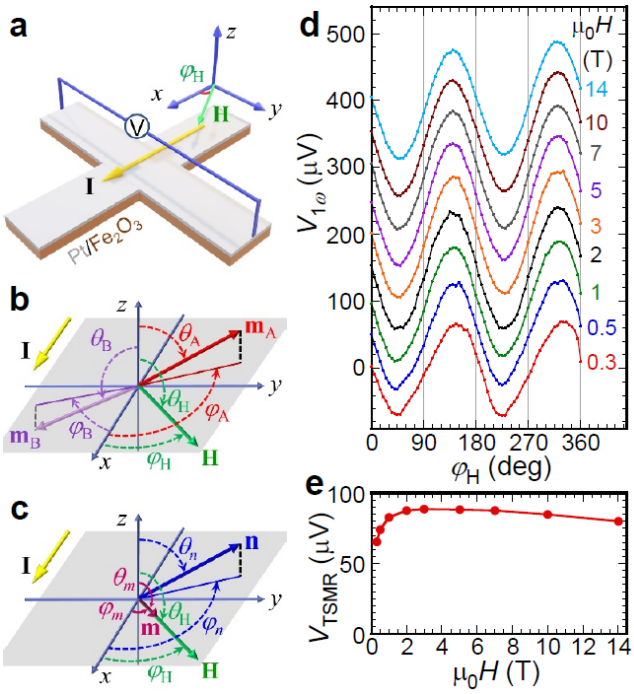

Figure 1. Schematics of **a**, a Pt/α-Fe_2O_3 Hall cross, **b**, two spin sublattices $\boldsymbol{m}_{\mathbf{A(B)}}$, and **c**, unit vector of Néel order $\boldsymbol{n}$ and net magnetization $\boldsymbol{m}$ of α-Fe_2O_3 in the presence of an in-plane magnetic field $\boldsymbol{H}$ within a spherical coordinate system with polar angle θ and azimuthal angle φ for each of the vectors. **d**, In-plane angular dependence of first harmonic Hall voltage $V_{1\omega}$ for a Pt(5 nm)/α-Fe_2O_3(30 nm) bilayer at different magnetic fields from 0.3 to 14 T and T = 300 K. **e**, Field dependence of transverse spin Hall magnetoresistance voltage V_{TSMR}.

In addition to the first harmonic signals, we simultaneously measure the second and third harmonic voltages. For $V_{2\omega}$, our modeling shows that it consists of two components, the field-like (FL) SOT and the spin Seebeck effect (SSE), which can be written as,

$$V_{2\omega} = V_{2\omega}^{\mathrm{FL}} + V_{2\omega}^{\mathrm{SSE}} = V_{\mathrm{TSMR}} \frac{H_{\mathrm{FL}}}{H} \cos(2\varphi_H) \cos\varphi_H + V_{\mathrm{SSE}} \cos\varphi_H, \qquad (2)$$

where H_{FL} is the effective field of filed-like torque and V_{SSE} is the SSE voltage. Figure 2a shows the in-plane angular dependent $V_{2\omega}$ at different magnetic fields from 1 to 14 T. Each curve in Fig. 2a is fitted by Eq. (2), such as those shown in Fig. 2b for $\mu_0 H$ = 5 T. We extract the magnitudes of these two contributions at different magnetic fields as shown in Figs. 2c and 2d. We find the differences between AFMs and their FM counterparts. For FMs, the SSE saturates when the total magnetization is aligned with the magnetic field, while the SSE in Pt/α-Fe_2O_3 linearly increases with H because when H exceeds the spin-flop field, the net magnetization in α-Fe_2O_3 is $\boldsymbol{m} = \chi_\perp \boldsymbol{H}$, resulting in $V_{SSE} \propto \boldsymbol{m} \propto \boldsymbol{H}$. The SSE in AFMs originates from the tilting-induced net magnetic

moment which is in parallel to the external field.

For the field-like torque shown in Fig. 2d, $V_{2\omega}^{\mathrm{FL}}$ first increases with field at $\mu_0 H < 1$ T and then decreases at higher fields. The inset of Fig. 2d gives the $1/\mu_0 H$ dependence of $V_{2\omega}^{\mathrm{FL}}$, which clearly shows that the $1/H$ dependence as predicted by Eq. (2) is valid at high fields. From the fitting, we obtain $H_{\mathrm{FL}} = 35$ Oe, which is consistent with previous reports, while the Oersted field contribution in our Hall cross is only ~5 Oe.

In our modeling of the harmonic signals for Pt/α-Fe_2O_3, a striking difference as compared with FMs is that the damping-like (DL) torque contribution does not appear in the second harmonic, but in the third harmonic voltage. A detailed study of the third harmonic voltage reveals that there are three terms in $V_{3\omega}$,

$$V_{3\omega} = V_{3\omega}^{\mathrm{DL}} + V_{3\omega}^{\mathrm{ME}} + V_{3\omega}^{\Delta \mathrm{R}}$$
$$= V_{\mathrm{TSMR}}\left(-\frac{H_{\mathrm{ex}}{H_{\mathrm{DL}}}^2}{4H(H+H_{\mathrm{DM}})\left(H_{\mathrm{K}}+H_{\mathrm{DM}}\left(\frac{H+H_{\mathrm{DM}}}{2H_{\mathrm{ex}}}\right)\right)} + \frac{H_{\mathrm{ex}}H_{\mathrm{ME}}}{4H(H+H_{\mathrm{DM}})}\right)\sin 4\varphi_{\mathrm{H}} + \frac{1}{8}\Delta V_{\mathrm{TSMR}} \sin 2\varphi_{\mathrm{H}}, \quad (3)$$

where $V_{3\omega}^{\mathrm{DL}}$, $V_{3\omega}^{\mathrm{ME}}$, and $V_{3\omega}^{\Delta \mathrm{R}}$ are the damping-like torque, magnetoelastic (ME) effect, and change of the resistivity (ΔR) term, respectively. H_{ex}, H_{DM}, H_{K}, H_{DL}, and H_{ME} are the exchange field, DMI effective field, easy-plane anisotropy field, damping-like torque effective field, and ME-induced effective easy-axis anisotropic field along $\boldsymbol{x}$, respectively. $V_{3\omega}^{\Delta \mathrm{R}}$ originates from the change of Pt resistivity due to the applied current. Equation (3) reveals why damping-like torque and ME only appear in the third harmonic voltage as ${H_{\mathrm{DL}}}^2$ and $H_{\mathrm{ME}} \propto I^2$, whereas in FMs, linear dependence of H_{DL} appears in the second harmonic voltage.

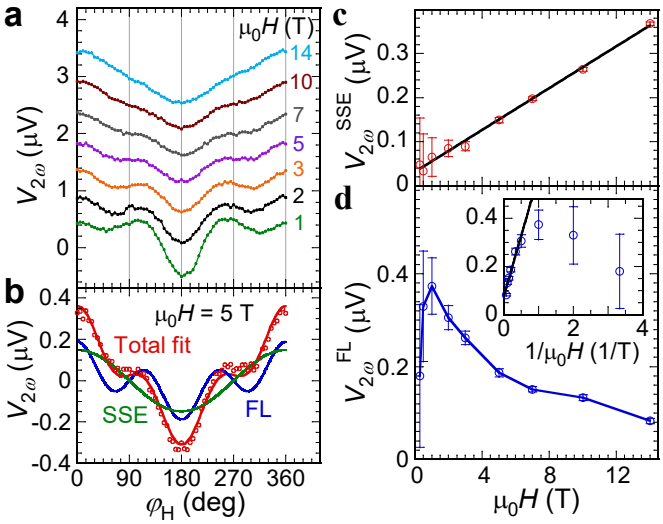

Figure 2. Second harmonic results. a, In-plane angular dependence of second harmonic Hall voltage $V_{2\omega}$ at different fields for a Pt(5 nm)/α-Fe_2O_3(30 nm) bilayer at 300 K. **b**, Angular dependence of $V_{2\omega}$ at 5 T with fitted contributions from the field-like torque and spin Seebeck effect. Field dependencies of **c**, $V_{2\omega}^{\mathrm{SSE}}$ and **d**, $V_{2\omega}^{\mathrm{FL}}$ where the inset shows the corresponding $1/H$ plots and linear fitting. $V_{2\omega}^{\mathrm{SSE}}$ exhibits a linear dependence of field. $V_{2\omega}^{\mathrm{FL}}$ shows a $1/H$ dependence at $\mu_0 H > 1$ T.

Figure 3a shows the angular dependence of $V_{3\omega}$ at different fields, which is fitted by Eq. (3). Figures 3b and 3c show the fitting of $V_{3\omega}$ for 0.3 and 10 T, respectively. At 0.3 T, the $V_{3\omega}^{\mathrm{DL}}$ and $V_{3\omega}^{\mathrm{ME}}$ contribution with a $\sin 4\varphi_{\mathrm{H}}$ dependence is comparable to the $V_{3\omega}^{\Delta \mathrm{R}}$ term with a $\sin 2\varphi_{\mathrm{H}}$ dependence. However, at 10 T, $V_{3\omega}^{\Delta \mathrm{R}}$ dominates the third harmonic voltage. Since $V_{3\omega}^{\mathrm{DL}}$ and $V_{3\omega}^{\mathrm{ME}}$ have the same angular dependence, they are combined as $V_{3\omega}^{\mathrm{DL+ME}}$, which shows a quick decay as the field increases.

To better understand the contribution from $V_{3\omega}^{\mathrm{DL}}$ and $V_{3\omega}^{\mathrm{ME}}$, we make the same harmonic measurement at lower temperatures. We find that $V_{3\omega}^{\mathrm{DL+ME}}$ decreases at lower temperatures and basically vanishes at 100 K. The effective anisotropic field of the magnetoelastic effect H_{ME} is

induced by thermoelastic stress Δσ. We use the finite-element simulation to estimate Δσ in our Hall cross at the corresponding temperatures, from which H_{ME} is obtained. We estimate that H_{ME} in our experiment is ~0.1 Oe at 300 K, while the damping-like torque effective field H_{DL} has the order of 1 Oe. One notes that this is an order of magnitude smaller than H_{FL}, which may be related to the insulating nature of Fe_2O_3.

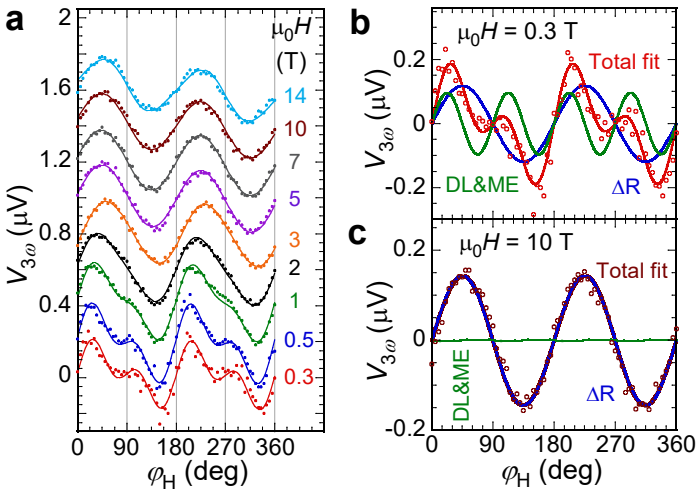

Figure 3. **Third harmonic results. a**, In-plane angular dependence of third harmonic Hall voltage $V_{3\omega}$ at different fields for a Pt(5 nm)/α-Fe_2O_3(30 nm) bilayer at 300 K. Angular dependencies of $V_{3\omega}$ at **b**, 0.3 T and **c**, 10 T with fitted contributions from the change of Pt resistivity (ΔR), damping-like torque and the magnetoelastic effect.

As harmonic measurements have been used in many FMs, we show that they also serve as a powerful tool in investigating current-induced effects in HM/AFM systems. We find that $V_{2\omega}^{\mathrm{FL}}$ and $V_{2\omega}^{\mathrm{SSE}}$ have similar in-plane angular dependence as those in FMs because the current-induced FL torque and SSE act similarly on AFMs as on FMs. The third harmonic voltage shows the key difference between AFMs and FMs where both DL torque and ME terms play an important role for AFMs. This work was funded primarily by this DOE grant and published in Nature Communications in June 2022.

Future Plans

In the coming year, we will be focusing on further DC and pulse electrical measurements of AFM films and structures, including Pt/α-Fe_2O_3 bilayers, MnTe films, and Pt/MnTe bilayers to gain deeper understanding of the spin interactions and electrical switching of antiferromagnetic heterostructures. In addition, we will investigate AFM films grown on piezoelectric single-crystal substrates (such as PMNT) for magnetoelectric control of AFM spins and domains using electrical and MOKE imaging techniques.

References

1. Garello, K., Miron, I. M., Avci, C. O., Freimuth, F., Mokrousov, Y., Blügel, S., Auffret, S., Boulle, O., Gaudin, G. & Gambardella, P. Symmetry and magnitude of spin–orbit torques in ferromagnetic heterostructures. *Nat. Nanotechnol.* **2013**, 8, 587-593.
2. Y. Cheng, E. Cogulu, R. D. Resnick, J. J. Michel, N. N. Statuto, A. D. Kent, and F. Y. Yang, "Third Harmonic Characterization of Antiferromagnetic Heterostructures," *Nat. Commun.* **13**, 3659 (2022).

Publications (2021-2023)

1. J. J. Michel, J. Flores, and F. Y. Yang, "Sub-Nanosecond Electrical Pulse Switching of an Easy Plane Antiferromagnetic Insulator," under review, arXiv:2211.07589.
2. Y. Cheng, J. Y. Tang, J. J. Michel, S. K. Chong, F. Y. Yang, R. Cheng, and K. L. Wang, "Unidirectional Spin Hall Magnetoresistance in Antiferromagnetic Heterostructures," *Phys. Rev. Lett.* **130**, 086703 (2023).
3. Q. C. Guo, A. D'Addario, Y. Cheng, J. Kline, I. Gray, H. F. H. Cheung, F. Y. Yang, K. C. Nowack, and G. D Fuchs, "Current-induced switching of thin film devices imaged using a scanning single-spin microscope," *Phys. Rev. Mater.* **7**, 064402 (2023).
4. J. M. Li, Y. H. Gu, Y. Takahashi, K. Higashi, T. Kim, Y. Cheng, F. Y. Yang, J. Kuneš, J. Pelliciari, A. Hariki, and V. Bisogni, "Single- and Multimagnon Dynamics in Antiferromagnetic α-Fe_2O_3 Thin Films," *Phys. Rev. X* **13**, 011012 (2023).
5. Y. Cheng, E. Cogulu, R. D. Resnick, J. J. Michel, N. N. Statuto, A. D. Kent, and F. Y. Yang, "Third Harmonic Characterization of Antiferromagnetic Heterostructures," *Nat. Commun.* **13**, 3659 (2022).
6. X. Kuang, S. Wu, Q. J. Ze, L. Yue, Y. Jin, S. M. Montgomery, F. Y. Yang, H. J. Qi, and R. K. Zhao, "Magnetic Dynamic Polymers for Modular Assembling and Reconfigurable Morphing Architectures," *Adv. Mater.* **33**, 2102113 (2021).
7. Y. Cheng, S. S. Yu, M. L. Zhu, J. Hwang, and F. Y. Yang, "Tunable topological Hall effects in noncollinear antiferromagnet Mn_3Sn/Pt bilayers," *APL Mater.* **9**, 051121 (2021).

Current Driven Switching of the Neel Vector

Fernando Ajejas[1], Felipe Torres[2, 3], Ali C. Basaran[1], Pavel Salev[1], and Ivan K. Schuller[1]
[1] University of California, San Diego, [2] Universidad de Chile, [3] Centro de Nanociencia y Nanotecnología (CEDENNA), Chile.

Keywords: spintronics/magnonics, thin film heterostructures, antiferromagnets, magnetotransport, magnetic imaging

Research Scope

Modifying and controlling electrically the properties of antiferromagnets (AFM) is an interesting basic research problem and a promising avenue for the development of novel spintronic technologies.[1] A specific implementation of this this task can take advantage of the proximity effect between different magnetic materials. In particular we are developing devices in which the spin configuration of AFM insulators is modified by pure spin currents generated in adjacent heavy metal (HM) layers.[2] We designed a trilayer, HM|AFM|FM heterostructure, where the top ferromagnetic (FM) layer is exchange coupled[3] to the AFM layer and thus can be used to monitor the changes in the AFM spin configuration. Magneto-optical Kerr effect and magneto-transport can be used to probe the FM hysteresis loops as a function of temperature (T) and applied current (I) which directly reflects the AFM spin configuration. The use of insulating AFMs allows us to rule out potential delirious effects which arise from the use of conducting AFMs.

Recent Progress

We have synthesized a HM (Pt, W, Au)/AFM (FeF_2)/FM(Ni) heterostructure to study the effect of spin current generated in the HM on the magnetic state of the AFM.[4] We showed that the exchange bias (H_{EB}) and coercivity (H_c) due to the bulk AFM spins at the AFM|FM interface can be strongly modified by the current applied to the HM layer [Fig. 1]. We showed that this is due to the spin-orbit torque generated at the HM|AFM interface that reaches the AFM|FM interface, modifying the amplitude and sign of H_{EB}. We found a critical current beyond which the effects on the H_{EB} and H_c are irreversible. The AFM blocking temperature is shifted and the Néel vector is switched once a critical current is overcome. Temperature-dependent control experiments using normal metals (NM) in NM|AFM|FM and without AFM in HM|FM confirmed that the effect is produced by the HM-induced spin orbit torque and is not caused by thermal heating, Oersted field, or other potentially spurious effects.

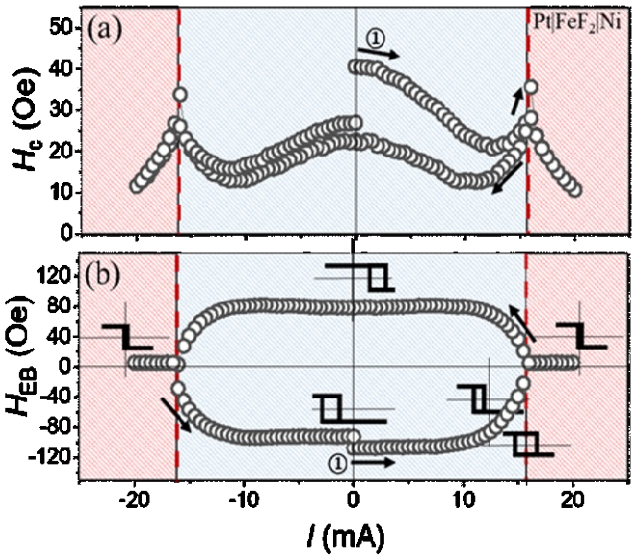

Figure 1: Pt|FeF_2|Ni (a) H_c and (b) H_{EB} as a function of the applied current I at 20 K. The arrows show the direction of the I cycle. The blue (red) area represents the region where the current effects are volatile (permanent). The dashed lines show the current where the magnetization is switched.

Future Plans

We will study the experimental systematics by investigating different insulating AFMs, different ferromagnets and by adding ion beam induced modification in the different layer of the heterostructures. We will also develop models based on microscopic theories to explain and predict the systematic behavior as a function of blocking temperature, orientation of the Neel vector, and angular dependence of the spin current.

References

1. V. Baltz, A. Manchon, M. Tsoi, T. Moriyama, T. Ono, and Y. Tserkovnyak, *Antiferromagnetic spintronics*, Rev. Mod. Phys. **90**, 15005 (2018).
2. D. Hou, Z. Qiu, and E. Saitoh, *Spin transport in antiferromagnetic insulators: progress and challenges*. NPG Asia Mater. **11**, 1 (2019)
3. Josep Nogues and Ivan K. Schuller, *Exchange Bias,* J. Magn. Magn. Mater. **192**, 203 (1999)
4. Fernando Ajejas, Felipe Torres, Ali C. Basaran, Pavel Salev, and Ivan K. Schuller, *Current-driven switching of Néel vector of an antiferromagnetic insulator thin film*, Adv. Elec. Mat. 2023 (in press)

Publications

1. Jun-young Kim, Joel Cramer, Kyujoon Lee, Dong-Soo Han, Dongwook Go, Pavel Salev, Pavel N. Lapa, Nicolas M. Vargas, Ivan K. Schuller, Yuriy Mokrousov, Gerhard Jakob, and Mathias Kläui, *Tuning Spin-Orbit Torques Across the Phase Transition in VO_2/NiFe Heterostructure,* Adv. Funct. Mater. **32**, 2111555 (2022)
2. Ali C. Basaran, C. Monton, J. Trastoy, R. Bernard, K. Bouzehouane, J.E. Villegas, Ivan K. Schuller, *Emergence of Exchange Bias and Giant Coercive Field Enhancement by Internal Magnetic Frustration in $La_{0.67}Sr_{0.33}MnO_3$ Thin Films*, J. Mag. Mag. Mat, **550**, 169077 (2022)
3. José Manuel Díez, José Luis F. Cuñado, Pavel Lapa, Raúl Solís, Icíar Arnay, Patricia Pedraz, Paolo Perna, Alberto Bollero, Rodolfo Miranda, Ivan K. Schuller, and Julio Camarero, *Interfacial exchange phenomena driven by ferromagnetic domains*, Adv. Mater. Interfaces. **9**, 2200331 (2022)
4. Christian T. Wolowiec, Juan Gabriel Ramírez, Min-Han Lee, Nareg Ghazikhanian, Nicolas M. Vargas, Ali C. Basaran, Pavel Salev, and Ivan K. Schuller, *Stress-tailoring magnetic anisotropy of V_2O_3/Ni bilayers,* Phys. Rev. Materials **6**, 064408 (2022)
5. C. Adda, H. Navarro, J. Kaur, M.-H. Lee, C. Chen, M. Rozenberg, S. P. Ong, and Ivan K. Schuller, *An optoelectronic heterostructure for neuromorphic computing: CdS/V_3O_5*, Appl. Phys. Lett. **121**, 041901 (2022)
6. Renjie Luo, Xuanhan Zhao, Liyang Chen, Tanner J. Legvold, Henry Navarro, Ivan K. Schuller, and Douglas Natelson, *Spin Seebeck effect at low temperatures in the nominally paramagnetic insulating state of vanadium dioxide,* Appl. Phys. Lett. **121**, 102404 (2022)
7. Parente, H. Navarro, N. M. Vargas, P. Lapa, Ali C. Basaran, E. M. González, C. Redondo, R. Morales, A. Munoz Noval, Ivan K. Schuller, and J. L. Vicent, *Unusual Magnetic Hysteresis and Transition between Vortex and Double Pole States Arising from Interlayer Coupling in Diamond-Shaped Nanostructure,* ACS Appl. Mater. Interfaces, **14**, 54961 (2022)
8. Alexander J. Breindel, Yuhang Deng, Camilla M. Moir, Yuankan Fang, Sheng Ran, Hongbo Laub, Shubin, Qiaoshi Zeng, Lei Shud, Christian T. Wolowiec, Ivan K. Schuller, Priscila F. S. Rosa, Zachary Fisk, John Singleton, and M. Brian Maple, *Probing FeSi, a d-electron topological Kondo insulator candidate, with magnetic field, pressure, and microwaves,* PNAS **120-8** e2216367120 (2023)
9. Ali C. Basaran, F. Ajejas, L. Fratino, S. Bag, T.D. Wang, E. Qiu, V. Rouco, I. Tenreiro, F. Torres, A. Rivera-Calzada, J. Santamaria, M. Rozenberg, and Ivan K. Schuller. *Light-Induced Decoupling of Electronic and Magnetic Properties in Manganites,* H. Navarro, Phys. Rev. Applied **19**, 044077 (2023)
10. Fernando Ajejas, Felipe Torres, Ali C. Basaran, Pavel Salev, Ivan K. Schuller, *Current-driven switching of Néel vector of an antiferromagnetic insulator thin film*, Advanced Electronic Materials (in press)

Oral Session 5

Title: Correlated States of Two-dimensional Electron Systems in AlAs Quantum Wells

Principal Investigator: M. Shayegan, Department of Electrical & Computer Engineering, Princeton University, Princeton, NJ, 08544

Keywords: spintronics/valleytronics, topology-quantum Hall, quantum wells, semiconductors, magnetotransport.

Research Scope

Two-dimensional (2D) carrier systems confined to modulation-doped semiconductor hetero-structures provide a nearly ideal testing ground for exploring new physical phenomena. At low temperatures and in the presence of a strong magnetic field, these systems exhibit fascinating, often unexpected, many-body states, arising from the strong electron-electron interaction.

Much of the work on clean 2D systems has been performed on 2D electrons in a remotely-doped *GaAs* quantum well. The goal of this project is to study the physics of 2D electrons confined to a remotely-doped *AlAs* quantum well. The 2D electrons in AlAs have parameters that are very different from those of the commonly-studied, GaAs 2D electrons: they have a much larger, anisotropic effective mass, a much larger effective Landé *g*-factor, and they occupy multiple conduction band valleys. Moreover, through varying the AlAs quantum well width, and also by applying uniaxial, in-plane strain, one can control the electron occupation in the different valleys. Demonstration of such control in AlAs quantum wells provided the first example of using the valley degree of freedom to change the electronic properties of an electron system and to make a functional device, and paved the way for the emerging field of "valleytronics."

We have had a very recent breakthrough in making AlAs quantum well samples with unprecedented quality. Through a systematic purification of the Al source material, we were able to optimize the growth conditions for AlAs quantum wells, and broke the world record (by a factor of eight) for the mobility of 2D electrons confined to these wells. The extremely high quality of these new samples, combined with the tunable valley degree of freedom, renders the AlAs 2D electron system a unique platform for studies of interaction-induced phenomena. Exploring such phenomena is the main goal of this research. For example, what role does the valley/spin degrees of freedom and effective mass anisotropy play in the competition between different correlated phases at high magnetic fields, namely the fractional quantum Hall liquid state and broken-symmetry states such as the Wigner crystal and stripe phases?

Moreover, the effective mass of electrons is about seven times larger in AlAs compared to GaAs, effectively making the AlAs 2D electrons much more dilute and therefore more interacting, even in the absence of a magnetic field. The parameter r_s, defined as the ratio of the Coulomb to kinetic (Fermi) energy, can indeed reach ~50 in our new AlAs samples (at a density of ~$1x10^{10}$ cm^{-2}) while still maintaining high enough quality to exhibit quantum Hall effect. These are prime samples to potentially exhibit the long-anticipated (since 1929) Bloch/Stoner spin and/or valley ferromagnetism of itinerant electrons.

In our project we study AlAs quantum well structures grown via state-of-the-art molecular beam epitaxy (MBE), and use low-temperature magneto-transport measurements to explore their novel physics. For sample fabrication, we collaborate closely with Dr. Loren Pfeiffer at Princeton

University who is a world expert in MBE, and Prof. Roland Winkler at the Univ. of Northern Illinois, who has expertise in calculating the energy band structure and Landau levels in various 2D systems.

Recent Progress

In a seminal work in 1929 Felix Bloch predicted that as the electron density is lowered in an ensemble of electrons, the exchange energy gained by aligning the electron spins should exceed the enhancement in the kinetic (Fermi) energy, leading to a (Bloch) ferromagnetic transition. At even lower densities, another transition to a (Wigner) solid, an ordered array of electrons, should occur. Experimental access to these regimes, however, has been limited because of the absence of a material platform that supports an electron system with very high quality (low disorder) and low density simultaneously.

In our study we explored the ground states of interacting electrons in an exceptionally clean, 2D electron system confined to a modulation-doped AlAs quantum well. We observe spontaneous ferromagnetism, for both the spin and valley degrees of freedom, followed by a transition to an *anisotropic* Wigner solid, in dilute, interacting, AlAs 2D electron systems [1-3]. Our findings, are highlighted in Fig. 1. The large electron effective mass in this system allows us to reach very large values of the interaction parameter r_s, defined as the ratio of the Coulomb energy to kinetic (Fermi) energy. As we lower the electron density via back-gate bias, we find a sequence of exotic phases and transitions: (*i*) a paramagnetic phase at large densities, $n > 6.0 \times 10^{10}$ cm^{-2} ($r_s < 21$), (*ii*) a spontaneous transition to a *valley-polarized* phase when n is lowered below 6.0×10^{10} cm^{-2} ($r_s > 21$), (*iii*) a transition to a ferromagnetic state at $n = 2.0 \times 10^{10}$ cm^{-2} ($r_s > 35$), and (*iv*) finally a phase with strongly nonlinear current-voltage characteristics, suggestive of a pinned Wigner solid, when $n < 1.8 \times 10^{10}$ cm^{-2} ($r_s > 38$).

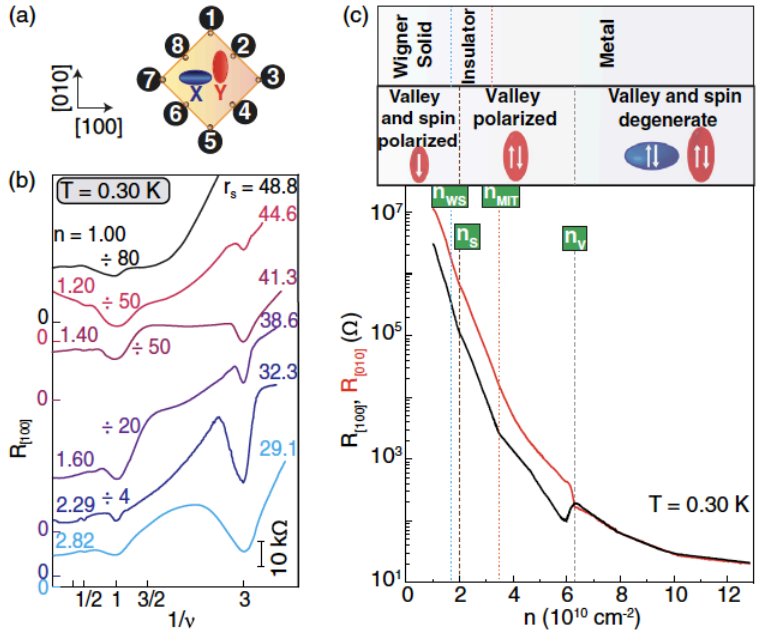

Fig. 1 Summary of various man-body states of AlAs 2D electrons observed in our studies. (From Ref. [3])

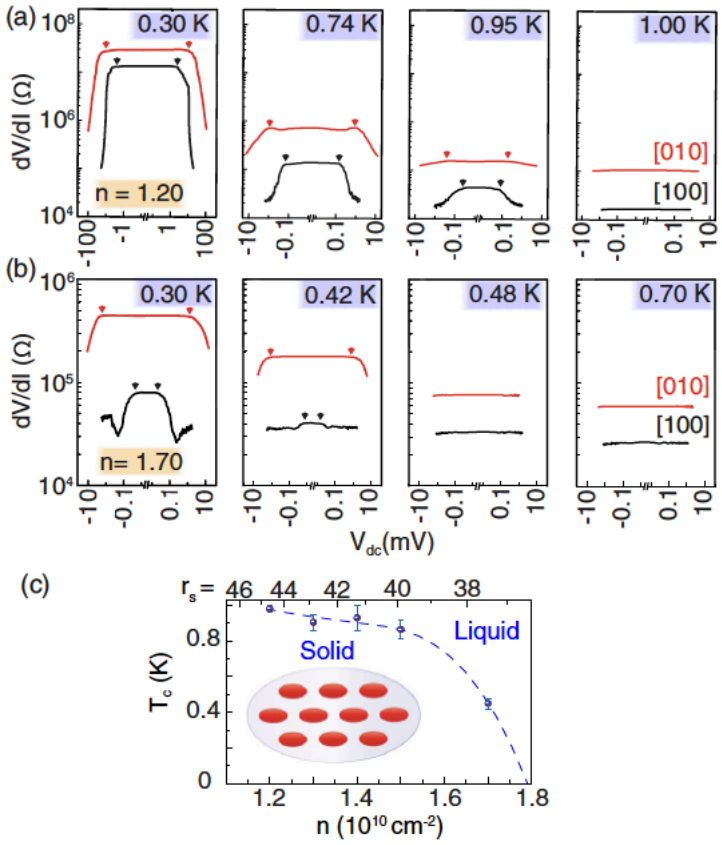

Fig. 2 Signatures of an *anisotropic*, pinned Wigner solid. Temperature dependence of the differential resistance (dV/dI) vs. applied *dc* voltage (V_{dc}) at (a) n = 1.2 x 10^{10} cm-2, and (b) n = 1.7 x 10^{10} cm^{-2}, measured along [100] and [010] crystallographic directions. (c) Critical temperature (T_c), below which the *I-V* characteristic becomes nonlinear, plotted vs electron density. The data suggest a drop in T_c with increasing density, extrapolating to 0 K as the onset density for the pinned Wigner solid formation (n = 1.80 x 10^{10} cm^{-2}) is reached. The dashed curve is a guide to the eye. The inset displays schematically an anisotropic WS; the shaded regions represent the electron charge distribution with anisotropic Bohr radii, reflecting the anisotropic electron effective mass. (From Ref. [3].

A very exciting surprise in our study has been that, before the 2D electron system makes the transition to a fully-spin-polarized state at $r_s \sim 35$, it reveals a sudden "valley-polarization" transition at higher densities ($r_s \sim 21$) [2]. The data, as summarized in Fig. 1(c), indicate a sudden anisotropy in resistances measured along [100] and [010] directions. Note that this transition is akin to the spin-polarization transition, except that here we see a transition in the valley degree of freedom. It is also noteworthy that the phenomenon and data demonstrate a quintessential example of a "valleytronic" field-effect type device: as we tune the density with a gate, we see a large change in the conductance of the device resulting from a change in the valley occupation.

Another noteworthy observation is that the 2D electron system at the lowest densities exhibits strongly non-linear current-voltage (*I-V*) characteristic, consistent with a pinned Wigner solid state [3] (see Fig. 2). Remarkably, this non-linear behavior is strongly *anisotropic*, with the current threshold for conduction along [010] being much larger than along [100], as seen in Figs. 2(a,b), suggesting the formation of an anisotropic Wigner solid. Our results stirred a bit of excitement, and our paper was featured in commentaries [3].

Our results and conclusions have been resoundingly confirmed in very recent theoretical quantum Monte Carlo calculations [4]. The calculated "phase diagram" presented in Fig. 1 of Ref. [4] shows that in a 2D system where the electrons have an anisotropic effective mass, such as our electron system in an AlAs quantum well, the mass anisotropy can indeed lead to the different phases we observe, including the spontaneously valley-polarized phase. The order in which we observe the different phases is also captured by the phase diagram of Ref. [4], although the r_s values at which the transitions take place do not agree with the experimental data quantitatively.

Future plans

We plan to continue our studies of 2D electrons in AlAs quantum wells. One problem of interest is the role of finite (non-zero) electron layer thickness. The non-zero thickness leads to a softening of the inter-electron Coulomb interaction, and can cause significant changes in the r_s values at which different transitions and phases are experimentally observed. We plan to fabricate, via molecular beam epitaxy, AlAs samples with different quantum well widths, and study their phases as a function of density, or equivalently, r_s.

Another interesting venue is to explore the evolution of the even-denominator fractional quantum Hall state at filling factor $\nu = ½$. Very recently, we observed a glimpse of such a state in an AlAs quantum well tilted magnetic fields [5]. This is very exciting as the quasi-particle excitations of the even-denominator fractional quantum Hall states are expected to obey non-Abelian statistics. We plan to focus further effort on this topic, e.g., design, fabricate, and study new samples that would exhibit the $\nu = ½$ state without the need for parallel magnetic fields.

References

1. Md. S. Hossain, K. A. Villegas-Rosales, M. K. Ma, Y. J. Chung, L. N. Pfeiffer, K. W. West, K. W. Baldwin, and M. Shayegan, *Observation of Spontaneous Ferromagnetism in a Two-Dimensional Electron System*, Proc. National Acad. Sciences (PNAS) **117**, 32244 (2020).

   See **Commentary:** Kyung-Su Kim and Steven A. Kivelson, *Discovery of an Insulating Ferromagnetic Phase of Electrons in Two Dimensions*, PNAS **118** (2) e2023964118 (2021).

2. Md. S. Hossain, M. K. Ma, K. A. Villegas-Rosales, Y. J. Chung, L. N. Pfeiffer, K. W. West, K. W. Baldwin, and M. Shayegan, *Spontaneous Valley Polarization of Itinerant Electrons*, Phys. Rev. Lett. **127**, 116601 (2021).

3. Md. S. Hossain, M. K. Ma, K. A. Villegas-Rosales, Y. J. Chung, L. N. Pfeiffer, K. W. West, K. W. Baldwin, M. Shayegan, R. Winkler, *Anisotropic Two-dimensional, Disordered Wigner Solid*, Phys. Rev. Lett. **129**, 036601 (2022). See **Featured in Physics:** *Squeezing a Wigner Solid*, by Allison Gasparini, *Physics* **15**, s93 (2022). And **Commentary** *Evidence of a new type of disordered quantum Wigner Solid*, by Ingrid Fadelli (Phys.org) on August 3, 2022; https://phys.org/news/2022-08-evidence-disordered-quantum-wigner-solid.html
4. Agnes Valenti, Vladimir Calvera, Steven A. Kivelson, Erez Berg, Sebastian D. Huber, *Nematic metal in a multi-valley electron gas: Variational Monte Carlo analysis and application to AlAs*, pre-print (2023); arXiv:2307.15119.
5. Md. Shafayat Hossain, Meng K. Ma, Y. J. Chung, S.K. Singh, A. Gupta, K. W. West, K. W. Baldwin, L. N. Pfeiffer, R. Winkler, and M. Shayegan, *Valley-tunable even-denominator fractional quantum Hall state in the lowest Landau level of an anisotropic system*, Phys. Rev. Lett. **130**, 126301 (2023). **[Editor's Suggestion]**

Ten Selected publications acknowledging DOE support; since September 2021:

1. Md. S. Hossain, M. K. Ma, K. A. Villegas-Rosales, Y. J. Chung, L. N. Pfeiffer, K. W. West, K. W. Baldwin, and M. Shayegan, "Spontaneous Valley Polarization of Itinerant Electrons," Phys. Rev. Lett. **127**, 116601 (2021).
2. Yoon Jang Chung, D. Graf, L. W. Engel, K. A. Villegas Rosales, P. T. Madathil,K. W. Baldwin, K. W. West, L. N. Pfeiffer, and M. Shayegan, "Correlated States of 2D Electrons near the Landau Level Filling $\nu = 1/7$," Phys. Rev. Lett. **128**, 026802 (2022).
3. Md. S. Hossain, M. K. Ma, K. A. Villegas-Rosales, Y. J. Chung, L. N. Pfeiffer, K. W. West, K. W. Baldwin, M. Shayegan, R. Winkler, "Anisotropic Two-dimensional, Disordered Wigner Solid," Phys. Rev. Lett. **129**, 036601 (2022).

   Featured in Physics: "Squeezing a Wigner Solid," by Allison Gasparini, *Physics* **15**, s93 (2022).

   https://physics.aps.org/articles/pdf/10.1103/Physics.15.s93

   Commentary "Evidence of a new type of disordered quantum Wigner Solid" by Ingrid Fadelli (Phys.org) on August 3, 2022; https://phys.org/news/2022-08-evidence-disordered-quantum-wigner-solid.html
4. Yoon Jang Chung, A. Gupta, K. W. Baldwin, K. W. West, M. Shayegan, and L. N. Pfeiffer "Understanding limits to mobility in ultra-high-mobility GaAs two-dimensional electron systems: The quest for 100 million cm^2/Vs and beyond," Phys. Rev. B **106**, 075134 (2022).
5. Chengyu Wang, A. Gupta, S. K. Singh, Y. J. Chung, L. N. Pfeiffer, K. W. West, K. W. Baldwin, R. Winkler, and M. Shayegan, "Even-denominator fractional quantum Hall state at filling factor $\nu = ¾$," Phys. Rev. Lett. **129**, 156801 (2022).

   [Editor's Suggestion] Also, **Featured in Physics:** "An Exotic Fractional Quantum Hall State," by Rachel Berkowitz, *Physics* **15**, s134 (2022).
6. Meng Ma, Chengyu Wang, Y. J. Chung, L. N. Pfeiffer, K. W. West, K. W. Baldwin, R. Winkler, and M. Shayegan, "Robust Quantum Hall Ferromagnetism near a Gate-tuned $\nu = 1$ Landau Level Crossing," Phys. Rev. Lett. **129**, 196801 (2022).
7. Md. Shafayat Hossain, Meng K. Ma, Y. J. Chung, S. K. Singh, A. Gupta, K. W. West, K. W. Baldwin, L. N. Pfeiffer, R. Winkler, and M. Shayegan, "Fractional quantum Hall valley ferromagnetism in the extreme quantum limit," Phys. Rev. B **106** (Letters), L201303 (2022).
8. Md. Shafayat Hossain, Meng K. Ma, Y. J. Chung, S.K. Singh, A. Gupta, K. W. West, K. W. Baldwin, L. N. Pfeiffer, R. Winkler, and M. Shayegan, "Valley-tunable even-denominator fractional quantum Hall state in the lowest Landau level of an anisotropic system," Phys. Rev. Lett. **130**, 126301 (2023). **[Editor's Suggestion]**
9. P. T. Madathil, K. A. Villegas Rosales, C. T. Tai, Y. J. Chung, L. N. Pfeiffer, K. W. West, K. W. Baldwin, and M. Shayegan, "Experiments on Delocalization and Universality of the Fractional Quantum Hall Plateau-to-Plateau Transitions," Phys. Rev. Lett. **130**, 226503 (2023).
10. Chengyu Wang, A. Gupta, Y. J. Chung, L. N. Pfeiffer, K. W. West, K. W. Baldwin, R. Winkler, and M. Shayegan, "Highly-Anisotropic Fractional Quantum Hall State at Even-Denominator Filling Factor $\nu = 3/2$, Phys. Rev. Lett. **131**, 056302 (2023).

Quantum Fluctuations in Narrow Band Systems – Thrust 1

Filip Ronning, Eric Bauer, Michihiro Hirata, Priscila Rosa, Allen Scheie, and Sean Thomas (Los Alamos National Lab)

Keywords: Magnetism, Topology, f-electron materials, Single crystals, Non-Fermi liquid behavior and charge dynamics

Research Scope

Coherence and topologically protected modes in quantum matter arise from highly entangled spin, charge, lattice, and orbital degrees of freedom. Narrow band systems, whose renormalized electronic bandwidth is comparable to other relevant energy scales in the material, inherently have strong interactions and a proliferation of quantum fluctuations. 4*f*- and especially 5*f*-materials possess strong Coulomb repulsion, large spin-orbit coupling, and multiple competing energy scales, which generate coherent narrow bands and topologically non-trivial states of matter. This complexity provides a rich environment for discovering new states of matter, as well as providing ideal representatives that enable the understanding of quantum matter that arises across the periodic table more generally. In thrust 1 we address how quantum fluctuations renormalize excitations in topologically trivial and non-trivial matter and will develop conceptual frameworks for understanding and controlling the consequences of quantum fluctuations in classes of electronically correlated systems. Currently, we are focusing on the role of magnetic frustration in renormalizing the electronic structure and generating instabilities towards new states of matter.

Recent Progress

Localized electrons such as *d*- and *f*-electrons possess strong quantum fluctuations as they interact with a sea of conduction electrons. At high temperatures scattering off these localized electrons is incoherent. Below a crossover scale known as the Kondo coherence scale the electronic structure acquires momentum dependence due to the coherent scattering from a lattice of these localized moments. Understanding the resulting narrow band renormalized electronic structure is key to unlocking the power of quantum materials. Using resonant inelastic X-ray scattering (RIXS) we have demonstrated how the bare electronic structure with eV energy scales is renormalized in the spin-orbit coupled J=5/2 and J=7/2 derived bands of the mixed valent material $CePd_3$ to a low energy electronic structure with an 11 meV bandwidth [1]. This work revealed the local character of the electronic renormalization in developing a lattice coherent low temperature electronic structure. $CePd_3$, however, is a mixed valent material far from magnetic instabilities. An open question is whether this local renormalization process persists in lower dimensional materials and/or systems with low temperature electronic instabilities. In support of this effort we have synthesized and characterized a quasi-1D compound, $YbFe_5P_3$, which appears to be in close proximity to a quantum critical point [2]. We have also begun spectroscopic investigation into CeRhSn and CeRhIn, two isostructural compounds where the cerium atoms occupy a distorted Kagome lattice. Both compounds are mixed valent materials, but the former is simultaneously

proximate to a quantum critical point. Our optical spectroscopy measurements show that the energy scale over which the electronic structure is renormalized is similar in both compounds, but the magnitude of spectral weight transfer is much stronger in the CeRhSn compound. We interpret this as evidence for anisotropic hybridization, which is significantly more pronounced in CeRhSn, and could explain the persistence of local moments to low energies.

We have also continued our exploration of clean narrow band gap materials, which are candidate correlated topological insulators due to the simultaneous presence of strong spin-orbit coupling and strong Coulomb interactions of the *f*-electrons. We performed thermopower measurements under pressure on SmB_6, which illustrated that the topologically protected surface state in this material is endowed with strong electronic correlations present in the bulk of the material [3]. Continuing our study of $Eu_5In_2Sb_6$, which illustrates colossal magnetoresistance, we showed that this candidate axion insulator also has a colossal piezoresistance [4], and through electron spin resonance measurements identified signatures of magnetic polarons controlling this physics, which shows a remarkable sensitivity to strain.

Future Plans

Our work on mixed valent $CePd_3$ demonstrated that inter-site correlations are insignificant for the coherent renormalized electronic structure for an isotropic material far from a magnetic instability. In the future we wish to determine the universality of this result by performing measurements on reduced dimensional and geometrically frustrated compounds such as $CeIr_3B_2$, $CeCo_2Ga_8$, and Ce*TX* (*T* = Rh, Pd; *X* = Sn, In). We will perform inelastic neutron scattering, optical spectroscopy, nuclear magnetic resonance, and La dilution studies to probe the momentum and energy dependence of the electronic renormalization to a coherent Kondo lattice due to the quantum fluctuations of the Ce *f*-electrons.

We recently reported our discovery of KU_2Te_6 – a trivial insulator with a narrow band gap of 130 meV [5]. A crystal field analysis demonstrated that the uranium 5*f*-electrons are localized in a non-magnetic ground state singlet. We will continue our materials exploration of layered narrow band gap 5*f*-materials with an eye towards observing strongly correlated topological materials. One such example will be to compare and contrast $UAgBi_2$ with $CeAgBi_2$ to understand the role of the more extended 5*f*-wavefunctions in uranium-based compounds relative to their 4*f*-cousins. Meanwhile, to determine the origin of the anomalous metal-insulator transition we found in $R_3Cd_2As_6$ (R=rare earth) crystals we will perform high resolution single crystal x-ray, transmission electron microscopy, nuclear quadrupole resonance, and magneto optical Kerr effect measurements.

References

1. M.C. Rahn, K. Kummer, A. Hariki, K.-H. Ahn, J. Kunes, A. Amorese, J.D. Denlinger, D.-H. Lu, M. Hashimoto, E. Rienks, M. Valvidares, F. Haslbeck, D. D. Byler, K. J. McClellan, E. D. Bauer, J.-X. Zhu, C. H. Booth, A.D. Christianson, J.M. Lawrence, F. Ronning, and M. Janoschek, *Kondo quasiparticle dynamics observed by resonant inelastic x-ray scattering*, Nature Communications **13**, 6129 (2022).

2. T. Asaba, S. Lee, S. Seo, K.E. Avers, S.M. Thomas, R. Movshovich, J.D. Thompson, P.F.S. Rosa, E.D. Bauer, F. Ronning, *Physical properties of $YbFe_5P_3$ with a quasi-one-dimensional crystal structure*, Physical Review B **104**, 195140 (2021).

3. S. Seo, Y. Luo, S.M. Thomas, Z. Fisk, O. Erten, P.S. Riseborough, F. Ronning, J.D. Thompson, and P.F.S. Rosa, *Persistence of correlation-driven surface states in SmB_6 under pressure*, Physical Review B **105**, 245150 (2022).

4. S. Ghosh, C. Lane, F. Ronning, E.D. Bauer, J.D. Thompson, J.-X. Zhu, P.F.S. Rosa, and S.M. Thomas, *Colossal Piezoresistance in Narrow-Gap $Eu_5In_2Sb_6$*, Physical Review B **106**, 045110 (2022).

5. M.M. Bordelon, S. S. Fender, S. M. Thomas, E.D. Bauer, and P.F.S. Rosa, *Structural anomaly and crystalline electric field excitations in low-dimensional KU_2Te_6*, Physical Review B **108**, 064406 (2023).

Publications (From 38 publications supported by this FWP over the past 2 years)

1. M.C. Rahn, K. Kummer, A. Hariki, K.-H. Ahn, J. Kunes, A. Amorese, J.D. Denlinger, D.-H. Lu, M. Hashimoto, E. Rienks, M. Valvidares, F. Haslbeck, D. D. Byler, K. J. McClellan, E. D. Bauer, J.-X. Zhu, C. H. Booth, A.D. Christianson, J.M. Lawrence, F. Ronning, and M. Janoschek, *Kondo quasiparticle dynamics observed by resonant inelastic x-ray scattering*, Nature Communications **13**, 6129 (2022).

2. M.M. Bordelon, S. S. Fender, S. M. Thomas, E.D. Bauer, and P.F.S. Rosa, *Structural anomaly and crystalline electric field excitations in low-dimensional KU_2Te_6*, Physical Review B **108**, 064406 (2023).

3. M.M. Bordelon, C. Girod, F. Ronning, K. Rubi, N. Harrison, J.D. Thompson, C. dela Cruz, S.M. Thomas, E.D. Bauer, and P.F.S. Rosa, *Interwoven atypical quantum states in $CeLiBi_2$*, Physical Review B **106**, 214433 (2022).

4. S. Ghosh, C. Lane, F. Ronning, E.D. Bauer, J.D. Thompson, J.-X. Zhu, P.F.S. Rosa, and S.M. Thomas, *Colossal Piezoresistance in Narrow-Gap $Eu_5In_2Sb_6$*, Physical Review B **106**, 045110 (2022).

5. M.M. Piva, L. Xiang, J.D. Thompson, S.L. Bud'ko, R.A. Ribeiro, P.C. Canfield, P.F.S. Rosa, *Effects of external pressure on the narrow-gap semiconductor $Ce_3Cd_2As_6$*, Physical Review *B* **105**, 094443 (2022).

6. Yu Liu, M.M. Bordelon, A. Weiland, P.F.S. Rosa, S.M. Thomas, J.D. Thompson, F. Ronning, and E.D. Bauer, *Physical properties of the layered f-electron van der Waals magnet Ce_2Te_5*, Physical Review Materials **6**, 094407 (2022).

7. S. Seo, Y. Luo, S.M. Thomas, Z. Fisk, O. Erten, P.S. Riseborough, F. Ronning, J.D. Thompson, and P.F.S. Rosa, *Persistence of correlation-driven surface states in SmB_6 under pressure*, Physical Review B **105**, 245150 (2022).

8. T. Asaba, S. Lee, S. Seo, K.E. Avers, S.M. Thomas, R. Movshovich, J.D. Thompson, P.F.S. Rosa, E.D. Bauer, F. Ronning, *Physical properties of $YbFe_5P_3$ with a quasi-one-dimensional crystal structure*, Physical Review B **104**, 195140 (2021).

9. Z. Lu, P. Hollister, M. Ozerov, S. Moon, E.D. Bauer, F. Ronning, D. Smirnov, L. Ju, and B.J. Ramshaw, *Weyl fermion magneto-electrodynamics and ultra-low field quantum limit TaAs*, Science Advances **8**, eabj1076 (2022).

10. C. Guo, A. Alexandradinata, C. Putzke, A. Estry, T. Tu, N. Kumar, F.-R. Fan, S. Zhang, Q. Wu, O.V. Yazyev, K.R. Shirer, M.D. Bachmann, H. Peng, E.D. Bauer, F. Ronning, Y. Sun, C. Shekhar, C. Felser, and P.J.W. Moll, *Temperature dependence of quantum oscillations from non-parabolic dispersions*, Nature Communications **12**, 6213 (2021); Nature Communications **14**, 2061 (2023).

Synthesis and Studies of Emergent Quantum Properties of Solids

I. R. Fisher[1,2], A. Kapitulnik[1,2,3] and S. A. Kivelson[1,2,3],

1. Stanford Institute for Materials and Energy Sciences, SLAC National Accelerator Laboratory, 2575 Sand Hill Road, Menlo Park, California 94025
2. Department of Applied Physics, Stanford University, Stanford, California 94305
3. Department of Physics, Stanford University, Stanford, California 94305

Keywords: Charge density wave; superconductivity; single crystals; transport; strain

Research Scope

An enduring aim of our FWP has been to discover and understand the nature, causes and consequences of emergent behavior in quantum materials, especially in relation to the occurrence of superconductivity. We incorporate synthesis, measurement and theory. Current efforts focus on (a) the occurrence and properties of CDW order in several families of quasi-two-dimensional compounds, including rare earth tritellurides and Kagome metals exhibiting electronic states with non-trivial topology; (b) the inter-relation of nematicity and superconductivity, in Fe-based superconductors and related materials; and (c) a more general investigation of the inter-relation of a variety of competing, coexisting and intertwined multi-component electronic orders (including in materials such as UTe_2, Sr_2RuO_4 etc., and in appropriate physical models). A pervasive recent emphasis has been the use of symmetry-breaking strain as a probe of, and tuning parameter for, a variety of emergent electronic phases.

Recent Progress

During this ECMP PIs meeting, we will present some of our work on charge density wave materials. We give a short overview of other key results below.

1. Charge density wave order

Our efforts have focused on two key areas: the possibility of emergent symmetries close to strain-tuned CDW bicritical points [1,7], and break-down of 'simple' transport in the vicinity of CDW phase transitions [9]. Additional work has explored the possibility of broken time reversal symmetry in CsV_3Sb_5 [4], the effects of disorder arising from intercalation in Pd_xErTe_3 [3], and nano-scale phase-slip domain walls in $NbTe_4$ [5].

1.1 Emergent symmetry near a CDW bicritical point: Symmetry plays a key role in determining the physical properties of materials. By Neumann's principle, the properties of a material remain invariant under the symmetry operations of the space group to which the material belongs. Continuous phase transitions are often associated with a spontaneous reduction in symmetry. Much less common are examples where proximity to a continuous phase transition can lead to an increase

in symmetry. Here, we find signatures of an emergent tetragonal symmetry close to a charge density wave (CDW) bicritical point in a fundamentally orthorhombic material, $ErTe_3$, for which two distinct CDW phase transitions are tuned via anisotropic strain [1]. $ErTe_3$ belongs to the orthorhombic space group Cmcm (no 63). The structure comprises bilayers of almost-square tellurium nets, which are separated along the b-axis by ErTe 'block' layers. At room temperature, the a and c lattice parameters are almost equal, a = 0.999c, and moreover, it is possible to tune the material from a > c to a < c using externally applied anisotropic strain. However, despite the near equivalence of the in-plane lattice parameters, the presence of a glide plane between the tellurium bilayers makes the material fundamentally orthorhombic. Thus, even when the material is strain-tuned to a point where the in-plane lattice parameters are exactly equal (a = c), the system does not possess a 4-fold rotational symmetry and hence can never be truly tetragonal. Nevertheless, as we find here, the presence of a strain-tuned CDW bicritical point in $ErTe_3$, which occurs at a critical strain where $a \neq c$, yields signatures of an emergent tetragonal symmetry associated with the critical fluctuations [1]. Remarkably, a thorough treatment of the fluctuations, which we develop in a separate article (submitted), reveals that under certain circumstances, this emergent symmetry becomes increasingly precise upon approach to criticality.

1.2 Breakdown of Wiedemann-Franz law and kinetic approximation near a charge density wave phase transition: Electrical and thermal transport measurements provide important information about electronic structure and scattering processes in complex quantum materials. When transport is dominated by weakly interacting elementary excitations, the kinetic approximation holds and thermal conductivity can be expressed as the sum of electronic and phononic contributions, $\kappa \approx \kappa_{el} + \kappa_{ph}$. Furthermore, for quasi-elastic scattering processes κ_{el} is related to electrical conductivity by the Wiedemann-Franz (WF) law, i.e. $\kappa_{el}/\sigma = L_0 T$, where L_0 is a universal constant. However, where a charge density wave transition takes place as a result of strong interactions the kinetic approximation may break down together with the WF law. Indeed, in an initial publication we examined the thermal diffusivity near the primary CDW transition in $ErTe_3$, concluding that the WF law does indeed break down. Here we report more detailed studies of two, a priori dissimilar CDW transitions, that of $ErTe_3$ with $T_{CDW} \approx 270K$ [9] and a Kagome-system CsV_3Sb_5 with $T_{CDW} \approx 94K$. In both cases and for each sample reported we measured the specific heat, thermal conductivity, resistivity and thermal diffusivity and compared the data to the above equations. We interpret our results as a breakdown of both the kinetic approximation and the WF law in the temperature regime near the phase transition. In fact, in both cases, well above the transition and below ~20 to 30 K from the transition, both the kinetic approximation and the WF law are satisfied again. We propose that these results point to a very strong electron-phonon coupling in the vicinity of the CDW transition, irrespective of its microscopic origin, suggesting a new state of matter that carries the entropy, which could be thought of as electron-phonon 'soup' (article in preparation).

2. Novel physics in Fe-based superconductors

All three PIs also contributed to three separate but inter-related ongoing studies which reveal new and unanticipated physics in the prototypical Fe-based superconductors $Ba(Fe_{1-x}Co_x)_2As_2$ and $Ba(Fe_{1-x}Cu_x)_2As_2$.

2.1 Additional phase transitions beneath the superconducting 'dome' in a prototypical Fe-based superconductor: The phase diagrams of the Fe-based superconductors have been well-established for quite some time, or at least this was widely believed to be the case. We reveal evidence for an unanticipated additional phase transition inside the superconducting state in the prototypical material $Ba(Fe_{1-x}Co_x)_2As_2$, based on extremely sensitive adiabatic elastocaloric effect measurements. The results point towards the possible onset of a multicomponent superconducting state for which the required degeneracy between the two components is not a strict requirement of symmetry. Proximity to the nematic phase transition (the effect happens near optimal doping, where the nematic phase boundary intersects T_c) possibly implies an important role for nematic order and/or fluctuations in inducing this new state.

2.2 Signatures of broken time reversal symmetry in the superconducting state of $Ba(Fe_{1-x}Co_x)_2As_2$: Motivated by the above observation, we systematically investigated the Kerr response across the phase diagram of $Ba(Fe_{1-x}Co_x)_2As_2$. We find ubiquitous signatures of broken time reversal symmetry several K below T_c for all superconducting compositions. Tentatively ascribed to vortex physics, the signatures have several remarkable properties. For example, we could follow the critical state of the vortex state by following the remanent magnetization measured via the Kerr effect at the center of the sample. Furthermore, we developed a simple phenomenology of the Kerr effect in the vortex state of a time-reversal symmetry breaking superconductor, which follows our previous studies of such state in UTe_2.

2.3 Dramatic effect of disorder on the nematic and superconducting states in $Ba(Fe_{1-x}Cu_x)_2As_2$: While Co-doped $BaFe_2As_2$ harbors a robust superconducting 'dome' with a maximum T_c of 25K, Cu-doping has always been a bit of a mystery, yielding only a 1K superconductor, possibly close to the implied antiferromagnetic quantum critical point. Here we reveal the profound effect that disorder has on the nematic phase transition in this material system, in contrast to a much weaker effect in Co-doped $BaFe_2As_2$. While for low dopant concentrations, the two families behave essentially identically, for compositions close to the antiferromagnetic quantum critical point long range nematic order (i.e. macroscopic orthorhombicity) appears to be suppressed for Cu-doped $BaFe_2As_2$. Our combined study, involving several thermodynamic and transport probes, as well as an extensive x-ray diffraction study performed at the APS, reveal a signature difference between the two materials, which could possibly also be associated with the presence/absence of superconductivity.

Future Plans

1. Novel experiments using strain. Building on our expertise, we are developing two new sets of measurements, driven by a joint post-doc collectively mentored/directed by the PIs. The first of these is to incorporate in-situ tunable strain into Kerr effect measurements, with the aim of probing the character (symmetry) of proposed multicomponent superconducting states in a number of different materials. The second general direction is to extend notions of strain tuning beyond linear response in a formal/rigorous way, in particular focusing on ways in which non-linear strain effects and their coupling to specific forms of 'hidden order' can be realized and fully symmetry-decomposed.

2. Density wave order. Current/ongoing research forms the thesis work of three of our students. Several natural follow-on lines of inquiry suggest themselves, including extension to other unidirectional orthorhombic CDW systems; the effect of CDW domain population (and possibly motion/dynamics) on sliding CDW dynamics under varying strain conditions; the application of strain techniques to hexagonal systems (for which the two doublet E_g representations provide new challenges and opportunities relative to tetragonal and orthorhombic systems); and the study of thermal diffusivity and deviations from the WD law in other related density wave materials.

3. Fe-based superconductors. We continue to test the presence of a possible multicomponent state inside the superconducting dome of representative '122' compounds, as well as other closely related materials. We will also further explore the character of the short range nematic correlations present in Cu-doped $BaFe_2As_2$. Complex diffuse scattering observed at the APS for higher concentrations requires considerable analysis, but we hope will provide deeper understanding of the evolution of the short-range correlations, which will be compared with experiments that directly probe the nematic susceptibility. In addition, preliminary dark field x-ray microscopy images obtained in collaboration with Z. Islam just before the APS shut down will take extensive effort to fully analyze, but (significantly) seem to show novel periodic modulation of the nematic domains for underdoped compositions, which will be explored in greater detail.

4. Other materials. During FY23 we began a series of exploratory elastocaloric effect measurements of the prototypical quantum-critical material $CePd_2Si_2$. Our initial observations are sufficiently promising for us to continue this line of inquiry, from which we anticipate obtaining a clearer understanding of the range over which quantum critical fluctuations are present (our measurements directly probe a Gruneissen 'ratio' in a single measurement; thus are extremely sensitive to this quantity, which follows certain universal power laws in the quantum critical regime). These observations are sufficiently exciting that we are already beginning to plan a series of related materials for which strain might even be able to fully traverse a quantum phase transition.

Publications (Sept 2021 – Sept 2023)

1. Anisha G. Singh, Maja D. Bachmann, Joshua J. Sanchez, Akshat Pandey, Aharon Kapitulnik, Jong Woo Kim, Philip J. Ryan, Steven A. Kivelson, Ian R. Fisher, *Emergent Tetragonality in a Fundamentally Orthorhombic Material*, arXiv:2306.14755
   URL: https://arxiv.org/abs/2306.14755

2. Xinyang Zhang, Mark Zic, Dong Chen, Chandra Shekhar, Claudia Felser, Ian R. Fisher, Aharon Kapitulnik, *Vortex phase diagram of kagome superconductor CsV_3Sb_5*, arXiv:2306.13297
   URL: https://arxiv.org/abs/2306.13297

3. Krishnanand Mallayya, Joshua Straquadine, Matthew Krogstad, Maja Bachmann, Anisha Singh, Raymond Osborn, Stephan Rosenkranz, Ian R Fisher, Eun-Ah Kim, *Bragg glass signatures in Pd_xErTe_3 with X-ray diffraction Temperature Clustering (X-TEC)*, arXiv:2207.14795
   URL: https://arxiv.org/abs/2207.14795

4. David R. Saykin, Camron Farhang, Erik D. Kountz, Dong Chen, Brenden R. Ortiz, Chandra Shekhar, Claudia Felser, Stephen D. Wilson, Ronny Thomale, Jing Xia, and Aharon Kapitulnik, *High Resolution Polar Kerr Effect Studies of CsV_3Sb_5: Tests for Time-Reversal Symmetry Breaking below the Charge-Order Transition*, Phys. Rev. Lett. **131**, 016901 – Published 7 July 2023
   URL: https://journals.aps.org/prl/abstract/10.1103/PhysRevLett.131.016901

5. J. A. Galvis, A. Fang, D. Jiménez-Guerrero, J. Rojas-Castillo, J. Casas, O. Herrera, A. C. Garcia-Castro, E. Bousquet, I. R. Fisher, A. Kapitulnik, and P. Giraldo-Gallo, *Nanoscale phase-slip domain walls in the charge density wave state of the Weyl semimetal candidate $NbTe_4$*, Physical Review B **107**, 045120 (2023) – Published 17 January 2023
   URL: https://link.aps.org/doi/10.1103/PhysRevB.107.045120

6. D. Jost, L. Peis, G. He, A. Baum, S. Gepraegs, J. C. Palmstrom, M. S. Ikeda, I. R. Fisher, T. Wolf, S. Lederer, S. A. Kivelson, R. Hackl, *Quantum critical fluctuations in an Fe-based superconductor*, Communications Physics **5**, Article number: 201 (2022) – Published: 09 August 2022
   URL: https://www.nature.com/articles/s42005-022-00981-5

7. J. A. W. Straquadine, M. S. Ikeda, and I. R. Fisher, *Evidence for Realignment of the Charge Density Wave State in $ErTe_3$ and $TmTe_3$ under Uniaxial Stress via Elastocaloric and Elastoresistivity Measurements,* Phys. Rev. X **12**, 021046 (2022) – Published 26 May 2022
   URL: https://journals.aps.org/prx/abstract/10.1103/PhysRevX.12.021046

8. Rafael M. Fernandes, Amalia I. Coldea, Hong Ding, Ian R. Fisher, P. J. Hirschfeld & Gabriel Kotliar, *Iron pnictides and chalcogenides: a new paradigm for superconductivity*, Nature **601**, 35 (2022) – Published 5 January 2022
   URL: https://www.nature.com/articles/s41586-021-04073-2

9. Erik D. Kountz, Jiecheng Zhang, Joshua A. W. Straquadine, Anisha G. Singh, Maja D. Bachmann, Ian R. Fisher, Steven A. Kivelson, and Aharon Kapitulnik, *Anomalous thermal transport and strong violation of Wiedemann-Franz law in the critical regime of a charge density wave transition*, Phys. Rev. B **104**, L241109 (2021) - Published 22 December 2021
   URL: https://journals.aps.org/prb/abstract/10.1103/PhysRevB.104.L241109

10. Matthias S. Ikeda, Thanapat Worasaran, Elliott W. Rosenberg, Johanna C. Palmstrom, Steven A. Kivelson, Ian R. Fisher, *Elastocaloric signature of nematic fluctuations*, PNAS **118** (37) e2105911118 (2021) – Published online September 9 2021
    URL: https://www.pnas.org/content/118/37/e2105911118

The Ground State of Geometrically Frustrated Magnets

Arthur P. Ramirez, University of California Santa Cruz

Keywords: magnetism, frustration, quantum limit, susceptibility, specific heat

Research Scope

Geometrically frustrated (GF) magnets undergo spin freezing at temperatures far below the mean-field estimate [1]. Such a suppression of ordering has made these materials candidates for the so-called quantum spin liquid, a theoretically predicted fully quantum-coherent state that can admit anyon excitations with their attendant quantum computing potential [2]. I will show that the response of GF magnets to disorder, as shown in Fig. 1, has two inescapable implications for the pure systems.

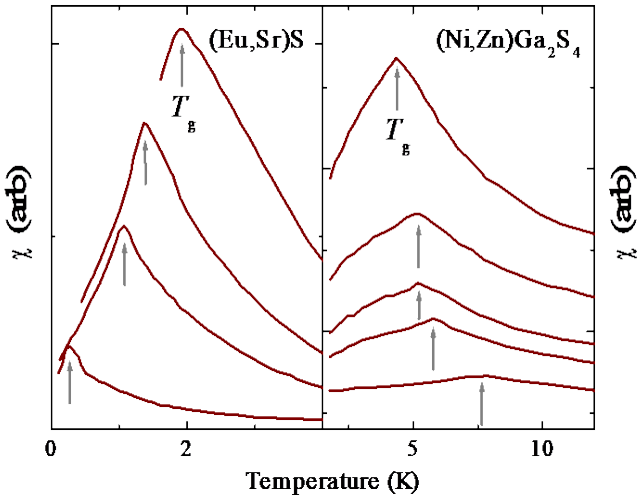

Fig 1. Left: Magnetic susceptibility for a conventional spin glass, (Eu,Sr)S vs temperature for different Eu concentrations. Right: Susceptibility of a geometrically frustrated spin glass, $(Ni,Zn)Ga_2S_4$ vs temperature for different Ni concentrations. From ref. 3.

First, the ground state of (3D) GF magnets mediates long-range interactions between defects. The most likely candidate for this interaction is the entropic interaction that results from the "eminuscent" state, a state well-described by the Coulomb representation [3]. The resulting spin glass freezing observed in GF magnets occurs among defect-induced quasispins, and does not described the intrinsic state. In other words, spin glass is a spectator state of the intrinsic GF ground state.

Second, the pure GF material possesses a previously unidentified, intrinsic, "hidden" energy scale at which the short-range order which produces the eminuscent state becomes established on cooling. This energy scale and its short-range order has already been characterized in a number of GF magnets. As shown in Fig. 2, for example, elastic short-range neutron scattering is seen in all relevant systems for which data exist. Data like these, considered along with the known entropy loss, construct a picture of the GF ground state in which virtually all of the spins are fully polarized, but in random directions beyond the nearest neighbor length scale. The resulting random internal field is not anticipated by theories of quantum spin liquids. We believe that, if a coherent quantum many-body state is to ensue in such systems, then it will be defined by the response of Goldstone-like local excitations that represent a small fraction of the full spin spectral weight.

Recent Progress

I will present recent results on Fe_2TiO_5 that demonstrate the interplay of spin glass physics and the nature of the geometrically frustrated ground state and that motivated the subject discussed here [4]. The quasispin in this system is not a vacancy, but rather a surfboard-shaped correlation region of Fe^{3+} ion. The exceedingly unusual anisotropic spin glass freezing observed in Fe_2TiO_5 is likely the result of a van der Waals-type interaction but in a magnetic context. I will also show results on specific heat of systems that exhibit the two-step loss of entropy that makes the ground state in geometrically frustrated systems unlikely to support a quantum coherent state. The low temperature field dependent specific heat is consistent with expectations of the Coulomb representation.

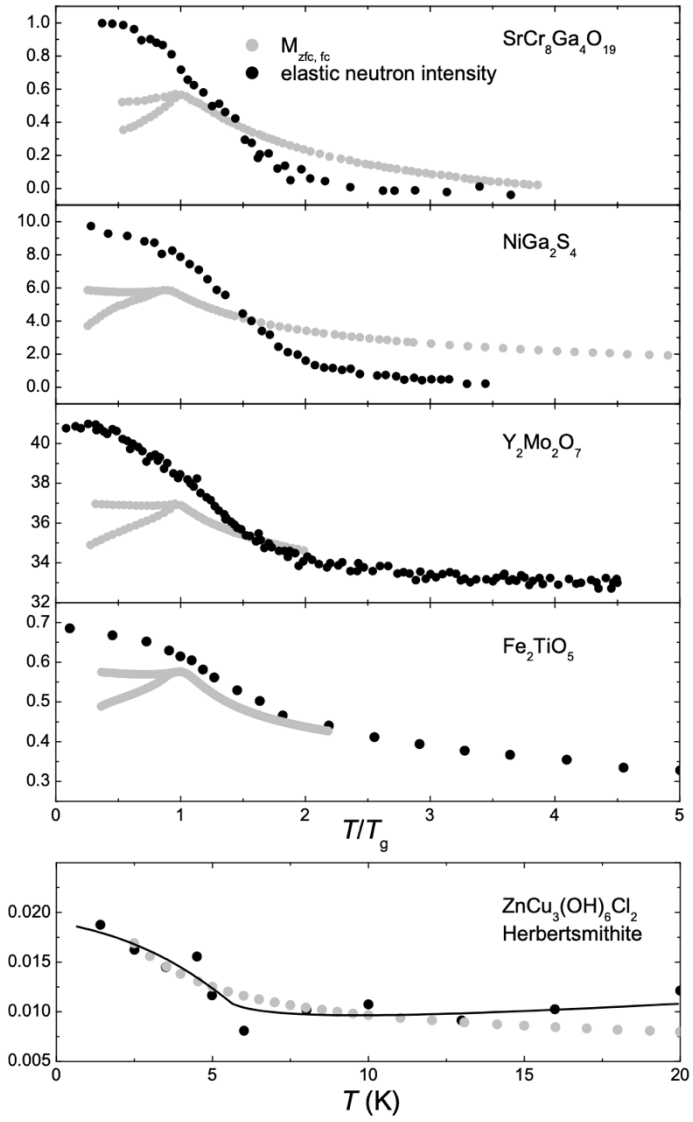

Fig. 2. Susceptibility at the spin glass freezing temperature (grey lines) and short wavelength neutron scattering (black dots) for GF magnets, showing the development of short-range order accompanying the SG state.

Future Plans

We will extend the above concepts to a survey of thermal and transport properties of the rare-earth gallium garnets. This compound series possess the hyperkagome lattice of corner-sharing triangles in 3D and should be a good complement to the rare-earth titanate pyrochlores.

We will also characterize the eminuscent state using its most readily defined order parameter, the "entropic susceptibility", given by $P_s \propto -\int_{T_{cr}}^{0}(\partial(C/T)/\partial M)dT$, where $T_{cr} \approx T^*$ is the crossover temperature that signals SRO.

References

[1] A. P. Ramirez, *Thermodynamic measurements on geometrically frustrated magnets*, Journal of Applied Physics **70**, 5952 (1991).

[2] L. Savary, and L. Balents, *Quantum spin liquids: a review*, Reports on Progress in Physics **80**, 016502, (2017).

[3] S. V. Syzranov, and A. P. Ramirez, *Eminuscent phase in frustrated magnets: a challenge to quantum spin liquids*, Nature Communications **13**, 2993, (2022).

[4] P. G. LaBarre, D. Phelan, Y. Xin, F. Ye, T. Besera, T. Siegrist, S. V. Syzranov, S. Rosenkranz, and A. P. Ramirez, *Fluctuation-induced interactions and the spin-glass transition in Fe_2TiO_5*, Physical Review B **103**, L220404, (2021).

Publications

P. G. LaBarre, D. Phelan, Y. Xin, F. Ye, T. Besera, T. Siegrist, S. V. Syzranov, S. Rosenkranz, and A. P. Ramirez, *Fluctuation-induced interactions and the spin-glass transition in Fe_2TiO_5*, Physical Review B **103**, L220404, (2021).

S. V. Syzranov, and A. P. Ramirez, *Eminuscent phase in frustrated magnets: a challenge to quantum spin liquids*, Nature Communications **13**, 2993, (2022).

Unusual ring-like magnons in novel class of Weyl magnets discovered.

Jak Chakhalian, **Rutgers University**

Keywords: topological materials**,** antiferromagnets, inelastic x-ray scattering, non-local magnons

Research Scope

Here we present the first in-depth investigation of magnetic ordering and magnon excitations in the synthetic lattice of [111]-oriented Y_2Ir2O_7 pyrochlore iridate. This compound belongs to a broad class of intermediately correlated electron systems known for their intricate interplay between spin and orbital degrees entwined with the frustrated Kagome and triangle motifs. A strong spin-orbit coupling matching electronic bandwidth and Hubbard U are defining features of these crystals.

Recent Progress

Our results combine state-of-the-art experimental techniques, XRMS and RIXS, and theoretical modeling to elucidate the unusual behavior of magnons in this complex quantum system. The experimental findings reveal the emergence of unconventional magnons in thin films of $Y_2Ir_2O_7$. These gapped magnon modes exhibit surprising spectral features. Specifically, RIXS data reveal the presence of essentially non-dispersive magnetic excitations that persist above the Neel transition temperature into the thermal cooperative paramagnetic phase. Those results along with the muon spin resonance data imply that across the Neel transition, non-local ring-like magnetic excitations are bound to the features of Kagome geometry decorated with non-collinear all-in-all-out spins. At the same time, the conventional linear spin wave theory shows difficulty in capturing this complex behavior.

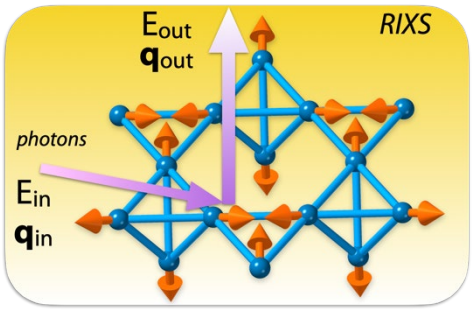

Figure 3. All-in-all-out (AIAO) spins on Kagome-triangular lattice along with the geometry of RIXS experiment

In addition, discovering a spin gap rules out the alternatively proposed XY ground state and the associated order-by-disorder in pyrochlore iridates. These experimental findings advance our understanding of the strong spin-orbit interaction in the artificial weekly correlated materials with complex magnetic interactions, topological fermions, and geometric frustration.

Future Plans

Based on our recent development of a new synthesis method (so-called hybrid solid state epitaxy or hSPE) for pyrochlores with 5d electrons like Ir, Re, and Os, we will continue the growth of a series of new synthetic Kagome lattices and their interfaces with Kagome superconductors and quantum spin liquids systems. Simultaneously, new synchrotron-based collaborative experiments at the DOE facilities (ALS and NSLS II) have been planned for Fall 2023-2024.

References

The manuscript has been submitted for publication in the Physical Review Letters.

Probing electronic and topological properties in 2D atomic crystals and their heterostuctures

Eva Y. Andrei, Department of Physics and Astronomy, Rutgers, the State University of NJ

Keywords: 2D and layered crystals, nanostructures, superconductivity, graphene, transport

Research Scope We study atomically thin crystals and their heterostructures using scanning tunneling microscopy and spectroscopy (STM, STS), planar tunneling, transport and magneto-transport. The scope and outcomes of our current research include: proximity induced charge density wave in graphene TaS2 heterostructures; observation of a strong self-alignment mechanism between magic angle bilayer graphene and hBN leading to broken sublattice symmetry and to the emergence of Chern insulators; observation of alternating light and heavy fermions as a function of band filling in magic angle twisted bilayer graphene; observation of superconductivity and superconductor-insulator transition in twisted trilayer graphene.

Recent Progress

Quantum-breakdown of superconductivity in Twisted Trilayer Graphene

The discovery of superconductivity in twisted graphene layers has made it possible to revisit and address long standing open questions about the nature of 2D superconductivity and about the superconducting to insulating transition in 2D. Using transport and magneto-transport measurements we studied the emergence of superconductivity in mirror-symmetric twisted trilayer graphene and its dependence on carrier density, temperature and magnetic field. We showed that on a temperature versus carrier density phase diagram the superconducting phase forms a dome with optimal doping at a filling of 2.25 electrons per moiré cell. Our findings include: (i) observation of a magnetically driven superconductor to insulator transition at ~400mT. The transition occurs at a sheet resistance, 6.54kΩ, that coincides with the quantum pair resistance $h/(2e^2)$, consistent with the formation of the theoretically proposed Bose insulator phase. The 2D Bose insulator is an intermediate phase between superconductivity and a Fermi insulator characterized by localized Cooper pairs coexisting with itinerant vortices. (ii) From scaling analysis of the magnetic field and temperature dependence of the resistivity we obtained a

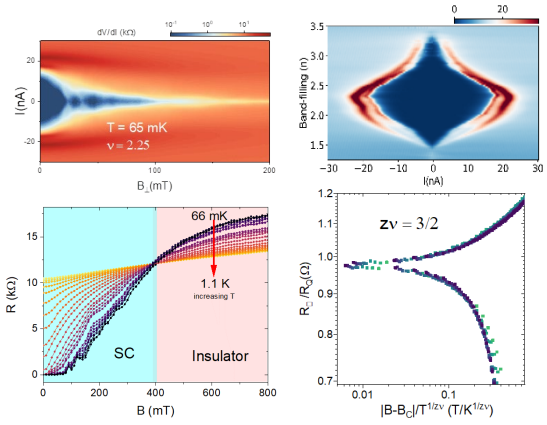

Figure 1. Top left: Frauenhofer oscillations provide evidence of superconducting phase coherence. Top right: resistance map plotted on the band-filling versus driving-current phase diagram shows the Superconducting dome (dark blue). Bottom left: Temperature dependence of resistance versus field curves shows SI transition at 400mT. Bottom right: Data collapse using critical scaling analysis shows a scaling exponent of 3/2.

critical scaling exponent, zν=3/2, which places trilayer graphene in the same universality class as High Tc superconductors. (iii) using Ahrenius analysis of the temperature and magnetic field dependence of the resistivity we discovered that the vortex pinning barriers are more than an order of magnitude lower than in any other material, making graphene the cleanest known superconductor.

Moiré Potential, Lattice Relaxation and Layer Polarization in Marginally Twisted MoS2 Bilayers. Twisted heterostructures of semiconducting transition-metal dichalcogenides (TMDs) offer unprecedented control over their electronic and optical properties via the spatial modulation of interlayer interactions and structural reconstruction. In this work we study the twist angle dependence of the electronic properties in twisted MoS2 bilayers using STM and STS. We find that the moiré pattern is dominated by lattice reconstruction for small angles (<2°), leading to large triangular domains with rhombohedral stacking. Local spectroscopy measurements reveal a strong alternating moiré-potential,100–200 meV, providing a direct signature of the vertical electric polarization intrinsic to rhombohedral stacked TMDs, which we directly demonstrated using spectroscopy maps and ambient piezoresponse measurements. Our results provide a microscopic perspective of this new class of interfacial ferroelectrics and offer a pathway for designing ferroelectric heterostructures.

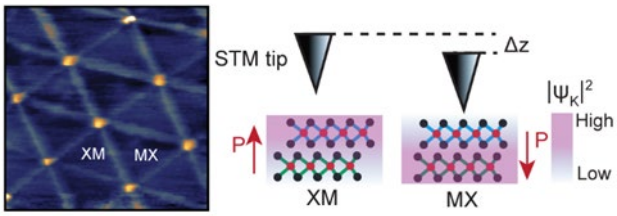

Figure 2. Left: STM image of the moiré lattice structure of Parallel-stacked (twist angle near 0°) twisted MoS2. Right top: schematic side-view of measurement setup. Right bottom: atomic registrations in the top and bottom MoS2 monolayers. X, M represent S and Mo atoms

Observation of Charge Density Wave Proximity Effect in Graphene on 1T-TaS_2 The proximity-effect, a phenomenon whereby materials in close contact appropriate each other's electronic-properties, is widely used in nano-scale devices to induce electron-correlations at heterostructure interfaces. Commonly observed proximity-induced correlation-effects include superconductivity, magnetism, and spin-orbit interactions. Thus far, however, proximity induced charge density waves (CDW) have not been explored, primarily because of screening in 3D metals and

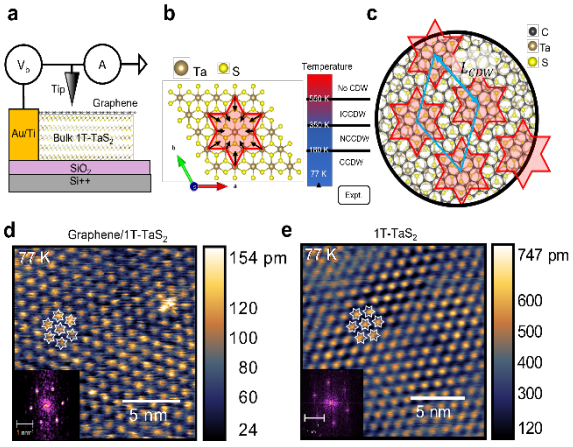

Figure 3. (a) Schematics of measurement setup. (b, left) Star-of-David (red) in TaS2. (b,right) CDW phases of TaS_2 as a function of temperature. (c) Schematics of graphene on TaS2. (d) STM topography and its 2D FFT(inset) showing proximity induced CDW in graphene. (e) STM topography and its 2D FFT(inset) of bulk TaS_2

defect scattering at interfaces. These drawbacks are mitigated in 2D atomic heterostructures where scattering is minimized due to the crystalline interfaces. We studied the appearance of a

CDW in graphene deposited on a 1T-TaS_2 (TaS_2) crystal. Using STM and STS to probe the interface between graphene and the TaS_2 crystal, together with theoretical-modeling, we demonstrated the existence of a proximity induced CDW within graphene induced by the commensurate CDW in the underlying TaS_2. Furthermore, we observed that graphene modifies the band structure at the surface of TaS_2, by providing mid-gap carriers and reducing the strength of electron correlations there. Using first-principle theoretical modeling we demonstrated that the mechanism underlying the proximity induced CDW is described by short range exchange interactions that are distinctly different from previously observed proximity effects.

Imaging Self-Aligned Moiré Crystals and Quasicrystals in Twisted-Graphene hBN Heterostructures. We studied the super-moiré structures created by placing twisted bilayer-graphene on hexagonal-Boron-Nitride using STM and theoretical modeling. These structures display a rich palette of readily observed moiré crystals and quasicrystals. We showed that these structures can be classified in a phase diagram comprising lines of commensurate moiré crystals embedded in a sea of moiré quasicrystals. The 1:1 commensurate moiré crystal is particularly interesting because its electronic properties are controlled by a topologically non-trivial band leading to the emergence of a Chern insulator and to the appearance of an anomalous quantum Hall effect (AQHE) at a band filling of 3 electrons per moiré cell. Remarkably we find that the 1:1 commensurate moiré crystal which should only exist at a single point on this phase-diagram rendering it practically undetectable, is much more common than previously believed. We found that there exists a self-alignment mechanism, which enables the 1:1 commensurate crystal to exist as far as 20% away from the rigid lattice commensuration-point. This provides direct evidence that a self-alignment mechanism may be responsible for the observation of the anomalous QHE in this system. We show that the self-alignment is driven by the competition between the van der Waals energy gain and the elastic energy cost of attaining the preferred stacking configuration. Our study reveals self-alignment as a previously neglected but fundamental property of twisted multilayer systems. Self-alignment reduces the sensitivity to twist angle disorder created during device fabrication and vastly increases the chances of achieving samples with desired global properties. Outside of the lines containing the self-aligned moiré crystals we observe a host of 2D quasicrystal. Quasicrystals are rarely found in nature, and their theoretically predicted correlated phases and topological properties remain largely unverified. Our

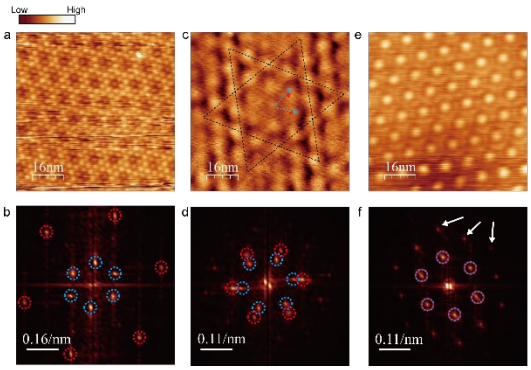

Figure 4. STM topography and FFT of double moiré patterns formed by superposing twisted graphene on hBN. (a,b) moiré quasicrystal; (c,d) Moiré crystal with moiré-of-moiré superstructure. (e,f) 1:1 aligned moiré crystal.

findings provide a new platform for creating and tuning 2D quasicrystals and for exploring their fascinating electronic properties.

Spectroscopic evidence for Landau degeneracy and massive quasiparticles in magic-angle twisted bilayer graphene

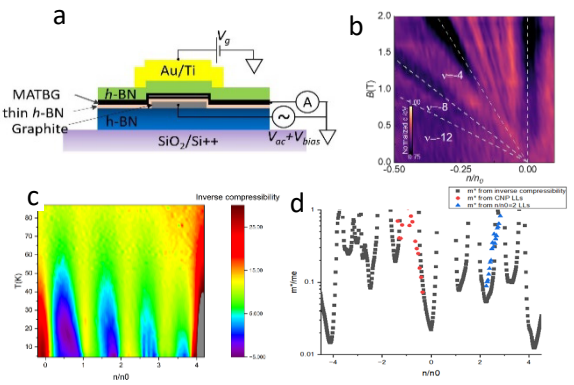

Figure 5. a) schematics of planar tunneling setup b) Field and doping dependence of differential conductance showing Landau levels emanating from the CNP. c) Inverse compressibility map as a function of temperature and filling. D) doping dependence of reduced effective mass extracted from inverse compressibility and Landau levels.

The flat band in magic-angle twisted bilayer graphene (MA-TBG) is soft and malleable, resulting in strong reconstruction as a function of band filling which leads to the emergence of correlated electron phases at integer filling per moiré cell. Earlier measurements using a single electron transistor technique interpreted the doping dependence of the inverse compressibility in terms of massless Dirac fermions arising from a conical band. However, recent theoretical work indicates that in the strong coupling limit relevant to this system, the band minimum is at the center of the Brillouin zone and is parabolic, resulting in massive rather than massless quasiparticles[1-3]. Using planar tunneling spectroscopy (Fig. 5a) we measured the doping dependence of the differential conductance, dI/dV_b, and of $dI/dV_g \propto d\mu/dn$ as a function of energy, carrier density and magnetic field, in MA-TBG samples. Here I is the tunneling current, V_b and V_g are the bias and gate voltages which control the energy and carrier density respectively, μ is the chemical potential, and $d\mu/dn$ is the inverse compressibility. In the presence of a magnetic field, we observe the Landau level sequence emanating from the charge neutrality point (CNP) (Fig. 5b) , from which we obtain a finite effective mass $m^*\sim0.17m_e$. Away from the CNP, where Landau levels are not easily discernible, we obtain the filling dependence of the effective mass $m^* = \frac{\pi^2\hbar^2}{2\pi}\left(\frac{d\mu}{dn}\right)^{-1}$ from the inverse compressibility (Fig. 4c,d). We find that doping dependence of our measured m* closely tracks the theoretical predictions, indicating that the heavy fermion model is a good starting point for understanding correlated phenomena in MA-TBG.

Future Plans

The symmetry of the superconducting wave function in graphene is one of the most important outstanding questions in the field and crucial for understanding the mechanism of superconductivity. To address this question we will use two experimental setups. i) a home built 300mK STM which is in the final stages of testing. We will use superconducting tips to enhance sensitivity so as to enable us to observe Andreev bound states and the shape of the superconducting gap. ii) Planar tunneling geometry with a superconducting top electrode acting as a tip. The

advantage of the setup is insensitivity to vibrations making it possible to use an existing dilution refrigerator equipped with a large magnetic field. The downside is lack of scanning ability.

References

1. Kang, J. Bernevig, B. A. Vafek, O., *Cascades between Light and Heavy Fermions in the Normal State of Magic-Angle Twisted Bilayer Graphen*e. Physical Review Letters **127**, 266402. (2021)
2. Song, Z.-D. Bernevig, B. A., *Magic-Angle Twisted Bilayer Graphene as a Topological Heavy Fermion Problem*. Physical Review Letters**, 129** 047601 (2022)
3. Călugăru, D. Borovkov, M. Lau, L. L. H. Coleman, P. Song, Z.-D. Bernevig, B. A., *Twisted bilayer graphene as topological heavy fermion: II. Analytical approximations of the model parameters.* Low Temperature Physics **49**, 640 **(**2023)

Publications

1. N. Tilak, M. Altvater, S-H Hung, C-J Won,G. Li, T. Kaleem, S-WCheong, C-H Chung , H-T Jeng, E. Y. Andrei, *Observation of Charge Density Wave Proximity Effect in Graphene on 1T-TaS2*, Nature Materials under review
2. X. Lai, D. Guerci, G. Li, Y.Jiang, J.Mao, K. Watanabe, T.Taniguchi, J. Wilson, J. H. Pixley and E.Y. Andrei, *Imaging Self-Aligned Moiré Crystals and Quasicrystals in Twisted-Graphene hBN Heterostructures,* preprint.
3. Nikhil Tilak, Guohong Li, Takashi Taniguchi, Kenji Watanabe, and Eva Y. Andrei. *Moiré Potential, Lattice Relaxation and Layer Polarization in Marginally Twisted MoS2 Bilayers*, Nano Letters **23**, 73 (2023)
4. R.S. Bisht, J. Park, H. Yu, C. Wu, N. Tilak, S. Rangan, T.J. Park, Y. Yuan, S. Das, U. Goteti, H.T. Yi, H. Hijazi, A. Al-Mahboob, J.T. Sadowski, H. Zhou, S. Oh, E.Y. Andrei, M.T. Allen, D. Kuzum, A. Frano, R.C. Dynes, S. Ramanathan, *Spatial Interactions in Hydrogenated Perovskite Nickelate Synaptic Networks*, Nano Letters **23**, 7166 (2023).
5. V. Bruevich, L. Kasaei, S. Rangan, H. Hijazi, Z. Zhang, T. Emge, E.Y. Andrei, R.A. Bartynski, L.C. Feldman, V. Podzorov, *Intrinsic (Trap-Free) Transistors Based on Epitaxial Single-Crystal Perovskites,* Advanced Materials, **34** 2205055 (2022).
6. M.A. Altvater, N. Tilak, S. Rao, G. Li, C.-J. Won, S.-W. Cheong, E.Y. Andrei, *Observation of a topological defect lattice in the charge density wave of 1T-TaS2*, Applied Physics Letters, **119** 121601(2021).
7. M.A. Altvater, N. Tilak, S. Rao, G. Li, C.-J. Won, S.-W. Cheong, E.Y. Andrei, Charge Density *Wave Vortex Lattice Observed in Graphene-Passivated 1T-TaS2 by Ambient Scanning Tunneling Microscopy*, Nano Letters, **21** 6132 (2021.
8. E.Y. Andrei, D.K. Efetov, P. Jarillo-Herrero, A.H. MacDonald, K.F. Mak, T. Senthil, E. Tutuc, A. Yazdani, A.F. Young, *The marvels of moiré materials*, Nature Reviews Materials, **6** 201 (2021)
9. N. Tilak, X. Lai, S. Wu, Z. Zhang, M. Xu, R.d.A. Ribeiro, P.C. Canfield, E.Y. Andrei, *Flat band carrier confinement in magic-angle twisted bilayer graphene,* Nature Communications, **12** 4180 (2021)
10. S. Wu, Z. Zhang, K. Watanabe, T. Taniguchi, E.Y. Andrei, *Chern insulators, van Hove singularities and topological flat bands in magic-angle twisted bilayer graphene*, Nature Materials, **20** 488 (2021)

Nanostructure Studies of Correlated Quantum Materials - Shot noise in a strange metal

Douglas Natelson, Rice University

Keywords: non-Fermi liquid behavior and charge dynamics; spintronics/magnonics; nanostructures; transport

Research Scope

This research program focuses on experiments that examine the emergent excitations that carry spin and charge in strongly correlated quantum materials. Nanostructure techniques originally developed for weakly interacting semiconductors and conventional metals can enable measurements that give microscopic insight into the emergent many-body excitations and quantum processes in quantum materials. Current research is concentrating on two open questions in such materials, the nature of current-carrying excitations in non-Fermi "strange metals", and the excitations responsible for angular momentum transport in strongly correlated insulators.

Ordinary metals are described by Landau Fermi liquid theory, in which the low energy excitations of the electronic system are long-lived quasiparticles (charge $|e|$, spin ½) that strongly resemble the electrons and holes used to describe the excitations of the non-interacting Fermi gas. The spectral function of the quasiparticles is sharply peaked as a function of energy, and the electrical resistivity of such metals varies as $\rho_0 + AT^2$ at low temperatures thanks to Umklapp scattering and electron-electron interactions, and the specific heat varies as T. In contrast, several material systems are strange metals[1], in which the low temperature resistivity varies as $\rho_0 + AT$ and there are logarithmic corrections to the specific heat. In strange metals, the inferred e-e scattering rate scales linearly in T, and scattering measurements reveal a very broad "incoherent" continuum rather than sharp electronic excitations[2], calling into question the applicability of the quasiparticle picture. Strange metallicity is often associated with quantum critical fluctuations above some quantum critical point. The example most relevant to the present research is the quantum critical strange metal $YbRh_2Si_2$, which exhibits non-Fermi liquid strange metal properties below a Kondo energy scale of about 25 K, near a magnetically driven quantum phase transition between two different Fermi liquid phases with heavy quasiparticles (low-field, small Fermi surface, Yb antiferromagnetically ordered vs. high field, large Fermi surface, paramagnet).

We are using charge shot noise to probe this strange metal, employing devices fabricated from epitaxial films of $YbRh_2Si_2$ grown on Ge substrates by our collaborators (Dr. Prof. Silke Paschen at TU Wien) [3]. Charge shot noise is the current fluctuations in a driven conductor due to the transport of charge by discrete carriers. For carriers of charge e with arrivals governed by Poisson statistics, the current noise per unit bandwidth is $S_{I,e} = 2eI \coth(eV/2k_BT)$ A^2/Hz, where I is the DC bias current. The Fano factor is the ratio of measured current noise to the Poissonian expectation, $F \equiv S_I/S_{I,e}$. In a diffusive constriction, the expected Fano factors predicted in weakly interacting Fermi liquids for weak and strong e-e scattering are 1/3 and $\sqrt{3}/4$, respectively, though the latter has never been observed unambiguously. Shot noise can be suppressed in long

constrictions by electron-phonon scattering, though there are measurements that can be performed to quantify the importance of this effect. Present experiments have examined shot noise in $YbRh_2Si_2$ nanowires and quantified the importance of electron-phonon scattering in this system. No broadly accepted, rigorous theoretical calculation exists for the shot noise in a strange metal, though the present work has stimulated theoretical efforts in this direction. Additional experiments in this effort are fabricating and measuring nanowires from two other important materials: $Sr_3Ru_2O_7$ (collaborator Prof. Tae Won Noh at Seoul National University) a different field-tunable quantum critical strange metal[4], and $YbAl_3$ (collaborator Prof. Kyle Shen at Cornell), a strongly interacting heavy fermion Fermi liquid.

In magnetic insulators, angular momentum may be transported in the absence of charge transport via exchange processes and spin-carrying excitations. For insulators with long-range magnetic order, the relevant excitations are magnons, quantized spin waves which each carry $\hbar$ of angular momentum. Thanks to the inverse spin Hall effect (ISHE), electrical detection is possible of magnons carrying appropriately directed spin. Interfacial exchange between the magnetic insulator and a strong spin-orbit coupled (SOC) metal can transfer angular momentum from magnons to the spin of the SOC metal conduction electrons, leading to an ISHE voltage. The spin Seebeck effect, in which a spin current is driven by a thermal gradient, may then be measured electrically this way[5]. Present investigations are examining the spin Seebeck response in three correlated materials: VO_2 (an unusual paramagnet, from Prof. Ivan Schuller at UCSD); V_2O_3 (a Mott insulator with an antiferromagnetic ground state, also from Prof. Schuller); and La_2CuO_4 (LCO, a Mott insulator with an antiferromagnetic ground state, from Dr. Ivan Bozovic at Brookhaven).

Recent Progress

We have measured charge shot noise in $YbRh_2Si_2$ nanowires fabricated from epitaxial thin films using a custom-built probe for a Quantum Design PPMS cryostat down to 3 K, well into the strange metal regime. In multiple devices, we have found that the shot noise is greatly reduced from the values expected for Fermi liquids, in contrast to noise measured in gold nanowires of similar dimensions, as shown in Fig. 1. By measuring tens of microns-long nanowires, we have quantified the phenomenological electron-phonon coupling parameter in this material, $\Gamma \approx 9 \times 10^9$ $K^{-3}m^{-2}$, comparable to the value found (and confirmed by our own measurements) for Au, 5×10^9 $K^{-3}m^{-2}$. These measurements show that electron-phonon scattering cannot be responsible for the suppression of shot noise in the $YbRh_2Si_2$ nanowires. These shot noise measurements are consistent with a lack of conventional quasiparticles in this strange metal. A complete lack of shot noise would be expected for charge transported by a continuous fluid, equivalent to a spectral function for electronic excitations that is completely featureless. This work has generated considerable theoretical interest.

In parallel with the experiments, we have worked with the group of Prof. Qimiao Si as they have performed a detailed theoretical analysis of the expected Fano factor for constrictions made

from a strongly interacting Fermi liquid (that is, with a strongly renormalized quasiparticle weight in the spectral function). That work (arxiv:2211.11735) shows that for any nonzero quasiparticle weight, the expected Fano factor for strong e-e scattering should be √3/4, unlike what is seen in our experiments.

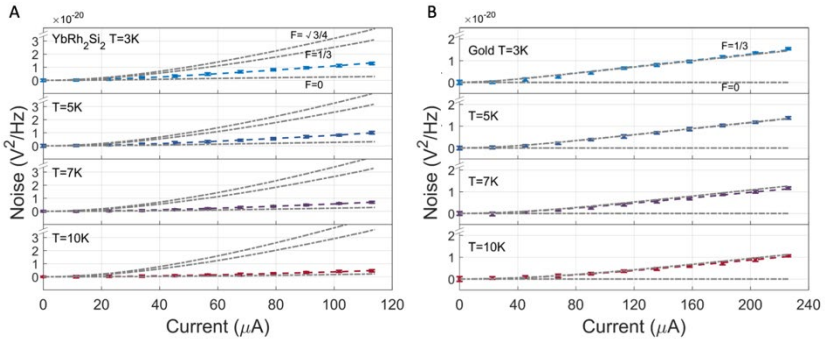

Figure 1. Comparison of shot noise in $YbRh_2Si_2$ nanowire (panel A) and a gold nanowire of similar dimensions (panel B). The noise in the non-Fermi liquid strange metal $YbRh_2Si_2$ nanowire is suppressed far below the expected level for either strongly interacting or weakly interacting Fermi liquids. This is the first measurement of shot noise in a strange metal and indicates that charge is not carried by discrete quasiparticles in this system.

Current experiments in this direction are focusing on fabrication and characterization of nanowires based on two other materials. For $Sr_3Ru_2O_7$, this material has a quantum critical strange metal regime at high fields (~ 8 T) and would be an excellent possible test for universality of the strange metal shot noise response measured thus far. So far, nanowires made from this material have suffered from significant $1/f$ noise that obscures any shot noise signature, but changes in fabrication protocol are continuing in the hopes of circumventing this. At the same time, we have been fabricating nanowires from $YbAl_3$ films, a heavy fermion Fermi liquid, with the intent of testing for the F=√3/4 expectation of noise in a strongly renormalized quasiparticle system.

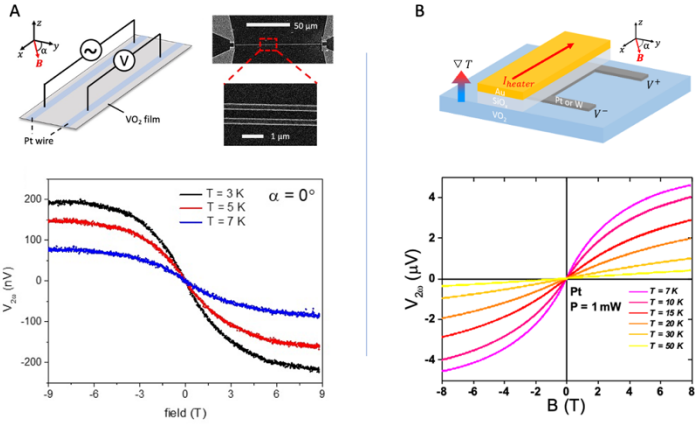

Figure 2. Spin Seebeck response in VO_2. (A) Nonlocal spin Seebeck measurement approach, with laterally displaced Pt wires for heating and ISHE detection of spin current. A signal is found that increases with decreasing temperature. (B) Local spin Seebeck measurement in vertical configuration. Again, a large SSE response is found, growing as T is decreased. The nature of the spin carrying excitations is currently unknown in this system.

In spin transport, we found nonlocal spin Seebeck response in devices fabricated on VO_2 films (collaborator Prof. Ivan Schuller at UCSD), as shown in Fig. 2a. Building on this work, we performed local spin Seebeck measurements on VO_2 films, finding a very large response that grows as temperature is decreased (Fig. 2b). These results are very surprising, as VO_2 is expected to be a spin Peierls-like system, lacking long range order and magnons to transport spin. Experiments are ongoing in devices fabricated on films of V_2O_3, which also show a pronounced spin Seebeck response with a

temperature dependence similar to that of another known antiferromagnet, MnF_2. We are in the process of beginning measurements on LCO films as well.

Future Plans

In the shot noise measurements, we have sent completed, already measured devices to our collaborators in Vienna who are attempting dilution refrigerator temperature measurements on the $YbRh_2Si_2$ nanowires. The goal of these lower temperature experiments is to perform shot noise measurements as a function of magnetic field tuning into and out of the quantum critical strange metal regime. That is also the goal of the $Sr_3Ru_2O_7$ experiments, if we can mitigate the $1/f$ noise issue associated with those samples. We will measure shot noise and electron-phonon coupling strength in $YbAl_3$ nanowires as well, as an attempt to observe shot noise in a Fermi liquid that has strong e-e scattering and quasiparticle weight renormalization. Given the opportunity, we also intend to fabricate nanowire devices for shot noise from Sr_2RuO_4, another strongly correlated material known to exhibit non-Fermi liquid response at higher temperatures but an apparent Fermi liquid ground state, as an interesting point of comparison.

We will continue to examine spin Seebeck response in VO_2 films of different thicknesses and preparations, to better constrain the possible mechanism of spin transport in its correlated insulating state. Similarly, we will expand upon our initial measurements in V_2O_3 to test for nonlocal spin Seebeck response and a quantitative understanding in terms of its known antiferromagnetic structure.

References

1. P.W. Phillips, N.E. Hussey, and P. Abbamonte, *Stranger than metals*, Science **377**(6602), eabh4273 (2022).
2. M. Mitrano, A.A. Husain, S. Vig, A. Kogar, M.S. Rak, S.I. Rubeck, J. Schmalian, B. Uchoa, J. Schneeloch, R. Zhong, G.D. Gu, and P. Abbamonte, *Anomalous density fluctuations in a strange metal*, Proc. Nat. Acad. Sci. US **115**(21), 5392-5396 (2018).
3. L. Prochaska, X. Li, D.C. MacFarland, A.M. Andrews, M. Bonta, E.F. Bianco, S. Yazdi, W. Schrenk, H. Detz, A. Limbeck, Q. Si, E. Ringe, G. Strasser, J. Kono, and S. Paschen, *Singular charge fluctuations at a magnetic quantum critical point*, Science **367**(6475), 285-288 (2020).
4. C.H. Mousatov, E. Berg, and S.A. Hartnoll, *Theory of the strange metal $Sr_3Ru_2O_7$*, Proc. Nat. Acad. Sci. US **117**(6), 2852-2857 (2020).
5. T. Kikkawa and E. Saitoh, *Spin Seebeck Effect: Sensitive Probe for Elementary Excitation, Spin Correlation, Transport, Magnetic Order, and Domains in Solids*, Ann. Rev. Cond. Matt. Phys. **14**(1), 129-151 (2023).

Publications

1. Renjie Luo, Xuanhan Zhao, Liyang Chen, Henry Navarro, Ivan K. Schuller, and Douglas Natelson, *Spin Seebeck effect at low temperatures in the nominally paramagnetic insulating state of vanadium dioxide*, Appl. Phys. Lett. **121**, 102404 (2022).

2. Renjie Luo, Tanner J. Legvold, Liyang Chen, and Douglas Natelson, *Nernst-Ettingshausen effect in thin Pt and W films at low temperatures*, Appl. Phys. Lett. **122**, 182405 (2023).

3. Liyang Chen, Dale T. Lowder, Emine Bakali, Aaron M. Andrews, Werner Schrenk. Monkia Waas, Robert Svagera, Gaku Eguchi, Lukas Prochaska, Yiming Wang, Chandan Setty, Shouvik Sur, Qimiao Si, Silke Paschen, and Douglas Natelson, *Shot noise in a strange metal*, arxiv:2206.00673 (submitted).

4. Yiming Wang, Chandan Setty, Shouvik Sur, Liyang Chen, Silke Paschen, Douglas Natelson, and Qimiao Si, *Shot noise as a characterization of strongly correlated metals*, arxiv:2211.11735 (submitted).

5. Renjie Luo, Tanner J. Legvold, Liyang Chen, Henry Navarro, Ali C. Basaran, Deshun Hong, Changjiang Liu, Anand Bhattacharya, Ivan K. Schuller, and Douglas Natelson, *Low temperature spin Seebeck effect in non-magnetic vanadium dioxide*, arxiv:2307.02594 (submitted).

6. Renjie Luo, Xuanhan Zhao, Tanner J. Legvold, Liyang Chen, Changjiang Liu, Deshun Hong, Anand Bhattacharya, and Douglas Natelson, *The challenges of measuring spin Seebeck noise*, arxiv:2307.11218 (submitted).

Emergent Quasiparticles in Graphene Heterostructure

Philip Kim, Department of Physics, Harvard University

Keywords: topology-quantum Hall, 2D and layered crystals, graphene, transport, magnetotransport, nanofabrication and 2D assembly

Research Scope

2-dimensional (2D) electronic systems realized in graphene-based van der Waals (vdW) atomic stacks have been a major material platform for realizing engineered quantum systems to study correlated many-body physical phenomena. The strong interaction between charged carriers promotes the unusual appearance of quasiparticles. In this project, we carry out a new set of experiments to explore novel physical effects associated with strong correlations occurring in graphene vdW heterostructures. Firstly, we are trying to probe the exchange statistics of abelian and non-abelian anyons in fractional quantum Hall (FQH) regimes using a locally-gated Fabry-Perot electron cavity. We also study the Andreev coupling of anyonic quasiparticles in FQH states hybridized with superconducting nanostructures. Novel device structures based on double-layer graphene heterostructures will also enable us to search for exotic pairing states between FQH states across vdW gaps. Additionally, we are developing experimental methodology such as radio-frequency (RF) wave reflectometry to probe quantum capacitance and kinetic inductance in correlated states. Finally, we extend our study of mesoscale quantum thermoelectric measurement to probe the transport entropy of non-Abelian anyons in even denominator FQH states that appear in bilayer graphene.

Recent Progress

<u>Demonstration of crossed Andreev reflection in the FQH state.</u>

Superconductivity and the FQH effect are two important scientific phenomena that stem from the interaction of electrons, each representing a unique, extreme state of matter. Superconductivity is a result of the pairing of electrons due to an attractive interaction, which gives rise to a quantum state that exhibits perfect conductance at the macroscopic level. This state, in which the charge carriers are Cooper pairs with twice the electron charge, is stabilized at low temperatures and low magnetic fields. On the other hand, the FQH effect develops from repulsive interactions, creating a collective state that conducts exclusively along its edges and has carriers with a fraction of the electron charge, making it distinct from other states. This state requires both low temperatures and ultra-pure materials, as well as intense magnetic fields, which are in direct contrast to the conditions for superconductivity.

The motivation for combining these two extreme states of matter is the possibility of parafermions, which are believed to occur in a system where superconductivity and the FQH effect coexist [1]. This combination forms a novel form of topological superconductor that offers unique

advantages over previous versions. Majorana fermions, an example of emergent quasiparticles based on proximitized systems, are expected to be the building blocks of advanced, fault-tolerant qubits in topological superconductor experiments. However, Majorana qubits have a significant limitation known as non-universality, meaning they cannot perform some quantum computability tasks [2]. To overcome this, unprotected qubit realizations must be included, which sacrifices fault-tolerance, in order to achieve universality. For a topological quantum computer to reach its full potential, universality must be achieved. This is where parafermions come into play, as they are able to provide this universality.

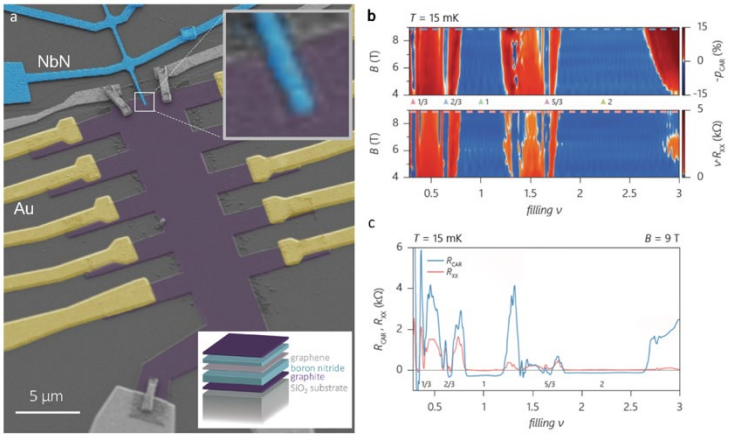

Fig. 1. The device and crossed Andreev reflection (CAR) in a FQH state. a, False color SEM image a typical device including a NbN superconductor <100 nm in width and ~1 μm in length (blue). **b,** probability of crossed Andreev reflection p_{CAR} and R_{xx} (normalized for different ν) as a function of filling and magnetic field B. **c,** CAR signal R_{CAR} and R_{xx} at B = 9 T from b. Small R_{xx} indicates negligible bulk conductance.

With the DOE/BES support, we construct high-quality graphene-based van der Waals devices with narrow superconducting niobium nitride (NbN) electrodes in which superconductivity and a robust FQH state coexist. We find a possible signature for crossed Andreev reflection (CAR) across the superconductor separating two FQH edges. Our observed CAR probabilities in the particle-like fractional fillings are markedly higher than those in the integer and hole-conjugate fractional fillings and depend strongly on temperature and magnetic field, unlike the other fillings. Further, we find a filling-independent CAR probability in integer fillings, which we attribute to spin-orbit coupling in NbN, allowing for Andreev reflection between spin-polarized edges. These results provide a route to realize novel topological superconducting phases in FQH-superconductor hybrid devices based on graphene and NbN.

Correlated electronic states in tunable flat bands in twisted multilayer graphene

Creating moire superlattices by twisting and stacking two layers of Van der Waals materials has proven to be an efficient method for promoting interaction effects and inducing exotic phases of matter. Following the discovery of superconductivity and correlated insulators in magic-angle twisted bilayer graphene (MA-TBG) [3], various two-dimensional materials have been utilized to create two-layer twisted systems and numerous novel phases. Reducing the energy bandwidth of electrons in a lattice below the energy of long-range Coulomb interaction promotes correlation effects in this method. Further tuning of the electronic properties of vdW moire superlattices is possible by modifying the interlayer coupling or band structure of constituent layers [4]. We investigated the emergence of electronic states in various forms of twisted multilayer graphene

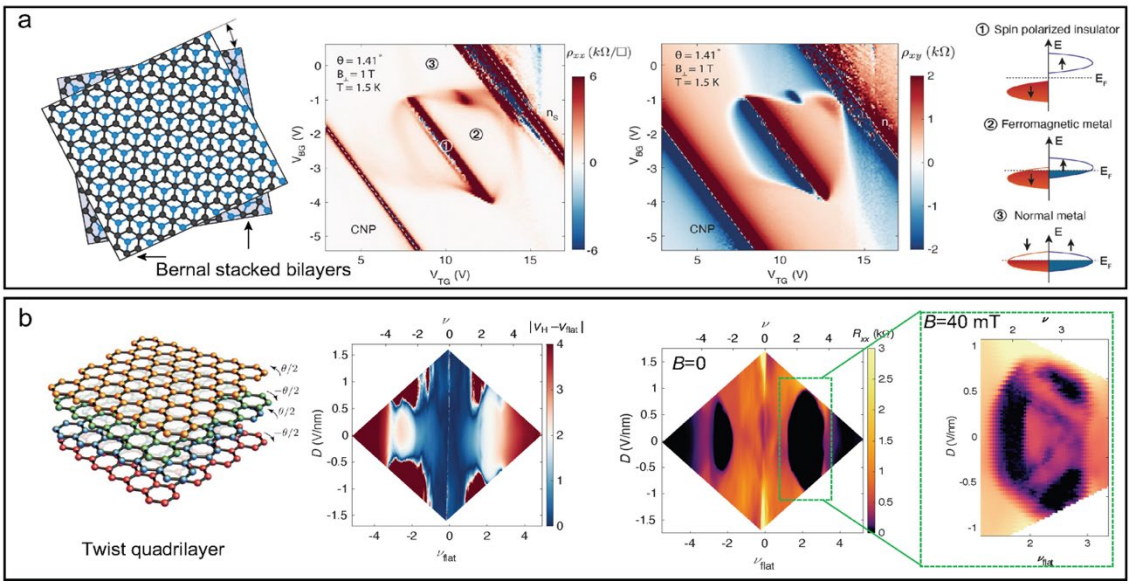

Fig. 2. Electronic transport measured in twisted multilayer graphene. a., Left panel shows a schematic of TDBG with a twist angle θ. Middle two panels display longitudinal resistivity and Hall resistance of the TDBG device around half-filling at T = 1.5 K and under perpendicular magnetic field $B_\perp$ = 1 T. The right panel shows illustration of electron orders for different regimes. The left half (right half) of the cartoon represents the band of spin down (up) electrons. **b.,** Left panel shows a schematic of 4 layer twisted graphene layer (TQG) with an alternating twist angle θ. Middle two panels display experimental phase diagram of normalized subtracted Hall filling density and longitudinal resistance as a function of flat banding filling (ν_{flat}) and displacement field. The right panel shows the zoomed in phase diagram taken at B = 40 mT.

with varying twist angles, including twisted double bilayer graphene (TDBG) and twisted quadrilayer graphene (TQG). Our research showed a flat band can be manipulated using electric fields perpendicular to the twist angle. Several correlated behaviors were observed, such as spin-polarized correlated insulators (illustrated in Fig. 2a) in TDBG and superconductivity and spontaneous flavor polarization in TQG (as shown in Fig. 2b).

Electronic thermal transport measurement in low-dimensional materials

Thermal transport plays a key role in the study of matter. From the first observation of Wiedemann and Franz, which linked heat and electronic transport, to recent experiments on topological materials, thermal transport has remained a discriminating predictor of material properties. Transport of heat is also crucial to modern technology, as limited heat dissipation in nanoscale systems is one of the primary obstacles to increasing processor performance. The recent introduction of low-dimensional materials has posed a problem for thermal measurement. These materials have strong electron interactions and topological effects that are expected to enhance exotic states of matter with novel applications in quantum sensing, computing, and energy harvesting. Existing methods for measuring heat transport are dominated by phonons, and the contribution of electrons has remained inaccessible. We developed fully electronic thermal transport measurement for low-dimensional materials like 2D van der Waals monolayers and 1D nanotubes by measuring thermal Johnson noise. Our new measurement approach isolates nonlocal

voltage fluctuations induced by electronic thermal transport. We show that graphene serves as an exceptional electronic thermometer that interfaces with van der Waals materials. We demonstrate outstanding sensitivity by measuring electronic thermal transport in a 1D carbon nanotube (NT), even in the quantum dot regime at low temperature (Fi g. 3). Signatures of interaction effects, not previously predicted, point to new insights that our technique is now able to reveal. Our results show that we can investigate low dimensional thermal transport with unprecedented sensitivity to electronic phenomena. Our method also allows the study of electronic heat transport in nanoscale devices, such as nanowires and molecular junctions.

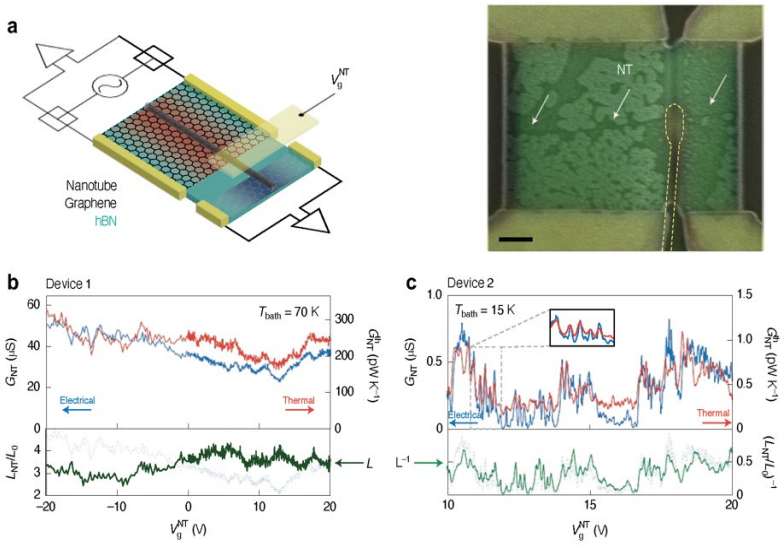

Fig. 3. Electronic thermal conductance of carbon NTs. a, Schematic of the device in which two graphene thermometers are bridged by a carbon NT (left). Composite optical and scanning electron microscopy image of the device (right). Scale bar, 1 μm. White arrows indicate the location of the NT. **b,** Two-point electrical and thermal conductance of a small-bandgap NT in Device 1 at different temperatures (top panels). The corresponding Lorenz ratio L_{NT}/L_0 is shown (dark green) in the lower panels, together with the electrical conductance shown in the respective upper panel (dotted light blue) to allow explicit comparison with L_{NT}/L_0.

Future Plans

We plan to investigate the following topics:

- Demonstration of quantum Hall interferometry in the FQH regime of graphene
- Andreev coupling of anyonic quasiparticles in FQH states
- Search for exotic pairing in double bilayer graphene FQH states
- RF reflectometry measurement for quantum capacitance and kinetic inductance
- Thermoelectric and transport entropy measurement in even denominator FQH states

References

1. J. Alicea and P. Fendley, *Topological Phases with Parafermions: Theory and Blueprints*, Annual Review of Condensed Matter Physics **7**, 119 (2016).

2. C. Nayak, S. H. Simon, A. Stern, M. Freedman, and S. Das Sarma, *Non-Abelian Anyons and Topological Quantum Computation*, Rev. Mod. Phys. **80**, 1083 (2008).

3. Y. Cao, V. Fatemi, S. Fang, K. Watanabe, T. Taniguchi, E. Kaxiras, and P. Jarillo-Herrero, *Unconventional Superconductivity in Magic-Angle Graphene Superlattices*, Nature **556**, 7699 (2018).

4. E. Khalaf, A. J. Kruchkov, G. Tarnopolsky, and A. Vishwanath, *Magic Angle Hierarchy in Twisted Graphene Multilayers*, Phys. Rev. B **100**, 085109 (2019)

Publications

1. X. Liu, J. I. A. Li, K. Watanabe, T. Taniguchi, J. Hone, B. I. Halperin, P. Kim, C. R. Dean, "Crossover between Strongly-coupled and Weakly-coupled Exciton Superfluids," Science 375, 205-209 (2022).

2. J. Waissman, L. E. Anderson, A. V. Talanov, Z. Yan, Y. J. Shin, D. H. Najafabadi, T. Taniguchi, K. Watanabe, B. Skinner, K. A. Matveev, P. Kim, "Measurement of Electronic Thermal Conductance in Low-Dimensional Materials with Graphene Nonlocal Noise Thermometry," Nature Nano. **17**, 166-173 (2022).

3. O. Gül, Y. Ronen, S. Y. Lee, H. Shapourian, J. Zauberman, Y. H. Lee, K. Watanabe, T. Taniguchi, A. Vishwanath, A. Yacoby, P. Kim, "Andreev reflection in fractional quantum Hall state," Phys. Rev. X **12**, 021057 (2022).

Emergent Topological Properties of Landau Flatbands

PI: Gabor Csathy, affiliation: Purdue University

Keywords: topology-quantum Hall, non-Fermi liquid behavior and charge dynamics, quantum wells, semiconductors, topological materials, magnetotransport, molecular beam epitaxy

Research Scope

The study of the quantum phases with topological order has permeated contemporary condensed matter physics. Most of the topological phases are single-particle in origin. Topological insulators and semiconductor-superconductor hybrid structures are examples of such systems. There is, however, a second group of topological phases that form because of strong electron-electron interactions. Materials with flat electronic bands naturally support these phases, since in these materials the kinetic energy is quenched. These flatband systems are currently under intense scrutiny, partly because of their rich physics and partly because of the hope that the interaction supported quantum entanglement stabilizes more intricate topological order. Topological phases in flatband systems hold the promise for applications in quantum memories and qubits, especially the ones that will be immune to noise.

Landau bands realized in the two-dimensional electron gas exposed to static magnetic fields are naturally flat and support an astonishingly large number of phases. Phases at half-filled bands are in particular very interesting and possess mysterious properties. One such phase at half filling is the paired fractional quantum Hall state forming due to *p*-wave pairing of composite fermions, the emergent particles of the fractional quantum Hall regime. The excitations of this paired state are thought to obey non-Abelian statistics. Another remarkable phase at half filling is the electronic nematic phase, an anisotropic phase that develops in otherwise isotropic samples. Beyond half-filling, the two-dimensional electron gas hosts a very large number of isotropic solids. Competition of topological phases with these traditional Landau phases will impact any application of the topological degree of freedom.

We seek to understand and control various aspects of flatband physics in the two-dimensional electron gas in GaAs/AlGaAs heterostructures in phases realized in the fractional quantum Hall regime. This system has a very rich history. Indeed, fractional quantum Hall states and a state that can be described as a *p*-wave superconductor were discovered in this system. This system continues to have an extremely high quality, due to progress in the growth technology it keeps improving, and it continues to exhibit new physics, even when it is compared to graphene. Its flat bands and high quality assure that the electron gas in GaAs/AlGaAs continues to exhibit novel phenomena.

Recent Progress

Several of our results make use of the most recent advance in molecular beam epitaxy technology [a]. The mobility of the two-dimensional electron gas in these new GaAs/AlGaAs heterostructures increased by more than a factor of 3 at densities less than $1x10^{11}/cm^2$ as compared to that of earlier generation of samples. In addition, we employ state of the art cryogenic techniques to cool this system to temperatures as low as 5 mK.

Pairing and nematicity in the fractional quantum Hall regime.

It has been known for some time that the paired fractional quantum Hall states compete with anisotropic phases called the quantum Hall nematic. We discovered earlier that when driven by hydrostatic pressure, there is a quantum phase transition from the ν=5/2 fractional quantum Hall state to the nematic. The diagram of this transition is shown in Fig.1. A puzzling aspect of our work is that in the more than three-decade long history of the ν=5/2 fractional quantum Hall state, during which experiments were performed at ambient pressure, a transition to the nematic was not seen prior to our experiments. This leaves one with the question what is the role of the pressure in inducing the observed phase transition?

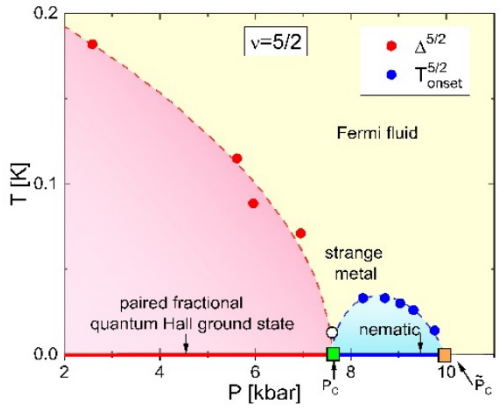

Fig.1 Quantum criticality at the filling factor ν=5/2.

A difficulty we had to overcome is the disentangling of pressure effects from density effects that occurred concomitantly. We conducted further experiments on the system and found a similar quantum phase transition at ν=7/2. We were thus able to demonstrate that this phase transition occurs in both spin branches of the so called second Landau level. A careful analysis of dependence of our data in terms of the Landau level mixing parameter **κ** and width of the quantum well **w/l$_B$** seen in Fig.2 revealed that the transition is driven by tuning of the electron-electron interactions, specifically the short-range part of this interaction [1]. As a final test, we were able to engineer a sample which had the right parameters for observing the nematic at ambient pressures. Tuning of the short-range part of the electron-electron interaction is possible in many two-dimensional materials and it presents an interesting pathway to manipulate the ground state of the system.

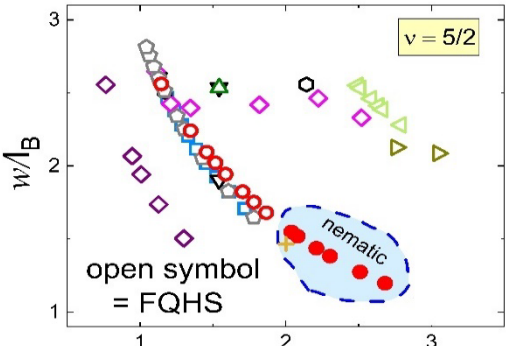

Fig.2 The ν=5/2 fractional quantum Hall state and the nematic in the w/l$_B$-κ space.

Finally, we emphasize that the transition can be understood as occurring between a *p*-wave superconductor and a nematic. Our results highlight the close connection between exotic superconductivity and nematicity and offer the insight that such a transition can be induced by tuning the short-range part of the electron-electron interactions.

Novel aspects of the interplay of single-electron localization and of collective localization in the topological regime.

The ν =1 integer quantum Hall state may be considered the first topological state. It was understood early on that Anderson-type of electron localization played a central role in the formation of the plateau. These ideas later led to understanding of the scaling for the plateau-to-plateau transition and the construction of the global phase diagram of the quantum Hall effect.

As the disorder level was reduced, it was understood that a second type of localization may also be present along the integer quantum Hall plateau. This second mechanism of localization is provided by the pinning of a collective phase, such as the Wigner solid. Even though evidence for the two distinct types of localization (Anderson-type single electron localization and pinning of the Wigner solid) was observed in various experiments, these two types of localization was not reported in widely employed magnetotransport measurements.

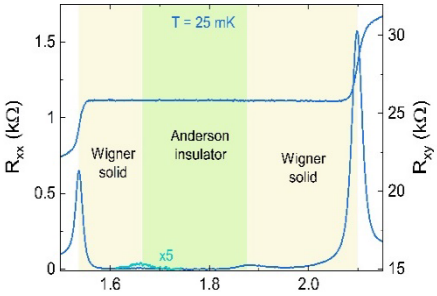

Fig.3 The Anderson insulator and the Wigner solid on the ν=1 plateau in transport measurements.

Our recent work has shown that in the newest generation of the highest mobility samples these two regions can be clearly distinguished [b]. Transport data is shown in Fig.3. Even though we do not fully understand why earlier samples did not exhibit these regimes, the new observations open up the possibility of new studies. We studied the electrical breakdown of the ν=1 plateau in the two different localization regimes [5]. We also investigated the temperature-dependent behavior on the plateau [7]. We found that the magnetoresistance is activated in both localization regimes. As shown in Fig.4, the activation energy $\mathbf{E_a}$ has local maxima in the center of the Anderson insulator and Wigner solid, but it has conspicuous minima at the boundary between the two phases.

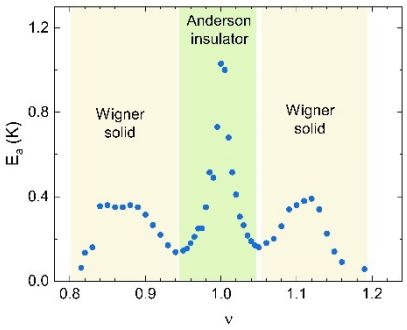

Fig.4 An unusual dependence of the activation energy E_a on the filling factor ν.

Advances in cryogenics: thermometry and sample cooling to the lowest dilution refrigerator temperatures.

Dilution refrigerators, widely used in the study of topological and quantum materials, routinely reach temperatures near 5 mK. However, measuring temperature at the low end of this scale continues to be fraught with difficulties. For example, it is well-known that the commonly used RuOx thermometers lose their sensitivity below about 25 mK. It is often assumed that the cause of loss of sensitivity is spurious rf radiation.

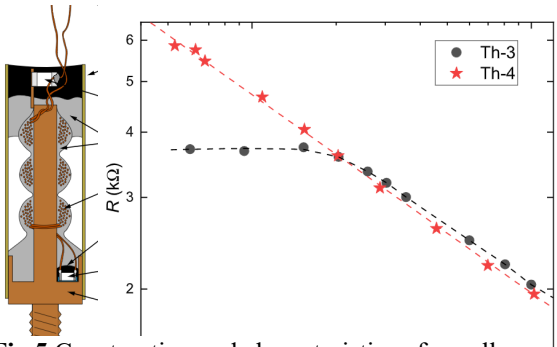

Fig.5 Construction and characteristics of a well-filtered RuOx thermometer that has an in-situ rf filter. We demonstrated that this thermometer operates down to 5 mK.

We have shown that rf filtering of the measurement wires does not necessarily solve this problem [4]. Indeed, when the measurement wires run through vacuum between the thermometer and the rf filter, the loss of sensitivity persists. However, then the rf filter is organically included in the thermometer's construction, as shown in Fig.5, and thermalization of the thermometer is recovered to the lowest temperatures. Furthermore, based on estimations of the magnitude of rf power, we concluded the source of this power is the black body radiation inside the vacuum can of the refrigerator. This discovery will impact not only thermometry, but also the cooling technology of samples to the low mK range.

Future Plans

Recent developments in the growth technology of the GaAs system yielded samples of extremely high mobility. These advances are bound to result in new discoveries and will support the study of known states under an expanded parameter space.

The existence of the quantum critical point in the paired-to-nematic transition impacts work and possible applications of non-Abelian fractional quantum Hall states. At the same time, lessons learned on this system open up numerous questions relevant not just for the electron gas, but also in other strongly correlated materials. We are currently working with our sample growers on new samples that will allow tuning this transition by gating, rather than by pressure. This avenue of inquiry will allow us to approach the critical point in a more controlled way and to obtain high quality data amenable for fitting to theory.

This approach will also allow us to investigate the strange metal properties of the Fermi sea near the critical point. We already know that the Fermi sea in this region is non-trivial. Above the critical point, the Fermi sea is ordinary as it is constitutes by electrons. However, below the critical pressure the Fermi sea is formed of emergent particles of the fractional quantum Hall effect, the composite fermions, whereas above it by electrons. It thus will be interesting to investigate details of this strange metal with unknown properties.

One of the most exciting consequences of the quantum critical point is the enhanced critical fluctuations of the order parameter and gauge fields near it. These enhanced fluctuations will undoubtedly induce novel effects. We will look for such effects associated with fluctuations. We also plan thermodynamic measurements of the paired fractional quantum Hall state. Such investigations are part of our long-term effort aimed at exploring unconventional collective behavior in topological systems and it is expected to lead to new insight of the behavior of related strongly correlated materials.

References

a. Yoon Jang Chung, K. A. Villegas Rosales, K. W. Baldwin, P. T. Madathil, K. W. West, M. Shayegan, and L. N. Pfeiffer, "*Ultra-high-quality two-dimensional electron systems*", Nature Materials 20, 632–637 (2021)

b. S. Myers, H. Huang, L.N. Pfeiffer, K.W. Baldwin, and G.A. Csathy, "*Magnetotransport patterns of collective localization near ν = 1 in a high-mobility two-dimensional electron gas*", Phys. Rev. B **104**, 045311 (2021).

Publications

1. K.A. Schreiber and G.A. Csathy, "*Competition of Pairing and Nematicity in the Two-dimensional Electron Gas*", Annual Review of Condensed Matter Physics **11**, 17 (2020) G.A. Csathy, chapter 5 entitled "*Exploring Quantum Hall Physics at Ultra-Low Temperatures and at High Pressures*" in the book *Fractional Quantum Hall Effects – New Developments*, edited by B.I. Halperin and J.K. Jain, World Scientific Publishing Co. (2020)

2. E. Kleinbaum, H. Li, N. Deng, G.C. Gardner, M.J. Manfra, and G.A. Csathy, "*Disorder broadening of even-denominator fractional quantum Hall states in the presence of a short-range alloy potential*", Phys. Rev. B **102**, 035140 (2020)

3. D. Ro, "*Multielectron bubble phases*", PhD Thesis (2020)

4. S.A. Myers, H. Li, and G.A. Csathy, "*A Ruthenium Oxide Thermometer for the Full Range of Dilution Refrigerator Temperatures*", Cryogenics **119**, 103367 (2021)

5. Haoyun Huang, S.A. Myers, L.N. Pfeiffer, K.W. West, K.W. Baldwin, and G.A. Csathy, "*Breakdown of the $\nu = 1$ integer quantum Hall effect in the single particle and collective localization regimes*", Solid State Communications **353**, 114876 (2022)

6. S.A. Myers, "*Transport signatures and energy scales of the collective insulator forming near integer quantum Hall plateaus*", PhD Thesis (2022)

7. S.A. Myers, Haoyun Huang, W. Hussain, L.N. Pfeiffer, K.W. West, and G.A. Csathy, "*Anomalous thermal activation in the Breakdown of the $\nu = 1$ integer quantum Hall effect in the single electron and collective localization regimes of the integer quantum Hall plateau*", manuscript submitted (2023)

Time, Momentum, and Energy Resolved Pump-Probe Tunneling Spectroscopy

H. M. Yoo[1] , M. Korkusinski[2] , D. Miravet[3] , K. W. Baldwin[2] , K. West[2] , L. Pfeiffer[2] , P. Hawrylak[3] , and R. C. Ashoori[1]

[1]Department of Physics, Massachusetts Institute of Technology
[2]Emerging Technologies Division, National Research Council of Canada, Ottawa
[3]Department of Physics, University of Ottawa
[4]Department of Electrical Engineering, Princeton University

Keywords General: topology-quantum Hall, **Material Forms:** Quantum Wells and Thin Film Heterostructures**, Material Classes:** Semiconductors, **Techniques:** Contactless Tunneling

Research Scope

Our project seeks to advance the use of two tunneling spectroscopies, contactless pulsed capacitance spectroscopy (CPTS), and momentum and energy resolved tunneling spectroscopy (MERTS)[1] in semiconductor quantum Hall systems. We are working to use CPTS, MERTS, and capacitance spectroscopy to examine phases of the 2D electronic system in high magnetic field (such as Wigner Crystal[2] and stripe and bubble phases) and unusual fractional quantum Hall states. We have used the methods to study the spin-polarizations over the broad phase diagram of the 2D system in magnetic field[3] and to study the exciton condensate phase.[4]

Recent Progress

Spectroscopy of nonequilibrium systems can uncover intricate relaxation mechanisms and exotic many-body interactions that are hidden in strongly correlated materials. Experimenters have extensively used pump-probe methods in ultra-fast optics for studying nonequilibrium phenomena in bulk materials. However, there remains a significant challenge in applying these spectroscopies to two-dimensional (2D) materials at low temperatures, home to a variety of intriguing correlated electronic phases such as superconducting and magnetic states.

In this work,[5] we have developed a time, momentum, and energy resolved pump-probe tunneling spectroscopy (Tr-MERTS) that allows high-energy resolution imaging of nonequilibrium states in a 2D electronic system in a strong applied magnetic field and at ultra-low temperatures. Tr-MERTS employs short-duty cycle RF pulses and easily functions in the millikelvin temperature range which has been inaccessible to previous pump-probe spectroscopy. In addition, electrical pulses utilized in Tr-MERTS are easily tunable and permit precise control of pumping electron densities. Finally, since the pumping energy can be tuned by the height of an applied pulse, electrons can be pumped into a specific energy state even for a system with equidistant energy levels.

Using Tr-MERTS, we visualize the time-dependent change of tunneling spectra in a wide range of filling factors, temperatures, and magnetic fields, all of which can tune the ground-state properties and hence the relaxation dynamics of excited electrons. We observe a substantially slowed-down relaxation process of spin-polarized electrons with lifetimes up to tens of microseconds when the system forms a ferromagnetic ground state. Furthermore, by precisely tuning the pumping electron density, we discover an unexpected splitting in the nonequilibrium energy spectrum in the vicinity of a ferromagnetic state. An exact diagonalization study of the system suggests that the splitting arises from a maximally spin-polarized higher energy state, distinct from a conventional equilibrium skyrmion. Furthermore, we observe time-dependent relaxation of the splitting, which we attribute to single-flipped spins forming topological spin textures. These results demonstrate the potential broad applicability of Tr-MERTS for exploring the nonequilibrium physics in Landau levels and other flat-band systems realized in emerging 2D materials.

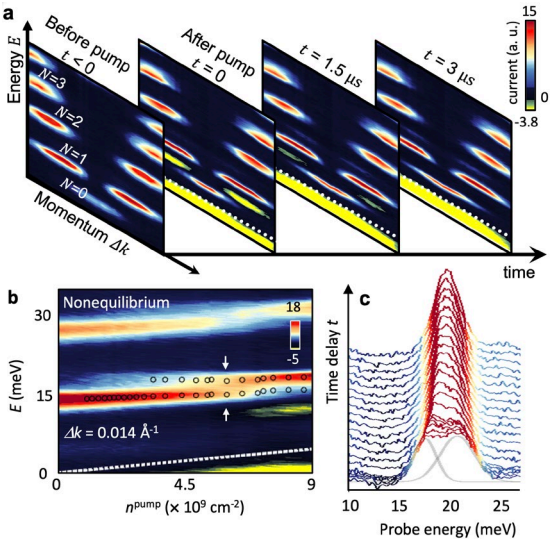

a, Tr-MERTS spectra measured as a function of time delay time (t). **b,** A momentum cut of the spectrum measured as a function of pumping density (n^{pump}). **c,** t dependence of a nonequilibrium splitting.

Future Plans

We are working to use these and related novel capacitance methods on a variety of TMD systems.

References

1. Jang J, Yoo HM, Pfeiffer LN, West KW, Baldwin KW, Ashoori RC (2017) Full momentum- and energy-resolved spectral function of a 2D electronic system. *Science*, **358**(6365):901–906. https://doi.org/10.1126/science.aam7073

2. Jang J, Hunt BM, Pfeiffer LN, West KW, Ashoori RC (2016) Sharp tunnelling resonance from the vibrations of an electronic Wigner crystal. *Nature Physics*, **13**:340.

3. Yoo HM, Baldwin KW, West K, Pfeiffer L, Ashoori RC (2020) Spin phase diagram of the interacting quantum Hall liquid. *Nature Physics*, https://doi.org/10.1038/s41567-020-0946-1

4. Jang J, Yoo HM, Pfeiffer LN, West KW, Baldwin KW, Ashoori RC (2021) Strong interlayer charge transfer due to exciton condensation in an electrically isolated GaAs quantum well bilayer. *Applied Physics Letters*, **118**(20):202110. https://doi.org/10.1063/5.0049595

5. Yoo HM, Korkusinski M, Miravet D, Baldwin KW, West K, Pfeiffer L, Hawrylak P, Ashoori RC (2023) Time, momentum, and energy resolved pump-probe tunneling spectroscopy of two-dimensional electron systems. https://doi.org/10.48550/arXiv.2304.12434

Publications (2021-2023)

1. Demir A, Staley N, Aronson S, Tomarken S, West K, Baldwin K, Pfeiffer L, Ashoori R (2021) Correlated Double-Electron Additions at the Edge of a Two-Dimensional Electronic System. Physical Review Letters, **126**(25):256802. https://doi.org/10.1103/PhysRevLett.126.256802

2. Jang J, Yoo HM, Pfeiffer LN, West KW, Baldwin KW, Ashoori RC (2021) Strong interlayer charge transfer due to exciton condensation in an electrically isolated GaAs quantum well bilayer. Applied Physics Letters, **118**(20):202110. https://doi.org/10.1063/5.0049595

3. Yoo HM, Korkusinski M, Miravet D, Baldwin KW, West K, Pfeiffer L, Hawrylak P, Ashoori RC (2023) Time, momentum, and energy resolved pump-probe tunneling spectroscopy of two-dimensional electron systems. https://doi.org/10.48550/arXiv.2304.12434

Poster Session 1

Optically Addressable Molecular Color Center Thin Films on Monolayer Graphene

PI James Rondinelli | Northwestern University
Co-PI David Awschalom | University of Chicago
Co-PI: Danna Freedman | Massachusetts Institute of Technology
Co-PI Mark Hersam | Northwestern University
Co-PI Jeffrey Long | UC Berkeley
Co-PI Michael Wasielewski |Northwestern University

Keywords: Molecular Approach to quantum information, quantum sensing, molecular qubits, 2D materials

Research Scope

Our team is employing chemical synthesis to create designer sensors, targeted for magnetic and electric field sensing of specific analytes. The initial focus of the proposal will be to design and modify molecular quantum sensors for integration with material targets. Our scientific approach exploits a feedback cycle involving the synthesis and measurement of quantum properties of materials with precise molecular design. Here, we will modulate charge, surface compatibility, read-out, and sensitivity through chemical synthesis (**Freedman**, **Long**, **Wasielewski**). We then will interrogate the coherence properties of these molecules (**Awschalom**, **Wasielewski**). Molecular design criteria will be established based on these outputs guided by computation (**Rondinelli**). In the final project phase, candidate molecular sensors will be tested in several proof-of-concept applications, where quantum sensors will be positioned in close proximity to state-of-the-art quantum materials using deposition, chemical tethering, and intercalation (**Hersam**, **Long**). Sensor information will be read out primarily with optically detected magnetic resonance (ODMR) (**Awschalom**, **Wasielewski**). Experimental design and sensing interpretations will be guided by electronic structure theory computations (**Rondinelli**). Key applications include sensing the orientation of the magnetic field in 2D magnets with high spatial precision, sensing the electric field of ferroelectrics and conductive metal–organic frameworks, and the high-risk target of combining magnetic and electric field sensors to search for quasiparticle excitations such as spinons.

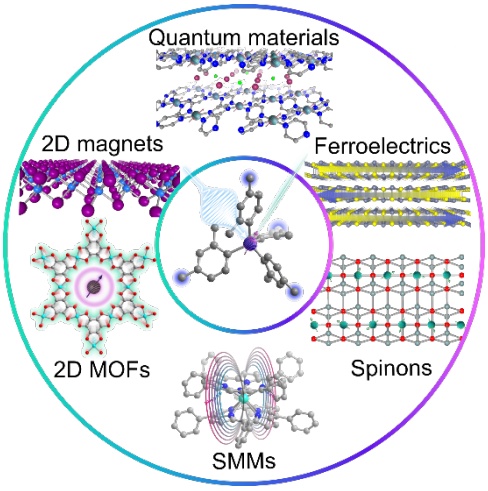

Figure 1 | Tunable optically addressable quantum sensors (center) offer integration with and nanoscale characterization of quantum materials such as 2D magnetic materials and ferroelectrics, 1D spin chains, biomaterials and single-molecule

Recent Progress (related to slide)

In previously published work, **Freedman** and **Awschalom** established Cr(IV)(*o*-tolyl)$_4$ as the first optically addressable molecular qubit.[3] Over the past year, **Hersam** explored co-deposition of Cr(*o*-tolyl)$_4$ and its spin-silent analog Sn(o-tolyl)$_4$ that acts as the host matrix to ensure isolated molecular qubits in a spin-dilute environment. When these molecules are co-deposited on SiO_2/Si substrates, they quickly form thick disordered islands, which are suboptimal for quantum sensing. In contrast, when these molecules are co-deposited on monolayer graphene substrates, smooth terraced films with consistent 1 nm steps are observed with atomic force microscopy. In addition, X-ray diffraction shows that the molecular films are highly oriented in the (110) out-of-plane direction. DFT calculations confirm that the (110) orientation of Sn(*o*-tolyl)$_4$ on graphene is the lowest energy configuration (**Rondinelli)**. The changes in the excited state energies and electronic structure in the film geometries were also computed.

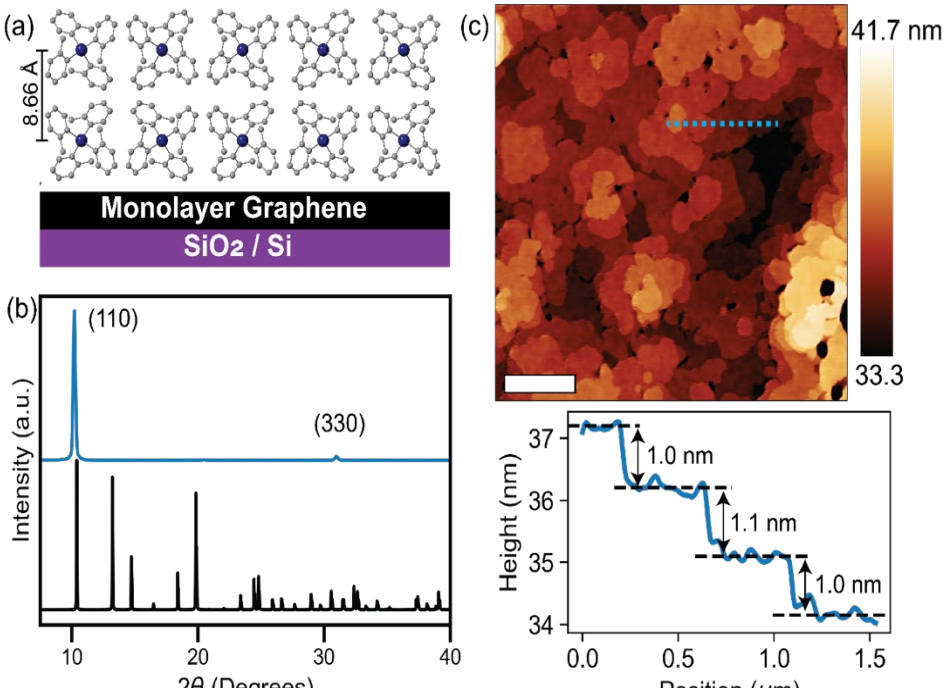

Figure 2 | (a) Schematic of a Sn(*o*-tolyl)$_4$ molecular qubit thin film in the (110) orientation on monolayer graphene. (b) X-ray diffraction (XRD) for a Sn(*o*-tolyl)$_4$ film on graphene shown in blue and simulated XRD pattern for Sn(*o*-tolyl)$_4$ shown in black. The (110) orientation is clearly dominant in the experimental data. (c) Atomic force microscope image of a Sn(*o*-tolyl)$_4$ film on graphene shows terraced growth with ~1 nm molecular steps (scale bar = 1 μm).

The molecular qubits remain optically active and microwave addressable following thermal deposition into highly order thin films. In particular, off-resonant photoluminescence (PL) measurements at 4 K show that the molecular qubit film on graphene possesses a sharp zero-phonon line (ZPL) with linewidth comparable to that of the molecular single crystal. The optical lifetime T_{opt} (8.3 μs) for the molecular qubit film is also comparable to the molecular single crystal (3 μs) (**Awschalom**). In addition, continuous wave electron paramagnetic resonance (CW-EPR) and pulse-EPR show that the molecular qubit thin films are microwave addressable (**Freedman)**. From CW-EPR, the molecular qubit film on graphene has strong angular dependence with respect to the magnetic field direction as expected for a highly-oriented film. Using pulse-EPR, the spin-lattice relaxation time T_1 and coherence time T_m were found to be 241±7 μs and 550±10 ns at 6 K, respectively. *Notably, T_1 (241 μs) is much longer than T_{opt} (8 μs) as is required for optically initializing the qubit state.*

While the critical quantum sensing properties of the molecular qubits are preserved in thin-film form, some differences are also observed. For example, from X-ray diffraction, the molecular qubit

films are found to be strained such that the molecular crystal lattice spacing in the (110) direction is elongated. Correspondingly, PL shows that the ZPL is shifted from 1025 nm to 1012 nm, and CW-EPR analysis reveals shifts in the ground state spin energy levels. DFT calculations by **Rondinelli** performed calculations to explain the subtle changes in the wavelength of the ZPL of the molecular crystal and thin film forms of Cr(*o*-tolyl)$_4$. **Rondinelli** found that changes in the excited state energy occur from a decrease in the molecules point group from S_4 to C_1, as experimental EPR results showing an increase in the E parameter suggested a change in the molecules symmetry. **Rondinelli** confirmed that these effects can be attributed to strain and changes in the local symmetry of Cr(*o*-tolyl)$_4$. These changes in the spin and optical properties of molecular qubits in the thin film environment suggest that surface engineering can be utilized to tune the properties of molecular qubits. Ongoing work is focused on demonstrating that optical addressability is retained in the molecular qubit films through optical spin-initialization and optically detected magnetic resonance (ODMR) (**Awschalom**).

Future Plans

Here, we propose using molecules developed by Freedman and Awschalom to not only seed the ALD and hence achieve CrI_3 ambient stability, but also sense magnetic fields in proximity to CrI_3 by optically reading out molecular color sensors, as recently shown by Freedman and Awschalom. Initially, Hersam will explore different methods of depositing these molecules on CrI_3 including gas-phase and solution-phase deposition in a controlled atmosphere glove box. If the molecular qubits do not effectively seed ALD growth, then PTCDA will be deposited on top of the molecular qubit layer as a seeding layer. Importantly, our controlled atmosphere glove boxes are directly interfaced with an ALD chamber and a thermal evaporation chamber, so all processing can occur without ambient exposure. In addition, by incorporating a spacer between the molecular qubit sensor and CrI_3, such as atomically thin hBN layers, we can spatially map the magnetic field with *a vertical resolution at the sub-nanometer scale.*

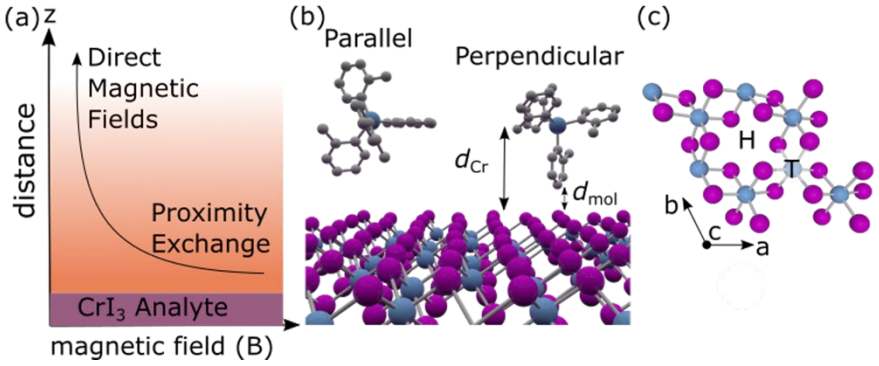

Figure 3 | Theory demonstrates potential for molecular color centers measuring the magnetic field of CrI_3

Publications

1 Wang, Y.; Ziebel, M. E.; Sun, L.; Gish, J. T.; Pearson, T. J.; Lu, X.; Thorarinsdottir, A. E.; Hersam, M. C.; Long, J. R.; Freedman, D. E.; Rondinelli, J. M.; Puggioni, D.; Harris, T. D. Strong Magnetocrystalline Anisotropy Arising from Metal–Ligand Covalency in a Metal–Organic Candidate for 2D Magnetic Order *Chem. Mater*. **2021**, *33*, 8712-8721.

2. Roesner, E.K.; Asheghali, D.; Kirillova, A.; Strauss, M.J.; Evans, A.M.; Becker, M.L., and Dichtel, W.R. Arene-Perfluoroarene Interactions Confer Enhanced Mechanical Properties to Synthetic Nanotubes *Chemical Science*, **2022**. 13, 8; 2475-2480. DOI: 10.1039/d1sc05932g

3. D. Lebedev, J. T. Gish, E. S. Garvey, T. K. Stanev, J. Choi, L. Georgopoulos, T. W. Song, H. Y. Park, K. Watanabe, T. Taniguchi, N. P. Stern, V. K. Sangwan, and M. C. Hersam, "Electrical interrogation of thickness-dependent multiferroic phase transitions in the 2D antiferromagnetic semiconductor NiI_2," *Adv. Funct. Mater.*, **33**, 2212568 (2023).

4. Nathan P. Bradshaw, Zoheb Hirani, Lidia Kuo, Siyang Li, Nicholas X. Williams, Vinod K. Sangwan, Lindsay E. Chaney, Austin M. Evans, William R. Dichtel, Mark C. Hersam Aerosol-Jet-Printable Covalent Organic Framework Colloidal Inks and Temperature-Sensitive Nanocomposite Films *Advanced Materials* https://doi.org/10.1002/adma.202303673

5. Fangbai Xie, Haochuan Mao, Chenjian Lin, Yuanning Feng, J. Fraser Stoddart, Ryan M. Young, and Michael R. Wasielewski Quantum Sensing of Electric Fields Using Spin-Correlated Radical Ion Pairs *J. Am. Chem. Soc.* 2023, 145, 27, 14922–14931

Search for 3D Topological Superconductors using Laser-Based Spectroscopy

Principal Investigator: David Hsieh
Mailing Address: 1200 E. California Blvd., MC 149-33, California Institute of Technology, Pasadena, CA 91125
E-mail: dhsieh@caltech.edu

Keywords: topology, single crystals, topological materials, optical spectroscopy, density functional theory

(i) Research Scope

The overarching goal of this program is to develop routes to realize a three-dimensional topological superconducting (3D TSC) state by identifying its precursor phases. It is theoretically proposed that the critical fluctuations of certain inversion symmetry breaking electronic phases[1] can mediate Cooper pairing in odd-parity channels and lead to topological superconductivity[2]. Therefore, 3D TSCs may potentially emerge upon suppressing these ordered phases to a critical point with external perturbations such as pressure or even light. We seek to test this hypothesis by deploying a suite of equilibrium and time-resolved optical probes operating under extreme conditions of high pressure and intense optical stimulation to identify and to characterize the predicted precursor phases in candidate materials.

(ii) Recent Progress

Under ambient conditions, elemental tellurium (Te) is a semiconductor with an inversion symmetry broken crystal structure composed of chiral chains of Te atoms oriented along the *c*-axis (Fig. 1A). Upon application of hydrostatic pressure, Te undergoes a semiconductor-to-metal transition and a series of different structural phase transitions, some of which are accompanied by the emergence of superconductivity at low temperature[3]. It has also been predicted that the metallic band structure at certain pressures may be topologically non-trivial. Therefore, Te is an intriguing candidate for hosting a 3D TSC. Since the pressure range where the highest superconducting critical temperature is reached is near 35 GPa, we first explored the possibility of controlling the crystallographic and electronic structures of Te using light.

Our study focused on a mechanism known as a light-induced inverse-Peierls distortion. The Peierls instability is a spontaneous symmetry-lowering lattice deformation that lifts the degeneracy of electronic states at the Fermi level in order to lower the overall system energy. Impulsive excitation by an intense laser pulse offers a potential out-of-equilibrium pathway to induce an inverse-Peierls transition. By optically de-populating states near the Fermi level, the energy increase due to the lattice distortion is no longer balanced by the energy decrease due to the lifting of band degeneracy. This triggers a sudden change in the potential energy surface of the lattice, generating a restoring force that drives coherent atomic motion reversing the Peierls distortion.

Elemental Te is a prototypical Peierls-distorted system whose band structure features Weyl nodes – topologically stable crossing points between non-degenerate bands in a crystal. The evolution from a Peierls distorted to non-distorted structure is parameterized by the chain radius x (measured in units of the inter-chain distance). By performing a combination of time-dependent density functional theory (DFT) calculations and ultrafast time-resolved optical second harmonic generation (SHG) polarimetry measurements, we showed that x transiently increases following impulsive optical excitation (Fig. 1B, C), amounting to a reversal of the Peierls distortion. By raising the transient value of x through increasing the excitation fluence, we discovered that Te undergoes a three-state switch from a Weyl semiconductor (x = 0.269) to a Weyl metal (x = 0.283), and finally to a Dirac metal (x = 0.333) once the Peierls distortion is completely reversed (Fig. 1A)[4].

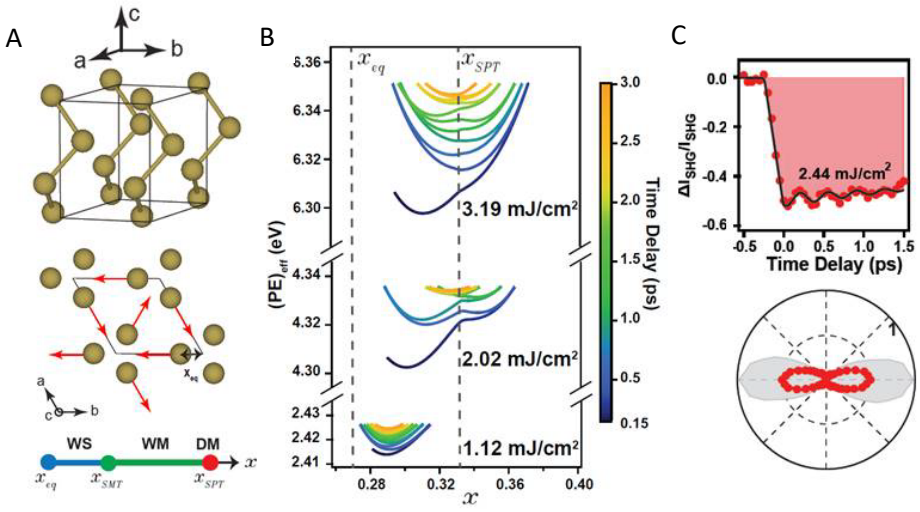

Fig 1: (A) Unit cell of Te from side and top views. Red arrows point along the Peierls distortion phonon coordinate x. Phase diagram as a function of x determined from DFT calculations (WS: Weyl semiconductor; WM: Weyl metal; DM: Dirac metal). (B) Time-dependent DFT calculated spatio-temporal trajectories of the potential energy at different excitation fluences showing different metastable x values. (C) Instantaneous SHG polarimetry pattern (bottom) measured after optical pumping. The static pattern (grey) is overlaid. Differential SHG intensity transient (top) acquired at the angle of maximum intensity in the polarimetry pattern, showing temporal stabilization of a metastable value of x.

Proof-of-principle experiments using ultrashort light pulses to create or annihilate Weyl nodes *in situ* were previously demonstrated in Dirac and type-II Weyl semimetal materials via impulsively driven lattice symmetry changes. However, such efforts focused on binary switching between semi-metallic states with and without Weyl nodes. Our results demonstrate the possibility of multi-state-switching. Moreover, they suggest that Peierls distorted systems are a fertile playground for exploring the interplay of ultrafast band topology control and ultrafast insulator-to-metal transitions, two hitherto separate areas of research.

(iii) Future Plans

Previous work from our group reported evidence of a 3D inversion breaking electronic liquid crystalline phase below a temperature T_c = 200 K in $Cd_2Re_2O_7$[5], a possible precursor to a 3D TSC. The technique used was optical SHG polarimetry, which probes electronic transitions at high energies in the visible spectral range. Probing electronic transitions at energies in the mid-infrared range may provide more insight into the nature of the low-energy instability across T_c. However, this energy range is technically more challenging for SHG measurements.

Recently, we have been working towards probing the photogalvanic effect (PGE) from $Cd_2Re_2O_7$ – a second-order nonlinear optical process that rectifies light to a DC current – that is readily measured using low energy incident light. In our experiment, mid-infrared light from a high-power CO_2 laser (10.6 μm wavelength) impinges on a $Cd_2Re_2O_7$ crystal. The DC electrical current generated through the PGE is then detected using metal contacts deposited onto the surface. Figure 2A shows an optical micrograph of a typical $Cd_2Re_2O_7$ device. The positioning of the contacts was guided by optical SHG microscopy measurements (Fig. 1B) to ensure that the contacts reside within a single crystallographic domain. By tracking the magnitude of the photocurrent as a function of the incident linear polarization, we observed clear modulations indicative of a linear PGE (Fig. 1C). For the remainder of this award, we plan to complete both linear and circular PGE measurements as a function of temperature to understand the detailed symmetries of the electronic phase below T_c.

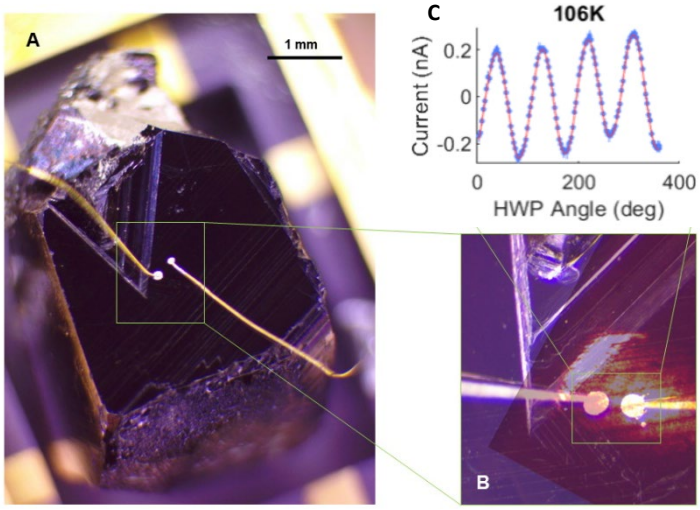

Fig. 2: (A) Microscope image of the $Cd_2Re_2O_7$ photogalvanic effect device used in our measurements. (B) Zoom-in near the contacts overlaid with an optical second harmonic generation image, verifying lead placement on a single crystallographic stripe domain. (C) Photocurrent amplitude as a function of incident light polarization, which is controlled by a half waveplate (HWP), acquired at T = 106 K.

(iv) References

1. Fu, L. Parity-Breaking Phases of Spin-Orbit-Coupled Metals with Gyrotropic, Ferroelectric, and Multipolar Orders. *Phys. Rev. Lett.* **115**, 026401 (2015).

2. Kozii, V. & Fu, L. Odd-Parity Superconductivity in the Vicinity of Inversion Symmetry Breaking in Spin-Orbit-Coupled Systems. *Phys. Rev. Lett.* **115**, 207002 (2015).

3. G. Parthasarathy and W. B. Holzapfel, High-pressure structural phase transitions in tellurium, *Phys. Rev. B* **37**, 8499(R) (1988).
4. H. Ning, O. Mehio, C. Lian, X. Li, E. Zoghlin, P. Zhou, B. Cheng, S. D. Wilson, B. M. Wong & D. Hsieh. Light-induced Weyl semiconductor-to-metal transition mediated by Peierls instability. *Phys. Rev. B* **106**, 205118 (2022).
5. Harter, J. W., Zhao, Z. Y., Yan, J.-Q., Mandrus, D. G. & Hsieh, D. A parity-breaking electronic nematic phase transition in the spin-orbit coupled metal $Cd_2Re_2O_7$. *Science* **356**, 295 (2017).

(v) Publications supported by BES

1. J. Orenstein, J. E. Moore, T. Morimoto, D. H. Torchinsky, J. W. Harter & D. Hsieh. Topology and symmetry of quantum materials via nonlinear optical responses. *Annu. Rev. Condens. Matter Phys.* **12**, 247 (2021).

2. C. Li, X. Li, T. Deshpande, X. Li, N. Nair, J. G. Analytis, D. M. Silevitch, T. F. Rosenbaum & D. Hsieh. High-pressure control of optical nonlinearity in the polar Weyl semimetal TaAs. *Phys. Rev. B* **106**, 014101 (2022).
3. H. Ning, O. Mehio, C. Lian, X. Li, E. Zoghlin, P. Zhou, B. Cheng, S. D. Wilson, B. M. Wong & D. Hsieh. Light-induced Weyl semiconductor-to-metal transition mediated by Peierls instability. *Phys. Rev. B* **106**, 205118 (2022).

Magnetometry Studies of Quantum Correlated Topological Materials in Intense Magnetic Fields

Lu Li, University of Michigan

Keywords: magnetism, single crystals, topological materials, magnetometry, magnetotransport

Research Scope

This project investigates the fundamental nature of quantum correlated topological materials by torque magnetometry in intense magnetic fields. The proposal aims to answer this question: does strong electronic interaction lead to novel topological quantum states? In particular, our proposal will address the following three questions: (a). Does strong electronic correlation help make a topological material? (b). Do topological insulators stay insulating or become semimetals under magnetic fields? (c). Does strong electronic correlation lead to new electronic and magnetic states? These questions test the hypothesis that, in quantum material, the strong electronic interaction creates unique topological quantum states.

This proposal aims to use advanced experimental torque magnetometry techniques to give conclusive evidence of the novel electronic and magnetic states in quantum correlated topological materials. Our research starts with magnetic torque and conductivity measurements in intense magnetic fields to explore the magnetic response of quantum correlated topological material. The material candidates include the following material families and their representative crystals: (1) mixed valence insulators: YbB_{12}, (2) noncentrosymmetric Weyl/Kondo insulators and semimetals: $Ce_3Bi_4(Pt_{1-x}Pd_x)_3$, (3) transition metal mixed valence insulator $FeSb_2$, (4) spin-orbit-coupled transition metal oxides: $Cd_2Re_2O_7$, and (5) Kondo exhaustion insulator: $YbIr_3Si_7$.
We hope to carry out the following tasks on these quantum correlated topological material candidates: (1). Detecting quantum oscillations of the bulk and the surface states in quantum correlated topological materials; (2). Revealing the origin of quantum oscillations in quantum correlated topological materials; (3). Searching for novel electronic and magnetic ground states in quantum correlated topological materials; (4). Resolving current-driven-magnetizations under magnetic fields in quantum correlated topological materials.

Recent Progress

(a). Resonant torque differential magnetometry with high frequency quartz oscillators (Review of Scientific Instruments 2022, Ref. [1])

Sensitive magnetometry has been a powerful probe for investigating quantum materials. Extreme conditions, such as sub-kelvin cryogenic temperatures and ultrahigh magnetic fields, demand further durability for sensitive magnetometry. However, significant mechanical vibrations and rapid magnetic field changes give enormous challenges to conventional magnetometry. This article presents a possible solution to this problem by developing a new magnetometry technique using high-frequency quartz oscillators. The technique takes advantage of the symmetry and geometry of mechanical vibration configurations of standard commercially available MHz quartz oscillators, and the setup keeps the high-quality factor resonance with the sample mounted on the oscillator. We further demonstrate the sensitivity of the technique using bismuth single crystals and a $Fe_{0.25}TaS_2$ ferromagnetic material. Quantum oscillations are observed in the magnetometry

response below 1 T, and the detected oscillation frequency is shown to come from the electron pockets of the bismuth.

(b). Hall Anomaly, Quantum Oscillations and Possible Lifshitz Transitions in Kondo Insulator YbB_{12}: Evidence for Unconventional Charge Transport (Physical Review X, 2022, Ref. [2])

Recently, magnetic quantum oscillations and metallic low- temperature thermal conductivity have been observed in the Kondo insulator YbB_{12}, whose resistivity is a few orders of magnitude higher than those of conventional metals. As yet, these unusual observations are not fully understood. Here we present a detailed investigation of the behavior of YbB_{12} under intense magnetic fields using both transport and torque magnetometry measurements. Our results support a novel two-fluid scenario in YbB_{12}: A Fermi-liquid-like fluid of charge-neutral quasiparticles coexists with charge carriers that remain in a non-metallic state. The former experience successive Lifshitz transitions and develop Landau quantization in applied magnetic fields, while scattering between both fluids allows the Shubnikov–de Haas effect to be observed in the electrical transport. The verification of this two-fluid scenario by the data in the current work strongly suggests that YbB_{12} represents a new phase of matter.

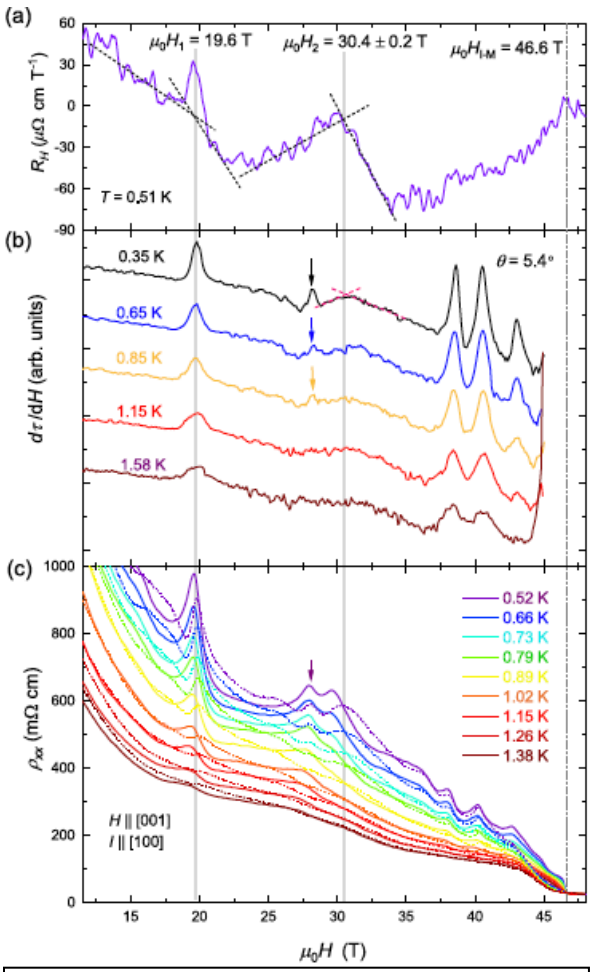

Figure 1. A comparison of the Hall effect, magnetic torque, and electrical resistivity, confirms the transitions at the same magnetic fields and the quantum oscillations in the Kondo insulator YbB_{12}. Taken from Ref. [2].

(c). Magnetic field effects on the quantum spin liquid behaviors of $NaYbS_2$ (Quantum Frontiers, 2022, Ref. [3])

Spin-orbit coupling is an important ingredient to regulate the many-body physics, especially for many spin liquid candidate materials such as rare-earth magnets and Kitaev materials. The rare-earth chalcogenides $NbYbCh_2$ (Ch = O, S, Se) is a congenital frustrating system to exhibit the intrinsic landmark of spin liquid by eliminating both the site disorders between Na^+ and Yb^{3+} ions with the big ionic size difference and the Dzyaloshinskii-Moriya interaction with the perfect triangular lattice of the Yb^{3+} ions. The temperature versus magnetic-field phase diagram is established by magnetization, specific heat, and neutron-scattering measurements. Notably, the neutron diffraction spectra and the magnetization curve might provide microscopic evidence for a series of spin configurations for in-plane fields, which include the disordered spin liquid state, 120° antiferromagnet, and one-half magnetization state. Furthermore, the ground state is suggested to be a gapless spin liquid from inelastic neutron scattering, and the magnetic field adjusts the spin orbit coupling. Therefore, the strong spin-orbit coupling in the frustrated quantum magnet substantially enriches low-energy spin

physics. This rare-earth family could offer a good platform for exploring the quantum spin liquid ground state and quantum magnetic transitions.

(d). Magnetic Breakdown and Spin-zero Effect in Quantum Oscillations in Kagome Metal CsV_3Sb_5 (Communications Materials, *under review*)

Magnetic fields shift electron energies via the Zeeman effect, with the proportionality given by the Lande g−factor. Conventional metals show that the g-factor may be enhanced for small electron orbits in the order of the inverse of the effective mass, a triumph of single-particle theory for massive Dirac bands. However, it is not clear how the Zeeman effect changes for correlated and topological quantum states. In the recently discovered Kagome metal CsV_3Sb_5, we determined the g-factor using spin-zeros in the magnetic quantum oscillations. The g-factor deduced is around an order of magnitude larger than the inverse of the effective mass. This large enhancement is visible only in magnetic breakdown orbits between conventional and concentrated Berry curvature Fermi pockets that host large orbital moments. Such Berry-curvature-generated large orbital moments are almost always concealed by the other effects; here, magnetic breakdown orbits due to proximity to a conventional Fermi-surface section allow them to be very visibly manifested in the magnetic quantum oscillations. Our results provide a unique example of the interplay between electronic correlations and more conventional electronic bands in quantum materials.

(e). Large Oscillatory Thermal Hall Effect in Kagome Metals (Nature Physics, *under review*)

The thermal Hall effect recently provided intriguing probes to the ground state of exotic quantum matters. These observations of a transverse effect without the Lorentz force lead to the debate on the origins of fermions versus bosons. The recent report of quantum oscillations (QOs) in Kitaev spin liquid points to a possible resolution. The Landau level quantization would most likely capture only the fermionic thermal transport effect. However, the quantum QOs in the thermal Hall effect are generally hard to detect. In this work, we report the observation of a large oscillatory thermal Hall effect of correlated Kagome metals. We detect a 180-degree phase change of the oscillation and demonstrate the phase flip as an essential feature for QOs in the thermal transport properties. More importantly, the oscillation amplitude of the thermal Hall effect is more profound than those in the longitudinal channel and electrical Hall effect. This result presents the oscillatory thermal Hall effect as a powerful probe to the correlated quantum materials.

(f). Quantum Oscillations Evidence for Topological Bands in Kagome Metal ScV_6Sn_6 (Physical Review B, *under review*)

Metals with kagome lattice provide bulk materials to host both the flat-band and Dirac electronic dispersions. A new family of kagome metals is recently discovered in AV_6Sn_6. However, there is no direct evidence supporting the Dirac electronic structures of this material. In the manuscript, we solve the problem by resolving the quantum oscillations in both electrical transport and magnetization in ScV_6Sn_6. The revealed orbits are consistent with the electronic band structure models. Furthermore, the Berry phase of a dominating orbit is revealed to be around π, providing direct evidence for the topological band structure. Our results demonstrate a rich physics and shed light on the correlated topological ground state of this kagome metal.

Future Plans

(a). Develop a current-driven-magnetization technique for quantum materials.
We aim to invent a new experimental technique to detect the current-driven-magnetization for quantum materials. Current-driven magnetization provides direct access to Berry curvature dipole, the critical quantity underlying the intrinsic nonlinear Hall effect, and other responses. Driving the sample with electrical currents leads to a displaced Fermi surface in momentum space with asymmetric electron distribution. For example, in Weyl Semimetals with Berry curvature dipole, the charge current will generate a measurable spin/orbital magnetization that is intimately related to the nonlinear Hall effect.

(b). Resolving the quantum oscillations in magnetization using resonant torque differential magnetometry for pulsed magnetic fields up to 65 T and 100 T.
The quantum oscillation pattern in the ultrahigh magnetic field has only been observed in the conduction channels. For a different comparison, we would need to resolve the oscillations in magnetization (the dHvA effect) using sensitive torque differential magnetometry [8] under pulsed magnets. Quantum oscillations in magnetic susceptibility create small oscillatory forces. Therefore, the magnetic force acting on a sample glued to a resonating cantilever will shift the resonating frequencies or broaden the resonance. We choose to use quartz tuning forks for the resonating cantilevers. Our preliminary experiment succeeded in running 192 kHz tuning forks to detect the M-H hysteresis loop of underdoped $YBa2Cu3O_{6.56}$ (YBCO). A tuning fork is glued to the heavy block ("qPlus" mode named for Atomic Force Microscopy), and a small AC voltage is applied to drive it to resonance. As the impedance changes, the resonance is observed in the current of the device.

The technical challenge still exists to resolve the quantum oscillations when the resonant frequency is too low and the frequency resolution in sliding FFT is about 10 Hz. And this resolution is still too large to determine quantum oscillations. To solve the problem, we have tested a range of quartz resonators with resonance frequencies in the 1.5-4 MHz range. In addition, we have built a current-voltage converter to detect excitation signals. Moreover, the tuning fork resonance is significantly damped by liquid Helium 3 when we tried to cool down samples to 0.4 K. This cold temperature is needed to resolve the dHvA effect for many materials. Therefore, we will build vacuum cells for tuning forks.

References

1. Guoxin Zheng, Dechen Zhang, Kuan-Wen Chen, J Singleton, and Lu Li. *Resonant torque differential magnetometry with high frequency quartz oscillators*, Review of Scientific Instruments, **93**, 063907 (2022)

2. Ziji Xiang, Kuan-Wen Chen, Lu Chen, Tomoya Asaba, Yuki Sato, Nan Zhang, Dechen Zhang, Yuichi Kasahara, Fumitoshi Iga, William A Coniglio, Yuji Matsuda, John Singleton, and Lu Li. *Hall anomaly, quantum oscillations and possible Lifshitz transitions in Kondo insulator YbB12: evidence for unconventional charge transport*, Physical Review X, **12**, 021050 (2022)

3. Jiangtao Wu, Jianshu Li, Zheng Zhang, Changle Liu, Yong Hao Gao, Erxi Feng, Guochu Deng, Qingy- ong Ren, Zhe Wang, Rui Chen, Jan Embs, Fengfeng Zhu, Qing Huang, Ziji Xiang, Lu Chen, Yan Wu, E. S. Choi, Zhe Qu, Lu Li, Junfeng Wang, Haidong Zhou, Yixi Su, Xiaoqun Wang, Gang Chen, Qingming Zhang, and Jie Ma. *Magnetic field effects on the quantum spin liquid behaviors of NaYbS2*, Quantum Frontiers, **1**, 13 (2022)

Publications

1. X. Rao, G. Hussain, Q. Huang, N. Li, W. J. Chu, H. L. Che, L. G. Chu, X. Zhao, Z. Dun, E. S. Choi, T. Asaba, L. Chen, Z. Xiang, L. Li, Y. H. Gao, J. Zhao, G. Chen, H. D. Zhou, and X. F. Sun, *Survival of itinerant excitations and quantum spin state transitions in $YbMgGaO_4$ with chemical disorder*, Nature Communications **12**, 4949 (2021)

2. Z. Xiang, L. Chen, K.-W. Chen, C. Tinsman, Y. Sato, T. Asaba, H. Lu, Y. Kasahara, M. Jaime, F. Balakirev, F. Iga, Y. Matsuda, J. Singleton, and Lu Li, *Unusual high-field metal in a Kondo insulator,* Nature Physics **17**, 788 (2021)

3. Xiaoran Liu, Sobhit Singh, Victor Drouin-Touchette, Tomoya Asaba, Jess Brewer, Qinghua Zhang, Yanwei Cao, Banabir Pal, Srimanta Middey, P. S. Anil Kumar, Mikhail Kareev, Lin Gu, D. D. Sarma, Padraic Shafer, Elke Arenholz, John W. Freeland, Lu Li, David Vanderbilt, and Jak Chakhalian, *Proximate Quantum Spin Liquid on Designer Lattice,* Nano Letters, **21**, 2010 (2021)

4. Y Sato, Z Xiang, Y Kasahara, S Kasahara, Lu Chen, C Tinsman, F Iga, J Singleton, NL Nair, N Maksimovic, JG Analytis, Lu Li, and Y Matsuda, *Topological surface conduction in Kondo insulator YbB12*, Journal of Physics D **54**, 404002 (2021)

5. Guoxin Zheng, Dechen Zhang, Kuan-Wen Chen, J Singleton, and Lu Li. *Resonant torque differential magnetometry with high frequency quartz oscillators*, Review of Scientific Instruments, **93**, 063907 (2022)

6. Ziji Xiang, Kuan-Wen Chen, Lu Chen, Tomoya Asaba, Yuki Sato, Nan Zhang, Dechen Zhang, Yuichi Kasahara, Fumitoshi Iga, William A Coniglio, Yuji Matsuda, John Singleton, and Lu Li. *Hall anomaly, quantum oscillations and possible Lifshitz transitions in Kondo insulator YbB12: evidence for unconventional charge transport*, Physical Review X, **12**, 021050 (2022)

7. Jiangtao Wu, Jianshu Li, Zheng Zhang, Changle Liu, Yong Hao Gao, Erxi Feng, Guochu Deng, Qingy- ong Ren, Zhe Wang, Rui Chen, Jan Embs, Fengfeng Zhu, Qing Huang, Ziji Xiang, Lu Chen, Yan Wu, E. S. Choi, Zhe Qu, Lu Li, Junfeng Wang, Haidong Zhou, Yixi Su, Xiaoqun Wang, Gang Chen, Qingming Zhang, and Jie Ma. *Magnetic field effects on the quantum spin liquid behaviors of NaYbS2*, Quantum Frontiers, **1**, 13 (2022)

8. Shirin Mozaffari, William R Meier, Richa P Madhogaria, Seoung-Hun Kang, John W Villanova, Hasitha W Suriya Arachchige, Guoxin Zheng, Yuan Zhu, Kuan-Wen Chen, Kaila Jenkins, Dechen Zhang, Aaron Chan, Lu Li, Mina Yoon, Yang Zhang, and David G Mandrus, *Universal sublinear resistivity in vanadium kagome materials hosting charge density waves,* arXiv preprint arXiv:2305.02393 (2023)

Chiral Materials and Unconventional Superconductivity

PIs: Qiang Li (Lead), Mengkun Liu, Weiguo Yin, and Genda Gu
Condensed Matter Physics & Materials Science Division, Brookhaven National Laboratory

Keywords: Chiral materials, Fe-based superconductors, magnetotransport, optical spectroscopy, ARPES

Research Scope

This program studies topological phases and charge transport properties in chiral materials and unconventional superconductors. A unique feature of chiral materials is that their low-energy quasi-particles possess an additional quantum number that goes by the name of handedness or chirality. The powerful notion of chirality underpins a wide palette of new and useful phenomena that may be utilized to construct a new type of qubit using chiral fermions in Dirac/Weyl semimetals, chiral edge current in graphene or topological insulators.[1] To this end, the program aims at providing the basic understanding of topological phase transition and chiral current under various stimulus. Unconventional superconductivity arises in superconductors hosting, for examples, Majorana zero mode, or order parameter with a non-zero angular momentum. To this end, the focus of the program is to look for the exotic states of matter, including pair density waves and topological superconductors. Our approach has been developed through synthesizing chiral materials and unconventional superconductors in both single crystals and thin film forms, and subsequently characterizing them using a range of techniques including transport, electron and optical spectroscopy. Experimental activities are strongly coupled with theory and computation efforts, providing new strategies for designing robust electronic materials for energy applications and quantum computing.

Recent Progress

Ultrafast Melting of Superconductivity in Fe-superconductors explored by tr-ARPES – The superconducting iron chalcogenides bring together superconductivity, topology, and magnetism in a single material. Superconductivity and topology offer the possibility of topological superconductivity, which in turn presents a platform for hosting Majorana fermions that are building blocks for topological quantum computing technology. Topological superconductivity has unconventional paring mechanism. One way to probe the pairing mechanism in superconductors is through optical pumping, whereby one pulse of light excites the material, and a subsequent pulse helps explore the properties of that excited state by time-resolved ARPES. We applied such techniques to an iron-chalcogenide superconductor, $FeSe_{0.45}Te_{0.55}$, as shown in Fig. 1 (a) and (b) below and above T_c respectively. We observed that following the initial decay, the system enters a metastable state in which the superconductivity disappears for timescales greater than 100 ps. Similar nonequilibrium behavior following photoexcitation has been observed in previous studies, but the relationship to superconductivity was unclear. Here, we clarify this understanding by modifying the experimental capabilities to allow for higher energy resolution, thereby gaining insight into the low-energy excitations. We identify, for the first time, the coherent peak associated with superconductivity and the associated energy gap, properties that were not evident in earlier studies. We found the filling of the superconducting gap occurring before the reduction of the superconducting peak, Fig. 1 (c) and (d), signaling the melting of

superconductivity on ultrafast timescales. We hypothesize that the orbital fluctuations directly caused by the pump-induced electronic redistribution are linked to double-stripe magnetic correlations known to compete with superconductivity. A better theoretical understanding of the precise electronic excitations and relaxation pathways would be crucial in understanding the mechanism of superconductivity in the iron-based superconductors.[2]

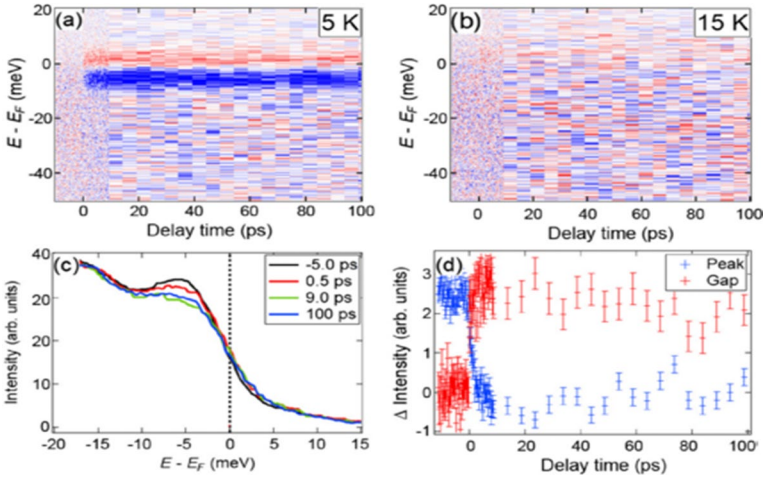

Fig. 1 Photoinduced changes to the k-integrated band structure of $FeSe_{0.45}Te_{0.55}$ below (a) and above (b) T_c. Red and blue lines indicate an intensity increase and decrease, respectively. (c) Energy distribution curves at various delay times. (d) Intensity dynamics just above and below E_F out to long delay times. The data were averaged over a 7-meV energy range. For clarity, the data below E_F were offset and normalized to match the change above E_F.[2]

Infrared Nano-Imaging of Dirac Magnetoexcitons in Graphene – Two-dimensional (2D) electron systems in strong magnetic fields are expected to exhibit quantized Hall conductivity, chiral edge currents, and distinctively collective modes referred to as magnetoplasmons and magnetoexcitons. Generating these propagating collective modes in charge-neutral samples and imaging them at their native nanometer length scales have thus far been experimentally elusive tasks. In this study, we visualize propagating magnetoexcition polaritons at their native length scales and report their magnetic-field-tunable dispersion in near-charge-neutral graphene. Our work is enabled by innovations in cryogenic near-field optical microscopy techniques that allow for the nano-imaging of the near-field responses of 2D materials under magnetic fields up to 7 Tesla. This novel nano magneto-optics approach represents a new paradigm for exploring and manipulating magnetopolaritons in specimens with low carrier doping via harnessing high magnetic fields. Fig. 2. show direct image of quantum Hall chiral edge currents due to the infrared Dirac magnetoexcitons (DiMEs) and controlled by the external magnetic field.[3]

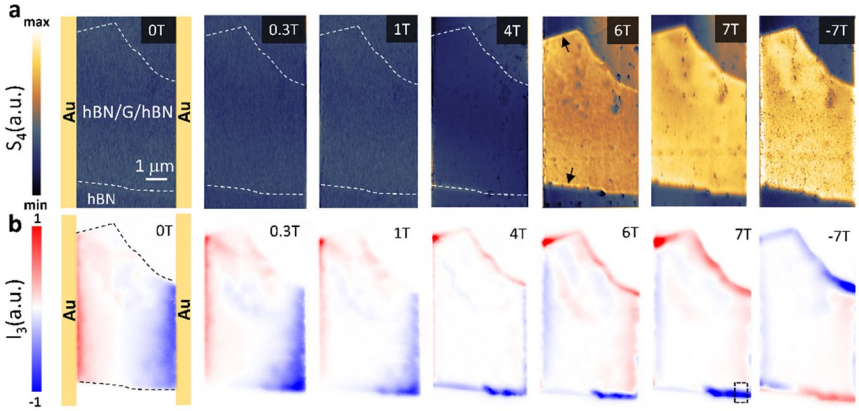

Fig. 2 Near-field scattering (a) and photocurrent (b) images of hBN encapsulated monolayer graphene as the magnetic field is tuned from 0 to 7 T. As the DiME is brought into resonance at 7 T, the graphene sheet becomes brighter (a), and an enhanced chiral edge current becomes apparent in (b), with the maximum current occurring at ±7 T.[3]

Robust and tunable Weyl phases in $ZrTe_5$ by infrared phonons – We used first-principles and effective Hamiltonian methods to study the effect of lattice distortions corresponding to the Raman and infrared phonon modes in $ZrTe_5$, a layered topological material close to the phase boundary between the strong and weak topological insulating (TI) phase. We found that all three types of zone-center infrared optical phonon modes can drive the system from the TI to a Weyl semimetal by breaking the global inversion symmetry. Fig. 3(a) shows the ground state band structure of the system around the Γ point. The system is initially in a strong TI phase, which is seen from the inversion of the band character in the figure. When the lattice is distorted corresponding to infrared optical phonon modes (the strength of such distortion is denoted by lattice distortion Q), after some critical value of lattice distortion, we get gapless phase with a pair of Weyl points (WPs), shown in Fig. 3(b). The Weyl phases are robust over a large value of lattice distortion Q, with distinct surface states (Fermi arc states). When the Weyl phase finally gaps out, the gapped phase is in a non-inverted regime (Weak TI). As shown in Fig. 3(c), we find that the critical value of lattice distortion necessary for the creation of a pair of Weyl points can be drastically reduced if our initial state is a Dirac semimetal (DSM) phase instead of a gapped TI phase. In the presence of the IR phonon mode distortion, one needs large value of Q to enter the Weyl regime (indicated by non-zero momentum transfer) but if one applies such IR distortion for the gapless Dirac phase, we immediately get Weyl phase. Such gapless Dirac phase can be obtained from A_g Raman phonon mode.[4]

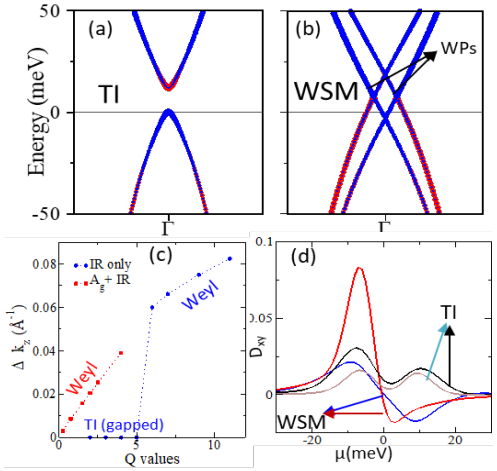

Fig. 3 (a), (b) Evolution of the band structure of $ZrTe_5$ around Γ point with an IR mode lattice distortion Q=0 as a TI (a) and Q=1.5 showing Weyl points (WPs) (b). (c) Distance between the WPs when pumping from TI (blue) or DSM (red) phase. (d) Berry curvature dipole moment as a function of chemical potential for TI and WSM phases.[4]

Anomalous Hall effect at the Lifshitz transition in $ZrTe_5$ – $ZrTe_5$ is a topological semimetal. The presence of a temperature-induced Lifshitz transition, in which the Fermi level goes from the conduction band to the valence band with increasing temperature, provides unique opportunities to study the interplay between Fermi-surface topology, dynamics of Dirac fermions, and Berry

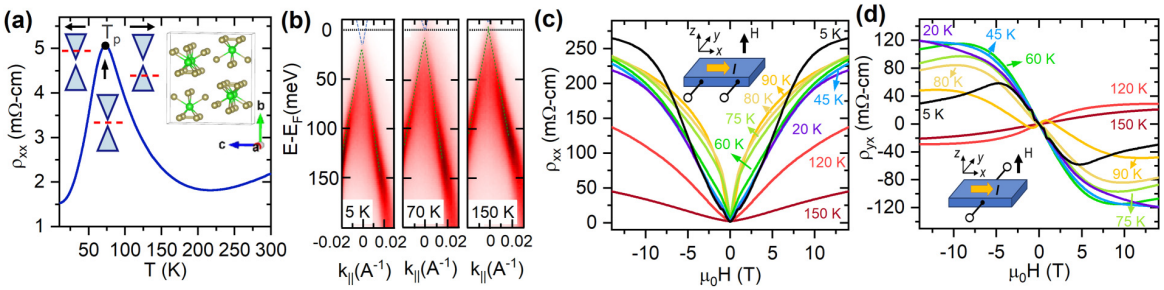

Fig. 4 (a) Temperature dependence of the longitudinal resistivity of $ZrTe_5$ along the a-axis. The resistivity peak at $T = T_p$ marks the temperature-induced Lifshitz transition. (b) The ARPES of the dispersion near the Γ point. The 70- and 150-K data were divided by the Fermi-Dirac function to make the data near the Fermi level clearer. (c, d) Longitudinal and transverse magnetoresistivity across the Lifshitz transition.[5]

curvature in one system. In a combined experimental and theoretical study, we show that a low-energy model can be used to understand the complicated Hall response and large anomalous Hall effect observed in $ZrTe_5$ over a wide range of temperature and magnetic field, as shown in Fig. 4 (d). We found that the Berry curvature induced anomalous Hall contribution dominates the Hall response in a narrow temperature window around the Lifshitz transition, away from which the orbital contribution dominates. Moreover, our results indicate that a topological phase transition coexists with the Lifshitz transition. Our model provides a unifying framework to understand the Hall effect in semimetals with large Zeeman splitting and nontrivial topology.[5]

Future Plans

Relationship between topology, strain, and transport properties in chiral materials and unconventional superconductors is a key research direction of this program. To this end, we will properly engineer, characterize, and understand strain-induced pseudo-magnetic fields and associated topological states in quantum materials. We will explore how pseudo-magnetic fields behave differently from real magnetic fields in topological materials. In addition, dynamic methods of topological controls using various coherent phonons will be investigated.

Interplay of topological orders, magnetism, and superconductivity is a planned study focused on the design, growth, and characterization of time reversal symmetry breaking topological materials and candidates for bulk topological superconductors. Our theoretical/computational effort will provide guiding principles for the selection of the most interesting material systems for crystal and thin film growth. A coordinated experimental effort is planned using combined ARPES + STM + IR/THz spectroscopy approach for investigating real space magnetic orders, momentum space topological orders and superconductivity in a range of quantum materials.

Ultrafast control of topological phase transitions is another planned study to exploit the unprecedented chiral response in topological materials to both internal and ex-ternal stimuli at vastly different time scales from steady-state to ultrafast. We aimed at using this response to design new materials and establish new topological control principles. To this end, we will characterize the photo-excited states and topological currents under various external and internal stimuli using combined time-resolved- (tr-) IR/THz and tr-ARPES, complemented by studies using time-dependent density function theory and dynamic method.

References

1. Q. Li, *Dynamics of chiral fermions in condensed matter systems,* a book chapter in the Proceedings of the Nobel Symposium 167: Chiral Matter, https://doi.org/10.1142/9789811265068_0007, (World Scientific, 2023).
2. D. Nevola, N. Zaki, J. M. Tranquada, W.-G. Yin, G. D. Gu, Q. Li, and P. D. Johnson, *Ultrafast Melting of Superconductivity in an Iron-Based Superconductor*, Phys. Rev. X **13**, 011001 (2023).
3. M. Dapolito, M. Tsuneto, W. Zheng, L. Wehmeier, S. Xu, X. Chen, J. Sun, Z. Du1, Y. Shao, R. Jing, S. Zhang, A. Bercher, Y. Dong, D. Halbertal, V. Ravindran, Z. Zhou, M. Petrovic, A. Gozar, G. L. Carr, Q. Li, A. B. Kuzmenko, M. M. Fogler, D. N. Basov, X. Du, M. Liu, *Infrared Nano-Imaging of Dirac Magnetoexcitons in Graphene*, Nature Nanotechnology https://doi.org/10.1038/s41565-023-01488-y (2023).
4. N. Aryal, X. Jin, Q. Li, M. Liu, A. M. Tsvelik, W. Yin, *Robust and tunable Weyl phases by coherent infrared phonons in $ZrTe_5$*, npj Computational Materials 8, **113** (2022).
5. P. M. Lozano, G. Cardoso, N. Aryal, D. Nevola, G. Gu, A. Tsvelik, W. Yin, and Q. Li, *Anomalous Hall effect at the Lifshitz transition in $ZrTe_5$*, Phys. Rev. B **106,** L081124 (2022).

Publications

1. M. Dapolito, M. Tsuneto, W. Zheng, L. Wehmeier, S. Xu, X. Chen, J. Sun, Z. Du1, Y. Shao, R. Jing, S. Zhang, A. Bercher, Y. Dong, D. Halbertal, V. Ravindran, Z. Zhou, M. Petrovic, A. Gozar, G. L. Carr, Q. Li, A. B. Kuzmenko, M. M. Fogler, D. N. Basov, X. Du, M. Liu, *Infrared Nano-Imaging of Dirac Magnetoexcitons in Graphene*, Nature Nanotechnology https://doi.org/10.1038/s41565-023-01488-y (2023).

2. T. Ren, P. M. Lozano, Q. Li, G. Gu, and A. M. Tsvelik, *Two types of superconducting pairs in stripe-ordered* $La_{2-x}Ba_xCuO_4$ *(x = 1/8): Evidence from the resistivity measurements* Phys. Rev. B **107**, 085118 (2023).

3. Y. Liu, H. Pi, K. Watanabe, T. Taniguchi, G. Gu, Q. Li, H. Weng, Q. Wu, Y. Li, and Y. Xu, *Gate-Tunable Multiband Transport in* $ZrTe_5$ *Thin Devices*, Nano Lett. **23**, 5334 (2023).

4. D. Nevola, N. Zaki, J. M. Tranquada, W.-G. Yin, G. D. Gu, Q. Li, and P. D. Johnson, *Ultrafast Melting of Superconductivity in an Iron-Based Superconductor*, Phys. Rev. X **13**, 011001 (2023).

5. S. Jois, J. L. Lado, G. Gu, Q. Li, and J. Lee, *Andreev Reflection and Klein Tunneling in High-Temperature Superconductor-Graphene Junctions* Phys. Rev. Lett. **130**, 156201 (2023).

6. N. Aryal, Q. Li, A. M. Tsvelik, W. Yin, *Topological Antiferromagnetic Semimetal for Spintronics: A Case Study of a Layered Square Net System* $EuZnSb_2$, Phys. Rev. B **106**, 235116 (2022).

7. P. Li, P. Qiu, Q. Xu, J. Luo, Y. Xiong, J. Xiao, N. Aryal, Q. Li, L. Chen and X. Shi, *Colossal Nernst power factor in topological semimetal* $NbSb_2$, Nature Communications **13**, 7612 (2022).

8. P. M. Lozano, Tianhao Ren, G. D. Gu, A. M. Tsvelik, J. M. Tranquada, and Q. Li, *Testing for pair-density-wave order in* $La_{1.875}Ba_{0.125}CuO_4$, Phys. Rev. B **106**, 174510 (2022).

9. P. M. Lozano, G. Cardoso, N. Aryal, D. Nevola, G. Gu, A. Tsvelik, W. Yin, and Q. Li, *Anomalous Hall effect at the Lifshitz transition in* $ZrTe_5$, Phys. Rev. B **106,** L081124 (2022).

10. N. Aryal, X. Jin, Q. Li, M. Liu, A. M. Tsvelik, W. Yin, *Robust and tunable Weyl phases by coherent infrared phonons in* $ZrTe_5$, npj Computational Materials **8**, 113 (2022).

Perfect Coulomb drag in a dipolar excitonic insulator

Kin Fai Mak, Cornell University

Keywords: Excitonic insulator, Coulomb drag measurements, exciton transport, 2D semiconductor bilayers

Research Scope

Excitonic insulators (EIs), which emerge in semiconductors with the electron-hole binding energy exceeding the band gap, are expected to host a suite of Bosonic phases of matter such as superfluids and supersolids. Coulomb-coupled electron-hole double layers built on two-dimensional semiconductors realize continuously tunable EIs. Although thermodynamic studies on double layer EIs have revealed the emergence of strongly correlated dipolar excitons, the transport of these excitons in the strong correlation regime remains elusive to date.

Recent Progress

We have demonstrated dipolar exciton transport in a double layer EI contacted by excitonic electrodes. Perfect Coulomb drag is observed in that a charge current in the electron layer induces an equal but opposite drag current in the hole layer. Correspondingly, the drag resistance diverges with decreasing temperature due to the thermally activated charge transport in the EI. With increasing exciton density beyond the Mott density, the drag resistance further shows an insulator-to-metal transition induced by the dissociation of excitons. The EI charge gap on the insulating side vanishes continuously towards the transition critical point while the metallic side shows a Fermi liquid drag with diverging effective mass at the Mott density. Our results open the door for the realization of excitonic circuitry and superfluidity.

Future Plans

Fabrication of multi-exciton-contact devices for demonstration of exciton superfluidity in both continuum systems and moiré lattices.

References

Manuscript in preparation.

Correlated Quantum Materials

Michael A. McGuire, David Mandrus, Andrew F. May, Brenden Ortiz, Jiaqiang Yan

Materials Science and Technology Division

Oak Ridge National Laboratory

Keywords: Magnetism, topology, 2D and layered crystals, single crystals, transition metal compounds

Research Scope

Correlated quantum materials with collective emergent behavior, such as quantum transport, superconductivity, and exotic magnetism, are expected to form the basis for next-generation energy and information technologies. Magnetism underlies many of the most interesting emergent behaviors, and its understanding is built upon careful experimental studies of magnetic order and interactions in high-quality crystals. The overarching goal of this project is to advance our understanding of correlated quantum materials through discovery, development, and investigation of model materials that exhibit magnetic order, topological order, and collective phenomena. Specifically, we aim to understand how structure and symmetry dictate magnetism and excitations in cleavable magnetic materials, to control topological states in materials with intrinsic magnetism, and to unlock emergent correlations in materials with flat bands. These goals are addressed by synthesis of high-quality crystals and investigation of their physical properties using electrical and thermal transport, specific heat, magnetization, and crystallographic measurements. The most interesting materials are pursued through collaborations involving theory, neutron scattering, angle resolved photoemission spectroscopy, and scanning tunneling microscopy. This research directly addresses the ability to control and exploit quantum mechanical behaviors targeting novel functionality, which is a priority research direction in the BES Basic Research Needs workshop report on Quantum Materials.

Recent Progress

Here we highlight progress made recently in cleavable magnetic materials and flat-band metals.

Cleavable magnetic materials. Research on cleavable van der Waals layered materials is driven by interests in the fundamental study of magnetism in low dimensions, adding functionality to novel devices, and potential applications in microelectronics and quantum information science. Fe_5GeTe_2 and related phases play key roles in this field, since they are metallic, ferromagnetic, and have magnetic ordering temperatures near room temperature. As part of our ongoing study of these complex and important 2D materials, we recently examined the effects of substituting arsenic for germanium as a route to tuning the magnetic properties without directly disturbing the magnetic sublattices [1]. Of particular interest is the sublattice of Fe1 atoms, which are closely bonded to the Ge atoms and remains magnetically disordered in Fe_5GeTe_2 to temperatures well below the

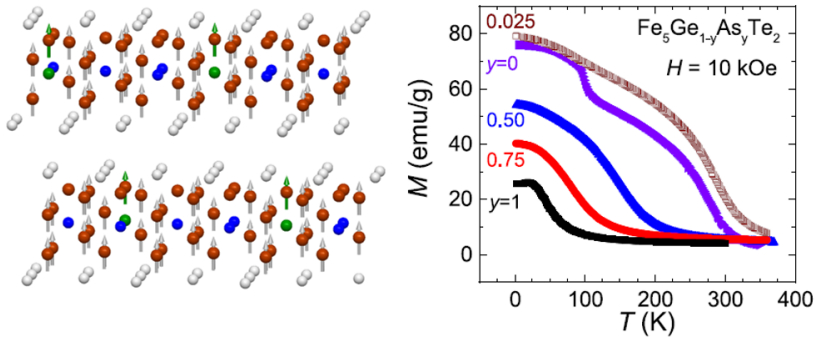

Figure 1. (left) Fe_5GeTe_2 contains magnetic Fe (dark red) slabs separated into 2D layers by Te atoms (white). (right) Magnetization measurements show that replacing increasing amounts of Ge (blue) with As (green) first strengthens the ferromagnetic alignment of the magnetic moments on Fe then pushes the compound into a competing antiferromagnetic phase.

bulk Curie temperature. This is seen in magnetization data in Figure 1 for y = 0, which shows magnetic order of most of the moments near 300 K and subsequent order of the Fe1 moments at the kink near 100 K. Tuning the crystal and electronic structure with only 2.5% As (y = 0.025 curve in Figure 1) quenches the magnetic fluctuations on the Fe1 site. As a result, the Fe1 moments order along with the other magnetic sublattices, and the Curie temperature of the compound is slightly increased. This work also led to the discovery of the new compound $Fe_{4.8}AsTe_2$, a van der Waals layered antiferromagnet with a Néel temperature of 46 K, and overall highlights the importance of chemical tuning to control the electronic and magnetic properties of these important materials.

Kagome metals and flat band systems. Continued and broad interest in kagome lattice compounds is motivated by their strongly frustrated magnetic lattice and more recently by related frustration/interference effects in their electronic properties. Over the last few years, CoSn (Figure 2) and related phases arose as model systems to study these effects and related ground states. Recently, we used the calculated electronic structure of non-magnetic CoSn to design a route to realizing a correlated ground state in this material [2]. A large peak in the density of states, associated with flat bands from the kagome lattice of Co atoms, is just below the Fermi level in CoSn. Based on simple electron counting, we used In substitution to lower the Fermi level into the flat band region and discovered the emergence of long range antiferromagnetic order in $CoSn_{1-x}In_x$ for x larger than about 0.3 (Figure 2). The Néel temperature reaches a maximum of 32 K for $x = 0.4$, the highest In content achieved in the study. Angle resolved photoemission spectroscopy confirmed that In substitution moved the Fermi level to coincide with the flat

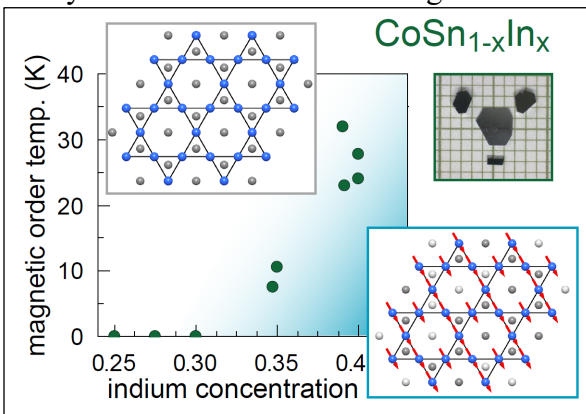

Figure 2. CoSn contains a kagome net of cobalt atoms (blue balls in upper left) that produces flat electronic bands. Replacing some of the tin with indium moves the Fermi energy into the flat bands and magnetic order emerges (lower right). Crystals grown for this study are shown on a mm grid in the upper right.

bands. This is also supported by electronic structure calculations, which showed the Fermi level in the flat band region and a fourfold increase in the density of states at the Fermi level in $CoSn_{0.67}In_{0.33}$. This was also confirmed with low temperature heat capacity measurements, which showed an increase in the Sommerfeld coefficient of more than a factor of five for $CoSn_{0.6}In_{0.4}$. Long range magnetic order was observed using neutron diffraction and magnetization measurements. The results show that the ordered moments lie in the plane of the kagome layers and give an A-type antiferromagnetic structure as the simplest model consistent with our data. This work shows a clear example of magnetism emerging from kagome flat bands in bulk crystals. Remarkably, we achieved this by substituting a non-magnetic element into a non-magnetic compound.

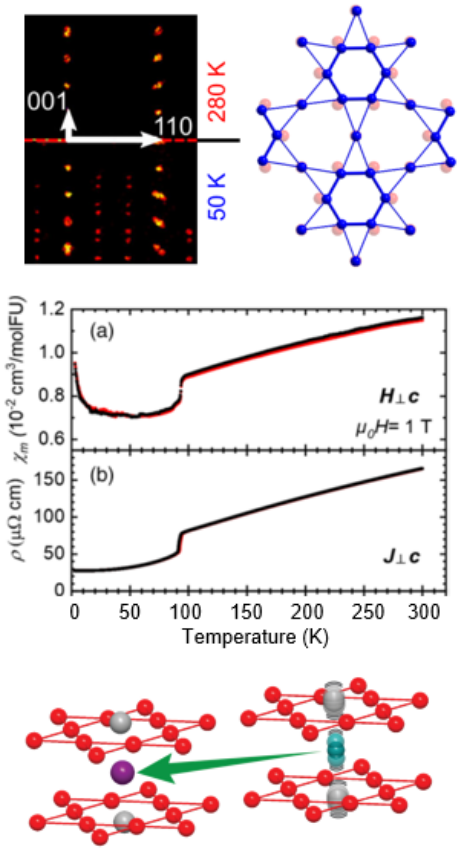

Figure 3. Evidence of a charge-density-wave-like transition in the kagome metal ScV_6Sn_6 is seen in x-ray diffraction (top), magnetic susceptibility, and resistivity (middle). An exaggerated representation of the distortion of the kagome net of V atoms that occurs at the transition is shown at the top right. (bottom) Replacing smaller Sc (blue) with a larger atom (purple) quenches rattling-like displacements and suppresses the associated structural distortion.

Other efforts on kagome materials have focused on the 166 family of compounds, and in particular ScV_6Sn_6 [3]. This is a large family of compounds structurally related to CoSn and adopting the $HfFe_6Ge_6$ structure type. We chose to study the Sc compound in part to avoid rare earth magnetism masking more subtle signatures associated with the kagome lattice. Crystals of this new compound were grown, and x-ray and neutron diffraction identified a structural phase transition below room temperature (Figure 3). The kagome net is distorted at the transition, and this is illustrated in Figure 3, in which the distortions are exaggerated to be easily seen. However, the primary atomic displacements occur out of the kagome plane and are associated with other elements in the structure. Effects of the distortion are seen in the magnetic and transport properties, shown in Figure 3. These measurements indicate a first order transition.

This phase transition has features similar to those seen in CsV_3Sb_5 and associated with a charge density wave. But very recently we have identified the driving force for the distortion to be closely related to the crystal structure itself [4]. This work also revealed an unusual correspondence between physical pressure and chemical pressure, which provides insight to understand the relationship between the crystal structure and the phase transition. Mechanical compression

(positive physical pressure) suppresses the structural transition in ScV_6Sn_6. Interestingly, we found that replacing some of the Sc with a larger element like Y (negative chemical pressure) also suppresses the transition. A careful look at the crystal structure revealed the link between these observations and the structural distortion. The structure contains chains of Sc and Sn atoms threaded through the kagome layers of V (Figure 3). The small size of Sc means the atoms in these chains are free to "rattle" along the chain direction. The freezing of these rattling motions results in the observed structural distortion at low temperature. Compressing the crystal or replacing Sc with a larger atom suppresses the rattling motion and the related low temperature distortion along with it. Identifying the underlying cause of this phase transition may help us understand similar transitions in other materials, including related kagome metal compounds.

Future Plans

Ongoing and future work on quasi-2D magnetic materials is moving toward mixed anion systems, with a particular emphasis on insulating antiferromagnets. Such systems offer a route to spintronic applications associated with magnon-driven effects, and understanding how to tune the magnetic properties is key to such future efforts to control the magnons in these materials. In the area of topological materials, we continue to study systems where magnetism and electronic topology are anticipated to be strongly intertwined. A particular emphasis is given to understanding how chemical substitutions can manipulate the magnetic order and anisotropy. This work is progressing in systems related to EuCuP, which is a member of a growing family of candidate topologically materials. For flat-band and kagome systems, we will continue to explore instabilities and emergent behaviors in $HfFe_6Ge_6$ family. Tuning the interaction strength between the kagome network can be achieved by altering bond distances, and integrating smaller atoms (e.g. silicides, borides) into the neighboring sublattices provides a means to develop wholly new systems while simultaneously tuning interaction energetics within the kagome network.

References

1. A. F. May, J. Yan, R. Hermann, M.-H. Du, and M. A. McGuire, *Tuning the room temperature ferromagnetism in Fe_5GeTe_2 by arsenic substitution*, 2D Mater. **9**, 015013 (2022). DOI 10.1088/2053-1583/ac34d9
2. B. C. Sales, W. R. Meier, D. S. Parker, L. Yin, J. Yan, A. F. May, S. Calder, A. A. Aczel, Q. Zhang, H. Li, T. Yilmaz, E. Vescovo, H. Miao, D. Moseley, R. P. Hermann, and M. A. McGuire, *Chemical control of magnetism in the kagome metal $CoSn_{1-x}In_x$: Magnetic order from nonmagnetic substitutions*, Chem. Mater. **34**, 7069 (2022). DOI 10.1021/acs.chemmater.2c01634
3. H. W. S. Arachchige, W. R. Meier, M. Marshall, T. Matsuoka, R. Xue, M. A. McGuire, R. P. Hermann, H. Cao, and D. Mandrus, *Charge Density Wave in Kagome Lattice Intermetallic ScV_6Sn_6*, Phys. Rev. Lett. **129**, 216402 (2022). DOI 10.1103/PhysRevLett.129.216402
4. W. R. Meier, R. P. Madhogaria, S. Mozaffari, M. Marshall, D. E. Graf, M. A. McGuire, H. W. S. Arachchige, C. L. Allen, J. Driver, H. Cao, and D. Mandrus, *Tiny Sc allows the chains to rattle: Impact of Lu and Y doping on the charge density wave in ScV_6Sn_6*, J. Am. Chem. Soc. accepted, arXiv:2306.07868, (2023).

Publications

This project published more than 60 papers in the last two years. Four are cited in References above and ten selected additional publications are listed here.

1. A. F. May, E. M. Clements, H. Zhang, R. P. Hermann, J. Yan, and M. A. McGuire, *Coupling of magnetism, crystal lattice, and transport in EuCuP and EuCuAs*, Phys. Rev. Mater. **7**, 064406 (2023). DOI: 10.1103/PhysRevMaterials.7.064406

2. J.-Q Yan, and M. A. McGuire, *Self-selecting vapor growth of transition metal halide single crystals*, Phys. Rev. Materials **7**, 013401 (2023). DOI: 10.1103/PhysRevMaterials.7.013401v.

3. M. A. McGuire, E. M. Clements, Q. Zhang, and S. Okamoto, *Double-Layer Kagome Metals Pt_3Tl_2 and Pt_3In_2*, Crystals **13**, 833 (2023). DOI: 10.3390/cryst13050833

4. T. Zhang, T. Yilmaz, E. Vescovo, H. X. Li, R. G. Moore, H. N. Lee, H. Miao, S. Murakami, and M. A. McGuire, *Endless Dirac nodal lines in kagome-metal $Ni_3In_2S_2$*, NPJ Computat. Mater. **8**, 155 (2022). DOI: 10.1038/s41524-022-00838-z

5. R. G. Moore, S. Okamoto, H. Li, W. R. Meier, H. Miao, H. N. Lee, M. Hashimoto, D. Lu, E. Dagotto, M. A. McGuire, and B. C. Sales, *Topological electronic structure evolution with symmetry-breaking spin reorientation in $(Fe_{1-x}Co_x)Sn$*, Phys. Rev. B **106**, 115141 (2022). DOI: 10.1103/PhysRevB.106.115141

6. H. Chen, S. Asif, M. Whalen, J. Tamara-Isaza, B. Luetke, Y. Wang, X. Wang, M. Ayako, S. Lamsal, A. F. May, M. A. McGuire, C. Chakraborty, J. Q. Xiao, and M. J. H. Ku, *Revealing room temperature ferromagnetism in exfoliated Fe_5GeTe_2 flakes with quantum magnetic imaging*, 2D Mater. **9**, 025017 (2022). DOI: 10.1088/2053-1583/ac57a9

7. Xun Li, Seung-Hwan Do, Jiaqiang Yan, Michael A McGuire, Garrett E Granroth, Sai Mu, Tom Berlijn, Valentino R Cooper, Andrew D Christianson, and Lucas Lindsay, *Phonons and phase symmetries in bulk $CrCl_3$ from scattering measurements and theory*, Acta Mater. **241**, 118390 (2022). DOI: 10.1016/j.actamat.2022.118390.

8. S. Gao, M. A. McGuire, Y. Liu, D. L. Abernathy, C. dela Cruz, M. Frontzek, M. B. Stone, and A. D. Christianson, *Spiral spin liquid on a honeycomb lattice*, Phys. Rev. Lett. **128**, 227201 (2022). DOI: 10.1103/PhysRevLett.128.227201

9. M. E. Manley, A. F. May, B. L. Winn, D. L. Abernathy, R. Sahul, and R. P. Hermann, *Phason-Dominated Thermal Transport in Fresnoite*, Phys. Rev. Lett. **129**, 255901 (2022). DOI: 10.1103/PhysRevLett.129.255901

10. W. R. Meier, J. R. Torres, R. P. Hermann, J. Zhao, B. Lavina, B. C. Sales, and A. F. May, *Thermodynamic insights into the intricate magnetic phase diagram of $EuAl_4$*, Phys. Rev. B 106, 094421 (2022). Editors' Suggestion. DOI 10.1103/PhysRevB.106.094421

Tuning magnetic topological insulators using defects

D. C. Johnston, L. Ke, R. J. McQueeney, P. P. Orth, B. G. Ueland, D. Vaknin
Ames National Laboratory and Iowa State University, Ames, Iowa 50011

Keywords: magnetism, topological materials, single crystals, polycrystalline materials, neutron scattering

Research Scope

Magnetic quantum materials promise to deliver new functionalities based on phenomena such as topological and spin-polarized transport, quantum-critical behavior, and unconventional superconductivity. Magnetism not only lies at the root of many of these fundamental phenomena, but it also provides a unique way to directly manipulate electronic charge carriers by controlling magnetic phases and excitations. We approach the overarching challenge to understand and exploit the close relationship between electronic charge and spin degrees-of-freedom in quantum materials by focusing on two research thrusts: (1) *flat electronic bands in itinerant magnets* which offer great tunability due to the proximity between various correlation-driven quantum phases; and (2) *magnetism in topological materials* where the magnetism controls the emergence of unique topologically-protected optical and transport phenomena. These thrusts share common challenges to understand fundamental issues of magnetism, including the development of itinerant magnetism, magnetic frustration, and the coupling between local moments and charge carriers. Our comprehensive research program combines the synthesis and discovery of novel magnetic quantum materials, the experimental characterization of their structural, magnetic, thermal, and electronic-transport properties, the determination of magnetic structure and excitations using neutron scattering techniques, and theoretical approaches that employ first-principles electronic-structure calculations, mean-field and linear spin-wave theory, atomistic spin-dynamics simulations, and analytical methods.

Recent Progress

In this meeting, we will present our recent progress in Thrust 2 that focuses on understanding magnetic phenomena in topological insulators. Our main result is that magnetic defects introduce competing ferromagnetic (FM) and antiferromagnetic (AFM) interactions in both dilute and intrinsic magnetic topological insulators. This competition can limit the effectiveness of how magnetic order couples to charge carriers, but it also provides a route for modifying the magnetic ground state through defect control.

Topological insulators (TIs) host Dirac-like surface electronic bands that are protected by time-reversal symmetry. The introduction of long-range magnetic order breaks time-reversal symmetry and generates a two-dimensional Chern insulator where gapped Dirac bands host dissipationless and spin-momentum locked edge states. A key experimental signature of a Chern insulator is the quantum anomalous Hall effect (QAHE).

One successful materials route develops magnetic TIs by introducing FM long-range order via the substitution of dilute concentrations of magnetic ions (such as Cr and V) into known TIs in the Bi_2Se_3 family. This has led to observation of the QAHE, although limited to temperatures well below the FM ordering temperature (T_C). The random nature of magnetic substitution and associated magnetic inhomogeneities has been hypothesized to introduce fundamental limitations to the onset-temperature of the QAHE. However, the magnetic interactions in the dilute case and why the QAHE is suppressed still remain poorly understood. One may even question how long-range magnetic interactions, necessary for FM order in dilute systems, can be mediated without a high density of conduction electrons.

To address these questions, we have synthesized single-crystal and polycrystalline samples of Mn-substituted magnetic TIs in the Bi_2Te_3 and SnTe families for detailed experimental studies. Magnetization, transport, x-ray diffraction, transmission electron microscopy, and wavelength-dispersive spectroscopy measurements are all consistent with randomly substituted Mn ions at the targeted concentrations.

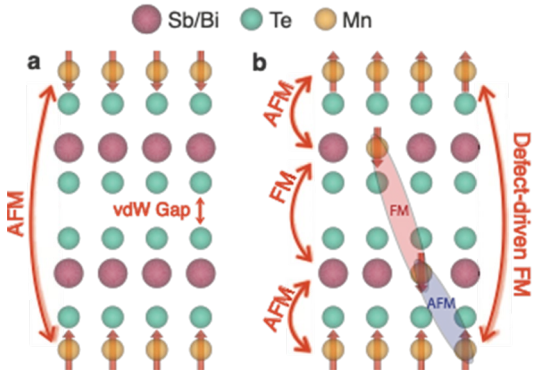

Figure. (a) Interlayer magnetic interactions in pristine antiferromagnetic $MnBi_2Te_4$. (b) New interlayer magnetic interactions in the presence of anti-site magnetic defects (colored ellipses) generate magnetic phase competition.

For low Mn concentrations that do not support long-range FM order, inelastic neutron scattering measurements on $(Sb_{0.97}Mn_{0.03})_2Te_3$ and $(Sn_{0.95}Mn_{0.05})Te$ reveal competing FM and AFM exchange interactions [1,2]. In both materials, strong AFM exchange leads to the formation of Mn-Mn spin dimers with a singlet ground state. The dimers are easily identified by their characteristic magnetic excitation spectrum. More detailed analysis of the momentum dependence of the scattering indicates that the dimers are formed via linear Mn-Te-Mn bonds among next-nearest-neighbor Mn ions, consistent with the Goodenough-Kanamori superexchange rule. In both materials, short-ranged and quasielastic FM spin correlations are observed, as expected for a paramagnetic fluctuations that occur close to FM order. The energy scale of these FM interactions are much smaller than the AFM dimer exchange. First-principles calculations were conducted to investigate the pairwise Mn-Mn magnetic interactions in various defect configurations for both materials, revealing the miscroscopic origin of the mangetic interaction as well as validating and enhancing the experimental data interpretation. In $(Sb_{0.97}Mn_{0.03})_2Te_3$, by combining experiments and calculations, we identify that the exchange pathways responsible for the key FM interactions occur within the Sb/Mn layers and across the van der Waals gap between Sb_2Te_3 layers.

Our most recent studies are investigating the magnetic excitations in single-crystals and powders of $(Sn_{0.9}Mn_{0.1})Te$ at higher Mn concentrations where long-range FM ordering occurs at $T_C = 12$ K. Two key observations are; (1) a FM resonance mode is observed that is associated the long-range

FM order, and (2) the AFM dimers persist in the FM-ordered state. Based on these results, we propose a two-component model for the magnetism, where strongly bound AFM dimer singlets interact weakly with a random framework of Mn spins that order via long-range magnetic interactions. This scenario outlines serious limitations in the development of robust FM order in dilute magnetic TIs.

These limitations have motivated the search for intrinsic magnetic TIs without substitutional disorder, leading to the discovery of the $MnBi_2Te_4$ family of AFM-TIs where quantized Hall conduction has been observed in applied magnetic fields. Also, the AFM order allows optical and electrodynamic responses to be augmented by topological magnetoelectric (axion) coupling. We have discovered long-range and competing magnetic interactions in the AFM-TI $MnBi_2Te_4$ using inelastic neutron scattering [3,4]. By employing a linear response method and incorporating the effects of electron correlations within Mn-3*d* electrons, we have calculated the dynamical transverse spin susceptibility and found it compares well with the measured spin-excitation spectra in $MnBi_2Te_4$. Through joint analysis of neutron and magnetization data, we find complex sources of magnetic anisotropy which include both single-ion anisotropy and anisotropic exchange. Since anisotropy significantly affects the magnetic ordering and, consequently, the material's symmetry, this information is relevant for understanding the development of topological axion and Chern phases in bulk and thin-film $MnBi_2Te_4$ in applied magnetic fields.

The intrinsic magnetic TIs are subject to chemical disorder in the form of anti-site mixing between Mn and Bi/Sb layers. The resultant magnetic defects have a strong AFM coupling to the main Mn layer (see Figure) leading to defect-induced ferrimagnetism with a compensated net magnetization. We found evidence for magnetic defect modes in $MnSb_2Te_4$ using inelastic neutron scattering and are able to characterize the nature of this coupling [5]. Surprisingly, the defect-induced FM and AFM interactions are the same as those found in the dilute Mn-doped Sb_2Te_3 materials [1,3] which establishes universal and transferable magnetic interactions within the broader family of Sb_2Te_3-$MnSb_2Te_4$ magnetic TIs (see Figure).

In summary, we have discovered that the magnetic interactions in what seem to be two distinct magnetic TI families, dilute and intrinsic, are closely related and can be understood within a unified picture. Morever, this research program has established that the magnetic ground states in magnetic **TIs can be controlled by magnetic defects.**

Future Plans

In the context of dilute magnetic TIs, there are two outstanding issues that we will address. The first is to obtain a better understanding of the long-range magnetic interactions that are responsible for FM order. We have evidence for collective FM magnon-like excitations in single crystals of Mn-doped SnTe. Analysis of these data will provide evidence neede to establish the range and strength of the pairwise magnetic interactions. The second issue concerns the generalization of these results to Cr- or V-doped dilute magnetic TIs, where the QAHE has been experimentally

observed. We hypothesize that singlet dimer formation will be found in all of these materials, and so we will pursue single crystal growth, characterization, and neutron-scattering experiments to prove this hypothesis. These experiments will be performed in parallel with first-principles calculations. A systematic *ab-initio* investigation of how magnetic interactions evolve with the continuous filling of 3d orbitals as dopants go from V to Mn can help determine the orbital pathways of magnetic interactions. More generally, our results demonstrate how the combined power of modern neutron sources and ab-initio electronic structure calculations enable a detailed understanding of dilute magnetic systems and we are currently planning to study the role of magnetic defects in other quantum materials.

For the intrinsic magnetic TIs, we are analyzing inelastic neutron scattering data on $MnSb_2Te_4$ single crystals where the magnetic spectrum is dominated by antisite Mn defects. These data can provide information about the interaction strength and range of defect-induced interactions, but their analysis requires numerical spin-dynamics simulations that account for chemical disorder. We are also studying the magnetic excitations in the $MnBi_4Te_7$ member, which is a magnetic TI with a large non-magnetic Bi_2Te_3 block that separates magnetic $MnBi_2Te_4$ layer blocks. Such "bulk-2D" systems provide a unique platform to explore the dimensional crossover of magnetism using inelastic neutron scattering, which is unparalleled in probing magnetic interactions in bulk systems.

References

1. Farhan Islam, Yongbin Lee, Daniel M. Pajerowski, JinSu Oh, Wei Tian, Lin Zhou, Jiaqiang Yan, Liqin Ke, Robert J. McQueeney, and David Vaknin, *Role of Magnetic Defects in Tuning Ground States of Magnetic Topological Insulators*, Adv. Mater. **25**, 2209951 (2023).

2. D. Vaknin, Santanu Pakhira, D. Schlagel, F. Islam, Jianhua Zhang, D. M. Pajerowski, C. Z. Wang, D. C. Johnston, and R. J. McQueeney, *Localized singlets and ferromagnetic fluctuations in the magnetic topological insulator* $Sn_{0.95}Mn_{0.05}Te$, Phys. Rev. B **101**, 140406(R) (2020).

3. Bing Li, D. M. Pajerowski, S. X. M. Riberolles, Liqin Ke, J.-Q. Yan, and R. J. McQueeney, *Quasi-two-dimensional ferromagnetism and anisotropic interlayer couplings in the magnetic topological insulator* $MnBi_2Te_4$, Phys. Rev. B **104***,* L220402 (2021).

4. Bing Li, J.-Q. Yan, D. M. Pajerowski, Elijah Gordon, A.-M. Nedić, Y. Sizyuk, Liqin Ke, P. P. Orth, D. Vaknin, and R. J. McQueeney, *Competing magnetic interactions in the antiferromagnetic topological insulator* $MnBi_2Te_4$*,* Phys. Rev. Lett. **124**, 167204 (2020).

5. S. X. M. Riberolles, Q. Zhang, Elija Gordon, N. P. Butch, Liqin Ke, J.-Q. Yan, and R. J. McQueeney, *Evolution of magnetic interactions in Sb-substituted* $MnBi_2Te_4$*,* Phys. Rev. B **104**, 064401 (2021).

Publications

1. Y. Lee, R. Skomski, X. Wang, P. P. Orth, Y. Ren, Byungkyun Kang, A. K. Pathak, A. Kutepov, B. N. Harmon, R. J. McQueeney, I. I. Mazin, and Liqin Ke, *Interplay between magnetism and band topology in Kagome magnets RMn_6Sn_6*, Phys. Rev. B **108**, 045132 (2023).

2. S. X. M. Riberolles, Tyler J. Slade R. L. Dally, P. M. Sarte, Bing Li, Tianxiong Han, H. Lane, C. Stock, H. Bhandari, N.J. Ghimire, D. L. Abernathy, P. C. Canfield, J. W. Lynn, B. G. Ueland, and R. J. McQueeney, *Orbital character of the spin-reorientation transition in $TbMn_6Sn_6$*, Nat. Commun. **14**, 2658 (2023).

3. Farhan Islam, Yongbin Lee, Daniel M. Pajerowski, JinSu Oh, Wei Tian, Lin Zhou, Jiaqiang Yan, Liqin Ke, Robert J. McQueeney, and David Vaknin, *Role of Magnetic Defects in Tuning Ground States of Magnetic Topological Insulators*, Adv. Mater. **25**, 2209951 (2023).

4. S. X. M. Riberolles, Tyler J. Slade, D. L. Abernathy, G. E. Granroth, Bing Li, Y. Lee, P. C. Canfield, B. G. Ueland, Liqin Ke, and R. J. McQueeney, *Low-Temperature Competing Magnetic Energy Scales in the Topological Ferrimagnet $TbMn_6Sn_6$*, Phys. Rev. X **12**, 021043 (2022).

5. Santanu Pakhira, Farhan Islam, Evan O'Leary, M.A. Tanator, Thomas Heitmann, Lin-Lin Wang, R. Prozorov, Adam Kaminski, David Vaknin, and D. C. Johnston, *A-type antiferromagnetic order in semiconducting $EuMg_2Sb_2$ single crystals*, Phys. Rev. B **106** 024418 (2022).

6. B. G. Ueland, Santanu Pakhira, Bing Li, A. Sapkota, N.S. Sangeetha, T. G. Perring, Y. Lee, Liqin Ke, D. C. Johnston, and R. J. McQueeney, *Carrier Tuning of Stoner ferromagnetism in $ThCr_2Si_2$-Type Cobalt Arsenides*, Phys. Rev. B **104**, L220410 (2021).

7. Bing Li, D. M. Pajerowski, S. X. M. Riberolles, Liqin Ke, J.-Q. Yan, and R. J. McQueeney, *Quasi-two-dimensional ferromagnetism and anisotropic interlayer couplings in the magnetic topological insulator $MnBi_2Te_4$*, Phys. Rev. B **104**, L220402 (2021).

8. S. X. M. Riberolles, Q. Zhang, Elijah Gordon, N. P. Butch, Liqin Ke, J.-Q. Yan, and R. J. McQueeney, *Evolution of magnetic interactions in Sb-substituted $MnBi_2Te_4$,* Phys. Rev. B **104**, 064401 (2021).

9. N.S. Sangeetha, Santanu Pakhira, Qing-Ping Ding, Lennard Krause, Hyung-Cheol Lee, Volodymyr Smetana, Anja-Verena Mudring, Bo Brummerstedt Iversen, Yuji Furukawa, and David C. Johnston, *First-order antiferromagnetic transitions of $SrMn_2P_2$ and $CaMn_2P_2$ single crystals containing corrugated-honeycomb Mn sublattices*, Proc. Nat. Acad. Sci. **118** e2108724118 (2021).

10. Santanu Pakhira, M.A. Tanatar, Thomas. Heitmann, David Vaknin, and D. C. Johnston, *A-type antiferromagnetic order and magnetic phase diagram of the trigonal Eu spin-7/2 triangular-lattice compound $EuSn_2As_2$*, Phys. Rev. B **104**, 174427 (2021).

Program Title: Dynamics and Driven States in Quantum Magnets

Principal Investigator: Thomas F. Rosenbaum, California Institute of Technology

Keywords: Magnetism, Single Crystals, Ferro/Antiferromagnets, Magnetic Susceptibility, Quantum Coherence

Research Scope

The order-disorder transition at a quantum phase transition intertwines the static and dynamical response of the material changing state, introducing new universality classes, amplifying the effects of disorder, and etching in high relief the role of quantum fluctuations. There are ample questions remaining about the character of such transitions and the nature of the competing quantum states. There are also opportunities to drive quantum materials out of equilibrium, with the possibility of new types of correlated and coherent order, and new ways to access the dynamical evolution of ground and excited states. We seek here to probe the critical modes at a quantum phase transition in both pure and disordered magnets, to quench the systems across their quantum critical points to reveal the means by which order grows, and to characterize avalanche domain wall dynamics in ferromagnets in the quantum tunneling regime. Moreover, by tuning the disorder and the quantum tunneling probability, it should be possible to study the competition between quantum entanglement and random field effects. We hope to elucidate the fundamental quantum physics as well as addressing the question of how best to use complex systems, such as magnetic solids with electronic and nuclear spin degrees of freedom, to process quantum information.

Recent Progress

(A) Quantum Barkhausen Noise. Although magnetism at the microscopic scale has been understood as a quantum phenomenon for nearly a century, macroscopic magnetic objects like domain walls are usually treated classically. There is good reason for this: in a conductor, the dissipative coupling to electrons rapidly suppresses domain wall tunneling, and even in an insulator, the coupling to phonons, paramagnetic impurities, and nuclear spins is enough to render the wall motion classical, except at microscopic scales. These mechanisms also suppress “chiral tunneling” between opposite chiralities for a given wall; for a Bloch wall, the chirality is simply the sense in which the magnetization winds in passing between the states on either side of the wall.

It is difficult to observe the dynamics of individual domain walls except in restricted geometries. More typically, one sees evidence of collective motion, either by imaging walls before and after this motion has occurred, or by measurements of the dynamic susceptibility or of the Barkhausen noise in the bulk magnet. The latter shows up in inductive measurements, arising from rapid jumps in the magnetization caused by the depinning of walls and their subsequent motion. Since the discovery of Barkhausen noise in 1919, a vast corpus of experimental work has accumulated, characterizing the influence on the noise of disorder, different magnetic interactions, and the proximity to phase transitions. However, all of this work has been done on thermally-activated wall motion – there have been no investigations of quantum Barkhausen noise, in which domain wall tunneling, rather than thermal excitation over barriers, dominates.

Our present work explores the quantum regime. Just as in the classical regime, inter-wall interactions, mediated by dipolar interactions, lead to collective wall dynamics and avalanche processes under the right conditions.

The choice of the right experimental system is critical. The domain wall structure needs to be simple and, to see quantum behavior, the crossover between classical thermal activation and quantum tunneling needs to be at sufficiently high temperature. An ideal system is the Ising magnet, $LiHo_xY_{1-x}F_4$, which has atomically sharp domain walls with uniaxial spin symmetry and in which strong crystal fields give an effective ground state doublet separated from the first excited state by a gap of 9.4 K. Moreover, the application of a transverse field introduces tunable quantum tunneling and random field pinning in the presence of disorder.

We plot in Fig. 1 two-dimensional histograms of Barkhausen event duration and area for temperatures at 15% and 95% of the Curie temperature (90 mK and 580 mK). The Barkhausen events we analyze correspond to changes in the magnetization of the largest and most strongly-pinned domains. The events separate into two distinguishable classes at low fields: one class that we label as "independent" that approximately spans a power-law with an exponent of ≈ 1.1 (close to the power of 1 indicative of avalanches) over approximately one decade of duration, and the second that we designate "cooperative" (highlighted by the red oval in Fig. 1a) that appears as an approximately Gaussian cluster over a more limited range of durations with higher areas for any given duration than events in the "independent" class. Furthermore, while the frequency of the "independent" events decreases only modestly with transverse field, the "cooperative" events are suppressed almost completely with a 200 Oe transverse field. We have plotted one sample event in each class in Fig. 1b, both marked by arrows on the 2D histograms in Fig. 1a, with the "cooperative" event in red and the "independent" event in orange.

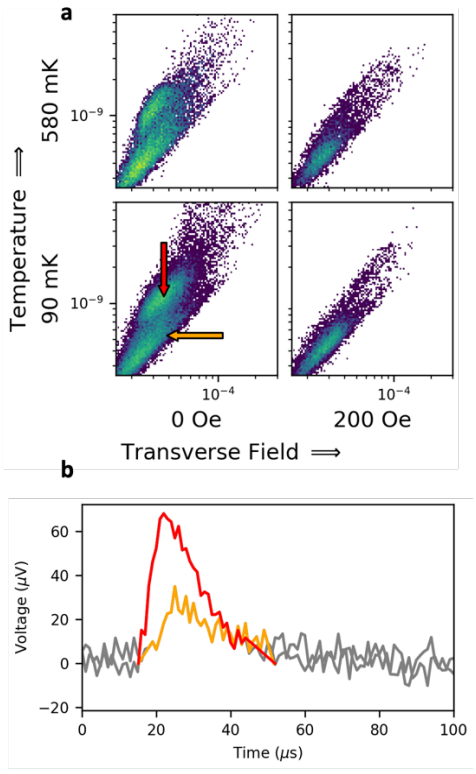

Fig. 1: Classes of events. **a** 2D histograms of event area (y-axis, V·sec) vs event duration (x-axis, sec) for low/high temperatures and transverse fields. **b** Sample events of each class: "independent" event in orange, and "cooperative" event in red as indicated by the colored arrows in **a**.

The event statistics show the same temperature independence, demonstrating that within these experimental parameters, the sample is deep within the quantum regime, where the dynamics are governed by quantum tunneling, rather than thermal activation, of spins. Given that both activation mechanisms are due to quantum tunneling (rather than one being quantum and the other thermal), it is not immediately obvious how there could be two different tunneling mechanisms, why they would have such dramatically different transverse field dependence, or how such a small 200 Oe field could suppress markedly either class of events.

Given this challenge, we have gone beyond the theoretical picture of a single independent wall tunneling and consider the interaction between walls. In so doing, we recover a phenomenological model, illustrated in Fig. 2, in which the two different activation mechanisms correspond, on one hand, to walls tunneling independently of each other and, on the other, to cooperative tunneling of pairs of walls. Co-tunneling of domain walls is strongly affected by the application of an external transverse field much smaller than the fields required to induce single-spin tunneling.

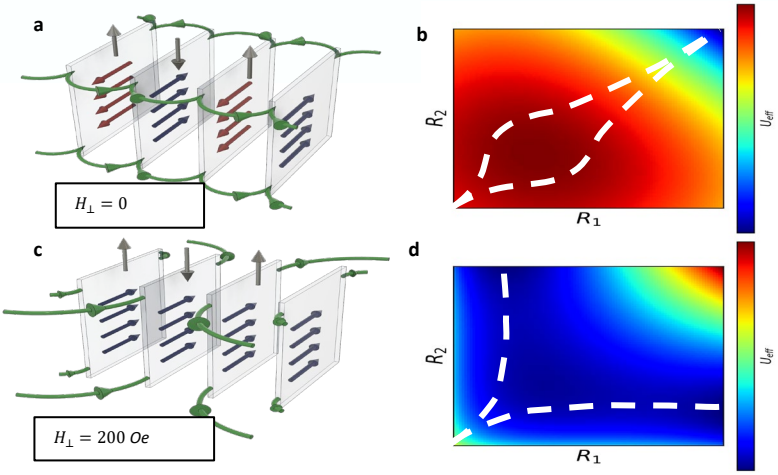

Fig. 2: Domain wall configurations (**a,c**) with corresponding interaction potentials (**b,d**). Vertical grey arrows designate bulk magnetization direction within a domain along the Ising axis, while the red/blue arrows designate the transverse polarizations within a Bloch wall. The green curved arrows designate the demagnetization fields. The tunneling potentials are a function of the radii of the two interacting plaquettes, R_1 and R_2, which interact through the dipolar interaction. **a** shows staggered polarizations of the domain walls at zero transverse field with corresponding attractive interaction in **b** causing R_1 and R_2 to grow together (as indicated by the tunneling paths shown in white). **c** shows all walls polarized in the same direction due to the transverse field, with corresponding repulsive interaction in **d**, causing plaquettes to grow independently from one another (as indicated by the tunneling paths shown in white).

Our work (Publication 1), venturing into the quantum regime, suggests that similar quantum effects should be observable in other systems where long-range interactions between microscopic degrees of freedom can cause correlated activation of macroscopic avalanches.

(B) Quantum Interference from Superposed Lattices. We have explored Shubnikov-de Haas (SdH) quantum oscillations of elemental Chromium in the spin density wave (SDW) ground state, with the motivation to work outside of the paradigm of three- (and two-) dimensional band structure. The electronic structure in the SDW state of Cr is determined by two sets of superposed reciprocal lattices – the lattice and the antiferromagnetic order. The incommensurate relationship between the two sets of lattices leads to a fractal-like electronic band structure in the 3D space. As the SDW state is a result of electron correlation, the precise band structure relies on gaps opening in the Fermi surface, which cannot be precisely calculated theoretically or computationally. This research thus relies heavily on both experimental exploration and qualitative theoretical considerations.

Our discovery reveals that phases of SdH oscillations can be of opposite sign (or equivalently, a pi-phase shift) when the current is running perpendicular versus parallel to the wave vector of the superlattice structure. This opposite phase behavior is contrasted by the same phase behavior of normal SdH orbits observed in both resistivity and conductivity channels. We deduce that this opposite phase behavior happens only for orbits built from both sets of reciprocal lattices and is attributed to quantum interference effects. This opposite phase behavior cannot be explained by either conventional SdH behavior or Berry phase arguments for Dirac orbits. Rather, we present (Publication 2) a qualitative model, including both elements of incoherent semi-classical transport and coherent quantum oscillations, to explain this new type of quantum transport phenomenon. Importantly, we believe that the underlying mechanism involving open and closed orbits on the Fermi surface can be engineered for many different materials of quantum and topological interest.

Future Plans

1. The avalanche domain wall dynamics that we measure (Publication 1) involve domains consisting ~10^{15} spins. Cryogenic amplifiers do not permit greater sensitivity. We hope to extend our Barkhausen noise measurements to capture tunneling of the smaller domains that constitutes most of the ferromagnetic hysteresis loop by developing appropriate SQUID amplifier techniques.

2. We propose to investigate the effects of disorder on the quantum phase transition in the Ising magnet in transverse field, $LiHo_xY_{1-x}F_4$. The critical exponents and scaling of the critical field in the quantum limit are different in the presence of disorder due to the introduction of local random fields. We plan to employ microwave spectroscopy to reveal the nature of the soft mode at the quantum phase transition as well as the critical excitations with increasing amounts of disorder. We recently detected the electronuclear soft mode in the pure system using microwave spectroscopy (Publication 5). It is unlikely to survive, but how and how much disorder, as represented by the random substitution of non-magnetic Yttrium for magnetic Holmium, is necessary to suppress the divergence is unknown.

3. The ability of a longitudinal magnetic field to permit soft mode absorption at finite frequency at the quantum phase transition (Publication 5) should open the door to quantum quench experiments, where we expect a microwave field to be able to tune the critical transverse field that separates paramagnet from quantum ferromagnet. A quantum quench is the rapid tuning of a quantum parameter, such as magnetic field, that drives a material out of equilibrium and creates excitations, e.g., quasiparticles, vortices, and magnetic domain walls. An area of particular focus and potential impact involves measuring quenches across a phase transition, which is believed to give rise to universal behavior irrespective of microscopic material details. The Kibble-Zurek effect predicts that the density of excitations created during a quench scales as a power-law that depends on the critical exponents associated with the phase transition and the dimensionality. We will test these predictions in the model quantum ferromagnet, $LiHo_xY_{1-x}F_4$, with varying amounts of disorder.

Publications

1. "Quantum Barkhausen Noise Induced by Domain Wall Co-Tunneling," C. Simon, D.M. Silevitch, P.C.E. Stamp, and T.F. Rosenbaum, manuscript submitted.
2. "Quantum Interference in Superposed Lattices," Y. Feng, Y. Wang, T.F. Rosenbaum, P.B. Littlewood, and H. Chen, manuscript submitted.

3. “Theory of Magnon Polaritons in Quantum Ising Materials,” R.D. McKenzie, M. Libersky, D.M. Silevitch, and T.F. Rosenbaum, Phys. Rev. A **106**, 043716 (2022).
4. “Discovery of Quantum Phases in the Shastry-Sutherland Compound $SrCu_2(BO_3)_2$ under Extreme Conditions of Field and Pressure,” Z. Shi, S. Dissanayake, P. Corboz, W. Steinhardt, D. Graf, D.M. Silevitch, H.A. Dabkowska, T.F. Rosenbaum, F. Mila, and S. Haravifard, Nature Commun. **13**, 2301 (2022).
DOI: 10.1038/s41467-022-30036-w.
5. “Direct Observation of Electronuclear Modes about a Quantum Critical Point,” M. Libersky, R.D. McKenzie, D.M. Silevitch, P.C.E. Stamp, and T.F. Rosenbaum, Phys. Rev. Lett. **127**, 207202 (2021).

Berry curvature engineering in superconductors

Badih Antoine Assaf, Yi-Ting Hsu, Xiaolong Liu, Xinyu Liu,

Keywords: Superconductivity, magnetotransport, molecular beam epitaxy, scanning tunneling microscopy.

Research Scope

This project aims to identify and tune experimental signatures of Berry curvature and inversion symmetry breaking (ISB) in superconductors. ISB is induced and tuned following three strategies: (i) by chemically tuning a ferroelectric distortion in $Ge_{1-x}In_xTe$, (ii) by varying the thickness of $NbSe_2$, (iii) by synthesizing interfaces of superconductors and semiconductors that host Rashba splitting. Signatures of Berry curvatures and ISB that we seek to identify include the anomalous Nernst effect, particle-hole asymmetry in the differential conductance, and tunneling evidence of mixed (s,p)-wave pairing.

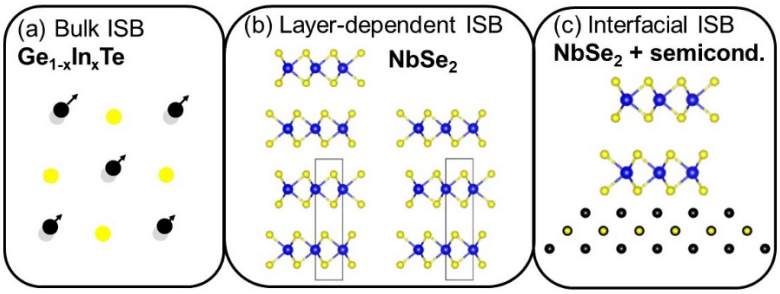

Figure 1. Proposed methods to tune ISB in 3D $Ge_{1-x}In_xTe$ and 2D $NbSe_2$

Recent Progress

GeTe and SnTe are known crystallize in a distorted rocksalt structure, which causes intrinsic ISB in the bulk. They are ideal to search for superconductivity with ISB, since alloying them with InTe, yields superconductivity with T_c exceeding 1.5K. But, alloying SnTe with InTe was seen to suppress the crystalline distortion, restoring a pristine cubic rocksalt structure. [1,2] We show potential evidence that ISB is more robust in thin films, and could coexist with superconductivity.

We find preliminary evidence of an enhanced upper critical field in thin $Sn_{0.7}In_{0.3}Te$ films grown by MBE. Despite prior knowledge that 100nm-$Sn_{0.7}In_{0.3}Te$ has a cubic crystal structure that has inversion symmetry and $H_{c2}<2T$, we find that in 8nm-$Sn_{0.7}In_{0.3}Te$, $H_{c2}>3T$ at 2K (Fig. 2(a,b) when the field is applied in the film plane. The extrapolation of the H_{c2} versus temperature to T=0, yields a large $H_{c2}(0)$ exceeding the Pauli limit (inset of Fig. 2(b)). This is not the case for 100nm films, grown under the same conditions, on the same substrate Fig. 2(c). We are carrying out additional measurements below 1K to determine if $H_{c2}(T\rightarrow0)$ indeed exceeds the Pauli limit. This thickness dependence of H_{c2} could be a consequence of inversion symmetry breaking caused by the substrate (Fig. 1(c)). It can also be due to intrinsic spontaneous ISB (Fig. 1(a)), stabilized in thin films, as

seen in prior studies of SnTe. [3] Scanning tunneling microscopy will further allow us to image the sample surface and search for evidence of the distorted rocksalt structure.

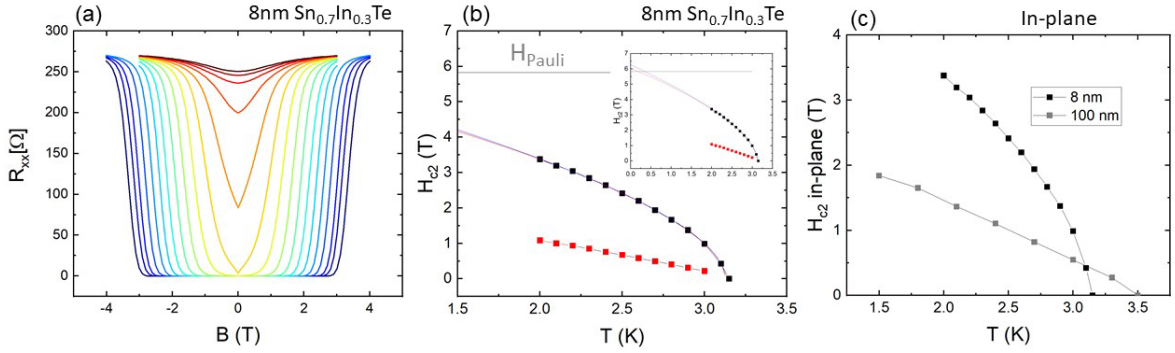

Figure 2. (a) Resistance versus magnetic field of an 8nm $Sn_{0.7}In_{0.3}Te$ film. (b) H_{c2} versus T extracting from the data shown in (a). Red: field applied out-of-plane. Black: field applied in-plane. The thin solid line is a fit using $Hc_2(T) = Hc_2(0)\left(1-\frac{T}{T_c}\right)^{\gamma}$. The grey represents the Pauli limit $1.85T_c$. (c) In-plane upper critical as a function of temperature for the 8nm film compared to a 100nm film from [1]

The low temperature scanning tunneling microscopy and spectroscopy system to be used has been in operation and good working order. As shown in Fig. 3, we have been able to prepare and visualize at the atomic scale a variety of materials including $FeSe_{0.45}Te_{0.55}$, FeSe, UTe_2, CsV_3Sb_5, and Cu(111), as well as clear signatures of quasiparticle interference. The next challenge that we will tackle, is the successful transfer of films grown in MBE for this project, into the STM.

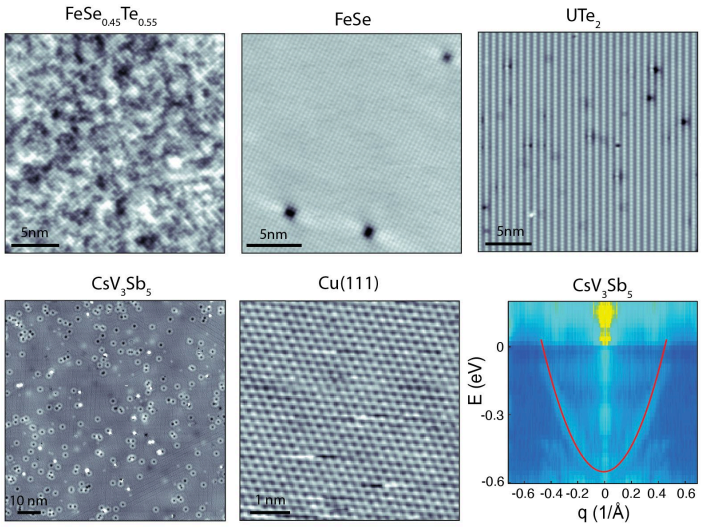

Figure 3. A series of atomically resolved surfaces of $FeSe_{0.45}Te_{0.55}$, FeSe, UTe_2, CsV_3Sb_5, and Cu(111) using low temperature scanning tunneling microscopy. The bottom right panel demonstrates clear extraction of the electron-like Sb pocket dispersion in CsV_3Sb_5 through quasiparticle interference imaging.

Future Plans

The findings on thin (Sn,In)Te motivate using this material to develop a device that we will use to measure the Nernst effect in the superconducting state and to search for signatures of particle-hole asymmetry in the different conductance using scanning tunneling spectroscopy, in the presence of ISB. A theoretical formalism of the Nernst effect caused by Berry curvature in ISB superconductors is also being developed. In parallel we will develop the synthesis of (Ge,In)Te, where the ferroelectric distortion is chemically tunable and expected to survive in the superconducting phase [4].

References

[1] J. Wang, W. Powers, Z. Zhang, M. Smith, B. J. McIntosh, S. K. Bac, L. Riney, M. Zhukovskyi, T. Orlova, L. P. Rokhinson, Y.-T. Hsu, X. Liu, and B. A. Assaf, *Observation of Coexisting Weak Localization and Superconducting Fluctuations in Strained $Sn_{1-x}In_xTe$ Thin Films*, Nano Lett **22**, 792 (2022).

[2] A. S. Erickson, J.-H. Chu, M. F. Toney, T. H. Geballe, and I. R. Fisher, *Enhanced Superconducting Pairing Interaction in Indium-Doped Tin Telluride*, Phys Rev B **79**, 024520 (2009).

[3] K. Chang, L. Junwei, L. Haicheng, N. Wang, K. Zhao, A. Zhang, F. Jin, Y. Zhong, X. Hu, W. Duan, Q. Zhang, L. Fu, Q.-K. Xue, X. Chen, and S.-H. Ji, *Discovery of Robust In-Plane Ferroelectricity in Atomic-Thick SnTe*, Science **353**, 274 (2016).

[4] M. Kriener, M. Sakano, M. Kamitani, M. S. Bahramy, R. Yukawa, K. Horiba, H. Kumigashira, K. Ishizaka, Y. Tokura, and Y. Taguchi, *Evolution of Electronic States and Emergence of Superconductivity in the Polar Semiconductor GeTe by Doping Valence-Skipping Indium*, Phys Rev Lett **124**, 047002 (2020).

Publications

None while SUPPORTED BY BES here.

Synthesis and Characterization of 2D Weyl Semimetals in Epitaxial Bismuthene

Guang Bian, University of Missouri

Keywords:

topology-quantum Hall, thin film heterostructures, topological materials, ARPES, molecular beam epitaxy

Research Scope

2D Weyl semimetal is a topological matter with topologically protected boundary states-Fermi string edge states [1]. It is also a solid-state realization of Weyl fermion states in 2D space with exotic topological features such as chiral anomaly and charge fractionalization. We aim to explore spin-valley locking, topological quantum criticality, and nonlinear electromagnetic properties of 2D Weyl fermion states.

Recent Progress

We synthesized monolayer bismuthene on SnS(Se) substrate and discovered 2D Weyl fermion states therein using techniques of MBE, ARPES and STM [1]. The linear band dispersion and canted spin texture of 2D Weyl fermion states were experimentally confirmed by our spin-resolved ARPES experiments.

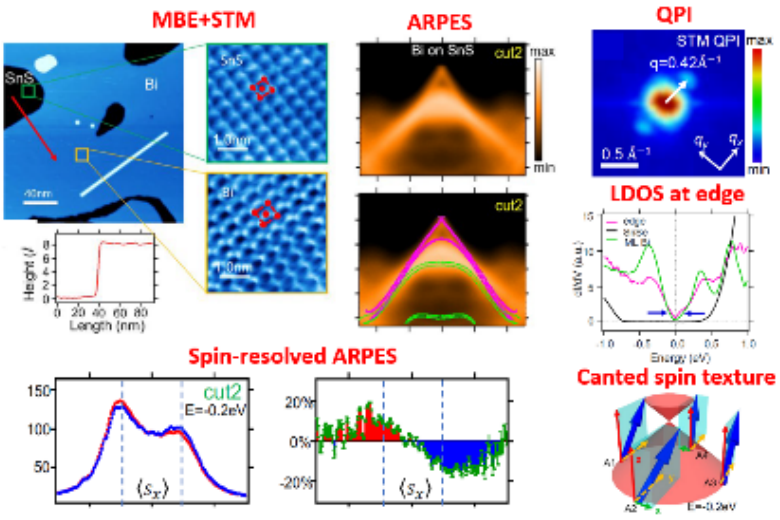

Experimental results taken from epitaxial monolayer bismuthene

Future Plans

We will test various material combinations for realizing 2D Weyl fermion states and investigate the electromagnetic properties of 2D Weyl fermion states using in- and ex-situ transport methods.

References

1. Q. Lu, P. V. S. Reddy, H. Jeon, A. R. Mazza, M. Brahlek, W. Wu, S. A. Yang, Jacob Cook, C. Conner, X. Zhang, A. Chakraborty, H.-J. Tien, C.-H. Tseng, P.-Y. Yang, S.-W. Lie, H. Lin, T.-C. Chiang, G. Vignale, A.-P. Li, T.-R. Chang, R. G. Moore, G. Bian, *Observation of 2D Weyl Fermion States in Epitaxial* Bismuthene, arXiv:2303.02971(2023)

Publications

This is a project newly funded by DES starting from August 2023. No publication has been produced yet.

In-Situ Cryo 4D STEM of Layered Correlated Materials

Judy J. Cha, Department of Materials Science and Engineering, Cornell University
Eun-Ah Kim, Department of Physics, Cornell University

Keywords: Charge density waves, 4D scanning transmission electron microscopy, machine learning, 2D and layered crystals, metal-insulator transitions

Research Scope

We combine cryogenic 4D scanning transmission electron microscopy (4D STEM), *in situ* transport measurements, and unsupervised machine learning to understand microscopically the phase transitions of charge density waves (CDWs) in layered transition metal chalcogenides at the nanoscale in real space. The microscopic understanding gained from the proposed research will be important for the device application of these layered materials as the CDW phase transitions of these materials show metal to insulator transitions useful for non-volatile memory and neuromorphic computing at atomic thickness.

Recent Progress

We have successfully carried out *in situ* 4D STEM experiments on 1T-TaS_2 flakes at variable cryogenic temperatures and studied the metal to insulator phase transitions and concurrent nearly commensurate (NC) to commensurate (C) CDW phase changes, induced by the application of voltage pulses.

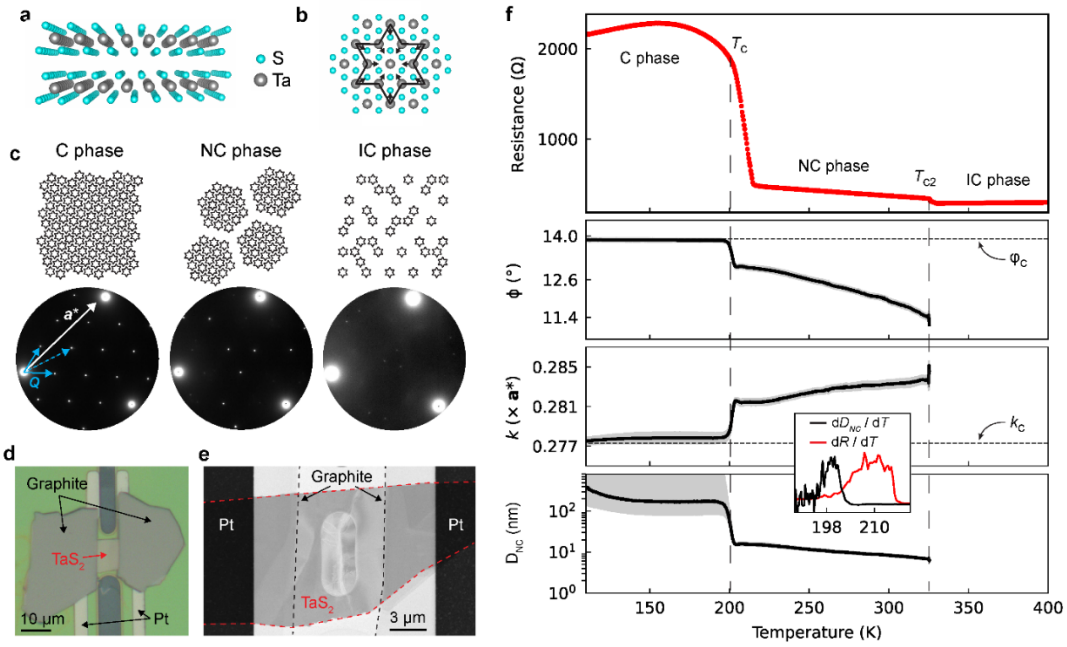

Figure 1 | TaS_2 structure and temperature dependent CDW behavior. Atomic structure of 1T-TaS_2 in cross-section (**a**) and plan-view (**b**). In **b**, the local CDW distortion is shown, which forms a Star-of-David structure. **c**. Illustration of the C, NC, and IC CDW phases, which exhibit different

orderings of the stars. Associated electron diffraction patterns are shown. For the C phase diffraction pattern, the Bragg vector ***a**** is shown, as well as two first order CDW ***Q*** vectors (solid line) and one 2nd order CDW vector (dotted line). The studied device imaged optically (**d**) and with STEM high angle annular dark field imaging (**e**). In the center of the STEM image is a through-hole in the SiN_x membrane, which allows for electron diffraction measurements. **f**. Temperature dependence of the TaS_2 resistance, CDW angle φ, CDW wavevector magnitude *k*, and the domain size D_{NC}. The shaded regions represent the standard error. The inset shows the temperature derivatives of the resistance and D_{NC}. For the inset, the *x*-axis units are temperature (K).

1T-TaS_2 exhibits an insulating C CDW phase and a metallic NC CDW phase below and above 200 K, respectively[1-3]. The phase transition can be driven by voltage pulses, promising for non-volatile memory applications and neuromorphic computing down to atomic thickness[2-4] (**Figure 1**).

Our main finding is that the voltage pulse-induced phase change in TaS_2 flakes is driven by Joule heating and the pulse-induced 'hidden' state is either the NC or incommensurate (IC) CDW phase. We believe our findings explain conflicting reports on the pulse-induced metal to insulator phase change of TaS_2 flakes for voltage pulses up to nanosecond time regime[2,4,5]. **Figure 2** shows the steady-state biasing to observe the CDW switching in TaS_2, where the temperature of the flake rises suddenly at the onset of the CDW switching voltage. A series of steady-state and pulsing experiments show clearly that the CDW switching and concurrent insulator-metal transition is driven by Joule heating, rather than purely field-driven[5].

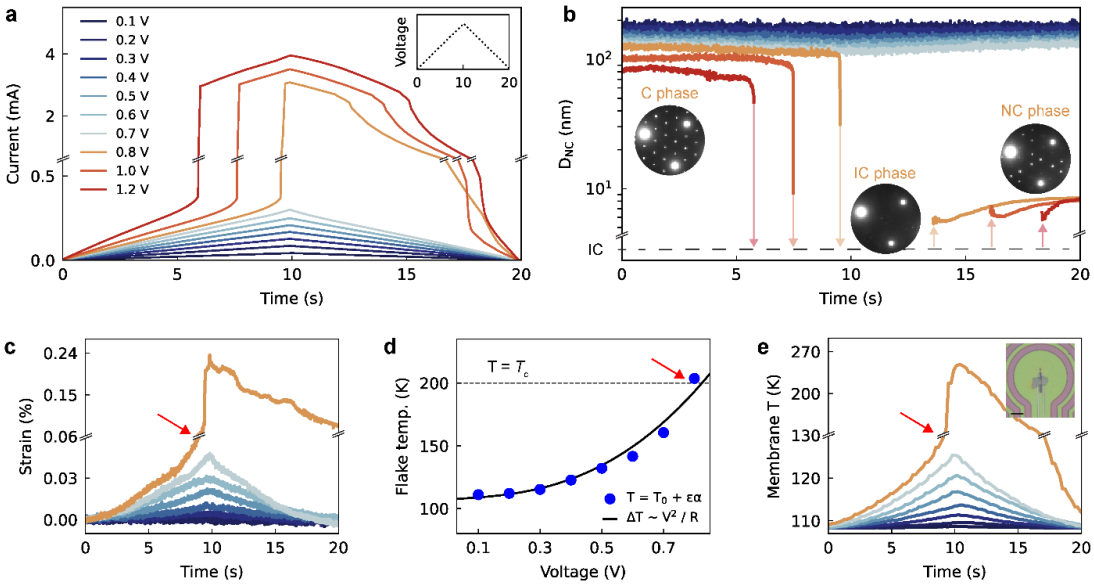

Figure 2 | Steady-state biasing and CDW switching. A. Current vs time during triangular voltage ramps with the maximum voltage ranging from 0.1 V to 1.2 V. The maximum voltage is reached at 10 s. Inset: example voltage profile, the *x*-axis is time (s). The color legend in **a** applies to **b**, **c,** and **e** as well. **B.** The measured CDW domain size D_{NC} during the voltage ramps. The insets show diffraction snapshots acquired during the 0.8 V ramp. **C.** Flake strain during the voltage ramps. **D.** Maximum flake temperature for voltage ramps from 0.1 to 0.8 V, calculated from the strain shown

in **c.** For the 0.8 V datapoint, we show the temperature immediately prior to the C to NC transition. T_0 is 110 K, ε is the strain, α is the effective coefficient of thermal expansion, and R is the flake resistance. **E.** Measured temperature of the SiN_x membrane during voltage ramps. The thermometer consists of a Pt coil encompassing the flake, pictured in the inset. Scale bar is 50 μm.

Figure 3 shows the pulsing experiments, where we demonstrate that the previously unknown, field-induced metallic state is a NC or IC CDW phase, depending on the degree of Joule heating induced by the voltage pulses.

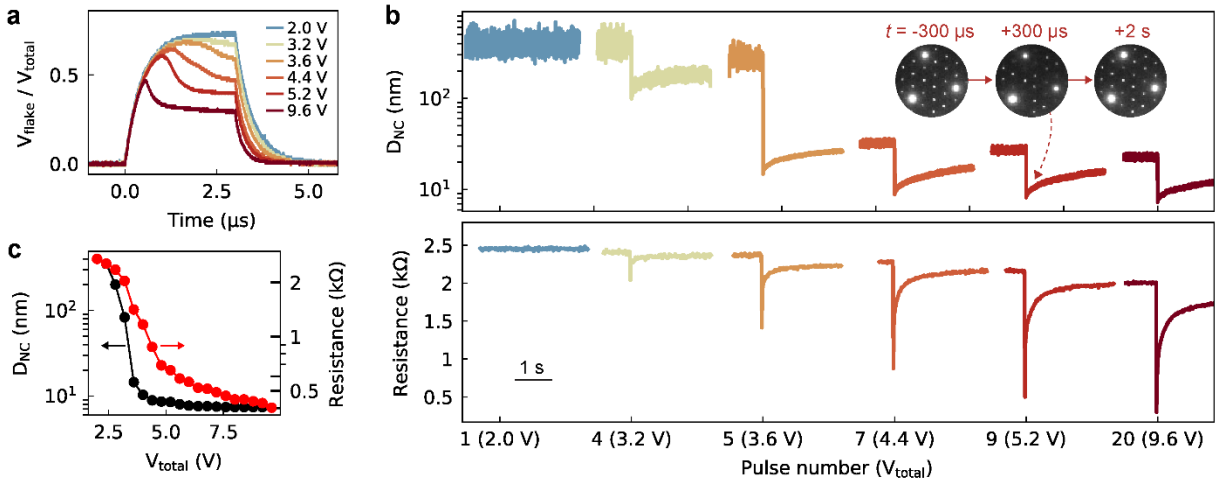

Figure 3 | Pulse induced CDW and resistive switching. a. V_{total} / V_{flake} during electric pulsing. Twenty consecutive pulses were performed in total, starting at 2.0 V and increasing by 0.4 V up to 9.6 V, with roughly 5 mins recovery time in between pulses. A representative set is shown here. **b.** Time-resolved CDW domain size D_{NC} and device resistance during pulsing. The scale bar shows 1 second. The measurement time resolutions are 300 μs for the CDW analysis and 12 ms for the device resistance. The diffraction data for the 9.6 V pulse is shown in Supplementary Video 5. **c.** Comparison of the CDW domain size D_{NC} (black) and the flake resistance (red) immediately after pulsing.

Further, we show that the boundaries between NC-CDW domains, known as discommensurations, are pinned at layer stacking disorders, i.e., dislocations, of TaS_2 flakes. This observation was uniquely enabled by *in situ* cryo 4D STEM maps where we followed the nucleation of the discommensurations during the CDW switching and found a one-to-one correlation between the networks of discommensurations and basal dislocations of TaS_2 flakes (**Figure 4**). Our finding represents the first realization of the direct link between the microstructure defects and electronic structures in TaS_2.

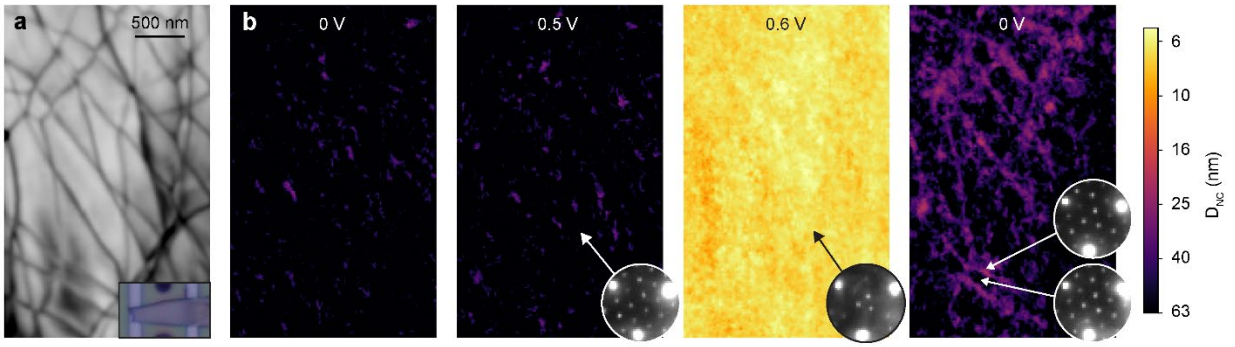

Figure 4 | Real-space CDW imaging during bias. a. Virtual STEM image which sums all the Bragg peak intensities. The dark lines are basal dislocations. The inset is an optical image of this flake. **b.** Maps of the CDW D_{NC} as a function of applied bias. The insets show cropped diffraction patterns, extracted from local regions of 3 x 3 pixels. For the post-bias dataset (right most image), the top diffraction pattern is extracted from a dislocation, and the bottom diffraction pattern is extracted from a non-defective region.

Future Plans

We are summarizing our findings in a manuscript, which we will submit in the Fall this year. We have also carried out a series of *in situ* 4D STEM experiments as a function of temperature during the CDW switching of TaS_2 flakes. Unsupervised machine learning algorithms are being applied to analyze the large data (~ terabyte and 5-dimensional datasets).

We are also fabricating nanobeams of TaS_2 using the electron beam in STEM as a nanoscale milling source. We will examine the stability of the C and NC CDWs in these nanobeam structures. Our hypothesis is that these CDW phases become unstable and disappear when the width of the TaS_2 flake is smaller than a critical nucleus size of the CDW domains.

References

1. J. Wilson, F. Di Salvo, and S. Mahajan, *Charge-density waves and superlattices in the metallic layered transition metal dichalcogenides,* Adv. Phys. **24**, 117–201 (1975).
2. M. J. Hollander *et al. Electrically driven reversible insulator–metal phase transition in 1T-TaS_2*, Nano Lett. **15**, 1861–1866 (2015).
3. A. W. Tsen *et al. Structure and control of charge density waves in two-dimensional 1T-TaS_2,* Proc. Natl. Acad. Sci. **112**, 15054–15059 (2015).
4. M. Yoshida, R. Suzuki, Y. Zhang, M. Nakano, and Y. Iwasa, *Memristive phase switching in two-dimensional 1T-TaS_2 crystal,* Sci. Adv. **1**, 1–7 (2015).
5. D. Mihailovic *et al. Ultrafast non-thermal and thermal switching in charge configuration memory devices based on 1T-TaS_2,* Appl. Phys. Lett. **119**, (2021).

Publications

This project started on July 1st, 2023. Thus, there are no publications to report to date.

Epitaxially-Imposed Control of Chiral Transport Phenomena

Matthew Brahlek, Oak Ridge National Laboratory

Keywords: Topology, Magnetism, Topological Superconductivity, Molecular Beam Epitaxy, Thin Film Heterostructures

Research Scope

The key research scope of this project is to create new heterostructured material paradigms to interrogate and discover new chiral phenomena. This includes chiral transport phenomena found in topological materials as well as emergent properties that can only be achieved in high-quality, well-designed interfaces synthesized by molecular beam epitaxy. We aim to probe these properties using advanced characterizations techniques including low temperature transport and spectroscopy to better understand the fundamental electronic properties as well as diffraction/reflectivity techniques (neutrons/x-rays) to link the observed phenomena to the underlying structures and designer defects.

Recent Progress

This is a new project so there are not any publications. However, we have initial data showing promising routes to address the Research Scope. Preliminary x-ray diffraction imaging (in figure on the right) has shown that we can create novel in-plane superlattices of the topological insulator Bi_2Se_3 with precisely created dislocation networks. We aim to extend this to the magnetic topological insulator $MnBi_2Te_4$ to explore emergent 1D quantized chiral edge states that may arise at the boundaries. We also have stabilized high-quality new thin film systems that exhibit unusual spin-momentum locking (altermagnet candidate MnTe) that can be integrated with superconductors to realize new exotic superconducting states.

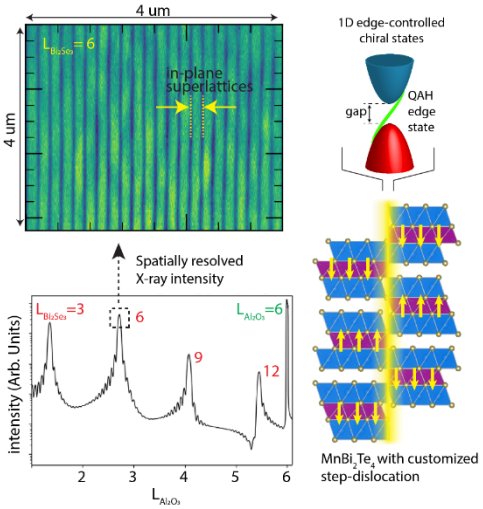

(left) Spatially resolved x-ray diffraction reveals in-plane superlattices composed of highly-order 1D dislocation arrays in topological insulator (TI) Bi_2Se_3. (right) Can these be extended to magnetic TIs and used to gain a new level of control over 1D quantized edge states?

Future Plans

An excite direction is centered around understanding how the topological and magnetic properties are modified at the precisely engineered dislocations boundaries. In particular, how do these local structures evolve with thickness, are the local electronic states modified near these boundaries and give rise to new topological states? We also aim to seek to understand the basic properties of thin film altermagnetic candidates by revealing their novel spin-moment locking and

understanding how they can be utilized at epitaxial interfaces to give rise to new phases of matter, e.g. novel superconductors.

Publications

(As this is a new project there are not any publications, but I listed some papers from other BES funded projects over the past two years.)

1. M. Brahlek, A. R. Mazza, A. Annaberdiyev, M. Chilcote, G. Rimal, G. B. Halász, A. Pham, Y.-Y. Pai, J. T. Krogel, J. Lapano, B. J. Lawrie, G. Eres, J. McChesney, T. Prokscha, A. Suter, S. Oh, J. W. Freeland, Y. Cao, J. S. Gardner, Z. Salman, R. G. Moore, P. Ganesh, T. Z. Ward, *Emergent magnetism with continuous control in the ultrahigh-conductivity layered oxide $PdCoO_2$,* Nano Letters 23, 16, 7279-7287 (2023).

2. M. Brahlek, R. G. Moore, *Surface-state limbo,* Nature Physics 4, 1-2 (2023). Nature Physics News & Views

3. R. G. Moore, T. Smith, X. Yao, Y.-Y. Pai, M. Chilcote, H. Miao, S. Okamoto, S. Oh, M. Brahlek, *Monolayer superconductivity and tunable topological electronic structure at the Fe(Te,Se)/Bi_2Te_3 interface,* Advanced Materials 35, 22, 2210940 (2023).

4. M. Brahlek, M. Gazda, V. Keppens, A. R. Mazza, S. J. McCormack, A. Mielewczyk-Gryń, B. Musico, K. Page, C. M. Rost, S. B. Sinnott, C. Toher, T. Z. Ward, A. Yamamoto, *What is in a name: Defining "high entropy" oxides,* APL Materials 10, 110902 (2022).

5. B. Sbierski, M. Geier, A.-P. Li, M. Brahlek, R. G. Moore, J. E. Moore, *Identifying Majorana vortex modes via non-local transport*, Physical Review B 106 (3), 035413 (2022).

6. M. A. McGuire, Y.-Y. Pai, M. Brahlek, S. Okamoto, R. G. Moore, *Electronic and topological properties of the van der Waals layered superconductor PtTe*, Physical Review B 105, 184514 (2022).

7. A. R. Mazza, J. Lapano, H. M. Meyer III, C. T. Nelson, T. Smith, Y.-Y. Pai, K. Noordhoek, B. J. Lawrie, T. R. Charlton, R. G. Moore, T. Z. Ward, M.-H. Du, G. Eres, M. Brahlek, *Surface-Driven Evolution of the Anomalous Hall Effect in Magnetic Topological Insulator $MnBi_2Te_4$ Thin Films*, Advanced Functional Materials 32, 2202234 (2022).

8. J. Zhang, Y.-Y. Pai, J. Lapano, A. R. Mazza, H. N. Lee, R. Moore, B. J. Lawrie, T. Z. Ward, G. Eres, V. R. Cooper, M. Brahlek, *Design and realization of Ohmic and Schottky interfaces for oxide electronics*, Small Science 2, 2100087 (2021).

9. J. Lapano, Y.-Y. Pai, A. R. Mazza, J. Zhang, T. Isaacs-Smith, P. Gemperline, L. Zhang, H. Li, H. N. Lee, H. Miao, G. Eres, M. Yoon, R. Comes, T. Z. Ward, B. J. Lawrie, M. McGuire, R. G. Moore, C. T. Nelson, A. May, M. Brahlek, *Self-regulated growth of candidate topological superconducting parkerite by molecular beam epitaxy*, APL Materials 9, 101110 (2021).

10. A. R. Mazza, E. Skoropata, J. Lapano, J. Zhang, Y. Sharma, B. L. Musico, V. Keppens, Z. Gai, M. Brahlek, A. Moreo, D. A. Gilbert, E. Dagotto, T. Z. Ward, *Charge doping effects on magnetic properties of single-crystal $La_{1-x}Sr_x(Cr_{0.2}Mn_{0.2}Fe_{0.2}Co_{0.2}Ni_{0.2})O_3$ ($0 \leq x \leq 0.5$) high-entropy perovskite oxides*, Physical Review B 104, 094204 (2021).

Macroscopic quantum states in antiferromagnets:
Bose-Einstein condensation of anti-ferro-magnons

Dmytro Bozhko, University of Colorado Colorado Springs (Principal Investigator);
Zbigniew Celinski, University of Colorado Colorado Springs (Co-Investigator);
Valentine Novosad, Argonne National Laboratory (Co-Investigator)

Keywords: spintronics/magnonics, single crystals/nanostructures, antiferromagnets, Brillouin light scattering, microwave spectroscopy

Research Scope

Bosons are particles of integer spin that support the formation of the fundamental macroscopic quantum object – Bose-Einstein condensate (BEC). It manifests itself in the spontaneous establishment of a macroscopic coherent state in an incoherent multiparticle system. The original theoretical predictions of the BEC phenomenon in an ideal atomic gas were done by A. Einstein and S.N. Bose in 1924, but the necessary experimental conditions for its observation were created only in 1995. Since then, BEC became a hot topic in experimental physics. Nowadays, BECs were experimentally observed in a variety of different systems, including real particles such as ultra-cold gases as well as quasiparticles like exciton-polaritons, photons, as well as in magnon systems of ferrimagnets, quantum magnets, and liquid ^{3}He. The BEC has already found its first applications in the field of quantum computing, making further investigations of this fascinating phenomenon necessary.

This proposal aims to realize a comprehensive study of anti-ferro-magnons' BEC (at microwave frequencies ranging from GHz to THz) and related phenomena in a range of antiferromagnetic (AFM) materials in a wide range of temperatures from ambient to the quantum limit. The range of materials for investigations includes but is not limited to $KMnF_3$, $KNi_xMn_{1-x}F_3$, NiO, and synthetic AFMs like Fe/Cu/Fe and Fe/Cr/Fe multilayers.

Recent Progress (preliminary results)

A newly discovered method of rapid cooling to achieve the BEC of magnons [1] in ferrimagnets is very universal and is applicable to any system of particles or quasiparticles. In a solid body, each quasi-particle system interacts with the phonon bath and these two systems stay in equilibrium in a quasi-stationary state. An instant (or close to instant) reduction in the phonon temperature results in a large excess of quasi-particles when compared to the equilibrium state at the new temperature. This kind of injection is incoherent and injects bosons over the entire energy spectrum. The consequent redistribution of the quasiparticles due to the multi-particle and particle-phonon scattering processes results in an increase in the chemical potential μ required for the BEC. The spectrum of anti-ferro-magnons in a classical fully-compensated AFM is in essence exchange-dominated and its properties could be derived using the same Holstein-Primakoff approach developed for ferromagnets. This similarity of the quantum representation of the problem gives

one the ability to apply analogous approaches for calculating the dynamics of anti-ferro-magnons. Also, it allows us to assume that the four-magnon scattering could be considered as one of the main mechanisms of nonlinear magnon scattering in AFMs. Of course, there are other scattering processes like three-magnon scattering and Cherenkov radiation, which will also contribute to the thermalization process, increasing its efficiency. Using the model developed in [1], we predict that BEC of anti-ferro-magnons could be achieved in low-anisotropy as well as synthetic AFMs. For the case of low-frequency AFMs, the rapid cooling model predicts, that the best conditions for observation of anti-ferro-magnon BEC could be achieved at low temperatures. A combination of decreased heat capacity with increased thermal conductivities of substrate materials (e.g., for MgO thermal conductivity at 3 K is practically the same as at 300 K), results in cooling rates not worth than those at room temperature. But the main improvement from the reduced temperature is a strong decrease in the magnon quantity required to achieve BEC. This results in a strikingly effective condensation, requiring a very small temperature change, even in the case of large Gilbert damping (with values of even up to 10^{-2}). The results of modeling performed for a low-frequency AFM are shown in the figure. Note also that in the case of low temperatures, the process appears

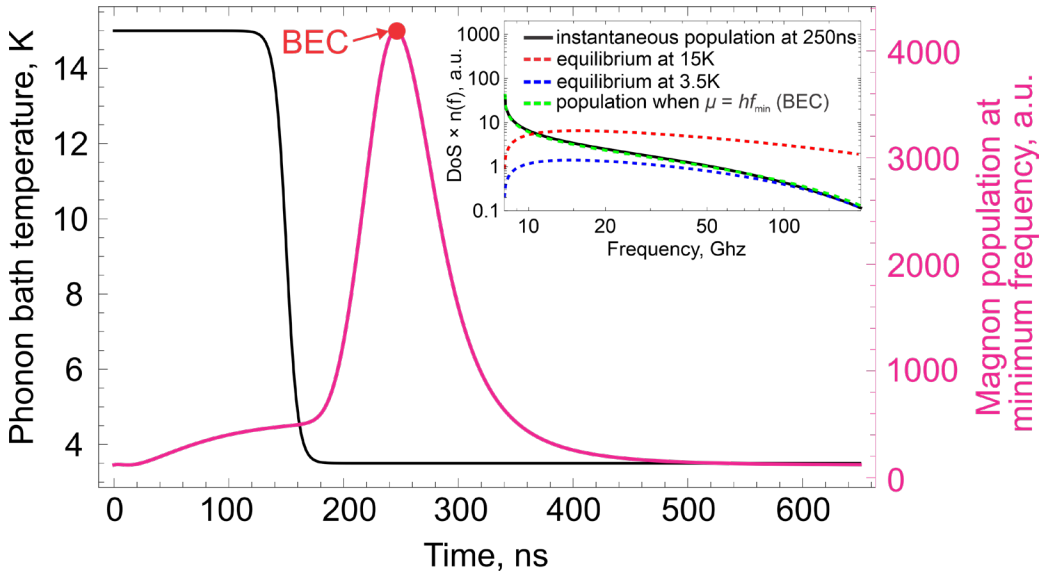

Results of modeling of BEC formation under rapid cooling at low temperatures. The time evolution of the temperature of the phonon system is shown by black line and the quasi-particle population at the lowest energy state is represented by magenta line. The inset shows the quasi-particle density as a function of frequency at 250 ns when BEC is achieved.

to be so effective that we can use realistic rates of temperature change in this simplified model, which was not possible in the original work performed at room temperature [1]. Therefore, the experimental realization of anti-ferro-magnons' BEC in the studied AFMs at low temperatures we consider as an easy to achieve experimental effort. At the same time, due to a simplified case of exchange spectrum with the global minimum located at zero wavevector, observation of BEC could be done using not only Brillouin light scattering but also conventional microwave techniques. The signal from a microwave antenna could be amplified and analyzed by a spectrum

analyzer, providing the frequency resolution down to one Hertz, which will allow us to ultimately answer the question about the coherency of the obtained BEC state.

Future Plans

The main scientific objectives of this 3-year proposal are:

1) Realization of AFM BEC through rapid cooling using a broad range of micro-structured AFMs with various Neel temperatures (T_N). BEC experiments will be carried out at low-temperature ($KMnF_3$ and $KNi_xMn_{1-x}F_3$) as well as at RT NiO.
2) Realization of microwave-pumped anti-ferro-magnetic BEC employing AFMs like $KMnF_3$ and $KNixMn_{1-x}F_3$ that exhibit AF resonances in tens of GHz below T_N.
3) Realization of magnon BEC in synthetic AFMs such as Fe/Cu/Fe and Fe/Cr/Fe through both parametric microwave pumping and rapid cooling techniques.
4) Observation of macroscopic quantum phenomena in AFMs: BEC supercurrents, Bogoliubov waves, magnon Josephson effect, and second sound.

Besides the four listed above scientific aims, the important objective of this proposal is to build significant research and educational capacity at UCCS to explore the quantum properties of magnetic systems that will allow to enhance quantum workforce development in DOE.

The proposed aims are going to be realized using a combination of various state-of-the-art fabrication and measurement techniques. The samples will be grown using molecular beam epitaxy and nanostructured using electron beam lithography and reactive ion etching. The AFM BEC will be detected using time-, space-, and wavevector-resolved Brillouin light scattering and microscopy, and microwave spectroscopy. To perform these measurements in a wide range of temperatures, the team will build a cryostat capable of reaching temperatures of 3 K together with optical and microwave access. Measurements of AFM dynamics in the single-quanta limit will be performed at ANL in the dilution ^{3}He-^{4}He fridge.

The outcomes of the proposal are offering breakthroughs in fundamental aspects of physics as well as applied material science. The first outcome is the experimental demonstration of fundamentally different from earlier achieved ways to create anti-ferro-magnonic BEC. The second one is to provide important insights into the properties of AFMs at low and ultra-low temperatures. Moreover, all the experimental efforts will serve the higher purpose to build the significant research capacity to explore quantum properties of matter at UCCS to provide research-backed education for training the new generation of the quantum workforce.

References

1. M. Schneider, T. Brächer, D. Breitbach, V. Lauer, P. Pirro, D. A. Bozhko, H. Y. Musiienko-Shmarova, B. Heinz, Q. Wang, T. Meyer, F. Heussner, S. Keller, E. T. Papaioannou, B. Lägel, T. Löber, C. Dubs, A. N. Slavin, V. S. Tiberkevich, A. A. Serga, B. Hillebrands, and A. V. Chumak, *Bose–Einstein Condensation of Quasiparticles by Rapid Cooling*, Nature Nanotechnology **15**, 457 (2020).

MXetronics: MXenes as Multifunctional Materials

Bhoj Raj Gautam, Fayetteville State University (Principal Investigator)
Daniel Autrey, Fayetteville State University (Co- Investigator)
Chandra Mani Adhikari, Fayetteville State University (Co- Investigator)
Shubo Han, Fayetteville State University (Co- Investigator)
Bishnu Prasad Bastakoti, North Carolina Agricultural and Technical State University (Co-Investigator)
Binod Kumar Rai, Savannah River National Laboratory (Co- Investigator)

Keywords: Semiconductors, transition metal compounds, optical spectroscopy, magnetism

Research Scope

Two-dimensional MXenes are a class of two-dimensional inorganic compounds with the chemical formula $M_{n+1}X_nT_x$, where M denotes an early transition metal, X indicates carbon, nitrogen or both, T is a surface termination group and n is an integer. MXenes are formed from selectively etching the A-layer from the three-dimensional ceramic MAX phase, which has the general formula, $M_{n+1}AX_n$, where A is a Group IIIA or IVA element. We synthesized $Ti_3C_2T_X$ MXene from Ti_3AlC_2 using a milder LiF/HCl solution and investigated its magnetic, optical, and electrochemical properties. The magnetic property of the resulting $Ti_3C_2T_X$ MXene was analyzed using a superconducting quantum interference device (SQUID)[1]. The electrochemical performances of $Ti_3C_2T_x$ MXene electrode were evaluated by cyclic voltammetry (CV) and electrochemical impedance spectroscopy (EIS) measurements. We also used the $Ti_3C_2T_x$ MXene as a charge transport layer to study the charge transport properties in organic solar cells. We used poly[(2,6-(4,8-bis(5-(2-ethylhexyl)thiophen-2-yl)-benzo[1,2-b:4,5-b0]dithiophene))-alt-(5,5-(10,30-di-2-thienyl-50,70-bis(2 ethylhexyl)benxo[10,20-c:40,50-c0]dithiophene-4,8-dione))](PBDB-T):3,9-bis(2-methylene-(3-(1,1-dicyanomethylene)-indanone))-5,5,11,11-tetrakis(4-hexylphenyl)-dithieno[2,3-d:20,30-d0]-s-indaceno[1,2-b:5,6-b0]-dithiophene (ITIC) blend as an active layer and studied the impact of charge transport layer on morphology, charge transfer and charge transport of this blend using optical spectroscopy and atomic force microscopy (AFM)[2-3].

Recent Progress

The extent of aluminum removal from Ti_3AlC_2 was controlled by performing two separate syntheses, one at ambient temperature (batch 1) and another at an elevated temperature for a longer reaction time (batch 2) and the extent of etching was determined by using X-ray diffraction (XRD). The (104) peak at 39° is vanishingly small as compared to Ti_3AlC_2 and $Ti_3C_2T_x$ Batch 1 samples indicating that Ti_3AlC_2 is transformed to $Ti_3C_2T_x$ MXene with less unreacted MAX phase in Batch 2 compared to Batch 1

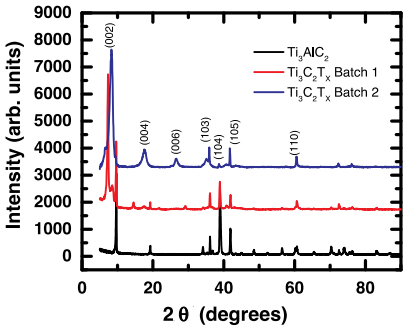

Figure 1. XRD patterns of Ti_3AlC_2 and $Ti_3C_2T_x$ MXenes.

(Figure 1). We observed a paramagnetic-antiferromagnetic (PM-AFM) phase transition in samples generated by both synthesis techniques that occurs at different Néel temperatures, indicating that the aluminum content mediates the magnetic transition **(Figure 2). Figure 3a** presents the CV curves of the sample at various scan rates in the potential range of 0.1 V to 0.55 V. The CV curves consists of a pair of strong and symmetric redox peaks. The increase in scan rate provides the shifting of anodic and cathodic peaks towards positive and negative potential slides, respectively. According to the EIS plot, $Ti_3C_2T_x$ MXene reveals higher charge transfer process across the electrode/electrolyte interface (**Figure 3b**). These promising results indicate the excellent electrode material for next generation energy storage devices.

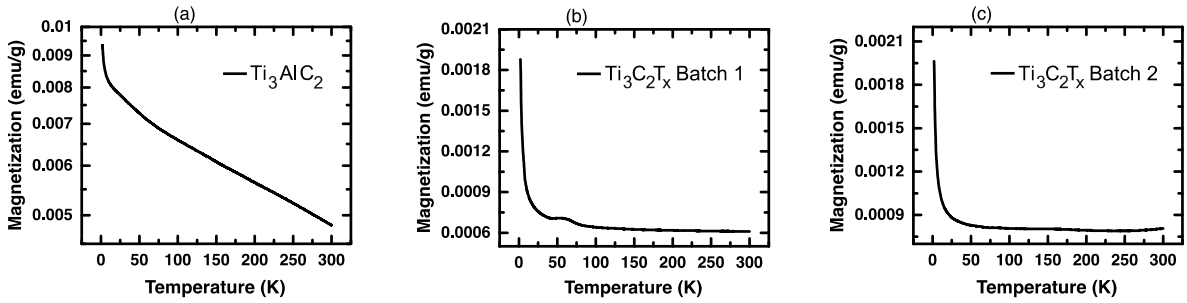

Figure 2. Magnetization versus temperature at 1000 Oe for (a)Ti_3AlC_2, (b) LiF/HCl etched $Ti_3C_2T_x$ Batch 1 and (c) Batch 2 samples.

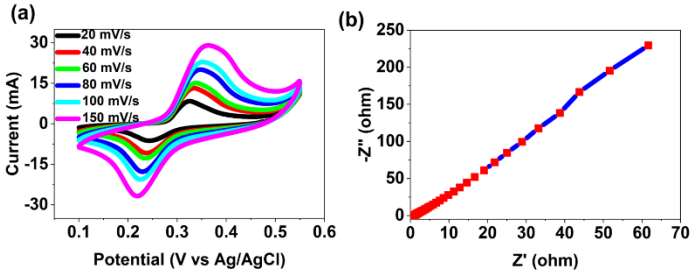

Figure 3. (a) CV and (b) EIS of $Ti_3C_2T_x$ MXene.

Morphology of PBDB:ITIC on poly (3,4-ethylene dioxythiophene): poly(styrenesulfonate) (PEDOT:PSS) charge transport layer shows root mean square (RMS) roughness of 15.7 nm and maximum height of 101 nm **(Figure 4a)** whereas PBDB:ITIC prepared on MXene layer has shown the RMS roughness 6.2 nm and maximum particle size up to 72.4 nm **(Figure 4b)**. Our results indicate that the charge transport layer underneath the active layer impacts the nanomorphology of PBDB-T:ITIC blend. This difference in morphology can cause differences in the performance of these solar cells. The current sensing atomic force microscopy (CSAFM) image showed a maximum current of 2.48 pA **(Figure 5a)** for PBDB-T:ITIC blend on PEDOT:PSS whereas it is *at a level of 45 pA (Figure 2b) for* PBDB-T:ITIC blend on MXene indicating that higher current is observed with MXene interface. This study will provide important information about the enhancement of current in MXene-based organic solar cells.

We used photoluminescence quenching and ultrafast femtosecond pump probe spectroscopy (**Figure 3**) to measure charge transfer and charge extraction in polymer blends using MXenes and PEDOT:PSS. Longer lifetime of ground state bleaching **(Figure 6a)** and high photoluminescence quenching **(Figure 6b)** by MXenes suggest great potential of this material

over benchmark PEDOT:PSS as a charge transport layer. This is further supported by the results of AFM measurement **(Figure 5)** where higher current is observed with MXene interface.

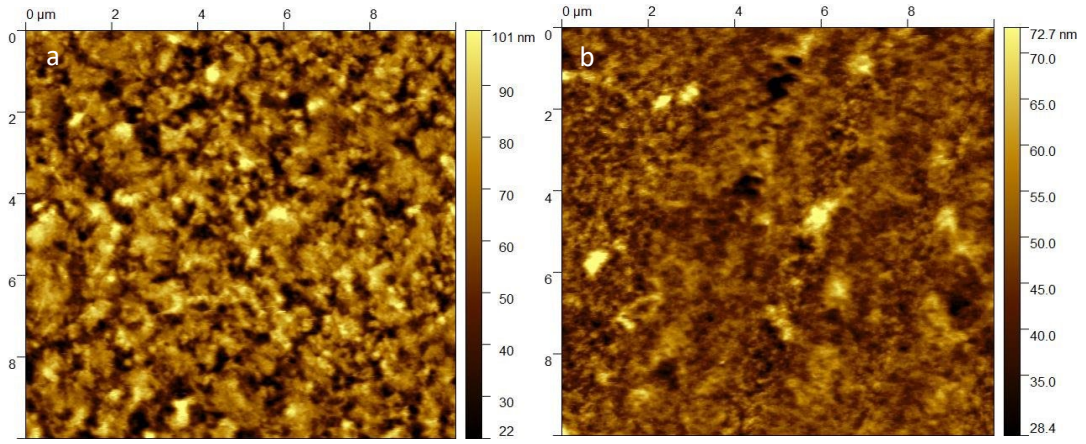

Figure 4. Atomic force microscopy topography image of (a) PBDB-T:ITIC film on PEDOT:PSS (b) PBDB-T:ITIC film on MXene.

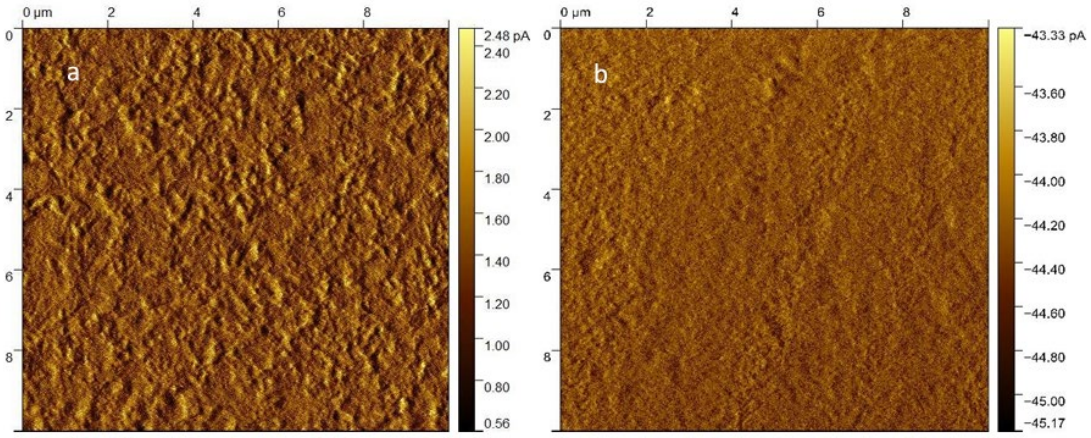

Figure 5. Current sensing atomic force microscopy image of (a) PBDB-T:ITIC film on PEDOT:PSS (b) PBDB-T:ITIC film on MXene.

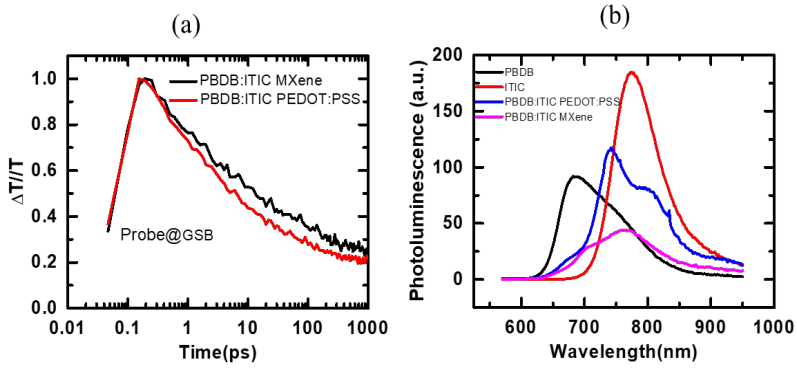

Figure 6 (a) Ground bleaching dynamics (a) and the photoluminescence quenching (b) of PBDB:ITIC blend in MXene and PEDOT:PSS layer

Future Plans

For the coming year, we are planning to work on the following projects.

1. We will study the effect of gamma radiation in magnetic and transport properties of Mxenes.
2. We will investigate the Impact of stoichiochemistry, dimensionality and surface functionalization in magnetic behavior of MXenes.
3. We will synthesize porous Mxene nanostructure using block copolymer as template and structure directing agent and study the electrochemical properties.
4. We will investigate the impact of surface functionalization on electronic and optical properties of Mxenes.
5. We will study the energy transfer process in MXene quantum dots for ratiometric fluorescence detection.

References

1. K. Allen-Perry, W. Straka, D. Keith, S. Han, L. Reynolds, B. Gautam, and D. E. Autrey, Tuning the Magnetic Properties of Two-Dimensional MXenes by Chemical Etching, *Materials* **14**, 694 (2021).

2. U. K. Aryal, H. Pazniak , T. Kumari , M. Weber, F. O.L. Johansson , N. Vannucchi, N. Witkowski , V. Turkovic, A. D. Carlo, and M. Madsen, 2D MXene-Based Electron Transport Layers for Nonhalogenated Solvent-Processed Stable Organic Solar Cells, *ACS Appl. Energy Mater.* **6**, 9, 4549–4558 (2023).

3. S. Jones, A. Ware, T. Wright, D. Keith, S. Han, D. Autrey, and B. Gautam, $Ti_3C_2T_x$ MXene Hole Transport Layer for Polymer Non-Fullerene Solar Cells, *Microsc. Microanal.* **28**, 926 (2022).

APS CUWiP+: Supporting the Success of All Undergraduate Women+ in Physics

Crystal Bailey, American Physical Society (Principal Investigator)

Farah Dawood, American Physical Society (Co-Investigator)

Keywords: Women, undergraduate, equity, diversity, inclusion.

Program Scope

Increasing the participation of women in physics is critical to addressing U.S. workforce needs in STEM. In 2020 only 25% of undergraduate physics degrees were earned by women, and over the last two decades this percentage has essentially plateaued. Nearly 75% of undergraduate women in a national sample reported experiencing sexual harassment in a physics environment; moreover, women who belong to multiple marginalized groups – such as women of color and those in the LGBTQ+ community, experience additional challenges due to negative climates and reduced access to mentors and peers who can relate to their experiences. The Conferences for Undergraduate Women in Physics (CUWiP) are a collaborative effort of physicists from around the country who organize about a dozen regional conferences annually with support from the American Physical Society (APS). The total number of participants has been close to 2,000 in recent years. By comparison, about 2,100 women graduate with a bachelor's degree in physics each year in the U.S (see Figure 1). The conferences provide an opportunity for women and gender minorities to hear inspirational talks by women and gender minority physicists; participate in workshops and panel discussions on summer research, graduate school, and physics careers; learn about issues facing women and gender minorities and strategies to help them thrive; and develop networks and informal mentoring relationships.

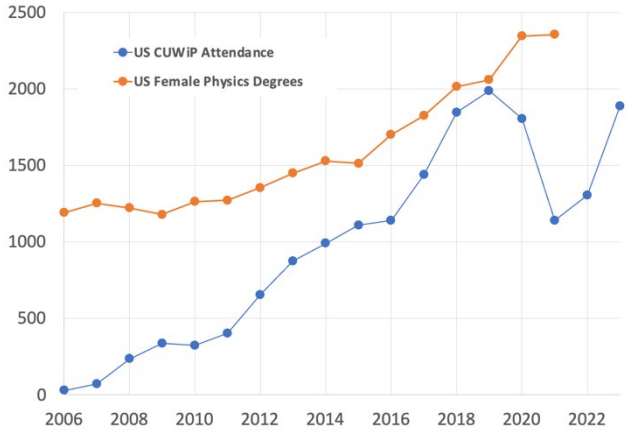

Figure 1: The number of US female physics degrees and the US CUWiP attendance since 2006

The goals of this project are to:

1. Deliver programming that strengthens identity and career choice in physics,
2. Establish community spaces that foster a sense of belonging, and
3. Support leadership development and sense of agency among participants

We will do this by organizing conferences for 2,000 participants annually for the next three years and providing support for conference organizers to plan events with effective and fully inclusive

programming. In addition, we will encourage participants to be active in local Women in Physics (WiP) groups, offer virtual programming throughout the year, and provide opportunities for leadership experience and skills development in building a community led by and for women and gender minorities in physics (a specific focus on the inclusion of gender minorities being signified by the "+" in CUWiP+).

Recent Progress

A return to in-person conferences following the pandemic took place across 14 sites located across the US on January 20 - 22, 2023. An aligned conference also took place in Canada, although no federal funds were used to support the activities outside of the United States. CUWiP was once again organized by 14 institutions with local organizing committees with guidance from the project National Organizing Committee (NOC-L). CUWiP also increased communication and networking opportunities for participants by creating a Women & Gender Minorities in Physics community as part of APS Engage, a social media networking tool.

The total number of US conference participants in 2023 was 1880, as compared to 1307 in 2022, 1139 in 2021 and 1806 in 2020 (the last time an in-person conference was held). Additionally, access was provided to 40 participants from all over the globe through a virtual conference held on February 11 - 12, 2023. Despite lower numbers in 2021 and 2022, due primarily to the conferences having to be converted to a virtual format during the pandemic, attendance in 2023 was comparable to 2020 which is an encouraging sign that the conference may continue to grow as we return to the in-person format.

Though the pandemic adversely affected conference attendance, it also afforded an opportunity to explore a non-synchronous, virtual format for the conferences. Advantages of this format include being able to offer year-round programming that could be accessed by individuals all around the world, who are not able to travel to the synchronous in-person event annually. Several program components were implemented to support the goals of professional development, networking, and contributing to the physics community. Leveraging the national scale of the virtual conference, a virtual lab tour of the Princeton Plasma Physics Laboratory (PPPL) and General Atomics (GA) was held at the virtual conference. Speakers and panelists were selected to bring experience from diverse areas of physics; session topics were chosen so that they would be inclusive to students with a variety of experiences and identities, including LGBTQ+, underrepresented ethnic and racial groups, and students with disabilities. The conference also featured presentations on a broad range of topics in science and technology both in academia and in industry. Attendees outside of the US (Canada and participants around the world) were able to live stream the keynote address by Nadya Mason.

A formal assessment of the project, which was conducted via pre- and post-conference surveys with 558 matched responses, revealed that participants show strong intentions to complete undergraduate degrees, build a sense of community among during the conference, have strong

interest in physics, and appear to be recovering from the anxiety that COVID ushered in. There were some negative shifts observed related to perceived competence and imposter syndrome; we will continue to closely monitor these metrics and implement recommendations by evaluators to create more of an emphasis on the positive aspects of a life in physics in conference programming.

Future Plans

Future plans include organizing the 2024 CUWiP+ at fourteen sites around the US:

- Boston College & Wellesley College
- City University of New York, Graduate Center
- Clemson University
- Georgia Institute of Technology
- Missouri University of Science & Technology
- Montana State University
- Stanford University & SLAC National Accelerator Laboratory
- Tulane University
- United States Military Academy, West Point
- University of Arizona
- University of Michigan, Ann Arbor
- University of Pennsylvania
- University of San Diego
- West Virginia University

We are further seeking to leverage points of connection with the Heising Simons funded Advancing Graduate Leadership (AGL) program, an APS initiative to provide professional skills development and leadership training to graduate women and gender minorities in physics. Graduate women and gender minorities who have received training and mentoring through the AGL program will participate in CUWiP+ conferences as mentors, panelists, and advisors. Doing so will not only give the AGL participants an opportunity to put their training into practice, but also will provide opportunities for near-peer mentoring between undergraduate CUWiP+ attendees and graduate mentors, which also contributes to higher rates of persistence.

Furthermore, we will implement an online virtual community, comprised of CUWiP+ attendees and AGL participants, which will allow both groups to interact throughout the year. We will broadcast select talks from the 2024 CUWiP+ so that high-quality content will reach a broader audience than attendees of a single conference. We will also provide points of contact (e.g. virtual coffee hours) between undergraduate participants and speakers as well as undergraduates and graduate mentors. We will also continue working with external evaluators to measure the impacts of the Conferences on attendees; we will also track participation in the online virtual community

to measure whether there is continued engagement with individual members as they transition between undergraduate and graduate physics programs.

Publications

1. M. Franklin, E. Brewe, A.R. Ponnock, *Examining reasons undergraduate women join physics*, Physical Review Education Research **19**, 010126 (2023).

Update on the activities of the National Academy of Sciences Condensed Matter and Materials Research Committee

Colleen N. Hartman, National Academy of Sciences

Keywords: Condensed matter; Materials Research, moiré physics, NASEM

Research Scope

The Condensed Matter and Material Research Committee (CMMRC) plays an active role within the condensed matter and materials research communities by serving as a conduit for interactions between these communities and the federal government and monitoring the health of and identifying critical new developments in these fields. Among the mechanisms that CMMRC can use to fulfill its charge are (1) organizing topical workshops around topical areas chosen in coordination with the sponsors and drafting workshop proceedings that summarize the presentations and ensuing discussions; (2) working with sponsoring agencies to propose workshops, other special forums such as meetings of experts, and report-generating ad hoc studies that relate to condensed matter and materials research, where needed; (3) providing long-term stewardship of reports that CMMRC helped to develop and that impact the condensed matter and materials research communities; (4) interacting with the professional societies and FACA committees for condensed matter and materials research; and (5) serving as a resource and providing expert advice to other standing committees in the BPA and other National Academies boards in the development of National Academies' activities that impact the condensed matter and materials research fields.

The primary responsibilities of the CMMRC Committee are to (1) monitor and assess the areas of condensed matter and materials research sciences, (2) identify and discuss issues of concern to the condensed matter and materials research communities, mainly connected with developments that impact research opportunities, and (3) guide federal agencies regarding their associated programs.

Recent Progress

One of the significant challenges in materials science has been developing materials that could survive and function in extreme environments, such as the high-radiation environments found in a fission or fusion reactor or the ultra-high temperature experienced by a hypervelocity vessel or a spacecraft traveling through Earth's atmosphere on its return to the planet's surface. To address this challenge, a 2-day workshop titled Materials in Extreme Environments: New Monitoring Tools and Data-Driven Approaches was held on October 5-6, 2022, at the National Academies of Sciences, Engineering, and Medicine. The workshop brought together an international collection of experts on testing and measuring materials in extreme environments and discovering and developing new materials.

The workshop proceedings recapped the presentations and discussions that took place during the two days of the workshop. What was unique about the workshop was how it brought together two different sets of tools to understand the behavior of materials in extreme environments. The

first set comprised various microscopes and other monitoring tools that could be used to characterize these materials, while the second consisted of new data analytics tools, such as machine learning capabilities. By combining observational tools with data analytics tools, it was possible to characterize the behavior of materials in extreme environments much more quickly and in greater detail than had been possible in the past. One particular focus of the workshop was how combining monitoring tools and data analytics could be applied better to understand materials processing approaches such as three-dimensional printing. It was noted that the workshop was structured so that the first day focused mainly on materials processing and manufacturing, while the second was primarily devoted to materials testing.

Future Plans

The Spring 2024 workshop planning is in full swing for the *Quantum Coherent Networks Workshop*. This public workshop will present a high-level authoritative view of quantum-coherent networks for physical scientists and policymakers seeking a general grasp of the subject and its potential. The workshop bridges AMO and condensed matter/materials science areas. In the coming weeks, a call for experts to serve on the planning committee will be issued, and community members are encouraged to apply. CMMRC members will meet in the fall to hear updates from DOE and NSF and break out into groups to discuss possible meeting topics for the follow-on workshop. This meeting will be Livestreamed and questions from the interested public will be taken.

Publications

National Academies of Sciences, Engineering, and Medicine, *Frontiers in Data Analytics and Monitoring Tools for Extreme Materials: Proceedings of a Workshop* (2023).

National Academies of Sciences, Engineering, and Medicine, *Frontiers in Synthetic Moiré Quantum Matter A Workshop (2022)*

National Academies of Sciences, Engineering, and Medicine, *Frontiers in Memristive Materials for Neuromorphic Processing Applications: A Workshop (2021)*

National Academies of Sciences, Engineering, and Medicine, *Frontiers in Synthetic Moiré Quantum Matter A Workshop (2022)*

Planar Systems for Quantum

PI: Jie Shan (Cornell University)
Co-PIs: Cory R. Dean (Columbia University)
James Hone (Columbia University)
Allan H. MacDonald (University of Texas at Austin)
Kin Fai Mak (Cornell University)
Tony F. Heinz (SLAC National Accelerator Laboratory/Stanford University)

Keywords: moiré physics, 2D and layered crystals, semiconductors, transport, optical spectroscopy.

Research Scope

The scope of this research program is to develop two-dimensional (2D) moiré materials as a quantum simulator to implement model Hamiltonians and their phase diagrams and dynamics. Specifically, we aim to (i) develop homogeneous moiré materials with controllable superlattice potential for quantum simulation; (ii) develop methods for continuous tuning of moiré parameters, including length and energy scales, and charge density; (iii) experimentally map the equilibrium quantum phase diagram of model many-body Hamiltonians such as the Hubbard models and compare with theory; and (iv) develop methods to dynamically control the many-body Hamiltonians and investigate non-equilibrium quantum dynamics.

Recent Progress

Band-structure engineering by forming moiré superlattices has been predicted to realize topological flat bands [1]. Our team has continued to build our strengths on the growth of high quality bulk crystals of semiconducting transition metal dichalcogenides (TMDs) and fabrication of moiré heterostructures and the development of techniques for forming contacts to TMD materials. These structures and devices have enabled us to realize a generalized Kane-Mele model in 60º-aligned $MoTe_2/WSe_2$ hetero-bilayers and demonstrated, as an initial result, a quantized Hall conductance in the absence of an external magnetic field when the moiré lattice is filled with one hole per unit cell [2]. More recently, we have observed thermodynamic evidence that small twist angle $MoTe_2$ bilayers support topological flat bands with appropriate band geometry to favor fractional Chern insulators at zero magnetic field [3].

We have also realized the Kondo lattice Hamiltonian in TMD moiré materials. The Kondo lattice, describing a matrix of local magnetic moments coupled via spin-exchange interactions to itinerant conduction electrons, is a prototype of strongly correlated quantum matter. Traditionally, Kondo lattices are realized in intermetallic compounds containing lanthanide or actinide. The complex electronic structure and limited tunability of both the electron density and exchange interactions in these bulk materials pose significant challenges to study Kondo lattice physics. The high tenability of the moiré materials opens new opportunities.

It has been shown previously that a Mott insulator with local magnetic moments can be realized in TMD moiré materials at half filling of the moiré band. The strong electronic interactions open a Mott gap with a fully filled Hubbard band. Our idea is to couple itinerant electrons to the lattice of local moments via the exchange interaction to realize the Kondo lattice. Figure 1a shows our original proposal based on three layer moiré superlattices at the interface between a WX_2 homobilayer and MoX_2 monolayer (X = S, Se). Under appropriate gating conditions, the interface WX_2 layer forms a triangular lattice of local moments that couple to itinerant electrons in the other WX_2 layer via a gate-tunable Kondo exchange interaction. Using a parton mean-field approach, we identify a range of twist angles which support a gate-tuned quantum phase transition between a heavy Fermi liquid with large anomalous Hall conductance and a chiral spin liquid coexisting with a light Fermi liquid and describe experimental signatures to distinguish among competing theoretical scenarios (Fig. 1b).

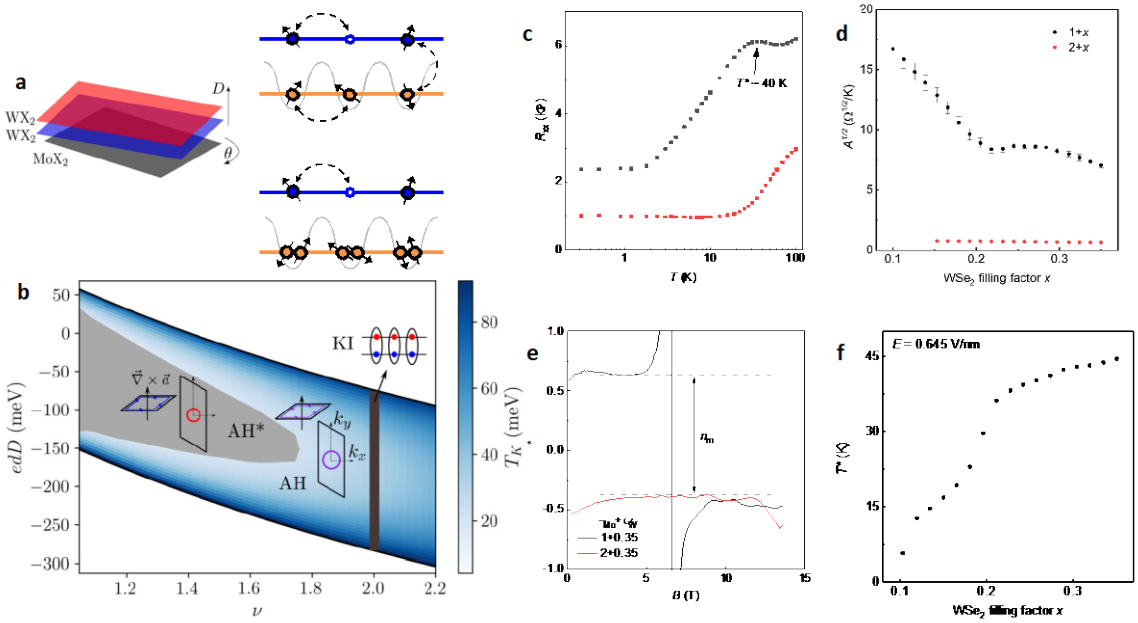

Figure 1 | Realization of a gate-controllable Kondo lattice. a, Left panel: schematic of a TMD trilayer Kondo lattice system proposed theoretically. The two active TMD layers (blue and red) experience moiré modulation potentials with different strengths so that one layer has flat bands and one has dispersive bands. Right panel: top shows a Kondo lattice and bottom shows a control experiment, in which the flat band is filled with two electrons, local moments and Kondo lattice are not present. **b,** Parton mean-field phase diagram as a function of the moiré band filling factor ν and the external displacement field D. KI: Kondo insulator; AH: anomalous Hall phase. **c,** Temperature dependence of the resistance of an AB-stacked $MoTe_2/WSe_2$ bilayer. Black ($\nu = 1 + x$, Kondo) and red ($\nu = 2 + x$, control experiment) correspond to the two schematics in **a**. A peak is observed for the Kondo lattice case at the Kondo temperature scale T^*. The low temperature part of dependence is described by AT^2, where coefficient $A^{1/2}$ is proportional to the effective mass in the Fermi liquid theory. **d,** Doping dependence of $A^{1/2}$ shows 10-20 times enhancement for the Kondo lattice case. **e**, Hall density as a function of magnetic field. The abrupt drop of the Hall density by 1 around 6 T is a manifestation of destruction of the Kondo singlet by the Zeeman effect. At the low fields, the charge carrier is a heavy fermion with a large Fermi surface. At high field, it is alight fermion with a small Fermi surface. **f,** The Kondo temperature can be continuously tuned by conduction electron density.

In the experiment, we realize a Kondo lattice in AB-stacked $MoTe_2/WSe_2$ moiré bilayers, in which the two TMD layers experience different moiré potentials. The band in $MoTe_2$ is relatively flat and the band in WSe_2 is relatively dispersive. The $MoTe_2$ layer is tuned to a Mott insulating state, supporting a triangular moiré lattice of local moments, and the WSe_2 layer is doped with itinerant conduction carriers. We observe heavy fermions with a large Fermi surface below the Kondo temperature (Fig. 1c,d). We also observe destruction of the heavy fermions by an external magnetic field with an abrupt decrease of the Fermi surface size and quasiparticle mass (Fig. 1e). We further demonstrate widely and continuously gate-tunable Kondo temperatures through the itinerant carrier density (Fig. 1f). Our study opens the possibility of in-situ access to the rich phase diagram of the Kondo lattice problem with exotic quantum criticalities in a single device.

Future Plans

We will continue the lines of on-going work, including the development of homogeneous moiré samples and devices and experimental techniques to probe the transport and thermodynamic properties of embedded samples. The combined theoretical and experimental efforts will particularly focus on the study of many-body quantum phenomena from strong electronic correlation and topology.

References

1. F. Wu, T. Lovorn, E. Tutuc, I. Martin, and A.H. MacDonald, "Topological insulators in twisted transition metal dichalcogenide homobilayers*," Phys. Rev. Lett.* **122,** 086402 (2019).
2. T. Li, S. Jiang, B. Shen, Y. Zhang, L. Li, Z. Tao, T. Devakul, K.Watanabe, T. Taniguchi, L. Fu, J. Shan, and K.F. Mak, "Quantum anomalous Hall effect from intertwined moiré bands," *Nature* **600,** 641–646 (2021).
3. Y. Zeng, Z. Xia, K. Kang, J. Zhu, P. Knüppel, C. Vaswani, K. Watanabe, T. Taniguchi, K. F. Mak, and J. Shan, "Thermodynamic evidence of fractional Chern insulator in moiré $MoTe_2$," *Nature* (2023). https://doi.org/10.1038/s41586-023-06452-3
4. A. Kumar, N. C. Hu, A. H. MacDonald, and A. C. Potter, "Gate-tunable heavy fermion quantum criticality in a moiré Kondo lattice", *Phys. Rev. B* **106,** L041116 (2022).
5. W. Zhao, B. Shen, Z. Tao, Z. Han, K. Kang, K. Watanabe, T. Taniguchi, K. F. Mak, and J. Shan, "Gate-tunable heavy fermions in a moiré Kondo lattice," *Nature* **616**, 61 (2023).

Publications

1. Y. Zeng, Z. Xia, K. Kang, J. Zhu, P. Knüppel, C. Vaswani, K. Watanabe, T. Taniguchi, K. F. Mak, and J. Shan, "Thermodynamic evidence of fractional Chern insulator in moiré $MoTe_2$," *Nature* (2023). https://doi.org/10.1038/s41586-023-06452-3

2. K. Kang, W. Zhao, Y. Zeng, K. Watanabe, T. Taniguchi, J. Shan and K. F. Mak, "Switchable moiré potentials in ferroelectric WTe_2/WSe_2 superlattices", *Nat. Nanotechnol.* **18,** 861 (2023).

3. W. Zhao, B. Shen, Z. Tao, Z. Han, K. Kang, K. Watanabe, T. Taniguchi, K. F. Mak, and J. Shan, "Gate-tunable heavy fermions in a moiré Kondo lattice," *Nature* **616**, 61 (2023).

4. Y. Tang, K. Su, L. Li, Y. Xu, S. Liu, K. Watanabe, T. Taniguchi, J. Hone, C.M. Jian, C. Xu, K. F. Mak, and J. Shan, "Frustrated magnetic interactions in a Wigner-Mott insulator," *Nat. Nanotechnol.* **18,** 233–237 (2023).

5. Y. Zeng, Z. Xia, R. Dery, K. Watanabe, T. Taniguchi, J. Shan, K.F. Mak, "Exciton density waves in Coulomb-coupled dual moiré lattices," *Nat. Mater.* **22**, 175–179 *(*2023).

6. M. Kuiri, C. Coleman, Z. Gao, A. Vishnuradhan, K. Watanabe, T. Taniguchi, J. Zhu, A. H. MacDonald & J. Folk, "Spontaneous time-reversal symmetry breaking in twisted double bilayer graphene", *Nat. Commun.* **13,** 6468 (2022).

7. Y. Xu, K. Kang, K. Watanabe, T. Taniguchi, K. F. Mak, and J. Shan, "A tunable bilayer Hubbard model in twisted WSe2," *Nat. Nanotechnol.* **17**, 934–939 (2022).

8. A. Kumar, N. C. Hu, A. H. MacDonald, and A. C. Potter, "Gate-tunable heavy fermion quantum criticality in a moiré Kondo lattice", *Phys. Rev. B* **106,** L041116 (2022).

9. Y. Tang, J. Gu, S. Liu, K. Watanabe, T. Taniguchi, J. C. Hone, K.F. Mak, and J. Shan, "Dielectric catastrophe at the Mott and Wigner transitions in a moiré superlattice," *Nat. Commun.* **13**, 4271 (2022).

10. X. Liu, J.I.A. Li, K. Watanabe, T. Taniguchi, J. Hone, B. I. Halperin, P. Kim, and C. R. Dean, "Crossover between strongly coupled and weakly coupled exciton superfluids", *Science* **375**, 205 (2022).

Dynamics of Electron Interactions in Superconductors and Other Novel Materials

Dan Dessau, University of Colorado Boulder

Keywords: Superconductivity, Non-Fermi Liquid Behavior and Charge Dynamics, ARPES, Cu-based superconductors, Topological Materials.

Research Scope

The goal of our project is to perform experimental studies of the electronic structure, electronic interactions and pairing in novel superconductors, and other novel materials, particularly topological and magnetic topological materials. We primarily utilize high-resolution angle-resolved photoemission (ARPES), pairing this with our own electronic structure calculations and with analysis of transport and other data.

Recent Progress

Though we have made good progress in both novel superconductors and magnetic topological materials, here we only discuss superconducting materials, or those materials believed to be near a superconducting instability.

Ni-based superconducting family – $Pr_4Ni_3O_8$. The discovery of superconductivity in planar nickelates raises the question of how the electronic structure and correlations of Ni^{1+} compounds compare to those of the Cu^{2+} cuprate superconductors. We perfomed an ARPES study of the trilayer nickelate $Pr_4Ni_3O_8$ (structure shown in Fig 1b), revealing a Fermi surface resembling that of the hole-doped cuprates but with critical differences. Specifically, the main portions of the Fermi surface are extremely similar to that of the bilayer cuprates (Fig 1a), with an additional piece that can accommodate additional hole doping. We find that the electronic correlations are about twice as strong in the nickelates as in the cuprates – for example the effective masses are ~ twice that of the cuprates (Fig 1d). We also find that the correlations are almost *k*-independent, indicating that they originate from a local effect, likely the Mott interaction, whereas cuprate interactions are somewhat less local. Nevertheless, the nickelates still demonstrate the strange-metal behavior in the electron scattering rates, which is also apparent in the measured

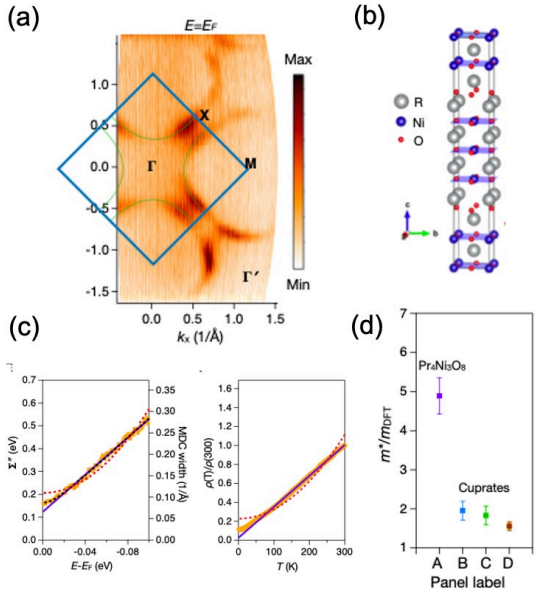

Fig 1 (a) Hole Fermi surface showing cuprate-like features (b) $Pr_4Ni_3O_8$ structure. (c) left: self-energy follows marginal Fermi liquid behavior; right: approximately T-linear resistivity (d) nickelate mass enhancement twice that of cuprates, potentially a signature of greater Mott character. From [1], performed with the Mitchell group.

resistivity (both shown in Fig 1c). Understanding the similarities and differences between these two families of strongly correlated superconductors is an important challenge. This work was done with the Mitchell group [1].

Ni-based superconducting family – $Ba_{1-x}Sr_xNi_2As_2$. $BaNi_2As_2$ is a structural analogue of the pnictide superconductor $BaFe_2As_2$, which like the iron-based superconductors, hosts a variety of ordered phases including charge-density waves (CDW), electronic nematicity, and superconductivity. Upon isovalent Sr substitution on the Ba site, the charge and nematic orders are suppressed, followed by a six-fold enhancement of the super- conducting transition temperature (T_c). To understand the mechanisms responsible for enhancement of T_c, we performed high-resolution ARPES measurements of the $Ba_{1-x}Sr_xNi_2As_2$ series, which agree well with our density functional theory (DFT) calculations throughout the substitution range. Analysis of our ARPES-validated DFT results indicates an electronic structure phase transition which we associate with the enhancement of nematic fluctuations, revealing unexpected connections to the iron-pnictide superconductors. This gives credence to a scenario in which nematic fluctuations drive an enhanced Tc. Work performed in collaboration with the Paglione group, and presently under review [2].

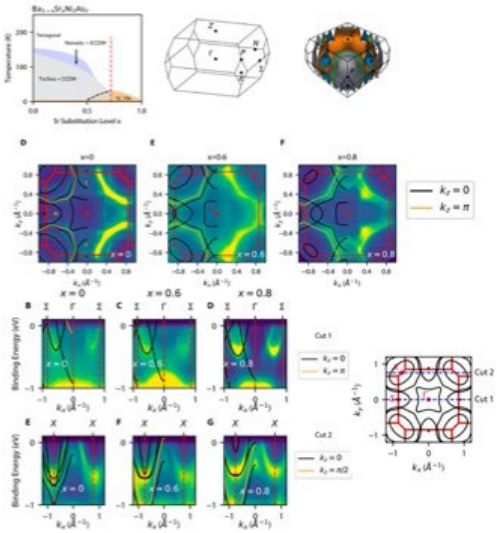

Fig 2. Evolution of Electronic Structure in Nematic Superconductor $Ba_{1-x}Sr_xNi_2As_2$, in collaboration with the Paglione group, under review [2]).

Cuprate Superconductors. In conventional s-wave superconductors, the shape of the Cooper pairs is commonly known to be isotropic. However, in high temperature superconductor cuprates, the d-wave gap symmetry naturally forms an anisotropic Cooper pair length scale. Here we use Angle-Resolved Photoemission Spectroscopy on a wide range of doping levels of $Bi_2Sr_2CaCu_2O_{8+x}$. For example, Fig 3 a-g shows a cut through the antinodal regime deep into the SC state, showing dramatically renormalized states that are gapped by the superconducting pairing. Utilizing new highly-constrained methods we developed that enable us to fit this data (Figs 3 h-n) as well as many cuts throughout the zone we are able to experimentally extract,

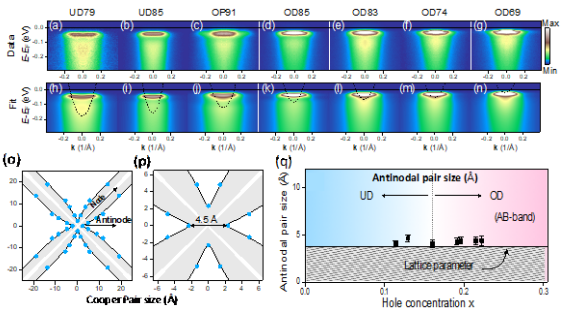

Fig 3. Hyper-local Cooper pairs in the antinodal direction of cuprate superconductors as obtained from ARPES. (a) – (g) Antinodal ARPES data from many different doping levels of $Bi_2Sr_2CaCu_2O_{8+x}$ measured in the SC state. [3]

for the first time, the shape of the Cooper pairs in a d-wave superconductor, shown to have a clover-like shape (Fig 3 o,p). Moreover, we find the pair length scale to be extremely short at the antinodal region where the pairing strength is maximized, with a length scale that is of the order of the in-plane lattice constant. This ultrashort pair length scale is ~ constant over a wide range of doping, which indicates that it is a fundamental characteristic of the pairing in cuprates. Work is ready for submission [3].

Other cuprate work of ours focussed on fitting electrical resistivity data as a function of temperature and for a wide range of dopings, sp as to extract power-law scattering rates and the temperature scales at which these scattering rates hold. This has lead to important new details in the doping phase diagram of the cuprate superconductors [4].

Pb-apatite framework as a generator of novel flat-band CuO based physics. A great amount of interest in the past few weeks has been focused on $CuPb_9(PO_4)_6O$ (Cu-doped lead apatite, aka LK-99), which was proposed to host room temperature superconductivity. A few weeks in, it now seems extremely unlikely that this compound actually hosts superconductivity. Nevertheless, our electronic structure calculations indicate that the electronic structure of this compound is very interesting, with the presence of CuO-based flat bands at the Fermi level if the original symmetry of the state can be maintained, i.e. if Jahn-Teller-style lattice distortions do not break the symmetry (Figs 4a,b). Following these observations, we proposed a new "road map" for obtaining new types of highly correlated electron physics, by placing Cu or Ni atoms in a framework of other atoms, as shown in Fig 4c-f. Therefore, finding an appropriate host structure for minimizing hybridization between the Cu (or Ni) and O while allowing them to still weakly interact should be a promising route for finding new interesting electronic phenomena, including high temperature superconductivity. From [5].

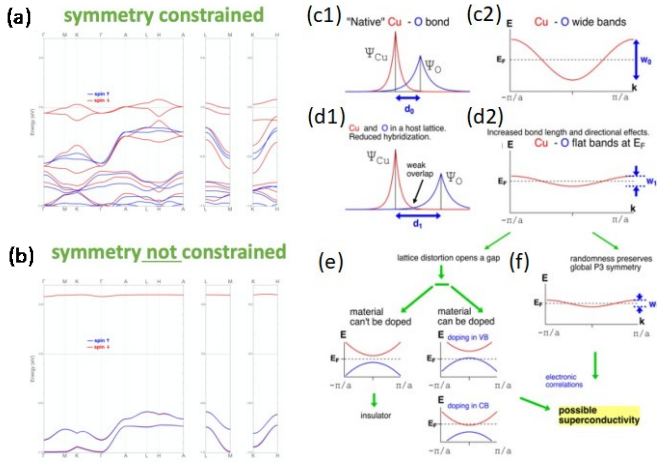

Fig 4. Calculated electronic structure of Cu-doped Pb-Apatite. (a) With the structure constrained to the nominally-observed P3 symmetry, the system has flat Cu-O bands at E_F that can support exotic physics. (b) With the constraints removed the system will tend to open gaps at E_F. (c)-(f) A "road map" for generating such flat band states by doping Ni or Cu into a general framework, with the final goal being high temperature superconductivity. From [5].

Magnetic topological materials - $MnBi_2Te_4$ and CuMnAs. While we don't have space in this abstract to discuss these results, we have published two papers on important magnetic topological materials. See the extended publication list.

Future plans. The landscape of novel superconductivity is as exciting and deep as ever, and ARPES has continued to advance in its ability to probe the most fundamental aspects of the electronic band structure, correlations, and pairing. Therefore, the future for ARPES of novel superconductors, especially when linked to increasingly sophisticated electronic structure calculations that can include the electronic correlations, is very bright. As an example we show a nearly-completed study of ours on the Fe-based superconductor YFe_2Ge_2. Heat capacity measurements on this material indicate a very large Sommerfeld coefficient, or mass enhancement. Our ARPES data (Fig 5) shows the nature of the greatly enhanced band masses and electronic correlations. In particular, we show that the "γ" band has an effective mass that is 40 times that of a free electron, which is the largest ever seen in an Fe-based superconductor. While our DFT-level electronic structure calculations are unable to account for the experimental data, our QSGW calculations, which explicitly include electronic correlations, do a superb job, as shown by the green lines in Fig 5b.

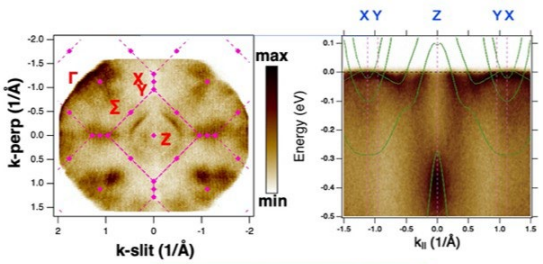

BAND	E_B (meV)	m_{eff} (m_e)	k_{F1} (1/Å)	v_F (eV Å)
α	25.05(46)	**6.64(8)**	0.2089(8)	0.24
β	61(1)	**16.1(2)**	0.507	0.241(2)
γ	-5.45(6)	**39.9(3)**	-	-

Fig 5. Flat bands at E_F in unconventional superconductor YFe_2Ge_2. Our ARPES data and QSGW-level electronic structure calculations (green lines panel b) show that this is the most strongly-correlated Fe-based superconductor [in progress].

We plan to continue to advance the state-of-the art of ARPES, coupled with the best electronic structure calculations, with the aim to unravel the nature and origins of novel superconductivity.

References

1. Haoxiang Li, Peipei Hao, Junjie Zhang, Kyle Gordon, A. Garrison Linn, Xinglong Chen, Hong Zheng, Xiaoqing Zhou, J.F. Mitchell, D. S. Dessau "Electronic structure and correlations in planar trilayer nickelate $Pr_4Ni_3O_8$" Sci Advances 9, eade4418 (2023)
2. D. M. Narayan, Peipei Hao, Rafał Kurleto, B. S. Berggren, A. G. Linn, C. Eckberg, M. Hashimoto, D. Lu, R. M. Fernandes, JP Paglione, D. S. Dessau "Evolution of Electronic Structure in Nematic Superconductor $Ba_{1-x}Sr_xNi_2As_2$" Under Review, Science Advances.
3. Haoxiang Li, Xiaoqing Zhou, Stephen Parham, Kyle N. Gordon, R. D. Zhong, J. Schneeloch, G. D. Gu, Y. Huang, H. Berger, G. B. Arnold, D. S. Dessau" Hyper-local Cooper pairs in the antinodal direction of cuprate superconductors" (Ready for submission)
4. Keiichi Harada, Yuki Teramoto, Tomohiro Usui, Kenji Itaka, Takenori Fujii, Takashi Noji, Haruka Taniguchi, Michiaki Matsukawa, Hajime Ishikawa, Koichi Kindo, Daniel S. Dessau, and Takao Watanabe "Revised phase diagram of the high-T_C cuprate superconductor Pb-doped $Bi_2Sr_2CaCu_2O_{8+\delta}$ revealed by anisotropic transport measurements" PHYSICAL REVIEW B **105**, 085131 (2022)
5. Rafal Kurleto, Stephan Lany, Dimitar Pashov, Swagata Acharya, Mark van Schilfgaarde, Daniel S. Dessau "Pb-apatite framework as a generator of novel flat-band CuO based physics", https://doi.org/10.48550/arXiv.2308.00698 (2023)

Publications (last 2 years)

1. Haoxiang Li, Peipei Hao, Junjie Zhang, Kyle Gordon, A. Garrison Linn, Xinglong Chen, Hong Zheng, Xiaoqing Zhou, J.F. Mitchell, D. S. Dessau "Electronic structure and correlations in planar trilayer nickelate $Pr_4Ni_3O_8$" Sci Advances 9, eade4418 (2023)
2. A. Garrison Linn, Peipei Hao, Kyle N. Gordon, Dushyant Narayan, Bryan S. Berggren, Nathaniel Speiser, Sonka Reimers, Richard P. Campion, Vıt Novak, Sarnjeet S. Dhesi, Timur K. Kim, Cephise Cacho, Libor Smejkal, Tomas Jungwirth, Jonathan D. Denlinger, Peter Wadley, and Daniel S. Dessau, "Experimental electronic structure of the electrically switchable antiferromagnet CuMnAs", NPJ Quantum Materials (2023) DOI 10.1038/s41535-023-00554-x
3. Keiichi Harada, Yuki Teramoto, Tomohiro Usui, Kenji Itaka, Takenori Fujii, Takashi Noji, Haruka Taniguchi, Michiaki Matsukawa, Hajime Ishikawa, Koichi Kindo, Daniel S. Dessau, and Takao Watanabe "Revised phase diagram of the high-T_c cuprate superconductor Pb-doped $Bi_2Sr_2CaCu_2O_{8+\delta}$ revealed by anisotropic transport measurements" PHYSICAL REVIEW B **105**, 085131 (2022)
4. Chaowei Hu, Anyuan Gao, Bryan Stephen Berggren, Hong Li, Rafał Kurleto, Dushyant Narayan, Ilija Zeljkovic, Dan Dessau, Suyang Xu, and Ni Ni "Growth, characterization, and Chern insulator state in $MnBi_2Te_4$ via the chemical vapor transport method" Phys. Rev. Materials 5, 124206 (2021)
5. Dimitar Pashov, Swagata Acharya, Stephan Lany, Daniel S. Dessau, Mark van Schilfgaarde "Multiple Slater determinants and strong spin-fluctuations as key ingredients of the electronic structure of electron- and hole-doped $Pb_{10-x}Cu_x(PO_4)_6O$" https://doi.org/10.48550/arXiv.2308.09900 (2023)
6. Rafal Kurleto, Stephan Lany, Dimitar Pashov, Swagata Acharya, Mark van Schilfgaarde, Daniel S. Dessau "Pb-apatite framework as a generator of novel flat-band CuO based physics", https://doi.org/10.48550/arXiv.2308.00698 (2023)

Poster Session 2

Digital Synthesis: A pathway to novel states of condensed matter

Anand Bhattacharya, Dillon Fong, Samuel Jiang (Argonne National Laboratory)

Self-identify keywords to describe your project: superconductivity, magnetism, spintronics, thin film heterostructures, transition metal compounds, molecular beam epitaxy, magnetotransport, scanning electron microscopy, x-ray scattering, spin transport.

Research Scope

In our program, we seek to create, explore and understand novel states of condensed matter and new functionalities that emerge at interfaces between different materials. These include collective states like interfacial magnetism and superconductivity, and interfacial topological states that may have relevance for spintronics and topological superconductivity. We seek to realize these states in materials synthesized with atomic layer-by-layer control using molecular beam epitaxy and related techniques. Thus, a significant part of our research is devoted to understanding growth processes that lead to these interfacial states and to improve our synthesis approaches. In the research presented here, we will focus on the formation of electron gases at the surfaces/interfaces of two perovskite oxides $SrTiO_3$ and $KTaO_3$, both 'quantum paraelectrics'. In $SrTiO_3$ the interfacial electron gas is superconducting for all known orientations – the [001], [110] and [111], with similar T_c's of approximately 0.2 – 0.3K. On the other hand, in $KTaO_3$, the superconductivity is highly orientation selective, with the [111] interface having a maximum T_c of 2.2 K, the [110] interface with maximum T_c of $\sim$ 1 K, while the [001] interface does not superconduct [Liu et al., *Science* 2021]. We have developed a theoretical model that explains this contrast [Liu et al., *Nat. Comm.* 2023]. Despite the striking similarities between dielectric properties of $SrTiO_3$ and $KTaO_3$, the striking orientation selectivity in $KTaO_3$ raises questions about its origin – these include the different spin-orbit couplings, and chemical/structural origins of the electron gas formation. In recent work, using a combined in-situ x-ray and ARPES study of $SrTiO_3$ films during growth, we unveiled a novel mechanism for the origin of two-dimensional electron gas formation in [001] oriented $SrTiO_3$, namely the formation of a TiO_2 double layer at the surface [Yan et al., *Adv. Mater*. 2022]. In our presentation (poster) we will explore these aspects in some detail.

Recent Progress

Orientation selective superconductivity in $KTaO_3$ interfaces and its origins: The mechanism for Cooper pairs to form in unconventional superconductors is often elusive because experimental signatures that connect to a specific pairing mechanism are rare. $KTaO_3$ is a quantum paraelectric and whose interfaces can become superconducting on doping with electrons [Liu et al., *Science* 2021]. We observe distinct dependences of the superconducting transition temperature T_c on carrier density n_{2D} for electron gases formed at $KTaO_3$ (111), (001) and (110) interfaces. For the (111) interface, a remarkable linear dependence of T_c on n_{2D} is observed over a range of nearly one order of magnitude. Further, our study of the dependence of superconductivity on gate electric

fields reveals the role of the interface in mediating superconductivity. We find that the extreme sensitivity of superconductivity to crystallographic orientation can be explained by pairing via inter-orbital interactions induced by an inversion-breaking transverse optical (TO1) phonon and quantum confinement. These TO1 phonons soften at low temperatures leading to a diverging dielectric constant and 'quantum paralectric' properties, and typically do not couple to electrons at the Fermi surface. The inter-orbital interaction makes this possible. The calculated dependence of T_c on n_{2D} using our proposed mechanism is also consistent with experimental findings. Our study may shed light on the pairing mechanism in other superconducting quantum paraelectrics and polar materials [Liu et al., *Nat. Comm.* 2023].

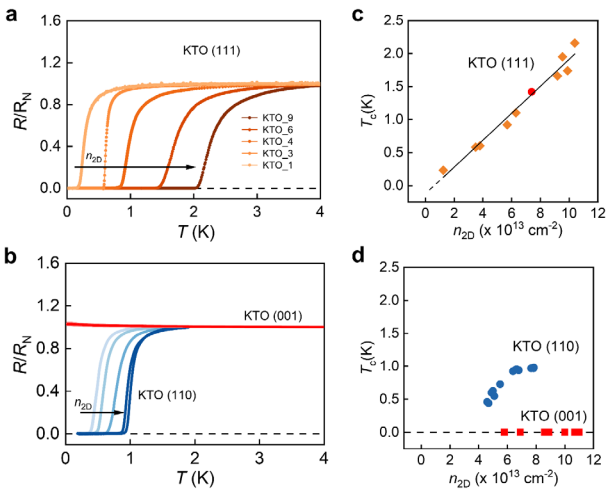

Fig. 1. The ratio of the resistance R_s/R_N vs. temperature measured for (a) KTO (111) samples (b) and KTO (001), (110) samples, with varying n_{2D}. The direction of the arrow indicates the increase of n_{2D}. **c, d** n_{2D} dependence of T_c for KTO (111) samples shown in (**a**) and KTO (001), (110) samples shown in (**b**), respectively.

Origin of the 2D Electron Gas at the $SrTiO_3$ surface: Bulk $SrTiO_3$ is a well-known band insulator and the most common substrate used in the field of complex oxide heterostructures. Its surface and interface with other oxides, however, have demonstrated a variety of remarkable behaviors distinct from those expected. In this work, using a suite of *in situ* techniques to monitor both the atomic and electronic structures of the $SrTiO_3$ (001) surface prior to and during growth, the disappearance and re-appearance of a 2D electron gas (2DEG) is observed after the completion of each SrO and TiO_2 monolayer, respectively. The 2DEG is identified with the TiO_2 double layer present at the initial $SrTiO_3$ surface, which gives rise to a surface potential and mobile electrons due to vacancies within the TiO_{2-x} adlayer. Much like the electronic reconstruction discovered in other systems, two atomic planes are required, here supplied by the double layer. The combined in situ scattering/spectroscopy findings resolve a number of longstanding issues associated with complex oxide interfaces, facilitating the employment of atomic-scale defect engineering in oxide electronics [Yan et al., *Adv. Mater.* 2022].

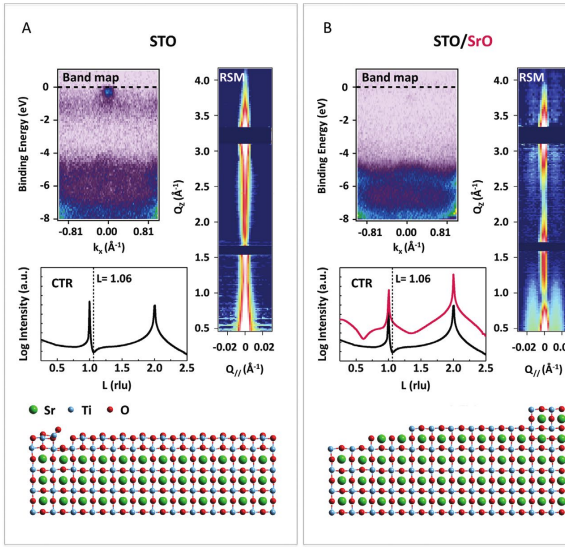

Fig. 2. Combined ARPES band maps and x-ray crystal truncation rods of $SrTiO_3$ (001) surfaces with (a) TiO_2 and (b) SrO terminations.

Future Plans

Understanding the structural and chemical origins of the 2D electron gas at interfaces of $KTaO_3$: Given our investigations $SrTiO_3$ interfaces and our findings in interfacial 2DEGs in $KTaO_3$, it is a logical progression to study the process of 2DEG formation at $KTaO_3$ surfaces in detail. In particular, we'd like to understand the following: (i) How diffusion processes for oxygen vacancies differ between $KTaO_3$ and $SrTiO_3$, and how does that influence electron gas formation (ii) Determine how the different orientations of $KTaO_3$ differ in the manner in which the electron gas forms. (iii) The degree to which inversion symmetry breaking near the interface leads to polar distortions at different interfaces, and determine its consequences for electronic structure.

With the impending upgrade of the APS to a more coherent source, it will be possible to investigate the dynamics of thin film growth processes, shining new light on the behavior of adatoms and 2D island nucleation during epitaxial growth.[1] We will conduct similar *in situ* X-ray photon correlation spectroscopy (XPCS) studies during the growth/reduction of different complex oxides including $KTaO_3$ and exploit the ability to transfer samples directly between the MBE system and a nearby angle-resolved photoemission system to measure the accompanying electronic structure.

Ongoing studies of interfacial superconductivity in $KTaO_3$: Our theoretical work (with Mike Norman) suggests several paths to tune superconductivity and probe its underlying mechanism. We have several ongoing/planned experiments to elucidate and perhaps also exploit the superconducting state found at $KTaO_3$ interfaces. These include: (i) Studies of the kinetic inductance of the superconducting electron gas at different interfaces of $KTaO_3$. (ii) Tunneling spectroscopy of the superconducting state in $KTaO_3$ 2DEGs in different orientations (iii) Creating novel electronic states in patterned 2DEGs and nano-wires made out of $KTaO_3$. (iv) THz spectroscopy of the two-dimensional interfacial states in $KTaO_3$ (with Haidan Wen). (v) Consequences of spin-momentum locking in $KTaO_3$ interfacial 2DEGs.

Reduction of $Nd_{0.8}Sr_{0.2}NiO_3$: The synthesis of epitaxial Sr-doped nickelates by pulsed laser deposition and the subsequent topotactic reduction procedure are the key processes essential to achieving superconductivity in nickelate heterostructures. Topotactic reduction, however, is a complex process involving breakdown of the hydride molecule, diffusion of the hydrogen throughout the oxide, and removal of particular ions from the octahedral framework of the perovskite to achieve the square-planar structure. Here, we will employ *in situ* synchrotron X-ray scattering to monitor the topotactic reduction process for $Nd_{0.8}Sr_{0.2}NiO_3$ films grown on $SrTiO_3$ (001) substrates.

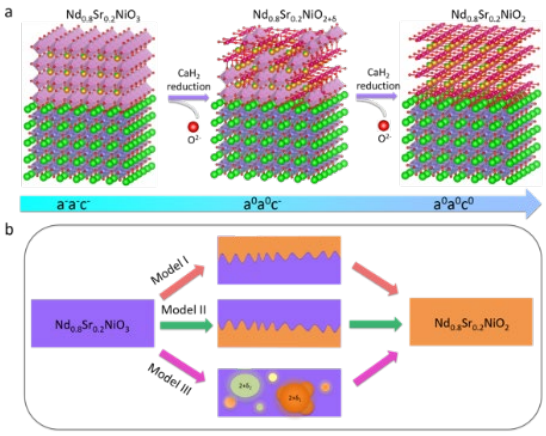

Fig. 3. Schematic of the reduction reaction for nickelate heterostructures illustrating different paths for the transformation and the change in crystal symmetry.

Charge-spin conversion in thin films of A15 compounds: The A15 family of compounds such as Ta_3Sb and Ti_3Pt have been predicted to have large intrinsic spin Hall conductivities because of the large spin Berry curvature of its electronic band structure, making them attractive for spintronic applications.[2] Due to the bulk superconductivity, the A15 superconductors are also promising candidates for the realization of topological superconductivity and Majorana fermions.[3] We have synthesized thin films of A15 phase Ta_3Sb by sputter deposition and using second-harmonic Hall measurements we have established that the material has very large spin-orbit torque and spin Hall conductivity.[4] We are also exploring the possible existence of unconventional superconductivity in mesoscale rings of A15 compounds.

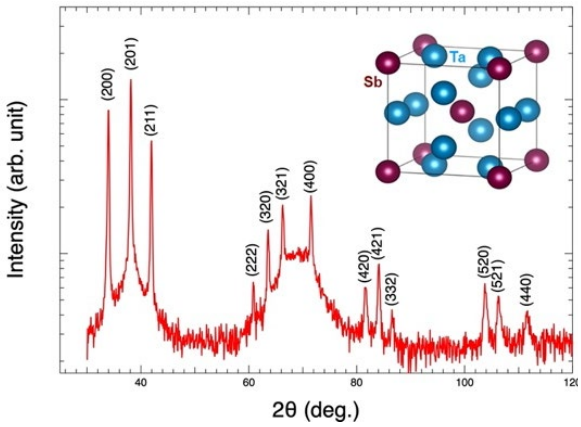

Fig. 4 X-ray diffraction pattern of a sputter-deposited Ta_3Sb thin film showing all the expected crystallographic peaks. Inset: Crystal structure of A15-type Ta_3Sb. (arXiv 2308.03220)

References

[1] G. Ju, D. Xu, M. J. highland, C. Thompson, H Zhou, J. A. Eastman, P. H. Fuoss, P. Zapol, H. Kim and G. B. Stephenson, Coherent x-ray spectroscopy reveals the persistence of island arrangements during layer-by-layer growth, *Nat. Phys.* **15**, 589 (2019).

[2] E. Derunova, Y. Sun, C. Felser, S. S. P. Parkin, B. Yan and M. N. Ali, Giant intrinsic spin Hall effect in W_3Ta and other A15 superconductors, *Sci Adv* **5**, eaav8575, (2019)

[3] M. Kim, C.-Z. Wang & K.-M. Ho, Topological states in A15 superconductors. *Physical Review B* **99**, 224506 (2019).

[4] J.S. Jiang, Q. Du, U. Welp, R. Chapai, H. Arava, Y. Liu, Y Li, J. Pearson, A. Bhattacharya, H. Park, A15 Phase Ta_3Sb films: Direct Synthesis and Giant Spin-Orbit Effects, arXiv:2308.03220.

Publications (10 most relevant)

1. Changjiang Liu, Xianjing Zhou, Deshun Hong, Brandon Fisher, Hong Zheng, Samuel Jiang, John Pearson, Dafei Jin, Michael R Norman, Anand Bhattacharya, Tunable superconductivity at the oxide-insulator/$KTaO_3$ interface and its origin, *Nature Communications* **14**, 951 (2023).

2. Q. Zhang, G. Hu, V. Starchenko, G. Wan, E. M. Dufresne, Y. Dong, H. Liu, H. Zhou, H. Jeen, K. Saritas, J. T. Krogel, F. A. Reboredo, H. N. Lee, A. R. Sandy, I. Calvo-Almazan, P. Ganesh, and D. D. Fong, Phase transition dynamics in a complex oxide heterostructures, *Phys. Rev. Lett.* **129,** 235701 (2022).

3. M. Yu, C. Liu, D. Yang, X. Yan, Q. Du, D. Fong, A. Bhattacharya, P. Irvin, and J. Levy, Nanoscale control of the metal-insulator transition at $LaAlO_3/KTaO_3(110)$ and $LaAlO_3/KTaO_3(111)$ interfaces, *Nano Lett.* **22,** 6062 (2022).

4. H. Liu, Y. Dong, M. Galib, Z. Cai, L. Stan, L. Zhang, A. Suwardi, J. Wu, J. Cao, C. K. I. Tan, S. K. R. S. Sankaranarayanan, B. Narayanan, H. Zhou, and D. D. Fong, Controlled Formation of Conduction Channels in Memristive Devices Observed by X-ray Multimodal Imaging, *Adv. Mater.* **34,** 2203209 (2022).

5. T. J. Park, S. Deng, S. Manna, A. N. M. Naiful Islam, H. Yu, Y. Yuan, D. D. Fong, A. A. Chubykin, A. Sengupta, S. K. R. S. Sankaranarayanan, and S. Ramanathan, Complex oxides for brain-inspired computing: A review, A*dv. Mater.* **34,** 2203352 (2022).

6. X. Yan, F. Wrobel, I-Cheng Tung, H. Zhou, H. Hong, F. Rodolakis, A. Bhattacharya, J. L. MChesney, and D. D. Fong, Origin of the 2D electron gas at the $SrTiO_3$ surface, *Adv. Mater.* **34,** 2200866 (2022).

7. H. Hong ; J. L. McChesney, F. Wrobel, X. Yan, Y. Li; A. Bhattacharya, A.; D. D. Fong. "In situ study on the evolution of atomic and electronic structure of $LaTiO_3/SrTiO_3$ system." *Physical Review Materials 6*, no. 1, L011401 (2022).

8. Y. Li, F. Wrobel, Y. Cheng, X. Yan, H. Cao, Z. Zhang, A. Bhattacharya, J. Sun, H. Hong, H. Zhou, H. Wang, and D. D. Fong, Self-healing growth of $LaNiO_3$ on a mixed-terminated perovskite surface, *ACS Appl. Mater. & Inter.* **14,** 16928 (2022).

9. Changjiang Liu, Yongming Luo, Deshun Hong, Steven S-L Zhang, Brandon Fisher, John E Pearson, J Samuel Jiang, Axel Hoffmann, Anand Bhattacharya, Voltage control of magnon spin currents in antiferromagnetic Cr_2O_3, *Science Advances* **7**, eabg1669 (2021).

10. M. Yu, C. Liu, D. Yang, X. Yan, Q. Du, D. D. Fong, A. Bhattacharya, P. Irvin, J. Levy, Nanoscale control of the metal-insulator transition at $LaAlO_3/KTaO_3$ interface, *Nano Lett. 22*, 15, 6062-6068 (2022).

Emerging Materials

John F. Mitchell (Argonne), Daniel Phelan (Argonne); Nirmal Ghimire (Notre Dame)

Keywords: magnetism, single crystals, transition metal compounds, topological materials, x-ray scattering

Research Scope

Emerging Materials pursues experimental studies of quantum materials, particularly correlated electron oxides, topological matter, and quantum magnetism. We specialize in designing and then growing target quantum materials—usually as single crystals—characterizing their magnetic, electrical, and thermodynamic properties, and leveraging synchrotron X-ray and neutron scattering techniques to investigate their vibrational, structural, and magnetostructural characteristics. An organizing principle of our research is the study of materials that either break or are poised to break degeneracies in structural, electronic, or magnetic degrees of freedom. Along these lines, our research divides into three focus areas: (1) *charge disproportionation and self-organization in correlated oxides*. Here, we study stripes, charge and spin density waves, and charge order, with an eye towards understanding how these forms of order emerge, behave, and respond, and how they relate to superconductivity; (2) *degeneracy breaking and chirality in topological and superconducting systems*. Here, we explore materials whose properties derive from either real- or *k*-space topology, such as magnetic textures or Weyl nodes. (3) *lifting spin degeneracies in quantum magnets*. Here, we probe the interplay between geometrical frustration, competing and frustrated exchange interactions, and randomness in magnets.

Recent Progress

***Competing Stripes and Metallic States*:** We have concentrated on nickelate materials to understand the formation and consequences of charge and spin stripes, as well as charge density waves (CDWs) and spin density waves (SDWs) in strongly correlated transition metal oxides. We identified the square-planar trilayer nickelate system, $R_4Ni_3O_8$, as a platform for investigating the evolution from a correlated metal ($Pr_4Ni_3O_8$) to a spin- and charge stripe

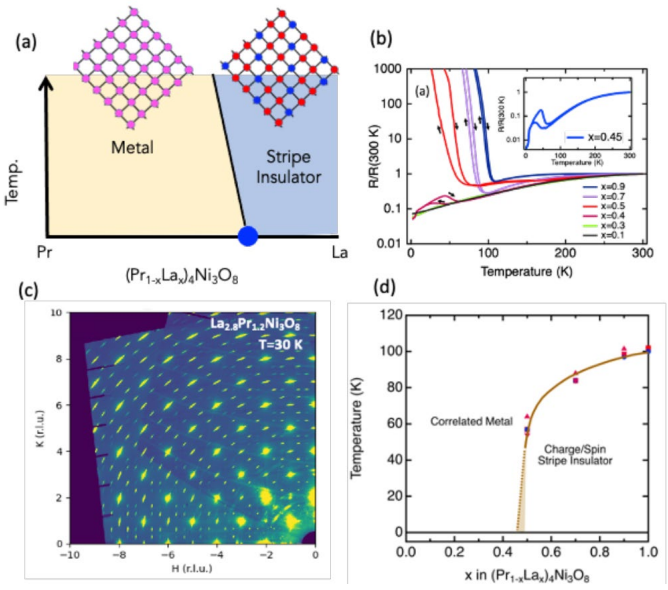

Fig. 1: Competing phases in $(Pr_{1-x}La_x)_4Ni_3O_8$. (a) schematic phase boundary indicating T=0 metal-insulator transition; (b) normalized resistivity vs. temperature; (c) single crystals X-ray diffraction for an x=0.7 specimen in the insulating phase showing superlattice spots; (d) experimental phase diagram.

insulator ($La_4Ni_3O_8$) [1]. We grew single crystals of $(Pr_{1-x}La_x)_4Ni_3O_8$, and then combined thermodynamic, transport, magnetic, and synchrotron X-ray single crystal diffraction measurements to locate the T=0 metal-insulator transition at $x \approx 0.45$. As both the transport data and the phase diagram show, this is a sharp, first-order-like transition both in T, and x (Fig. 1(b,d)). X-ray diffraction (Fig. 1(c)) shows the superlattice for an x=0.7 with in-plane $\boldsymbol{q}$=(1/3,1/3), confirming the persistence of the charge stripe phase found in the x=1.0 endmember. Remarkably, the correlation length in the NiO_2 planes seems unaffected by the substitution. Rather than a continuous, second-order-like process that might have harbored a quantum critical point, our findings collectively favor a percolation scenario (i.e., electronically inhomogeneous) for the transition. One would predict in this case that vestigial signatures of the charge- and spin-stripe phase should persist into the metallic region of the phase diagram.

Fermi surface 'building blocks' in the Kagome superconductor CsV_3Sb_5: The recently discovered Kagome lattice compounds AV_3Sb_5 (CVS, A = K, Rb, Cs) offer a complex interplay of superconductivity, charge density wave (CDW) order and non-trivial topology of the electronic band structure. We performed quantum oscillation measurements in pulsed magnetic fields up to 86 T, using the tunnel diode technique [2]. The high-field data reveal a sequence of magnetic breakdown orbits that allowed us to construct a model for the folded Fermi surface of CsV_3Sb_5, shown in Fig. 2(a,b) The dominant features are large triangular Fermi surface sheets that cover almost half the folded Brillouin zone, highlighted in magenta (ϖ band with a frequency of 1943 T) and green (ξ_2 band at 804 T). These orbits act as "building blocks" that combine one-by-one to form a series of approximately equally spaced frequencies that dominate the high-field oscillation spectrum shown in Fig. 2(c). In addition to charting this folded Fermi surface, we have extracted the Berry phases of the electron orbits from Landau level fan diagrams near the quantum limit without the need for extrapolations, thereby unambiguously establishing the non-trivial topological character of several electron bands in this Kagome lattice superconductor.

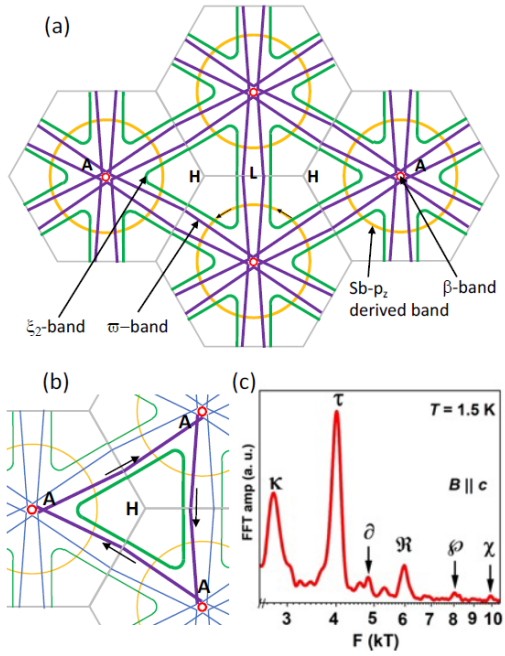

Fig. 2: (a) Schematic of the 2x2 reconstructed Fermi surface of CsV_3Sb_5 for $k_z = \pm\pi/c$ in repeated zones. Capital letters refer to Brillouin zone points (b) Enlarged schematic of the ξ_2 and ϖ orbits. (c) High-frequency section of the oscillation spectrum at 1.5 K on a log field scale. The κ orbit corresponds to the sum of the ξ_2 and ϖ orbits, while the τ orbit represents two basic triangular ϖ units. Correspondingly, ℜ, ℘, and $\mathcal{X}$ contain 3, 4 and 5 triangular building blocks. ∂ is the sum of ξ_2 and τ.

Surfing on geometrically frustrated magnets: Fe_2TiO_5, in which Fe^{3+} spins lie on double corrugated chains with frustrated exchange interactions (Fig 3(a)), exhibits an anisotropic spin-glass transition. This anisotropy is unexpected given the notionally L=0 outer shell ($3d^5$) configuration of Fe^{2+}. Collaborating with Art Ramirez at UC-Santa Cruz and Stephan Rosenkranz at Argonne, we undertook a campaign to understand the unusual magnetism in this compound. First, we discovered via neutron diffraction that nanoscale antiferromagnetic spin clusters, whose elliptical shape inspired the nickname "surfboards," emerge during cooling, leading to non-Curie Weiss like susceptibility [3]. We proposed that transverse fluctuations of surfboard magnetization promote the uniaxial freezing, expressing a magnetic van der Waals-like interaction. Turning to inelastic neutron scattering, we observed an overdamped zero-energy mode associated with the spin freezing on THz timescales, but we also unexpectedly found remanent fluctuating correlations below T_g, probably a consequence of disorder in the system [4]. Finally, we investigated the effect of introducing magnetic vacancies via Ga substitution on the Fe^{3+} sites [5]. Our idea here was to modulate both disorder and relative exchange interactions through the magnetic vacancy concentration. We grew a large, Ga-doped single crystal that was used for neutron diffraction measurements (Fig. 3(b)). This study revealed that as the vacancy concentration is initially increased, the surfboards remain, but they shrink in size, while T_g drops in concert, corroborating changes in the heat capacity and magnetic susceptibility.

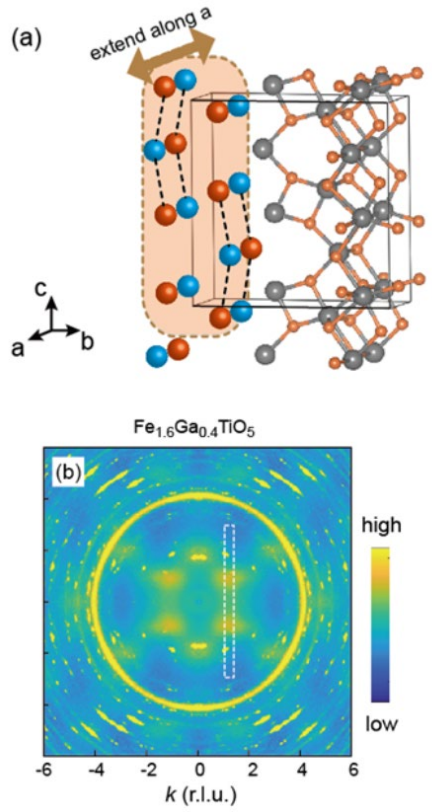

Fig. 3: Neutron diffuse scattering in Fe_2TiO_5 (a) Crystal structure of Fe_2TiO_5. Larger spheres represent Fe/Ti atoms. Small spheres represent oxygen atoms. A "surfboard" region is highlighted; within this region the red and blue denote ordered spins parallel and antiparallel to the a-axis. (b) Neutron diffraction data. The intense "blobs" near the center are modeled in real space as surfboards.

Other Accomplishments: Mapped Fermi surface of $Pr_4Ni_3O_8$ confirming similarity to overdoped cuprates; identified magnetization-driven Lifshitz transition in YMn_6Sn_6; characterized superconducting behavior in eight-fold degenerate Ta_3Sb; measured and modeled antiferromagnetic order and spin dynamics in $Tb_2Ir_3Ga_9$; explored the gap structure of the topological superconductor candidate Ti_3Sb.

Future Plans

Charge disproportionation and self-organization in correlated oxides: We will use nickel oxides as a platform to probe nematicity and its evolution from correlated metals in pristine stripe phases, and to pursue contrarian routes to superconductivity in bulk nickelates. We will also explore new views on electron-phonon instabilities in charge separated perovskite superconductors.

Degeneracy breaking and chirality in topological and superconducting systems: We will probe the effects of symmetry breaking and chirality on topological electronic behaviors coupled to magnetism in novel Kagome lattice systems, deterministically control degenerate Weyl nodes using symmetry-breaking fields, test predictions for controlling Berry phase and anomalous Hall effects in perovskite oxides, and sculpt artificial structures from bulk crystals designed to manifest non-reciprocal transport in chiral domain states with an eye toward chiral superconductivity.

Lifting spin degeneracies in quantum magnets: We will synthesize new families of spin chain systems based on rare square planar Ni^{2+} structures to understand their spin states, short- and long-range magnetic ordering, and possible Haldane spin-gap physics; and we will study short-range magnetic order in a family of pentagonal lattices with controllable exchange pathways to test models of hidden energy scales in frustrated magnets.

References

[1] X. Chen, H. Zheng, D. Phelan, H. Zheng, S. Lapidus, M.J. Krogstad, R. Osborn, S. Rosenkranz, and J.F. Mitchell. *Competing charge/cpin-stripe and correlated metal phases in trilayer nickelates* $(Pr_{1-x}La_x)_4Ni_3O_8$, Chem. Mater. **34**, 4560 (2022).

[2] R. Chapai, M. Leroiux, V. Oliverio, D. Vignolles, N. Bruyuant, M.P. Smylie, D.Y. Chung, M.G. Kanatzidis, W.-K. Kwok, J.F. Mitchell, and U. Welp, *Magnetic breakdown and topology in the Kagome superconductor* CsV_3Sb_5 *under high magnetic field*, Phys. Rev. Lett. **130**, 126401 (2023).

[3] P.G. LaBarre, D. Phelan, Y. Xin, F. Ye, T. Besara, T. Siegrist, S.V. Syzranov, S. Rosenkranz, and A.P. Ramirez, *Fluctuation-induced interactions and the spin-glass transition in* Fe_2TiO_5, Phys. Rev. B **103**, L220404 (2021).

[4] Y. Li, P.G. LaBarre, D.M. Pajerowski, A.P. Ramirez, S. Rosenkranz, and D. Phelan, *Neutron scattering study of fluctuating and static spin correlations in the anisotropic spin glass* Fe_2TiO_5", Phys. Rev. B **107**, 014405 (2023).

[5] Y. Li, D. Phelan, F. Ye, H. Zheng, E. Krivyakina, A. Samarakoon, P.G. LaBarre, J. Neu, T. Siegrist, S. Rosenkranz, S.V. Syzranov, and A.P. Ramirez, *Evolution of magnetic surfboards and spin glass behavior in* $(Fe_{1-p}Ga_p)_2TiO_5$, accepted to J. Phys. Condens. Matt. (2023).

Publications

1. R. Chapai, M. Leroiux, V. Oliverio, D. Vignolles, N. Bruyuant, M.P. Smylie, D.Y. Chung, M.G. Kanatzidis, W.-K. Kwok, J.F. Mitchell, and U. Welp, *Magnetic breakdown and topology in the Kagome superconductor CsV_3Sb_5 under high magnetic field*, Phys. Rev. Lett. **130**, 126401 (2023).

2. R. Chapai, M.P. Smylie, H. Hebbeker, D.Y. Chung, W.-K. Kwok, J.F. Mitchell, and U. Welp, *Superconducting properties and gap structure of the topological superconductor candidate Ti_3Sb*, Phys. Rev. B **107**, 104504 (2023).

3. Y. Li, P.G. LaBarre, D.M. Pajerowski, A.P. Ramirez, S. Rosenkranz, and D. Phelan, *Neutron scattering study of fluctuating and static spin correlations in the anisotropic spin glass Fe_2TiO_5*, Phys. Rev. B **107**, 014405 (2023).

4. H. Li, P. Hao, J. Zhang, K. Gordon, A. Garrison Linn, X. Chen, H. Zheng, X. Zhou, J.F. Mitchell, and D.S. Dessau, *Electronic structure and correlations in planar trilayer nickelate $Pr_4Ni_3O_8$*, Science Advances **9**, eade4418 (2023).

5. X. Chen, H. Zheng, D. Phelan, H. Zheng, S. Lapidus, M.J. Krogstad, R. Osborn, S. Rosenkranz, and J.F. Mitchell. *Competing charge/spin-stripe and correlated metal phases in trilayer nickelates $(Pr_{1-x}La_x)_4Ni_3O_8$*, Chem. Mater. **34**, 4560 (2022).

6. B. X. Wang, M.J. Krogstad, H. Zheng, R. Osborn, S. Rosenkranz, and D. Phelan, *Active and passive defects in tetragonal tungsten bronze relaxor ferroelectrics*, J. Phys.: Condens. Matter **34**, 405401 (2022).

7. R. Chapai, A. Rydh, M.P. Smylie, D.Y. Chung, H. Zheng, A.E. Koshelev, J.E. Pearson, W.-K. Kwok, J.F. Mitchell, and U. Welp, *Superconducting properties of the spin Hall candidate Ta_3Sb with eightfold degeneracy*, Phys. Rev. B **105**, 184510 (2022).

8. P.P. Orth, D. Phelan, J. Zhao, H. Zheng, J.F. Mitchell, C. Leighton, and R.M. Fernandes, *Essential role of magnetic frustration in the phase diagrams of doped cobaltites*, Phys. Rev. Mater. **6**, L071402 (2022).

9. Y. Shen, JSears, G. Fabbris, J. Li, J. Pellicari, I. Jarrige, X. He, I. Bozovic, M. Mitrano, J. Zhang, J.F. Mitchell, A.S. Botana, V. Bisogni, M.R. Norman, S. Johnston, and M.P.M. Dean, *Role of oxygen states in the low valence nickelate $La_4Ni_3O_8$*, Phys. Rev. X **12**, 011055 (2022).

10. K.M. Taddei, L. Yi, L.D. Sanjeewa, Y. Li, J. Xing, C. de la Cruz, D. Phelan, A.S. Sefat, and D.S. Parker, *Single pair of Weyl nodes in the spin-canted structure of $EuCd_2As_2$*, Phys. Rev. B **105**, L140401 (2022).

Magnetism and Topology in Kagome and van der Waals Systems

Ming Yi, Rice University

Keywords: magnetism, topology, 2D and layered crystals, transition metal compounds, topological materials, ARPES

Research Scope

The scope of this project is to advance the understanding of the nature of low dimensional magnetism in correlated quantum materials via the measurement of the single-particle spectral function through angle-resolved photoemission spectroscopy (ARPES). With advanced understanding, we also aim to explore the control and tuning of the magnetism. We have been primarily targeting two material families, the van der Waals (vdW) ferromagnets and the kagome magnets. The vdW magnets are a class of materials that exhibit long range magnetic order even down to the 2D limit. They provide a rich platform for probing low dimensional magnetism and are also known to be highly susceptible to tuning due to the vdW nature. Amongst the vdW magnets, we have been exploring both the semiconducting members $Cr_2Ge_2Te_6$ and $Cr_2Si_2Te_6$, as well as the metallic family Fe_nGeTe_2 (n=3, 5). The kagome system is a structural family consisting of corner-sharing triangles that exhibit geometric frustration. Analogous to the magnetic frustration on kagome insulators, when realized in the metallic regime, the geometric frustration on a kagome lattice leads to a destructive interference of the electronic wavefunction such that the kinetic energy is quenched, leading to flat electronic bands in addition to dispersive bands that exhibit singularities including Van Hove Singularities (VHSs) and Dirac crossings. The large density of states associated with the flat bands as well as the VHSs could lead to electronic instabilities that result in emergent electronic orders. In recent years, a wide range of correlated phases have been reported in kagome metals, including magnetism, charge density wave, nematicity, and superconductivity. We have been focusing on metallic kagome systems that exhibit magnetism, in particular hexagonal FeGe, with the goal of deepen understanding of the origin of magnetism as well as its interaction with the other electronic orders associated with the kagome lattice.

Recent Progress

1. van der Waals ferromagnets

The $Cr_2Ge_2Te_6$ system is electrically insulating and exhibits a Curie temperature T_C of 65 K. We have recently found a clear response of the electronic structure to a dimensional crossover in the form of two distinct temperature scales marking onsets of modifications in the electronic structure. Combined with neutron scattering, density functional theory calculations, and Monte Carlo simulations, we find that the electronic system can be consistently understood to respond sequentially to the distinct temperatures at which in-plane and out-of-plane spin correlations exceed a characteristic length scale. Our findings reveal the sensitivity of the orbital-selective

electronic structure for probing the dynamical evolution of local moment correlations in vdW insulating magnets [1].

The Fe_nGeTe_2 (n=3, 5) (FGT) systems, in contrast, are metallic and exhibit a combination of local moments and itinerant magnetism. The 312 members (Fe_3GeTe_2 and Fe_3GaTe_2) are isostructural yet exhibit Curie temperatures differing by a factor of ~1.5, with the Ga version having a T_C of 360K and the Ge version having a T_C of 220K. Through detailed temperature dependence of the electronic structure of these two systems across their respective T_Cs, we find the modifications to the electronic structure to deviate strongly from a Stoner-type itinerant magnetism, and instead evidences a large contribution from local moments [2].

The 512 member of the FGT system is even more interesting. Building off from our previous ARPES measurements of the 512 system in the past two years, we have finally come to a consistent understanding of the dichotomy of the electronic structure of this system after a comprehensive collaboration with scanning tunneling microscopy (STM), density functional theory (DFT), second harmonic generation (SHG), synchrotron-based X-Ray diffraction (XRD), and theoretical model [3]. We find an electronic phase switching between a magnetic Dirac nodal line phase and a topological flat band phase in $Fe_{5-\delta}GeTe_2$ using thermal annealing and quenching. We demonstrate that the switching of electronic properties is associated with a crystal symmetry change driven by an Fe site ordering that is modified in the thermal annealing process. With random occupancy of the Fe sites, inversion symmetry is globally preserved, leading to the observation of magnetic Dirac nodal lines. When the Fe site occupancy orders, inversion symmetry is broken and the Dirac degeneracy is lifted (Fig. 1). Moreover, the ordered Fe sites form a clover sublattice that is protected by chiral symmetry and harbors geometric frustration, resulting in topological flat bands. We further demonstrate that this switching is non-volatile and reversibly controlled via thermal annealing and quenching. Our work not only reveals a rich variety of quantum phases emergent in 2D van der Waals ferromagnets, but also uncovers the potential of utilizing site occupancy as a novel degree of

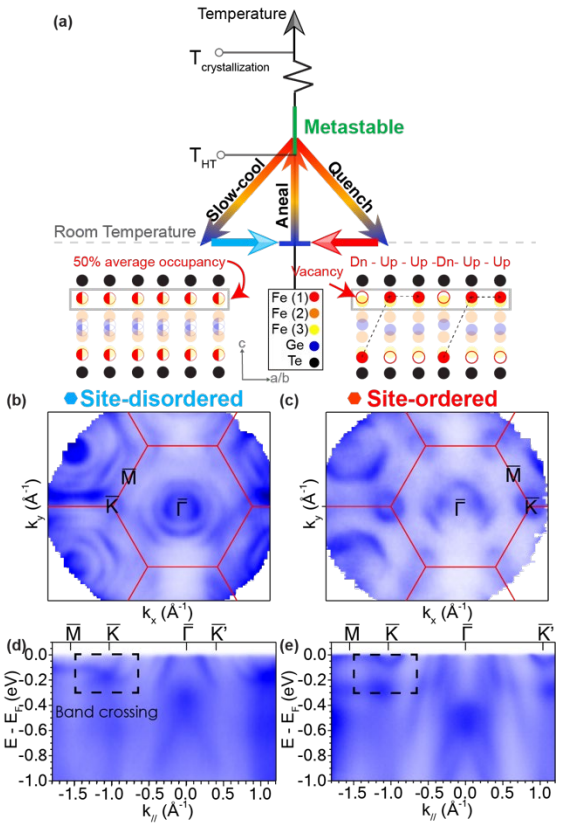

Figure 4 Electronic switching in Fe_5GeTe_2. (a) Two stable phases exist in Fe_5GeTe_2, one with 50% random occupation of Fe(1) site (site-disordered) and the other with up-down-down occupation of Fe(1) sites (site-ordered). The two phases can be reversibly switched via a thermal process. (b), (c) Measured Fermi surfaces of site-disordered and site-ordered phases, respectively. (d)-(e) Band dispersions for the two phases. Adapted from Ref. [3].

freedom for tuning symmetry and therefore topology in quantum materials for the realization of exotic emergent phases.

2. Magnetism in Kagome Lattices

In the past year, we have also expanded our material platforms to kagome magnets. In particular, we have extensively explored the kagome magnet FeGe. Made of corner sharing triangles in 2D, kagome lattice materials are hosts of a plethora of correlated electronic phases including exotic magnetism, charge density wave (CDW), nematicity and superconductivity. One of the most intensely studied order in the past few years is a 2x2 CDW order, which has been theoretically predicted to occur in kagome lattices due to the nesting of VHSs in the band structure. In the past year, we discovered the presence of such a CDW order in a magnetic kagome lattice, FeGe [4]. Through comprehensive study via ARPES, neutron scattering, magnetotransport, STM, we come to understand that the magnetic order of the Fe moments helps to bring to the chemical potential the VHSs to enable such a CDW order [5].

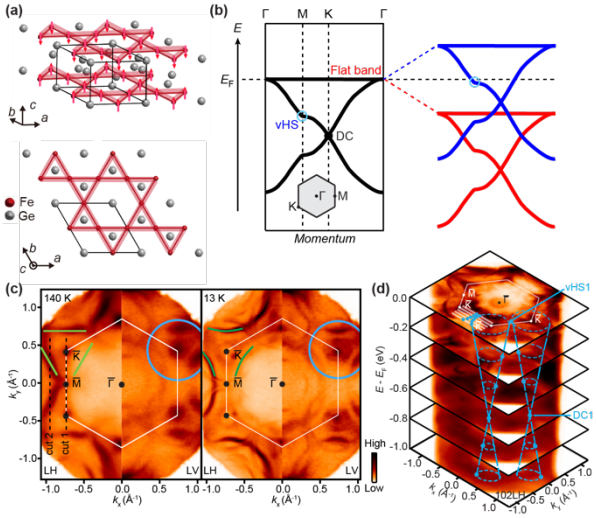

Figure 5 Magnetic kagome FeGe. (a) Lattice structure of kagome FeGe and the A-type AFM order of the Fe sites. (b) Schematic of the effect of the A-type AFM order on the kagome tight binding band structure: band splitting into the spin majority and spin minority states within each ferromagnetic layer. (c) Measured Fermi surfaces across the CDW transition. The green and blue lines mark the Fermi pockets formed by the VHSs. (d) 3D electronic structure showing the VHS at M and Dirac points at K points of the Brillouin zone. Adapted from Ref. [5].

Future Plans

1. van der Waals ferromagnets

Having established the switchable electronic phases in Fe_5GeTe_2, our goal for next year is two-fold. First, we plan to use temperature dependence measurements to probe the microscopic origin of the magnetism in the distinct electronic phases. In our preliminary data, we observe very distinct behaviors of the electronic structures in the two electronic phases. In the phase with random Fe occupation, we observe a very sudden coherence-incoherence transition at 100K. In the phase with ordered Fe vacancies, we observe no such transition, but instead observe the merging together of two spin-polarized flat bands across T_C—the only compound amongst the FGT family that exhibits such indication that itinerant electrons contribute to magnetism. The distinct behavior of the electronic structure for these otherwise iso-stoichiometric phases suggest that the Fe(1) site ordering plays a crucial role in dictating the magnetic order in FGT. The second goal for this material is to explore laser heating to switch between the two electronic phases. This can be carried out by the combination of micro-ARPES and a laser source with a small beamspot. The motivation

is that the key distinction of the two types of crystal structure is that of inversion symmetry, which can directly affect the formation of skyrmions and other spin textures, with potentials for spintronics applications.

2. Magnetism in Kagome lattices

Very recently, it was reported that with post-growth annealing, the phase transitions in FeGe can be substantially modified. In one extreme, the CDW order can be completely suppressed while in the other extreme the CDW order can be tuned to a long-range order. This surprisingly strong and effective tunability of the CDW order provides an opportunity to understand the origin of the CDW order in kagome magnets. One of our immediate goals is to compare the electronic structure, the lattice structure, and the magnetic order of kagome FeGe processed under different annealing conditions.

In a parallel direction, we plan to work on the magnetic kagome systems in thin film form. We have recently established molecular beam epitaxy capability in our lab connected in vacuo to our ARPES system. We plan to carry out the study of the effect of magnetic order on the electronic structure in magnetic kagome thin films and work on growing FeGe in thin film form. In contrast to bulk FeGe crystals where attempts at doping have been largely unsuccessful, doping or chemical substitution in epitaxial thin film form could be easier. If successful, this would allow us to gain a tuning knob for perturbing the magnetism and CDW order in FeGe.

References

1. H. Wu, J.-X. Zhu, L. Chen, M. W. Butcher, Z. Yue, D. Yuan, Y. He, J. S. Oh, J. Huang, S. Wu, C. Gong, S.-K. Mo, J. Denlinger, D.H. Lu, M. Hashimoto, M. B. Stone, Al. I. Kolesnikov, S. Chi, J. Kono, A. Nevidomskyy, R. J. Birgeneau, P. Dai, M. Yi, *Two-Step Electronic Response to Magnetic Ordering in a van der Waals Ferromagnet,* (under review).

2. H. Wu, C. Hu, Y. Xie, B. G. Jang, J. Huang, Y. Guo, S. Wu, C. Hu, Z. Yue, Y. Shi, Z. Ren, T. Yilmaz, E. Vescovo, C. Jozwiak, A. Bostwick, E. Rotenberg, A. Fedorov, J. D. Denlinger, C. Klewe, P. Shafer, D. Lu, M. Hashimoto, J. Kono, R. J. Birgeneau, X. Xu, J.-X. Zhu, P. Dai, J.-H. Chu, and M. Yi, *Spectral Evidence for Local-Moment Ferromagnetism in van der Waals Metals Fe_3GaTe_2 and Fe_3GeTe_2*, arXiv: 2307.00441.

3. H. Wu, L. Chen, P. Malinowski, J. Huang, Q. Deng, K. Scott, B. G. Jang, J. P. C. Ruff, Y. He, X. Chen, C. Hu, Z. Yue, J. S. Oh, X. Teng, Y. Guo, M. Klemm, C. Shi, Y. Shi, C. Setty, T. Werner, M. Hashimoto, D. Lu, T. Yilmaz, E. Vescovo, S.-K. Mo, A. Fedorov, J. D. Denlinger, Y. Xie, B. Gao, J. Kono, P. Dai, Y. Han, X. Xu, R. J. Birgeneau, J.-X. Zhu, E. H. da Silva Neto, L. Wu, J.-H. Chu, Q. Si, and M. Yi, *Reversible Non-Volatile Electronic Switching in a Near Room Temperature van der Waals Ferromagnet*, arXiv: 2307.03154.

4. X. Teng, L. Chen, F. Ye, E. Rosenberg, Z. Liu, J.-X. Yin, Y.-X. Jiang, J. S. Oh, M. Z. Hasan, K. J. Neubauer, B. Gao, Y. Xie, M. Hashimoto, D. Lu, C. Jozwiak, A. Bostwick, E. Rotenberg, R. J. Birgeneau, J.-H. Chu, M. Yi, P. Dai, *Discovery of charge density wave in a correlated kagome lattice antiferromagnet*, Nature **609**, 490 (2022).

5. X. Teng, J. S. Oh, H. Tan, L. Chen, J. Huang, B. Gao, J.-X. Yin, J.-H. Chu, M. Hashimoto, D. Lu, C. Jozwiak, A. Bostwick, E. Rotenberg, G. E. Granroth, B. Yan, R. J. Birgeneau, P. Dai, M. Yi, *Magnetism and charge density wave order in kagome FeGe*, Nat. Phys. **19**, 814-822 (2023).

Publications (2022-2023)

1. X. Teng, J. S. Oh, H. Tan, L. Chen, J. Huang, B. Gao, J.-X. Yin, J.-H. Chu, M. Hashimoto, D. Lu, C. Jozwiak, A. Bostwick, E. Rotenberg, G. E. Granroth, B. Yan, R. J. Birgeneau, P. Dai, M. Yi, *Magnetism and charge density wave order in kagome FeGe*, Nat. Phys. **19**, 814-822 (2023).

2. J. Huang, Y. Guo, M. Yi, *Electron Correlations and Nematicity in the Iron-Based Superconductors,* Synchrotron Radiation News (2023). Invited review.

3. A. Böhmer, J.-H. Chu, S. Lederer, M. Yi, *Nematicity and nematic fluctuations in iron-based superconductors*, Nat. Phys. **18**, 1412 (2022). Invited perspective.

4. J.-X. Yin, Y.-X. Jiang, X. Teng, Md. S. Hossain, S. Mardanya, T.-R. Chang, Z. Ye, G. Xu, M. Michael Denner, T. Neupert, B. Lienhard, H.-B. Deng, C. Setty, Q. Si, G. Chang, Z. Guguchia, B. Gao, N. Shumiya, Q. Zhang, T. A. Cochran, D. Multer, M. Yi, P. Dai, M. Z. Hasan, *Discovery of charge order and corresponding edge state in kagome magnet FeGe*, Phys. Rev. Lett. **129**, 166401 (2022).

5. X. Teng, L. Chen, F. Ye, E. Rosenberg, Z. Liu, J.-X. Yin, Y.-X. Jiang, J. S. Oh, M. Z. Hasan, K. J. Neubauer, B. Gao, Y. Xie, M. Hashimoto, D. Lu, C. Jozwiak, A. Bostwick, E. Rotenberg, R. J. Birgeneau, J.-H. Chu, M. Yi, P. Dai, *Discovery of charge density wave in a correlated kagome lattice antiferromagnet*, Nature **609**, 490 (2022).

6. H. Wu, A. M. Hallas, X. Cai, J. Huang, J. S. Oh, V. Loganathan, A. Weiland, G. T. McCandlesss, J. Y. Chan, S.-K. Mo, D. Lu, M. Hashimoto, J. Denlinger, R. J. Birgeneau, A. H. Nevidomskyy, G. Li, E. Morosan, M. Yi, *Nonsymmorphic symmetry-protected band crossings in a square-net metal* $PtPb_4$, npj Quantum Materials, **7**, 31 (2022).

7. J. Huang, R. Yu, Z. Xu, J.-X. Zhu, J. S. Oh, Q. Jiang, M. Wang, H. Wu, T. Chen, J. D. Denlinger, S.-K. Mo, M. Hashimoto, M. Michiardi, T. M. Pedersen, S. Gorovikov, S. Zhdanovich, A. Damascelli, G. Gu, P. Dai, J.-H. Chu, D. Lu, Q. Si, R. J. Birgeneau, M. Yi, *Correlation-driven electronic reconstruction in* $FeTe_{1-x}Se_x$, Commun. Phys. **5**, 29 (2022).

Anomalous Proximatized Transport in Metal/Quantum Magnet Heterostructure

PIs: Haidong Zhou (University of Tennessee), Jian Liu (University of Tennessee)

Keywords: magnetism, spintronics/magnonics, thin film heterostructures, antiferromagnets, magnetotransport,

Research Scope

The overarching goal of our project is to address the grand challenge of "metallizing quantum magnets", where emergent electronic phenomena are induced as quantum mechanical consequences of exotic spin states and excitations in insulating magnets. Our approach in this investigation focuses on (i) materials synthesis by both single crystal and epitaxial growth, and (ii) transport characterizations complemented by other necessary analysis. The specific directions include (i) synthesizing geometrically frustrated quantum magnets with strong quantum spin fluctuations and topological magnons, (ii) exploring the electronic response to these collective spin dynamics with various external controls; (iii) materials discovery of new quantum magnets in forms of crystals, films, and heterostructures.

Recent Progress

Anomalous Proximatized Transport in Metal/Quantum Magnet Heterostructure. We finished the magnetoresistance (MR) studies of $Bi_2Ir_2O_7/Dy_2Ti_2O_7$ (BIO/DTO) heterostructures in which the BIO film was epitaxially deposited directly on the DTO single crystal. We observed that the spin-ice rule-breaking transition in insulating DTO leads to an MR anomaly in the conducting BIO. This MR feature of BIO faithfully tracks this field-induced transition of DTO as a function of the field direction and temperature. Since this transition corresponds to magnetic monopole condensation, these results demonstrate a novel heteroepitaxial approach for electronically probing the transition between exotic insulating spin states, laying out a blueprint for the metallization of frustrated quantum magnets by proximitized transport. Our work was published in Nature Communications (NC **14**, 1404 (2023)) and selected as the Editor's highlight.

By leveraging with this new approach, we replaced DTO with $Yb_2Ti_2O_7$ (YbTO) in the heterostructure such that the carriers in BIO are influenced by quantum spin ice physics instead of classical spin ice. The heavy interests on quantum spin ice root in the underlying strong quantum spin fluctuations (QSFs). First, the quantum fluctuations are highly correlated and entangled, involving tunneling between distinct collective spin states with nearly degenerate energies. Such quantum dynamics is beyond the conventional picture of spin-wave excitations. The exotic magnetic phases of quantum spin liquids (QSL) [1] are prominent examples, where QSFs completely suppress conventional magnetic orders to facilitate topological orders [2]. Second, such magnetic systems promise future applications in quantum devices as the tunneling mechanism bypasses the energy barrier necessary for reorienting the magnetic moments in conventional spintronics [3]. However, most of the known quantum magnets with strong QSFs are good insulators and thus incompatible with the electronic integrated-circuit technology. Our approach demonstrated in the BIO/DTO heterostructure provides a solution to **"*electronically*"** probe and harness the quantum effects of insulating quantum magnets.

We constructed a heterostructure of a metallic BIO film epitaxially deposited on an YbTO single crystal (Fig. 1(a)). We found strong proximity effects between the electric transport in BIO and the quantum magnetism in YbTO, supported by the scaling behaviors of the resistance and its sensitivity to the anisotropic QSFs. In particular, the observed $1/T$ dependence (Fig. 1(b)) and large negative $1/\sqrt{B}$ magnetoresistance (Fig. 1(c)) in the low-temperature regime do not conform to the expectation based on electrons scattering by coherent spin waves, but point to the decisive role of QSFs. The MR also shows a clear response to the QSFs of the field-

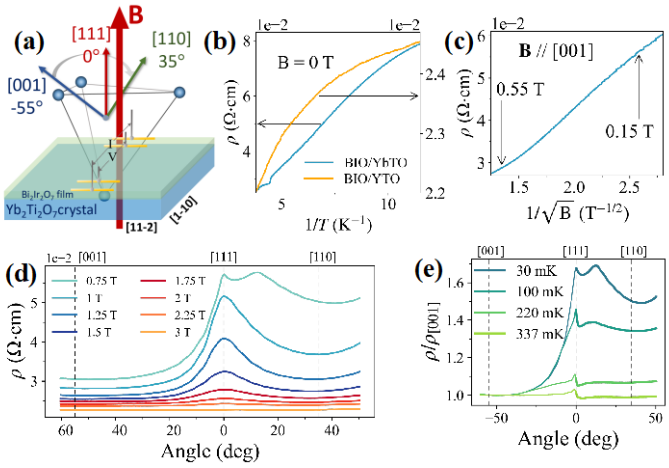

Figure 1 (a) Schematic diagram of the BIO/YbTO heterostructure. (b) $1/T$ dependence of the resistivity for BIO/YbTO and BIO/YTO at zero field. Here, BIO/YTO is a reference heterostructure with BIO film deposited on $Y_2Ti_2O_7$ crystal, which is nonmagnetic. (c) $1/\sqrt{B}$ dependence of the resistivity of BIO/YbTO at 0.03 K. Magnetic field (B) was applied along [001] axis. (d) Angle dependence of the resistivity of BIO/YbTO at 0.03 K with several selected fields. (e) Angle dependence of the normalized resistivity of BIO/YbTO at several temperatures with B = 0.75 T.

induced magnetic phase transitions (Fig. 1(d, e)). Compared with the MR anomaly due to the field-induced transition in BIO/DTO, the MR response here in BIO/YbTO is much stronger and covers a much wider field range, capturing the distinction between classical spin system and quantum spin system. The MR response here also persists to relatively high temperatures, capturing the so-called reentrance behavior of YbTO which has been believed to be a signature of QSFs due to proximity to a quantum spin liquid phase. *To our knowledge, this is the first time to report such anomalous transport behavior through the mechanism of QSFs scattering of electrons at the interface.* Our study thus further demonstrates the heteroepitaxial approach for realizing strong coupling between the electronic transport and the QSFs, opening up exciting possibilities for future proximitized transport studies of insulating quantum magnetism. The manuscript of this work has been submitted for peer-review.

Pyrochlore heterostructures of topological magnonic states We continued our efforts to synthesize the heterostructure built on single crystals of pyrochlore $Lu_2V_2O_7$ (LVO), which is a ferromagnet with topological magnon bands [4]. So far, we have successfully grown high-quality single crystals of LVO. We have tested the BIO thin film growth on LVO but found that the growth condition of the BIO film may affect the level of oxygen in the LVO crystal and degrade the oxidation state of the V^{4+} ions. Instead, we found that it is possible to grow $Bi_2Ru_2O_7$ (BRO), another nonmagnetic pyrochlore metal, on LVO. Our preliminary results show that the growth of BRO can be done under reducing gas atmosphere to preserve the LVO properties. Next step is to optimize the condition for depositing BRO on top of LVO to achieve high quality heterostructure.

Spatial spin modulation due to competing anisotropy in Sr_2IrO_4 tuned by in situ B_{2g} strain We finished the *in situ* strain studies on Sr_2IrO_4. In this work, we demonstrate that competing anisotropy of B_{1g} and B_{2g} symmetry leads to an emergent magnetic modulation consisting of 12 IrO_2 planes in Sr_2IrO_4. In particular, we applied shear strain to distort the *ab*-plane of Sr_2IrO_4 and induce B_{2g} anisotropy that is *orthogonal* to the spontaneous B_{1g} anisotropy (Fig. 2(a)). Surprisingly, this leads to translational symmetry-breaking along the c-axis, and the emergence of a tri-quadrupole-layer (TQL) state (Fig. 2(b, c)). The induced anisotropy not only has an orthogonal symmetry but is also at the quartic order, which is higher than the spontaneous one and has not been observed before. These characters are crucial in stabilizing new emergent states in the mechanism of competing anisotropy. More interestingly, the TQL state can be well captured in transport measurement of elasto-magnetoresistance, indicating the remarkable sensitivity of the charge carriers to the magnetic competition despite the Mott insulating state. Our tuning of magnetic anisotropy of different irreducible point group representations adds to the list of recently found controllable rotational symmetry-breaking phases in quantum materials, such as electronic nematicity, quadrupolar order, and unconventional superconductivity. Our work was published in Physical Review Letters (PRL **129**, 027203(1-7) (2022)).

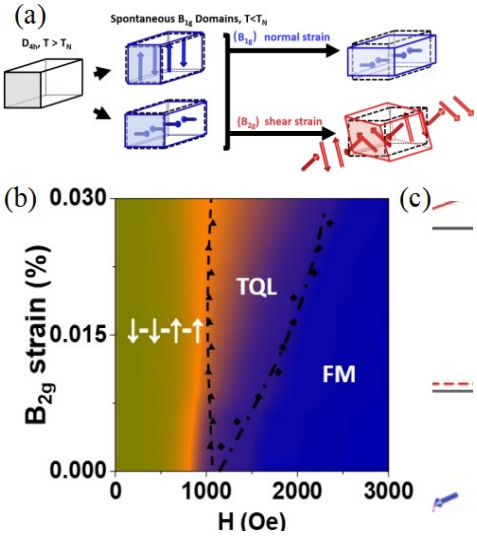

Figure 2 (a) schematic showing symmetry-breaking of a tetragonal material by spontaneous magnetic anisotropy and competition with shear-induced anisotropy. (b) phase diagram of Sr_2IrO_4 under tunable in-situ shear strain and magnetic field. (c) schematic of the TQL spin modulation.

Continuum spin excitations in an ordered antiferromagnet For a magnetic insulator, it is intriguing to ask whether its localized magnetic moments can show magnetic continuum alongside spin waves in a spin-ordered state, while the common sense is that these two features are incompatible. Meanwhile, if such system indeed exists, its magnetic properties should be easily tuned by external driving forces like magnetic field due to its delicate ordered state. The answer to this question has become a new direction to search for QSLs.

During our efforts to search for epitaxy-compatible quantum magnets, we successfully grew high quality of single crystals $K_2Ni_2(SO_4)_3$, which is a langbeinite with two sets of spin-1 Ni^{2+}-trillium lattice interconnecting in three-dimensional (3D) space. Although it orders around 1.0 K, our inelastic neutron scattering measurement on single crystals clearly shows a dominant excitation continuum (Fig. 3), which exhibits a distinct temperature-dependent behavior from that of spin waves, and is rooted in strong quantum spin fluctuations. Further using the self-consistent-gaussian- approximation method, we determined the fourth- and fifth-nearest neighbor exchange interactions are dominant. These two bonds together form a unique three-dimensional

network of corner-sharing tetrahedra, which we name as “hyper-trillium” lattice. Our results provide direct evidence for the existence of QSL features in $K_2Ni_2(SO_4)_3$ and highlight the potential for the hyper-trillium lattice to host frustrated quantum magnetism. The manuscript of this work (arXiv:2303.16384) has been submitted for peer-review.

Future Plans

We will move forward on the directions we have embarked on and continue leveraging our

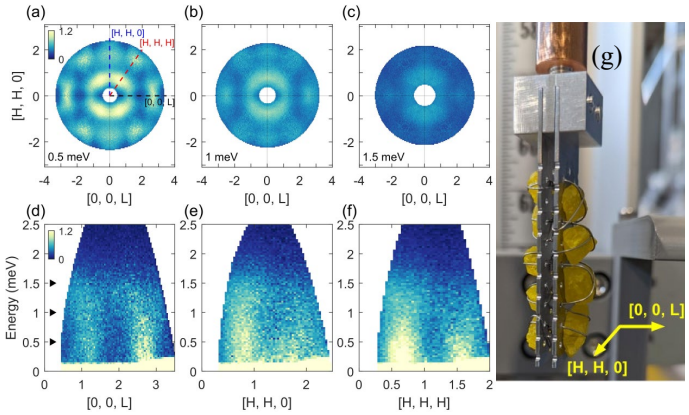

Figure 3 (a)-(c) Constant energy slices of the (H, H, L) plane at 0.1 K for $K_2Ni_2(SO_4)_3$. (d)-(f) Energy dependence of the magnetic continuum along high-symmetric directions [dashed lines in (a)]. The right triangles indicate in (d) energy positions where the slices in (a)-(c) were taken. (g) Single crystal array used in the neutron scattering experiment.

capabilities of synthesizing and characterizing novel materials. In particular, our main focus will be (i) exploiting the BIO/YbTO heterostructure to investigate the debated role of site disorder in affecting the QSFs and the long-range order in YbTO; (ii) identifying other metallic films that would exhibit the QSF-driven proximatized transport behaviors in a heterostructure with YbTO; (iii) examining the proximatized transport behaviors in other QSL candidates, such as $Tb_2Ti_2O_7$; (iv) exploring proximatized transport behaviors driven by topological properties of the insulating magnets, such as $Lu_2V_2O_7$ which is known to host the topological magnons excitations; (v) synthesis of other frustrated magnets to explore the possibility of new heterostructures. We also plan establish micro-fabrication capability to make devices on our heterostructures, which is crucial for measuring Hall effect and other delicate transport properties at ultralow temperatures.

References

1. L. Balents, *Spin liquids in frustrated magnets*, Nature **464**, 199-208 (2010).

2. Y. Kasahara, T. Ohnishi, Y. Mizukami, O. Tanaka, S. Ma, K. Sugii, N. Kurita, H. Tanaka, J. Nasu, Y. Motome, T. Shibauchi,and Y. Matsuda, *Majorana quantization and half-integer thermal quantum Hall effect in a Kitaev spin liquid*, Nature **559**, 227-331 (2018).

3. S. A. Wolf, D. D. Awschalom, R. A. Buhrman, J. M. Daughton, S. Von Molnar, M. L. Toukes, A. Y. Chtchelkanova, and M. Treger, *Spintronics: a pin-based electronics vision for the future*, Science **294**, 1488-1495 (2001).

4. A. Mook, J. Henk, and I. Mertig, *Tunable magnon Weyl points in ferromagnetic pyrochlores*, Physical Review Letters **117**, 157204(1-6) (2016).

Publications

1. L. Xiang, R. Dhakal, M. Ozerov, Y. Jiang, B. S. Mou, A. Ozarowski, Q. Huang, H. D. Zhou, J. Fang, S. M. Winter, Z. Jiang, and D. Smirnov, *Disorder-enriched magnetic excitations in a Heisenberg-Kitaev quantum magnet $Na_2Co_2TeO_6$*, Physical Review Letters **131**, 076701(1-6) (2023).

2. Y. Jiang, T. Zhao, L. Zhang, Q. Chen, H. D. Zhou, M. Ozerov, D. Smirnov, and Z. Jiang, *Revealing temperature evolution of the Dirac band in $ZrTe_5$ via magnetoinfrared spectroscopy*, Physical Review B **108**, L041202(1-7) (2023).

3. H. Zhang, C. K. Xing, K. Noordhoek, Z. Liu, T. Zhao, L. Horak, Q. Haung, L. Hao, J. Yang, S. Pandey, E. Dagotto, Z. Jiang, J. H. Chu, Y. Xin, E. S. Choi, H. D. Zhou, and J. Liu, *Anomalous magnetoresistance by breaking ice rule in $Bi_2Ir_2O_7/Dy_2Ti_2O_7$ heterostructure*, Nature Communications **14**, 1014(1-7) (2023).

4. S. Pandey, H. Zhang, J. Yang, A. F. May, J. Sanchez, Z. Liu, J. H. Chu, J. W. Kim, P. J. Ryan, H. D. Zhou, and J. Liu, *Controllable emergent spatial spin modulation in Sr_2IrO_4 by in situ shear strain*, Physical Review Letters **129**, 027203(1-7) (2022).

5. Z. Morgan, H. D. Zhou, B. C. Chakoumakos, and F. Ye, *rmc-discord: reverse Monte Carlo refinement of diffuse scattering and correlated disorder from single crystals*, Journal of Applied Crystallography **54**, 1867-1885 (2021).

6. J. Wang, Y. Jiang, T. Zhao, Z. Dun, A. L. Miettinen, X. Wu, M. Mourigal, H. D. Zhou, W. Pan, D. Smirnow, and Z. Jiang, *Magneto-transport evidence for strong topological insulator phase in $ZrTe_5$*, Nature Communications **12**, 6758(1-7) (2021).

7. N. Li, R. R. Neumann, S. K. Guang, Q. Huang, J. Liu, K. Xia, X. Y. Yue, Y. Sun, Y. Y. Wang, Q. J. Li, Y. Jiang, J. Fang, J. Jiang, X. Zhao, A. Mook, J. Henk, I. Mertig, H. D. Zhou, and X. F. Sun, *Magnon-phonon driven thermal hall effect in a Heisenberg-Kitaev antiferromagnet*, arXiv:2201.11396.

8. W. Yao, Q. Huang, T. Xie, A. Podlesnyak, A. Brassington, C. Xing, R. S. D. Mudiyanselage, W. Xie, S. Zhang, M. Lee, V. S. Zapf, X. Bai, D. A. Tennant, J. Liu, and H. D. Zhou, *Continuous spin excitations in the three-dimensional frustrated magnet $K_2Ni_2(SO4)_3$*, arXiv:2303.16384.

2D magnetic spin LED

Xiao-Xiao Zhang, Department of Physics, University of Florida

Keywords: 2D material; Optical spectroscopy; Spintronics.

Research Scope

Here we explore the valley index manipulation with the spin tuning ability from 2D magnet-semiconductor heterostructures (e.g., CrI_3 and 1L WSe_2). Magnetic insulating crystals provide spin filtering and realize vertical spin-polarized injection into the 2D semiconductor, which can be read out via spin-valley coupled electroluminescence (EL) in monolayer transition metal dichalcogenide (TMD). We investigated the magnetic field dependence of the EL to elucidate the correlation between the spin polarization of the magnetic layer and EL helicity. Through our measurements, we also identify the critical role of a thin dielectric tunneling layer in preserving the interlayer spin injection polarization.

Recent Progress

Figure 1a shows the currently investigated device structure and a typical device microscope image. The top gate voltage tunes the WSe_2 doping, and a vertical bias electric field can tune the band alignment and drive carrier injection through the interlayer interface.

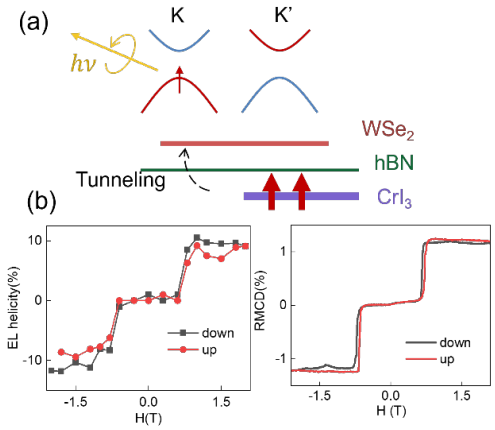

Figure 1. (a) Schematics of the device structure. The insulating hBN is < 3nm in thickness. WSe_2 is monolayer, and CrI_3 is bilayer. (b) The left panel: WSe_2 EL helicity as a function of the out-of-plane magnetic field. Right panel: Magnetic circular dichroism of the bilayer CrI_3 layer. The step changes in EL helicity correspond the layer spin-flip transition of the CrI_3 layer. The measurement is taken at 4K.

When applying a bias voltage between the WSe_2 and CrI_3 layers, holes can tunnel through the magnetic insulating layer CrI_3 and thin hBN layer into the n-doped WSe_2 and give rise to EL signals. The relative band alignment between these two materials is extracted through the separate gate and bias voltage dependence of the EL spectra.

As shown in Fig. b, the EL helicity follows the net magnetization of the CrI_3 layer. Notably, in the CrI_3 AFM state (-0.6 T to 0.6T), EL helicity remains zero. This contrasts the previously studied case of photo-excited charge transfer from TMD to the CrI_3 layer, where only the topmost CrI_3 layer magnetization determines the spin-polarized charge transfer process(1). With the addition of hBN tunneling barrier in this project, the spin transfer is no longer solely determined by the

distorted band alignment between the TMD and the topmost magnetic layer but relies on the net magnetization of the 2D magnetic layer.

The measured EL helicity at the CrI_3 FM state is comparable to the degree of valley polarization measured from the circularly polarized photoluminescence with near-resonant excitation conditions, which indicates a high degree of spin polarization preservation in the charge injection process. The less-than-unity emission helicity can be attributed to the rapid exciton valley exchange rate, which also gives rise to depolarization in the valley-polarized photoluminescence(2).

In comparison, we have also fabricated an EL device CrI_3/WSe_2, that is otherwise identical but without the hBN insulating layer. While the EL signal can be observed under similar bias and gate voltage conditions, they don't show observable helicity as a function of the magnetic field. This contrast demonstrates that the hBN layer can effectively reduce the conductance mismatch(3) during the spin transfer process, therefore significantly increasing the degree of spin polarization.

Our measurements provide the first example of spin light emitting diode (LED) that is completely based on 2D crystals. The results also provide insights into key device parameters to maintain a high degree of spin polarization transfer within 2D heterostructures.

Future Plans

One immediate goal is to investigate the electrical tunability in such spin LED structures. The spin-flip transition field in bilayer CrI_3 has been shown to be susceptible to both an out-of-plane electrical field and doping differences. By further constructing gating and electrode layers, we aim to simultaneously modulate the CrI_3 magnetization to switch the helicity of the EL signals.

In the long term, we will use the established high degree of spin-polarization injection to probe the non-equilibrium spin dynamics in 2D magnets through optical excitation of valley-spin polarized carriers in TMD layers, which corresponds to a reverse process of the spin injection presented in the recent progress. The spin torque motions due to the pulsed spin currents will be investigated as a function of in-plane and out-of-plane magnetic fields with time-resolved Magneto-optic Kerr effect (tr-MOKE). This project will include different types of 2D magnetic crystals to study the impacts of different magnetic anisotropy and exchange interactions.

References

1. Zhong D., Seyler K.L., Linpeng X., Wilson N.P., Taniguchi T., Watanabe K., McGuire M.A., Fu K.-M.C., Xiao D., Yao W., & Xu X. *Layer-resolved magnetic proximity effect in van der Waals heterostructures. Nature Nanotechnology.* **15**(3):187-191. (2020).
2. Yu T. & Wu M.W. *Valley depolarization due to intervalley and intravalley electron-hole exchange interactions in monolayer ${\text{MoS}}_{2}$. Physical Review B.* **89**(20):205303. (2014).
3. Rashba E.I. *Theory of electrical spin injection: Tunnel contacts as a solution of the conductivity mismatch problem. Physical Review B.* **62**(24):R16267-R16270. (2000).

Publications

The manuscript for this project is still in preparation.

High temperature quantum valley Hall effect

Jun Zhu, Department of Physics, Penn State University

Keywords: topology-quantum Hall, graphene, transport, nanofabrication

Research Scope

Edge states born out of non-trivial bulk topology are excellent platforms to explore the fundamental physics of low dimensions and develop ballistic quantum electronics elements that may be useful in quantum information science and engineering. Helical edge states associated with the quantum spin Hall effect and quantum valley Hall effect are particularly valuable because their presence does not require a magnetic field. However, owing to material challenges, achieving a robust resistance quantization, the hallmark of a topological edge state, has proven to be difficult for helical edge states.

Recent Progress

As a manifestation of the quantum valley Hall effect, bilayer graphene supports valley-momentum locked kink states at the line junction of two oppositely gapped bulk regions created by lithography. In prior works, we demonstrated the existence of the kink states [1] and the operations of a topological valley valve and tunable electron beam splitter [2]. In this work, we improved on the device quality to achieve precisely quantized resistance plateaus to within 1% of $h/4e^2$ at zero magnetic field. Most remarkably, the quantum valley hall effect persists to high temperatures of tens of Kelvin, with the plateau resistance drops by approximately 1% at 12 K and 3% at ~50 K. The quantization is also robust over a large dc bias range of tens of mV. We demonstrate operation of an in situ programmable topological switch with an on/off ratio of 200. These results are a significant step forward in advancing the understanding and applications of topological edge states.

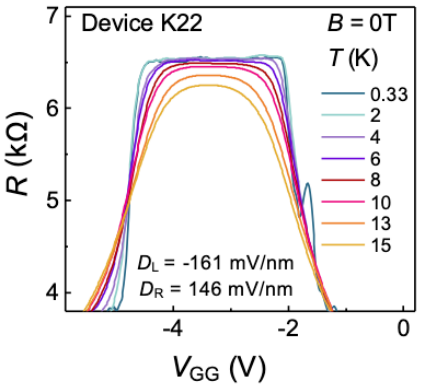

Figure 1: Experimental signatures of quantum valley Hall effect: two-terminal resistance quantized to h/4e^2 at zero magnetic field and its temperature dependence. Huang et al, submitted.

Future Plans

Future plans include coupling the kink states with superconductors using Josephson junction devices and exploring the evolution of the kink states from helical to chiral edge states in a magnetic field.

References

[1] J. Li, K. Wang, K. J. McFaul, Z. Zern, Y. F. Ren, K. Watanabe, T. Taniguchi, Z. H. Qiao, and J. Zhu, *Gate-controlled topological conducting channels in bilayer graphene*, Nature Nanotechnology **11**, 1060 (2016).

[2] J. Li, R. X. Zhang, Z. X. Yin, J. X. Zhang, K. Watanabe, T. Taniguchi, C. X. Liu, and J. Zhu, A valley valve and electron beam splitter, Science **362**, 1149 (2018).

[3] Ke Huang, Hailong Fu, Kenji Watanabe, Takashi Taniguchi, and Jun Zhu, *High-Temperature Quantum Valley Hall Effect with Quantized Resistance and a Topological Switch*, submitted to Science

Publications

None

Topological Engineering in Carbon-Based Nanostructures

Prof. Dr. Felix R. Fischer

Department of Chemistry, University of California, Berkeley, CA 94720, U.S.A.

Materials Sciences Division, Lawrence Berkeley National Laboratory, Berkeley, CA 94720, U.S.A.

Kavli Energy NanoSciences Institute at the University of California Berkeley and the Lawrence Berkeley National Laboratory, Berkeley, California 94720, U.S.A.

Bakar Institute of Digital Materials for the Planet, Division of Computing, Data Science, and Society, University of California, Berkeley, CA 94720, USA.

Keywords: topology, nanostructures, graphene, scanning tunneling microscopy, nanofabrication and 2D assembly

Research Scope

This research program lays the scientific foundation for the rational bottom-up design, isolation, and investigation of symmetry protected topological (SPT) electron spin qubits embedded in graphene nanoribbons and their integration with atomically precise low dimensional logic architectures that hold the key to unlocking scalable quantum materials for next-generation computing and sensing. Our effort will reveal the fundamental correlations between real space molecular architecture, local spin densities, energy dispersion and level alignments that underpin key operational parameters of SPT qubits and will benchmark their intrinsic performance against established molecular and solid-state devices. Long decoherence times, sharp energy transitions, and highly tunable exchange interactions between entangled states all represent critical device parameters that can be tuned with atomic precision through a scalable bottom-up manufacturing technique. Access to topologically engineered molecular qubits is guided at every stage by theory and validated by experiment at the ensemble and single molecule level. Our research activities not only push the boundaries of quantum materials design and synthesis but innovate spin-sensitive scanning probe microscopy tools that provide an unprecedented level of detail from the direct observation of quantum structures and dynamic processes at the scale of a single atom. While our proposed research activities represent hypothesis-driven fundamental scientific investigations, we embrace a comprehensive materials design approach that delivers technological solutions that can be translated into smart manufacturing.

Recent Progress

(1) Engineering Robust Metallic Zero-Mode States in Olympicene Graphene Nanoribbons:[1] Metallic graphene nanoribbons (GNRs) represent a critical component in the toolbox of low-dimensional functional materials technology serving as 1D interconnects capable

of both electronic and quantum information transport. The structural constraints imposed by on-surface bottom-up GNR synthesis protocols along with the limited control over orientation and sequence of asymmetric monomer building blocks during the radical step-growth polymerization has plagued the design and assembly of metallic GNRs. Here we report the regioregular synthesis of GNRs hosting robust metallic states by embedding a symmetric zero-mode superlattice along the backbone of a GNR. Tight-binding electronic structure models predict a strong nearest-neighbor electron hopping interaction between adjacent zero-mode states resulting in a dispersive metallic band. First principles DFT-LDA calculations confirm this prediction and the robust, metallic zero-mode band of olympicene GNRs (oGNRs) is experimentally corroborated by scanning tunneling spectroscopy.

(2) Fermi Level Engineering of Nitrogen Core-Doped Armchair Graphene Nanoribbons:[2] Substitutional heteroatom doping of bottom-up engineered 1D graphene nanoribbons (GNRs) is a versatile tool for realizing low-dimensional functional materials for nanoelectronics and sensing. Previous efforts have largely relied on replacing C–H groups lining the edges of GNRs with trigonal planar N-atoms. This type of atomically-precise doping however only results in a modest realignment of the valence band (VB) and conduction band (CB) energies. Here we report the design, bottom-up synthesis, and spectroscopic characterization of nitrogen core-doped 5-atom-wide armchair-GNRs (N_2-5-AGNRs) that yield much greater energy-level shifting of the GNR electronic structure. Here the substitution of C-atoms with N-atoms along the backbone of the GNR introduces a single surplus π-electron per dopant that populates electronic states associated with previously unoccupied bands. First principles DFT-LDA calculations confirm that a sizeable shift in Fermi energy (~1.0 eV) is accompanied by a broad reconfiguration of the band structure, including the opening of a new band gap and the transition from a direct to an indirect semiconducting bandgap. Scanning tunneling spectroscopy (STS) lift-off charge transport experiments corroborate the theoretical results and reveal the relationship between substitutional heteroatom doping, Fermi level shifting, electronic band structure, and topological engineering for this new N-doped GNR.

(3) Controlled Catalyst Transfer Polymerization in Graphene Nanoribbon Synthesis:[3] Exercising direct control over the unusual electronic structures arising from quantum confinement effects in graphene nanoribbons (GNRs) is intimately linked to geometric boundary conditions imposed by the structure of the ribbon. Besides composition and position of substitutional dopant atoms, the symmetry of the unit cell, width, length, and termination of a GNR govern its electronic structure. Here we present a rational design that integrates each of these interdependent variables within a modular bottom-up synthesis. Our hybrid chemical approach relies on a catalyst transfer polymerization (CTP) that establishes uniform control over length, width, and end-groups. Complemented by a surface-assisted cyclodehydrogenation step, uniquely enabled by matrix-assisted direct (MAD) transfer protocols, geometry and functional handles encoded in a polymer template are faithfully mapped onto the structure of the corresponding GNR. Bond-resolved

scanning tunnelling microscopy (BRSTM) and spectroscopy (STS) validate the robust correlation between polymer template design and GNR electronic structure.

(4) Five-Membered Rings Create Off-Zero Modes in Nanographene:[4] The low-energy electronic structure of nanographenes is known to be tunable through zero-energy π-electron states typically referred to as zero-modes. Customizable electronic and magnetic structures have been engineered by coupling zero-modes through exchange and hybridization interactions. The manipulation of the absolute energy of such states, however, has not yet received significant attention. We find that attaching a five-membered ring to a zigzag edge hosting a zero-mode perturbs the energy of that mode and turns it into an *off-zero* mode: a localized state with distinctive electron-accepting character. Whereas the end states of typical 7-atom-wide armchair graphene nanoribbons (7-AGNRs) lose their electrons when physisorbed on Au(111) (due to its high work function), converting them to off-zero modes by introducing cyclopentadienyl five-membered rings allows them to retain their single-electron occupation. This approach enables the magnetic properties of 7-AGNR end states to be explored using scanning tunneling microscopy (STM) on a gold substrate. Off-zero mode end states coupled across short nanoribbons transition from a closed shell (nonmagnetic) configuration for $n \leq 4$ to an open shell (paramagnetic) configuration for $n \geq 5$ repeating anthracene units.

(5) Topological Engineering of Molecular Quantum Dots in Nanographenes: Topological phases in laterally-confined low-dimensional nanographenes have emerged as versatile design tools used to imbue otherwise unremarkable materials with exotic band structures ranging from topological semiconductors, quantum dots, to intrinsically metallic bands. The periodic boundary conditions that come to define the topology of a given lattice have thus far prevented the translation of this technology to the zero-dimensional (0D) domain of small molecular structures. Here, we describe the synthesis of a discrete polycyclic aromatic hydrocarbon (PAH) featuring two localized zero modes (ZMs) formed by the topological junction interface between a trivial and non-trivial phase within a single molecule. First-principles density functional theory calculations predict a strong hybridization between adjacent ZMs that gives rise to an exceptionally small topologically protected HOMO-LUMO gap. Scanning tunneling microscopy and spectroscopy corroborate the molecular structure of 9/7/9-double quantum dots and reveal an experimental quasi-particle gap of 0.16 eV corresponding to a small molecule long-wavelength infra-red (LWIR) absorber. The access to topologically engineered ultra-low bandgap nanographenes paves the way toward the realization IR sensitized photovoltaics and LWIR detectors based on carbon nanotechnology.

Future Plans

Phase two (year 2) of this continuing program will see the tuning of the exchange coupling between symmetry protected topological states by structural design and/or doping to access the weakly coupled regime of two interacting S =1/2 SPT quantum dots by modulation the exchange coupling t and the on-site energy U. We will use ensemble-based ESR and advanced single

molecule STM ESR techniques to explore energy transitions, decoherence lifetimes τ_{dec}, and exchange interactions J in molecularly defined SPT qubits.

References

1. R. D. McCurdy, A. Delgado, J. Jiang, J. Zhu, E. C. H. Wen, R. E. Blackwell, G. C. Veber, S. Wang, S. G. Louie, F. R. Fischer, *Robust Metallic Zero-Mode States in Olympicene Graphene Nanoribbons*, *J. Am. Chem. Soc.* ***145,*** 15162–15170 (**2023)**.

2. E. C. H. Wen, P. H. Jacobse, J. Jiang, Z. Wang, S. G. Louie, M. F. Crommie, F. R. Fischer, *Fermi Level Engineering in Nitrogen Core Doped Armchair Graphene Nanoribbons*, *J. Am. Chem. Soc.* **145**, *accepted* (2023).

3. S. H. Pun, A. Delgado, C. Dadich, F. R. Fischer, *Controlled Catalyst Transfer Polymerization in Graphene Nanoribbon Synthesis*, Chem, *under review* (2023). arXiv:2304.07394

4. P. H. Jacobse, M. C. Daugherty, K. Čerņevičs, Z. Wang, R. D. McCurdy, O. V. Yazyev, F. R. Fischer, M. F. Crommie, *Five-Membered Rings Create Off-Zero Modes in Nanographene*, ACS Nano, *under review* (2023).

5. K. Slicker, A. Delgado, J. Jiang, A. Cronin, R. E. Blackwell, S. G. Louie, F. R. Fischer, *Topological Engineering of Molecular Quantum Dots in Nanographenes*, in preparation (2023).

Publications

1. R. D. McCurdy, A. Delgado, J. Jiang, J. Zhu, E. C. H. Wen, R. E. Blackwell, G. C. Veber, S. Wang, S. G. Louie, F. R. Fischer, *Robust Metallic Zero-Mode States in Olympicene Graphene Nanoribbons*, *J. Am. Chem. Soc.* ***145,*** 15162–15170 (**2023)**.

2. E. C. H. Wen, P. H. Jacobse, J. Jiang, Z. Wang, S. G. Louie, M. F. Crommie, F. R. Fischer, *Fermi Level Engineering in Nitrogen Core Doped Armchair Graphene Nanoribbons*, *J. Am. Chem. Soc.* **145**, *accepted* (2023).

3. S. H. Pun, A. Delgado, C. Dadich, F. R. Fischer, *Controlled Catalyst Transfer Polymerization in Graphene Nanoribbon Synthesis*, Chem, *under review* (2023). arXiv:2304.07394

4. P. H. Jacobse, M. C. Daugherty, K. Čerņevičs, Z. Wang, R. D. McCurdy, O. V. Yazyev, F. R. Fischer, M. F. Crommie, *Five-Membered Rings Create Off-Zero Modes in Nanographene*, ACS Nano, *under review* (2023).

5. K. Slicker, A. Delgado, J. Jiang, A. Cronin, R. E. Blackwell, S. G. Louie, F. R. Fischer, *Topological Engineering of Molecular Quantum Dots in Nanographenes*, in preparation (2023).

Two Dimensional Heavy Fermions in the van der Waals Metal CeSiI

Xavier Roy and Abhay Pasupathy

Keywords: Magnetism, non-Fermi liquid behavior and charge dynamics, 2D and layered crystals, magnetotransport, scanning tunneling microscopy

Research Scope

Dimensionality has emerged as an important tuning handle in the study of correlated materials, especially heavy fermion materials.[1] Traditional platforms for reducing dimensionality in intermetallic heavy fermion materials rely on crystal structure engineering or epitaxial growth,[2] but the study of such materials at the two-dimensional (2D) limit remains challenging. To this end, van der Waals (vdW) materials that can be mechanically exfoliated represent ideal candidates for studying heavy fermions at the monolayer limit; such materials would additionally enable exploration of the Kondo lattice phase space using tuning handles developed for other 2D materials, including electrostatic and electrochemical gating, strain, and twist angle.[3] To date, however, there are no examples of a vdW metal hosting Kondo lattice physics. We have identified the antiferromagnetic van der Waals metal, CeSiI, as a host of two-dimensional heavy fermions.[4] Using a combination of thermodynamic and spectroscopic measurements, we find evidence for an enhancement in the electron effective mass and for strong hybridization between conduction and 4*f* electrons persisting well above the Néel temperature T_N = 7.5 K. Angle-resolved photoemission spectroscopy (ARPES) and magnetotransport measurements additionally reveal signatures of a quasi-2D electronic structure arising from the vdW crystal structure. The weak interactions between vdW layers enables mechanical exfoliation of CeSiI to the ultra-thin limit, where we observe quantitative changes in the magnetotransport behavior arising from reduced dimensionality. In totality, these results demonstrate CeSiI as a new platform for studying Kondo lattice physics at the 2D limit.

Recent Progress

The crystal structure of CeSiI consists of an intermetallic $[CeSi]^+$ core, featuring a nearly planar honeycomb layer of Si sandwiched between two triangular layers of Ce, and iodide capping layers that define the vdW gap.[4] This material was identified on the basis of its Zintl-Klemm formalism, $(Ce^{3+})(Si^-)(I^-)(e^-)$, where the presence of a free electron implies metallic character and the possibility of strong Kondo coupling. Heat capacity measurements reveal a substantial

enhancement in the Sommerfeld coefficient compared to the non-magnetic, isostructural compound LaSiI, and bulk transport measurements reveal a downturn in the resistivity below $T^* \sim 50$ K, associated with the transition from incoherent Kondo scattering at high temperature to coherent heavy Bloch states at low temperature.

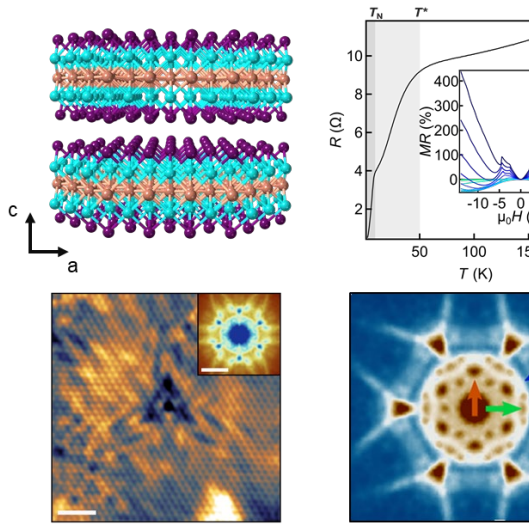

(Top left) Crystal structure of CeSiI, highlighting the van der Waals gap in the layered structure. (Top right) Temperature and magnetic field dependence of resistivity revealing signatures of Kondo coupling and magnetic ordering. (Bottom left) STM topographic image showing standing wave oscillations around a lattice defect. (Bottom right) Quasiparticle interference of CeSiI revealing nodal hybridization.

Scanning tunneling spectroscopy (STS) and ARPES measurements provide further evidence for Kondo coupling persisting to high-temperature in CeSiI. STS measurements reveal a temperature-dependent, Fano-like feature near the Fermi energy that is not observed for LaSiI. Similarly, while ARPES measurements reveal nearly identical dispersive bands for both CeSiI and LaSiI, spectra for CeSiI additionally reveal flat bands at and below the Fermi energy associated with Ce 4f resonances. Below ~80 K, we observe signatures of a hybridization gap at the intersection of flat and dispersive bands in CeSiI, consistent with the single-ion Kondo temperature $T_K = 78$ K extracted from STS measurements.

The quasi-2D electronic structure of CeSiI, derived from its layered vdW crystal structure, was probed by ARPES and magnetotransport measurements. While the Fermi surface of CeSiI, as probed by ARPES, is complex and contains multiple electron and hole pockets in the $\bar{K} - \bar{\Gamma} - \bar{M}$ plane, it is largely unchanged in the k_z direction, indicative of a quasi-2D electronic structure. Magnetotransport measurements in bulk CeSiI additionally reveal Shubnikov–de Haas oscillations at high magnetic fields. Angle-dependent measurement of these oscillations reveal that they remain in phase with increasing amplitude as the field is tilted away from the crystallographic stacking axis, providing additional evidence for a quasi-2D Fermi surface.

The vdW crystal structure of CeSiI enables us to routinely obtain micron-scale, few-layer flakes via mechanical exfoliation. Transport measurements on a fifteen-layer flake retain signatures of Kondo lattice physics and are qualitatively similar to measurements on bulk flakes. In contrast, measurements on a four-layer flake reveal changes in field-induced magnetic transitions, suggestive of changes in the Kondo coupling induced by reduced dimensionality. While the air sensitivity of CeSiI makes measurements on even thinner flakes challenging, these initial results near the 2D limit imply that it may be possible to tune the Kondo lattice ground state

of CeSiI through exfoliation alone and illustrate that CeSiI represents a tunable, vdW platform for the study of Kondo physics in two dimensions.

In our exploration of the effects of reduced dimensionality on the electronic structure of CeSiI, we have additionally uncovered signatures of momentum-dependent electron masses arising from highly anisotropic electronic interactions. Specifically, quasiparticle interference (QPI) measurements on cleaved surfaces of bulk CeSiI reveal that the Fermi surface is characterized by discrete spots with high spectral intensity. Through comparison with measurements on isostructural LaSiI, we demonstrate that these QPI patterns can be explained by nodal heavy fermion hybridization in the 2D planes, highlighting the possibility to observe new emergent phenomena derived from the anisotropic electronic and crystalline structure of CeSiI.

Future Plans

Having established CeSiI as a host of two-dimensional heavy fermions, our ongoing work is focused on tuning its Kondo physics in the bulk and at the 2D limit. The ternary composition of CeSiI enables modulation of its properties via substitution at its three different lattice sites; for example, substitution of La for Ce allows us to weaken the Kondo coupling and to study single-ion Kondo physics at the dilute Ce limit, whereas substitution on the Si or I site may enable electron and hole doping or generation of chemical pressure. By accessing the quantum critical point through chemical substitution, we will be able to directly study the effects of dimensionality in the quantum critical regime.

Further, we will explore the ability to use techniques developed for other 2D materials to tune the ground state of CeSiI. In particular, current efforts are focused on improving existing methods for the handling of extremely air-sensitive 2D materials, which will enable us to probe the properties of CeSiI at the monolayer limit. We will then explore the ability to tune Kondo coupling via ionic gating, strain, van der Waals charge transfer, and heterostructure engineering, which will be probed via transport in addition to spectroscopic methods.

Finally, we will attempt to better understand the magnetic structure of CeSiI. A recent neutron investigation identified an incommensurate antiferromagnetic structure at zero magnetic field, but the detailed magnetic structure could not be resolved.[5] CeSiI displays two field-induced metamagnetic transitions below 5 T, and the absence of magnetic saturation up to 9 T may imply additional magnetic transitions at even higher fields. Understanding the ground state magnetic structure, as well as the evolution of the magnetic structure under applied fields, may provide a route to new exotic phenomena. For example, one possible magnetic ground state is a cycloidal structure in which an electric polarization becomes symmetry allowed, potentially enabling CeSiI to act as a heavy fermion multiferroic.

References

1. P. Monthoux, D. Pines, and G. G. Lonzarich, *Superconductivity without phonons*, Nature **450**, 1177 (2007).

2. Y. Mizukami, H. Shishido, T. Shibauchi, M. Shimozawa, S. Yasumoto, D. Watanabe, M. Yamashita, H. Ikeda, T. Terashima, H. Kontani, and Y. Matsuda. *Extremely Strong-Coupling Superconductivity in Artificial Two-Dimensional Kondo Lattices*, Nat. Phys. **7**, 849 (2011).

3. K. S. Novoselov, A. Mishchenko, A. Carvalho, and A. H. Castro Neto, *2D Materials and van der Waals Heterostructures*, Science, **353**, 461 (2016).

4. H. Mattausch and A. Simon, *Si_6, Si_{14}, and Si_{22} Rings in Iodide Silicides of Rare Earth Metals*, Angew. Chem. Int. Ed. **37**, 499 (1998).

5. R. Okuma, C. Ritter, G. J. Nilsen, Y. Okada, *Magnetic Frustration in a van der Waals Metal CeSiI*, Phys. Rev. Mater. **5**, L121401 (2021).

Publications

Publications supported by the ECMP program:

1. V. A. Posey, S. Turkel, M. Rezaee, A. Devarakonda, A. K. Kundu, C. S. Ong, D. G. Chica, R. A. Vitalone, R. Jing, S. Xu, D. R. Needell, E. Meirzadeh, M. L. Feuer, A. Jindal, T. Valla, P. Thunström, T. Yilmaz, E. Vescovo, D. Graf, X.-Y. Zhu, A. Scheie, A. F. May, O. Eriksson, D. N. Basov, C. R. Dean, A. Rubio, P. Kim, M. E. Ziebel, A. J. Millis, A. N. Pasupathy, X Roy, "Two-dimensional heavy fermions in the van der Waals metal CeSiI", in revision at *Nature*.

2. S. Turkel, V. A. Posey, C. S. Ong, A. K. Kundu, D. G. Chica, P. Thunström, O. Eriksson, A. Rubio, A. J. Millis, X. Roy, A. N. Pasupathy, "Nodal hybridization in a two-dimensional heavy fermion material", in revision at *Nature Physics*.

First Observation of Coupled Ferroelectricity and Superconductivity in Few-layer Superconductors

PI: Daniel Rhodes, University of Wisconsin Madison, Co-PI: Xiaofeng Qian, Texas A&M University

Keywords: superconductivity, ferroelectrics, 2D and layered crystals, transition metal compounds, magnetotransport

Research Scope

Recently we have demonstrated, for the first time, an unambiguous coupling between ferroelectricity and superconductivity in a single material, bilayer T_d-$MoTe_2$ [1]. This material presents the first opportunity to study the fundamental mechanism underpinning how the internal polarization can coexist with superconductivity. Previous attempts to study the interplay between ferroelectricity and superconductivity (SC) have used ferroelectric (FE) perovskite oxides. However, disorder in the oxides leads to spatially separated polar and superconducting regions that vary with temperature and doping and creates a complex energy landscape, making it difficult to connect theory with experiment. Our discovery of the coexistence of superconductivity and ferroelectricity in a transition metal chalcogenide is made possible by the unique mechanism of ferroelectricity in bilayer T_d-$MoTe_2$, whereby flipping of the sign of polarization in an out-of-plane electric field can be achieved even at high carrier densities. The ferroelectric switching occurs via interlayer sliding ferroelectricity. We show that for dual-gated devices of bilayer T_d-$MoTe_2$ at low temperatures, where sliding ferroelectricity and SC are both present, sweeping electric field in forward and reverse bias directions results in a hysteretic transition to and from the superconducting state. The superconducting transition coincides with flipping of the polarization, indicating an interplay between ferroelectricity and SC. We have proposed a Fermi surface nesting model to explain the hysteretic behavior of SC with FE switching. Currently, we are exploring the impacts of FE switching on the symmetry of the superconducting state, the electronic band structure, and the in-plane magnetotransport properties. In the future, we will expand our understanding of the interplay between FE and SC by studying the electron-phonon coupling and the effect of interlayer interactions on the internal polarization.

Recent Progress

Bilayer $MoTe_2$ has a noncentrosymmetric crystal structure, giving rise to an out-of-plane, interlayer dipole moment. Concomitant with the weak van der Waals bonding between layers, electric fields can couple to this dipole moment and an interlayer sliding process will ensue until polarization is switched, known as sliding ferroelectricity (SFE). The SFE process in $MoTe_2$ is

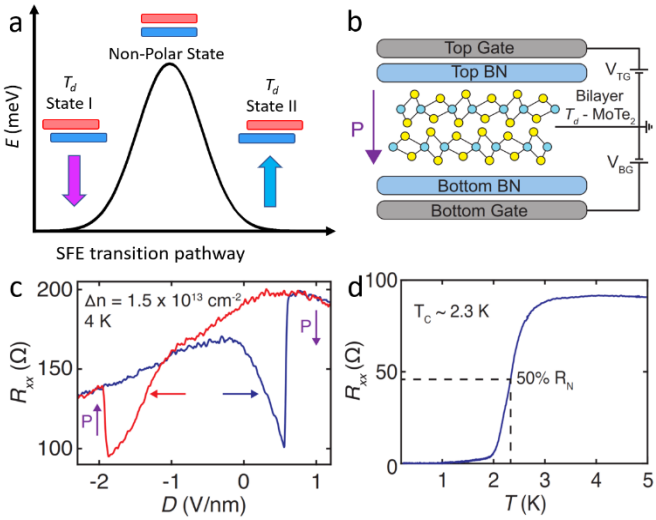

Fig. 1: a, Transition pathway for SFE. **b,** Schematic for bilayer T_d-$MoTe_2$ device. **c,** Hysteretic behavior of the longitudinal resistance (R_{xx}) with ferroelectric switching when applying an out-of-plane electric field. **d,** Superconducting transition with temperature.

akin to flipping the flake over, so that the resulting internal polarization after interlayer sliding has occurred is the same magnitude as the starting state, but opposite in sign [2] (see Fig. 1a). Our previous results on bilayer $MoTe_2$ indicated that it is a superconductor with a superconducting critical temperature of 2.5 K [3]. Given that bilayer $MoTe_2$ is predicted to exhibit SFE and is a superconductor, we investigated bilayer $MoTe_2$ in an effort to understand the interplay between FE and SC we investigated bilayer MoTe2 using a dual gate geometry. As shown in Fig. 1b, bilayer MoTe2 is encapsulated in hexagonal boron nitride (BN), which serves as dielectric layers for applying out-of-plane electric fields and tuning the carrier density. Upon cooling below 60 K we observe a hysteresis emerging in the resistance as a function of the displacement field, which we attribute to the switching of polarization as $MoTe_2$ transits along the SFE transition pathway. In the same geometry, we also observe a drop in resistance down to zero at 2.5 K (Fig. 1d) as expected, proving that this system is a viable playground for exploring the interplay of SFE and SC.

By further cooling bilayer $MoTe_2$ into the superconducting state, we can observe a clear indication of the coupling of SFE switching and SC by examining the out-of-plane electric field response, as shown in Fig. 2a. Starting from D<-2 V/nm (blue curve) with the bilayer in T_d state I, both the displacement field and the $MoTe_2$ polarization point in the same direction. On decreasing the magnitude of the displacement field and then flipping its sign, SC emerges gradually - resulting in a drop of the bilayer $MoTe_2$ resistance to zero. Bilayer $MoTe_2$ remains superconducting until the out-of-plane electric field switches the crystal to T_d state II, at which point the polarization sign flips and bilayer $MoTe_2$ transitions to the normal state. The behavior on the downward sweep (red curve, Fig. 2a) of displacement field is similar, displaying a hysteresis which we expect is from SFE. Given the observed hysteresis, the interplay between SFE and SC can be used to produce a superconducting switch driven by electric field, as illustrated in Fig. 2b. We show that a positive (negative) electric field pulse of appropriate intensity can drive a transition

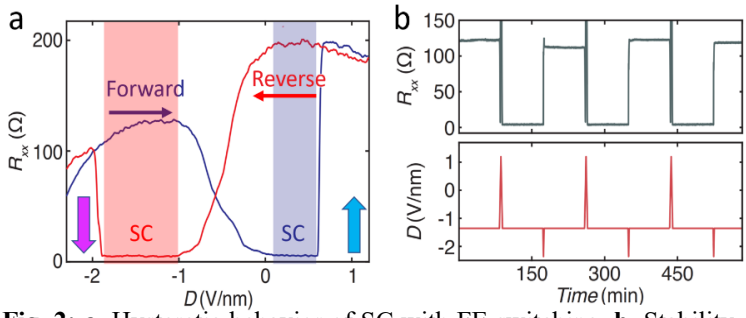

Fig. 2: a, Hysteretic behavior of SC with FE switching. **b,** Stability of the superconducting and normal state upon switching polarization directions.

to the superconducting (normal) state. Once switching from one state to another has been established, the resistance of bilayer $MoTe_2$ remains fixed indefinitely.

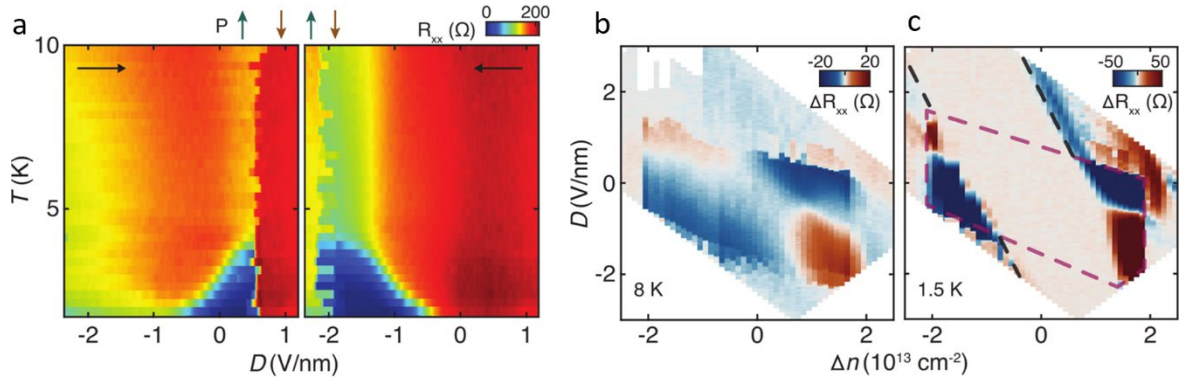

Fig. 3: a, Temperature evolution of the coupled ferroelectric and superconducting behavior at $\Delta n = 1.5\times10^{13}$ cm^{-2}. An increase in T_c is observed just before FE switching. The internal polarization is marked with arrows on top. **b**, ΔR_{xx} between displacement field sweep directions showing regions of ferroelectricity at 8 K and its evolution with doping. **c**, At 1.5 K, highlighting the regions of SC. The largest difference in resistance occurs at dopings with hysteretic superconductivity. The magenta dashed line represents the hysteretic region in the normal state. The black dashed line represents the boundary of the field-driven superconductivity.

To explore the interplay between SFE switching and SC more carefully, we performed displacement field sweeps at different temperatures, summarized in Fig. 3a, for the two sweep directions. For the forward direction (left panel, Fig. 3a), as the displacement field is lowered from a high absolute value to a low value, a superconducting transition emerges at low temperatures. On continuing to sweep the displacement field through zero, T_c continues to increase until the displacement field switches the polarization, at which point SC is lost. In both sweep directions, the maximum T_c is therefore seen just before a switching event. This continuous tuning of T_c prior to switching shows that the mechanism for the superconducting state is intimately tied to the internal electric field of the sample. The observed FE and SC behaviors described above are also density dependent. To understand the region of ferroelectricity in the carrier doping versus displacement field phase diagram, we have performed sweeps of the displacement field, similar to Fig. 2a, at various doping levels, both in the superconducting state and in the normal state. Taking the difference in resistance (ΔR_{xx}) between the forward and backward displacement field sweep directions. From these diagrams we can identify when hysteretic switching is observed in bilayer $MoTe_2$. The results in the normal state ($T = 8$ K) and in the superconducting state ($T = 1.5$ K) are shown in Fig. 2b and 2c, respectively. In the normal state, we observe that the hysteretic switching in our samples is limited to a doping range of $\Delta n = \pm2\times10^{13}$ cm^{-2}. We also observe that the hysteretic superconductivity occurs in parts of the phase diagram that are close to the boundary where field-driven superconductivity intersects with the normal state ferroelectric behavior. This phenomenology suggests that it is the total internal electric field in the sample that controls superconductivity: the polarization of bilayer $MoTe_2$, when flipped, can turn the superconducting phase on or off if bilayer $MoTe_2$ is sufficiently close to the field-driven superconducting transition.

Supported by theory, we surmise that the coupling between SFE and SC is driven by a Fermi surface nesting picture, where nesting between electron and hole pockets is enhanced, via an increase in hole carrier density from charge transfer between layers, as bilayer $MoTe_2$ approaches the point at which polarization switches. However, multiple mechanisms can lead to changes in the superconductivity as strong electric fields, required for flipping the polarization, are applied and carrier densities are tuned, obscuring contributions from interlayer charge transfer: 1) the strong electric fields can shift the bands of the electronic band structure near the Fermi level and change the relative carrier densities in each layer – inducing SC. 2) The weak interlayer bonding that allows for SFE can change with electric field and carrier doping [4], causing structural phase transitions which can change T_c [5]. Changes to interlayer bonding can also lead to stacking disorder, creating regions of differing polarization – affecting the evolution of FE domains and its interplay with SC, and smearing out any related phonon modes. 3) The frequencies of soft phonon modes associated with the SFE transition could change with electric field and thus change the pairing strength of Cooper pairs.

Future Plans

To resolve these complexities, we plan to: (1) Study the effects of ferroelectricity on the electronic transport properties of superconductivity in detail using magnetotransport measurements, initially in few-layer T_d-$MoTe_2$ encapsulated in BN (as in Fig. 1b) and later extend these same efforts to other Td-structured superconductors (TDSCs). Measurements of the superconducting transition, both by resistance and tunneling current, as a function of magnetic field angle (in- and out-of-plane) will allow us to extrapolate how FE impacts the symmetry of the superconducting order parameter and extract the spin-orbit coupling strength and orientation of the TdSC. Experimental results will be compared to the density functional theory calculated electronic band structure that includes interactions with an electric field, allowing us to create a feedback loop between theory and experiment and improve understanding of how electronic contributions to SC evolve through the SFE transition pathway. We will also measure the polarization directly, using a graphene layer, throughout the FE switching process. Investigating TdSC heterostructures via Raman spectroscopy and second-harmonic generation with temperature and electric field will reveal additional changes in crystal symmetry, allow us to verify the existence of polar phonon modes associated with SFE, and evaluate whether changes in superconducting behavior are related to changes in ionic fluctuations from these polar phonon modes. (2) Reveal **t**he interplay between interlayer coupling, SC, and ferroelectricity via hydrostatic pressure. Changes to the interlayer coupling, *i.e.,* interlayer charge transfer and orbital interactions, can have profound consequences on SFE. Increasing the interlayer coupling could increase the amount of charge transfer and lock the polarization in one direction, allowing for independent tuning of the electric field without polarization flipping across all carrier densities, enabling us to disentangle Rashba effects from those of interlayer charge transfer caused by SFE. Increased interlayer coupling may also lead to

a phase transition from a non-centrosymmetric T_d structure to a centrosymmetric T' structure, quenching SFE at all temperatures. We will change interlayer coupling by applying hydrostatic pressure to induce substantial changes to the interlayer distance in few-layer TdSCs. We will perform measurements of the doping-, electric field-, and magnetic-field dependent phase diagrams with applied hydrostatic pressure to determine the resulting the spin-orbit coupling and spin texture, coherence length, and any additional changes to the superconducting transport behavior. We will also calculate the hydrostatic pressure-dependent electronic band structure and density of states of few-layer TdSCs using many-body perturbation theory and including spin-orbit coupling. Comparing the differences in the values of various parameters measured and calculated in (2) to those of (1) will close the feedback loop and be used to guide further experiments to accurately determine the mechanism for hysteretic superconductivity in ferroelectric 2D TdSCs.

References

1. A. Jindal, A. Saha, Z. Li, T. Taniguchi, K. Watanabe, J. C. Hone, T. Birol, R. M. Fernandes, C. R. Dean, A. N. Pasupathy, and D. A. Rhodes, *Coupled ferroelectricity and superconductivity in bilayer T_d-$MoTe_2$*, Nature **613**, 48 (2023).

2. X. Liu, Y. Yang, T. Hu, G. Zhao, C. Chen, and W. Ren, *Vertical ferroelectric switching by in-plane sliding of two-dimensional bilayer WTe_2*, Nanoscale **11**, 18575 (2019)

3. D. A. Rhodes, A. Jindal, N. F. Q. Yuan, Y. Jung, A.Antony, H. Wang, B. Kim, Y. C. Chiu, T. Taniguchi, K. Watanabe, K. Barmak, L. Balicas, C. R. Dean, X. Qian, L. Fu, A. N. Pasupathy, and J. Hone. *Enhanced Superconductivity in Monolayer T_d-$MoTe_2$*, Nano Lett. **21**, 2505 (2021)

4. Y. Dai, Q. Zheng, M. E. Ziffer, D. Rhodes, J. Hone, J. Zhao, and X. Y. Zhu, *Ultrafast Ferroelectric Ordering on the Surface of a Topological Semimetal $MoTe_2$*, Nano Lett. **21**, 9903 (2021)

5. J. G. Si, W. J. Lu, H. Y. Lv, B. C. Zhao, and Y. P. Sun, *Pressure controllable phase transition in $MoTe_2$ by the interlayer band occupancy*, Phys. Lett. A **383**, 126016 (2019).

Publications

1. A. Jindal, Z. Li, A. Strasser, Y. He, W. Zheng, D. Graf, T. Taniguchi, K. Watanabe, L. Balicas, X. Qian, A. N. Pasupathy, and D. A. Rhodes, *Two-Fold Anisotropic Superconductivity in Bilayer T_d-$MoTe_2$*, in preparation (2023).

Moiré Magnetism in Twisted 2D Magnets

Liuyan Zhao, University of Michigan – Ann Arbor

Keywords: magnetism, moiré physics, 2D and layered crystals, nanofabrication and 2D assembly, optical spectroscopy

Research Scope

Moiré superlattice, formed by twisting two two-dimensional (2D) atomic crystals, emerges as one of the most powerful venues to design new physical properties of 2D material systems. While it has achieved tremendous success in controlling the charge degree of freedom (DoF) and realizing a wealth of novel quantum electronic phases, the potential and the power of moiré superlattice in modifying the spin DoF and engineering the magnetic phases have remained much less explored. Very recently, the moiré engineering of magnetism becomes experimentally feasible thanks to the recent discoveries of and progresses in 2D magnetism in atomically thin crystals. In the proposed project, we identify this unique opportunity brought by 2D magnetic atomic crystals and moiré superlattice to experimentally explore moiré magnetism in hetero/homo-structures of 2D magnetic atomic crystals. We aim at realizing, understanding, and controlling nontrivial magnetic orders and collective magnetic excitations in moiré magnets, through developing ultra-sensitive symmetry-resolved and ultrafast time-resolved nonlinear optical spectroscopy and microscopy, in addition to using conventional linear optics. Specifically, we will undertake three major tasks – (i) realizing noncollinear spin textures in moiré magnetic superlattices, and investigating its coupling to moiré crystalline structures; (ii) accessing topological and correlated magnetic excitations in moiré magnetic superlattices, and exploring their dependencies on the external magnetic field; and (iii) controlling moiré magnetic orders and collective excitations with ultrafast optical excitations, and researching the impact of optical field characteristics on the transient or metastable magnetic orders and excitations. The success of this project will not only provide a promising route to design and engineer 2D magnetism for future microelectronics and quantum electronics, but also a new set of symmetry-, time-, and spatial-resolved nonlinear optical techniques for investigating static, dynamic, and even out-of-equilibrium properties of symmetry-breaking phases in 2D.

Recent Progress

The Zhao group pioneers in the study of moiré magnetism, using twisted double bilayer CrI_3 as a material platform. CrI_3 is a van der Waals (vdW) layered magnetic materials, whose interlayer magnetic exchange coupling is proven to depend on the interlayer stacking geometry – ferromagnetic (FM) interlayer exchange coupling for the rhombohedral (R) stacking and antiferromagnetic (AFM) for the monoclinic (M) one. Bilayer CrI_3 is a layered AFM with zero total magnetization. Twisted double bilayer CrI_3 contains two bilayer CrI_3 with uniform AFM interlayer coupling within each bilayer and moiré modulated interlayer exchange coupling at the interface between the two bilayers. The key progresses are listed as follows:

- We managed to fabricate high-quality moiré superlattices of twisted double bilayer CrI_3[1,2,3]. In collaboration with Prof. Robert Hovden's group, we imaged the moiré superlattices with both selected are electron diffraction (SAED) and dark-field transmission electron microscopy (DF-TEM). The presence of moiré superlattices is confirmed by the superlattice peaks in the SAED pattern, and the high quality of moiré superlattices is revealed by the real-space DF-TEM image. Please see Figure R1 below for both data sets.

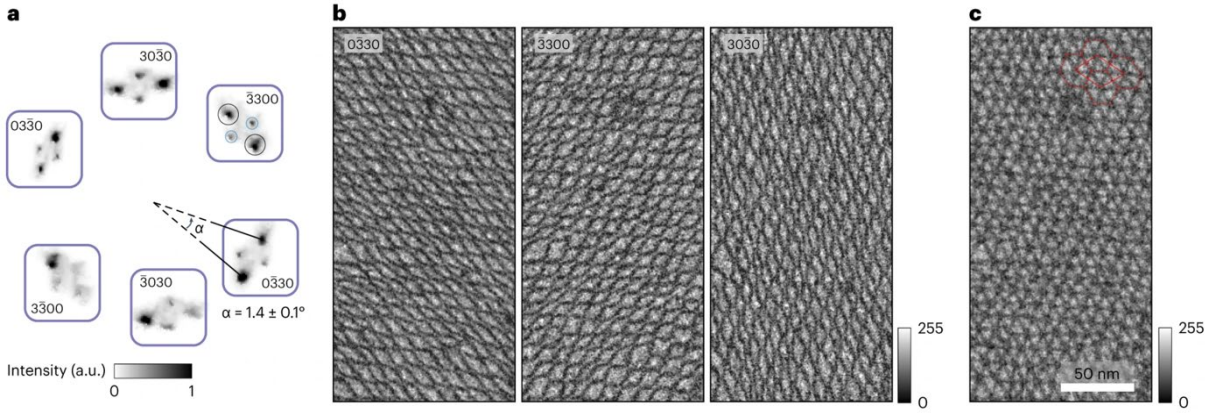

Figure R1 Moiré superlattices imaged by SAED and DF-TEM. (a) SAED pattern for a twisted double bilayer CrI_3, with a twist angle measured to be $\alpha = 1.4 \pm 0.1^o$. Dark and light blue circles highlight the Bragg and moiré superlattice peaks. (b) DF-TEM images for individual pairs of Bragg-moiré superlattice peaks. (c) A composite DF-TEM image made of summing up the three images in (b), showing the high-quality of moiré superlattices.

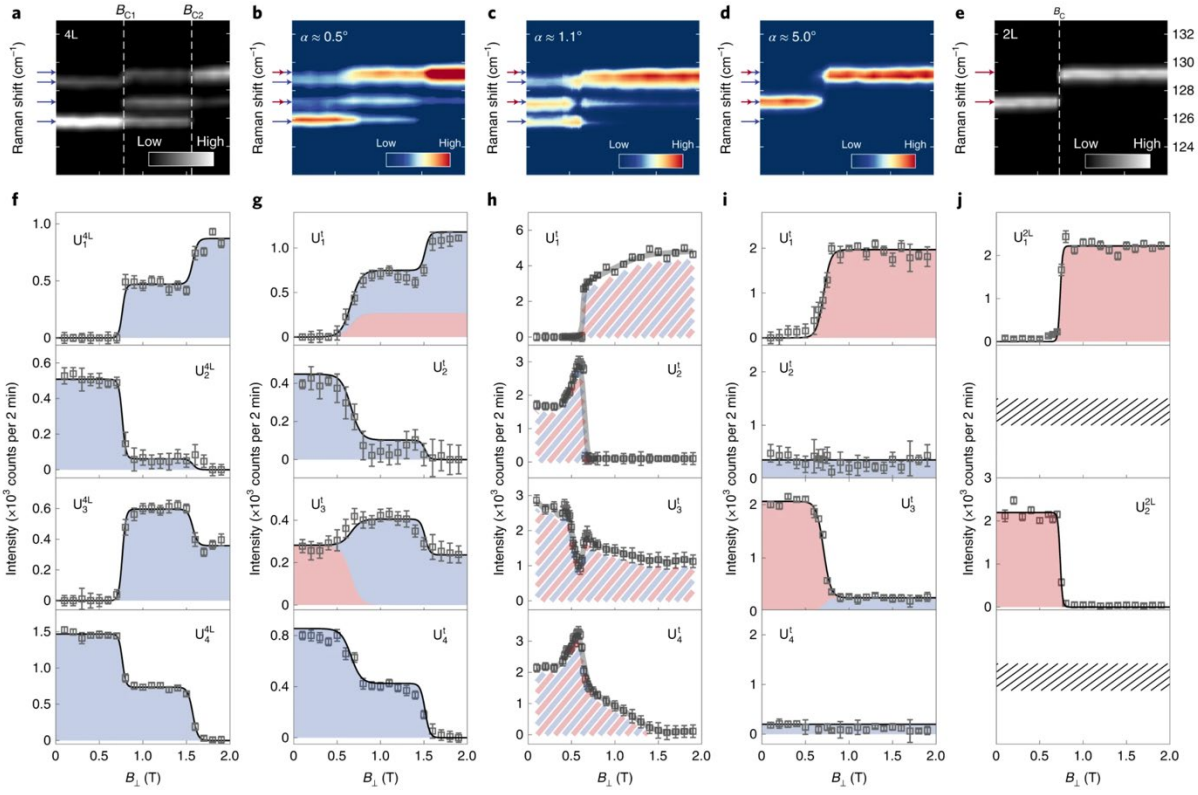

Figure R2 Magneto-Raman spectroscopy of twisted double bilayer CrI_3. (a-e) False color map of magnetic field dependent Raman spectroscopy for four-layer, 0.5°, 1.1°, 5.0° twisted double bilayer, and bilayer CrI_3. (f-j) Magnetic field dependence of fitted Raman mode intensities in (a-e).

- We performed magneto-Raman spectroscopy of twisted double bilayer CrI_3[2], at very small twist angle $\alpha = 0.5^o$, intermediate angle, 1.1^o, and very large angle 5^o. We found that while the small and large twist angle samples are dominated by features of natural bilayer and four-layer CrI_3 (i.e., a linear superposition of bilayer and four-layer data can fit the data of 0.5^o and 5^o samples), the intermediate twist angle sample is in stark contrast to them by showing multiple features that are absent in bilayer and four-layer samples. This suggests the uniqueness of magnetism in the intermediate twist angle samples (Figure R2).
- We performed magnetic circular dichroism (MCD) of twisted double bilayer CrI_3[3], with a careful twist angle dependence. Our analysis separates the collinear and noncollinear spin contributions to MCD. An unexpected net magnetization and a noncollinear spin texture emerge in a wide twist angle range, 0.5° – 5.0° and peaks at 1.1°. Both features are not present in bilayer or four-layer, or any homogenous stacking of two bilayer CrI_3 (Figure R3).

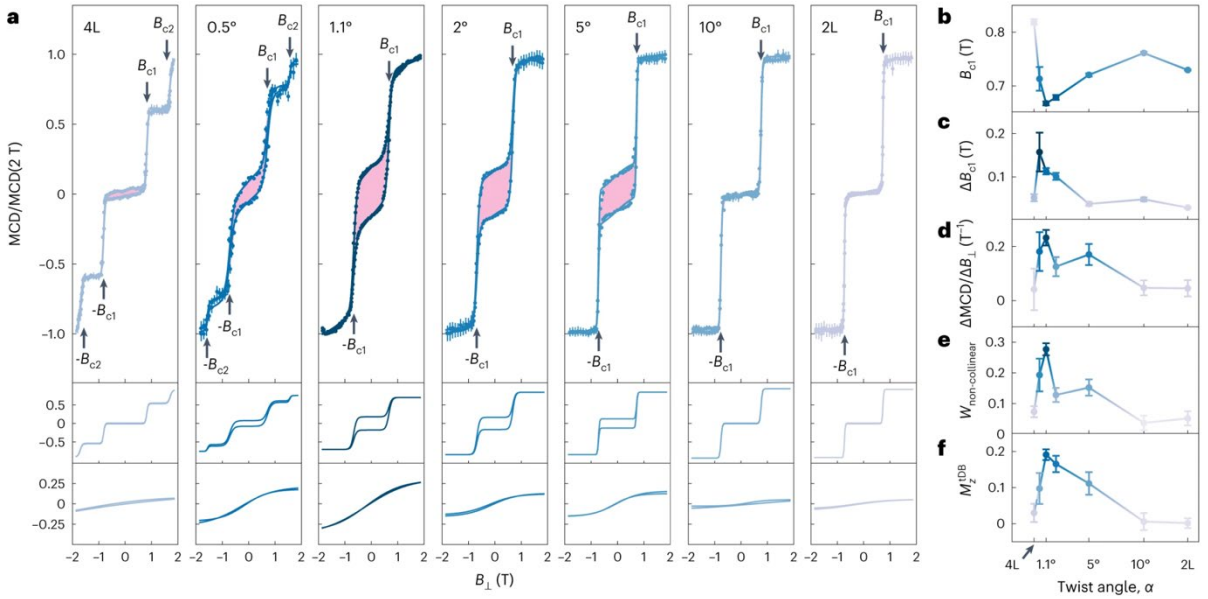

Figure R3 Magnetic circular dichroism of twisted double bilayer CrI_3. (a) Normalized MCD data and fits under out-of-plane magnetic field sweeping from +2T to -2T and back to +2T, for four-layer, 0.5°, 1.1°, 2°, 5°, 10° twisted double bilayer, and bilayer CrI_3 (top panel) and the separated collinear (middle panel) and noncollinear (bottom panel) contributions. (b-f) Twist angle dependence of fitted parameters, showing 1.1° being the special twist angle that maximize the moiré impact.

Future Plans

Towards the goals of this project, we have the following three plans for the coming year, with the first two on the scientific aspect and the third one from the technical perspective.

- First, we plan to work on the H-stacked twisted double bilayer CrI_3, i.e., twist angle around 180°. Because of the 3-fold, rather than the 6-fold, rotational symmetry of CrI_3 layers, there is clear distinctions between R-stacked (~ 0°) and H-stacked (~ 180°) twisted double bilayer CrI_3. From the first principle calculations [4], the moiré interlayer exchange potential is drastically different between R-stacked and H-stacked cases, and suggests a more stable moiré magnetic

superlattice for the H-stacked case. We have fabricated H-stacked twisted double bilayer CrI_3 with a twist angle of 181° and examined with SAED and DF-TEM measurements, showing a higher moiré superlattice quality than the R-stacked counterpart (i.e., 1° twist angle). Further optical spectroscopy measurements will be performed in this system with a careful twist angle dependence study.

- Second, we plan to investigate the moiré magnons of both R-stacked and H-stacked twisted double bilayer CrI_3. Recently, we have finished a careful study of layer-number dependent magnons in natural few-layer CrI_3, which sets the foundation for the study of moiré magnons in the twisted double bilayer CrI_3. In addition, the research on the magnetic ground states in R-stacked and H-stacked twisted double bilayer CrI_3 also provides the essential piece of information for the study of moiré magnons. Magneto-Raman spectroscopy and time-resolved optical spectroscopy will be used for this study, with a particular focus on 1° and 181° twist angles.
- Third, we plan to use magnetic second and third harmonic generation (MS/THG) rotation anisotropy (RA) to directly couple to the complex spin textures in twisted double bilayer CrI_3 and resolve their full point symmetry evolutions across the magnetic phase transitions, upon varying the temperature and the external magnetic field. Currently, we have achieved the sub-photon counting detection sensitivity for both SHG and THG and will practice them on this challenging systems of twisted double bilayer CrI_3.

In addition to these major research activities from the Zhao group, we further plan to collaborate with Prof. Rita C. Du's group at Georgia Institute of Technology to perform scanning and wide-field NV magnetometry measurements on twisted double trilayer CrI_3 of the H-stacked case, based on our recent successful collaboration on the R-stacked geometry[5].

References

1. S. H. Sung, Y. M. Goh, H. Yoo, R. Engelke, H. Xie, K. Zhang, Z. Li, A. Ye, P. B. Deotare, E. B. Tadmor, A. J. Mannix, J. Park, L. Zhao, P. Kim, and R. Hovden, *Torsional Periodic Lattice Distortions and Diffraction of Twisted 2D Materials*, Nature Communications **13**, 7826 (2022)
2. H. Xie*, X. Luo*, G. Ye*, Z. Ye, H. Ge, S. H. Sung, E. Rennich, S. Yan, Y. Fu, S. Tian, H. Lei, R. Hovden, K. Sun, R. He, and L. Zhao, *Twist engineering of the two-dimensional magnetism in double bilayer chromium triiodide homostructures*, Nature Physics **18**, 30 (2022)
3. H. Xie*, X. Luo*, Z. Ye*, Z. Sun*, G. Ye, S.-H. Sung, H. Ge, S. Yan, Y. Fu, S. Tian, H. Lei, K. Sun, R. Hovden, R. He, and L. Zhao, *Evidence of Noncollinear Spin Texture in Magnetic Moiré Superlattices*, Nature Physics, **19**, 1150 (2023)
4. F. Zheng, *Magnetic Skyrmion Lattices in a Novel 2D-Twisted Bilayer Magnet*, Advanced Functional Materials, **33**, 2206923 (2022)
5. M. Huang*, Z. Sun*, G. Yan, H. Xie, G. Ye, H. Lu, J. Zhou, S. Yan, S. Tian, H. Lei, R. He, H. Wang, L. Zhao, and C. Du, Revealing intrinsic domains and fluctuations of moiré magnetism by a wide-field quantum microscope, Nature Communications, **in press** (2023)

Ultrafast Control of Topological Transport in Quantum Materials

James McIver, Columbia University in the City of New York

Keywords: light-matter phenomena, topology, 2D and layered crystals, transition metal compounds, ultrafast optoelectronics

Research Scope

This new research program will deliver pathways to on-demand topological transport in bulk quantum materials using femtosecond pulses of light. Experimental protocols will be developed to create and control novel non-equilibrium topological states. The ultrafast transport dynamics of these states will be directly captured using a chip-scale optoelectronic device architecture. The results will further our understanding of out-of-equilibrium topological phenomena in solids and enable transformative functionalities in next-generation, energy efficient technologies.

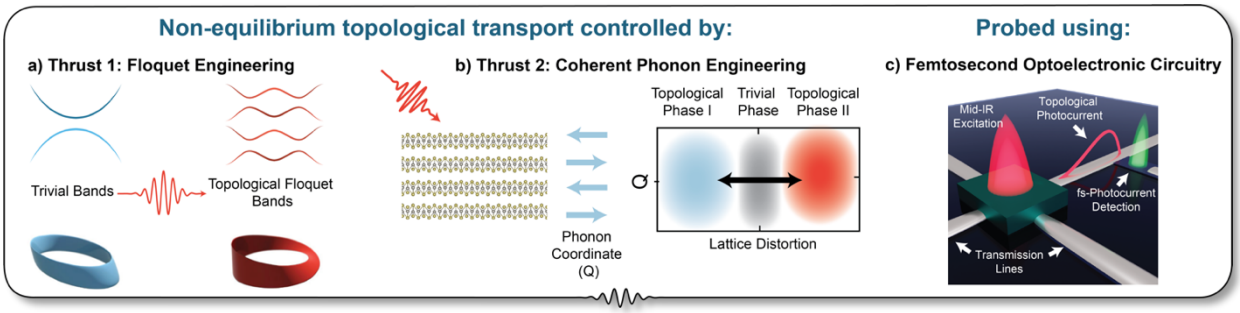

Figure 1. Pathways to controlling topological transport in quantum materials: (a) The creation of photon-dressed Floquet states and (b) the optical generation of coherent phonons can manipulate electronic topology. c) Femtosecond optoelectronic circuitry captures ultrafast topological transport responses on their characteristic timescales.

This research program encompasses two thrusts. In the first, coherent light-matter interaction will be used to design topological transport responses via the creation of photon-dressed Floquet states. Novel bi-chromatic driving schemes in which specific material symmetries can be broken or restored to induce topological transport responses will be developed [1]. This new set of driving protocols will be used to engineer ultrafast magnetotransport phenomena with no equilibrium counterparts, in an effort to perfect tools for controlling material topology with light [2]. The overarching goal of this thrust will be accomplished by the achievement of three well-defined sub-goals. **Thrust 1-1** will realize a Floquet-Weyl semimetal state by breaking time-reversal symmetry with circularly polarized light. **Thrust 1-2** will develop bi-chromatic optical drives with highly manipulable polarizations to program a variety of other broken symmetry Floquet states and characterize their induced transport properties. **Thrust 1-3** will probe the emergence of topologically protected axial transport predicted to occur when Floquet states are induced in the presence of a magnetic field.

The second research thrust will develop routes to creating metastable changes in material topology by targeting specific coherent phonons. The goal is to drive materials through distinct topological

phases, each with their own unique transport signature, using strongly driven displacive phonons to change the structure of the crystal lattice, either transiently or permanently. **Thrust 2-1** will investigate the ultrafast transport signatures of phonon-Berry curvature coupling upon the excitation of coherent phonons in topological materials (see recent progress, Figure 2). **Thrust 2-2** will extend this work to dynamically steer semimetals between different topological phases and capture their transport transients by selectively exciting shear modes with symmetry-matching polarization states. **Thrust 2-3** will discover phononic pathways to induce persistent and reversibly switchable topological metastability and capture the transport properties of these hidden phases (see recent progress, Figure 3).

Recent Progress

Although funding for this project has yet to commence, my group has promising preliminary results on two of the proposed goals in Thrust 2.

Thrust 2-1: Signatures of direct coupling between phonon oscillations induced by ultrafast optical excitation and quantum geometric transport have been observed. Figure 2 shows the measurement of light-induced changes in the nonlinear Hall effect in thick exfoliated flakes of $MoTe_2$ (a Type-II Weyl semimetal) under optical excitation conditions known to drive an inter-layer shear phonon. Oscillations in the nonlinear Hall effect are observed at ~200 GHz, which is the known frequency of the interlayer shear mode.

Preliminary interpretation: the nonlinear Hall effect is proportional to the magnitude of the Berry curvature dipole, which is related to the separation and tilt of the Weyl nodes in k-space. As the phonon oscillates, the separation between Weyl node pairs are known to oscillate [3,4], which is the possible source of the coherent oscillations observed in the nonlinear Hall effect signal.

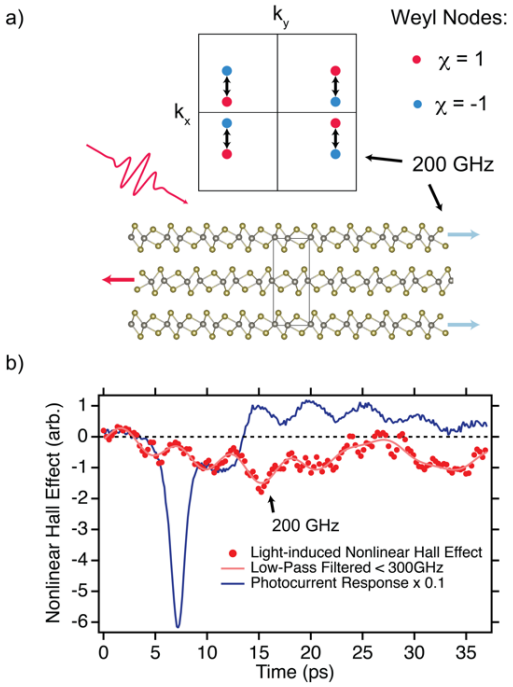

Figure 2a) Schematic of Weyl node oscillations induced by coherent phonons in $MoTe_2$. b) Measurement of the time-resolved changes in the nonlinear Hall effect as the coherent interlayer shear mode oscillates.

Thrust 2-3: While characterizing the coupling between coherent phonon dynamics and the nonlinear Hall effect, my group discovered that T_d-$MoTe_2$ undergoes a persistently metastable phase transition, whereby the nonlinear Hall effect disappears after photoexciting the material strongly enough. Following guidance from theory collaborators, it was found that, depending on the pulse polarization and wavelength, single groups of pulses (10 pulses per group) can either

destroy or revive the nonlinear Hall effect, without appreciably changing the overall sample resistance. Upon thermal cycling, the metastable, non-topological phase remains (i.e. the nonlinear Hall signal is still absent in this metastable phase). This is shown in Figure 3: the nonlinear Hall effect can be destroyed and revived with pulses of femtosecond light, showing that ultrafast, permanent switching of topological transport observables is indeed possible. The photo-induced phase transitions observed here were stable over long timescales (at least days).

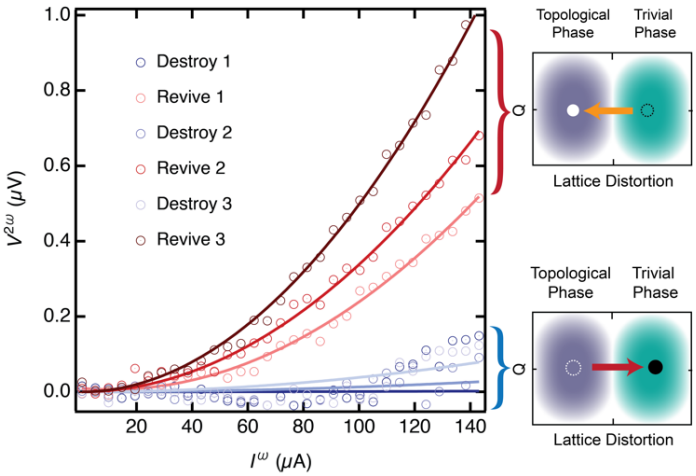

Figure 3: By driving the lattice with laser pulses possessing different properties (polarization/wavelength etc.) the topological phase of the material can be switched, as shown by monitoring the nonlinear Hall effect.

Taken together, these preliminary results show that coherently excited phonons may be a reliable route to switch between different topological allotropes of layered quantum materials. Given that the mechanism for inducing single-pulse, light-induced phase transitions is not known, more work needs to be done to understand this structural distortion mechanism, and to what extent it can be controlled. This is elaborated on in the future plans for Thrust 2-3 below.

Future Plans

Thrust 1: Technical development of bi-chromatic, multi-symmetry breaking pulses of light will commence at the start of the funding period. This light-source development is required to achieve the aims in Thrust 1-2 and 1-3. Once the development is completed, my group will execute Thrust 1-1 and 1-2, as they are similar experiments that can be performed on the same sample. Namely, the light-induced changes to the longitudinal and (nonlinear) Hall conductivities will be characterized in a nodal-line semimetal as a function of different light-induced broken symmetries, including time-reversal (Thrust 1-1) and inversion (Thrust 1-2). Together, both experiments will fulfill my plan to demonstrate that materials can be tuned coherently through multiple Floquet-engineered topological states by tailoring the photonic field used to drive the material out of equilibrium.

Following these experimental achievements, my group will create and capture coherent, out-of-equilibrium topological magnetotransport responses in the same class of materials. It is predicted that in a magnetic field, changes to the out-of-plane conductivity will couple with a strong magnetic field to create an axial vector potential that will drive a new type of topological transport [2]. It is within my group's capabilities to measure this response and it is planned to do so upon the completion of the other objectives in Thrust 1.

Thrust 2: The key deliverables of Thrust 2 have begun to germinate (see Recent Progress). As this program grows, my group will continue to build on this success to understand exactly how to use coherent phonons to control material topology, either transiently (Thrusts 2-1 and 2-2) or permanently (Thrust 2-3). In the former case, light-induced changes to the nonlinear Hall effect will be monitored under strong optical driving to characterize and understand the coupling between coherent phonons and topological transport. My hope is to drive WTe_2 and/or $ZrTe_5$ through a transient topological phase change, monitored by the ultrafast destruction and recovery of ultrafast nonlinear Hall currents.

In Thrust 2-3, my group will expand on our preliminary data and deliver roads to femtosecond switching of persistent metastable topological phases. A persistent, switchable metastability in a topological transport observable has already been demonstrated. However, how this switching mechanism functions, and to what degree it can be controlled, will next be explored. With collaborative support from theory colleagues, this metastable switching will be characterized, pulse-by-pulse, as a function of laser wavelength and polarization state. This will seed the development of new coherent phonon engineering protocols to control material properties with switching times comparable to single femtosecond pulses of light.

References

1. Trevisan, T. V., Arribi, P. V., Heinonen, O., Slager, R.-J. & Orth, P. P. *Bicircular Light Floquet Engineering of Magnetic Symmetry and Topology and Its Application to the Dirac Semimetal Cd3As2*. Phys. Rev. Lett. **128**, 066602 (2022).
2. Ebihara, S., Fukushima, K. & Oka, T. Chiral pumping effect induced by rotating electric fields. Phys. Rev. B **93**, 155107 (2016).
3. Sie, E. J., Nyby, C. M., Pemmaraju, C. D., Park, S. J., Shen, X., Yang, J., Hoffmann, M. C., Ofori-Okai, B. K., Li, R., Reid, A. H., Weathersby, S., Mannebach, E., Finney, N., Rhodes, D., Chenet, D., Antony, A., Balicas, L., Hone, J., Devereaux, T. P., Heinz, T. F., Wang, X. & Lindenberg, A. M. *An ultrafast symmetry switch in a Weyl semimetal.* Nature **565,** 61–66 (2019).
4. Guan, M.-X., Wang, E., You, P.-W., Sun, J.-T. & Meng, S. Manipulating Weyl quasiparticles by orbital-selective photoexcitation in WTe2. Nat. Commun. **12,** 1885 (2021).

Heterogeneous Integration of 2D-3D Materials for Energy Efficient Electronics

Nihar R. Pradhan[1], Anirudha V. Sumant[2], Jerzy Leszczynski[1], Dinesh Kumar Sengottuvelu[3], Mohammed Majdoub[3], Sasan Nouranian[4] and Ahmed Al-Ostaz[5]

[1] Department of Physics, Chemistry & Atmospheric Science, Jackson State University, Jackson, Mississippi, 39217, USA
[2] Center for Nanoscale Materials, Argonne National Laboratory, 9700 South Cass Avenue, Lemont, Illinois 60439, USA
[3] Center for Graphene Research and Innovation, C06 Jackson Avenue Center, University of Mississippi, Mississippi 38677, USA
[4] Department of Chemical Engineering, University of Mississippi, Mississippi, 38677 USA
[5] Department of Civil Engineering, University of Mississippi, Mississippi, 38677 USA

Keywords: 2D and layered crystals, thin film heterostructures, transition metal compounds, nanofabrication and 2D assembly

Research Scope

The integration of 2D and 3D materials has emerged as a promising avenue to develop innovative technological solutions with enhanced performance and reduced energy consumption in the semiconductor industry. Through this project, we aim to understand the interface science and materials synthesis, and to integrate multi-dimensional materials to form 2D-3D, 2D-2D, and 0D-2D heterostructures. Our goal is to develop in-depth understanding of how these interfaces works that will help us to develop design rules that governs the functionality of the devices and will enable fabrication of devices with unprecedented properties that can be applied in a wide range of functional applications. Specifically, our research is focused on the following areas:
(i) Integration of two-dimensional (2D) semiconductor transition metal dichalcogenides (TMDs) with diamond (3D) with high thermal conductivity and carrier mobility. This integration is expected to produce new phenomena with enhanced properties.
(ii) Integration of 2D-2D and 2D-infrared (IR) absorbing polymer (3D) with 0D quantum dots (QDs) of TMDs to develop photosensor and optoelectronic applications in a broader spectral range, particularly to push the limit to the IR sensing technology.
(iii) Our interest to explore the fundamental physics at the interface of different heterogeneous materials system using computational DFT study. We will investigate the charge transfer phenomena at the interface as a function of defects, lattice mismatch, contact effect on 2D-2D, 2D-3D and metal contacts etc.
(iv) Phonon transport properties will be explored at different 2D-2D and 2D-3D interfaces to explore the thermal transport properties of such hetero integrated systems.

Recent Progress:

We recently got the grant awarded in August 2023. Given below are some of the preliminary results from the earlier work, which is the basis for the new proposed work:

Enhanced rectification in n-MoS_2/p-CVD Diamond heterostructure: A wafer scale of high quality amorphous diamond films were grown using CVD technique on a Si/SiO_2 wafer. Several exfoliated MoS_2 flakes were transferred on the diamond film in ambient conditions and 2-contact devices were fabricated as shown in the Figure-1. We demonstrated the diamond (p-type)/MoS_2 (n-type) can create heterostructure *p-n* junctions with high current rectification ratio and operating at large current density (>10^3 $A.cm^{-2}$).

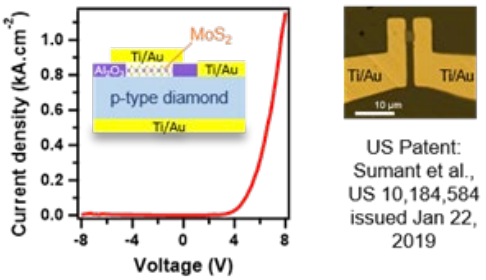

Figure-1: *n*-MoS_2/*p*-type CVD Diamond heterostructure shows enhanced rectification current. Fabricated device is shown on the right. (Ref. 1)

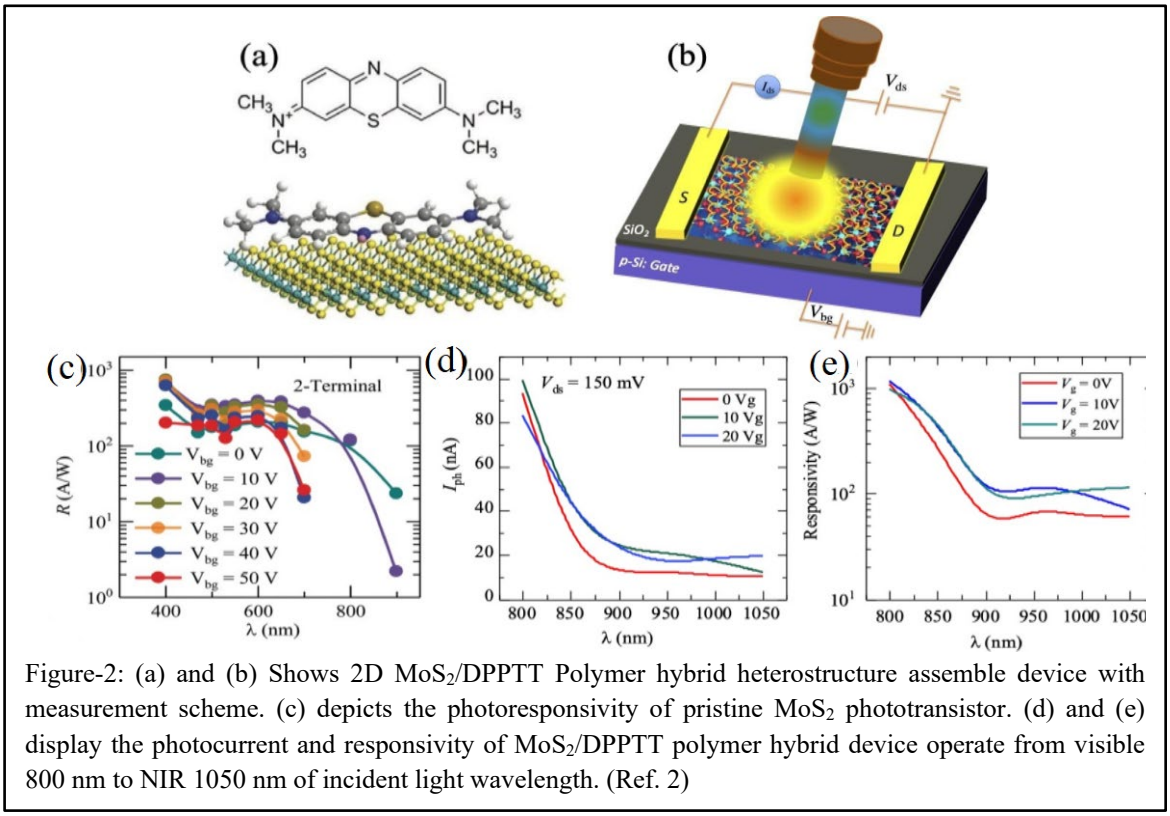

Figure-2: (a) and (b) Shows 2D MoS_2/DPPTT Polymer hybrid heterostructure assemble device with measurement scheme. (c) depicts the photoresponsivity of pristine MoS_2 phototransistor. (d) and (e) display the photocurrent and responsivity of MoS_2/DPPTT polymer hybrid device operate from visible 800 nm to NIR 1050 nm of incident light wavelength. (Ref. 2)

High responsivity NIR photosensor in MoS_2/Polymer hybrid integrated structure:
Developing high responsivity thin film photosensor working at broad spectral range, particularly NIR to IR wavelength is one of the great interest and challenge. We recently explored the photoconductivity of MoS_2 and NIR absorbing DPPTT polymer hybrid heterostructure materials which shows extremely high photoconductivity at NIR region, from l = 800 nm to 1050 nm. Figure-2 (c) shows the photoresponsivity of pristine MoS_2 phototransistor (Pradhan et al. *Nanoscale* (2020) 12, 22904) which provide high photoresponse in the visible wavelength of the solar spectrum and it fails to show responsivity above or NIR wavelength due to the band edge absorption. On the other hand, when the surface of such visible sensitivity 2D systems (MoS_2) passivated with the NIR absorbing polymer, the hybrid device (MoS_2/DPPTT polymer) yields

much more sensitivity and extend photoresponse capability to the NIR region. Figure 2 (d) shows the photocurrent measured from the MoS_2/DPPTT polymer device shows high photocurrent ~20 nA at incident wavelength of 1050 nm in the NIR region. The extracted photoresoonsivity from the same polymer/2D hybrid integrated device shows high responsivity, R~100 A/W where pristine MoS_2 does not show any responsivity due to the band edge absorption.

Future Plans:

We have plan to explore the interface physics in diverse members of layered van der Waals materials with 2D-3D, 2D-2D and 2D-0D hetero integrated materials in close collaboration among the DOE EPSCoR family of Jackson State University (JSU), University of Mississippi (UM), and Argonne National Laboratory (ANL). Our immediate plans in the project are, *Year-1:* (i) to grow the high-quality diamond film and 0D, 2D materials such as transition metal dichalcogenides using CVD and CVT system, (ii) integrate some of these 2D materials with varying electronic properties such as n-type MoS_2, p-type WSe_2 and ambipolar crystals with 3D diamond film and (iii) explore the various electronic and optical properties to understand the interface charge transfer dynamics in hetero integrated devices. Simultaneously, exploring the computation technique to simulate the charge transfer mechanism between different 0D, 2D and 3D (diamond) systems. *Year-2*: (i) We plan extend the synthesis more 2D materials family and explore the intrinsic interface properties. Emphasis will be given to 0D-2D-3D multi-layered integrated system for optoelectronic properties and ambipolar/diamond heterostructure for high power, energy efficient electronic applications. Role of different contact materials and their interface charge transfer mechanism will be studied to understand the charge transfer properties where the applications for energy efficient electronics could be enhanced. A phonon transport studies will be theoretical explored to understand the thermal transport behavior of these hetero integrated systems, which is one of the crucial parameters to develop energy efficient electronics.

References

1. A. V Sumant and K. K. Kovi, Systems and methods for forming diamond heterojunction junction devices, US Patent 10,186,584 (2019).
2. R. W. Don, P. Das, Z. Ma, U. M. Kuruppu, D. Feng, B. Shook, M. K. Gangishetty, M. C. Stefan, N. R. Pradhan, and C. N. Scott, Vinyl-Flanked Diketopyrrolopyrrole Polymer/MoS2 Hybrid for Donor–Acceptor Semiconductor Photodetection, *Chem. Mater.* 35, 12, 4691–4704 (2023)

Exciton Dynamics in 2D WSe_2 Samples

Birol Ozturk, Morgan State University

Can Ataca, University of Maryland Baltimore County

Keywords: 2D exciton and light-matter phenomena

Research Scope

The nitrogen-vacancy (NV) color center defect in diamond has been widely used in quantum sensing experiments. Defects in two-dimensional (2D) transition metal dichalcogenides (TMDs) semiconductors are relatively less characterized and not well understood compared to defects in diamond. As wide band- gap semiconductors, 2D TMDs are potentially a host for defect energy states within the band-gap and rigorous characterization of defect properties will lead to their utilization in a wide range of quantum devices and applications.

Recent Progress

In this preliminary study, we performed structural and optical characterization of mechanically exfoliated and Chemical Vapor Deposition (CVD) grown WSe_2 samples. We have observed band-gap emission in the photoluminescence (PL) spectra from monolayer WSe_2 samples at room temperature. We extensively investigated the optical properties of defect states in these WSe_2 samples at cryogenic temperatures and observed shifting of excitonic peaks to higher energies with decreasing temperature. Intensities of excitonic PL peaks did not increase uniformly with increasing excitation laser power, where dark exciton intensities increased more compared to free excitonic PL peaks. Excitonic peaks from exfoliated WSe_2 monolayer samples shifted to lower energies compared to CVD grown samples due to substrate effects.

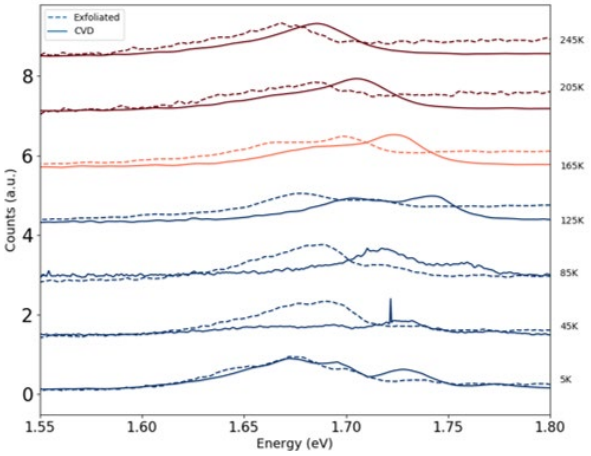

Comparison of PL spectra from exfoliated and CVD WSe_2 samples at different temperatures.

Future Plans

We plan to collect PL spectra from the WSe_2 and other 2D semiconductor samples with a high resolution spectrometer to better identify the exitonic peaks. We plan to perform optically detected magnetic resonance (ODMR) measurements to verify the possibility of using PL spectra from defects in these 2D semiconductors in quantum sensing experiments. We will also perform computational simulations to determine the quantum properties of defects in 2D semiconductors, including zero field splitting frequencies and Debye-Weller factors.

References

1. Liu, Xiaolong and Mark C. Hersam, *2D materials for quantum information science*, Nature Reviews Materials **4**.10, 669-684 (2019).

2. J. Huang, T. B. Hoang, and M. H. Mikkelsen, *Probing the origin of excitonic states in monolayer WSe2*, Scientific reports, **6**(1), 1-7 (2016).

3. S. Tongay, J. Suh, C. Ataca, W. Fan, A. Luce, J.S. Kang, J. Liu, C. Ko, R. Raghunathanan, J. Zhou, and F. Ogletree, *Defects activated photoluminescence in two-dimensional semiconductors: interplay between bound, charged and free exciton*, Scientific reports, **3**(1), p.2657 (2013).

4. X. X. Zhang, Y. You, S.Y.F. Zhao, and T. F. Heinz, T. F, *Experimental evidence for dark excitons in monolayer WSe_2*. Physical review letters, **115**(25), 257403 (2015).

Incommensurate Interfaces in Intercalated Quantum Materials

Joe Checkelsky, MIT

Keywords: 2D and layered crystals, single crystals, transport

Research Scope

The objective of this study is to realize new types of incommensurate interfaces in bulk crystals with equilibrium (via direct synthesis) and nonequilibrium (post-synthesis) intercalated structures. The goals are to realize new behavior in terms of materials and devices that support modulated magnetism, topology, superconductivity, multiferroic behavior, and other emergent phenomena. The efforts involve materials synthesis, structural and electrical characterization, and modeling of physical properties. Discoveries herein could offer new platforms for energy saving technology based on incommensurate interfaces.

Recent Progress

Incommensurate materials are systems which lack true crystalline periodicity and have long been a subject of study in condensed matter physics (*1*). Realized in structural, magnetic, and charge density modulation systems, such materials extend the notion of crystallinity and are potential platforms for exotic phases of quantum beyond conventional solids. These systems have been revisited after recent advances in van der Waals (vdW) heterostructures, which have demonstrated the capability of incommensurate structures to support correlated electronic phases (*2*). Realizing such potential in bulk crystal systems offers opportunities for scalability and new methods of structural control.

The transition metal dichalcogenides (TMDs) have played a key role in the recent developments in vdW heterostructures. We have recently investigated these materials in the bulk form via synthesis of layered variants which in the synthesis process combine TMD layers with spacer layers (see Fig. 1) (*3*). These materials are bulk materials grown by a chloride catalyzed reaction and produce single crystals of half millimeter lateral size. In our initial report (*3*), the materials was found to have a spacer layer which had

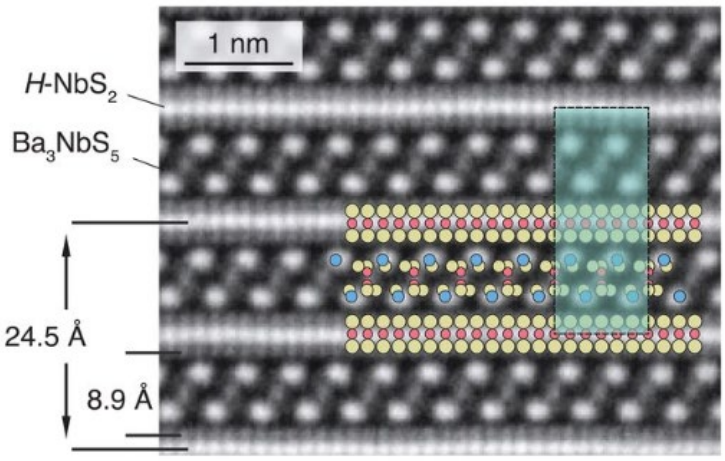

Fig. 1 – Transmission electron microscope image of layered TMD system (from (3)).

exactly three times the lattice constant of the TMD layer, yielding a commensurate structure with a zone-folded band structure. Recent efforts have focused on the further synthesis of natural van der Waals (vdW) super lattices with structural modulation. These are potentially material in which electronic transport of high mobility conducting layers is modulated by structural deformation, representing a natural crystal analog of vdW heterostructure with incommensurate structure. These are a natural foil to *ex-situ* intercalation and may represent an approach to modulating more complex "parent" electronic structures (see below).

In terms of simulating the electronic properties of these materials, significant insight is provided by the modulation of the 2D layer electronic structure with the symmetry of the spacer layer (see Fig. 2). The zone folding that occurs in these materials can lead to changes in the hierarchy of bands, leading to changes in *e.g.* the importance of different types of spin-orbit effects at the Fermi surface. A current question of interest is to what extend the emergent electronic behavior of these systems is determined by the TMD versus the spacer layer- it is therefore of significant interest to realize different spacer layers with the same TMD. Furthermore, the chemical combability of different layer types and the ability to control the stacking structure (in terms of number of layers and relative orientation) is also being investigated.

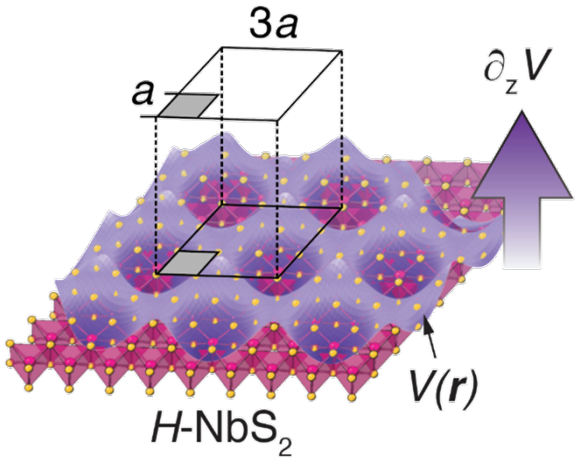

Fig. 2 – Depiction of modulation of TMD layer with spacer potential.

In terms of *ex-situ* preparation of incommensurate structures, we have investigated molecular intercalation into graphite and other layered systems. In contrast to the majority of prior graphite intercalation compound (GIC) studies (*4*), we have employed a two-step intercalation procedure that minimizes unwanted chemical reactions. The Raman spectroscopy in Fig. 3(b) shows that no discernible chemical disorder is introduced in the oxidation process (as suggested by the absence of the D band which often appears in such systems). In

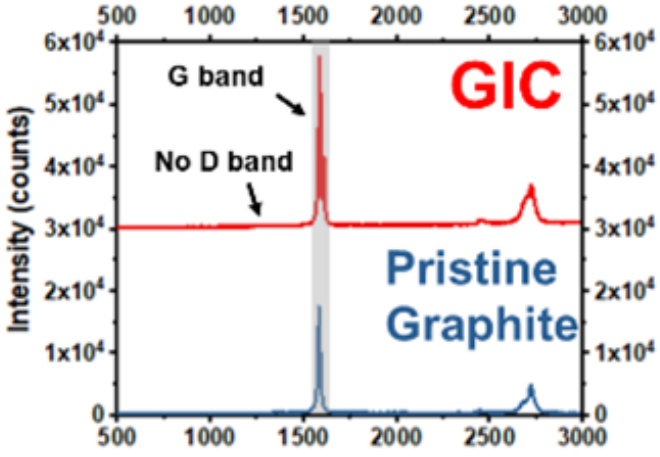

Fig. 3 – Raman spectroscopy of synthesized GIC compound compared to pristine graphite.

comparison with the GICs explored extensively in prior literature, this allows charge-neutral organic species to be intercalated. This is a key consideration as intercalation can act to either decouple or more strongly couple layers depending the chemical interaction between the intercalant and the active layer in addition to the geometry (*e.g.* size) of the intercalant. In the case of minimal charge transfer, a natural expectation is a relatively decoupling of the conducting layers that leads to stronger quasi-2D behavior.

In terms the lateral structure formed by the intercalants, we have performed scattering experiments including synchrotron Wide angle X-ray scattering (see Fig. 4). A series of structural changes are observed upon lowering temperature. An outstanding challenge is to control the distribution and homogeneity of such a superlattice on a macroscopic scale. With a refined structural model, a key goal is to develop an understanding of the modulated electronic structure of these systems. This follows previous work in superlattice systems based on transition metal dichalcogenide systems with crystalline intergrown layers (*3*).

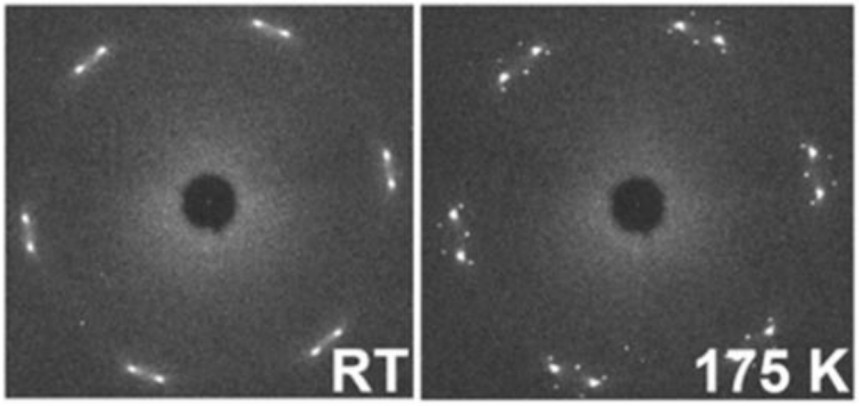

Fig. 4 – Synchrotron wide-angle X-ray scattering of GIC.

To experimentally probe the resulting electronic structure, one well-established method is via quantum oscillations. As in other GICs, there are pronounced quantum oscillations observed in the form of Shubnikov-de Haas and de Haas-Van Alphen effects in these compounds. Here, we have focused on improving material quality with the aim of being able to resolve quantum oscillations at high temperature, including potentially across the ordering transitions of the intercalants. As shown in Fig. 5, the quantum oscillations of the lightest mass bands can be resolved above 100 K. By employing techniques with improvised sensitivity and higher magnetic fields, a key goal is to map the electronic structure of

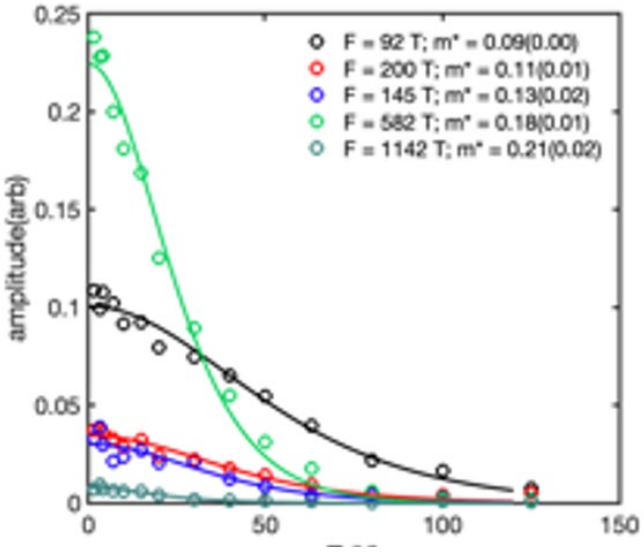

Fig. 5 – Amplitude of quantum oscillations as a function of temperature of GIC fit for effective mass.

these GICs across the ordering transitions. This would allow for a direct probe of the evolution of the Fermi surfaces in these systems and an examination of the development of long-range order of the intercalants on the overall electronic properties of these materials. Thermodynamic measurements of these materials are also of significant interest to map structural phase transitions that may occur, including for different intercalants with varying degrees of charge transfer and size of intercalant. Finally, the role of chiral intercalants has recently been discussed in the literature and may allow additional degrees of freedom to be introduced in the material design of intercalated systems.

Future Plans

For as-grown materials, developing an understanding of which TMDs are most amenable to these structural forms is a key target. Significant insight can be provided by the study of misfit systems (*5*); we plan to build on this large body of literature in this development. In terms of physical phenomena, finding active layers which connect to *e.g.* frustrated magnetism or excitonic behavior would potentially enable scalable platforms for such phenomena recently explored in the literature for few-layer vdW heterostructures. This could potentially open the study of such systems to tools that require macroscopic samples (*e.g.* neutron scattering). For post-synthesis intercalation, developing methods to improve the range of coherence of GICs and improving their electronic quality is a focus for future work. Additionally, extending these studies to other layered hosts including the TMDs is of significant interest.

References

1. S. Van Smaalen, *Incommensurate crystal structures*, Crystallogr. Rev. **4**, 79 (1995).

2. E. Y. Andrei, D. K. Efetov, P. Jarillo-Herrero, A. H. MacDonald, K. F. Mak, T. Senthil, E. Tutuc, A. Yazdani, A. F. Young, *The marvels of moiré materials*, Nat. Rev. Mater. **6**, 201 (2021).

3. A. Devarakonda, H. Inoue, S. Fang, C. Ozsoy-Keskinbora, T. Suzuki, M. Kriener, L. Fu, E. Kaxiras, D. C. Bell, and J. G. Checkelsky, *Clean 2D superconductivity in a bulk van der Waals superlattice*, Science 370, 231 (2020).

4. M. S. Dresselhaus, *Intercalation in Layered Materials*, Springer US, (1986).

5. A. Meerschaut, *Misfit layer compounds*. Current Opinion in Solid State and Materials Science **1**, 250-259 (1996).

Publications

A. Devarakonda, T. Suzuki, S. Fang, J. Zhu, D. Graf, M. Kriener, L. Fu, E. Kaxiras, and J. G. Checkelsky, *Signatures of bosonic Landau levels in a finite-momentum superconductor*, Nature **599**, 51 (2021).

D. Azoury, E. Baldini, A. Devarakonda, J. Li, S. Fang, P. Williams, R. Comin, J. G. Checkelsky, and N. Gedik, *Probing charge order of monolayer $NbSe_2$ within a bulk crystal*, arXiv:2308.02772 (2023).

Criteria and impact of electronic growth modes of metals on MoS_2

Timothy E. Kidd, Pavel V. Lukashev, Paul M. Shand, Andrew J. Stollenwerk

Keywords: 2D and layered crystals, nanostructures, transition metal compounds, scanning tunneling microscopy, magnetotransport

Research Scope

From an applications perspective, the ability to form high quality metallic contacts is crucial to integrating 2D semiconductors like MoS_2 into a device configuration. The general challenge is that the van der Waals surface of these materials is quite inert, which inhibits strong bonding and epitaxial growth. Furthermore, the lattice mismatch typically exceeds 8%, which leads to significant strain for most growth processes. In this research project, we explore the physics found at the interface between metals and layered semiconductors to determine optical growth processes to harness their potential applications.

In this work, have explored different combinations of meal and layered semiconductors to determine the properties essential for forming useful metallic contacts for devices. In varying the combinations of layered substrates and deposited metals, we are able to explore film growth modes with respect to properties including surface diffusion, bonding energies, lattice mismatch, and surface free energy. Our initial work focused on the noble metals, based on our discovery of electronic growth in the Au/MoS_2 system.1 This electronic growth mode, also seen in other noble metals, led to the self-assembly of quantized features correlated to the Fermi surface topography of the metal. Furthermore, these films had an abrupt interface with no determinantal signatures of strain from the large (~8%) lattice mismatch. As we explored other systems, we have developed a better understanding of the microscopic origins of this quantized electronic growth and also discovered new phenomena with potential in the area of spintronics and catalysis.

Recent Progress

In the past two years, we have discovered three distinct growth modes for metals on semiconducting layered dichalcogenide substrates. The noble metals Au, Ag, and Cu all exhibit very similar features at nanometer scale coverages. In each system, the metals form features with quantized heights correlated to their electronic structure, abrupt interfaces, and have surfaces that are atomically flat. These metals all share very similar Fermi surface topographies and lattice constants. The largest difference in their microscopic properties is Au bonds directly above the sulfur atoms at the surface for sulfur based dichalcogenide substrates, while in all other cases these metals bond in the hollow site surrounded by three sulfur atoms. For comparison, we examined

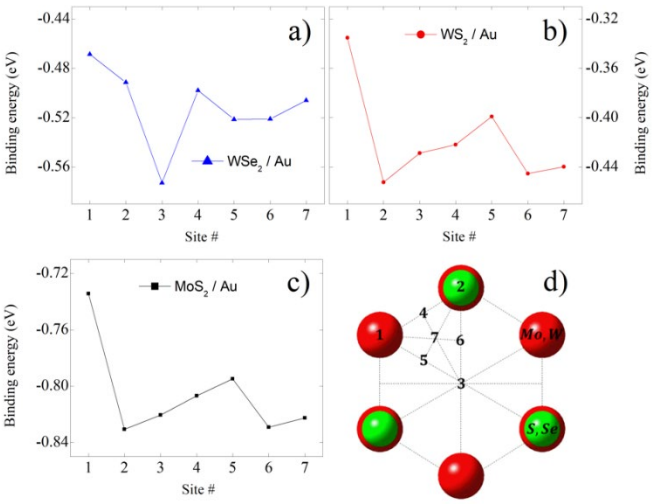

Figure 1. Density functional theory calculations of the binding energy of an Au atom on various layered semiconductor substrates.

MoS_2, WS_2, $MoSe_2$, and WSe_2 substrates using density functional theory calculations. For each system, the calculations show the difference in binding energy for nearby sites is quite small, indicated easy diffusion of metal ions on the dichalcogenide surface even at room temperature.[2] This was especially true for the Au/MoS_2 system (Fig. 1), which exhibited the strongest electronic growth, with quantized heights seen up to a film thickness of 7 nm. Additionally, in the Au/MoS_2 system, deposition above 8 nm thickness resulted in atomically flat films with a high degree of uniformity.[3] As an optimal system, we further probed the details of the Au/MoS_2 interface.

To explore the robustness of the Au/MoS_2 system and its potential for device applications, we explored the use of sputtering for film growth. In our studies of fundamental properties, we deposit the metals on freshly exfoliated surfaces using molecular beam epitaxy in ultra-high vacuum chambers on single crystal substrates. To test the impact of disorder, we instead used a sputtered MoS_2 film on a standard, unprocessed, silicon wafer as our substrate for Au deposition. Upon this film, we sputtered gold films of various thickness to explore surface roughness. The silicon wafers with native oxide had a surface roughness of roughly 200 pm as measured by atomic force microscopy. The optimal MoS_2 film thickness was found to be 2 molecular layers, with surface roughness slightly less than the silicon wafer. Sputtering Au onto this MoS2 film resulted in even flater surface morphologies. While these films did not display the single crystal characteristics found using single crystal substrates, the lowest measured surface roughness was found to be 72 nm (Fig. 2), which is quite near the resolution lmit of our microscope. As for the samples grown on single crystals, these ultra-flat surfaces were

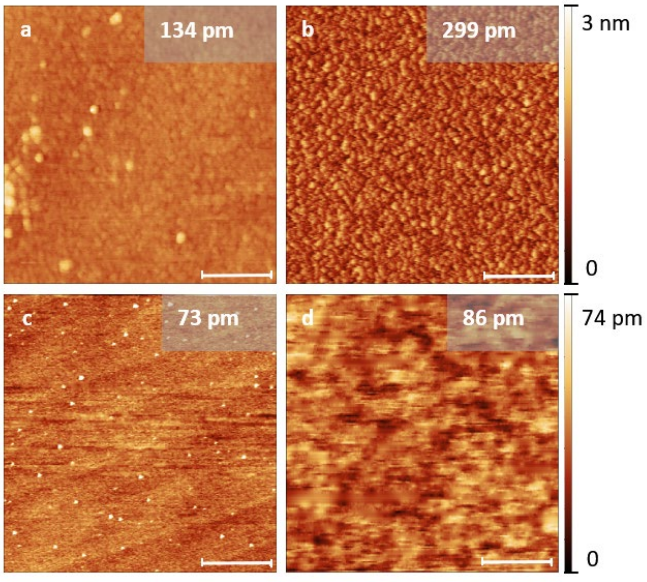

Figure 2. Topography measurements of Au films deposited onto a 2 monolayer MoS_2 film. The horizontal scale bar in each image is 500 nm. The RMS surface roughness is indicated within each image. Au film thicknesses are a) 2.9 nm Gold. b) 7.8 nm Gold. c) 12 nm Gold. d) 15 nm Gold.

only found for Au films thicker than the quantization limit of 7 nm. This indicates that even for growth under such relatively crude conditions, electronic growth modes could have a significant impact.

We also explored deposition using Ni, Co, Pd, and Pt. In Pd and Pt, there were some signs of limited electronic growth,[4] but only for isolated nanostructures. These metals, as compared to Au, Ag, and Cu, have significantly stronger binding energies to the substrate and very different Fermi surface topographies. Of interest was the fact the size of the nanostructures remained unchanged over a range of deposition coverages. Rather than aggregate to form plateaus or larger structures, the surface was simply populated with more nanostructures at higher coverages. Given their use in catalysis, these systems could find use in applications requiring size uniformity and high surface areas.

The Ni and Co films appeared exactly as one might expect for metals deposited on an inert system. These systems followed a standard Volmer-Weber growth pattern forming irregular clusters. However, their magnetic properties were quite interesting. We determined that there is an anomalous magneto-transport effect in these films at room temperature[5] and significant hybridization between the metal film and semiconducting substrate.[6] In measuring magnetization, we have been able to link the magnetotransport behavior to the formation of a spin glass at the interface. For example, at low temperatures the Ni/MoS_2 system behaves as a normal ferromagnetic film with standard magnetotransport through the interface. However, near room temperature, this system shows significant time dependent properties as a spin glass and a significant anisotropy in magnetotransport. This asymmetry shows some variation between samples, and so we expect some strong dependence on the initial film formation that we have not yet determined.

Future Plans

We have determined three areas of interest: magnetic interfaces, electronic growth, and nanostructured catalysts. We have also seen that at least some interesting properties can persist even within highly disordered systems such as the sputtered MoS_2 substrates. One general avenue of research will be to explore the impact of finite layer substrates. In the next year, we will be bringing a thin film growth system online which will be able to deposit ordered single and finite layer dichalcogenide materials as well as heterojunctions to further explore dimensional confinement. We anticipate this will not only enable integration to standard device specifications but also explore hybridization effects and their impact on truly 2D materials.

We are also introducing research into the potential for the Au/MoS2 system as a substrate for science in surface enhanced Raman spectroscopy and self-assembled organic molayers with thiol anchors. Using temperature and deposition coverage as parameters, surface roughness can be tuned very finely, which should complement research in these areas. In the magnetic films, we will be performing cross-sectional transmission electron microscopy with collaborators at Ames

laboratory to better understand the interface structure and control the magnetoresistance anisotropy. In the area of nanostructures (Pd, Pt, Ag, Cu, Au) we will use the microprobe system at Brookhaven Laboratory to test catalytic potential as a function of size, density, and substrate.

References

Put the list of references here using Times New Roman 10 pt. Please limit to no more than 5 papers. Provide full citation, including title and full author list.

1. T. E. Kidd, J. Weber, R. Holzapfel, K. Doore, and A. J. Stollenwerk, *Three-dimensional quantum size effects on the growth of Au islands on MoS_2*. Appl. Phys. Lett. **113**, 191603 (2018)
2. T. E. Kidd, P. Kruckenberg, C. Gorgen, P.V. Lukashev, A.J. Stollenwerk, *Criteria for electronic growth of Au on layered semiconductors*. Journal of Applied Physics, **132** 245301 (2022)
3. T.E. Kidd, J. Weber, E. O'Leary, A.J. Stollenwerk, *Preparation of ultrathin gold films with subatomic surface roughness* Langmuir **37**, 9472-9477 (2021)
4. T. E. Kidd, S. Skylar, S. Roberts, R. Carlile, P. V. Lukashev, A. J. Stollenwerk, *Electronic Growth of Pd(111) nanostructures on MoS_2*, J. App Phys, **129**, 174303 (2021)
5. T.E. Kidd, P.M. Shand, A.J. Stollenwerk, C. Gorgen, Y. Moua, L. Stuelke, P.V. Lukashev, *Large-field Magnetoresistance of nanometer scale nickel films grown on molybdenum disulfide.* AIP Advances **12** 035233 (2022)
6. A.J. Stollenwerk, L. Stuelke, L. Margaryan, T.E. Kidd, P.V. Lukashev, *First principles study of nearly strain-free Ni/WSe2 and Ni/MoS2 interfaces*, Journal of Physics: Condensed Matter **33** 425001 (2021)

Publications

1. P.V. Lukashev, T. E. Kidd, H.A. Harms, C. Gorgen, *Linear zipper defects on the surface of MoS_2*.Surface Science, under review (2023)
2. T. E. Kidd, P. Kruckenberg, C. Gorgen, P.V. Lukashev, A.J. Stollenwerk, *Criteria for electronic growth of Au on layered semiconductors*. Journal of Applied Physics, **132** 245301 (2022)
3. T.E. Kidd, P.M. Shand, A.J. Stollenwerk, C. Gorgen, Y. Moua, L. Stuelke, P.V. Lukashev, *Large-field Magnetoresistance of nanometer scale nickel films grown on molybdenum disulfide.* AIP Advances **12** 035233 (2022)
4. T.E. Kidd, P.V. Lukashev, L. Stuelke, C. Gorgen, S. Roberts, G. Gu, A.J. Stollenwerk, *Diffusion energy barrier of Au on Bi_2Se_3: theory and experiment*, Physica Scripta **96** 125708 (2021)
5. A.J. Stollenwerk, L. Stuelke, L. Margaryan, T.E. Kidd, P.V. Lukashev, *First principles study of nearly strain-free Ni/WSe2 and Ni/MoS2 interfaces*, Journal of Physics: Condensed Matter **33** 425001 (2021)
6. T.E. Kidd, J. Weber, E. O'Leary, A.J. Stollenwerk, *Preparation of ultrathin gold films with subatomic surface roughness* Langmuir **37**, 9472-9477 (2021)
7. T. E. Kidd, S. Skylar, S. Roberts, R. Carlile, P. V. Lukashev, A. J. Stollenwerk, *Electronic Growth of Pd(111) nanostructures on MoS_2*, J. App Phys, **129**, 174303 (2021)

Exploring Chirality-Spin Interplay Enabled by the Inorganic Chiral Nanostructures

Min Ouyang, University of Maryland- College Park

Keywords: spins, nanostructures, light-matter phenomena, scanning probe microscopy, chirality

Research Scope

The interplay between chirality and spin in inorganic solids has important implications in understanding and controlling fundamental magnetism with emerging applications in various fields, including Spintronics. The overall scope of this project is to develop a new class of inorganic nanostructures that can possess well-defined structural chirality and can be utilized as a foundation to explore various chirality entangled phenomena in condensed matters, and to characterize, understand inorganic chirality and explore intrinsic spin-chirality coupling. This project has adopted a multi-pronged experimental approach to achieve our goals by combining novel optical-atomic force microscopy (AFM) and low-temperature femtosecond optical spectroscopy with chemically synthesized chiral inorganic nanostructures. Knowledges as well as materials advancement and characterization of chiral inorganic nanostructures may enable new technology of such as next generation of magnetic storage and quantum information processing by using structural chirality.

Recent Progress

During the grant period (2022-2024), we have achieved substantial progresses in materials development of colloidal chiral nanostructures, characterization of chirality at the nanoscale and intrinsic spin-chirality coupling, with a few selected results highlighted below:

• Tuning geometric chirality in chiral metallic and their hybrid nanostructures by controlled crystal symmetry breaking.

While organic chiral molecules containing cyclic or dihedral point groups and their induced chirality-dependent phenomena have been extensively studied, exploration of inorganic chiral solids has been limited due to their structural complexity with involvement of many atoms as well as lack of understanding of underlying chiral mechanisms. We have developed a facile and general bottom-up synthetic strategy for achieving chiral metal (e.g., Au, Pd) nanostructures with different morphology and fine chirality control (Figure 1)[1]. The underlying chiral mechanism enabled by the chiral boundary morphology is proposed and substantiated by theoretical modeling and finite element method (FEM) simulation. These colloidal chiral metal nanostructures have manifested robust chirality that can be further used as building blocks towards formation of more complex chiral nanostructures. During the grant period, we have also achieved a new class of chiral hybrid metal-semiconductor nanostructures that can allow integration of chirality with other properties and functionalities[2]. Our achievement of chiral metal and their hybrid nanostructures have paved

the way to engineer nanoscale inorganic chirality and thus investigate various chirality entangled effects with new technological applications.

• Emerging experimental approach towards chirality and chiral electromagnetic field imaging with nanoscale spatial resolution.

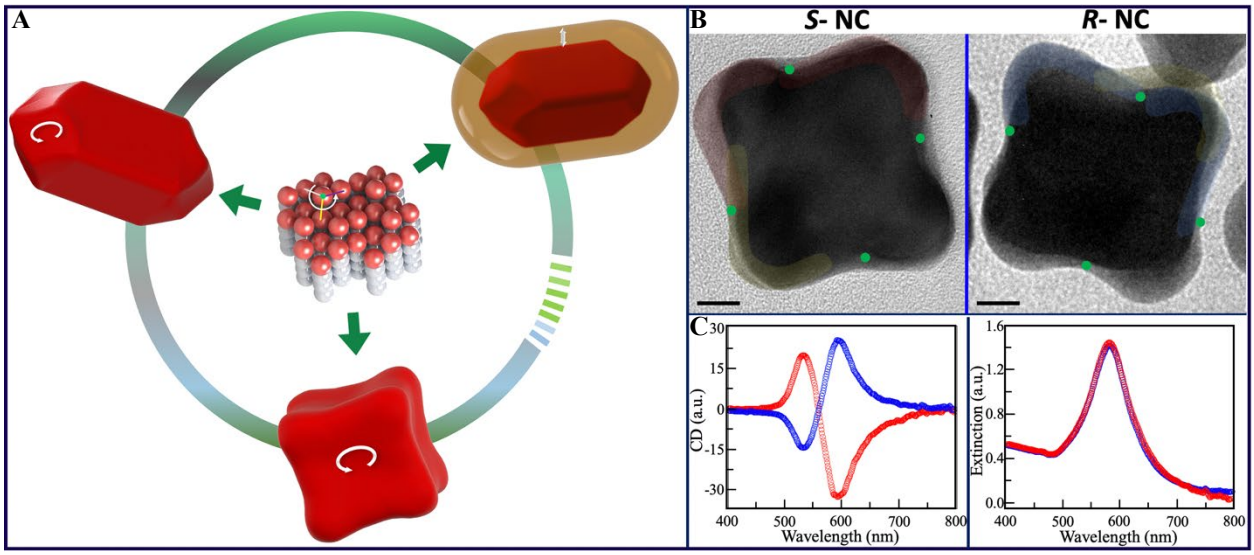

Figure 1. (A) Induced structural chirality by the broken crystal symmetry. (B) Typical TEM images of *S*- and *R*- chiral Au nanocubes. Scale bar, 10nm. (C) The CD (left) and absorption (right) spectroscopy of *S*- (red curve) and *R*- (blue curve) chiral Au nanocubes.

Characterization of structural chirality in condensed matter systems has been extremely challenging. Typical characterization technical is based on far- field optical spectroscopy, i.e., circular dichroism (CD) spectroscopy by measuring different absorptions of chiral objects between left- and right- circularly polarized light. Nevertheless, due to the fundamental optical diffraction limit, spatial resolution of CD is in the range of micron-meters. We have developed a novel experimental tool to enable direct optical chirality imaging by combining the AFM with chiral photothermal effect (unpublished). Enabled by this newly developed technique, we have demonstrated during the current grant period a spatial resolution of chiral imaging down to 10 nm. This technique has been applied to investigate and understand chirality of our synthesized chiral Au nanocubes with one example presented in the Figure 2.

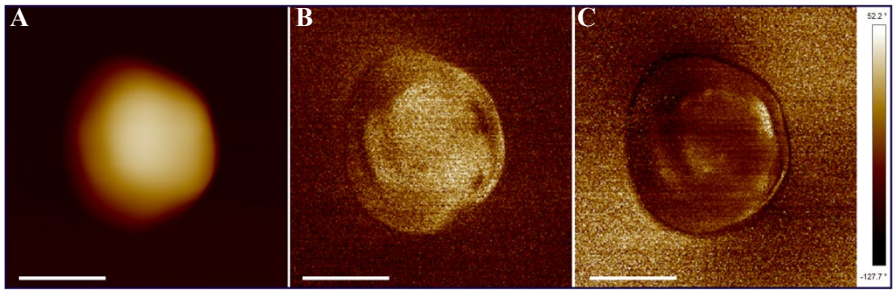

Figure 2. Topographic (A), near- field absorption (B) and chiral (C) images that are acquired simultaneously on a chiral Au nanocubes by our newly developed optical-AFM technique. (B) and (C) were acquired at 633 nm. Scale bar, 100 nm

• Exploring chirality-dependent spin polarizations in the chiral metal-semiconductor hybrid nanostructures.

During the grant period, we have utilized chiral Au-CdS hybrid nanostructures as a model system to investigate spin-chirality coupling at the low temperature (4K). We have employed time-resolved Faraday rotation (TRFR) femtosecond spectroscopy to explore spin dynamics of achiral semiconductor (CdS), when being coupled to a localized chiral plasmonic field originated from the Au core nanoparticles[3]. We have performed a series of control measurements by comparing chiral and achiral Au-CdS nanostructures, and we have observed that while for achiral Au-CdS nanostructures spin excitation with linearly polarized excitation in TRFR measurements has led to null TRFR signals because the spin-up and spin-down excitons are cancelled out, a clear chirality-dependent TRFR oscillation has been unambiguously observed from the left-handed and right-handed chiral Au-CdS core-shell nanostructures under the excitation of linearly polarized light. This observation has provided the firs evidence of chiral light-matter interactions through interfacial coupling, which is fundamentally different from the chirality-induced spin polarization observed in organic molecules.

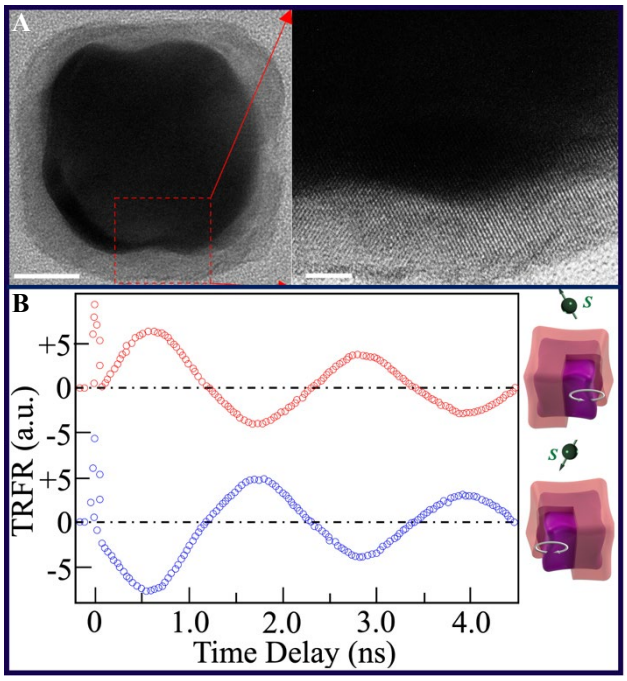

Figure 3. (A) TEM image of chiral Au-CdS hybrid nanostructure (left) and high- resolution image (right) showing single crystalline semiconductor shells. (B) The TRFR spectra of left- and right- handed hybrid nanostructures.

Future Plans

We will continue our achievements in both growth and characterizations of chiral nanoscale condensed matter systems and optical chirality-entangled spin measurements, with particular focus on understanding chirality mechanism and chirality-spin coupling. More specifically, we will optimize our newly developed nanoscale chirality imaging and combine with theoretical simulation to elucidate chirality imaging mechanism (Figure 2). We will also continue our chirality-spin measurements on the chiral Au-CdS nanostructures by tuning its structural parameters (e.g., semiconductor shell thickness and chiral core size) and investigate systematically structure-spin property relationship to elucidate the underlying mechanism of results presented in Figure 3. The outcome of this new study should enable unexplored nanoscale spin physics and magnetism, and open up new horizons of spin control beyond the conventional semiconductors Spintronics.

References

1. H. Liu, A.E. Vladar, P.-P. Wang and M. Ouyang, *Tuning Geometric Chirality in Metalic and Hybrid Nanostructures by Controlled Nanoscale Crystal Symmetry Breaking*, J.Am.Chem.Soc. **145**, 749-7503 (2023).

2. K. Lee, J.T. Zhang, H. Liu and M. Ouyang, *Injective Morphology Imprinting Synthesis of Anisotropic Inorganic Hybrid Nanostructures and Enabled Applications*, Nature Materials (under review) (2023).

3. P.-P. Wang, H. Liu and M. Ouyang, *All- Optical Localized Plasmons Enabled Spin Manipulation and Applications*, Nature Nanotechnology (under review) (2023).

Probing the origins of Chirality Induced Spin Selectivity via transport measurements

Meenakshi Singh, Colorado School of Mines

Keywords: Spintronics, nanostructures, hybrid organic inorganic perovskites, semiconductors, magnetotransport

Research Scope

Chirality induced spin selectivity (CISS) generates spin polarization in electron currents passing through a chiral molecule. Since its discovery almost two decades ago, CISS has been experimentally observed in a number of spectroscopic and tunneling magnetoresistance measurements. The theoretical foundations of CISS however, remain a subject of intense debate: helicity, chirality, substrate effects, interface effects, inelastic scattering processes, and many-body effects have all been highlighted as the critical factor governing CISS. One reason for this lack of consensus is that most CISS materials are delicate molecular systems that display spin filtering behavior under exacting conditions. This limits the types of geometries these systems can be integrated into for experimental enquiry. ***Our proposal, premised on the recent discovery the CISS system (Methylbenzylammonium)$_2$Pb$_{1-x}$Sn$_x$I$_4$, aims to provide key experimental insights needed to consolidate the theoretical foundations of CISS.*** The key properties of this system that make it ***fundamentally different from other CISS systems and ideal for integration into flexible transport platforms are its semiconducting nature and its ability to be spun coated into oriented thin films.*** We will develop processes to integrate (MBA)$_2$Pb$_{1-x}$Sn$_x$I$_4$ into a variety of transport measurement geometries and characterize charge and spin transport in these systems. The objectives of the proposed experiments are to ***measure critical parameters for CISS systems including spin-orbit coupling strength, prevalence of spin-flip scattering, and interaction with other spin orders such as superconductivity.***

Recent Progress

We have made Hall-bar devices and measured in-plane transport. The conductivity values match expectations. Magnetization measurements in a SQUID-MPMS system confirm the absence of ferromagnetism (figure 1).

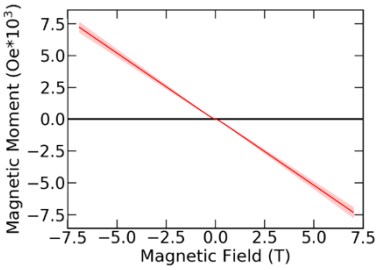

Figure 1: Magnetic moment of a 50 nm thick (R-MBA)$_2$SnI$_4$ film at 300 K.

Future Plans

(MBA)$_2$Pb$_{1-x}$Sn$_x$I$_4$ is semiconducting, highly tunable, and solution processable. We will capitalize on these unique features to make Hall bars, multi-terminal measurement platforms, and superconducting hybrids with (MBA)$_2$Pb$_{1-x}$Sn$_x$I$_4$. Temperature dependent magnetoresistance measurements in such geometries have been the workhorse of experimental Condensed Matter Physics and have elucidated phenomena ranging from superconductivity to topological insulators. We will apply this powerful toolkit to CISS systems. For example, measurements of non-local spin

transport on Hall bars will allow us to *experimentally determine spin-orbit coupling strength*, which is the major source of controversy in understanding CISS. Measurements of spin currents with ferromagnetic leads in various orientations will allow us to *experimentally determine spin transport efficiency*. Finally, measurements of supercurrents in superconductor-ferromagnet-CISS hybrids will enable us to *examine theoretical predictions of triplet superconductivity in CISS-superconductor hybrids.*

References

1. Lu, H., Xiao, C., Song, R., Li, T., Maughan, A. E., Levin, A., Brunecky, R., Berry, J. J., Mitzi, D. B., Blum, V., and Beard, M. C., *"Highly Distorted Chiral Two-Dimensional Tin Iodide Perovskites for Spin Polarized Charge Transport."*, Journal of the American Chemical Society **142**, 13030–13040 (2020).
2. Naaman, R., Paltiel, Y., and Waldeck, D., *"Chiral molecules and the electron spin."*, Nature Reviews Chemistry **3**, 250 –260 (2019).

Intervalley coherence and spin orbit coupling in rhombohedral trilayer graphene

Andrea Young, University of California Santa Barbara

Keywords: Magnetism, superconductivity, 2D materials, transport, scanning probe microscopy.

Research Scope

Our program seeks to understand the interplay between magnetism and superconductivity in correlated two dimensional materials using scanned probe microscopy based on nanoscale superconducting quantum interference devices. Our sensors are nanoscale SQUIDs fabricated at the apex of a quartz tube, and can be made as small as 30nm in diameter; moreover, they boast flux sensitivities near the quantum limit enabling, in principle, single spin detection. We have built two working instruments operating at 300mK and 1.5K, respectively, and are working on a 20mK machine to bring this technique to bear on a wide range of heterostructures over a large range of temperatures and magnetic fields. Under this phase of the program, our science focus is on rhombohedral multilayer graphene, which we previously discovered hosts superconducting and magnetic states similar to `magic-angle' graphene but without disorder induced by inhomogenous stacking

Recent Progress

Rhombohedral graphene multilayers show a cascade of magnetic and superconducting states when electrostatically doped through a gate-tuned van Hove singularity[1-4]. Rhombohedral graphene provides a highly reproducible and nearly disorder free platform to explore the emergence of superconductivity in a strongly interacting electron system, and a wide range of contrasting theoretical proposals have emerged to describe the interplay of correlated electron phenomena. However, a lack of experimental constraints on the emergent orders, and precise microscopic Hamiltonian has stymied theoretical progress.

In our recent progress, we used local magnetometry combined with electronic compressibility measurements to reveal a quarter-metal phase with a single fermi surface characterized by in-plane spin polarization but a vanishing out-of-plane orbital moment in rhombohedral trilayer graphene. We identify this new phase with an inter-valley coherent (IVC) phase with real-space charge density wave order. The inter-valley coherent phase competes with valley imbalanced (VI) orbital ferromagnets, in which electrons condense preferentially into one of the two inequivalent momentum space valleys. Remarkably, the competition between IVC and

VI phases is highly sensitive to intrinsic spin-orbit coupling, which suppresses the in-plane spin susceptibility of the VI phases and leads to distinct new correlated phases with hybrid VI-IVC character.

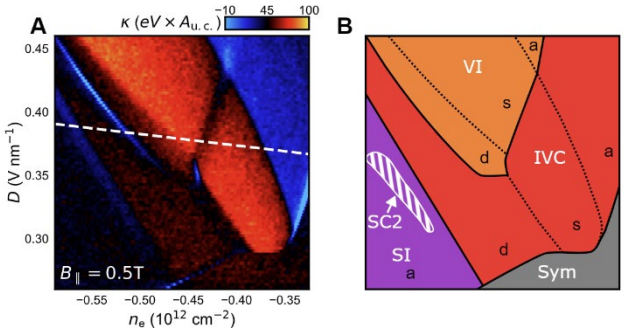

Intervalley coherent quarter metal in rhombohedral trilayer graphene. ***A,*** *Inverse compressibility, $\kappa = \partial\mu/\partial n_e$ as a function of carrier density n_e and applied displacement field D at T \approx 20mK and $B_\parallel = 5T$.* ***B,*** *Schematic phase diagram. Sym is a symmetric state; VI and IVC, are quarter metals with a single fermi surface; SI is a spin polarized, valley unpolarized state with two fermi surfaces. Dashed lines indicate Lifshitz transitions between disjointed (d), simple (s) and annular (a) fermi surfaces as marked by lower case labels. There is a superconducting pocket (SC2) at the boundary between the IVC and SI phases as marked.*

Figure panel A shows the inverse compressibility κ for hole doping in the vicinity of the `quarter metal' phase previously identified to have a single Fermi surface by Zhou et al [1]. In the current work, we have improved both thermalization ad sensitivity to allow us to resolve more phases in the same type of sample. Several features associated with phase transitions are visible in panel A, which is measured under an applied magnetic field of $B_\parallel$= 0.5T to polarize the electron spins into the plane. The transitions fall into two categories. First order transitions are marked by a negative dip in compressibility, and are associated with a change in isospin order. Steps in κ, in contrast, are associated with Lifshitz transitions where the fermi surface topology changes.

Panel B shows our proposed assignment of spin- and valley orders to the parameter space spanned in panel A. We identify four distinct regimes of isospin polarization. At the lowest values of n_e D, the system is in a paramagnetic phase with full isospin symmetry (Sym). At the highest values of n_e, the system is a spin-imbalanced (SI) ferromagnet, with identical, spin-polarized fermi surfaces in the two valleys. Spin-triplet superconductivity was reported at the extreme low-$|n_e|$ end of this `half-metal' SI phase. At high D and intermediate n_e, we identify two competing phases, both of which are spin polarized. In the valley imbalanced (VI) phase, the ground state conserves particle number in each of the two valleys but the net valley polarization is finite—the fermi surfaces in the contrasting valleys have different sizes. In the intervalley coherent (IVC) phase, in contrast, valley charge is not conserved, and fermi surfaces have k-dependent valley polarization resulting from the hybridization of the two valleys. Within each of these distinct isospin polarization regimes, Lifshitz transitions separate regions with simple (s), disjoint (d), or annular (a) topology of the Fermi sea.

While we do not elaborate on it in this abstract, our paper (in preparation) shows how the IVC/VI boundary directly reveals the presence of intrinsic spin orbit coupling. Notably, the value of 370 mK is non-negligible when compared to the energy differences between different magnetic states—expected to be in the few Kelvin range—and considerably larger than superconducting pairing energy inferred from the transition temperature. Crucially, the existence of spin orbit coupling lowers the symmetry of the single-particle Hamiltonian, making a number of new ground

states more likely. For example, the competition between spin orbit coupling and ferromangetic Hund's coupling naturally gives rise to spin polarized but valley-imbalanced half metals. However, theoretical treatments to date have typically neglected the effects of intrinsic spin orbit coupling entirely. It is likely that finite spin orbit coupling plays a key role in the physics of low-temperature interacting electron phases present in twisted and rhombohedral graphene systems. Indeed, a number of previous reports in Bernal bilayer and twisted double bilayer are consistent with finite spin-orbit coupling.

Future Plans

WSe2 support plays an important role in encouraging superconducting behavior; for example, in Bernal bilayer graphene is increases Tc by an order of magnitude [4]. This effect has remained enigmatic but is presumably tied to the enhanced spin orbit coupling. Having revealed the effects of intrinsic spin orbit coupling in the current reporting period, in the next award period plan to use nanoSQUID on tip microscopy and capacitance to directly probe the effects of induced spin orbit coupling in WSe2-supported rhombohedral trilayer. Transport measurements, we believe, may reveal significantly enhanced Tc.

References

1. Haoxin Zhou, Tian Xie, Areg Ghazaryan, Tobias Holder, James R. Ehrets, Eric M. Spanton, Takashi Taniguchi, Kenji Watanabe, Erez Berg, Maksym Serbyn & Andrea F. Young. *Half- and quarter-metals in rhombohedral trilayer graphene.* Nature 598, 429 (2021).

2. Haoxin Zhou, Tian Xie, Takashi Taniguchi, Kenji Watanabe & Andrea F. Young. *Superconductivity in rhombohedral trilayer graphene.* Nature 598, 434 (2021).

3. Haoxin Zhou, Ludwig Holleis, Yu Saito, Liam Cohen, William Huynh, Caitlin L. Patterson, Fangyuan Yang, Takashi Taniguchi, Kenji Watanabe, Andrea F. Young. *Isospin magnetism and spin-polarized superconductivity in Bernal bilayer graphene. Science 375, 774–778 (2022).*

4. Yiran Zhang, Robert Polski, Alex Thomson, Étienne Lantagne-Hurtubise, Cyprian Lewandowski, Haoxin Zhou, Kenji Watanabe, Takashi Taniguchi, Jason Alicea & Stevan Nadj-Perge. *Enhanced superconductivity in spin–orbit proximitized bilayer graphene.* Nature 613 268, (2023).

Publications

1. Haoxin Zhou, Ludwig Holleis, Yu Saito, Liam Cohen, William Huynh, Caitlin L. Patterson, Fangyuan Yang, Takashi Taniguchi, Kenji Watanabe, Andrea F. Young. *Isospin magnetism and spin-polarized superconductivity in Bernal bilayer graphene. Science 375, 774–778 (2022).*

Ultrafast and high-endurance switching of sliding ferroelectrics

Kenji Yasuda[1†*], Evan Zalys-Geller[1†], Xirui Wang[1], Kenji Watanabe[2], Takashi Taniguchi[2], Raymond Ashoori[1], and Pablo Jarillo-Herrero[1]

[1]Department of Physics, Massachusetts Institute of Technology, Cambridge, Massachusetts
[2]National Institute for Materials Science, Tsukuba, Japan.

Keywords: General: ferroelectrics, moiré physics **Material Forms:** 2D and layered crystals, nanostructures **Material Classes:** transition metal compounds, ferroelectrics and multiferroics. **Techniques:** transport, pulsed electrical measurements, nanofabrication and 2D assembly

Research Scope

The broad scope of this work under the QIS program involves theoretical, materials development, and measurement methods towards the creation of topological systems capable of supporting topological qubits in transition metal dichalcogenide (TMD) materials. Successes include: theoretical predicting the occurrence of a flat band in small angle twisted WSe_2 hosting an interaction driven Haldane and Mott insulators;[1] using theory to develop of a recipe for creating topological bands in AB stacked TMD bilayers;[2] study of the band structure driven thermoelectric response of $ZrTe_5$[3], a transition metal dichalcogenide that may host topologically nontrivial ground states; and observation of ferroelectric properties and moiré structure in rhombohedral stacked TMDs.[4]

Recent Progress

We have worked in two realms to broaden the scope of potentially topological materials. In one effort, we have focused on growing TMDs with potentially topological properties, while in the other we have worked on creating new "twistronic" materials functionality by creating layer-by-layer stacks with a twist between the layers. In this regard, the Jarillo-Herrero group and the Fu groups (with primary funding from our QIS grant) produced a breakthrough in ferroelectricity in twisted TMD layers.[4] Ultrathin semiconducting transition metal dichalcogenides (TMDs) such as MoSe2 hold promise for next generation electric and optoelectronic devices thanks to their extremely rich properties such as thickness dependent band gap, strong Coulomb interactions and spin-valley locking. These properties are further enriched by employing unique degrees of freedom in van der Waals (vdW) heterostructures with non-equilibrium stacking configurations. For example, varieties of emergent phenomena such as interlayer excitons, moiré excitons, and correlated insulating states have been recently discovered in heterobilayers of TMDs. Jarillo-Herrero and Fu discovered a new emergent property in semiconducting rhombohedral-stacked bilayer TMDs: ferroelectricity. The exfoliated bilayer TMD is non-ferroelectric because the adjacent layers are stacked antiparallel to each other.

We have adopted pulsed electronic methods (initially used for pulsed capacitance measurements) to study ferroelectricity and ferroelectric switching rates in bilayer rhombohedral stacked hBN structures. Figure 1 shows the basics of the measurement technique and data. We investigated switching kinetics over 10 orders of magnitude in time: from 1 ns to 10 s for up to down polarization switching and from 1 ns to 5 s for down to up polarization switching. We employed different measurement configurations for three different time scales: Above 1 ms, we used the Function Generator DS345 (Stanford Research Systems) through the DC port of the bias tee. Between 10 ns and 10 µs, we used the Data Timing Generator DTG5274 (Tektronix) via the RF port of the bias tee (See Fig. S1). Below 10 ns, we utilized the DTG5274 with an additional 16 dB attenuator and the amplifier Model 5865 (Picosecond Pulse Labs) through the RF port of the bias tee to apply a voltage pulse greater than 2.5 V.

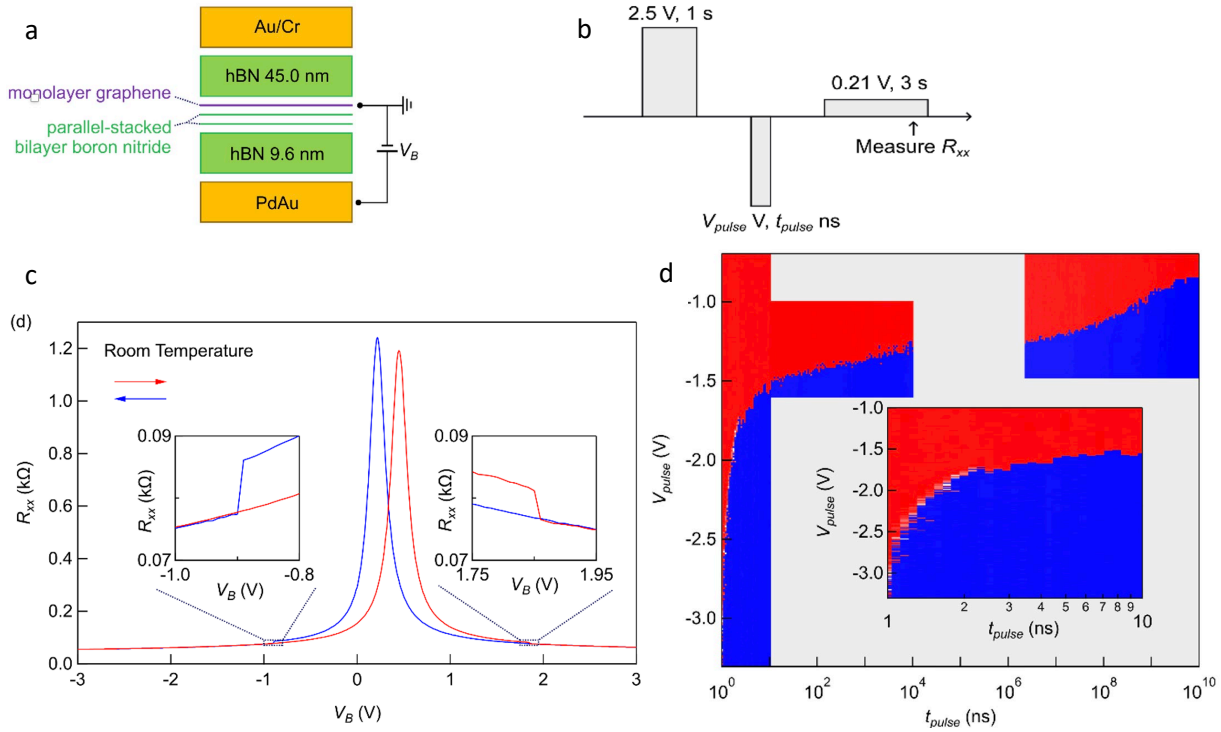

Figure 1: a) Schematic of the side view of the ferroelectric field-effect transistor. b) Illustration of the measurement procedure for the results shown in (d). c) Resistance of monolayer graphene R_{xx} as a function of the back gate voltage. The red and blue curves correspond to forward and backward scans, respectively. The inset shows the enlarged view at the ferroelectric switching voltages. d) Resistance of monolayer graphene R_{xx} measured at $V_B = 0.21$ V after the application of negative voltage pulse of V_{pulse} V and t_{pulse} ns. The inset shows the enlarged view from 1ns to 10ns.

We observed that the critical voltage for polarization switching increases as the pulse width decreases. Meanwhile, we can still achieve polarization switching with a pulse width as short as 1 ns for both up-to-down and down-to-up polarization transitions. We note that the switching speed of 1 ns is only limited by the instrumentation, and further investigation is required to examine the ultimate switching speed. The rapid switching observed at the nanosecond scale rivals the state-

of-the-art values for FeFET devices, suggesting potential applications in nonvolatile devices operating in the GHz frequency range.

Future Plans

If the polarization switching occurs via the domain wall motion of a single domain, the domain wall speed is as high as 1000 m/s, by dividing the device size of around 1 μm by the pulse width of 1 ns. This is close to the speed of shear phonon modes, which is theoretically predicted to be the physical limitation of the domain wall motion. Real-space imaging will be invaluable for understanding the dynamics of ferroelectric switching in sliding ferroelectricity from both fundamental and application perspectives.

References

1. Devakul T, Crépel V, Zhang Y, Fu L (2021) Magic in twisted transition metal dichalcogenide bilayers. *Nature Communications*, 12(1):6730. https://doi.org/10.1038/s41467-021-27042-9

2. Zhang Y, Devakul T, Fu L (2021) Spin-textured Chern bands in AB-stacked transition metal dichalcogenide bilayers. *Proceedings of the National Academy of Sciences*, 118(36):e2112673118. https://doi.org/10.1073/pnas.2112673118

3. Zhu J, Lee C, Mahmood F, Suzuki T, Fang S, Gedik N, Checkelsky JG (2022) Comprehensive study of band structure driven thermoelectric response of ZrTe 5. *Physical Review B*, 106(11):115105. https://doi.org/10.1103/PhysRevB.106.115105

4. Wang X, Yasuda K, Zhang Y, Liu S, Watanabe K, Taniguchi T, Hone J, Fu L, Jarillo-Herrero P (2022) Interfacial ferroelectricity in rhombohedral-stacked bilayer transition metal dichalcogenides. *Nature Nanotechnology*, 17(4):367–371. https://doi.org/10.1038/s41565-021-01059-z

Publications (2021-2023)

1. Zhang Y, Devakul T, Fu L (2021) Spin-textured Chern bands in AB-stacked transition metal dichalcogenide bilayers. Proceedings of the National Academy of Sciences, **118**(36):e2112673118. https://doi.org/10.1073/pnas.2112673118

2. Devakul T, Crépel V, Zhang Y, Fu L (2021) Magic in twisted transition metal dichalcogenide bilayers. Nature Communications, **12**(1):6730. https://doi.org/10.1038/s41467-021-27042-9

3. Li T, Jiang S, Shen B, Zhang Y, Li L, Tao Z, Devakul T, Watanabe K, Taniguchi T, Fu L, Shan J, Mak KF (2021) Quantum anomalous Hall effect from intertwined moiré bands. Nature, **600**(7890):641–646. https://doi.org/10.1038/s41586-021-04171-1

4. Wang X, Yasuda K, Zhang Y, Liu S, Watanabe K, Taniguchi T, Hone J, Fu L, Jarillo-Herrero P (2022) Interfacial ferroelectricity in rhombohedral-stacked bilayer transition metal

dichalcogenides. Nature Nanotechnology, **17**(4):367–371. https://doi.org/10.1038/s41565-021-01059-z

5. Devakul T, Fu L (2022) Quantum Anomalous Hall Effect from Inverted Charge Transfer Gap. Physical Review X, **12**(2):021031. https://doi.org/10.1103/PhysRevX.12.021031

6. Barrera SC de la, Aronson S, Zheng Z, Watanabe K, Taniguchi T, Ma Q, Jarillo-Herrero P, Ashoori R (2022) Cascade of isospin phase transitions in Bernal-stacked bilayer graphene at zero magnetic field. Nature Physics, **18**(7):771–775. https://doi.org/10.1038/s41567-022-01616-w

7. Zhu J, Lee C, Mahmood F, Suzuki T, Fang S, Gedik N, Checkelsky JG (2022) Comprehensive study of band structure driven thermoelectric response of $ZrTe_5$. Physical Review B, **106**(11):115105. https://doi.org/10.1103/PhysRevB.106.115105

8. Paul N, Zhang Y, Fu L (2023) Giant proximity exchange and flat Chern band in 2D magnet-semiconductor heterostructures. Science Advances, 9(8):eabn1401. https://doi.org/10.1126/sciadv.abn1401

Author
Index

Adhikari, Chandra Mani 279
Ahn, Charles H..... 38
Ajejas, Fernando 185
Al-Ostaz, Ahmed 345
Analytis, James 109
Andrei, Eva Y. 206
Ashoori, R. C. 226
Ashoori, Raymond 367
Assaf, Badih Antoine 265
Autrey, Daniel..... 279
Awschalom, David..... 230
Bailey, Crystal..... 283
Baldwin, K. W. 226
Balicas, Luis..... 169
Basaran, Ali C. 185
Basov, D. N. 96
Bastakoti, Bishnu Prasad 279
Bauer, Eric 31, 193
Bauers, Sage..... 120
Bhattacharya, Anand..... 299
Bian, Guan 268
Birgeneau, Robert 109
Bockrath, Marc 61
Bozhko, Dmytro..... 276
Brahlek, Matt 77
Brahlek, Matthew..... 274
Bud'ko, Sergey 13
Butov, Leonid 100
Canfield, Paul..... 13
Cava, Robert 88
Celinski, Zbigniew..... 276
Cha, Judy J. 270
Chakhalian, Jak 205
Chan, Mun..... 53
Chang, Cui-Zu..... 91
Checkelsky, Joe..... 350
Crommie, Michael 104
Crooker, Scott 53
Csathy, Gabor 221
Dawood, Farah..... 283
Dean, Cory R. 289
Dessau, Dan 293
Eom, Chang-Beom..... 66
Eres, Gyula..... 77
Fiete, Gregory 139
Finkelstein, Gleb 72
Fischer, Felix R. 324
Fisher, I.R..... 197
Fong, Dillon 299
Fowlie, Jennifer..... 34
Freedman, Danna 230
Frolov, Sergey..... 58
Furukawa, Yuji 13
Gautam, Bhoj Raj..... 279
Ghimire, Nirmal..... 304
Gu, Genda 243
Hadjipanayis, George..... 139
Han, Shubo..... 279
Harrison, Neil..... 53
Hartman, Colleen N. 287
Hawrylak, P..... 226
Heinz, Tony F. 289
Hersam, Mark 230
Hirata, Michihiro..... 31, 193
Hoffmann, Axel 159
Hone, James 289
Hsieh, David 234
Hsu, Yi-Ting 265
Hu, Jin 48
Hwang, Harold Y. 34
Jaime, Marcelo 53
Jarillo-Herrero, Pablo..... 367
Jiang, Samuel 299
Jiang, Zhigang..... 144
Johnston, D.C. 255
Kaminski, Adam 13
Kapitulnik, A..... 197
Ke, L. 255
Kidd, Timothy E. 354
Kim, Eun-Ah..... 270
Kim, Philip..... 216
Kim, Stephan..... 88
Kivelson, S.A. 197
Korkusinski, M. 226
Lanzara, Alessandra..... 104, 109
Lau, Chun Ning (Jeanie) 61
Lee, Dunghai..... 109
Lee, Ho Nyung..... 77
Lee, Minhyea 136
Lei, Shiming..... 88
Leszczynski, Jerzy 345
Lewis, Laura H..... 139

Li, Lu 238
Li, Qi 43
Li, Qiang 243
Li, Yi 159
Liu, Jian 314
Liu, Mengkun 243
Liu, Xiaolong 265
Liu, Xinyu 265
Long, Jeffrey 230
Louie, Steven 104
Lukashev, Pavel 354
MacDonald, Allan H. 289
Madhavan, Vidya 10
Majdoub, Mohammed 345
Mak, Kin Fai 249, 289
Mandrus, David 250
Manfra, Michael J. 125
Maple, M. Brian 25
May, Andrew F. 250
McGuire, Michael A. 250
McIver, James 341
McQueeney, R.J. 255
Miao, Hu 77
Miravet, D. 226
Mitchell, John F. 304
Moore, Joel 109
Natelson, Douglas 211
Ni, Chaoying 139
Ni, Ni 17
Nouranian, Sasan 345
Novosad, Valentine 159, 276
Ojeda-Aristizabal, Claudia 129
Ong, N. Phuan 88
Orenstein, Joseph 109
Orth, P.P. 255
Ortiz, Brenden 250
Ouyang, Min 358
Ozturk, Birol 348
Paglione, Johnpierre 21
Palmstrom, Johanna 53
Pan, Wei 83
Pasupathy, Abhay 328
Pfaff, Wolfgang 159
Pfeiffer, L. 226
Phelan, Daniel 304
Pradhan, Nihar R. 345
Prozorov, Ruslan 13
Qian, Xiaofeng 332
Qiu, Zi Q. 104
Raghu, Srinivas 34
Rai, Binod Kumar 279
Ralph, Dan 154
Ramesh, R. 109
Ramirez, Arthur P. 202
Rhodes, Daniel 332
Rondinelli, James 230
Ronning, Filip 31, 193
Rosa, Priscilla 53
Rosenbaum, Thomas F. 260
Rossi, Enrico 83
Roy, Xavier 328
Salev, Pavel 185
Sapkota, Aashish 13
Scheie, Allen 31, 193
Schiffer, Peter 150
Schleife, André 159
Schoop, Leslie 88
Schuller, Ivan K. 185
Sengottuvelu, Dinesh Kumar 345
Shabani, Javad 83
Shan, Jie 289
Shand, Paul M. 354
Shayegan, M. 188
Shekhter, Arkady 53
Singh, Meenakshi 362
Singleton, John 53
Slade, Tyler 13
Smirnov, Dmitry 144
Smith, Arthur R. 164
Staunton, Julie B. 139
Stollenwerk, Andrew J. 354
Sumant, Anirudha V. 345
Tanatar, Makariy 13
Taniguchi, Takashi 367
Thomas, Sean 31, 193
Torres, Felipe 185
Ueland, B.G. 255
Vaknin, D. 255
Wang, Feng 104
Wang, Linlin 13
Wang, Xirui 367
Ward, T. Zac 77

Wasielewski, Michael 230
Watanabe, Kenji 367
West, K. 226
Wu, Mingzhong 134
Xu, Xiaoshan 175
Yan, Jiaqiang 250
Yang, Fengyuan 180
Yasuda, Kenji 367
Yi, Ming 309
Yin, Weiguo 243
Yoo, H. M. 226
Young, Andrea 364
Zaletel, Mike 104
Zalys-Geller, Evan 367
Zettl, Alex 104
Zhang, Xiao-Xiao 319
Zhao, Liuyan 337
Zhou, Haidong 314
Zhou, You 115
Zhu, Jun 322
Zuo, Jian-Min 159

Participant

List

Full Name	Institution	Email Address
Charles Ahn	Yale University	charles.ahn@yale.edu
Eva Andrew	Rutgers	eandrei@physics.rutgers.edu
Ray Ashoori	Massachusetts Institute of Technology	ashoori@mit.edu
Badih Assaf	University of Notre Dame	bassaf@nd.edu
Crystal Bailey	American Physical Society	bailey@aps.org
Luis Balicas	Florida State University	balicas@magnet.fsu.edu
Dmitri Basov	Columbia University	db3056@columbia.edu
Sage Bauers	National Renewable Energy Laboratory	sage.bauers@nrel.gov
Anand Bhattacharya	Argonne National Laboratory	anand@anl.gov
	University of Missouri	biang@missouri.edu
Marc Bockrath	Ohio State University	bockrath.31@osu.edu
Dmytro Bozhko	University of Colorado, Colorado Springs	dbozhko@uccs.edu
Matthew Brahlek	Oak Ridge National Laboratory	brahlekm@ornl.gov
Leonid Butov	University of California, San Diego	lvbutov@physics.ucsd.edu
Paul C. Canfield	Ames National Laboratory / Iowa State University	canfield@ameslab.gov
Claudia Cantoni	U.S. Department of Energy	claudia.cantoni@science.doe.gov
Judy Cha	Cornell University	jc476@cornell.edu
Mun Chan	Los Alamos National Laboratory	mchan@nsf.gov
Cui-Zu Chang	Pennsylvania State University	cxc955@psu.edu
Joe Checkelsky	Massachusetts Institute of Technology	checkelsky@mit.edu
Gabor Csathy	Purdue University	gcsathy@purdue.edu
Dan Dessau	University of Colorado	Dessau@Colorado.edu
Chang-Beom Eom	University of Wisconsin, Madison	EOM@ENGR.WISC.EDU
Gleb Finkelstein	Duke University	gleb@duke.edu

Full Name	Institution	Email Address
Felix R. Fischer	University of California, Berkeley	ffischer@berkeley.edu
Ian Fisher	Stanford University	irfisher@stanford.edu
Michael Fitzsimmons	U.S. Department of Energy	michael.fitzsimmons@science.doe.gov
Danna Freedman	Massachusetts Institute of Technology	danna@mit.edu
Sergey Frolov	University of Pittsburgh	frolovsm@pitt.edu
Bhoj Gautam	Fayetteville State University	bgautam@uncfsu.edu
Neil Harrison	Los Alamos National Laboratory	nharrison@lanl.gov
Colleen Hartman	National Academies of Sciences, Engineering, and Medicine	chartman@nas.edu
Frances Hellman	University of California, Berkeley/Lawrence Berkeley National Laboratory	fhellman@berkeley.edu
Michi	Los Alamos National Laboratory	mhirata@lanl.gov
Axel Hoffmann	University of Illinois, Urbana-Champaign	axelh@illinois.edu
David Hsieh	California Institute of Technology	dhsieh@caltech.edu
Yi-Ting Hsu	University of Notre Dame	yhsu2@nd.edu
Jin Hu	University of Arkansas	jinhu@uark.edu
Harold Hwang	Stanford Linear Accelerator Center	hyhwang@stanford.edu
Debdeep Jena	Cornell University	djena@cornell.edu
Adam Kaminski	Ames National Laboratory	adamkam@ameslab.gov
Tina Kaarsberg	U.S. Department of Energy	tina.kaarsberg@ee.doe.gov
Helen Kerch	U.S. Department of Energy	helen.kerch@science.doe.gov
Tim Kidd	University of Northern Iowa	tim.kidd@uni.edu
Philip Kim	Harvard University	pkim@physics.harvard.edu

Full Name	Institution	Email Address
Jeanie Lau	The Ohio State University	lau.232@osu.edu
Ho-Nyung	Oak Ridge National Laboratory	hnlee@ornl.gov
Minhyea Lee	University of Colorado Boulder	minhyea.lee@colorado.edu
Laura	Northeastern University	lhlewis@northeastern.edu
Lu Li	University of Michigan	luli@umich.edu
Yi Li	Argonne National Laboratory	yili@anl.gov
Qiang Li	Brookhaven National Laboratory/Stony Brook University	qiangli@bnl.gov
Xinyu Liu	University of Notre Dame	xliu2@nd.edu
Xiaolong Yu	University of Notre Dame	xliu33@nd.edu
Kin Fai Mak	Cornell University	kinfai.mak@cornell.edu
Michael Manfra	Purdue University	mmanfra@purdue.edu
Brian Maple	UC San Diego	mbmaple@ucsd.edu
Michael McGuire	Oak Ridge National Laboratory	mcguirema@ornl.gov
James McIver	Columbia University	jm5382@columbia.edu
Robert McQueeney	Ames National Laboratory/Iowa State University	mcqueeney@ameslab.gov
Claudia Mewes	U.S. Department of Energy	claudia.mewes@science.doe.gov
Tim Mewes	U.S. Department of Energy	tim.mewes@science.doe.gov
John Mitchell	Argonne National Laboratory	mitchell@anl.gov
Vijay Narayanan	IBM Research	vijayna@us.ibm.com
Douglas Natelson	Rice University	natelson@rice.edu
Ni Ni	University of California, Los Angeles	nini@physics.ucla.edu
Valentine Novosad	Argonne National Laboratory	novosad@anl.gov

Full Name	Institution	Email Address
Claudia Ojeda-Aristizabal	California State University Long Beach	Claudia.Ojeda-Aristizabal@csulb.edu
N. Phuan Ong	Princeton University	npo@princeton.edu
Joseph Orenstein	University of California, Berkeley/Lawrence Berkeley National Laboratory	jworenstein@lbl.gov
Min Ouyang	University of Maryland	mouyang@umd.edu
Birol Ozturk	Morgan State Univeristy	birol.ozturk@morgan.edu
Johnpierre Paglione	University of Maryland, College Park	paglione@umd.edu
Mick Pechan	U.S. Department of Energy	michael.pechan@science.doe.gov
Danny Phelan	Argonne National Laboratory	dphelan@anl.gov
Nihar Pradhan	Jackson State University	nihar.r.pradhan@jsums.edu
Xiaofeng Qian	Texas A&M University	feng@tamu.edu
Dan Ralph	Cornell University	dcr14@cornell.edu
Art Ramirez	University of California, Santa Cruz	apr@ucsc.edu
Brad Ramshaw	Cornell University	bradramshaw@cornell.edu
Dan Rhodes	University of Wisconsin, Madison	darhodes@wisc.edu
Filip Ronning	Los Alamos National Laboratory	fronning@lanl.gov
Thomas Rosenbaum	California Institute of Technology	tfr@caltech.edu
Enrico Rossi	William & Mary	erossi@wm.edu
Xavier Roy	Columbia University	xr2114@columbia.edu
Peter Schiffer	Princeton University	peter.schiffer@yale.edu
Ivan Schuller	University of California, San Diego	ischuller@ucsd.edu
Andy Schwartz	U.S. Department of Energy	andrew.schwartz@science.doe.gov
Athena Sefat	U.S. Department of Energy	athena.sefat@science.doe.gov
Mansour Shayegan	Princeton University	shayegan@princeton.edu
Meenakshi Singh	Colorado School of Mines	msingh@mines.edu

Full Name	Institution	Email Address
Dmitry Smirnov	National High Magnetic Field Laboratory	smirnov@magnet.fsu.edu
Arthur R. Smith	Ohio University	smitha2@ohio.edu
Julie Staunton	University of Warwick	J.B.Staunton@warwick.ac.uk
Mark Stiles	National Insitute of Standards and Technology	mark.stiles@nist.gov
Sean Thomas	Los Alamos National Laboratory	smthomas@lanl.gov
Susan Trolier-McKinstry	Pennsylvania State University	stmckinstry@psu.edu
Feng Wang	Lawrence Berkeley National Laboratory	fengwang76@berkeley.edu
Mingzhong Wu	Colorado State University	mwu@colostate.edu
Xiaoshan Xu	University of Nebraska, Lincoln	xiaoshan.xu@unl.edu
Fengyuan Yang	The Ohio State University	yang.1006@osu.edu
Ming Yi	Rice University	mingyi@rice.edu
Andrea Young	University of California, Santa Barbara	afy2003@ucsb.edu
Ian Young	Intel Corporation	ian.young@intel.com
Xiao-Xiao Zhang	University of Florida	xxzhang@ufl.edu
Liuyan Zhao	University of Michigan, Ann Arbor	lyzhao@umich.edu
Haidong Zhou	University of Tennessee	hzhou10@utk.edu
You Zhou	University of Maryland, College Park	youzhou@umd.edu
Jun Zhu	Pennsylvania State University	jxz26@psu.edu